NATURAL PRODUCTS AND HEPATIC HEALTH: LIGHT AND SHADOWS

EDITED BY: Silvia Di Giacomo, Antonella Di Sotto, Oscar Briz and Annabella Vitalone

PUBLISHED IN: Frontiers in Pharmacology

frontiers Research Topics

frontiers

ISSN 1664-8714
ISBN 978-2-88974-529-6
DOI 10.3389/978-2-88974-529-6

About Frontiers

Frontiers is more than just an open-access publisher of scholarly articles: it is a pioneering approach to the world of academia, radically improving the way scholarly research is managed. The grand vision of Frontiers is a world where all people have an equal opportunity to seek, share and generate knowledge. Frontiers provides immediate and permanent online open access to all its publications, but this alone is not enough to realize our grand goals.

Frontiers Journal Series

The Frontiers Journal Series is a multi-tier and interdisciplinary set of open-access, online journals, promising a paradigm shift from the current review, selection and dissemination processes in academic publishing. All Frontiers journals are driven by researchers for researchers; therefore, they constitute a service to the scholarly community. At the same time, the Frontiers Journal Series operates on a revolutionary invention, the tiered publishing system, initially addressing specific communities of scholars, and gradually climbing up to broader public understanding, thus serving the interests of the lay society, too.

Dedication to Quality

Each Frontiers article is a landmark of the highest quality, thanks to genuinely collaborative interactions between authors and review editors, who include some of the world's best academicians. Research must be certified by peers before entering a stream of knowledge that may eventually reach the public - and shape society; therefore, Frontiers only applies the most rigorous and unbiased reviews.
Frontiers revolutionizes research publishing by freely delivering the most outstanding research, evaluated with no bias from both the academic and social point of view. By applying the most advanced information technologies, Frontiers is catapulting scholarly publishing into a new generation.

What are Frontiers Research Topics?

Frontiers Research Topics are very popular trademarks of the Frontiers Journals Series: they are collections of at least ten articles, all centered on a particular subject. With their unique mix of varied contributions from Original Research to Review Articles, Frontiers Research Topics unify the most influential researchers, the latest key findings and historical advances in a hot research area! Find out more on how to host your own Frontiers Research Topic or contribute to one as an author by contacting the Frontiers Editorial Office: frontiersin.org/about/contact

NATURAL PRODUCTS AND HEPATIC HEALTH: LIGHT AND SHADOWS

Topic Editors:
Silvia Di Giacomo, Sapienza University of Rome, Italy
Antonella Di Sotto, Sapienza University of Rome, Italy
Oscar Briz, University of Salamanca, Spain
Annabella Vitalone, Sapienza University of Rome, Italy

Citation: Di Giacomo, S., Di Sotto, A., Briz, O., Vitalone, A., eds. (2022). Natural Products and Hepatic Health: Light and Shadows. Lausanne: Frontiers Media SA. doi: 10.3389/978-2-88974-529-6

Table of Contents

frontiers in Pharmacology

EDITORIAL
published: 25 February 2022
doi: 10.3389/fphar.2022.868207

Editorial: Natural Products and Hepatic Health: Light and Shadows

Silvia Di Giacomo[1]*, *Oscar Briz*[2,3], *Annabella Vitalone*[1] and *Antonella Di Sotto*[1]

[1]Deptartment of Physiology and Pharmacology "V. Erspamer", Sapienza University of Rome, Rome, Italy, [2]Laboratory of Experimental Hepatology and Drug Targeting (HEVEFARM), IBSAL, University of Salamanca, Salamanca, Spain, [3]Center for the Study of Liver and Gastrointestinal Diseases (CIBERehd), Carlos III National Institute of Health, Madrid, Spain

Keywords: herbal extracts, hepatoprotection, hepatotoxicity, liver disease, gut microbiota, waste, polyphenols, antioxidant

Editorial on the Research Topic

Natural Products and Hepatic Health: Light and Shadows

The liver is an essential organ for survival, being involved in the regulation of several physiological functions, including synthesis and storage of nutrients, detoxication, and decomposition of xenobiotics and toxicants, along innate immunity (Marin et al., 2020). Hepatic ailments often compromise global wellness, leading to severe reactions and troubles, and sometimes to death (Zhang et al., 2018). Indeed, with approximately 2 million deaths per year worldwide, liver diseases represent one of the major causes of death globally and a major threat to public health; among them, viral hepatitis is the most common while nonalcoholic fatty liver disease (NAFLD) is the most rapidly growing contributor to mortality and morbidity. The NAFLD increased incidence seems also to contribute to the risk of cirrhosis and liver cancer (Asrani et al., 2019).

In the past decades, several efforts have been made to fight liver diseases; however, limitations in finding more effective hepatoprotective drugs than the currently available medications still exist. This strengthens the importance to discover novel therapeutic options, which can also tackle the socioeconomic burden of these diseases (Wang et al., 2021).

In this context, a renewed strategy is represented by plant-based natural products, which provide a wide range of new and unique bioactive molecules for drug discovery (**Figure 1**). These phytochemicals can be responsible for the healing properties of the extracts both by acting synergistically within the phytocomplex or as pure compounds. Moreover, herbal by-products and waste could be exploited as renewable sources of bioactive natural substances (Di Sotto et al., 2019).

However, "all that glitters is not gold"! Indeed, searching for new drug candidates from natural products is often limited by some issues that can also raise safety concerns. Particularly, the complexity and variability of phytochemical composition could lead to unpredictable and unexpected effects, along with possible interactions with concomitantly administered drugs (**Figure 1**). In this context, using phytochemically characterized and standardized herbal extracts can allow to partially control the undesired effects and achieve reproducible bioactivities (Thomford et al., 2018).

The complex picture described above is, at least in part, the cause of the contrasting evidence about the relationship between natural products and hepatic health. Indeed, while some preclinical

OPEN ACCESS

Edited and reviewed by:
Angelo A. Izzo,
University of Naples Federico II, Italy

***Correspondence:**
Silvia Di Giacomo
silvia.digiacomo@uniroma1.it

Specialty section:
This article was submitted to Gastrointestinal and Hepatic Pharmacology, a section of the journal Frontiers in Pharmacology

Received: *02 February 2022*
Accepted: *11 February 2022*
Published: *25 February 2022*

Citation:
Di Giacomo S, Briz O, Vitalone A and Di Sotto A (2022) Editorial: Natural Products and Hepatic Health: Light and Shadows. Front. Pharmacol. 13:868207. doi: 10.3389/fphar.2022.868207

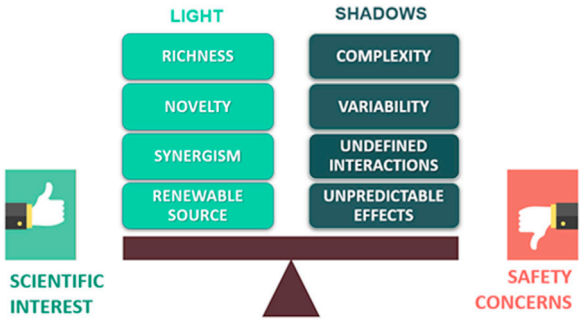

FIGURE 1 | Scheme of the possible advantages and issues related to the use of plant-based natural products in drug discovery.

and clinical studies underpin a potential interest in botanicals to manage liver diseases (Wang et al., 2020), others highlight safety concerns associated with their use (Ippoliti et al., 2021). In line with this evidence, the articles collected within the Research Topic "Natural Products and Hepatic Health: Light and Shadows" can contribute to the advancement of our knowledge about the impact of botanicals on hepatic health. Particularly, some articles tried to provide solid scientific bases to the traditional use of certain botanicals. Yang et al. have studied the antihyperlipidemic effect of the Traditional Chinese Medicine (TCM) formula Qing Gan San (QGS) in a rat model of metabolic associated fatty liver disease. QGS exhibited hepatoprotective effects and lowered lipid accumulation in the liver, likely through the inhibition of sterol regulatory element-binding protein-1. Similarly, the TCM formula Liuweiwuling was found endowed with *in vitro* and *in vivo* hepatoprotective properties, mediated by anti-apoptotic, anti-inflammatory, and antioxidant effects (Gao et al.); esculetin, luteolin, schisandrin A and schisandrin B were highlighted to be the major bioactive phytochemicals. The pharmacological power of TCM formulas in liver diseases has been also described by Fu et al.; notably, they highlighted that TCM can relieve liver diseases through the modulation of several pathways among which Nrf2, NF-κB, PI3K/Akt, and IL-6/STAT3, leading to antiinflammatory, antioxidant and antiviral effects.

Nowadays, several studies have shown that liver health is strictly connected to gut microbiota homeostasis (Minemura and Shimizu, 2015). In this context, Zhang et al. studied the changes in gut microbiota induced by the TCM Yinchen Wuling powder and showed that this formula was able to increase the abundance of eubacteria, and modulate inflammation and immune function, thus improving liver health. Similarly, Yu et al. underpinned the anti-cholestatic effects of the TCM formula Zhuyu Pill, mediated by changes in amino acid metabolism, steroid hormone biosynthesis, and bile secretion, along with an increase in fecal eubacteria. A specific focus on the hepatoprotection by chlorogenic acid, through the modulation of gut microbiota and glucagon-like peptide-1, has been addressed by Shi et al. in an *in vivo* NAFLD model.

Herbal by-products and waste have been also approached as a source of hepatoprotective agents. In this context, the hepatoprotective effects of different extracts from *Punica granatum* L. peels, known to be a rich source of polyphenols, have been evaluated by Ali et al. in a rat model of carbon tetrachloride–induced liver injury. The tested samples affected the inflammatory and oxidative response, and the liver enzyme levels; such effects were like those of the standard silymarin. Similarly, Feng et al. investigated the potential usefulness of a polysaccharide-based extract from the *Schisandra chinensis* (Turcz.) Baill. caulis in a rat model of HFD-induced NAFLD. Interestingly, the extract was found able to improve the liver enzyme levels and lipid parameters, through the regulation of metabolic pathways, and oxidative stress inhibition.

Mixtures of different herbal extracts as possible remedies to fight liver diseases have been approached too. Particularly, Frigerio et al. dealt with the anticholesterolemic activity of a commercial formulation based on a blend of artichoke, caigua, and fenugreek extracts. The product was found able to reduce total and free cholesterol, and to increase bile acid synthesis, acting similarly to red yeast rice, thus strengthening the interest in its nutraceutical role. Chen et al. also highlighted the ability of a fixed mixture of geniposide and chlorogenic acid to blunt the hepatic *de novo* lipogenesis, by inhibiting stearoyl-CoA desaturase-1, in an *in vivo* model of NAFLD.

At last, in line with the importance to address the possible safety concerns related to botanical use, Stati et al. critically evaluated recent cases of hepatotoxicity linked to *Curcuma longa* L. food supplements. According to previously published evidence (Vitalone et al., 2011; Frenzel and Teschke, 2016), the authors pointed out that other factors related to the subject susceptibility or to the product composition and bioavailability should be considered in the causality assessment as possible contributors of liver damage.

Altogether the results of the articles collected in the present Research Topic greatly improve our knowledge about the effects of herbal products on liver function and the mechanisms involved, and suggest possible future developments in nutraceutical and pharmacological fields. However, more outstanding research, as those here collected, and clinical trials are still needed to clarify the opportunities and pitfalls of natural products in liver diseases so putting light in the shadows.

AUTHOR CONTRIBUTIONS

SDG, OB, AV, and ADS surveyed and designed this Research Topic. SDG and ADS wrote and drafted the editorial manuscript. OB and AV revised the manuscript critically. All authors contributed to the article and approved the submitted version.

ACKNOWLEDGMENTS

We wish to thank all the authors contributing to this Frontiers Research Topic and all the reviewers who have helped to make it solid.

REFERENCES

Asrani, S. K., Devarbhavi, H., Eaton, J., and Kamath, P. S. (2019). Burden of Liver Diseases in the World. *J. Hepatol.* 70 (1), 151–171. doi:10.1016/j.jhep.2018.09.014

Di Sotto, A., Locatelli, M., Macone, A., Toniolo, C., Cesa, S., Carradori, S., et al. (2019). Hypoglycemic, Antiglycation, and Cytoprotective Properties of a Phenol-Rich Extract From Waste Peel of Punica granatum L. var. Dente di Cavallo DC2. *Molecules* 24 (17), 3103. doi:10.3390/molecules24173103

Frenzel, C., and Teschke, R. (2016). Herbal Hepatotoxicity: Clinical Characteristics and Listing Compilation. *Int. J. Mol. Sci.* 17 (5), 588. doi:10.3390/ijms17050588

Ippoliti, I., Menniti-Ippolito, F., Mazzanti, G., and Di Giacomo, S. (2021). Suspected Adverse Reactions to Performance Enhancing Dietary Supplements: Spontaneous Reports from the Italian Phytovigilance System. *Phytother. Res.* 35 (6), 3246–3261. doi:10.1002/ptr.7040

Marin, J. J. G., Serrano, M. A., Monte, M. J., Sanchez-Martin, A., Temprano, A. G., Briz, O., et al. (2020). Role of Genetic Variations in the Hepatic Handling of Drugs. *Int. J. Mol. Sci.* 21 (8), 2884. doi:10.3390/ijms21082884

Minemura, M., and Shimizu, Y. (2015). Gut Microbiota and Liver Diseases. *World J. Gastroenterol.* 21 (6), 1691–1702. doi:10.3748/wjg.v21.i6.1691

Thomford, N. E., Senthebane, D. A., Rowe, A., Munro, D., Seele, P., Maroyi, A., et al. (2018). Natural Products for Drug Discovery in the 21st Century: Innovations for Novel Drug Discovery. *Int. J. Mol. Sci.* 19 (6), 1578. doi:10.3390/ijms19061578

Vitalone, A., Di Giacomo, S., Di Sotto, A., Franchitto, A., Mammola, C. L., Mariani, P., et al. (2011). Cassia Angustifolia Extract Is Not Hepatotoxic in an *In Vitro* and *In Vivo* Study. *Pharmacology* 88 (5-6), 252–259. doi:10.1159/000331858

Wang, R., Tang, R., Li, B., Ma, X., Schnabl, B., and Tilg, H. (2021). Gut Microbiome, Liver Immunology, and Liver Diseases. *Cell Mol. Immunol.* 18 (1), 4–17. doi:10.1038/s41423-020-00592-6

Wang, X., Zhang, Z., and Wu, S. C. (2020). Health Benefits of Silybum marianum: Phytochemistry, Pharmacology, and Applications. *J. Agric. Food Chem.* 68 (42), 11644–11664. doi:10.1021/acs.jafc.0c04791

Zhang, H. Y., Wang, H. L., Zhong, G. Y., and Zhu, J. X. (2018). Molecular Mechanism and Research Progress on Pharmacology of Traditional Chinese Medicine in Liver Injury. *Pharm. Biol.* 56 (1), 594–611. doi:10.1080/13880209.2018.1517185

Conflict of Interest: The authors declare that the research was conducted in the absence of any commercial or financial relationships that could be construed as a potential conflict of interest.

frontiers in Pharmacology

ORIGINAL RESEARCH
published: 04 May 2021
doi: 10.3389/fphar.2021.653641

Geniposide and Chlorogenic Acid Combination Improves Non-Alcoholic Fatty Liver Disease Involving the Potent Suppression of Elevated Hepatic SCD-1

Cheng Chen[1], *Xin Xin*[1], *Qian Liu*[1], *Hua-Jie Tian*[1], *Jing-Hua Peng*[1], *Yu Zhao*[1], *Yi-Yang Hu*[1,2,3]* *and Qin Feng*[1,2,3]*

[1]*Institute of Liver Diseases, Shuguang Hospital Affiliated to Shanghai University of Traditional Chinese Medicine, Shanghai, China,* [2]*Shanghai Key Laboratory of Traditional Chinese Clinical Medicine, Shanghai, China,* [3]*Key Laboratory of Liver and Kidney Diseases, Shanghai University of Traditional Chinese Medicine, Ministry of Education, Shanghai, China*

OPEN ACCESS

Edited by:
Antonella Di Sotto,
Sapienza University of Rome, Italy

Reviewed by:
Ning-Ning Liu,
Shanghai Jiao Tong University, China
Feng Shen,
Shanghai Jiaotong University, China
Romina Mancinelli,
Sapienza University of Rome, Italy

***Correspondence:**
Qin Feng
fengqin@shutcm.edu.cn
Yi-Yang Hu
yyhuliver@163.com

Specialty section:
This article was submitted to Gastrointestinal and Hepatic Pharmacology, a section of the journal Frontiers in Pharmacology

Received: *14 January 2021*
Accepted: *15 April 2021*
Published: *04 May 2021*

Citation:
Chen C, Xin X, Liu Q, Tian H-J, Peng J-H, Zhao Y, Hu Y-Y and Feng Q (2021) Geniposide and Chlorogenic Acid Combination Improves Non-Alcoholic Fatty Liver Disease Involving the Potent Suppression of Elevated Hepatic SCD-1. Front. Pharmacol. 12:653641. doi: 10.3389/fphar.2021.653641

Background: Non-alcoholic fatty liver disease (NAFLD), characterized by the excessive accumulation of hepatic triglycerides (TGs), has become a worldwide chronic liver disease. But efficient therapy keeps unsettled. Our previous works show that geniposide and chlorogenic acid combination (namely the GC combination), two active chemical components combined with a unique ratio (67.16:1), presents beneficial effects on high-fat diet-induced NAFLD rodent models. Notably, microarray highlighted the more than 5-fold down-regulated SCD-1 gene in the GC combination group. SCD-1 is an essential lipogenic protein for monounsaturated fatty acids' biosynthesis and serves as a key regulatory enzyme in the last stage of hepatic *de novo* lipogenesis (DNL).

Methods: NAFLD mice model was fed with 16 weeks high-fat diet (HFD). The pharmacological effects, primarily on hepatic TG, TC, FFA, and liver enzymes, et al. of the GC combination and two individual components were evaluated. Furthermore, hepatic SCD-1 expression was quantified with qRT-PCR, immunoblotting, and immunohistochemistry. Finally, the lentivirus-mediated over-expressed cell was carried out to confirm the GC combination's influence on SCD-1.

Results: The GC combination could significantly reduce hepatic TG, TC, and FFA in NAFLD rodents. Notably, the GC combination presented synergetic therapeutic effects, compared with two components, on normalizing murine hepatic lipid deposition and disordered liver enzymes (ALT and AST). Meanwhile, the robust SCD-1 induction induced by HFD and FFA in rodents and ALM-12 cells was profoundly blunted, and this potent suppression was recapitulated in lentivirus-mediated SCD-1 over-expressed cells.

Abbreviations: NAFLD, non-alcoholic fatty liver disease; MAFLD, metabolic dysfunction-associated fatty liver disease; SCD-1, stearoyl-CoA desaturase-1; GC, geniposide and chlorogenic acid; QHD, Qushi Huayu Decoction; DNL, de novo lipogenesis; TG, triglyceride; TC, total cholesterol; FFA, free fatty acid; T2DM, type 2 diabetes mellitus; FBG, fasting blood glucose; IR, insulin resistance; ALT, alanine aminotransferase; AST, aspartate transaminase; HFD, high-fat diet; AML-12, alpha mouse liver 12.

Conclusion: Taken together, our data prove that the GC combination shows a substantial and synergetic anti-lipogenesis effect in treating NAFLD, and these amelioration effects are highly associated with the potent suppressed hepatic SCD-1 and a blunted DNL process.

Keywords: non alcoholic fatty liver disease, metabolic associated fatty liver disease 1, stearoyl-CoA desaturase-1, *de novo* lipogenesis, geniposide, chlorogenic acid

INTRODUCTION

Non-alcoholic liver disease (NAFLD), newly named metabolic dysfunction-associated fatty liver disease (MAFLD), is the leading chronic liver disease, affecting approximately 1.7 billion individuals worldwide (Eslam et al., 2020;). Nowadays, NAFLD and its complications pose a tremendous health burden not only in western countries but also in developing countries, for instance, in China (Zhou et al., 2020). NAFLD is characterized by the excessive accumulation of triglycerides (TGs) in hepatocytes without alcoholic abuse (Rinella, 2015). The mechanism of NAFLD is still not fully understood. The "multiple hits" is considered an influential contributor to severe NAFLD and NASH development. Notably, hepatic *de novo* lipogenesis (DNL) is a fundamental biosynthetic pathway within liver, leading to the lipids secreted and stored by hepatocytes, which involves a sequence of fatty acid synthetase. Among these fatty acid synthetases, SCD-1 is a terminal enzyme controlling the DNL, and the induction of SCD-1 is highlighted to be a key player in the pathogenesis and progression of NAFLD (Jensen-Urstad and Semenkovich, 2012; Sanders and Griffin, 2016).

Our previous research has identified that the recipe composed of atractylodes macrocephala polysaccharide, chlorogenic acid, and geniposide (namely the ACG recipe), derived from traditional Chinese medicine Qushi Huayu Decoction (QHD) (Tang et al., 2013; Feng et al., 2013; Peng et al., 2018; Leng et al., 2020; Feng et al., 2017), presents the therapeutic effects on NAFL rodent by improving hepatic lipid deposition and inflammation (Meng et al., 2016). Atractylodes macrocephala polysaccharide (A), chlorogenic acid (C), and geniposide (G), these three components were identified as the primary active ingredients in QHD (Meng et al., 2016), and they were randomly but in a formulaic way selected and combined by uniform design. For further simplifying these three natural products compounded ACG recipe. These three components were also screened by the consistent design. Finally, the regression equation $Y = 71.966–19.798 \times X4 + 18.687 \times X1 \times X4$ isolated from *artemisia capillaries Thunb*, might exhibit the most potent protective effects against hepatic lipid deposition. This unique combination of geniposide and chlorogenic acid was named as the GC combination.

Notably, the GC combination presents multi-therapeutic effects on improving NAFLD by reducing gut inflammation, evaluating gut barrier function, and anti-oxidative stress in NAFL rodent (Peng et al., 2018; Feng et al., 2017). However, whether the GC combination is directly involved in the hepatic lipid synthesis process and its specific molecular mechanism still keeps unclear. Preliminarily, microarray assay reported that stearoyl-CoA desaturase-1 (SCD-1) hits the No. 1. among the biomarkers influenced by the GC combination, and it was surprisingly five times down-regulated. SCD-1 is a crucial enzyme for monounsaturated fatty acids' biosynthesis and serves as a key regulatory enzyme in the last stage of hepatic DNL (Liu et al., 2017a; Kumar et al., 2020). Its primary substrates C16:0 and C18:0, and products palmitoleic acid (C16:1) and oleic acid (C18:1) are the most abundant fatty acids in TGs, cholesterol esters, and membrane phospholipids (Poloni et al., 2015). In humans and rodents, SCD-1 is mainly expressed in liver and adipose tissue. SCD-1 deficiency protects against high-fat-, high-carbohydrate-, and leptin deficiency-induced obesity and hepatic steatosis (Miyazaki et al., 2009). On the contrary, SCD-1 level was aggravated 10- to 15-fold in animal models after fed with a high-glucose and high-fat diet (Basciano et al., 2009). Simultaneously, SCD-1 inhibitors represent a potential treatment for NAFLD (Rotman and Sanyal, 2017).

Here, we evaluate the pharmacological effects of the GC combination in the NAFLD model. We primarily focus on the hepatic index correlated with lipid and glucose metabolism. Meanwhile, based on the microarray assay results, SCD-1 is expected as a potential therapeutic target of the GC combination for ameliorating hepatic lipid accumulation in NAFLD. We further explore the effect of the GC combination on SCD-1 in free fatty acids induced and lentivirus transfected SCD-1 over-expressed cells. Our data show the apparent amelioration effects of GC combination by removing hepatic lipid accumulation on HFD induced fatty liver. Moreover, the GC combination presents a robust suppression effect on hepatic SCD-1 *in vivo* and *in vitro*, which highly blunts the DNL process. Since SCD-1 and DNL play an essential role in lipid metabolism in NAFLD, suppressed SCD-1 expression could be a reason to clarify the therapeutic effects of the GC combination.

MATERIALS AND METHODS

Drug Preparation

Geniposide (drug purity was 98%, lot number CY101018) derived from *Gardenia jasminoides Ellis*, Chlorogenic acid (drug purity was 98%, lot number GY0900705) derived from *artemisia capillaries Thunb*, all drugs were purchased from Shanghai Winherd medical technology Co., Ltd., Shanghai, China. The high-performance liquid chromatography (HPLC) analysis of two drugs is presented in **Supplementary Figure S1**, and the method was described previously (Feng et al., 2013). The ratio of geniposide (G) and chlorogenic acid (C) in the GC combination is 67.16:1.

Animal Experimental Design

The protocols for animal studies were reviewed and approved by the Animal Studies Ethics Committee of Shanghai University of

Traditional Chinese Medicine (NO. PZSHUTCM190621014). The rat experiment was identified before (Meng et al., 2016). Here, Fifty 6 week-old male C57BL/6J mice were purchased from the Shanghai Laboratory Animal Center (Shanghai, China). Animals were maintained at room temperature on a 12h:12h light-dark cycle in the animal center of the Shanghai University of Traditional Chinese Medicine.

After acclimation for 1 week, Fifty C57BL/6J mice were randomly divided into normal diet group (ND, $n = 10$) and high-fat diet group ($n = 40$). The mice in the high-fat diet group were fed a 60.0% kcal fat diet (D12492i, Research Diets, New Brunswick), and the mice in the normal diet group were fed a 10.0% kcal control diet (D12450B, Research Diets, New Brunswick). After 12 weeks on the respective diets, mice in the HFD group were further randomized into four groups: HFD group (HFD), HFD plus the GC group (HFD + GC), HFD plus the G (HFD + G), and the C group (HFD + C), 10 mice in each group. In the following 4 weeks, the mice were administrated with different drugs by gavage once per day. The G (90 mg/kg per day), the C (1.34 mg/kg per day) and, the GC combination [(90 mg G + 1.34 mg C)/kg per day] were dissolved in drinking water, and HFD group mice received an equal volume of drinking water. All the animals were sacrificed for tissue collection at the end of the 16th week.

Microarray Data Analysis

RNA samples were subjected to transcriptome analysis using Affymetrix Rat Genome 230 2.0 Array. Microarray data is available at PubMed under accession number GSE87432. The MicroArray Suite 5 (MAS5) was used for data normalization in consideration that MAS5 makes use of the "Perfect Match – Mismatch" signals and that expression values determined from MAS5 are not on a logarithmic scale. Pathway analysis was performed with the Ingenuity Pathways Analysis (IPA; Ingenuity Systems, Inc., Redwood City, CA, www.ingenuity.com). Input lists included DEGs between experimental groups (False Discovery Rate < 0.05, *t*-test) (Feng et al., 2017).

Measurement of Triglyceride, Total Cholesterol, and Free Fatty Acid Content in Liver Tissue

The wet liver (approx. 100 mg) was homogenized in 1.5 ml of ethanol-acetone (1:1) and kept at 4°C for 12 h. Afterward, the sample was centrifuged at 3,000 rpm for 15 min, and the suspension was collected for the determination of triglyceride content and total cholesterol by using biochemistry assay kits (Dongou Biology Technique Co. Ltd., Zhejiang, China). To measure the amount of hepatic FFA content, we use 100 mg wet liver tissue of each sample. The samples were homogenized in 0.9 ml saline and centrifuged at 3,500 rpm for 15 min. The suspension was collected for the determination of FFA content by using commercial kits (Nanjing Jiancheng Institute of Biotechnology, Nanjing, China) according to the manufacturer's instructions.

Serum Biochemical Parameter Analysis

The analysis of alanine aminotransferase (ALT) and aspartate aminotransferase (AST) was measured by commercial kits (Nanjing Jiancheng Institute of Biotechnology, Nanjing, China) according to the manufacturer's instructions. Fasting blood glucose (FBG) was determined with a blood glucose meter (Roche diagnostic GmbH, Germany). Fasting insulin (FI) level was measured using the Mouse Insulin ELISA (ALPCO, America). The homeostasis model assessment of basal insulin resistance (HOMA-IR) was calculated using the formula FBG (mM) × FI (mM)/22.5.

Histological Examination and Assessment

Sections of the liver samples (4 μm thick) or the frozen liver tissues (5 μm thick) were stained with hematoxylin-eosin (H and E) or oil red O. They were examined under the light microscope (Olympus Medical Systems Corp, Tokyo, Japan) (Tang et al., 2013). The cells were washed with PBS twice, fixed with 10% formalin at room temperature for 30 min, and stained with a freshly prepared working solution of Oil-Red O (Sigma, St. Louis, MO, United States) at room temperature for 30 min. The cells were observed in an Olympus microscope and documented. The concrete operating steps were followed by the previous studies (Feng et al., 2013).

Cell Culture and Experimental Design *In Vitro*

AML-12 cells established from mouse hepatocytes (CD1 strain, line MT 42) were purchased from the Institutes of Biochemistry and Cell Biology, Shanghai Institutes for Biological Sciences, CAS, Shanghai, China. The cells were maintained in complete growth Dulbecco's Modified Eagle's Medium/Ham's F-12 growth medium (DMEM/F-12 medium, GIBCO BRL) 1:1 with 10% fetal bovine serum (FBS; GIBCO-BRL, Grand Island, NY), ITS (1.0 mg/ml insulin, 0.55 mg/ml transferring, 5 ug/ml selenium, Sigma) and 40 ng/ml dexamethasone, at 37°C in a humidified incubator with 5% CO_2.

The experiment started when the cells grew to 60–70% confluence. Cellular steatosis was induced by a mixture of 0.3 mM FFA (the ratio of oleate to palmitate is 2:1) in DMEM/F-12 containing 10% FBS for 24 h. Then the cells were divided into different groups as control group (CO), FFA group (FFA), FFA +200 μm GC group (FFA + GC) group. After the cells were incubated with respective drugs for another 24 h, the cells were stained with Oil-Red O and imaged. The cytotoxicity of the GC combination was measured by CCK-8 kit (Sigma, 96992), following the manufacturer's instructions.

Lentiviral Construction and Cell Transfection

All lentiviral constructs were prepared by Shanghai GeneChem Co., Ltd (Shanghai, China). Lentivirus GV287-SCD-1transfection was conducted following the manufacturer's instructions. Generally, the AML-12 cells were infected with the GV287-SCD-1 or the control lentivirus GFP. The lentivirus vector and packaging plasmid mixes were transfected into AML-12 cells using Lipofectamine 2000 (Invitrogen Life Technologies, Carlsbad, CA, United States). Following 6–8 h incubation, the viruses were removed and replaced with a fresh medium. Three-

days post-transfection, GFP expression was observed using a fluorescence microscope.

Measurement of Cellular Triglyceride Content

The intracellular TG was extracted and purified using the method by Heider and Boyett (Heider and Boyett, 1978). The content of TG was determined with a biochemistry assay kit (Dongou Biology Technique Co. Ltd., Zhejiang, China), according to the manufacturer's instructions.

Quantitative Real-Time PCR

Custom primers were designed following our previous work (Feng et al., 2017). Primers were characterized by melting curve analysis, agarose gel electrophoresis, and DNA sequencing and synthesized at Eurofins MWG Operon (Huntsville, Alabama). Animal tissues were stored at −80 °C after soaking with RNA later (Qiagen, Valencia, CA). Total RNA isolated using the RNA Extraction kit (Cat# 9769, TaKaRa, Japan) was used to prepare cDNA with the RevertAid First Strand cDNA Synthesis kit (#K1622, Thermo). Quantitative qRT-PCR was performed on an iCycler iQ real-time detection system (Bio-Rad Laboratories) using SYBR Green (iQ SYBR Green Supermix, Bio-Rad Laboratories). Relative expression of each gene was calculated with β-actin or GAPDH as the housekeeping gene. Primer sequences were listed in **Supplementary Table S3**.

Western Blot Analysis

Liver tissue and AML-12 cells were homogenized in a lysis buffer (150 mM NaCl, 1% Nonidet P- 40, 0.1% SDS, 50 mM Tris-HCl pH 7.4, 1 mM EDTA, 1 mM PMSF, 1x Roche complete mini protease inhibitor cocktail). The supernatants were collected after centrifugation at 10,000 g at 4°C for 15 min. Protein concentration was determined using a BCA protein assay kit (Beyotime Institute of Biotechnology, Jiangsu, China). Equal amounts of protein were separated by 10% SDS gel electrophoresis (SDS-PAGE) under denaturing and nonreducing conditions and transferred to a PVFD membrane. The membrane was blocked with 5% non-fat milk in TBST at room temperature for 1 h and then incubated with primary antibody at 4°C overnight (antibody information was presented in **Supplementary Table S2**.). After thrice washing in TBST, the blots were incubated with horseradish-coupled secondary antibody. The signals were visualized using an enhanced chemical luminescent (ECL) system (Pierce Biotechnology, Inc., Rockford, IL, United States) and recorded in the chemiluminescence imaging system (ChemiScope 3500 mini, Xiang Ying, China).

Immunohistochemistry Staining

Paraffin-embedded liver tissues were prepared when sacrificed the mice. Briefly, after dewaxing, liver sections were submitted to antigen retrieval and further blocked using a blocking solution. The section was rinsed in PBS for 5 min, three times, and then incubated with the primary antibody (1:100 dilution) overnight at 4°C. Following washing in PBS, the sections were incubated with secondary antibody for 1 h.

Statistical Analysis

Statistical analysis was performed using GraphPad Prism version 5.0 (GraphPad Software, La Jolla, CA). Data are expressed as mean ± standard deviation. Data were analyzed using the *t*-test or one-way analysis of variance and the least significant difference test, and $p < 0.05$ was considered statistically significant.

RESULTS

The GC Combination, a Simplified Prescription of the ACG Recipe, Ameliorates the Hepatic Triglyceride Accumulation and Impairs the Elevated Liver Enzymes in Non-Alcoholic Fatty Liver Rats

Our previous data (Meng et al., 2016) has verified the therapeutic effects of the recipe composed of atractylodes macrocephala polysaccharide, chlorogenic acid, and geniposide (named ACG) on the experimental non-alcoholic fatty liver (NAFL). Here, the GC combination, only two components simplified from the ACG recipe, presented similar powerful ameliorations on hepatic TG accumulation (**Figure 1A**) as well as liver enzymes (**Figures 1B,C**) in NAFL rat models (HFD). What's more, the GC combination showed more potent effects for reversing the pathologically elevated liver enzymes. The AST (aspartate transaminase) level of the GC group was even significantly lower than the ACG group level (**Figure 1C**).

The GC Combination Markedly Ameliorates Lipid and Glucose Metabolism Serum Index and Normalizes the Liver Functional Enzymes

We next arranged mice experiments to elucidate whether the GC combination attenuates the HFD induced fatty liver. Meanwhile, for further identifying the individual effects of the G and C, the same dosage intervention separated from the GC combination was performed. Fifty mice were fed with a high-fat diet for 12 weeks and following with or without the respective pharmacological intervention for another 4 weeks.

As shown before, the GC combination did not significantly affect food intake (Peng et al., 2018). After 4 weeks of treatment, the body weight and liver weight of mice in each treatment group were notably lower than those in the HFD group (**Figures 2A,B**). Meanwhile, the disordered serum HDL-C (high-density lipoprotein cholesterol) (**Figure 2C**) and LDL-C (low-density lipoprotein cholesterol) (**Figure 2D**) were normalized. The elevated serum ALT (alanine transaminase) and AST (**Figures 2E,F**) levels were also significantly reversed. Although the serum insulin level (data not shown) did not show a significant difference among the treatment groups, the GC combination

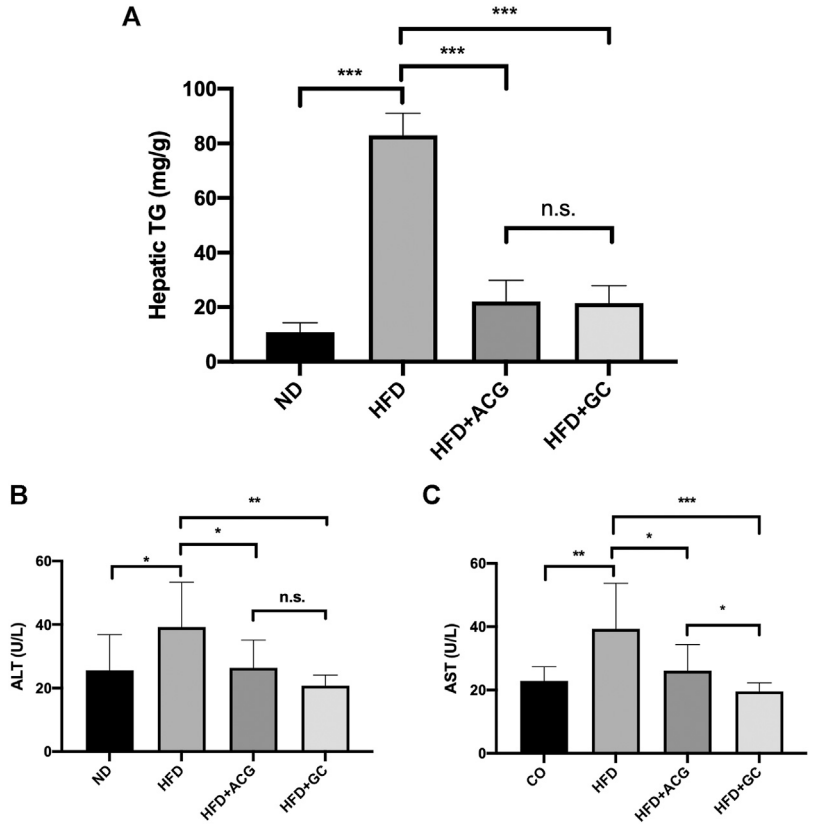

FIGURE 1 | The GC combination ameliorates the hepatic triglyceride (TG) accumulation and impairs the elevated alanine aminotransferase (ALT) and aspartate transaminase (AST) levels in NAFL rats. **(A)** Hepatic TG content in rats ($n = 9$) **(B,C)** serum ALT and AST ($n = 9$). $^{*}p < 0.05$, $^{**}p < 0.01$, $^{***}p < 0.001$, n.s. = no significant.

strongly decreased the FBG (fasting blood glucose) (**Figure 2G**) and HOMA-IR (homeostatic model assessment-insulin resistance) (**Figure 2H**). Notably, comparing with the geniposide (G) or chlorogenic acid (C) alone, the GC combination showed a significant synergetic effect on normalizing the serum lipids and the blood glucose level, and reversing the increased AST and ALT induced by HFD.

The GC Combination Markedly Ameliorates Hepatic Steatosis in Non-Alcoholic Fatty Liver Mice and Presents Significant Synergetic Effects than Each Component

Attractively, grievous hepatic steatosis in NAFL mice was markedly attenuated after 4 weeks of the GC treatment, as demonstrated by H&E and Oil Red O staining (**Figure 3A**). With 16 weeks HFD feeding, steatosis and ballooning of hepatocytes and inflammatory cells infiltration were readily observed in lobules with hematoxylin and eosin (H&E) staining. Typical macrovesicular steatosis was showed in centrilobular regions. Consistently, as visualized in Oil Red O staining, dramatically increased lipid deposition occupied much of the cytoplasm of hepatocytes. However, after 4 weeks treating with the GC combination, the steatosis of hepatocytes is reversed, and rarer ballooning degeneration and inflammatory infiltration were showed. In line with the pathological changes in the liver section, the significantly reversed level of hepatic triglyceride (TG) (**Figure 3B**), total cholesterol (TC) (**Figure 3C**), and free fatty acid (FFA) (**Figure 3D**) were also presented in the GC treatment group. Again, even the pathological and biochemical ameliorations were also demonstrated in the G or C individual treatment group; the GC treatment showed remarkably synergetic effects on suppressing the hepatic lipid content.

SCD-1 Is the Most Significant Differential Gene Down-Regulated by the GC Combination in NAFL Rats, and the Expression Is Consistently Suppressed in the NAFL Mice Model

The microarray analysis was performed to search the potential therapeutic targets. The volcano plot highlighted that SCD-1 was the most attractive differential gene (**Figure 4A**) down-regulated (more than 5-fold down-regulated) by the GC combination in the liver tissue of NAFL rats ($n = 3$). The top five differential genes in rat liver tissue analyzed by microarray between the HFD and the GC combination treatment groups were presented in the **Supplementary Table S1**. For confirming the eye-catching result, the real-time PCR test was performed to identify the

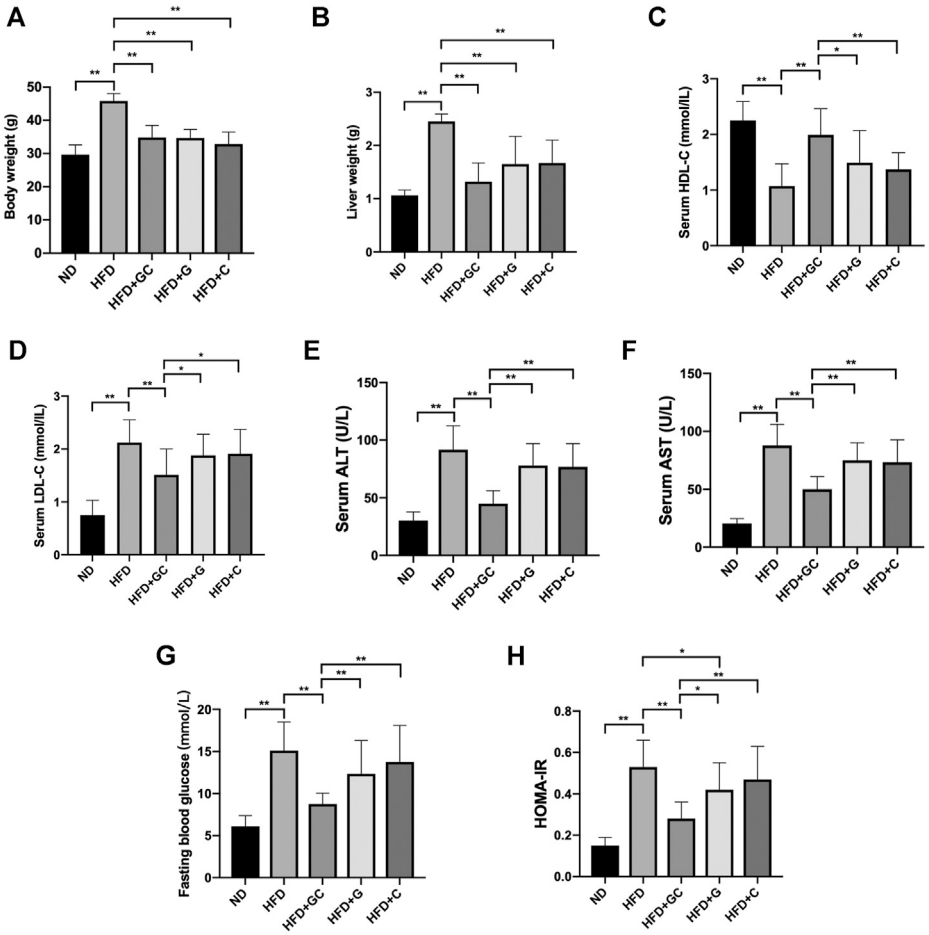

FIGURE 2 | The GC combination reverses biochemical parameters in NAFL mice. The mice body weight **(A)**, liver weight **(B)**. The level of serum HDL-C **(C)** and LDL-C **(D)**, serum ALT **(E)** and AST **(F)**, fasting blood glucose **(G)**, and HOMA-IR **(H)** in the mice from each group (n = 10). $^{*}p < 0.05$, $^{**}p < 0.01$.

SCD-1 mRNA expression. The GC combination dramatically suppressed the SCD-1 mRNA expression (**Figure 3B**). Meanwhile, the SCD-1 transcriptional (**Figure 3C**) and translational (**Figure 3D**) levels in the liver of NAFL mice were also suppressed by the GC combination. Consistent with the immunoblotting result, SCD-1 was positively stained with the brown area around the ballooning lipid droplets in hepatocytes by immunohistochemistry staining (**Figure 4E** and **Supplementary Figure S2**), but the GC combination stably blunted the SCD-1 expression.

Since SCD-1 acts as a key mediator in the hepatic DNL process, SCD-1 might be the potential therapeutic target of the GC combination in improving hepatic lipid accumulation in NAFL rodent models.

The GC Combination Markedly Ameliorates Cellular Steatosis and Reverses Up-Regulated SCD-1 in FFA-Exposed AML-12 Cells

To investigate the effect of the GC combination on FFA-induced lipid accumulation in AML-12 cells, we exposed the cells to a 0.3 mM FFA mixture with the presence or absence of the 200 μm GC combination. We first determined the concentration dependence of the cytotoxic effects of the GC in AML-12 cells by CCK8 assay. In 24 h, cell viability was not affected by the GC combination (**Supplementary Figure S3A**) up to 400 μm. Meanwhile, 48 h GC combination exposure (medium contained the GC combination was refreshed at 24 h), cell viability was not affected either (data not shown). In addition, 0.3–0.5 mM FFA mixture significantly increased cellular TG content in AML-12 cells (**Supplementary Figure S3B**). Hence, a 0.3 mM FFA mixture was used to induce the steatosis in AML-12 cells. Dramatically red-stained cytoplasmic lipid droplets accumulation induced by FFA mixture was confirmed by Oil-red O staining, but the accumulation was significantly reversed by the GC combination treatment (**Figure 5A**). Furthermore, the intracellular TG content was measured; the induced TG level was dramatically attenuated by the GC combination (**Figure 5B**). Meanwhile, the SCD-1 expression was activated, in transcriptional and translational levels, by FFA mixture exposure after 24 h. But the induced SCD-1 induction was significantly reversed by the GC combination (**Figures 5C–E**).

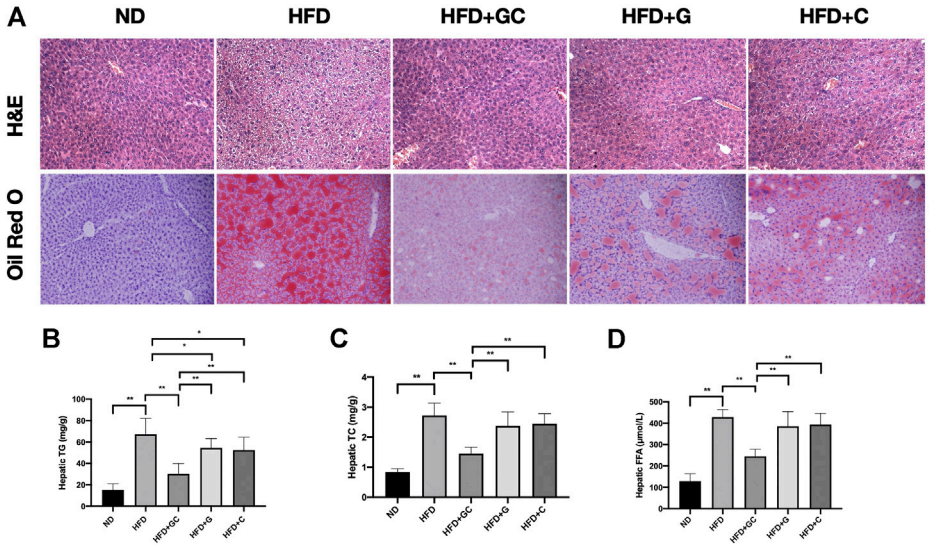

FIGURE 3 | The GC combination ameliorates hepatic fat deposition induced by high-fat diet (HFD). **(A)** H&E and Oil Red O staining for liver sections (200 times of magnification). Hepatic TG, TC, and FFA content in each group (n = 10) **(B,C,D)**. *p < 0.05, **p < 0.01.

Together, *in vitro* data demonstrate that the GC combination significantly impaired the intracellular TG deposition, and it also suppressed the FFD induced SCD-1.

The GC Combination Strongly Attenuates SCD-1 Expression in SCD-1 Overexpressed AML-12 Cells

To further confirm whether the GC combination has a strong suppression effect on SCD-1, the lentivirus SCD-1 was used to stably overexpress SCD-1 in AML-12 cells and following with the presence or absence of the GC combination treatment. The overexpression of SCD-1 was initially confirmed by real-time PCR and western blotting tests. The significant up-regulated SCD-1 level stably presented in SCD-1 overexpressed AML-12 cells (OE), comparing with the non-insect vector control (NC) (**Figures 6A,B**). Subsequently, SCD-1 overexpressed cells were directly exposed to the GC combination treatment for 24 h. As expected, the GC combination significantly revered the lentivirus-mediated SCD-1 overexpression as before (**Figures 6C–E**).

Above all, the GC combination showed a powerful suppressing effect on hepatic SCD-1 expression and consequently triggered the hepatic DNL process impairment. These effects highly contribute to the amelioration of hepatic lipid accumulation in NAFLD models (**Figure 7**).

DISCUSSION

We here prove that the GC combination, composed of geniposide and chlorogenic acid, presents potent amelioration effects in treating non-alcoholic liver disease *in vivo* and *in vitro*. In the beginning, we focused on hepatic lipid accumulation changes in the presence or absence of the GC combination in the NAFL model and further compared the pharmacological effects with two individuals of the GC combination. After clarifying the ameliorating impacts, microarray analysis was performed to identify the potential therapeutic targets, and SCD-1 suppression was highlighted by microarray. Finally, two strategies for confirming the influence of the GC combination on SCD-1 in FFA triggered and lentivirus-mediated SCD-1 overexpressed cells were performed.

The pathogenesis of NAFLD is multifactorial, and its understanding still keeps incomplete. Nowadays, a multiple-hit hypothesis that implicates a myriad of factors acting in a parallel and synergistic manner in individuals with genetic predisposition is the more accepted understanding (Arab et al., 2018). A disturbed lipid and glucose homeostasis, increased lipid peroxidation, liver injury, and gut microbiota disorder triggered inflammation et al., drive the disease progression.

In our previous research, four weeks of the GC combination treatment significantly improve the hepatic inflammatory condition (Peng et al., 2018; Feng et al., 2017). HFD triggered hepatic IL-1β, TNF-a, LPB, TLR4 induction were significantly blunted. Meanwhile, the plasma LPS level and the F4/80, the biomarker of the Kupffer cell, were also dramatically down-regulated. And we also found that the GC combination had a significant impact on the gut microbiome structure and ameliorated colonic injury and incidence of inflammatory cell infiltration (Peng et al., 2018). The same, the hepatic glutathione level in NAFL rats was significantly up-regulated after the GC treatment, which highly elucidated that the GC combination presented the anti-oxidative stress function (Feng et al., 2017). To sum up, the GC combination displayed multi-therapeutic effects on NAFLD improvement, and these different targeting mechanisms highly interact with each other and make synergistic amelioration influences.

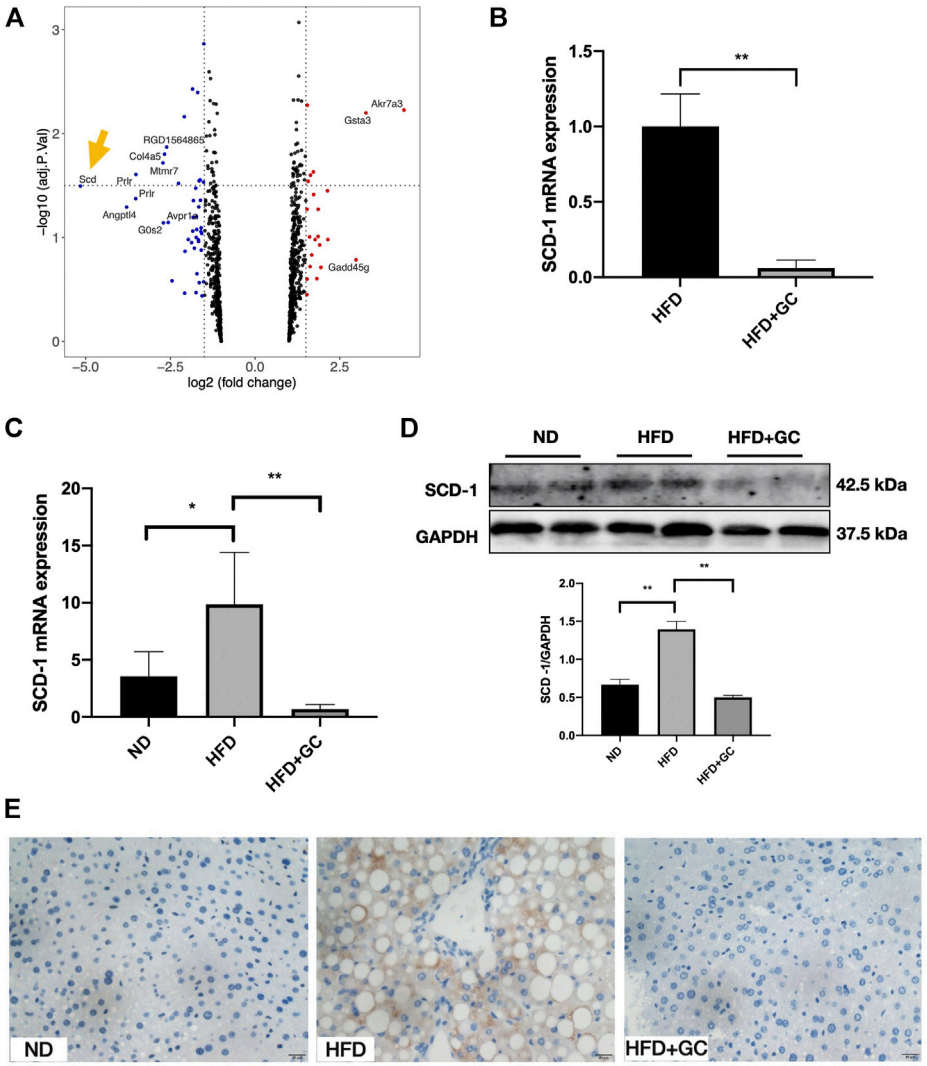

FIGURE 4 | SCD-1 is the most significant differential gene highlighted in microarray and significantly down-regulated by the GC combination. **(A)** Volcano Plot for differential gene expression between HFD and HFD + GC group in the liver of rats ($n = 3$), logFC < 1 was deleted during the analysis. SCD-1 mRNA expression in rat **(B)** and mice **(C)** liver tissues was verified by real-time PCR analysis. SCD-1 protein expression in mice liver was detected by immunoblotting **(D)** and immunohistochemistry **(E)** (Brown area, 400 times of magnification), and the relative expression levels of proteins were corrected by GAPDH. $^{*}p < 0.05$, $^{**}p < 0.01$.

Importantly, lipid accumulation in hepatocytes is the key pathological feature of NAFLD. On the other hand, lipid metabolic disorder is the most direct etiology of this disease (Chen et al., 2019). Increased TG deposition in the liver reflects an input/output imbalance of hepatic FFA metabolism (Rotman and Sanyal, 2017). Our previous non-alcoholic steatohepatitis (NASH) with liver fibrosis mice models amply proved that a long term (30 weeks) of high fat, high carbohydrate diet crazily induced hepatic lipid deposition, even triggered liver fibrosis in mice liver (Xin et al., 2020). Here, mice continuously fed with a high-fat diet for 16 weeks ending up with NAFLD, characterized by markedly increased hepatocytes TG content, FFAs accumulation, and simultaneously companied by severe insulin resistance. Attractively, the GC combination presented a significant anti-lipogenic effect on the NAFL rodent's liver and steatosis cell model. Moreover, compared with the G or C individual pharmacological intervention, the GC combination showed significantly stronger amelioration effects on hepatic lipid and glucose metabolism, and liver function normalization (ALT and AST). The synergetic effects were demonstrated by combining the G and C with a unique ratio (67.16:1). It should be noticed that the chlorogenic acid or geniposide individual treatment did not show any significant suppressing effects on the disordered hepatic TC or FFA accumulation. Still, this hepatic lipid deposition attenuation effect was dramatically enhanced with this unique combination.

Accordingly, three sources of FFAs are known to contribute to TG accumulation in the fatty liver. 25% come from the DNL process, the second major contributor of FFAs in hepatocytes (Donnelly et al., 2005; Chen et al., 2019). Besides, DNL is also

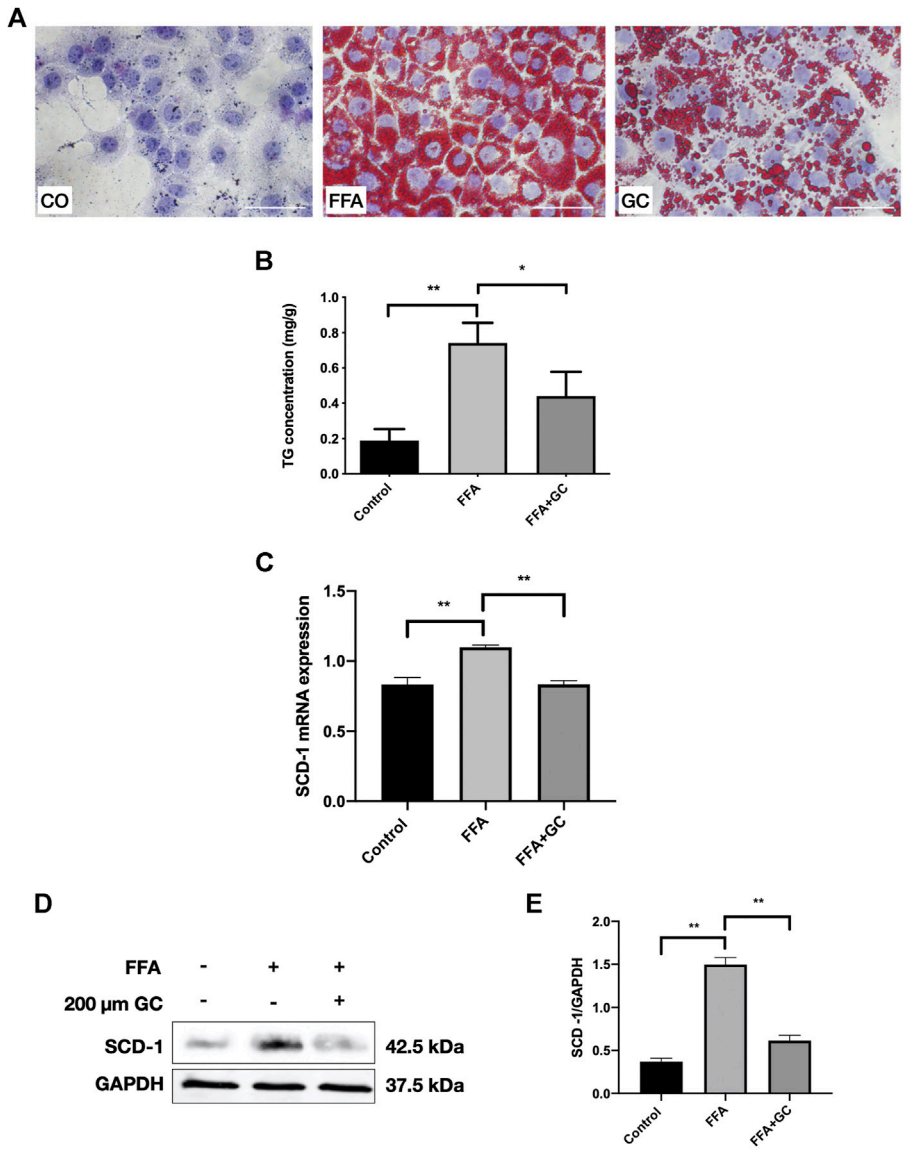

FIGURE 5 | The GC combination ameliorates lipid droplet accumulation and reverses up-regulated SCD-1 induced by free fatty acid (FFA) in AML-12 cells. **(A)** Oil Red O staining of AML-12 cells (400 times of magnification). **(B)** intracellular TG content. **(C)** SCD-1 mRNA expression in cells was detected by qRT-PCR. **(D)** SCD-1 protein levels in cells were detected by immunoblotting, and the relative expression levels **(E)** of proteins were corrected by GAPDH. $^{*}p < 0.05$, $^{**}p < 0.01$.

increased under the condition of insulin resistance. And *vice versa*, the DNL rate would provide an early warning of the possible development of type 2 diabetes mellitus (T2DM) (Ameer et al., 2014). Here, the significantly decreased hepatic FFAs content and attenuated fasting blood glucose level *in vivo* strongly proved that the disordered hepatic DNL process went back to normal with the GC combination treatment.

During the DNL process, even several primary enzymes (e.g., acetyl-CoA carboxylase and fatty acid synthase) promote its going, and hepatic SCD-1 plays a critical role in the generation of monounsaturated FAs from saturated FAs, which is the last stage of DNL to form the FFAs (Chen et al., 2019). Increasing research demonstrated that suppressed SCD-1 expression and enzyme activity or SCD-1 knock out to make a great contribution to NAFLD amelioration (Ntambi et al., 2002; Biddinger et al., 2006; Miyazaki et al., 2007; Sampath et al., 2009). More importantly, SCD-1 activity was a predictor of the development of metabolic syndrome, and the expression of SCD-1 was associated with hepatic steatosis in humans (Warensjö et al., 2005; Poloni et al., 2015). In our present study, 16 weeks HFD robustly triggered the up-regulation of hepatic SCD-1 in NAFL rats and mice. Similarly, FFA also induced the SCD-1 expression in AML-12 cells.

Although the clinical burden of NAFLD is increasing rapidly, unfortunately, there are no FDA-approved effective drugs thus

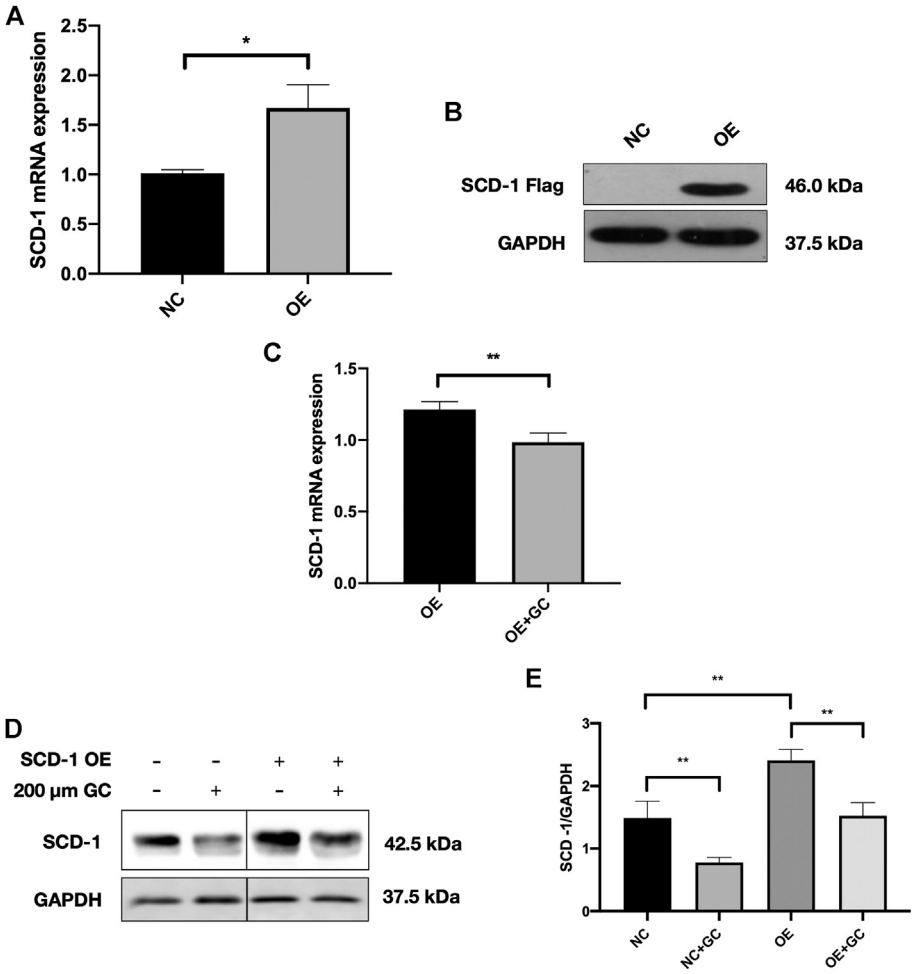

FIGURE 6 | The GC combination dramatically suppresses the SCD-1 expression in SCD-1 over-expressed cell models **(A,B)** SCD-1 mRNA and protein levels in lentivirus transfected SCD-1 over-expressed AML-12 cells (OE). The same vector without the SCD-1 insert was used as control (NC). **(C)** SCD-1 mRNA expression in cells was detected by qRT-PCR. **(D)** SCD-1 protein levels in cells were detected by immunoblotting, and the relative expression levels of proteins **(E)** were corrected by GAPDH. $^{*}p < 0.05$, $^{**}p < 0.01$.

far. As a potential therapeutic target of NAFLD, SCD-1 inhibitor investigation attract attention (Rotman and Sanyal, 2017; Friedman et al., 2018; Chen et al., 2019). Again, the microarray assay provided us with a clue that SCD-1 might be a therapeutic target of the GC combination. Both *in vivo* and *in vitro* data strongly proved that the GC combination presents a potent suppressing effect on hepatic SCD-1 expression. Furthermore, this kind of solid suppression effect was demonstrated in the SCD-1 overexpressed cell model. Even SCD-1 expression was stably promoted by lentivirus transfection, and the GC combination undoubtedly reversed this up-regulation on transcriptional and translational levels. Above all, it has become clear that the GC combination reversed the hepatic lipid deposition in NAFL *in vivo* and *in vitro* models. More importantly, these effects are highly contributed to the robustly suppressed hepatic SCD-1 expression.

However, SCD-1, as the downstream regulator in hepatic lipid synthesis, is controlled by a sequence of upstream targets. Logically, suppressed SCD-1 either comes from the direct modulation of the GC combination or is influenced by its upstream targets, or both possibilities exist simultaneously. Accordingly, the known major upper-stream regulators of SCD-1 are leptin receptor (Lep-R) and sterol regulatory element-binding protein (SREBP)-1c (Biddinger et al., 2006). The leptin receptor bind with Leptin will further suppress SCD-1 expression. With the primary exploration, GC treatment significantly induced Lep-R expression *in vivo* and *in vitro* (data not shown). On the other hand, the n-terminal part of mature SREBP-1c will be translocated into the nucleus, which binds with the sterol regulatory elements (SRE) and further promotes the SCD-1 transcription (Ntambi, 1999; Ferré and Foufelle, 2007). Simultaneously, the GC combination blunted nSREBP-1c expression in NAFL models (data not shown). The exact mechanisms of the SCD-1 regulation with the GC combination will be deeply understood in our following research. The same, the specific

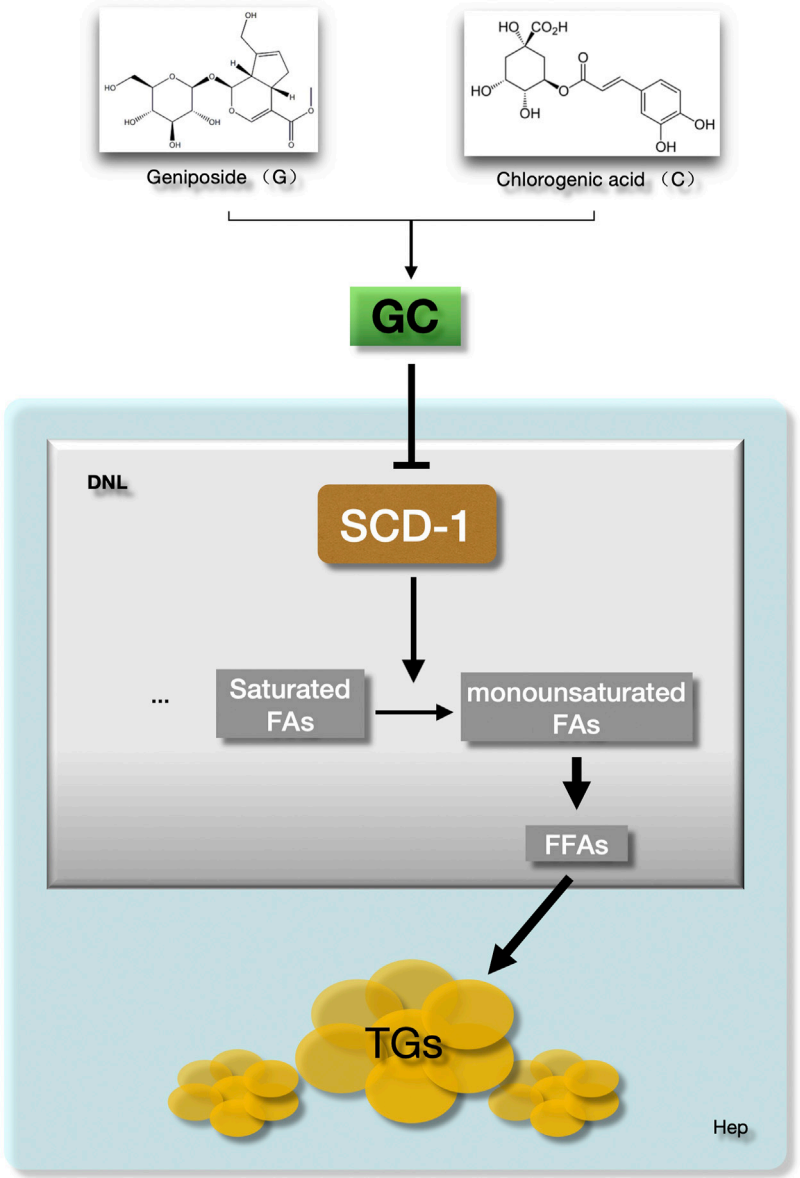

FIGURE 7 | The GC combination ameliorates hepatic fat deposition by suppressing SCD-1. SCD-1 promotes the last stage of *de novo* lipogenesis to form the free fatty acid in hepatocytes. The GC combination was demonstrated to suppress the hepatic SCD-1expression, which highly impairs the DNL process and further attenuate the hepatic lipid deposition in NAFLD models. GC, Geniposide and chlorogenic acid combination, SCD-1, Stearoyl CoA desaturase-1, DNL, *de novo* lipogenesis, FFAs, Free fatty acids, TGs, Triglycerides.

mechanism(s) of the interaction between these two active ingredients in the GC combination to trigger these pharmacological synergetic impacts should be answered in the future.

Finally, natural active components attracted from herbs or food demonstrated promising therapeutic effects on NAFLD, such as EGCG (Chen et al., 2018) extracted from green tea and caffeine (J Martins, 2017) present multiple pharmacological effects in treating NAFLD. Except for making an effect on SCD-1, geniposide and chlorogenic acid have also been reported to ameliorate NAFLD by up-regulating PPAR-α (Liu et al., 2017b), GLP-1R expression (Zhang et al., 2016) et al. in hepatocytes. Nowadays, the current understanding of the pathophysiology of NAFLD provides a strong rationale for combination therapeutics for this disease (Rotman and Sanyal, 2017). The GC combination, to some extent, indicates a preliminary idea of combination therapy and also provides a promising choice of natural active components in treating NAFLD.

In summary, our data demonstrate that the GC combination presents inspiring pharmacological effects on ameliorating NAFLD, especially on impairing the lipogenesis in hepatocytes. Moreover, these therapeutic advantages are highly

attributed to the dramatically suppressed hepatic SCD-1 expression and impaired *de novo* lipogenesis process.

DATA AVAILABILITY STATEMENT

The raw data generated in this study can be found in NCBI using the accession number GSE87432.

ETHICS STATEMENT

The animal study was reviewed and approved by Animal Studies Ethics Committee of Shanghai University of Traditional Chinese Medicine.

AUTHOR CONTRIBUTIONS

QF, CC, and Y-YH designed this study. CC and XX performed the experiments. CC and QF analyzed the data. CC wrote the manuscript. QF revised the manuscript and supported the research. All authors critically participated in the discussion and commented on the manuscript.

FUNDING

This work was supported by National Science Foundation of China (No.81573668, to Q. F.) National Science & Technology Major Project 'Key New Drug Creation and Manufacturing Program', China (No. 2019ZX09201001-001-002, to Q. F.), Shanghai Science and Technology Development Funds (No.18401933100, to Q. F.)

ACKNOWLEDGMENTS

We thank Xin Sun (Shanghai University of TCM), Na Jiang (Shanghai University of TCM) for providing technical assistance. We appreciate Chen Li (Charité–Universitätsmedizin Berlin) and Yang Liu (Universität Hamburg) for providing useful discussion.

SUPPLEMENTARY MATERIAL

The Supplementary Material for this article can be found online at: https://www.frontiersin.org/articles/10.3389/fphar.2021.653641/full#supplementary-material.

REFERENCES

Ameer, F., Scandiuzzi, L., Hasnain, S., Kalbacher, H., and Zaidi, N. (2014). De Novo lipogenesis in Health and Disease. *Metabolism*. 63 (7), 895–902. doi:10.1016/j.metabol.2014.04.003

Arab, J. P., Arrese, M., and Trauner, M. (2018). Recent Insights into the Pathogenesis of Nonalcoholic Fatty Liver Disease. *Annu. Rev. Pathol. Mech. Dis.* 13, 321–350. doi:10.1146/annurev-pathol-020117-043617

Basciano, H., Miller, A . E., Naples, M., Baker, C., Kohen, R., Xu, E., et al. (2009). Metabolic Effects of Dietary Cholesterol in an Animal Model of Insulin Resistance and Hepatic Steatosis. *Am J Physiol Endocrinol Metab.* 297 (2), E462–E473. doi:10.1152/ajpendo.90764.2008

Biddinger, S. B., Miyazaki, M., Boucher, J., Ntambi, J. M., and Kahn, C. R. (2006). Leptin Suppresses Stearoyl-CoA Desaturase 1 by Mechanisms Independent of Insulin and Sterol Regulatory Element-Binding Protein-1c. *Diabetes*. 55 (7), 2032–2041. doi:10.2337/db05-0742

Chen, C., Liu, Q., Liu, L., Hu, Y. Y., and Feng, Q. (2018). Potential Biological Effects of (-)-Epigallocatechin-3-Gallate on the Treatment of Nonalcoholic Fatty Liver Disease. *Mol. Nutr. Food Res.* 62 (1), 1700483. doi:10.1002/mnfr.201700483

Chen, Z., Yu, Y., Cai, J., and Li, H. (2019). Emerging Molecular Targets for Treatment of Nonalcoholic Fatty Liver Disease. *Trends Endocrinol. Metab.* 30 (12), 903–914. doi:10.1016/j.tem.2019.08.006

Donnelly, K. L., Smith, C. I., Schwarzenberg, S. J., Jessurun, J., Boldt, M. D., and Parks, E. J. (2005). Sources of Fatty Acids Stored in Liver and Secreted via Lipoproteins in Patients with Nonalcoholic Fatty Liver Disease. *J. Clin. Invest.* 115 (5), 1343–1351. doi:10.1172/jci23621

Eslam, M., Newsome, P. N., Sarin, S. K., Anstee, Q. M., Targher, G., Romero-Gomez, M., et al. (2020a). A New Definition for Metabolic Dysfunction-Associated Fatty Liver Disease: An International Expert Consensus Statement. *J. Hepatol.* 73 (1), 202–209. doi:10.1016/j.jhep.2020.03.039

Eslam, M., Sanyal, A. J., George, J., Sanyal, A., Neuschwander-Tetri, B., Tiribelli, C., et al. (2020b). MAFLD: A Consensus-Driven Proposed Nomenclature for Metabolic Associated Fatty Liver Disease. *Gastroenterology*. 158 (7), 1999–2014. doi:10.1053/j.gastro.2019.11.312

Feng, Q., Gou, X. J., Meng, S. X., Huang, C., Zhang, Y. Q., Tang, Y. J., et al. (2013). Qushi Huayu Decoction Inhibits Hepatic Lipid Accumulation by Activating AMP-Activated Protein Kinase *In Vivo* and *In Vitro*. *Evid. Based Complement. Alternat Med.* 2013, 184358. doi:10.1155/2013/184358

Feng, Q., Liu, W., Liu, W., Baker, S. S., Li, H., Chen, C., et al. (2017). Multi-targeting Therapeutic Mechanisms of the Chinese Herbal Medicine QHD in the Treatment of Non-alcoholic Fatty Liver Disease. *Oncotarget*. 8 (17), 27820–27838. doi:10.18632/oncotarget.15482

Ferré, P., and Foufelle, F. (2007). SREBP-1c Transcription Factor and Lipid Homeostasis: Clinical Perspective. *Horm. Res. Paediatr.* 68 (2), 72–82. doi:10.1159/000100426

Friedman, S. L., Neuschwander-Tetri, B. A., Rinella, M., and Sanyal, A. J. (2018). Mechanisms of NAFLD Development and Therapeutic Strategies. *Nat. Med.* 24 (7), 908–922. doi:10.1038/s41591-018-0104-9

Heider, J. G., and Boyett, R. L. (1978). The Picomole Determination of Free and Total Cholesterol in Cells in Culture. *J. Lipid Res.* 19 (4), 514–518. doi:10.1016/s0022-2275(20)40725-4

J Martins, I. (2017). Nutrition Therapy Regulates Caffeine Metabolism with Relevance to NAFLD and Induction of Type 3 Diabetes. *Diabetes Metab. Disord.* 4 (1), 1–9. doi:10.24966/dmd-201x/100019

Jensen-Urstad, A. P. L., and Semenkovich, C. F. (2012). Fatty Acid Synthase and Liver Triglyceride Metabolism: Housekeeper or Messenger? *Biochim Biophys Acta.* 1821 (5), 747–753. doi:10.1016/j.bbalip.2011.09.017

Kumar, M., Coria, A. L., Cornick, S., Petri, B., Mayengbam, S., Jijon, H. B., et al. (2020). Increased Intestinal Permeability Exacerbates Sepsis through Reduced Hepatic SCD-1 Activity and Dysregulated Iron Recycling. *Nat. Commun.* 11 (1), 483. doi:10.1038/s41467-019-14182-2

Leng, J., Huang, F., Hai, Y., Tian, H., Liu, W., Fang, Y., et al. (2020). Amelioration of Non-alcoholic Steatohepatitis by Qushi Huayu Decoction Is Associated with Inhibition of the Intestinal Mitogen-Activated Protein Kinase Pathway. *Phytomedicine*. 66, 153135. doi:10.1016/j.phymed.2019.153135

Liu, X. L., Cao, H. X., Wang, B. C., Xin, F. Z., Zhang, R. N., Zhou, D., et al. (2017a). miR-192-5p Regulates Lipid Synthesis in Non-alcoholic Fatty Liver Disease through SCD-1. *World J Gastroenterol.* 23 (46), 8140–8151. doi:10.3748/wjg.v23.i46.8140

Liu, Q., Zhu, L., Cheng, C., Hu, Y.-Y., and Feng, Q. (2017b). Natural Active Compounds from Plant Food and Chinese Herbal Medicine for Nonalcoholic Fatty Liver Disease. *Curr. Pharm. Des.* 23 (34), 5136–5162. doi:10.3748/wjg.v23.i11.1964

Meng, S. X., Liu, Q., Tang, Y. J., Wang, W. J., Zheng, Q. S., Tian, H. J., et al. (2016). A Recipe Composed of Chinese Herbal Active Components Regulates Hepatic

Lipid Metabolism of NAFLD *In Vivo* and *In Vitro*. *Biomed. Res. Int.* 2016, 1026852. doi:10.1155/2016/1026852

Miyazaki, M., Flowers, M. T., Sampath, H., Chu, K., Otzelberger, C., Liu, X., et al. (2007). Hepatic Stearoyl-CoA Desaturase-1 Deficiency Protects Mice from Carbohydrate-Induced Adiposity and Hepatic Steatosis. *Cel Metab.* 6 (6), 484–496. doi:10.1016/j.cmet.2007.10.014

Miyazaki, M., Sampath, H., Liu, X., Flowers, M. T., Chu, K., Dobrzyn, A., et al. (2009). Stearoyl-CoA Desaturase-1 Deficiency Attenuates Obesity and Insulin Resistance in Leptin-Resistant Obese Mice. *Biochem. Biophysical Res. Commun.* 380 (4), 818–822. doi:10.1016/j.bbrc.2009.01.183

Ntambi, J. M., Miyazaki, M., Stoehr, J. P., Lan, H., Kendziorski, C. M., Yandell, B. S., et al. (2002). Loss of Stearoyl-CoA Desaturase-1 Function Protects Mice against Adiposity. *Proc. Natl. Acad. Sci.* 99 (17), 11482–11486. doi:10.1073/pnas.132384699

Ntambi, J. M. (1999). Regulation of Stearoyl-CoA Desaturase by Polyunsaturated Fatty Acids and Cholesterol. *J. Lipid Res.* 40 (9), 1549–1558. doi:10.1016/s0022-2275(20)33401-5

Peng, J. H., Leng, J., Tian, H. J., Yang, T., Fang, Y., Feng, Q., et al. (2018). Geniposide and Chlorogenic Acid Combination Ameliorates Non-alcoholic Steatohepatitis Involving the Protection on the Gut Barrier Function in Mouse Induced by High-Fat Diet. *Front. Pharmacol.* 9, 1399. doi:10.3389/fphar.2018.01399

Poloni, S., Blom, H., and Schwartz, I. (2015). Stearoyl-CoA Desaturase-1: Is it the Link between Sulfur Amino Acids and Lipid Metabolism? *Biology*. 4 (2), 383–396. doi:10.3390/biology4020383

Rinella, M. E. (2015). Nonalcoholic Fatty Liver Disease. *JAMA* 313 (22), 2263–2273. doi:10.1001/jama.2015.5370

Rotman, Y., and Sanyal, A. J. (2017). Current and Upcoming Pharmacotherapy for Non-alcoholic Fatty Liver Disease. *Gut* 66 (1), 180–190. doi:10.1136/gutjnl-2016-312431

Sampath, H., Flowers, M. T., Liu, X., Paton, C. M., Sullivan, R., Chu, K., et al. (2009). Skin-specific Deletion of Stearoyl-CoA Desaturase-1 Alters Skin Lipid Composition and Protects Mice from High Fat Diet-Induced Obesity. *J. Biol. Chem.* 284 (30), 19961–19973. doi:10.1074/jbc.m109.014225

Sanders, F. W. B., and Griffin, J. L. (2016). De Novo lipogenesis in the Liver in Health and Disease: More Than Just a Shunting Yard for Glucose. *Biol. Rev.* 91 (2), 452–468. doi:10.1111/brv.12178

Tang, Y., Meng, S., Feng, Q., Li, X., Wang, W., Peng, J., et al. (2013). Screening and Validation of a Chinese Medicine Recipe in the Treatment of Fatty Livers. *Univ. Tradit. Chin. Med.*, 53–57.

Warensjö, E., Risérus, U., and Vessby, B. (2005). Fatty Acid Composition of Serum Lipids Predicts the Development of the Metabolic Syndrome in Men. *Diabetologia*. 48 (10), 1999–2005. doi:10.1007/s00125-005-1897-x

Xin, X., Cai, B. Y., Chen, C., Tian, H.- J., Wang, X., Hu, Y. Y., et al. (2020). High-trans Fatty Acid and High-Sugar Diets Can Cause Mice with Non-alcoholic Steatohepatitis with Liver Fibrosis and Potential Pathogenesis. *Nutr. Metab. (Lond)* 17, 40. doi:10.1186/s12986-020-00462-y

Zhang, Y., Ding, Y., Zhong, X., Guo, Q., Wang, H., Gao, J., et al. (2016). Geniposide Acutely Stimulates Insulin Secretion in Pancreatic β-cells by Regulating GLP-1 receptor/cAMP Signaling and Ion Channels. *Mol. Cell Endocrinol.* 430, 89–96. doi:10.1016/j.mce.2016.04.020

Zhou, J., Zhou, F., Wang, W., Zhang, X. J., Ji, Y. X., Zhang, P., et al. (2020). Epidemiological Features of NAFLD from 1999 to 2018 in China. *Hepatology*. 71 (5), 1851–1864. doi:10.1002/hep.31150

Conflict of Interest: The authors declare that the research was conducted in the absence of any commercial or financial relationships that could be construed as a potential conflict of interest.

frontiers in Pharmacology

ORIGINAL RESEARCH
published: 30 June 2021
doi: 10.3389/fphar.2021.693048

Chlorogenic Acid Improves NAFLD by Regulating gut Microbiota and GLP-1

Ameng Shi[1†], *Ting Li*[2†], *Ying Zheng*[3†], *Yahua Song*[3], *Haitao Wang*[4], *Na Wang*[4], *Lei Dong*[3] *and Haitao Shi*[3*]

[1]Department of Ultrasound, The Second Affiliated Hospital of Xi'an Jiaotong University, Xi'an, China, [2]Department of Geriatric Respiratory and Endocrinology (The Third Unit of Cadre's Ward), The Second Affiliated Hospital of Xian Jiaotong University, Xi'an, China, [3]Department of Gastroenterology, The Second Affiliated Hospital of Xi'an Jiaotong University, Xi'an, China, [4]Department of Pharmacy, The Second Affiliated Hospital of Xi'an Jiaotong University, Xi'an, China

Our previous studies have shown that chlorogenic acid (CGA) could significantly improve acute and chronic liver injury through antioxidant and anti-inflammatory activities. However, its effect on non-alcoholic fatty liver disease (NAFLD) are not entirely clear. This study aims to explore the effect of CGA on NAFLD induced by high-fat diet (HFD) and whether it regulates the gut microbiota and Glucagon-like peptide-1 (GLP-1). NAFLD mice were established by HFD and treated with or without CGA. Serum transaminase, fasting blood glucose (FBG), blood lipids, insulin, GLP-1 and lipopolysaccharide (LPS) were detected. Liver histology was evaluated with Hematoxylin-eosin staining. Toll like receptor 4 (TLR4) signaling pathway was analyzed with western blot and inflammatory cytokines were detected with real-time PCR. The content of gut microbiota were determined with real-time PCR of the bacterial 16S rRNA gene. Expressions of intestine tight junctional protein were examined with immunohistochemistry. CGA could alleviate HFD-induced hepatic steatosis and inflammation, reduce serum transaminase, FBG and blood lipids, increase insulin sensitivity. CGA also could reverse HFD-induced activation of TLR4 signaling pathway and expression of tumor necrosis factor-α (TNF-α) and interleukin-6 (IL-6) in liver. Meanwhile, CGA increased the content of Bifidobacterium and reduced the content of *Escherichia coli* in feces. Furthermore, CGA could increase the expression of tight junction proteins Occludin and zonula occludens-1 (ZO-1) in intestinal tissue. Moreover, CGA could the level of LPS and increased the level of GLP-1 in portal vein. These results indicated that CGA protected against HFD-induced hepatic steatosis and inflammation probably through its anti-inflammatory effects associated with regulation of gut microbiota and an increase of GLP-1 secretion and thus could be used as a potential drug for prevention and treatment of NAFLD.

Keywords: chlorogenic acid, non-alcoholic fatty liver disease, gut microbiota, glucagon-like peptide-1, anti-inflammatory

OPEN ACCESS

Edited by:
Silvia Di Giacomo,
Sapienza University of Rome, Italy

Reviewed by:
Laura Grasa,
University of Zaragoza, Spain
Sara Baldassano,
University of Palermo, Italy

***Correspondence:**
Haitao Shi
shihaitao7@163.com

[†]*These authors have contributed equally to this work*

Specialty section:
This article was submitted to Gastrointestinal and Hepatic Pharmacology, a section of the journal Frontiers in Pharmacology

Received: *09 April 2021*
Accepted: *18 June 2021*
Published: *30 June 2021*

Citation:
Shi A, Li T, Zheng Y, Song Y, Wang H, Wang N, Dong L and Shi H (2021) Chlorogenic Acid Improves NAFLD by Regulating gut Microbiota and GLP-1. Front. Pharmacol. 12:693048. doi: 10.3389/fphar.2021.693048

INTRODUCTION

Non-alcoholic fatty liver disease (NAFLD) has become the world's most common chronic liver disease and is the main cause of end-stage liver disease (Mikolaevi et al., 2021). It is generally believed that NAFLD is associated with abnormal glucose and lipid metabolism, insulin resistance, inflammation, oxidative stress and imbalanced gut microbiota. To date, no evidence-based drug

has been approved for the treatment of NAFLD (Campbell et al., 2021). Thus, revealing the pathogenesis of NAFLD and finding more effective therapeutic targets and drugs are challenges in the field of fatty liver research.

Gut *microbiota* imbalance participates in the occurrence and development of NAFLD (Aron-Wisnewsky et al., 2020). The structure of the gut microbiota in NAFLD patients is significantly different from that in the healthy population, which manifests as a reduction in beneficial bacteria (such as *Bifidobacterium* and *Lactobacillus*) and an increase in harmful bacteria (such as *Escherichia coli* and *Enterococcus*) (Dai et al., 2020). Overgrowth of the gut *microbiota* promotes the development of obesity and insulin resistance, which can damage the intestinal mucosa barrier function and allow endotoxins to travel to the liver, where they can induce or exacerbate liver inflammation and oxidative stress damage, leading to occurrence and progression of hepatic steatosis, inflammation and fibrosis (Akash et al., 2019).

Glucagon-like peptide-1 (GLP-1) is an important incretin and its receptor GLP-1R is widely distributed in tissues such as liver, pancreas, brain, heart and intestine. GLP-1 can increase liver fatty acid oxidation and insulin sensitivity by binding to GLP-1R, thereby improving NAFLD (Areti et al., 2020). Short-chain fatty acids (SCFA), a metabolic product of the gut *microbiota*, can regulate the secretion of GLP-1 (Bayer et al., 2018). Therefore, regulating gut *microbiota* and increasing the secretion of GLP-1 have become a new research direction for the treatment of NAFLD. Many studies have investigated the mechanism and feasibility of this therapeutic approach (Akash et al., 2019).

Chlorogenic acid (CGA) is a phenolic compound that is abundant in plants such as coffee, *eucommia ulmoides* and *honeysuckle*. CGA has antioxidative, anti-inflammatory, antitumor, antihypertensive and lipid-lowering functions (Shi et al., 2013). Our previous studies have shown that CGA can significantly improve carbon tetrachloride-induced acute liver injury and chronic liver injury through antioxidant and anti-inflammatory activities (Shi et al., 2013; Dong et al., 2016; Shi et al., 2017). It is also reported that CGA might also increase insulin sensitivity by increasing the secretion of GLP-1 (Mccarty, 2005; Faraji, 2019), however, the mechanism is not entirely clear. This study aims to explore the effect of CGA on NAFLD induced by HFD and whether it regulates the gut microbiota and Glucagon-like peptide-1 (GLP-1).

MATERIALS AND METHODS

Reagents

CGA (#C3878) was purchased from Sigma-Aldrich (St. Louis, United States). CGA was resolved in dimethyl sulfoxide and then sterile filtered before used and dissolved in distilled water. Rabbit-anti-mouse polyclonal primary antibodies against Toll like receptor 4 (TLR4), nuclear transcription factor-κB (NF-κB), p-NF-κB, inhibitor of NF-κB-α (IκB-α), *p*-IκB-α, β-actin, zonula occludens-1 (ZO-1), and Occludinwere purchased from Proteintech group. Goat-anti-rabbit secondary antibodies were purchased from Cell Signaling Technology.

Experimental Animals

6-week-old male C57BL/6 mice (19.48 ± 2.32 g) were supplied by the Laboratory Animal Center of Xi'an Jiaotong University (Xi'an, China) and housed under specific pathogen-free conditions with free access to water. 24 mice were randomly divided into four groups ($n = 6$): Control:fed with a standard chow diet and treated with the same amount of distilled water; CGA:fed with a standard chow diet and treated with CGA (60 mg/kg, orally once a day); high-fat diet (HFD):fed with a high-fat diet and treated with the same amount of distilled water; HFD + CGA:fed with a high-fat diet and treated with CGA (60 mg/kg, orally once a day). HFD consists of 50% regular diet, 10% lard, 7.5% sucrose, 5% milk powder, 2.5% egg yolk powder, 15% soybean powder, and 10 drops of cod liver oil/100 g, which was similar to our previous approach (Li et al., 2019). The dosage and administration of CGA were chosen according our previous studies (Shi et al., 2013; Shi et al., 2017). After 12 w of feeding and 12 h of fasting, all mice were sacrificed by an intravenous administration of pentobarbital (1%, 50 mg/kg). Liver tissue, intestinal tissue at the ileum and *caecum*, portal vein serum and stool specimens were collected using sterilizing tubes after 12 w feeding and were immediately frozen in liquid nitrogen and stored at −80°C.

Blood Analysis and Enzyme-linked Immunosorbent Assay

Serum transaminase, fasting blood glucose (FBG) and blood lipids including total cholesterol (TC) and triglyceride (TG) were analyzed by a biochemistry analyzer (Olympus AU2700, Japan). Sandwich Enzyme-linked immunosorbent assay (ELISA) (R and D Systems, Minneapolis, MN, United States) was used to analyze the content of fasting insulin (FINS), lipopolysaccharide (LPS and GLP-1) according to the manufacturer's instructions. The homeostasis model assessment-estimated insulin resistance (HOMA-IR) index was calculated as fasting plasma glucose level (mmol/L) × fasting insulin level (mIU/L)/22.5 (Matthews et al., 1985). ELISA assay protocol: after placed at 4°C overnight, whole blood samples were centrifuged at 1,000 g for 20 min to prepare serum. 100°µl of standard or sample were added to the standard hole and sample hole in ELISA plate, no reagent added to blank hole. After fully mixed, the reaction plate was incubated at 37°C for 120°min; the reaction plate was washed 4–6 times; 100 µl of the first antibody working solution was added and incubated at 37°C for 60°min; after washed, 100 µl of enzyme labeled antibody working solution was added and incubated at 37°C for 30°min; after washed, 100 µl of substrate working solution was added and reacted at 37°C in dark for 15°min; 100 µl termination solution were added and the absorbance were measured at 450 nm within 30 min. The standard curve was made and the content of target protein (FINS, LPS and GLP-1) was calculated.

Hematoxylin-Eosin Staining

Liver tissues fixed in 10% formaldehyde were cleared in xylene, dehydrated with gradient ethanol, embedded in paraffin, and serially sectioned at 5 µm. Sections were dewaxed with xylene, dehydrated with gradient ethanol, stained with Harris's hematoxylin for 5 min, differentiated with 0.1% hydrochloric

TABLE 1 | Primer sequences used for gut microbiota and inflammatory cytokines.

Microbiota/genes	Sequences
Bifidobacterium	Forward: 5′-GGGTGGTAATGCCGGATG-3′
	Reverse: 5′-TAAGCGATGGACTTTCACACC-3′
Lactobacillus	Forward: 5′-AGCAGTAGGGAATCTTCCA-3′
	Reverse: 5′-CACCGCTACACATGGAG-3′
Escherichia coli	Forward: 5′-GTTAATACCTTTGCTCATTGA-3′
	Reverse: 5′-ACCAGGGTATCTAATCCTGTT-3′
Enterococcus	Forward: 5′-CCCTTATTGTTAGTTGCCATCATT-3′
	Reverse: 5′-ACTCGTTGTACTTCCCATTGT-3′
TNF-α	Forward: 5′-GCATGATCCGCGACGTGGAA-3′
	Reverse: 5′-AGATCCATGCCGTTGGCCAG-3′
IL-6	Forward: 5′-ACCCCAATTTCCAATGCTCTC-3′
	Reverse: 5′-AACGCACTAGGTTTGCCGAG-3′
β-actin	Forward: 5′-GGCTGTATTCCCCTCCATCG-3′
	Reverse: 5′-CCAGTTGGTAACAATGCCATGT-3′

acid alcohol, stained with 1% eosin for 2 min, dehydrated by gradient ethanol, cleared in xylene, mounted with neutral gum, and observed and photographed under a microscope. NAFLD Activity Score (NAS) defined as the sum of steatosis, lobular inflammation and ballooning was used to evaluate improvement in liver histology (Kleiner et al., 2005).

Western Blot

The total protein of liver tissues stored at 80°C was extracted using RIPA protein lysis buffer (Beyotime, Shanghai, China). Samples of 50 μg of protein were mixed with gelloading buffer, boiled for 5 min, and loaded on 10% polyacrylamide gels. After electrophoresis, the proteins were transferred to PVDF membranes (Millipore, Billerica, MA, United States). Non-specific antibody binding was blocked by preincubation of the membranes in 1× Tris-buffered saline (TBS) containing 5% skimmed milk for 2 h at room temperature. The membranes were incubated overnight at 4°C with rabbit-anti-mouse primary antibodies TLR4 (1:500), IκB-α(1:500), p-IκB-α(1:500), NF-κB (1: 400), p-NF-κB (1:400) and β-actin (1:1,000) in 1 × TBS containing 5% skimmed milk. After washing, they were incubated for 2 h at room temperature with goat-anti-rabbit secondary antibody at a 1:2,000 dilution. Positive bands were detected using an ECL plus chemiluminescence detection kit (Millipore, Billerica, MA, United States). The results were analyzed using Gel-pro Analyzer 4.0 software (Media Cybernetics, CA, United States), normalized to β-actin.

Real-Time PCR

The mRNA expression of TNF-α and IL-6 in liver tissues were detected with real-time PCR. Total RNA from liver tissues was extracted using a TRIzol kit (Invitrogen, Los Angeles, CA, United States) according to the manufacturer's protocol and synthesized into cDNA using a RevertAid™ First Strand cDNA Synthesis Kit (Fermentas, Thermo Scientific Molecular Biology, Waltham, MA, United States). The primer sequences of TNF-α and IL-6 are shown in **Table 1**. The real-time PCR was performed on an ABI 7,500 Real-Time Detection System using the SYBR Premix Ex Taq II qRT-PCR Kit (TaKaRa) to obtain the cycle threshold (CT) values. The applied PCR conditions were: preliminary denaturation at 95°C for 30°s, followed by 40 cycles at 95°C for 5°s and 60°C for 30°s. The relative expression levels of target genes were calculated using the $2^{-\Delta\Delta CT}$ method (Livak and Schmittgen, 2002), β-actin was used as an internal control.

The stool counts of *Bifidobacterium*, *Lactobacillus*, *Escherichia coli* and *Enterococcus* were determined from real-time PCR of the bacterial 16S rRNA gene. Total DNA was isolated from the fecal samples using a DNeasy Blood and Tissue Minikit (Qiagen, Germany) accroding to the manufacturer's protocols. The primer sequences of Bifidobacterium, Lactobacillus, *Escherichia coli* and *Enterococcus* used are shown in **Table 1**. The real-time PCR was performed similar to the above. CT values and standard curve were obtained by amplifying 10-fold serially diluted plasmids. Each amplification efficiency was also determined. The number of *Bifidobacterium*, *Lactobacillus*, *Escherichia coli* and *Enterococcus* copies were calculated based on their standard curves, respectively.

Immunohistochemistry

Liver and intestine tissues fixed in formalin and then embedded in paraffin were cut into 5-μm sections. After deparaffinized and rehydrated, the sections were antigen retrieved in the sodium citrate buffer solution and serum blocked. Then the sections were incubated with primary antibodies at 4°C overnight. The applied primary antibody: rabbit-anti-mouse polyclonal against ZO-1 (1: 100) and Occludin (1:100). After washing with phosphate-buffered saline (PBS) the next day, biotin-labeled secondary antibody (1:500) and streptavidin-biotin-peroxidase were added dropwise, followed by 3,3′-diaminobenzidine staining, counterstaining by hematoxylin, dehydration by gradient alcohol, clearing in xylene, and mounting with neutral gum. The primary antibody was replaced by PBS as a negative control. The slides were scanned at 100 × under light microscope (Olympus, Tokyo, Japan). Five fields were randomly selected for each slide. Image-Pro Plus 6.0 software (Media Cybernetics, Maryland United States) was used to calculate the ratio of the positively stained area to the area of the field of view, and the mean density from the five fields was taken.

Statistical Analysis

SPSS 17.0 was used for statistical analysis. All data showed normal distribution and are expressed as the mean ± standard deviation. Comparisons between multiple groups were performed using one-way analysis of variance (ANOVA). The LSD-*t* test was used for comparisons between groups. $p < 0.05$ was considered statistically significant.

RESULTS

Effect of Chlorogenic Acid on the Liver Pathology

In the negative control group and CGA control group, the liver cells were arranged neatly, and the morphology of the hepatic lobule was regular. In the HFD group, the liver cells were disorderly and showed obvious steatosis, mainly with microbubble-like lipid droplets, accompanied by a large amount of inflammatory cell infiltration and patchy necrosis. The degree of hepatic steatosis was lesser in the CGA treatment group than the HFD group, and there

TABLE 2 | Quantitation analysis of gut microbiota in fecal samples by real-time PCR (Mean ± SD).

Group	*Bifidobacterium*	*Lactobacillus*	*Escherichia coli*	*Enterococcus*
Control	8.45 ± 0.29	6.39 ± 0.33	8.44 ± 0.29	7.44 ± 0.34
CGA	8.62 ± 0.31[a]	6.41 ± 0.19	8.09 ± 0.13[a]	7.39 ± 0.33
HFD	8.05 ± 0.38[a]	5.83 ± 0.39[a]	8.71 ± 0.26[a]	8.46 ± 0.15[a]
HFD + CGA	8.32 ± 0.26[b]	5.85 ± 0.23	8.13 ± 0.36[b]	8.45 ± 0.31

Data were expressed as log_{10} (copy/g feces).
[a]p < 0.05 as compared with the control group.
[b]p < 0.05 as compared with the HFD group.

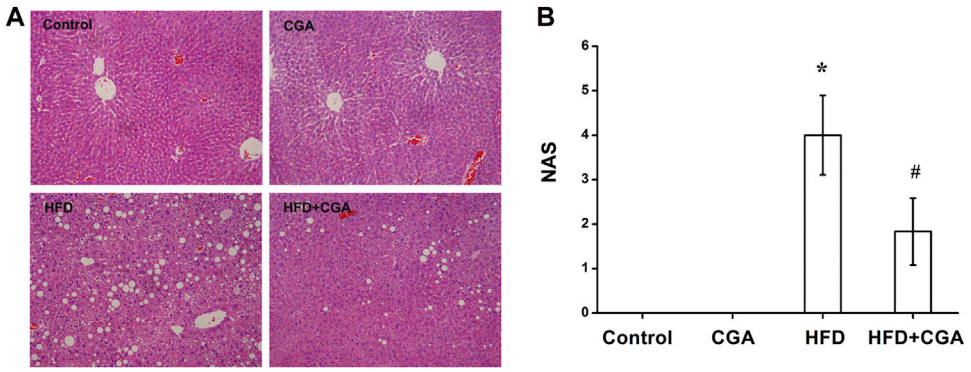

FIGURE 1 | Effect of CGA on liver tissue pathology. **(A)** Hematoxylin-eosin staining for liver sections (200×). **(B)** NAS in four groups. Data are presented as the mean ± SD. *p < 0.05 as compared with the control group; #p < 0.05 as compared with the HFD group.

were significantly fewer inflammatory cells (**Figure 1A**). NAS defined as the sum of steatosis, lobular inflammation and ballooning was used to evaluate hepatic steatosis and inflammation. Compared with HFD group, the NAS score was significantly lower in HFD + CGA group (p < 0.05) (**Figure 1B**).

Effect of Chlorogenic Acid on Serum Transaminase, Fasting Blood Glucose, Blood Lipids and Insulin Resistance

To evaluate the effect of CGA on metabolic characteristics of NAFLD mice, serum transaminase, FBG, blood lipids and fasting insulin were detected. Serum transaminase, FBG, blood lipids and HOMA-IR of the control group and CGA control group were in the normal range. The mice in the HFD group showed significantly elevated serum transaminase, FBG, blood lipids and HOMA-IR (p < 0.05). After treatment with CGA, the serum transaminase, FBG, blood lipids and HOMA-IR significantly decreased (p < 0.05) (**Figure 2**).

Effect of Chlorogenic Acid on Liver Inflammation

TLR4 signaling pathway is an important pathway related to liver inflammation in NAFLD. TNF-α and IL-6 were two major inflammatory cytokines. We further evaluated the effect of CGA on liver inflammation in NAFLD. Compared with the control group, the HFD group had significantly higher protein expression of TLR4, p-NF-κB, and p-IκB-α in the liver (p < 0.05), and the mRNA expression levels of TNF-α and IL-6 were significantly increased (p < 0.05). After CGA treatment, the protein expression of TLR4, p-NF-κB, and p-IκB-α and mRNA expression of TNF-α and IL-6 were all decreased (p < 0.05). However, the CGA itself had no significant effect on the expression of TLR4 signaling pathway and inflammatory cytokines (**Figure 3**).

Effect of Chlorogenic Acid on Gut Microbiota

In order to elucidate the mechanism of CGA improving liver inflammation, we examined the effect of CGA on gut-liver axis, and the gut microbiota was detected. Compared with the control group, the HFD group had more *Escherichia coli* and *Enterococcus* and less *Bifidobacterium* and *Lactobacillus* (p < 0.05). Treatment with CGA increased the content of Bifidobacterium, reduced the content of *Escherichia coli* (p < 0.05). However, CGA had no significant effect on the content of *Lactobacillus* and *Enterococcus* (**Table 2**).

Effect of Chlorogenic Acid on the Expression of Intestine Tight Junction Proteins

The gut microbiota plays an important role in integrity maintenance of intestinal mucosal barrier and intestinal tight junction protein is the principal determinant of mucosal barrier. Compared with the control group, the expression of the tight

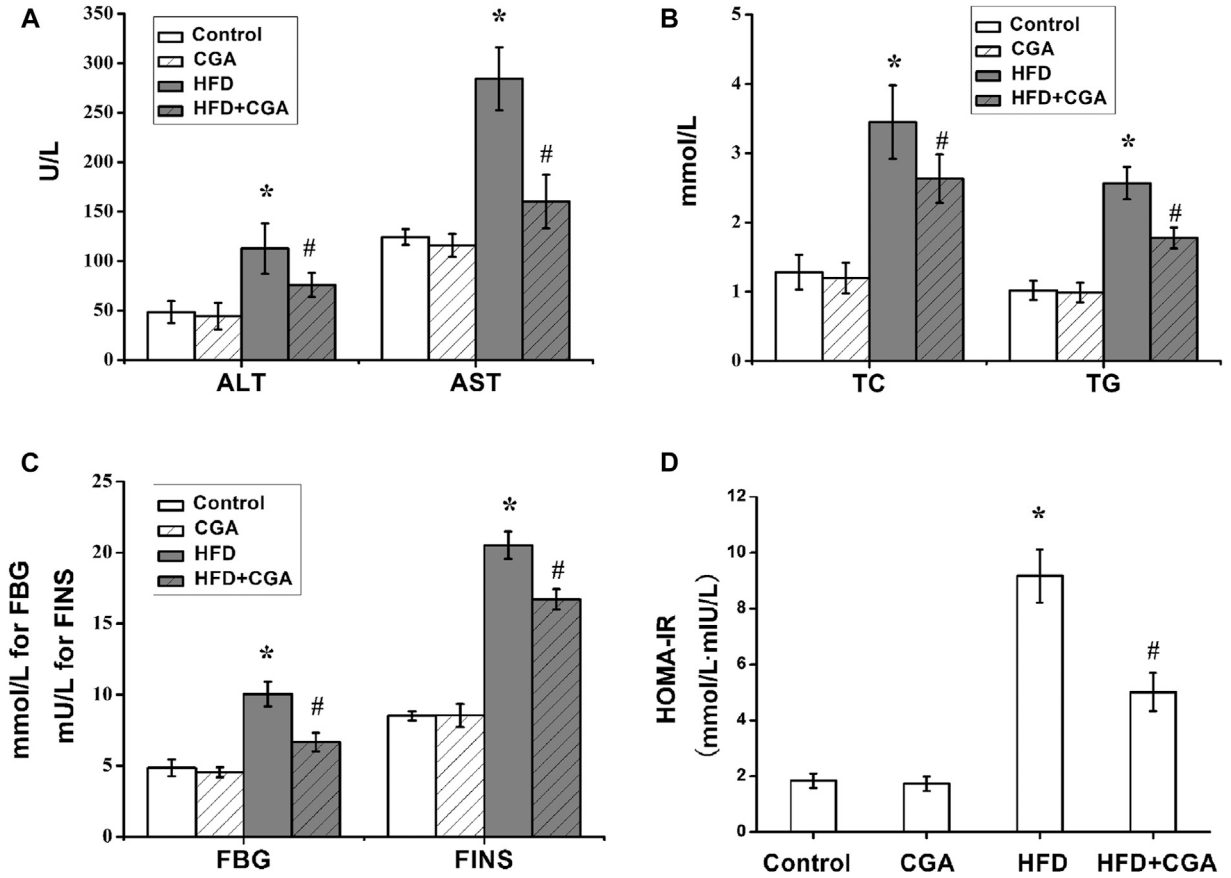

FIGURE 2 | Effect of CGA on serum transaminase, fasting blood glucose (FBG) and blood lipids and insulin resistance. **(A)** serum transaminase; **(B)** blood lipids including total cholesterol (TC) and triglyceride (TG); **(C)** FBGand FINS; **(D)** HOMA-IR. Data are presented as mean ± SD. *$p < 0.05$ as compared with the control group; #$p < 0.05$ as compared with the HFD group.

junction protein Occludin and ZO-1 in the HFD group were downregulated ($p < 0.05$), and the expression of Occludin and ZO-1 were increased after CGA treatment ($p < 0.05$). However, the CGA itself had no significant effect on the expression of the tight junction proteins (**Figure 4**).

Effect of Chlorogenic Acid on the Level of Lipopolysaccharide in the Portal Vein

Disruption of gut microbiota and intestinal mucosal barrier leads to the increase of mucosal permeability and the entry of endotoxin into the liver. Therefore, we examined the level of LPS in portal vein. Compared with the control group, the level of LPS in portal vein significantly in the HFD group was increased ($p < 0.05$), and the level of LPS was reduced after CGA treatment ($p < 0.05$). However, CGA itself had no significant effect on the level of LPS (**Figure 5**).

Effect of Chlorogenic Acid on the Level of GLP-1 in the Portal Vein

Gut microbiota and its metabolites can increase the secretion of GLP-1, which thus improve insulin resistance, hepatic steatosis and inflammation. Compared with the control group, the level of GLP-1 in portal vein significantly in the HFD group was decreased ($p < 0.05$), and the level of GLP-1 was increased after CGA treatment ($p < 0.05$). However, CGA itself had no significant effect on the level of LPS (**Figure 6**).

DISCUSSION

NAFLD seriously endangers people's health when it develops into fatty hepatitis, liver cirrhosis and even liver cancer. In recent years, the influence of gut microbiota as a "microbial organ" on human health has received extensive attention. Gut microbiota disturbances can be a manifestation of certain diseases and can also cause or exacerbate diseases, such as obesity, diabetes mellitus, metabolic syndrome, inflammatory bowel disease and tumors (Illiano et al., 2020). Gut microbiota dysregulation plays an important role in the occurrence and progression of NAFLD (Dai et al., 2020). Overgrowth of the gut microbiota leads to dysfunction of the intestinal mucosal barrier, resulting in the translocation of endotoxins to the liver, where they bind to their specific receptors CD14 and TLR4 on Kupffer cells. They release a

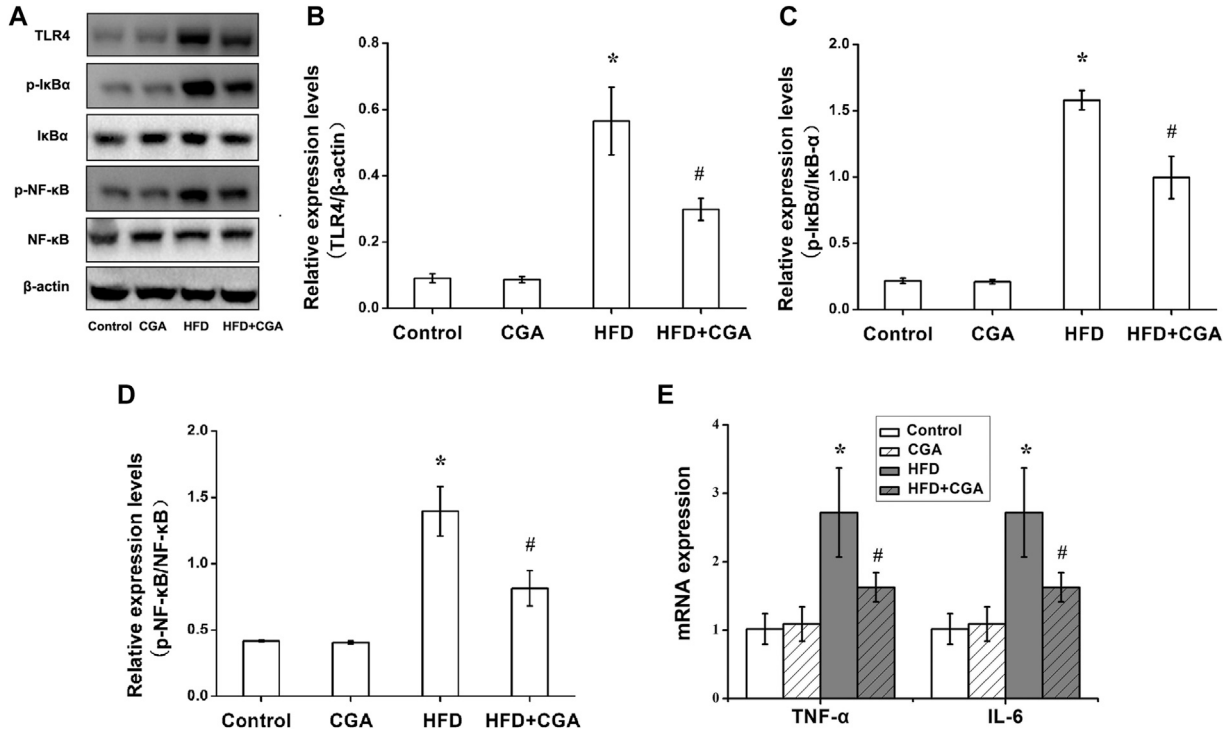

FIGURE 3 | Effects of CGA on the TLR4/NF-κB signaling pathway and inflammatory cytokines in the liver. **(A)** TLR4/NF-κB signaling pathway analyzed with western blot. **(B)** TLR4 expression. **(C)** *p*-IκBα/IκBα expression **(D)** p-NF-kB/NF-kB expression. **(E)** expression of TNF-α and IL-6 analyzed with real-time PCR. Data are presented as mean ± SD. $^{*}p < 0.05$ as compared with the control group; $^{\#}p < 0.05$ as compared with the HFD group.

series of oxygen free radicals and inflammatory cytokines by activating downstream signaling pathways such as NF-κB to cause changes in the liver microenvironment, which induces or aggravates inflammation and oxidative stress damage in the liver (Hussain et al., 2020). Therefore, the gut microbiota, intestinal mucosal barrier, endotoxins and NAFLD are interrelated.

Incretins are a class of intestinal hormones in the human body, including GLP-1 and glucose-dependent insulinotropic peptide (GIP). GLP-1 is a product of the translation and posttranslational processing of the proglucagon gene. It is secreted by L cells of the small intestine and the large intestine and is rapidly degraded by dipeptidyl peptidase 4 (DPP-4) (Brierley et al., 2021). By binding to GLP-1R, GLP-l regulates not only glucose metabolism but also lipid metabolism (Karstoft et al., 2015; Lutz and Osto, 2016). An abnormal incretin system is present in NAFLD patients. It is found that nondiabetic NAFLD and non-alcoholic steatohepatitis (NASH) patients had lower GLP-1 than healthy controls (Christine et al., 2014). The mechanisms by which GLP-1 improves NAFLD include direct and indirect effects (Teshome et al., 2020). GLP can activate AMP-activated protein kinase (AMPK) to increase liver lipid oxidation, improve insulin sensitivity and inhibit liver fat synthesis. GLP-1 also regulates feeding neurotransmitters through central GLP-1R, leading to anorexia and reduced food intake, leaving less material for liver fat synthesis. Through gastric GLP-1R, GLP-1 inhibits gastric emptying and improves satiety, thereby indirectly reducing food intake.

There is clear evidence that the gut microbiota is related to the incretin effect, the gut microbiota does affect the differentiation and apoptosis of intestinal epithelial cells (Demidova et al., 2020). Adding prebiotics to the diet can increase the amount of bifidobacterial in the distal gut, increase the fermentation of dietary fiber, promote the differentiation of colonic L cells, and increase the secretion of GLP-1. Short-chain fatty acids, among the metabolites of gut microbiota, can regulate GLP-1 secretion, thereby improving diet-induced obesity and insulin resistance (Jiao et al., 2020). This study shows that CGA could increase the contents of *Bifidobacterium* and reduced the *Escherichia coli* in NAFLD mice, suggesting its promoting effect on GLP-1 secretion may be related with its effect on these gut microbiota. Some studies have shown that CGA could increase the diversity of gut microbiota (Song et al., 2019; Yan et al., 2020), while others have shown that the CGA treated mice showed similar microbial structure compared to that of the HFD mice (He et al., 2020). Based on these researches and our study, we speculated that CGA could regulate composition of gut microbiota under different pathological conditions as a different way. There is a certain negative correlation between coffee consumption and the occurrence and progression of chronic liver diseases, including fatty liver and liver fibrosis. Some epidemiological studies found that the risk of NAFLD in patients who drank coffee was significantly lower than that in patients who did not and a significantly decreased risk of liver fibrosis among NAFLD patients who drank coffee (Bambha et al.,

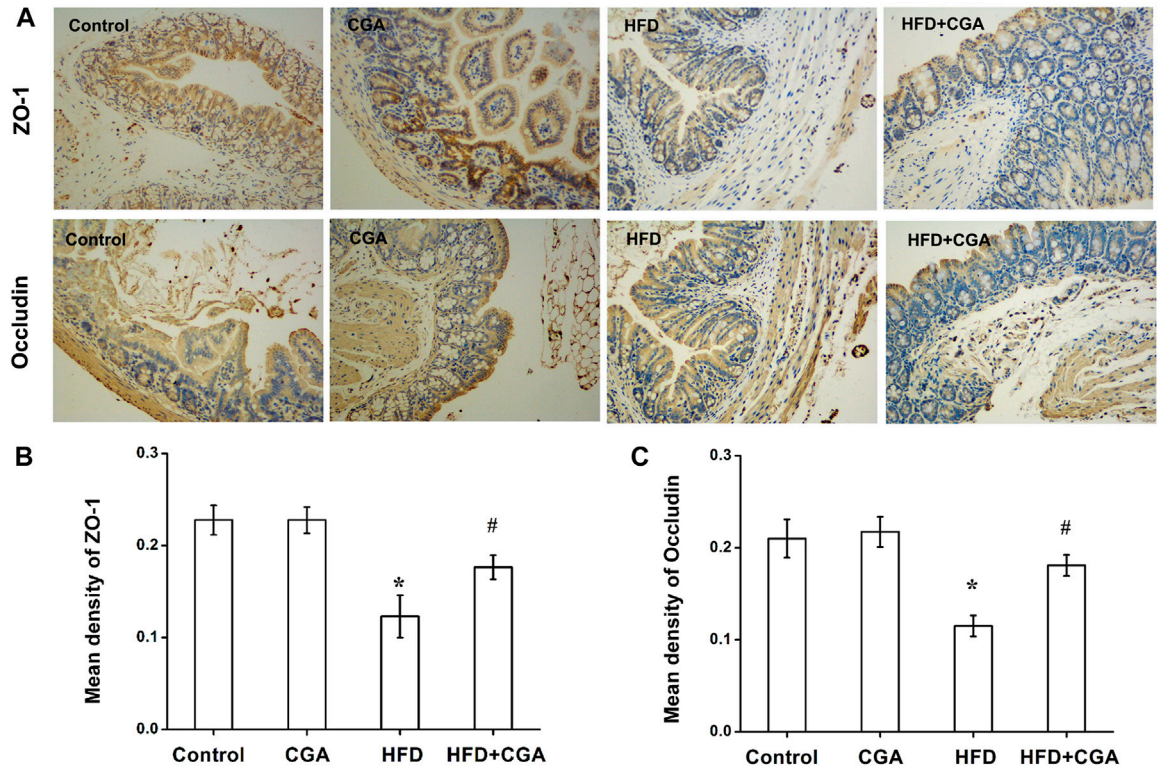

FIGURE 4 | Effect of CGA on the expression of intestinal tight junction protein. **(A)** Immunohistochemical staining of ZO-1 and Occludin (100×) **(B)** Mean density of ZO-1 analyzed with Image-Pro Plus. **(C)** Mean density of Occludin analyzed with Image-Pro Plus. Data are presented as mean ± SD. $^{*}p < 0.05$ as compared with the control group; $^{\#}p < 0.05$ as compared with the HFD group.

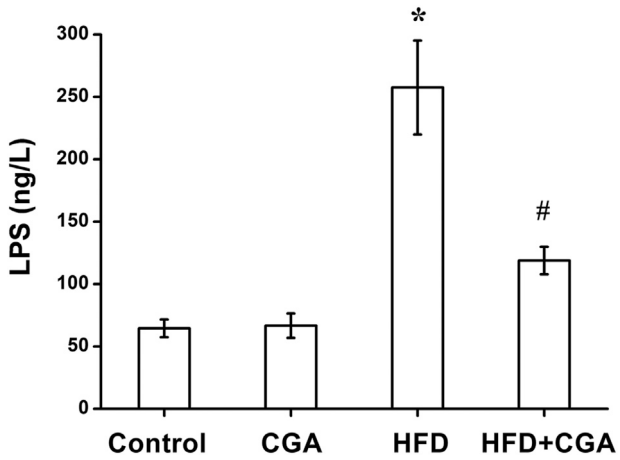

FIGURE 5 | Effect of CGA on the level of LPS in portal vein. Data are presented as mean ± SD. $^{*}p < 0.05$ as compared with the control group; $^{\#}p < 0.05$ as compared with the HFD group.

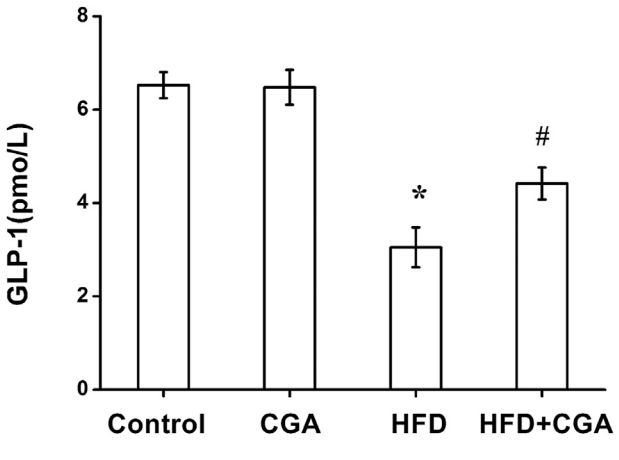

FIGURE 6 | Effect of CGA on the level of GLP-1 in portal vein. Data are presented as mean ± SD. $^{*}p < 0.05$ as compared with the control group; $^{\#}p < 0.05$ as compared with the HFD group.

2015; Wijarnpreecha et al., 2017; Calabro et al., 2020). Vitaglione et al.found that coffee supplementation prevented HFD-induced NAFLD in mice by reducing hepatic fat deposition and modulating pathways of the gut-liver axis and gut microbiota (Vitaglione et al., 2019). It remains unclear which ingredients of coffee play these roles. One recent study showed that caffeic acid, one compound of coffee, prevents non-alcoholic fatty liver disease induced by a high-fat diet through reverting the imbalance in the gut microbiota and related

lipopolysaccharide-mediated inflammation (Hnm et al., 2021). CGA is a polyphenolic compound found in high amounts in coffee. CGA has significant antioxidant, anti-inflammatory, lipid-lowering, and hypoglycemic effects. Our and other's studies showed that CGA can improve acute and chronic liver injury caused by various reasons (Dong et al., 2016; Shi et al., 2017; Kim et al., 2018; Abbas et al., 2020; Hu et al., 2020). Chlorogenic acid can also improve NAFLD through its antioxidant, anti-inflammatory, lipid-lowering activities (Alqarni et al., 2019; Zamani-Garmsiri et al., 2020). However, there are few studies on the effect of CGA on gut microbiota, intestinal mucosal barrier, short-chain fatty acids and GLP-1 in NAFLD patients or animal models. Xie M found CGA can alleviate colitis in HFD-induced obesity through its anti-inflammatory effects associated with changes in gut microbiota composition and an increase in the production of short-chain fatty acids (Xie et al., 2021). Mccarty MF found that CGA could increase GLP-1 secretion, thereby reducing the risk of diabetes (Mccarty, 2005). This study showed that CGA significantly improved liver damage, reduced FBG and blood lipids, improved insulin resistance, and reduced hepatic steatosis and inflammation in NAFLD mice. We also found that CGA regulated the gut microbiota, improved intestine mucosal barrier, reduced LPS levels, and increased GLP-1, suggesting that CGA could improve hepatic steatosis and inflammation by enhanceing the proportions of beneficial bacteria to increase the level of GLP-1. In the research method, the mice received CGA and HFD at the same time, so our results could better explain the potential protective and preventive effects of CGA in the development of NAFLD. If we gave CGA intervention after NAFLD model was established, it could better explain its therapeutic effect. This needs to be further studied in the future.

CONCLUSION

In summary, these results indicate that CGA protects against HFD-induced hepatic steatosis and inflammation probably through its anti-inflammatory effects associated with regulation of certain gut microbiota and an increase of GLP-1 secretion and thus can be used as a potential drug for the prevention and treatment of NAFLD. Meanwhile, this study also elucidated the new mechanism of anti-inflammatory effect of CGA from gut-liver axis. However, the mechanism of CGA regulating gut microbiota and GLP-1 needs further study.

DATA AVAILABILITY STATEMENT

The datasets presented in this study can be found in online repositories. The names of the repository/repositories and accession number(s) can be found in the article/ Supplementary Material.

ETHICS STATEMENT

The animal study was reviewed and approved by the ethics committee of the second affiliated hospital of Xi'an Jiao Tong University, Xi'an, China. Written informed consent was obtained from the owners for the participation of their animals in this study.

AUTHOR CONTRIBUTIONS

AS, TL, and HS developed the conception and design of the study. AS, TL, and YZ conducted the experiments and wrote the article. YZ, YS, HW, and NW performed the data analysis. LD and HS revised the article. All authors read and approved the final article.

FUNDING

This study was supported by National Key Research and Development Program of China during the 13th Five-Year Plan Period (2018YFC1311504), Key Research and Development Program of Shaanxi Province (2017SF-100) and the Fundamental Research Funds for the Central Universities (xjj2018132).

REFERENCES

Abbas, N. A. T., Awad, M. M., and Nafea, O. E. (2020). Silymarin in Combination with Chlorogenic Acid Protects against Hepatotoxicity Induced by Doxorubicin in Rats: Possible Role of Adenosine Monophosphate-Activated Protein Kinase Pathway. *Toxicol. Res.* 9 (6), 771–777. doi:10.1093/toxres/tfaa080

Akash, M. S. H., Fiayyaz, F., Rehman, K., Sabir, S., and Rasool, M. H. (2019). Gut Microbiota and Metabolic Disorders: Advances in Therapeutic Interventions. *Crit. Rev. Immunol.* 39 (4), 223–237. doi:10.1615/CritRevImmunol.2019030614

Alqarni, I., Bassiouni, Y. A., Badr, A. M., and Ali, R. A. (2019). Telmisartan And/or Chlorogenic Acid Attenuates Fructose-Induced Non-alcoholic Fatty Liver Disease in Rats: Implications of Cross-Talk between Angiotensin, the Sphingosine Kinase/Sphingoine-1-Phosphate Pathway, and TLR4 Receptors. *Biochem. Pharmacol.* 164, 252–262. doi:10.1016/j.bcp.2019.04.018

Sofogianni, A., Filippidis, A., Chrysavgis, L., Tziomalos, K., and Cholongitas, E. (2020). Glucagon-like Peptide-1 Receptor Agonists in Non-alcoholic Fatty Liver Disease: An Update. *World J. Hepatol.* 12 (8), 493–505. doi:10.4254/wjh.v12.i8.493

Aron-Wisnewsky, J., Vigliotti, C., Witjes, J., Le, P., Holleboom, A. G., Nieuwdorp, J. M., et al. (2020). Gut Microbiota and Human NAFLD: Disentangling Microbial Signatures from Metabolic Disorders. *Nat. Rev. Gastroenterol. Hepatol.* 17, 279–297. doi:10.1038/s41575-020-0269-9

Bambha, K., Wilson, L. A., Unalp, A., Loomba, R., Neuschwander-Tetri, B. A., Brunt, E. M., et al. (2015). Coffee Consumption in NAFLD Patients with Lower Insulin Resistance Is Associated with Lower Risk of Severe Fibrosis. *Liver Int.* 34 (8), 1250–1258. doi:10.1111/liv.12379

Bayer, C. C., Nordskov, G., Berit, S., Ove, D. L., Marie, R. M., and Juul, H. J. (2018). The Impact of Short Chain Fatty Acids on GLP-1 and PYY Secretion from the Isolated Perfused Rat colon. *Am. J. Physiol. Gastr. L.* 315 (1), G53–G65. doi:10.1152/ajpgi.00346.2017

Brierley, D. I., Holt, M. K., Singh, A., de Araujo, A., McDougle, M., Vergara, M., et al. (2021). Central and Peripheral GLP-1 Systems Independently Suppress Eating. *Nat. Metab.* 3 (2), 258–273. doi:10.1038/s42255-021-00344-4

Calabrò, A., Procopio, A. C., Primerano, F., Larussa, T., Luzza, F., Di Renzo, L., et al. (2020). Beneficial Effects of Coffee in Non-alcoholic Fatty Liver Disease: A Narrative Review. *Hepatoma Res* 2020 (10), 69. doi:10.20517/2394-5079.2020.63

Campbell, P., Symonds, A., and Barritt, A. S. (2021). Therapy for Nonalcoholic Fatty Liver Disease: Current Options and Future Directions. *Clin. Ther.* 43, 500–517. doi:10.1016/j.clinthera.2021.01.021

Christine, B., Meyer-Gerspach, A. C., Blaser, L. S., Lia, J., Steinert, R. E., Heim, M. H., et al. (2014). Glucose-Induced Glucagon-like Peptide 1 Secretion Is Deficient in Patients with Non-alcoholic Fatty Liver Disease. *PLoS One* 9 (1), e87488. doi:10.1371/journal.pone.0087488

Dai, X., Hou, H., Zhang, W., Liu, T., Li, Y., Wang, S., et al. (2020). Microbial Metabolites: Critical Regulators in NAFLD. *Front. Microbiol.* 11, 567654. doi:10.3389/fmicb.2020.567654

Demidova, T. Y., Lobanova, K. G., and Oinotkinova, O. S. (2020). Gut Microbiota Is a Factor of Risk for Obesity and Type 2 Diabetes. *Terapevticheskii Arkhiv* 92 (10), 97–104. doi:10.26442/00403660.2020.10.000778

Shi, H., Shi, A., Dong, L., Lu, X., Wang, Y., Zhao, J., et al. (2016). Chlorogenic Acid Protects against Liver Fibrosis *In Vivo* and *In Vitro* through Inhibition of Oxidative Stress. *Clin. Nutr.* 35 (6), 1366–1373. doi:10.1016/j.clnu.2016.03.002

Faraji, H. (2019). The Effect of Coffee-Enriched Chlorogenic Acid on Insulin, GIP and GLP-1 Levels in Healthy Humans: A Systematic Review. *Prog. Nutr.* 21 (4), 744–751. doi:10.23751/pn.v21i4.6557

He, X., Zheng, S., Sheng, Y., Miao, T., Xu, J., Xu, W., et al. (2020). Chlorogenic Acid Ameliorates Obesity by Preventing Energy Balance Shift in High-fat Diet Induced Obese Mice. *J. Sci. Food Agric.* 101 (2), 631–637. doi:10.1002/jsfa.10675

Hnm, A., Qi, Z. A., Ryy, A., Wqt, A., Hxl, A., Smw, A., et al. (2021). Caffeic Acid Prevents Non-alcoholic Fatty Liver Disease Induced by a High-Fat Diet through Gut Microbiota Modulation in Mice. *Food Res. Int.* 143, 110240. doi:10.1016/j.foodres.2021.110240

Hu, F., Guo, Q., Wei, M., Huang, Z., Shi, L., Sheng, Y., et al. (2020). Chlorogenic Acid Alleviates Acetaminophen-Induced Liver Injury in Mice via Regulating Nrf2-Mediated HSP60-Initiated Liver Inflammation. *Eur. J. Pharmacol.* 883, 173286. doi:10.1016/j.ejphar.2020.173286

Hussain, M., Umair Ijaz, M., Ahmad, M. I., Khan, I. A., Bukhary, S. U. F., Khan, W., et al. (2020). Gut Inflammation Exacerbates Hepatic Injury in C57BL/6J Mice via Gut-Vascular Barrier Dysfunction with High-Fat-Incorporated Meat Protein Diets. *Food Funct.* 11 (10), 9168–9176. doi:10.1039/d0fo02153a

Illiano, P., Brambilla, R., and Parolini, C. (2020). The Mutual Interplay of Gut Microbiota, Diet and Human Disease. *FEBS J.* 287 (5), 833–855. doi:10.1111/febs.15217

Jiao, A., Yu, B., He, J., Yu, J., Zheng, P., Luo, Y., et al. (2020). Short Chain Fatty Acids Could Prevent Fat Deposition in Pigs via Regulating Related Hormones and Genes. *Food Funct.* 11 (2), 1845–1855. doi:10.1039/c9fo02585e

Karstoft, K., Mortensen, P. S., and Knudsen, H. S. (2015). The Direct Effect of Incretin Hormones on Glucose Metabolism. *FASEB j.* 27, 748. doi:10.1096/fasebj.27.1_supplement.lb748

Kim, H., Pan, J. H., Kim, S. H., Lee, J. H., and Park, J.-W. (2018). Chlorogenic Acid Ameliorates Alcohol-Induced Liver Injuries through Scavenging Reactive Oxygen Species. *Biochimie* 150, 131–138. doi:10.1016/j.biochi.2018.05.008

Kleiner, D. E., Brunt, E. M., Van Natta, M., Behling, C., Contos, M. J., Cummings, O. W., et al. (2005). Design and Validation of a Histological Scoring System for Nonalcoholic Fatty Liver Disease. *Hepatology* 41, 1313–1321. doi:10.1002/hep.20701

Li, T., Yan, H., Geng, Y., Shi, H., Li, H., Wang, S., et al. (2019). Target Genes Associated with Lipid and Glucose Metabolism in Non-alcoholic Fatty Liver Disease. *Lipids Health Dis.* 18 (1), 211. doi:10.1186/s12944-019-1154-9

Livak, K. J., and Schmittgen, T. D. (2002). Analysis of Relative Gene Expression Data Using Real-Time Quantitative PCR and the 2−ΔΔCT Method. *Methods* 25 (4), 402–408. doi:10.1006/meth.2001.1262

Lutz, T. A., and Osto, E. (2016). Glucagon-like Peptide-1, Glucagon-like Peptide-2, and Lipid Metabolism. *Curr. Opin. Lipidol.* 27 (3), 257–263. doi:10.1097/MOL.0000000000000293

Matthews, D. R., Hosker, J. P., Rudenski, A. S., Naylor, B. A., Treacher, D. F., and Turner, R. C. (1985). Homeostasis Model Assessment: Insulin Resistance and ?-cell Function from Fasting Plasma Glucose and Insulin Concentrations in Man. *Diabetologia* 28, 412–419. doi:10.1007/BF00280883

Mccarty, M. F. (2005). A Chlorogenic Acid-Induced Increase in GLP-1 Production May Mediate the Impact of Heavy Coffee Consumption on Diabetes Risk. *Med. Hypotheses* 64 (4), 848–853. doi:10.1016/j.mehy.2004.03.037

Mikolaevi, I., Kaniaj, T. F., and Targher, G. (2021). Nonalcoholic Fatty Liver Disease - a Growing Public Health Problem. *Croat. Med. J.* 62 (1), 1–3. doi:10.3325/cmj.2021.62.1

Shi, H., Dong, L., Jiang, J., Zhao, J., Zhao, G., Dang, X., et al. (2013). Chlorogenic Acid Reduces Liver Inflammation and Fibrosis through Inhibition of Toll-like Receptor 4 Signaling Pathway. *Toxicology* 303 (1), 107–114. doi:10.1016/j.tox.2012.10.025

Shi, A., Shi, H., Wang, Y., Liu, X., Cheng, Y., Li, H., et al. (2017). Activation of Nrf2 Pathway and Inhibition of NLRP3 Inflammasome Activation Contribute to the Protective Effect of Chlorogenic Acid on Acute Liver Injury. *Int. Immunopharmacology* 54, 125–130. doi:10.1016/j.intimp.2017.11.007

Song, J., Zhou, N., Ma, W., Gu, X., Chen, B., Zeng, Y., et al. (2019). Modulation of Gut Microbiota by Chlorogenic Acid Pretreatment on Rats with Adrenocorticotropic Hormone Induced Depression-like Behavior. *Food Funct.* 10, 2947–2957. doi:10.1039/C8FO02599A

Teshome, G., Ambachew, S., Fasil, A., and Abebe, M. (2020). Efficacy of Glucagon-like Peptide-1 Analogs in Nonalcoholic Fatty Liver Disease: A Systematic Review. *Hepat. Med.* 12, 139–151. doi:10.2147/HMER.S265631

Vitaglione, P., Mazzone, G., Lembo, V., D'Argenio, G., Rossi, A., Guido, M., et al. (2019). Coffee Prevents Fatty Liver Disease Induced by a High-Fat Diet by Modulating Pathways of the Gut-Liver axis. *J. Nutr. Sci.* 8, e15. doi:10.1017/jns.2019.10

Wijarnpreecha, K., Thongprayoon, C., and Ungprasert, P. (2017). Coffee Consumption and Risk of Nonalcoholic Fatty Liver Disease. *Eur. J. Gastroenterol. Hepatol.* 29 (2), e8–e12. doi:10.1097/MEG.0000000000000776

Xie, M. G. F. Y., Fei, Y. Q., Wang, Y., Wang, W. Y., and Wang, Z. (2021). Chlorogenic Acid Alleviates Colon Mucosal Damage Induced by a High-Fat Diet via Gut Microflora Adjustment to Increase Short-Chain Fatty Acid Accumulation in Rats. *Oxidative Med. Cell Longevity* 2021, 1–18. doi:10.1155/2021/3456542

Yan, Y., Zhou, X., Guo, K., Zhou, F., and Yang, H. (2020). Chlorogenic Acid Protects against Indomethacin-Induced Inflammation and Mucosa Damage by Decreasing Bacteroides-Derived LPS. *Front. Immunol.* 11, 1125. doi:10.3389/fimmu.2020.01125

Zamani-Garmsiri, F., Ghasempour, G., Aliabadi, M., Hashemnia, S. M. R., Emamgholipour, S., and Meshkani, R. (2020). Combination of Metformin and Chlorogenic Acid Attenuates Hepatic Steatosis and Inflammation in High-Fat Diet Fed Mice. *IUBMB Life* 73 (1), 252–263. doi:10.1002/iub.2424

Conflict of Interest: The authors declare that the research was conducted in the absence of any commercial or financial relationships that could be construed as a potential conflict of interest.

frontiers in Pharmacology

ORIGINAL RESEARCH
published: 05 July 2021
doi: 10.3389/fphar.2021.680081

Prediction of Srebp-1 as a Key Target of Qing Gan San Against MAFLD in Rats via RNA-Sequencing Profile Analysis

Bendong Yang[1], Jingyue Sun[2], Shufei Liang[1], Peixuan Wu[1], Rui Lv[1], Yanping He[1], Deqi Li[1], Wenlong Sun[1] and Xinhua Song[1]**

[1]School of Life Sciences, Shandong University of Technology, Zibo, China, [2]Key Laboratory of Novel Food Resources Processing, Ministry of Agriculture and Rural Affairs/Key Laboratory of Agro-Products Processing Technology of Shandong Province/Institute of Agro-Food Science and Technology, Shandong Academy of Agricultural Sciences, Jinan, China

Metabolism-associated fatty liver disease (MAFLD) is the most common chronic liver disease worldwide, and the use of traditional Chinese medicines (TCMs) to treat this disease has attracted increasing attention. The Qing Gan San (QGS) formula comprises *Polygonatum sibiricum,* the peel of *Citrus reticulata Blanco,* the leaves of *Morus alba L, Cichorium intybus, Glycyrrhiza uralensis Fisch,* and *Cirsium setosum.* The present study aimed to uncover the anti-hyperlipidaemic effects, hepatic fat accumulation-lowering effects and mechanisms of QGS in high-fat diet-induced MAFLD rats. QGS significantly reduced the levels of total cholesterol and triglycerides in both serum and liver tissue and partially protected hepatic function. Additionally, QGS significantly ameliorated hepatic lipid accumulation with histopathology observation, as demonstrated by H&E and oil red O staining. RNA sequencing was used to further investigate the key genes involved in the development and treatment of MAFLD. Hierarchical clustering analysis showed that the gene expression profiles in rats with MAFLD were reversed to normal after QGS treatment. QGS had 222 potential therapeutic targets associated with MAFLD. Enrichment analysis among these targets revealed that QGS affected biological functions/pathways such as the regulation of lipid metabolic processes (GO: 0019216) and the non-alcoholic fatty liver disease pathway (hsa04932), and identified Srebp-1 as a key regulator in the synthesis of cholesterol and triglycerides. Subsequently, both immunofluorescence and Western blot analyses demonstrated that QGS suppressed the transfer of Srebp-1 to the nucleus from the cytoplasm, suggesting that the activation of Srebp-1 was inhibited. Our study reveals the effects and mechanisms of QGS in the treatment of MAFLD and provides insights and prospects to further explore the pathogenesis of MAFLD and TCM therapies.

Keywords: traditional Chinese medicines, SREBP-1, Qing Gan San, RNA sequencing, metabolism-associated fatty liver disease

OPEN ACCESS

Edited by:
Silvia Di Giacomo,
Sapienza University of Rome, Italy

Reviewed by:
Doha Mohamed,
National Research Center, Egypt
Damjana Rozman,
University of Ljubljana, Slovenia

****Correspondence:***
Wenlong Sun
512649113@qq.com
Xinhua Song
892442572@qq.com

Specialty section:
This article was submitted to Gastrointestinal and Hepatic Pharmacology, a section of the journal Frontiers in Pharmacology

Received: *13 March 2021*
Accepted: *08 June 2021*
Published: *05 July 2021*

Citation:
Yang B, Sun J, Liang S, Wu P, Lv R, He Y, Li D, Sun W and Song X (2021) Prediction of Srebp-1 as a Key Target of Qing Gan San Against MAFLD in Rats via RNA-Sequencing Profile Analysis. Front. Pharmacol. 12:680081. doi: 10.3389/fphar.2021.680081

Abbreviations: ALT, plasma alanine aminotransferase; AST, aspartate aminotransferase; CVD, cardiovascular disease; DEGs, differentially expressed genes; GO, Gene Ontology; H&E, hematoxylin and eosin; HDL-C, high-density lipoprotein cholester; HFD, high-fat diet; KEGG, Kyoto Encyclopedia of Genes and Genomes; LDL-C, low-density lipoprotein cholesterol; MAFLD, metabolism-associated fatty liver disease; NC, normal control; NASH, non-alcoholic steatohepatitis; QGS, Qing Gan San; Srebp-1, sterol regulatory element-binding protein-1; T2DM, Type 2, diabetes mellitus; TC, total cholesterol; TCMs, traditional Chinese medicines; TG, triglycerides; TNF-α, tumor necrosis factor-α.

INTRODUCTION

Metabolism-associated fatty liver disease (MAFLD), characterized by hepatic lipid accumulation without excessive alcohol consumption, has become a common metabolic liver disease with a global prevalence of ~25% (Friedman et al., 2018). Recent studies have demonstrated that metabolic syndrome, which typically involves obesity, hyperglycaemia, dyslipidaemia, and hypertension, is a critical risk factor for the progression of MAFLD (Huang, 2009). Additionally, MAFLD is strongly associated with chronic diseases such as cardiovascular disease (CVD) and type 2 diabetes mellitus (T2DM) (Mikolasevic et al., 2016). Although knowledge concerning the pathogenesis of MAFLD has expanded rapidly in recent years, approved drugs by the Food and Drug Administration are lacking. Exercise and diet remain dominant options for treating MAFLD, and few people can maintain a regulated lifestyle for a long time (Friedman et al., 2018). Thus, more available therapeutic strategies are required to suit the various demands of MAFLD patients.

Traditional Chinese medicines (TCMs) are widely used to prevent and treat chronic diseases in China. The QGS formula is effective for MAFLD treatment through long-term clinical experience. The QGS formula comprises six herbs: *Polygonatum sibiricum*, the peel of *Citrus reticulata Blanco*, the leaves of *Morus alba L*, *Cichorium intybus*, *Glycyrrhiza uralensis Fisch*, and *Cirsium setosum*. These herbs have good effects against hepatic steatosis and related pathologies, but few studies have investigated the polysaccharide constituents of herbs that influence mechanisms against MAFLD (Yang et al., 2015; Guo et al., 2016; Peng et al., 2018; Wu et al., 2018; Wang et al., 2019; Gou et al., 2020). In our study, the efficacy of QGS polysaccharide in treating MAFLD was comprehensively estimated.

In recent decades, RNA sequencing techniques involving high-throughput screening and the identification of targets have greatly expanded the application of TCMs (Arendt et al., 2015). In a previous study, Huang-Qi San, a Chinese herbal formula, improved lipid accumulation and provided protective effects against hepatic steatosis in high-fat diet-fed rats via the analysis of RNA sequence data (Li et al., 2020). Additionally, the GeneCards database can enable a deep understanding of how TCMs influence important targets involved in the occurrence and progression of MAFLD (Fishilevich et al., 2017). Herein, RNA sequencing was used as an efficient strategy to identify target genes and metabolism.

The present study was designed to clarify the efficacy of QGS against MAFLD in rats. The compositions and structures of QGS were analyzed by ion chromatography and infrared radiation, respectively. Using a rat model of MAFLD induced by high-fat diet feeding, we investigated the effects of QGS in rats with MAFLD and clarified the potential underlying mechanisms via the combination with RNA sequencing and the GeneCards database.

MATERIALS AND METHODS

Preparation and Quality Control of QGS

For QGS preparation, *Polygonatum sibiricum*, the leaves of *Morus alba L, Cichorium intybus*, *Cirsium setosum,* the peel of *Citrus reticulata Blanco*, and *Glycyrrhiza uralensis Fisch* were purchased from Tongrentang Chinese Medicine Co., Ltd. (Beijing, China) and then ground in a grinder and mixed at a 15:10:10:10:6:6 ratio. The processing steps were performed as described in a previous study with minor modifications (Zhang et al., 2018). Briefly, the powder mixture was extracted with boiling distilled water three times (1:10, w/v), and then the supernatant was deoiled with ligroin (10:1, v/v) to remove small molecules. Subsequently, the solution was concentrated and precipitated with 75% ethanol. After being stored for 24 h, the mixture was centrifuged at 4°C at 4,500 rpm/min for 10 min, and the extract was dried with a vacuum freeze dryer for further analysis. The production was calculated to be 36.81%, and measurement of the main components (polysaccharides, polyphenols, proteins and galacturonic acid) was performed.

Quality control was also conducted by ion chromatography using a Dionex CarboPac^{TM} PA20 (3 × 150) column and an electrochemical detector. The mobile phases comprised 1) H_2O and 2) 250 mM NaOHC (50 mM NaOH and 500 mM NaOAc). The flow rate was 0.3 ml/min, and the column temperature was set to 30°C. Glucose, galactose, chlorinated galactosamine, rhamnose, arabinose, and xylose were prepared as standards to establish calibration curves to perform quantitative analysis. To prepare the QGS solution, 0.01 g of QGS was weighed and dissolved in a volume of 10 ml of trifluoroacetic acid for 3 h at 120°C. Subsequently, the aqueous acid solution was dried under nitrogen. The powder was redissolved in 5 ml of double-distilled water, and then 100 μL was pipetted into 900 μL of deionized water. The mixture was centrifuged at 12,000 rpm for 5 min, and the supernatant was used for ion chromatography analysis. Additionally, infrared radiation spectra were detected using a Fourier transform infrared apparatus, the wavenumbers of which are reported in cm^{-1}. The polysaccharide molecular weight was investigated using high-performance gel permeation chromatography.

Animal Experiment and Sample Collection

Male Sprague-Dawley rats (8 weeks old, weighing 180–220 g) were purchased from the Shandong Laboratory Animal Center (Jinan, China) with the permission number SCXK 2014-0007. All the animal procedures were performed in accordance with the Guidelines for the Care and Use of Laboratory Animals of Shandong University of Technology and were permitted by the Animal Ethics Committee of Shandong University of Technology. The rats were first housed at 25 ± 0.5°C under a 12 h light/dark cycle for adaptation for one week. Next, the rats were randomly divided into three groups (n = 6 per group): normal control (NC) group, high-fat diet (HFD) group, and QGS treatment (QGS) group. The high-fat diet comprised 20% protein, 35% carbohydrate, and 45% fat as a percent of total calories (**Supplementary Table S1**). The rats in the HFD and QGS groups were given a high-fat diet for 12 weeks continuously, while the NC group was fed a normal diet (Keaoxieli, Beijing, China). The rats in the QGS group received 100 mg/ml of QGS extract at 8:00 am for the last 8 weeks until sacrifice, while the rats in the NC and HFD groups received equal amounts of saline as a control.

During the last week, the body weight and food intake of the rats in each group were recorded. At the end of the experimental period, blood samples were collected and centrifuged at 3,000 rpm for 5 min at 4°C. The samples were then preserved at −80°C for further analysis. Liver samples were also collected, frozen with liquid nitrogen and stored at −80°C.

Measurement of Serum Biochemical Indexes

After fasting for 16 h, the TC and TG levels in both plasma and liver samples, as well as the low-density lipoprotein cholesterol (LDL-C) and high-density lipoprotein cholesterol (HDL-C) levels in plasma, were assayed immediately using commercial kits (Jiancheng, Nanjing, China). Additionally, the plasma alanine aminotransferase (ALT) and aspartate aminotransferase (AST) levels were also determined directly using commercial kits.

Histopathological Analysis

Hematoxylin and eosin (H&E) staining was performed to observe the degree of fat accumulation in the liver. The liver tissues were fixed with formalin, embedded in paraffin, cut into 3 μm-thick slices, stained with H&E and then observed using a light microscope at ×40.0 magnification. Additionally, liver cryosections were stained with oil red O and counterstained with hematoxylin to visualize the lipid droplets using an optical microscope at ×40.0 magnification.

RNA Sequencing Analysis

RNA sequencing was conducted using homogenized liver tissue (three replicates each for the NC, HFD, and QGS groups). Total RNA was extracted using TRIzol reagent (Qiagen, Germany) according to the manufacturer's instructions. RNA sequence library construction was performed using the Illumina TruSeq^{TM} RNA Sample Prep Kit method. The concentration, purity, and quality of the RNA were evaluated using the Agilent Bioanalyzer system (Agilent, United States) with the criteria of a 28S:16S ratio >1.5 and a 260/280 absorbance ratio between 1.8 and 2.1. Subsequently, the Illumina NovaSeq 6,000 platform (LC Science, United States) was employed for quantification and sequencing according to a standard sequencing protocol.

The sequencing data were quality controlled using fastx_toolkit_0.0.14 to generate clean data. The clean data were mapped to the rat reference genome (*Rattus_norvegicus*, version Rnor_6.0) using HISAT2 and then were assembled via StringTie software. Next, transcript quantification was performed using RSEM with the FPKM method to produce read counts. The read counts were determined to generate a gene expression profile with DESeq2, in which the default filter conditions were used (p-adjust < 0.05 and | log2 FC | ≥ 1).

Protein Isolation and Western Blot Analysis

As previously described (Sun et al., 2020), sterol regulatory element-binding protein-1 (Srebp-1) and Lamin B1 or β-actin protein in both the nucleus and cytoplasm were extracted with kits, and the protein samples were separated by 10% SDS–polyacrylamide gel electrophoresis. Next, the protein samples were transferred to a PVDF membrane (0.22 μm), which was blocked with 5% skim milk for 4 h at room temperature. Subsequently, the membrane was incubated with primary antibodies, including Srebp-1 (1:1,000), β-actin (1:2,000), and Lamin B1 (1:2,000), which were diluted in Tris-buffered saline with Tween-20 containing 5% skim milk at 4°C overnight. The immune complexes were recognized by a secondary antibody (1:2,000) conjugated to horseradish peroxidase (ProteinTech, Chicago, United States). Peroxidase activity was visualized using an enhanced chemiluminescence kit (Solarbio, Beijing, China). Densitometric analysis of the immunoblots was performed using ImageJ software.

Immunofluorescence Staining

Liver sections were fixed with 4% paraformaldehyde for 15 min at 37°C. Next, the sections were blocked with 2% BSA for 30 min. Subsequently, the sections were incubated with an anti-Srebp-1 antibody (1:100) overnight at 4°C. The sections were then washed and re-incubated with an FITC-labelled secondary antibody (1:100) (ProteinTech, Chicago, United States) for 1 h. Finally, immunofluorescence was observed using a fluorescence microscope after staining with DAPI for 5 min.

Statistical Analysis

Statistical analysis was conducted using GraphPad Prism 8, and the results were presented as means ± standard error of the mean. One-way ANOVA was used for multiple comparisons. Post-hoc testing was conducted using Dunnett's test method. Significant differences were accepted for $^{*}p < 0.05$, $^{**}p < 0.01$, and $^{***}p < 0.001$.

RESULTS

Determination and Analysis of QGS Extract Components

The determination of the main components of the QGS extract is essential to clarify the mechanisms. The QGS extract was collected, and the contents of polysaccharides, polyphenols, proteins and galacturonic acid were assessed. The ratio of QGS polysaccharides was up to 75.5%, and the ratio of galacturonic acid was 18.1% in QGS polysaccharides, while the polyphenols and proteins were only 6.5 and 12.1%, respectively (**Table 1**).

Additionally, the monosaccharide composition and polysaccharide linkage mode of QGS were investigated. The monosaccharide composition of QGS was detected using an ion spectrometer (Thermo Fisher, United States) (**Figure 1A**). The results suggested that the glucose: xylose: galactose: galactosamine hydrochloride: rhamnose: arabinose molar ratio was 0.896:0.028:0.024:0.018:0.014:0.014. Thus, glucose is recognized as the main monosaccharide in QGS polysaccharides. Additionally, high-performance gel permeation chromatography with a calibration curve of dextran standards (log MW = −0.2078x + 12.968; R^2 = 0.993) calculated that the average molecular weight was 5,735 kDa. Furthermore, Fourier transform infrared spectroscopy identified

TABLE 1 | Polysaccharide, polyphenol, protein, and glycuronic contents. The data are presented as means ± SEM.

Term	Content (mg/ml)	Sample concentration (mg/ml)	Ratio (%)
Polysaccharides	0.0755 ± 0.002	0.1	75.5
Polyphenols	0.0065 ± 0.001	0.1	6.5
Protein	0.0121 ± 0.001	0.1	12.1
Glucuronic acid	0.0137 ± 0.001	0.1	13.7

the bands at 868 cm^{-1} and 817.96 cm^{-1} as the β-glycosidic bond and α-glycosidic bond deformation modes, respectively.

QGS Ameliorates Dyslipidaemia in MAFLD Model Rats

The design and procedures of the animal experiment are shown in **Figure 2A**. Food intake was decreased in the HFD group compared with that in the NC group, while no difference was found after QGS treatment. Additionally, the body weight was significantly increased in the HFD group compared with that in the NC group, and it was slightly reduced by QGS intervention (**Figures 2B,C**). Because MAFLD is closely associated with dyslipidaemia, the plasma lipid levels in each group were measured. Compared with the NC group, the HFD group exhibited markedly higher plasma levels of both TC and TGs (**Figure 2D**). By contrast, the levels of TC and TGs were reduced significantly by QGS administration. Additionally, the LDL-C level showed trends toward growth in the HFD group that was reversed following QGS intervention. The levels of HDL-C were increased in the HFD group induced by a high-fat diet and continued to grow with QGS administration. These results suggest that QGS may attenuate dyslipidaemia induced by a high-fat diet.

QGS Regulates Excessive Lipid Accumulation in the Livers of MAFLD Rats

Excessive fat accumulation in the liver is a dominant sign of MAFLD. We investigated the levels of TC and TGs in the liver. QGS obviously attenuated the degrees of TC and TGs in the liver (**Figure 3A**). Additionally, H&E and oil red O staining were employed for histopathological observation. Histopathological change in the liver was observed between the HFD and NC groups (**Figures 3B,C**). More lipid droplets were observed in the HFD group than in the NC group. Daily oral administration of QGS for 8 weeks greatly ameliorated the abovementioned pathological abnormalities caused by high-fat diet feeding. Thus, we conclude that QGS could partially ameliorate hepatic lipid accumulation.

Hepatic Gene Expression Profiles Among the NC, HFD, and QGS Groups

Raw data were loaded into NCBI (BioProject ID: PRJNA726732), and a normalized gene expression matrix was produced and submitted for further analysis (**Supplementary Table S4**). Gene expression profile analysis was performed using hierarchical clustering. The gene expression profile trend of the QGS group was closer to that of the NC group than to that of the HFD group (**Figure 4A**). According to methods described in previous reports (Hong et al., 2019), 3031 differential genes were identified using RESM software (P-adjust $<$ 0.05 and $|\log FC| >$ 1) in three pairwise comparisons: NC vs. HFD, HFD vs. QGS, and NC vs. QGS. The results are shown with a Venn diagram (http://www.funrich.org/) in **Figure 4B**. Furthermore, when our RNA sequencing data intersected with target genes involved in MAFLD from the GeneCards database (1,051 genes, searched with the key word "MAFLD"; **Supplementary Table S2**), 222 differentially expressed genes (DEGs) were screened and identified as potential therapeutic targets for MAFLD at subsequent analysis (**Supplementary Table S3**).

GO Functional Enrichment and KEGG Pathway Analysis

The 222 DEGs were subjected to Gene Ontology (GO) functional enrichment and Kyoto Encyclopedia of Genes and Genomes (KEGG) pathway enrichment analyses (**Figure 5**). The terms regulation of lipid metabolic process (GO: 0019216), lipid localization (GO: 0010876), and response to nutrient levels (GO: 0031667) were significantly enriched in the biological process category. The terms endoplasmic reticulum lumen (GO: 0005788), secretory granule lumen (GO: 0034774), and cytoplasmic vesicle lumen (GO: 0060205) were enriched in the cellular component category. The terms signaling receptor activator activity (GO: 0030546), receptor ligand activity (GO: 0048018), and cytokine receptor binding (GO: 0005126) were enriched in the molecular function category. KEGG pathway enrichment analysis was also performed using these DEGs and revealed that the non-alcoholic fatty liver disease pathway (hsa04932) and the tumor necrosis factor (TNF) signaling pathway (hsa04668) terms were enriched for 24 genes and 23 genes, respectively (**Table 2**).

Screening of Srebp-1 as a Key Regulator of Lipogenesis

To determine the hub genes, we examined the intersection of genes participating in the MAFLD pathway and target genes. Eleven genes were upregulated in HFD and downregulated with QGS treatment or downregulated in HFD and upregulated with QGS treatment, and were collected as target genes (**Table 3**). Only Srebp-1 was upregulated by high-fat diet feeding, downregulated after QGS intervention

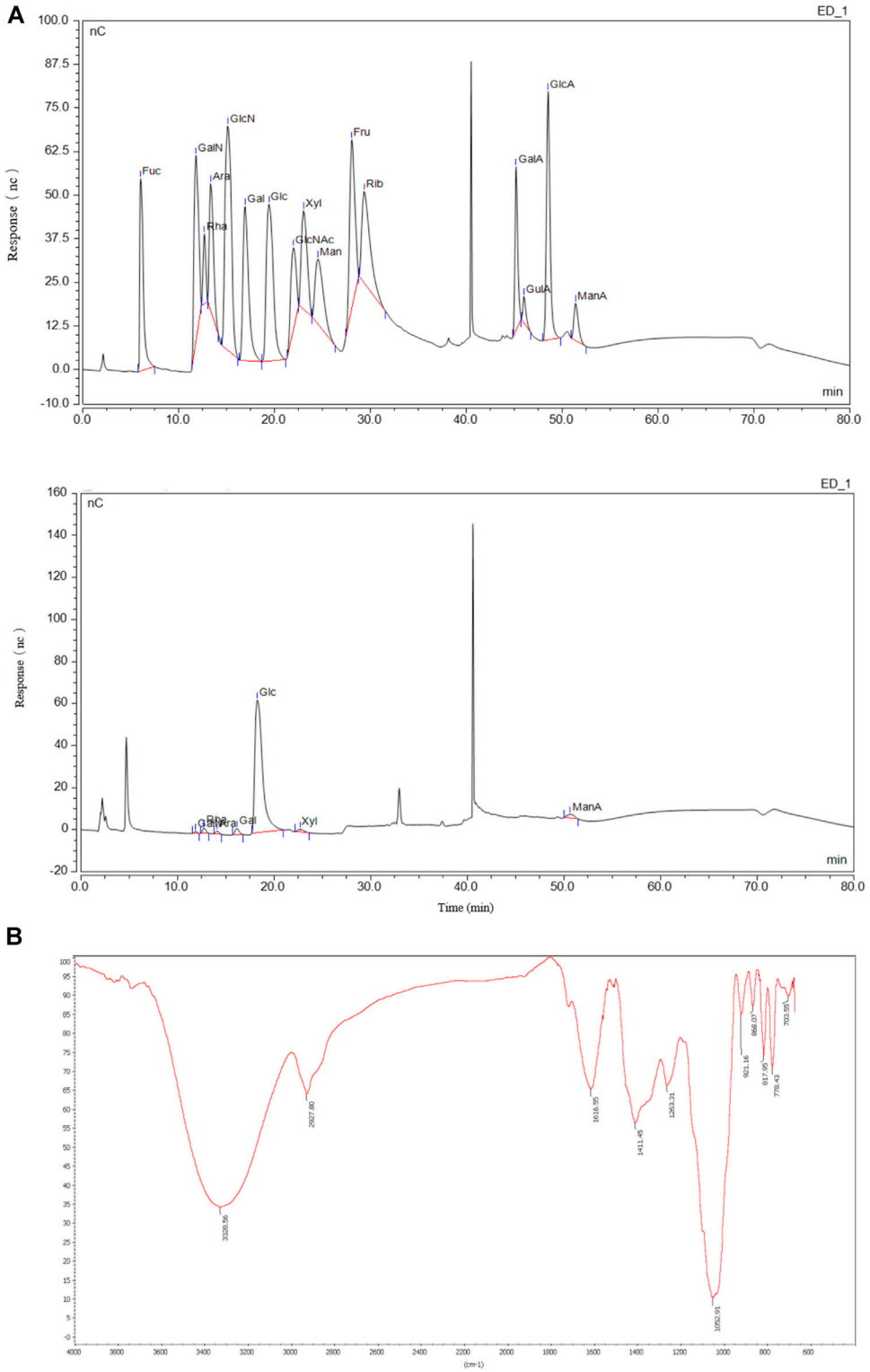

FIGURE 1 | Monosaccharide compositions and structure of QGS. **(A)** The monosaccharide standard (upper panel) and QGS sample (lower panel) were measured with HPIEC. **(B)** The structure of QGS was determined by fourier transform infrared spectroscopy.

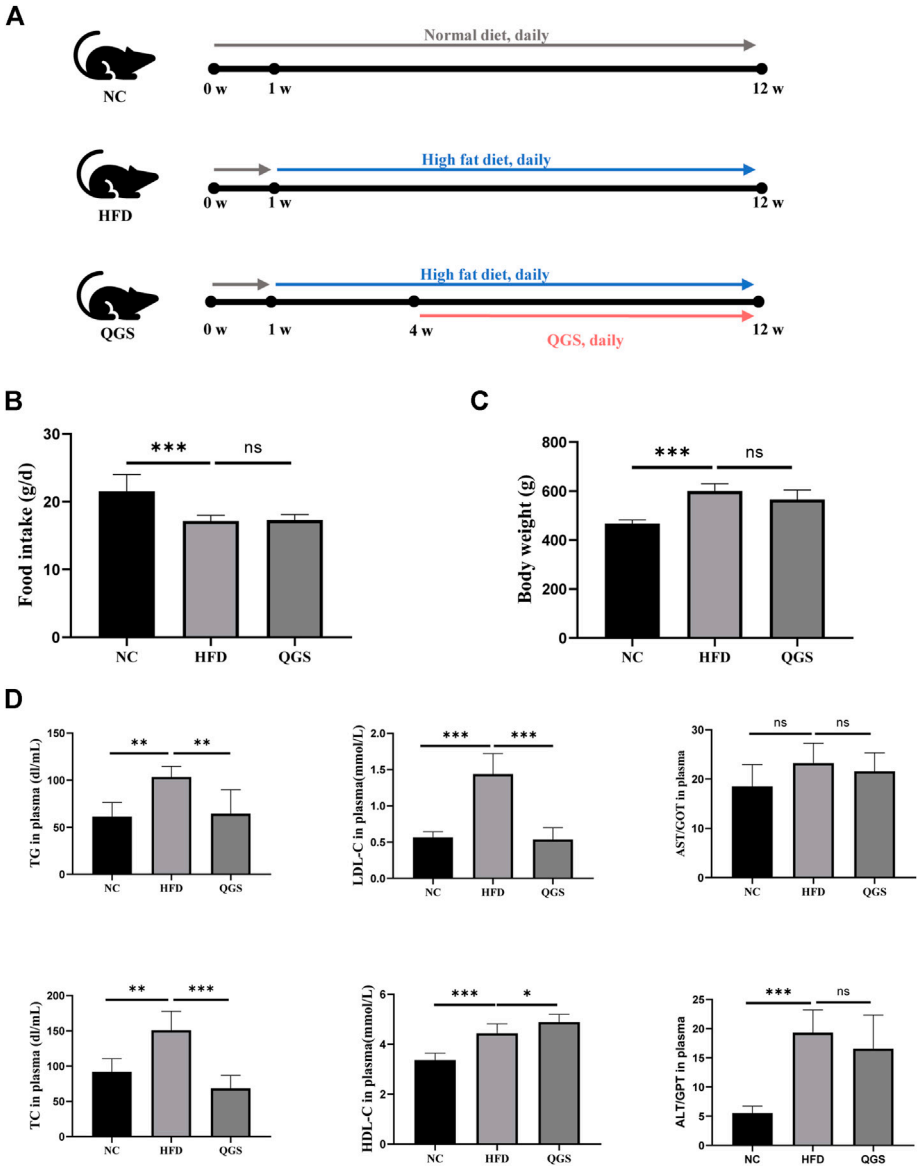

FIGURE 2 | Effects of QGS on MAFLD in rats. **(A)** Flow cytometry. **(B)** Food intake of rats at the 8th week. **(C)** Body weight of rats at the 8th week. **(D)** Measurements of TC, TG, LDL-C, HDL-C, AST, and ALT in plasma. The data are presented as means ± SEM; ns, no significant difference, $^{*}p < 0.05$, $^{**}p < 0.01$, $^{***}p < 0.001$, vs. the HFD group.

and involved in the MAFLD pathway (**Figure 6**). Therefore, Srebp-1 may be a key regulator associated with MAFLD treatment after QGS intervention.

Validation of the Western Blot and Immunofluorescence Analyses

The expression and localization of Srebp-1 were verified by Western blotting and immunofluorescence. A clear difference was observed between each group: the expression of Srebp-1 was higher in the HFD group than in the NC group, whereas the expression of Srebp-1 was decreased after QGS treatment (**Figures 7A,B**). A significantly greater proportion of Srebp-1 was recruited to the nucleus in the HFD group than in the NC group, but intervention with QGS reversed this trend. The expression of Srebp-1 in the nucleus was significantly increased in the HFD group (**Figures 7C,D**). QGS treatment significantly decreased the expression of Srebp-1 in the nucleus. Moreover, the expression of Srebp-1 in the cytoplasm was lower in the HFD group than in the NC and QGS groups. These results indicate that QGS treatment changes the expression of Srebp-1 in the nucleus and cytoplasm.

DISCUSSION

MAFLD, formerly known as NAFLD, which encompasses a spectrum of diseases, including simple steatosis, non-alcoholic

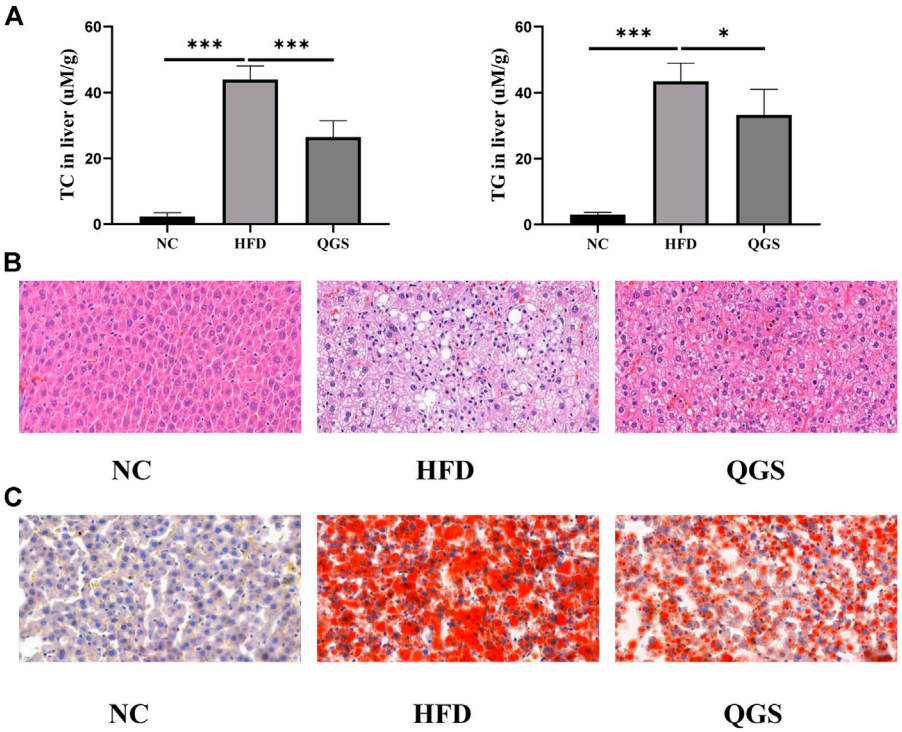

FIGURE 3 | Levels of lipid accumulation in the liver. **(A)** Levels of TC and TG in the liver. **(B)** Hematoxylin and eosin staining of liver tissue at ×40.0 magnification. **(C)** Oil red O staining of liver tissue at ×40.0 magnification. The data are presented as means ± SEM. ns, no significant difference. *$p < 0.05$, **$p < 0.01$, ***$p < 0.001$, vs. the HFD group.

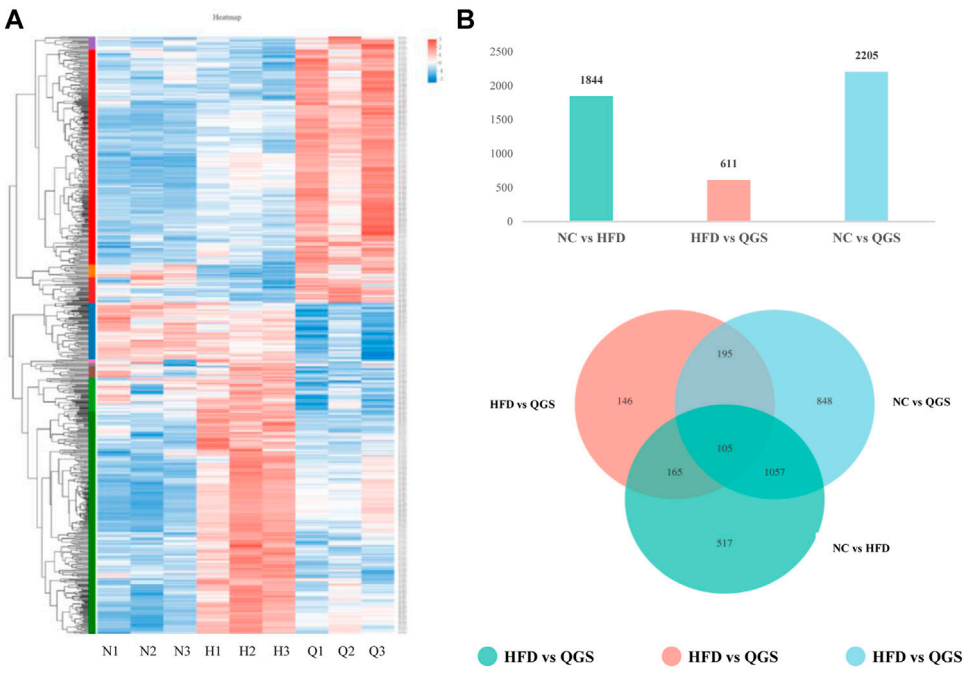

FIGURE 4 | Differential expression gene analysis. **(A)** Hierarchical clustering. Red represents high expression of genes, while blue represents low expression of genes. The left part is a dendrogram of gene clustering, and the lower part is the name of the sample (N, NC group; H, HFD group; Q, QGS group). **(B)** The upper panel presents numbers in three pairwise comparisons; the lower panel shows the Venn diagram showing the number of DEGs in the three pairwise comparisons.

TABLE 2 | The results of GO and KEGG enrichment analyses.

Term	ID	Count
Biology process		
Regulation of lipid metabolic process	GO: 0019216	44
Response to nutrient levels	GO: 0031667	44
Lipid localization	GO: 0010876	41
Molecular function		
signaling Receptor activator activity	GO: 0030546	31
receptor ligand activity	GO: 0048018	30
cytokine Receptor binding	GO: 0005126	22
Cellular component		
secretory granule lumen	GO: 0034774	25
cytoplasmic vesicle lumen	GO: 0060205	25
vesicle lumen	GO: 0031983	25
KEGG enrichment analysis		
Non-alcoholic fatty liver disease	hsa04932	24
TNF signaling pathway	hsa04668	23
Salmonella infection	hsa05132	22

steatohepatitis, cirrhosis, and hepatocellular carcinoma, has become a major hepatic metabolic disease worldwide (Tilg, 2017). MAFLD is closely associated with several diseases, including chronic kidney disease, T2DM, and CVD. The pathogenic causes of MAFLD are multifactorial, and known factors include genetics, the environment, and metabolic syndrome, which contribute to the occurrence and progression of MAFLD (Targher and Byrne, 2015; Valenti and Baselli, 2019). Because of the complicated pathogenesis of MAFLD, agents approved by the Food and Drug Administration for MAFLD are lacking (Friedman et al., 2018). Therefore, exploration of effective and safe novel strategies to treat MAFLD is valuable.

The beneficial effects of TCMs have long been proven to treat chronic metabolic diseases (Liu et al., 2015), such as Ganpi (modern name: MAFLD). The details of the mechanisms and bioactive components of most TCMs have not yet been elucidated. Similarly, the anti-hyperlipidaemic mechanisms of QGS, which has a long history of clinical use to treat this disease, have not been fully investigated. In our study, the extract of QGS was collected and identified to contain mainly polysaccharides, which comprised 75.5% of the total extract composition. Additionally, the ratio of galacturonic acid in the QGS polysaccharide was 18.1%, suggesting that it was an acidic polysaccharide. Additionally, proteins and polyphenols were determined to be present in smaller proportions. Thus, polysaccharides are the main bioactive ingredient. This finding is consistent with other reports that polysaccharides are the main contributors to the lipid-lowering effects of *Polygonatum sibiricum* (National Pharmacopoeia Committee, 2010) and *Morus alba L* (Wen et al., 2019). Furthermore, the monosaccharide composition was measured, and glucose exhibited a molar ratio of 0.896, indicating that it is the main monosaccharide in QGS. In the infrared spectra, peaks at 3,328 and 2,927 cm^{-1} were identified as absorption peaks of polysaccharides, and the modes of linkage among monosaccharides were identified as β-glycosidic bonds and α-glycosidic bonds. A previous study showed that α-/β-glycosidic bonds in polysaccharides are strongly associated with antioxidant activity (Chen and Huang, 2018). Excess oxidant stress is a crucial cause of hepatic damage and results in simple steatosis. Thus, the effect of QGS in the treatment of MAFLD may be attributed to its antioxidant properties (Ferramosca et al., 2017).

In our animal experiments, the high-fat diet provided more energy than the normal diet, and the consumption of food intake was lower in the HFD group than in the NC group and exhibited no difference between the HFD and QGS groups. Additionally, the level of body weight in the HFD group was increased significantly after feeding the high-fat diet but slightly decreased with QGS administration. Thus, QGS could mainly influence the metabolism of TC and TGs against the development of MAFLD. QGS polysaccharides lowered the levels of TC and TGs in both plasma and liver tissue and reduced the LDL-C levels in plasma. Additionally, QGS polysaccharides slightly ameliorated liver injury by decreasing the plasma AST and ALT levels in rats with MAFLD. Overall, these data indicate that QGS possesses beneficial effects in treating hepatic lipid accumulation and liver injury. The results of chemical indexes are enhanced by H&E and oil red O staining results of liver tissue.

To investigate the potential functional mechanism of QGS, obtaining target genes related to the progression and treatment of MAFLD was necessary. RNA sequencing, a new strategy to screen DEGs between sample groups, has been widely performed to identify potential genes involved in the development and treatment of MAFLD (Govaere et al., 2020). In our study, DEGs between the NC and HFD groups, the HFD and QGS groups, and the NC and QGS groups were identified using DESeq2 (Love et al., 2014). Subsequently, a clustering heatmap was created for the DEGs and indicated that QGS reversed the trends in gene expression induced by high-fat diet feeding, causing the expression profile in the QGS group to be similar to that in the NC group. The altered genes associated with different processes should be further analyzed to obtain more information concerning the development of MAFLD.

To determine which biological functions and metabolic pathways involved in MAFLD were affected by QGS treatment, GO and KEGG enrichment analyses were performed. the terms lipid metabolic process (GO: 0019216) and response to nutrient levels (GO: 0031667) were enriched in the biological process category. These processes are tightly involved in lipogenesis. Hepatic lipid metabolism is usually associated with the

TABLE 3 | Screening of target genes.

Treatment comparison	Gene count	Gene information
NC-HFD: Upregulated and HFD-QGS: Downregulated	9	SREBP1, CYBA, PLTP, YCP2, CTSS, CFD, CCL21, TMSB4X, SLC40A1
NC-HFD: Downregulated and HFD-QGS: Upregulated	2	HSPH1, SOCS2

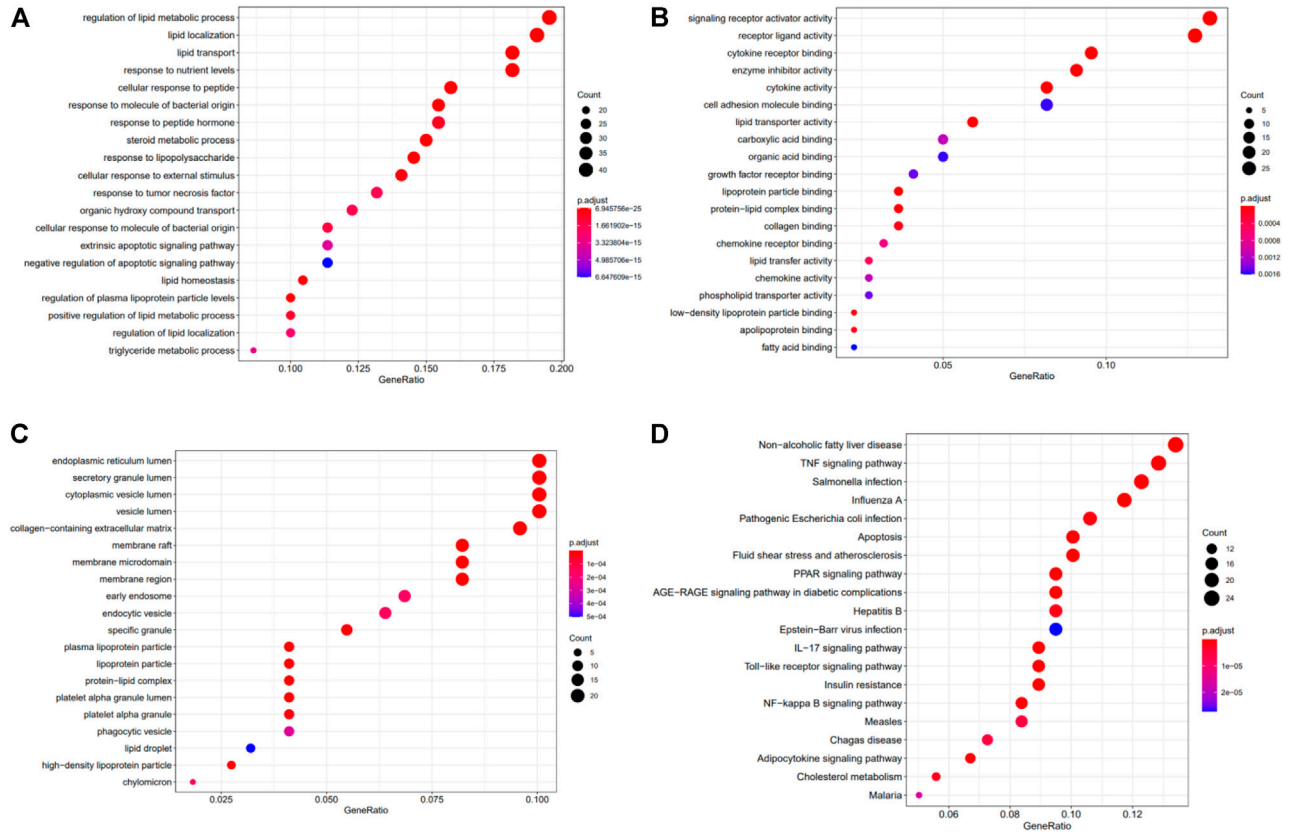

FIGURE 5 | The results of GO and KEGG analyses of the crosstalk genes. GO analysis of the 222 hub genes comprised three aspects: **(A)** biological process, **(B)** cellular components, and **(C)** molecular function. **(D)** KEGG pathway analysis of the 222 potential target genes.

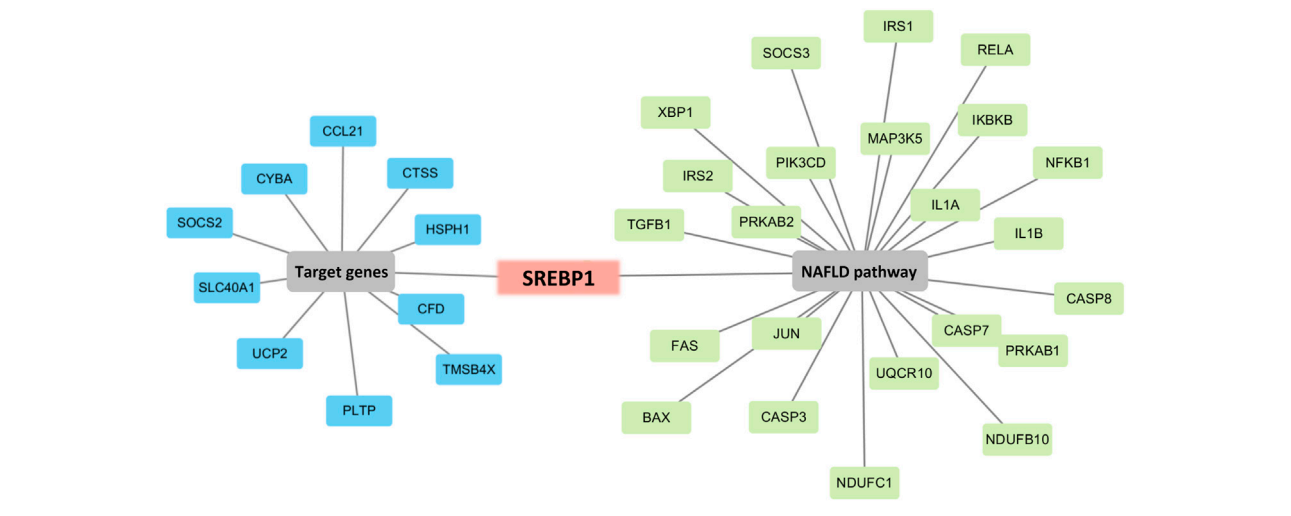

FIGURE 6 | Screening of the key regulated gene. Combining target genes with MAFLD pathway genes, only Srebp-1 was screened out. The blue box represents target genes, the green box represents genes participating in the MAFLD pathway, and the red box represents genes involved in both the target genes and the MAFLD pathway.

occurrence and treatment of MAFLD. Disruption of the balance of lipid metabolism in the liver can lead to lipid accumulation and consequently MAFLD (Pei et al., 2020). In our study, excess intake of a high-fat diet disrupted the balance of cholesterol and TG synthesis and led to dyslipidaemia. Additionally, the DEGs were mostly enriched in the non-alcoholic fatty liver disease pathway

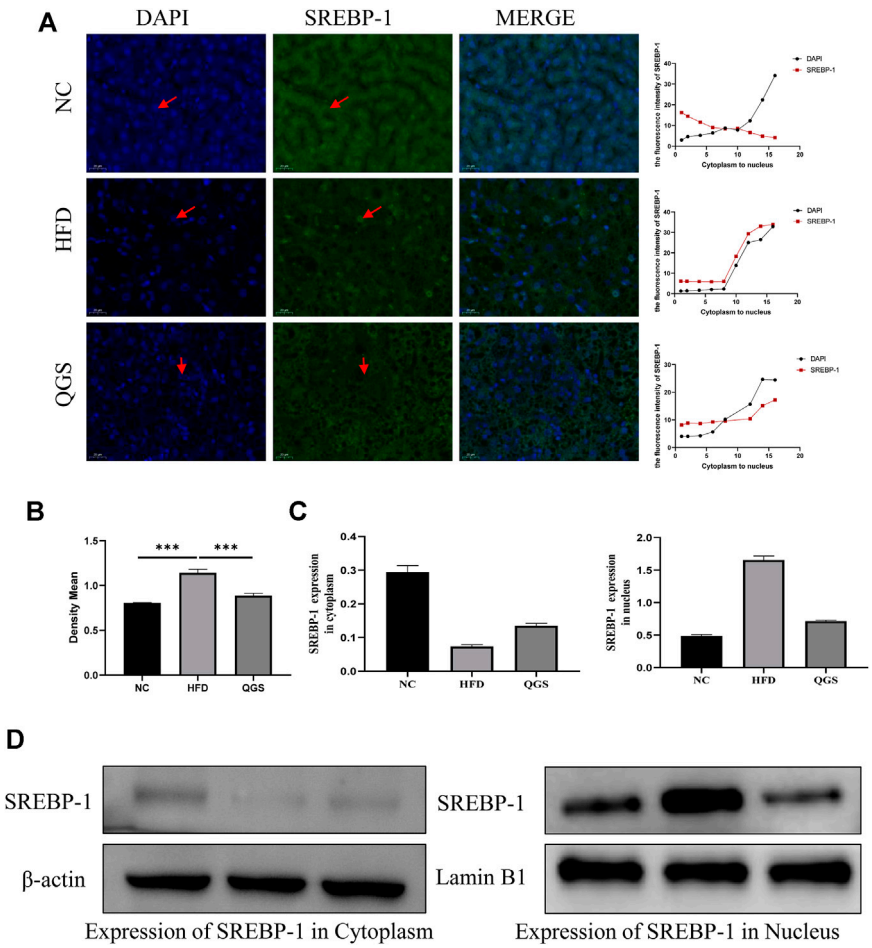

FIGURE 7 | Effects of QGS on the expression of Srebp-1 in the cytoplasm and nucleus. **(A)** Immunofluorescence staining for Srebp-1 in liver tissue (original magnification, ×200). The line chart presents the trend of expression from the cytoplasm to the nucleus. **(B)** The relative protein expression in immunohistochemistry was quantified using ImageJ software. The results are represented as the density mean (density mean = integrated density/area). **(C,D)** The expression levels of Srebp-1 in the cytoplasm and nucleus were detected by Western blotting. β-actin and Lamin B1 were used as loading controls.

(hsa04932), which is a crucial signaling pathway for the regulation of MAFLD. In our study, 24 genes regulated by QGS were mapped to the non-alcoholic fatty liver disease pathway. Only the expression of Srebp-1 was downregulated by QGS treatment after high-fat diet-mediated model construction. Srebp-1, a transcription factor, affects the activity and expression of fatty acid synthase (Wang et al., 2020). Additionally, the TNF signaling pathway (hsa04668) was also enriched and affected inflammation in MAFLD. Recent studies suggest that anti-inflammatory agents may be useful for MAFLD treatment (Wang et al., 2021). Thus, QGS may intervene in TNF-α to drive the progression of MAFLD to NASH, and verification for this purpose will be performed in future studies.

Srebps have two isoforms: Srebp-1 and Srebp-2. Srebp-1 preferentially activates the transcription of genes required for fatty acid and triglyceride synthesis. By contrast, Srebp-2 regulates the transcription of genes related to cholesterol synthesis and uptake (DeBose-Boyd and Jin, 2018). Lipid droplets, formed with triglycerides that are digested in the form of fatty acids in the liver, store neutral lipids during times of energy excess, whose prolonged storage leads to MAFLD (Nina L. Gluchowski et al., 2017; Sahini and Borlak, 2014). Srebp-1 acts as a crucial regulator of lipogenesis progression by affecting fatty synthesis genes and adjusting the levels of TGs in the plasma and liver. Thus, in our study, we investigated the activation of Srebp-1 in the liver of MAFLD rats with or without QGS intervention. A high-fat diet was used to promote the expression and activation of Srebp-1 and then the consequent transfer of Srebp-1 to the nucleus from the cytoplasm (Hao et al., 2010; Moon, 2017). When Srebp-1 enters the nucleus, it combines with the promoter region of fatty acid synthesis and related genes associated with lipogenesis, leading to the synthesis of TGs and formation of lipid droplets in the liver (Porstmann et al., 2005). Many studies have proven that inhibition of the expression and activation of Srebp-1 is an efficient method for MAFLD amelioration (Ziamajidi et al., 2013). In our study, immunofluorescence and Western blotting demonstrated that less Srebp-1 was recruited to the nucleus in the QGS group than in the HFD group, indicating that activation of Srebp-1 was

inhibited and that the expression of related genes such as fatty-acid synthase and acetyl-coenzyme A carboxylase was suppressed (DeBose-Boyd and Jin, 2018). Thus, QGS contributed to the inhibition of lipogenesis and amelioration of lipid accumulation in the liver. Although Srebp-1 was predicted as an important target gene in MAFLD rats with QGS intervention, limitations persist because of the measurement method, and further biological verification is required. The lipid accumulation-lowering and anti-inflammatory effects may be associated with the expression and activation of Srebp-1. However, the mechanism by which the QGS formula treats MAFLD rats has not been fully explained. Thus, we will examine the biological function of QGS from various perspectives in future studies.

Furthermore, our results were supported by several previous studies. Multiple studies have also demonstrated that polysaccharides from *Polygonatum sibiricum and Morus alba L* exhibit hypolipidaemic activity by inhibiting the progression of cholesterol and TG synthesis (C-G Liu et al., 2017; Yang et al., 2015). Likewise, *Cichorium intybus* polysaccharides inhibit lipogenesis by modulating AMPK (Wu et al., 2018). Some studies have also supported that the expression of Srebp-1 and fatty acid synthase is significantly decreased following treatment with the ethanol extract of *Polygonatum sibiricum* (Ko et al., 2015) and *Cichorium intybus* polysaccharide (Ziamajidi et al., 2013). Notably, ethanol extracts of *Citrus reticulata Blanco* can ameliorate lipid accumulation in the liver (Ke et al., 2020). These findings are consistent with our experimental results, suggesting that QGS polysaccharide ameliorates high-fat diet-induced disorders of lipid metabolic processes in rats. Furthermore, previous studies have shown that *Glycyrrhiza uralensis Fisch* extract mitigates TNF-α overproduction in rats with MAFLD (Jung et al., 2016; Gou et al., 2020). *Cirsium setosum* extract exerts obvious anti-inflammatory effects, and this herb is also often utilized to prevent cardiovascular disease (Wang et al., 2019). Thus, QGS may protect against inflammation resulting from lipid accumulation, a finding that must be comprehensively investigated in further studies.

Recent studies have demonstrated that CVD is the major cause of death in MAFLD patients (Athyros et al., 2017). For MAFLD/NASH patients with a high CVD risk, statins, as first-line drugs for lowering the lipid content, have been widely utilized. However, treatment resistance and intolerance are the main limitations of statin use with long-term administration (Doumas et al., 2019). Importantly, statins have no effects on hepatic fat accumulation. Herein, the QGS formula comprising six herbs obviously mitigated excess lipid accumulation in the liver. In a subsequent study, the combination of QGS and statins probably became an adjunct therapeutic strategy for MAFLD patients with CVD risk and expanded the application of QGS in clinical practice.

The presence of MAFLD in T2DM patients is strongly correlated with more severe dyslipidaemia and insulin resistance in hepatic and adipose tissue than in T2DM patients without MAFLD (Tilg et al., 2017). An explanation for the association between liver lipid accumulation and insulin resistance is that liver fat accumulation is directly generated from excess lipid availability and leads to insulin resistance (Roden, 2006). However, first-line blood glucose-lowering drugs, such as metformin, obviously decrease both hepatic and peripheral insulin resistance but have no effects on reducing liver fat accumulation (Tilg et al., 2017). The QGS formula significantly ameliorates liver fat accumulation by inhibiting the expression and activation of Srebp-1 and might alleviate insulin resistance by reducing fat accumulation. The QGS formula, as a supplemental therapeutic strategy to blood glucose-lowering drugs such as metformin, may be a novel lipid-reducing therapeutic strategy to treat T2DM patients with MAFLD.

CONCLUSION

Our data suggest that QGS effectively lowers lipids in both serum and liver and partly protects liver function in MAFLD rats. The lipid-lowering effects are mediated by decreased TC and TG production by regulating the expression and activation of Srebp-1.

DATA AVAILABILITY STATEMENT

The data presented in the study are deposited in the NCBI repository, accession number (PRJNA726732).

ETHICS STATEMENT

The animal study was reviewed and approved by the Animal Ethics Committee of Shandong University of Technology.

AUTHOR CONTRIBUTIONS

Experimental design: WS, XS, and BY; Network pharmacology assay: BY and WS and; Animal experiment: SL, YH, and LR; Polysaccharide analysis: PW, DL, and JS; Pathway analysis: WS and BY; Manuscript Writing: WS and BY. All data were generated in-house, and no paper mill was used. All authors agree to be accountable for all aspects of work and for ensuring the integrity and accuracy of the data.

FUNDING

The Major Scientific and Technological Innovation Project of Shandong, China (NO. 2019JZZY020612), Zibo School-City Integrated Development Project (2018ZDXC10), National Natural Science Foundation of China (81903878), Natural Science Foundation of Shandong Province (ZR2019BH049).

SUPPLEMENTARY MATERIAL

The Supplementary Material for this article can be found online at: https://www.frontiersin.org/articles/10.3389/fphar.2021.680081/full#supplementary-material

REFERENCES

Arendt, B. M., Comelli, E. M., Ma, D. W. L., Lou, W., Teterina, A., Kim, T., et al. (2015). Altered Hepatic Gene Expression in Nonalcoholic Fatty Liver Disease Is Associated with Lower Hepatic N-3 and N-6 Polyunsaturated Fatty Acids. *Hepatology*. 61, 1565–1578. doi:10.1002/hep.27695

Athyros, V. G., Alexandrides, T. K., Bilianou, H., Cholongitas, E., Doumas, M., Ganotakis, E. S., et al. (2017). The Use of Statins Alone, or in Combination with Pioglitazone and Other Drugs, for the Treatment of Non-alcoholic Fatty Liver Disease/non-Alcoholic Steatohepatitis and Related Cardiovascular Risk. An Expert Panel Statement. *Metabolism*. 71, 17–32. doi:10.1016/j.metabol.2017.02.014

Chen, L., and Huang, G. (2018). Extraction, Characterization and Antioxidant Activities of Pumpkin Polysaccharide. *Int. J. Biol. macromolecules*. 118, 770–774. doi:10.1016/j.ijbiomac.2018.06.148

DeBose-Boyd, R. A., and Ye, J. (2018). SREBPs in Lipid Metabolism, Insulin Signaling, and beyond. *Trends Biochemical Sciences*. 43, 358–368. doi:10.1016/j.tibs.2018.01.005

Doumas, M., Imprialos, K., Dimakopoulou, A., Stavropoulos, K., Binas, A., Athyros, V. G., et al. (2019). The Role of Statins in the Management of Nonalcoholic Fatty Liver Disease. *Curr Pharm Des.* 24, 4587–4592. doi:10.2174/1381612825666190117114305

Ferramosca, A., Di Giacomo, M., and Zara, V. (2017). Antioxidant Dietary Approach in Treatment of Fatty Liver: New Insights and Updates. *World J Gastroenterol*. 23, 4146–4157. doi:10.3748/wjg.v23.i23.4146

Fishilevich, S., Nudel, R., Rappaport, N., Hadar, R., Plaschkes, I., Iny Stein, T., et al. (2017). GeneHancer: Genome-wide Integration of Enhancers and Target Genes in GeneCards. *Database (Oxford).* 2017, bax028. doi:10.1093/database/bax028

Friedman, S. L., Neuschwander-Tetri, B. A., Rinella, M., and Sanyal, A. J. (2018). Mechanisms of NAFLD Development and Therapeutic Strategies. *Nat. Med.* 24, 908–922. doi:10.1038/s41591-018-0104-9

Gluchowski, N. L., Becuwe, M., Walther, T. C., and Farese, R. V. (2017). Lipid Droplets and Liver Disease: from Basic Biology to Clinical Implications. *Nat. Rev. Gastroenterol. Hepatol.* 14, 343–355. doi:10.1038/nrgastro.2017.32

Gou, S. H., He, M., Li, B. B., Zhu, N. Y., and Ni, J. M. (2020). Hepatoprotective Effect of Total Flavonoids from Glycyrrhiza Uralensis Fisch in Liver Injury Mice. *Nat. Prod. Res.* 34, 1–5. doi:10.1080/14786419.2020.1824223

Govaere, O., Cockell, S., Tiniakos, D., Queen, R., Younes, R., Vacca, M., et al. (2020). Transcriptomic Profiling across the Nonalcoholic Fatty Liver Disease Spectrum Reveals Gene Signatures for Steatohepatitis and Fibrosis. *Sci. Transl. Med.* 12, eaba4448. doi:10.1126/scitranslmed.aba4448

Guo, J., Tao, H., Cao, Y., Ho, C.-T., Jin, S., and Huang, Q. (2016). Prevention of Obesity and Type 2 Diabetes with Aged Citrus Peel (Chenpi) Extract. *J. Agric. Food Chem.* 64, 2053–2061. doi:10.1021/acs.jafc.5b06157

Hao, J., Liu, S. X., Wei, J. Y., Yao, H. Y., and Duan, H. J. (2010). [High Fat Diet Induced the Expression of SREBP-1, TGF-Beta1 and Alpha-SMA in Renal Tubular Cells and Extracellular Matrix Accumulation in Wistar Rats]. *Zhongguo Ying Yong Sheng Li Xue Za Zhi* 26, 307–311.

Hong, W., Li, S., Wu, L., He, B., Jiang, J., and Chen, Z. (2019). Prediction of VEGF-C as a Key Target of Pure Total Flavonoids from Citrus against NAFLD in Mice via Network Pharmacology. *Front. Pharmacol.* 10, 582. doi:10.3389/fphar.2019.00582

Huang, P. L. (2009). A Comprehensive Definition for Metabolic Syndrome. *Dis. models Mech.* 2, 231–237. doi:10.1242/dmm.001180

Jung, J. C., Lee, Y. H., Kim, S. H., Kim, K. J., Kim, K. M., Oh, S., et al. (2016). Hepatoprotective Effect of Licorice, the Root of Glycyrrhiza Uralensis Fischer, in Alcohol-Induced Fatty Liver Disease. *BMC Complement. Altern. Med.* 16, 19. doi:10.1186/s12906-016-0997-0

Ke, Z., Zhao, Y., Tan, S., Chen, H., Li, Y., Zhou, Z., et al. (2020). Citrus Reticulata Blanco Peel Extract Ameliorates Hepatic Steatosis, Oxidative Stress and Inflammation in HF and MCD Diet-Induced NASH C57BL/6 J Mice. *J. Nutr. Biochem.* 83, 108426. doi:10.1016/j.jnutbio.2020.108426

Ko, J. H., Kwon, H. S., Yoon, J. M., Yoo, J. S., Jang, H. S., Kim, J. Y., et al. (2015). Effects ofPolygonatum Sibiricumrhizome Ethanol Extract in High-Fat Diet-Fed Mice. *Pharm. Biol.* 53, 563–570. doi:10.3109/13880209.2014.932393

Li, Y., Wang, C., Jin, Y., Chen, H., Cao, M., Li, W., et al. (2020). Huang-Qi San Improves Glucose and Lipid Metabolism and Exerts Protective Effects against Hepatic Steatosis in High Fat Diet-Fed Rats. *Biomed. Pharmacother.* 126, 109734. doi:10.1016/j.biopha.2019.109734

Liu, C. G., Ma, Y. P., and Zhang, X. J. (2017). Effects of mulberry Leaf Polysaccharide on Oxidative Stress in Pancreatic β-cells of Type 2 Diabetic Rats. *Eur. Rev. Med. Pharmacol. Sci.* 21, 2482–2488.

Liu, S. H., Chuang, W. C., Lam, W., Jiang, Z., and Cheng, Y. C. (2015). Safety Surveillance of Traditional Chinese Medicine: Current and Future. *Drug Saf.* 38, 117–128. doi:10.1007/s40264-014-0250-z

Love, M. I., Huber, W., and Anders., S. (2014). Moderated Estimation of Fold Change and Dispersion for RNA-Seq Data with DESeq2. *Genome Biol.* 15, 550. doi:10.1186/s13059-014-0550-8

Mikolasevic, I., Milic, S., Racki, S., Zaputovic, L., Stimac, D., Radic, M., et al. (2016). Nonalcoholic Fatty Liver Disease (NAFLD)-A New Cardiovascular Risk Factor in Peritoneal Dialysis Patients. *Perit Dial. Int.* 36, 427–432. doi:10.3747/pdi.2014.00223

Moon, Y. A. (2017). The SCAP/SREBP Pathway: A Mediator of Hepatic Steatosis. *Endocrinol. Metab.* 32, 6–10. doi:10.3803/EnM.2017.32.1.6

National Pharmacopoeia Committee (2010). *Chinese Pharmacopoeia*. Beijing: China Medical Science Press

Pei, K., Gui, T., Kan, D., Feng, H., Jin, Y., Yang, Y., et al. (2020). An Overview of Lipid Metabolism and Nonalcoholic Fatty Liver Disease. *Biomed. Research International.* 2020, 1–12. doi:10.1155/2020/4020249

Peng, C. H., Lin, H. T., Chung, D. J., Huang, C. N., and Wang, C. J. (2018). Mulberry Leaf Extracts Prevent Obesity-Induced NAFLD with Regulating Adipocytokines, Inflammation and Oxidative Stress. *J. Food Drug Anal.* 26, 778–787. doi:10.1016/j.jfda.2017.10.008

Porstmann, T., Griffiths, B., Chung, Y.-L., Delpuech, O., Griffiths, J. R., Downward, J., et al. (2005). PKB/Akt Induces Transcription of Enzymes Involved in Cholesterol and Fatty Acid Biosynthesis via Activation of SREBP. *Oncogene*. 24, 6465–6481. doi:10.1038/sj.onc.1208802

Roden, M. (2006). Mechanisms of Disease: Hepatic Steatosis in Type 2 Diabetes-Pathogenesis and Clinical Relevance. *Nat. Rev. Endocrinol.* 2, 335–348. doi:10.1038/ncpendmet0190

Sahini, N., and Borlak, J. (2014). Recent Insights into the Molecular Pathophysiology of Lipid Droplet Formation in Hepatocytes. *Prog. Lipid Res.* 54, 86–112. doi:10.1016/j.plipres.2014.02.002

Sun, W., Liu, P., Wang, T., Wang, X., Zheng, W., and Li, J. (2020). Baicalein Reduces Hepatic Fat Accumulation by Activating AMPK in Oleic Acid-Induced HepG2 Cells and High-Fat Diet-Induced Non-insulin-resistant Mice. *Food Funct.* 11, 711–721. doi:10.1039/c9fo02237f

Targher, G., and Byrne, C. D. (2015). A Perspective on Metabolic Syndrome and Nonalcoholic Fatty Liver Disease. *Metab. Syndr. Relat. Disord.* 13, 235–238. doi:10.1089/met.2015.1502

Tilg, H. (2017). How to Approach a Patient with Nonalcoholic Fatty Liver Disease. *Gastroenterology*. 153, 345–349. doi:10.1053/j.gastro.2017.06.016

Tilg, H., Moschen, A. R., and Roden, M. (2017). NAFLD and Diabetes Mellitus. *Nat. Rev. Gastroenterol. Hepatol.* 14, 32–42. doi:10.1038/nrgastro.2016.147

Valenti, L. V. C., and Baselli, G. A. (2019). Genetics of Nonalcoholic Fatty Liver Disease: A 2018 Update. *Curr Pharm Des.* 24, 4566–4573. doi:10.2174/1381612825666190119113836

Wang, H. C., Bao, Y. R., Wang, S., Li, T. J., Meng, X. S., and Meng, X. S. (2019). Simultaneous Determination of Eight Bioactive Components of Cirsium Setosum Flavonoids in Rat Plasma Using Triple Quadrupole LC/MS and its Application to a Pharmacokinetic Study. *Biomed. Chromatogr.* 33, e4632. doi:10.1002/bmc.4632

Wang, H., Humbatova, A., Liu, Y., Qin, W., Lee, M., Cesarato, N., et al. (2020). Anne-Marie Calza, Armand Bottani, Janine Altmüller, Andreas Buness, Shuxia Yang, Xiujuan Sun, Lin Ma, Kerstin Kutsche, Karl-Heinz Grzeschik, Regina C. Betz, and Zhimiao Lin. (Mutations in SREBF1, Encoding Sterol Regulatory Element Binding Transcription Factor 1, Cause Autosomal-Dominant IFAP Syndrome. *Am. J. Hum. Genet.* 107, 34–45. doi:10.1016/j.ajhg.2020.05.006

Wang, H., Mehal, W., Nagy, L. E., and Rotman, Y. (2021). Immunological Mechanisms and Therapeutic Targets of Fatty Liver Diseases. *Cell Mol Immunol.* 18, 73–91. doi:10.1038/s41423-020-00579-3

Wen, P., Hu, T. G., Linhardt, R. J., Liao, S. T., Wu, H., and Zou, Y. X. (2019). Mulberry: A Review of Bioactive Compounds and Advanced Processing Technology. *Trends Food Sci. Technology*. 83, 138–158. doi:10.1016/j.tifs.2018.11.017

Wu, Y., Zhou, F., Jiang, H., Wang, Z., Hua, C., and Zhang, Y. (2018). Chicory (Cichorium Intybus L.) Polysaccharides Attenuate High-Fat Diet Induced Non-alcoholic Fatty Liver Disease via AMPK Activation. *Int. J. Biol. macromolecules*. 118, 886–895. doi:10.1016/j.ijbiomac.2018.06.140

Yang, J. X., Wu, S., Huang, X. L., Hu, X. Q., and Zhang, Y. (2015). Hypolipidemic Activity and Antiatherosclerotic Effect of Polysaccharide ofPolygonatum Sibiricumin Rabbit Model and Related Cellular Mechanisms. *Evid Based. Complement. Altern. Med.* 2015, 1–6. doi:10.1155/2015/391065

Zhang, F., Ran, C., Zheng, J., Ding, Y., and Chen, G. (2018). Polysaccharides Obtained from Bamboo Shoots (Chimonobambusa Quadrangularis) Processing By-Products: New Insight into Ethanol Precipitation and Characterization. *Int. J. Biol. macromolecules*. 112, 951–960. doi:10.1016/j.ijbiomac.2018.01.197

Ziamajidi, N., Khaghani, S., Hassanzadeh, G., Vardasbi, S., Ahmadian, S., Nowrouzi, A., et al. (2013). Amelioration by Chicory Seed Extract of Diabetes- and Oleic Acid-Induced Non-alcoholic Fatty Liver Disease (NAFLD)/non-alcoholic Steatohepatitis (NASH) via Modulation of PPARα and SREBP-1. *Food Chem. Toxicol.* 58, 198–209. doi:10.1016/j.fct.2013.04.018

Conflict of Interest: The authors declare that the research was conducted in the absence of any commercial or financial relationships that could be construed as a potential conflict of interest.

frontiers in Pharmacology

ORIGINAL RESEARCH
published: 27 July 2021
doi: 10.3389/fphar.2021.713197

Comprehensive Analysis of Fecal Microbiome and Metabolomics in Hepatic Fibrosis Rats Reveal Hepatoprotective Effects of Yinchen Wuling Powder From the Host-Microbial Metabolic Axis

Yumeng Zhang[1†], Min Zhao[1†], Xue Jiang[1], Qiaoyu Qiao[1], Tingting Liu[1], Chunjie Zhao[1] and Miao Wang[2]**

[1]School of Pharmacy, Shenyang Pharmaceutical University, Shenyang, China, [2]School of Life Science and Biopharmaceutics, Shenyang Pharmaceutical University, Shenyang, China

OPEN ACCESS

Edited by:
Oscar Briz,
University of Salamanca, Spain

Reviewed by:
Xuan Chen,
Fujian Agriculture and Forestry University, China
Wuwen Feng,
Chengdu University of Traditional Chinese Medicine, China

***Correspondence:**
Chunjie Zhao
lab433@163.com
Miao Wang
wangmiao_77111@hotmail.com

†These authors have contributed equally to this work

Specialty section:
This article was submitted to Gastrointestinal and Hepatic Pharmacology, a section of the journal Frontiers in Pharmacology

Received: 22 May 2021
Accepted: 19 July 2021
Published: 27 July 2021

Citation:
Zhang Y, Zhao M, Jiang X, Qiao Q, Liu T, Zhao C and Wang M (2021) Comprehensive Analysis of Fecal Microbiome and Metabolomics in Hepatic Fibrosis Rats Reveal Hepatoprotective Effects of Yinchen Wuling Powder From the Host-Microbial Metabolic Axis. Front. Pharmacol. 12:713197. doi: 10.3389/fphar.2021.713197

Hepatic fibrosis (HF) is a typical consequence in the development of multiple chronic liver diseases, which is intimately related to the composition and metabolic status of gut microbiota. A myriad of evidence has indicated that traditional Chinese medicine can treat HF by regulating gut microbiota. Yinchen Wuling powder (YCWLP) is a famous traditional Chinese medicine prescription, which has been used to relieve liver diseases for thousands of years. YCWLP has demonstrated protective function on HF, but its effect on the alterations of gut microbiota is still unclear, and its explicit therapeutic mechanism also needs to be further elucidated. In this study, 16S rRNA gene sequencing and fecal metabolomics analysis were combined to investigate the influence of YCWLP on gut microbiota in HF rats and the interactions between gut microbiota and host metabolism. The results showed that YCWLP treatment significantly improved the disorder of multiple organ indices, HF-related cytokines and plasma LPS induced by HF. Masson's trichrome stainings also showed that YCWLP treatment could significantly alleviate the severity of HF in rats. Additionally, YCWLP could reverse the significant changes in the abundance of certain genera closely related to HF phenotype, including *Barnesiella* [*Ruminococcus*] and *Christensenella*. Meanwhile, YCWLP significantly increased the abundance of *Bifidobacterium*, *Coprococcus* and *Anaerostipes*, which are closely related to butyrate production. Metabolomics and Spearman's correlation analysis showed that YCWLP could regulate the disorder of arginine biosynthesis, sphingolipid metabolism and alanine, aspartate and glutamate metabolism in HF rats, and these regulations were intimately related to *Barnesiella*, [*Ruminococcus*], *Christensenella, Coprococcus* and *Anaerostipes*. By explaining the biological significance of the above results, we concluded that YCWLP might ameliorate HF by regulating the imbalance of gut microbiota, increasing the abundance of butyrate-producing bacteria to reduce ammonia production, promote ammonia degradation, and regulate pro-inflammatory cytokines and immune function.

Keywords: Yinchen Wuling powder, hepatic fibrosis, 16S rRNA gene sequencing, fecal metabolomics, correlation analysis, butyrate

INTRODUCTION

Hepatic fibrosis (HF) is the pathological basis of the progress of diverse chronic liver diseases, which is characterized by excessive deposition of extracellular matrix (ECM). The development of HF into cirrhosis will seriously endanger human health (Williams, 2006). Nevertheless, HF is pathologically reversible, and early treatment can effectively prevent its further development (Pinzani and Rombouts, 2004). In the past few decades, innumerable treatment modalities targeting HF have been studied, but these methods have hardly achieved substantial results.

Liver and intestine originate from the same germ layer, so liver and intestinal microecology are intimately related not only in anatomical position, but also in function. The liver directly interacts with the gut through the bile secretion system and hepatic portal, which is called the "gut-liver axis" (Wahlstrom et al., 2016). Accumulating numbers of researches have shown that gut microbiota is significantly related to chronic liver disease progression (Li et al., 2020). The occurrence of HF is usually accompanied by microbiome dysbiosis and the impairment of the intestinal barrier. The excessive growth of small intestine bacteria leads to the accumulation of a large number of toxic substances such as endotoxin and ammonia. These pathogens and toxins enter the liver through the damaged intestine and portal vein, bind with toll-like receptors (TLRs), and then activate the liver immune cells, produce inflammatory cytokines, induce the liver innate immune response, and finally aggravate the progress of HF (Guo and Friedman, 2010; Seki and Schnabl, 2012). Additionally, gut microbiota also participates in the occurrence, development and treatment of liver diseases through host-microbe metabolic axes (Nicholson et al., 2012). In recent years, it has become a research hotspot to prevent and treat HF by ameliorating gut microbiota disorder (Dhiman et al., 2014). It is of great significance to investigate the mechanism of drug therapy of HF with gut microbiota as the target.

Yinchen Wuling powder (YCWLP) is a famous traditional Chinese medicine (TCM) prescription for the treatment of liver diseases recorded in *Synopsis of the Golden Chamber* written by Zhang Zhongjing, a famous physician in the Eastern Han Dynasty. It is composed of *artemisia Capillaris Herba*, *Polyporus Umbellatus*, *Alismatis Rhizoma*, *Atractylodes Macrocephalae Rhizoma stir-fried with wheat bran*, *Poria* and *Cinnamomi Ramulus*. In modern clinics, it is commonly used in the treatment of icteric hepatitis (Ma, 2020), hepatic fibrosis (Chen, 2012), non-alcoholic fatty liver disease (Liu and Zhao, 2011) and other diseases. In our previous study, we investigated the hepatoprotective effects and underlying mechanism of YCWLP on CCl_4-induced HF (Zhang et al., 2021). After 8 weeks of intervention, YCWLP could significantly reduce the serum aspartate transaminase (AST), alanine transaminase (ALT), hyaluronidase (HA), laminin (LN), type Ⅳ collagen (CIV) and N-terminal propeptide of procollagen type III (PIIINP) of HF rats. The histopathological analysis also showed that YCWLP could protect hepatocytes and reduce the degree of HF. Additionally, the metabolomic analysis of plasma, urine and liver samples also indicated that the mechanisms underlying the effects of YCWLP might be through reducing ammonia accumulation, promoting energy metabolism, reducing oxidative stress, protecting cell membrane and regulating intestinal flora metabolism. We have noticed that the mechanism of YCWLP in the treatment of HF might be related to gut microbiota. The increasing number of evidence also suggests that TCMs may be used as prebiotics to regulate the composition of gut microbiota and the metabolic phenotype of the host, and further as a new source for drug leads in gut microbiota-targeted disease management (Xu et al., 2015; Chang et al., 2017; Yu et al., 2017). Therefore, this study further elucidated the mechanism of YCWLP in the treatment of HF from the perspective of gut microbiota.

Fecal metabolomics can better reflect the intestinal-related metabolites, its association with the functional readout of the intestinal microbiome is of great value for the understanding of the microbiota-metabolism interactions (Zierer et al., 2018). Therefore, in this study, 16S rRNA gene sequencing analysis was used to analyze the changes of gut microbiota in CCl_4-induced HF rats and the intervention effect of YCWLP. Furthermore, the interaction between gut microbiota and host metabolism was explored by combining 16S rRNA gene sequencing with fecal metabolomics to elucidate the mechanism of YCWLP in the treatment of HF.

MATERIALS AND METHODS

Drugs and Chemicals

Artemisia Capillaris Herba (batch number: 190301; source: Hebei, China), Polyporus Umbellatus (batch number: 1808079; source: Liaoning, China), Alismatis Rhizoma (batch number: 190705; source: Sichuan, China), Atractylodes Macrocephalae Rhizoma stir-fried with wheat bran (batch number: 200622; source: Anhui, China), Poria (batch number: 190601; source: Anhui, China) and Cinnamomi Ramulus (batch number: 190401; source: Guangxi, China) were purchased from Shenyang Guoyaoda Pharmacy (Shenyang, China) and authenticated by Prof. Jia from Shenyang Pharmaceutical University (Shenyang, China).

HPLC grade acetonitrile, HPLC grade methanol and LC/MS grade formic acid were purchased from Fisher Scientific (Fair Lawn, NJ, United States). Analytical grade dibasic sodium phosphate and sodium dihydrogen phosphate were obtained from Kemeo Regent Co., Ltd (Tianjin, China). Sodium 3-trimethylsilyl-propionate [2,2,3,3,d_4] (TSP) and deuteroxide (D_2O) were supplied by Merck Drugs & Biotechnology (Darmstadt, Germany). Purified water was bought from Wahaha Co., Ltd. (Hangzhou, China). Masson's trichrome staining kit was purchased from Beijing Solarbio Science & Technology Co., Ltd. Platelet derived growth factor (PDGF), transforming growth factor-β1 (TGF-β1), tissue inhibitor of matrix metalloproteinases-1 (TIMP-1), α-smooth muscle actin (α-SMA) and lipopolysaccharide (LPS) assay ELISA kits were provided by Jiangsu Meimian Industrial Co., Ltd. (Jiangsu, China).

Preparation of Yinchen Wuling Powder Suspension

All crude herbal medicines were ground into powder and then sieved through a 60 mesh stainless steel sieve. The dosage of each

drug in YCWLP used in this study was in accordance with the record of "*Synopsis of the Golden Chamber*". 6 g YCWLP contained: 4.000 g of Artemisia Capillaris Herba, 0.375 g of Polyporus Umbellatus, 0.625 g of Alismatis Rhizoma, 0.375 g of Atractylodes Macrocephalae Rhizoma stir-fried with wheat bran, 0.375 g of Poria and 0.250 g of Cinnamomi Ramulus. The above herbs were then mixed with 60 ml normal saline to obtain the YCWLP suspension (0.1 g/ml). Besides, the suspension was prepared before each administration and mixed evenly before each rat was given intragastric administration.

Animal Experiments

18 male Sprague-Dawley (SD) rats (200 ± 20 g) supplied by the Experimental Animal Center of Shenyang Pharmaceutical University (Liaoning, China) were maintained in an environmentally controlled room (12/12 light-dark cycle, 20–25°C, 40%–70% relative humidity) with *ad libitum* access to food and water. All animal protocols in this study were approved by the Medical Ethics Committee of Shenyang Pharmaceutical University and in accordance with the guidelines of the National Institutes of Health on Animal Care (2004).

After 1 week of acclimation, all animals were randomly divided into three groups (n = 6): the control group (CON group), the hepatic fibrosis group (HF group) and the YCWLP treatment group (YCWLP group, 2 g/kg/d). The rats in the HF and YCWLP groups were orally administrated with 40% (v/v) CCl_4 (dissolved in soybean oil, 2 ml/kg) twice a week for 13 weeks, whereas the CON rats obtained the same dose of soybean oil with the same procedure. Since the 6th week, the rats in the YCWLP group were administered with YCWLP suspension once daily for 8 weeks, while the rats in the CON and HF groups received an equivalent volume of normal saline.

Sample Collections and Preparation

At the end of the 13th week, fecal samples within 12 h were collected on ice using sterilized metabolism cages under specific pathogen-free (SPF) conditions for metabolomics analysis. As for 16S rRNA gene sequencing analysis, fecal samples from each group were simultaneously obtained under sterile conditions in a laminar flow bench. The specific operation steps were as follows: disinfect the perianal area and tails of rats with 75% alcohol cotton, and collect fecal samples with aseptic freezing tubes using the tail-lifting method. All fecal samples above were stored at −80°C for further analysis immediately after collection.

Then, all rats were fasted overnight before the blood of the orbital venous plexus was collected and transferred to heparinized tubes. The plasma samples were obtained by centrifuging at 1,100 g for 15 min, and the supernatants were stored at −80°C for the determination of LPS. After all rats were sacrificed under ether anesthesia, the liver, spleen and thymus of each rat were removed and washed with pre-cooled normal saline. These organs were weighed after wiping dry and the organ indexes were calculated based on the percentages of organs to body weights. Finally, the liver of each rat was divided into two parts. One part was immediately snap-frozen in liquid nitrogen and stored at −80°C for the analysis of HF-related cytokines and the other part was fixed in 10% formaldehyde for Masson's trichrome staining.

Masson's Trichrome Staining

The liver tissues were fixed in 10% formaldehyde for 24 h, embedded in paraffin and cut into 5 μm sections, then stained with Masson's trichrome staining kit according to the manufacturer's instructions. The liver histological and fibrotic changes were assessed by two pathologists who were blinded to the treatment protocol. The degree of HF was scored using the Ishak scoring system after observation under a biological microscope (Andruszkow et al., 2019).

HF-Related Cytokines in Liver

After thawed at 4°C, 1.0 g liver tissue of each rat was immersed in 10.0 ml PBS (Na_2HPO_4–NaH_2PO_4, 0.01 M, pH = 7.4) followed by homogenized adequately to obtain liver tissue homogenate. Then, the homogenate was centrifugated at 1,100 g for 20 min and the supernatant was used to measure the activities of PDGF, TGF-β1, TIMP-1 and α-SMA by commercially available kits according to the manufacturer's instructions. The optical density values of PDGF, TGF-β1, TIMP-1 and α-SMA were all measured at 450 nm by a microplate reader.

Lipopolysaccharide

Plasma LPS was detected using a commercially available kit according to the manufacturer's instructions, and the optical density value of each plasma sample was detected by a microplate reader at 450 nm.

Fecal Metabolomics Analysis

^{1}H NMR Analysis

After thawed at 4°C, 200 mg feces of each sample was extracted with 1.0 ml pre-cooled PBS (Na_2HPO_4-NaH_2PO_4, 0.2 M, pH = 7.4) by ultrasound for 30 min. After centrifuged at 11,600 g for 10 min at 4°C, the supernatant was obtained. Finally, 450 μl supernatant was mixed with 100 μL TSP D_2O solution (1.0 mg/ml) and transferred to a 5 mm NMR tube for ^{1}H NMR analysis.

All fecal samples were analyzed at 298.2 K using Bruker AV 600 MHz superconducting Fourier transform NMR spectrometer (Bruker, Karlsruhe, Germany) with a one-dimensional water pre-saturated standard NOESYPR 1D pulse sequence. The pre-saturation method was used to suppress the water peak. Deuterium (D_2O) + water (H_2O) was used for field frequency locking and TSP was used as chemical shift reference (^{1}H, 0.00ppm). ^{1}H NMR spectra were measured with 64 scans into 64 K data points over a spectral width of 12,019 Hz and a relaxation delay of 2 s. An exponential function corresponding to a line broadening factor of 0.3 Hz was applied to all acquired free induction decays (FIDs) before Fourier transformation.

The obtained ^{1}H NMR spectra were manually phased and baseline corrected using MestReNova 6.1.1 software (Mestrelab Research, United States) with TSP as the reference. The integral interval was δ 0–10.0 with an integral spacing of 0.04 ppm. Moreover, in order to eliminate the influence of water peak, the integral value of δ 4.7–5.2 was removed.

UPLC-MS Metabolomics Analysis

After thawed at 4°C, 250 mg of each fecal sample was mixed with 1.0 ml pre-cooled water, extracted by ultrasound for 20 min, and then centrifuged at 11,600 g for 10 min at 4°C to obtain the supernatant. 400 μl pre-cooled methanol and 400 μl pre-cooled acetonitrile that act as the extraction solvent were successively added to the precipitation, and the above steps were repeated after each addition of solvent. Finally, the supernatant obtained was mixed and centrifuged at 11,600 g for 10 min at 4°C, and filtered through a 0.22 μm microporous membrane for UPLC-MS analysis. Furthermore, 10 μl of each fecal supernatant was mixed to obtain a quality control (QC) sample.

UPLC analysis was conducted on the Waters ACQUITY UPLC system (Waters Corp., Milford, United States). Chromatographic peaks were separated on a universal XB C18 column (150 mm × 2.1 mm, 1.8 μm; Kromat, United States) at the temperature of 35°C. The mobile phase composed of 0.1% (v/v) formic acid-water (A) and 0.1% (v/v) formic acid-acetonitrile (B), the flow rate was 0.2 ml/min and the elution procedure was set as follows: 5–30% (B) in 0–8 min, 30–60% (B) in 8–10 min, 60–90% (B) in 10–15 min, 90–5% (B) in 15–15.1 min, 5% (B) in 15.1–20 min. The sample injection volume was set at 5 μl. MS analysis was carried out on the Waters Quattro mass spectrometer coupled with a triple quadrupole mass analyzer (Waters Corp., Milford, MA, United States) in positive ion mode. The MS conditions were as follows: the cone voltage was 35 V; the capillary voltage was 3.2 kV; the desolvation temperature was 350°C; the source temperature was 120°C; the desolvation flow rate was 600 L/h; the cone gas flow rate was 50 L/h; the collision energy was 10–30 eV. In addition, the mass range was set from 100 to 1,000 Da with full scan mode.

The repeatability and stability of the UPLC-MS platform were evaluated using QC samples by the method described in our previous study (Zhang et al., 2021). Finally, the original data were imported into Markerlynx V4.1 (Waters Corp., Milford, United States) for peak deconvolution and normalization and a matrix including mass, retention time and corresponding peak areas of all the detected peaks was obtained.

Data Processing and Analysis

The normalized data were imported into SIMCA-P 13.0 (Umetrics, Umea, Sweden) for principal component analysis (PCA) and orthogonal projection to latent structure discrimination analysis (OPLS-DA). The loading plots generated by OPLS-DA were used to screen the key fecal metabolites between the CON and HF groups and between the HF and YCWLP groups, respectively. The key metabolites were selected according to the variable importance in projection (VIP) values (>1.2) and the *p*-values (<0.05), and identified by matching the chemical shift (^{1}H NMR) and the m/z (UPLC-MS) with the available databases such as HMDB (http://www.hmdb.ca), KEGG (http://www.genome.jp), METLIN (http://metlin.scripps.edu) and MassBank (http://www.massbank.jp) and the related literature (Chen et al., 2018; Santiago et al., 2019; Liu et al., 2020). In addition, the 7-fold cross-validation method and permutation test (999 permutations) were used to validate the models used in this study. Finally, the key metabolites were imported into MetaboAnalyst 5.0 (http://metpa.metabolomics.ca) for metabolic pathways analysis.

16S rRNA Gene Sequencing Analysis

Fecal samples were sent to Beijing Microread Genetics Co., Ltd (Beijing, China) for 16S rRNA gene sequencing. Total genomic DNA was extracted using the QIAamp Fast DNA Stool Mini Kit (Qiagen, Frankfurt, Germany) according to the manufacturer's protocols. The concentration of DNA was detected by Nanodrop One (Thermofisher, Waltham, Massachusetts, United States), and the purity was detected by 1% agarose gel electrophoresis. The V3-V4 hypervariable regions of the bacteria 16S rRNA gene were amplified with primers 341F (5′- CCTACGGGNBGCASCAG-3′) and 805R (5′- GACTACNVGGGTATCTAATCC-3′) by Veriti 96 Well Thermal Cycler (Thermofisher, Waltham, Massachusetts, United States). The PCR products were purified by adding an equal volume of MagPure A3 XP (Magen) and quantified by the Qubit® 2.0 Fluorometer (Effendorf, Hamburg, Germany) using KAPA Library Quant (Illumina) DNA Standards and Primer Premix Kit (Kapa Biosystems, Boston, Massachusetts, United States) according to the manufacturer's protocols. At last, the library was sequenced on the IlluminaHiseq 2,500 (Illumina, San Diego, California, United States) platform (PE250) to generate single-end reads.

The original sequencing data in fastq format were filtered by removing the low-quality base sequence using FASTQC (https://www.bioinformatics.babraham.ac.uk/projects/fastqc/), and then merged by HTQC (Version 1.92.3) to generate high-quality clean reads. Then, the chimera sequences were detected and removed by Mothur (Versions 1.38.1) software to obtain effective tags. The effective tags with at least 97% sequence similarity were clustered using Usearch61 method in QIIME (Version 1.9.1) software to obtain the operation taxonomic units (OTUs). The PyNAST (Python Nearest Alignment Space Termination) method in RDP Classifier (http://sourceforge.net/projects/rdp-classifier/, Version 2.2) was used to compare the representative sequences of each OTU with the GreenGenes database (http://greengenes.secondgenome.com/) to obtain the species classification information. Moreover, the relative abundance of species at each taxonomic level was calculated, including phylum, class, order, family and genus.

Alpha diversities such as Chao1 index, Shannon index, Simpson index, PD_whole_tree and rarefaction curve were calculated by QIIME and displayed by R software (Version 3.2.2) to identify the community richness and diversity. Principal coordinate analysis (PCoA), unweighted pair-group method with arithmetic mean (UPGMA), non-metric multidimensional scaling analysis (NMDS) and analysis of similarities (ANOSIM) were performed to analyze the beta diversity between groups by using QIIME software and ggplot2 package in R software (Version 3.2.2). Welch's *t*-test (SPSS, Version 19.0) was used to screen species with significant differences at each level between the CON and HF groups and between the HF and YCWLP groups (p-value < 0.05), respectively. In addition, the linear discriminant analysis (LDA) effect size measurement (LefSe) analysis based on Kruskal-Wallis rank-sum test and Wilcoxon rank-sum test was conducted to identify the abundant taxonomy with significant differences among the three experimental groups.

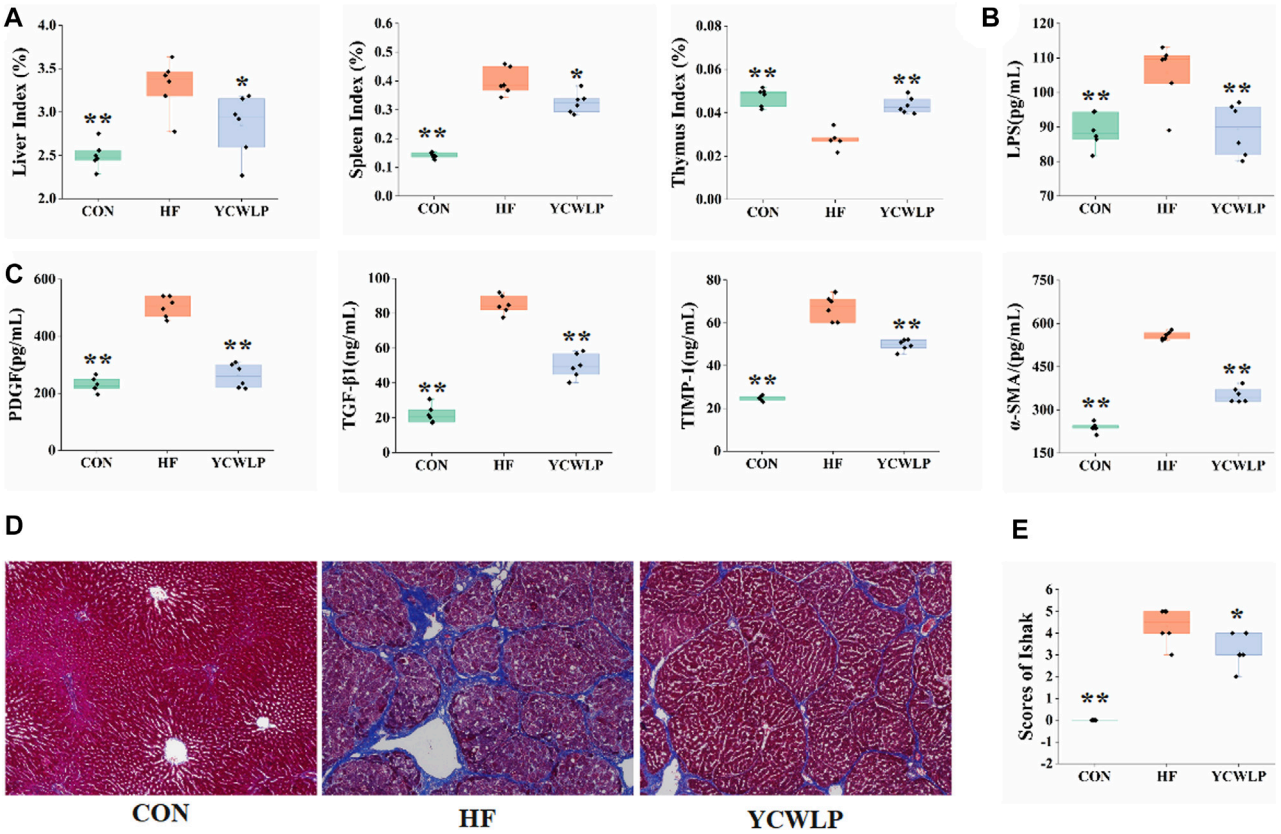

FIGURE 1 | Effect of YCWLP on the CCl_4–induced HF (n = 6). **(A)** Liver, spleen and thymus indices; **(B)** LPS in the plasma samples; **(C)** The expression of PDGF, TGF-β1, TIMP-1 and α-SMA in the liver samples. **(D)** Masson's trichrome staining of rat liver tissue. Magnification ×100; **(E)** Ishak scores based on Masson's trichrome staining of rat liver tissue. Significant difference compared with the HF group: * p-value < 0.05; ** p-value < 0.01.

Statistical Analysis

All data were expressed as mean ± standard errors of the means. The multiple organ indices, HF-related cytokines, plasma LPS, Ishak scores and fecal metabolites were analyzed by one-way ANOVA test. In 16S rRNA analysis, Welch's t-test and LefSe analysis were used to screen the species with significant abundance differences between the experimental groups. A p-value < 0.05 was considered statistically significant. To calculate the correlation coefficient between the pharmacodynamic data, key fecal metabolites and gut microbiota at the genus level, Spearman's correlation analysis was performed using SPSS 19.0 software and the corresponding heatmaps were visualized using Origin (Version 2018).

RESULTS

Yinchen Wuling Powder Attenuates CCl_4-Induced Hepatic Fibrosis

In a previous study, we investigated the effect of YCWLP on serum AST, ALT, HA, LN, CIV and PIIINP in HF rats (Zhang et al., 2021). The detailed data of these indicators were used for further Spearman's correlation analysis with gut microbiota in this study (**Supplementary Table S1**). Furthermore, the effects of YCWLP on multiple organ indices, HF-related cytokines and plasma LPS were also investigated in this study. As the results, the liver index, the spleen index (**Figure 1A**, p-value < 0.01, respectively), the liver levels of PDGF, TGF-β1, TIMP-1 and α-SMA (**Figure 1C**, p-value < 0.01, respectively), and the plasma level of LPS (**Figure 1B**, p-value < 0.01) were significantly increased in the HF group compared with the CON group. And the YCWLP treatment significantly reduced the liver index, the spleen index (**Figure 1A**, p-value < 0.05, respectively), the liver levels of PDGF, TGF-β1, TIMP-1 and α-SMA (**Figure 1C**, p-value < 0.01, respectively), and the plasma level of LPS (**Figure 1B**, p-value < 0.01) in HF rats. However, compared with the CON group, the thymus index of the HF group was significantly decreased (**Figure 1A**, p-value < 0.01). Meanwhile, this change was recovered after the YCWLP treatment (**Figure 1A**, p-value < 0.01). The detailed data of these indices were listed in **Supplementary Table S1** for further Spearman's correlation analysis with gut microbiota.

Masson's trichrome staining was used to observe the pathological changes of liver tissue among the experimental groups. As shown in **Figure 1D**, large amounts of collagen fibers proliferated in the portal area of HF rats, with obvious fiber bridging and nodules. After treatment, the proliferation of collagen fibers in the YCWLP group was significantly reduced,

and there was occasional fiber bridging between the portal regions. Additionally, the Ishak score analysis of hepatic fibrosis confirmed that the hepatic fibrosis score of the YCWLP group was significantly lower than that of the HF group (**Figure 1E**). Thus, these results indicated that YCWLP could alleviate the severity of HF in CCl_4-induced rats.

Yinchen Wuling Powder Modulated Fecal Metabolism in HF Rats

Representative ^{1}H NMR spectra of the fecal samples of the CON, HF and YCWLP groups were shown in **Supplementary Figure S1A**. 46 endogenous metabolites in the fecal samples were ultimately assigned according to the ^{1}H NMR spectra and listed in **Supplementary Table S2**. Total ion chromatograms (TICs) of each group were overlaid and shown in **Supplementary Figure S1B**. After normalization of the QC sample data, the extracted ion chromatographic peaks of six ions were selected for method validation. The relative standard deviations (RSDs) of the retention time (RT) and peak areas of the selected ions were calculated and listed in **Supplementary Table S3**. All values were less than 10%, indicating that the developed method with good repeatability and stability was suitable for the following research.

According to the 3D PCA score plots of both ^{1}H NMR and UPLC-MS (**Figures 2A,D**), the segregations were visible between the CON and HF groups, which indicated that the fecal metabolic profile of HF rats changed significantly. After treatment, the YCWLP group showed a restorable trend and partially coincided with the CON group. In addition, OPLS-DA analysis was also performed to visualize the metabolic alterations occurring between the CON and HF groups and between the HF and YCWLP groups, respectively. As the result, there were significant distinctions between the CON and HF groups (**Figures 2B,E**) as well as between the HF and YCWLP groups (**Figures 2C,F**). The above results indicated the hepatoprotective effects of YCWLP against CCl_4-induced HF, which were consistent with the pharmacodynamic and pathological studies. According to the parameters of 7-fold cross-validation (**Supplementary Table S4**) and permutations tests of PLS-DA (**Supplementary Figures S2E–H**), the PCA and OPLS-DA models used in this study were robust.

Based on the loading plots produced by OPLS-DA analysis (**Supplementary Figures S2A–D**), a total of 57 key metabolites significantly altered between the CON group and the HF group were identified (**Supplementary Table S5**). Moreover, there were 50 key metabolites significantly changed between the HF group and the YCWLP group (**Supplementary Table S6**). Among them, 42 fecal metabolites changed due to CCl_4-treatment could be reversed by YCWLP (**Supplementary Table S7**), and these metabolites were considered to be the key metabolites of YCWLP affecting HF.

Key metabolites with significant differences between the CON and HF groups and between the HF and YCWLP groups were imported into the MetaboAnalyst 5.0 to screen the meaningful metabolic pathways (p-value < 0.05, impact value >0.1), respectively. As shown in **Figures 2G,H**, three metabolic pathways were selected as the most meaningful metabolic pathways, which were significantly disordered in HF rats and regulated by YCWLP, including arginine biosynthesis, sphingolipid metabolism and alanine, aspartate and glutamate metabolism. Therefore, these three metabolic pathways might be related to the potential mechanism of YCWLP in the treatment of HF.

16S rRNA Gene Sequencing Analysis

Overall Structural Modulation of Gut Microbiota by Yinchen Wuling Powder Treatment

A total of 337,264 clean reads were obtained from 15 fecal samples (5 in each group), and each sample produced an average of 22,484 ± 788 clean reads. Rarefaction curves of each sample tended to be flat within a certain number of sequences sampled, which indicated that the sequencing depth of each sample in this study was adequate (**Supplementary Figure S3**). As shown in alpha diversity analysis, the Chao1 and Shannon indices were significantly lower in the HF group than those in the CON group (**Supplementary Figure S4A, Table S8**, p-value < 0.01, respectively), whereas there were no significant differences in the Simpson and PD_whole_tree indices between these two groups. Compared with the HF group, the Shannon index of the YCWLP group was significantly increased (**Supplementary Figure S4A, Table S8**, p-value < 0.05). The results indicated that the richness and diversity of the gut microbiota were significantly reduced after CCl_4 treatment, which was consistent with the previous research (Li et al., 2020), and the YCWLP treatment could significantly improve the gut microbiota diversity of HF rats.

Then, unweighted UniFrac-based-PCoA, NMDS and UPGMA were performed to analyze the changes in gut microbiota community structures among different groups. As shown in PCoA analysis, the gut microbiota profiles of the CON, HF and YCWLP groups were separated obviously with the total variances of PC1 16% and PC2 11% (**Supplementary Figure S4B**). The NMDS analysis depicted that the HF group was clearly separated from the CON group, and the YCWLP group was located in the middle of them and showed a trend away from the HF group and close to the CON group (**Supplementary Figure S4D**). The stress value was less than 0.2, which indicated that the NMDS analysis was able to accurately reflect the difference between samples (Clarke, 1993). Moreover, the hierarchical clustering analysis of UPGMA also manifested that the distance between the YCWLP group and the CON group was shorter than that between the YCWLP group and the HF group (**Supplementary Figure S4C**). The results above indicated that YCWLP could ameliorate the dysbiosis of the gut microbiota induced by CCl_4. In addition, according to the ANOSIM analysis (**Supplementary Figure S4E**), the results of R-value > 0, p < 0.01 showed that the difference between the groups was significantly greater than that within the group, indicating that the grouping of this study was meaningful.

Differential Gut Microbiota in Hepatic Fibrosis and Yinchen Wuling Powder-Treated Rats

The top ten gut microbiota in the relative abundance at the phylum, class, order and family levels were shown in

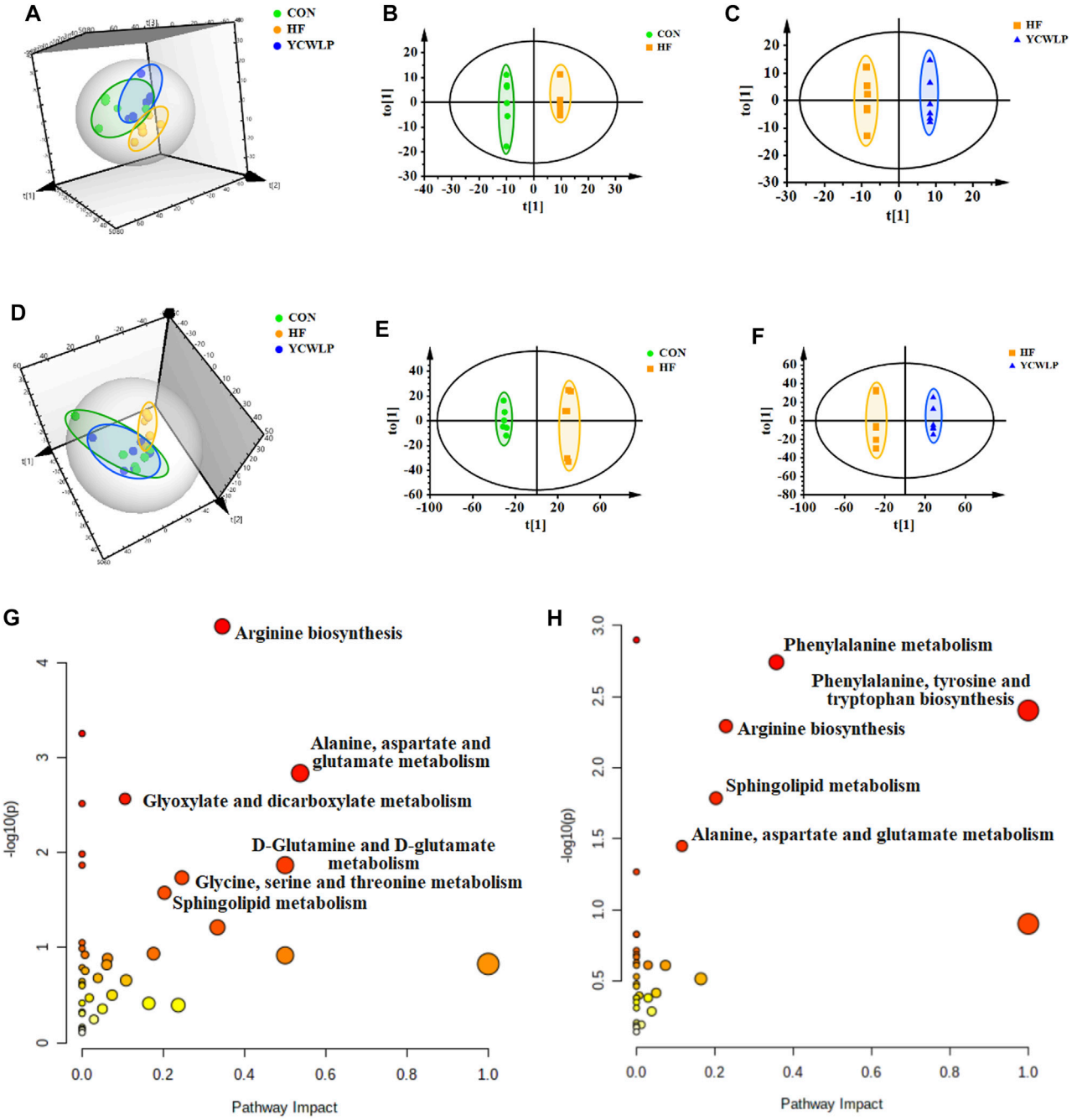

FIGURE 2 | Multivariate data analysis and the metabolic pathway analysis of the fecal samples. 3D PCA score plots of the CON, HF and YCWLP groups based on ^{1}H NMR **(A)** and UPLC-MS **(D)**, respectively; OPLS-DA score plots of the CON and HF groups based on ^{1}H NMR **(B)** and UPLC-MS **(E)**, respectively; OPLS-DA score plots of the HF and YCWLP groups based on ^{1}H NMR **(C)** and UPLC-MS **(F)**, respectively. Meaningful pathway analysis based on the key fecal metabolites between the CON and HF groups **(G)** and between the HF and YCWLP groups **(H)**, respectively (p-value < 0.05, impact-value > 0.1).

Supplementary Figure S5A and the species with significant changes at each level were evaluated and shown in **Supplementary Figure S5B**. At the phylum level, compared with the CON group, the relative abundance of *Firmicutes*, *Chloroflexi*, *Gemmatimonadetes*, TM7 and *Tenericutes* of the HF group were significantly increased, while the relative abundance of *Bacteroidetes* was significantly decreased. Compared with the HF group, YCWLP treatment could significantly restore the relative abundance of *Gemmatimonadetes*. At the class level, the relative abundance of *Acidobacteria-6*, *Acidimicrobiia*, *Ktedonobacteria*, TM7-1, *Gemmatimonadetes*, *Clostridia*, *Deltaproteobacteria,* TM7-3

and *Mollicutes* in the HF group were significantly higher than those in the CON group, whereas *Bacteroidia* and *Actinobacteria* were significantly lower. After treatment, the relative abundance of *Acidobacteria-6, Acidimicrobiia, Ktedonobacteria*, TM7-1 and *Gemmatimonadetes* in the YCWLP group were significantly restored. At the order level, the relative abundance of *Bacteroidales* and *Actinomycetales* were significantly lower and the relative abundance of *Acidimicrobiales*, *Clostridiales*, *Desulfovibrionales,* CW040 and RF39 were significantly higher in the HF group than those in the CON group. In addition, the relative abundance of *Acidimicrobiales* was significantly reversed by YCWLP treatment. At the family level, the reduced abundance of Prevotellaceae, Micrococcaceae, Streptococcaceae and Peptococcaceae, and the increased abundance of Ruminococcaceae, [Barnesiellaceae], Dehalobacteriaceae, F16, Desulfovibrionaceae and Thermomonosporaceae were observed in HF rats. Compared with the HF group, YCWLP significantly restored the relative abundance of Thermomonosporaceae in HF rats. Interestingly, the relative abundance of *Bifidobacteriales* at the order level and Bifidobacteriaceae at the family level were significantly increased after YCWLP treatment.

At the genus level, the top ten genera in the relative abundance were shown in **Figure 3A**. The Welch's *t*-test showed that a total of 19 genera changed significantly among the experimental groups (**Figure 3C**), and their specific relative abundance was shown in **Supplementary Figure S6**. Among them, 15 genera were significantly changed due to the CCl_4 treatment. In detail, we observed significantly decreased abundance of *Rothia*, *Prevotella*, *Streptococcus*, *Robinsoniella*, rc4-4, *Butyricicoccus*, *Faecalibacterium* and *Christensenella*, and significantly increased abundance of *Oscillospira, Bilophila, Desulfovibrio, Barnesiella*, *Dehalobacterium*, *Roseburia* and [*Ruminococcus*] in HF rats compared with the CON rats. After treatment, three genera including *Christensenella* [*Ruminococcus*] and *Barnesiella* were significantly reversed by YCWLP (**Figure 3B**). In addition, YCWLP treatment also significantly increased the relative abundance of *Anaerostipes, Coprococcus*, *Bifidobacterium* and *Allobaculum* in HF rats (**Figure 3D**).

The LEfSe analysis, which emphasizes the statistical significance and biological correlation, was also performed to search for biomarkers with statistical significance among the CON, HF and YCWLP groups (**Figures 3E,F**). In this study, the discriminative features of the bacterial taxa were identified with an LDA score >2.0. According to the ranked bacterial taxa, the HF rats were enriched with p_Tenericutes, c_Mollicutes, o_RF39, f_Thermomonosporaceae, g_Oscillospira, g_Roseburia, g_Desulfovibrio and g_[Ruminococcus], which suggested that the changes of these gut microbiota might promote the deterioration of HF. After treatment, the rats of the YCWLP group were enriched with p_TM7, c_TM7_3, o_CW040, o_Bifidobacteriales, f_F16, f_Bifidobacteriaceae, g_Coprococcus, g_Anaerostipes and g_Bifidobacterium. Combined with the differential gut microbiota analyzed by Welch's *t*-test at the genus level (**Figures 3B,D**), it can be concluded that [*Ruminococcus*] played the most significant role in YCWLP treatment. We also noticed that *Bifidobacterium* as a well-known probiotic was significantly increased after YCWLP treatment, together with *Coprococcus* and *Anaerostipes* which were the characteristic genera for the rats of the YCWLP group, might also be responsible for YCWLP treatment.

Hepatic Fibrosis-Related Genera Regulated by Yinchen Wuling Powder

The correlations between 19 genera that changed significantly among the experimental groups (**Figure 3C**) and 14 HF-related pathological indices (**Supplementary Table S1**) were conducted by Spearman's correlation analysis. The results were summarized in **Supplementary Table S9** and presented as a heatmap (**Figure 4A**). In general, there were 13 genera closely related to the phenotype of HF (≥4 pathological indices were closely correlated with certain genus). Among them, *Desulfovibrio*, *Bilophila*, *Oscillospira* [*Ruminococcus*], *Dehalobaterium*, *Barnesiella* and *Roseburia* showed significant positive correlations with the pathological changes, while *rc4-4*, *Rothia*, *Faecalibacterium*, *Robinsoniella*, *Christensenella* and *Butyricicoccus* showed significant negative correlations. Of these 13 genera, *Christensenella, [Ruminococcus]* and *Barnesiella* could be significantly reversed by YCWLP in HF rats. Therefore, these three genera might be the targets of YCWLP in the treatment of CCl_4-induced HF.

Correlations Between Gut Microbiota and Fecal Metabolites

Spearman's correlation analysis was also conducted to analyze the correlations between the 19 significant changed genera and 42 key fecal metabolites that could be reversed by YCWLP (**Supplementary Table S7**). As shown in **Figure 4B** and **Supplementary Table S9**, [*Ruminococcus*] showed a negative correlation with citrulline and positive correlations with the metabolites related to sphingolipid metabolism. *Christensenella* was negatively correlated with sphingosine and positively correlated with L-Glutamine. *Barnesiella* was positively correlated with sphingosine.

DISCUSSION

In this study, we further verified the therapeutic effect of YCWLP on HF using Masson's trichrome staining. Additionally, the effects of YCWLP on multiple organ indices, HF-related cytokines and plasma LPS in HF rats were also investigated, so as to provide evidence for the exploration of the therapeutic mechanism of YCWLP. The results showed decreased levels of the liver and spleen indices and an increased level of the thymus index following YCWLP treatment. The spleen is mainly involved in humoral immunity, while the thymus is mainly involved in cellular immunity. The callback effect of YCWLP on these indices reflected its hepatoprotective and immunomodulatory effects. Compared with the HF group, YCWLP could significantly reduce the expression of PDGF, TGF-β1, TIMP-1 and α-SMA

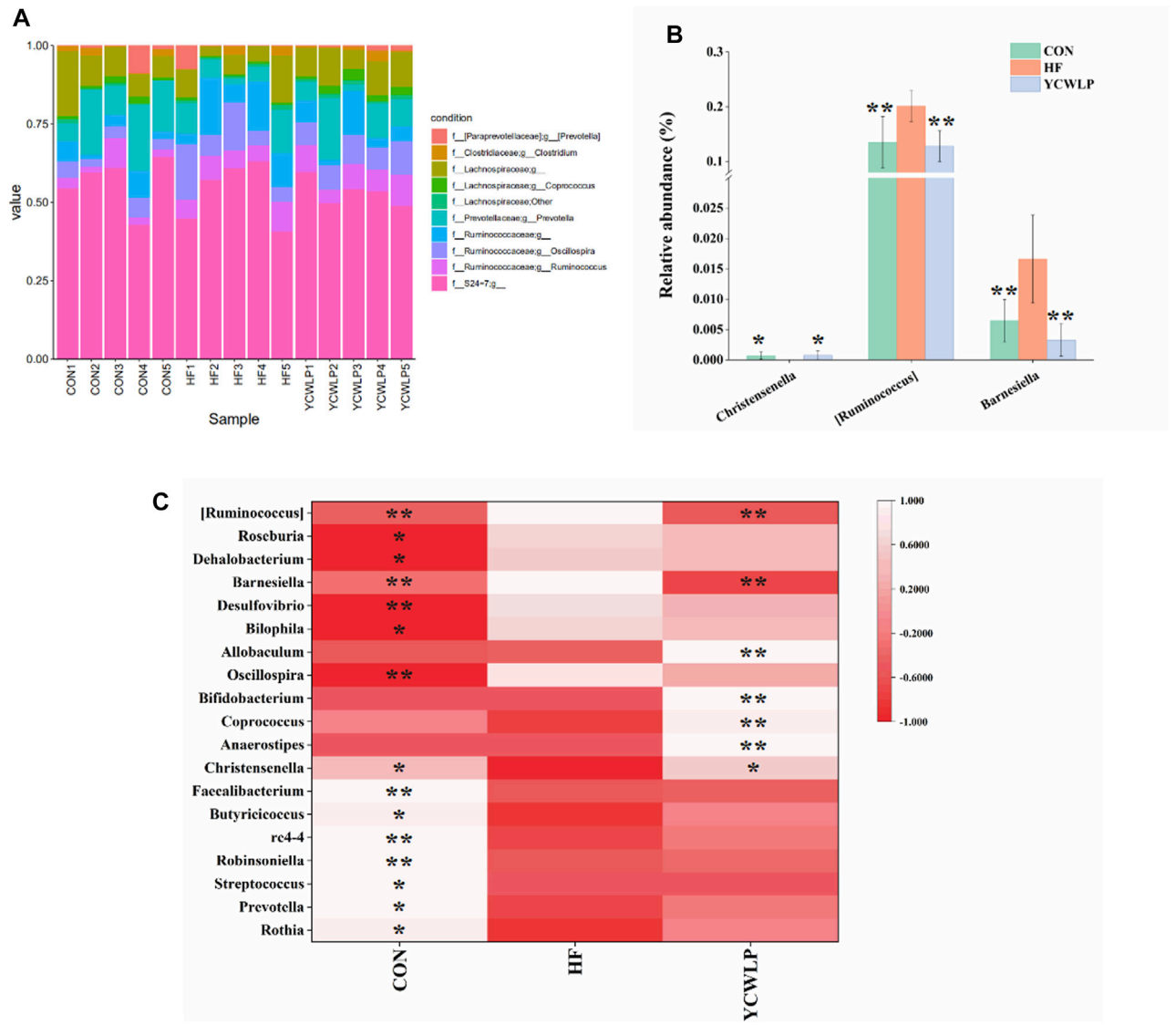

FIGURE 3 | Differences of gut microbiota composition among the CON, HF and YCWLP groups. **(A)** Top ten gut microbiota in the relative abundance at the genus level; **(B)** The relative abundance of *Christensenella* [*Ruminococcus*] and *Barnesiella*; **(C)** Heatmap of genera with significant variations; **(D)** The relative abundance of *Anaerostipes*, *Coprococcus*, *Bifidobacterium* and *Allobaculum*; **(E)** Cladogram generated by the LEfSe analysis; **(F)** Linear discriminant analysis (LDA) scores of the discriminative taxa. The letters p, c, o, f and g represented phylum, class, order, family and genus, respectively. Significant difference compared with the HF group: * p-value < 0.05; ** p-value < 0.01.

in the liver. These cytokines mainly participate in the activation of hepatic stellate cells (HSCs), and the production and degradation of extracellular matrix (ECM), which indicated that the anti-fibrosis mechanism of YCWLP might be related to inhibiting HSC activity and reducing ECM synthesis. In addition, YCWLP could restore the level of LPS in plasma of HF rats, indicating that YCWLP could protect the intestinal tract and reduce the release of LPS from liver cells into blood circulation.

It has been proved that the therapeutic mechanism of YCWLP on HF is related to gut microbiota (Zhang et al., 2021). In this study, multiomics was used to investigate the effect of YCWLP on gut microbiota in HF rats and the interaction between gut microbiota and host metabolism. 16S rRNA sequencing showed that the diversity and richness of gut microbiota in HF rats were both significantly decreased. YCWLP treatment could significantly improve the diversity of gut microbiota in rats with HF, but had no significant effect on the richness. PCoA and NMDS analysis indicated significant differences in gut microbiota composition among the CON, HF and YCWLP groups. In UPGMA analysis, the beta diversity of the YCWLP-treated rats showed a greater similarity to the rats in the CON group than those in the HF group. Spearman's correlation analysis was performed on the 19 genera with significant changes among the experimental groups and 14 HF-related pathological indices. Finally, 13 genera were identified to be intimately related to HF phenotype, from which strong positive relationships were

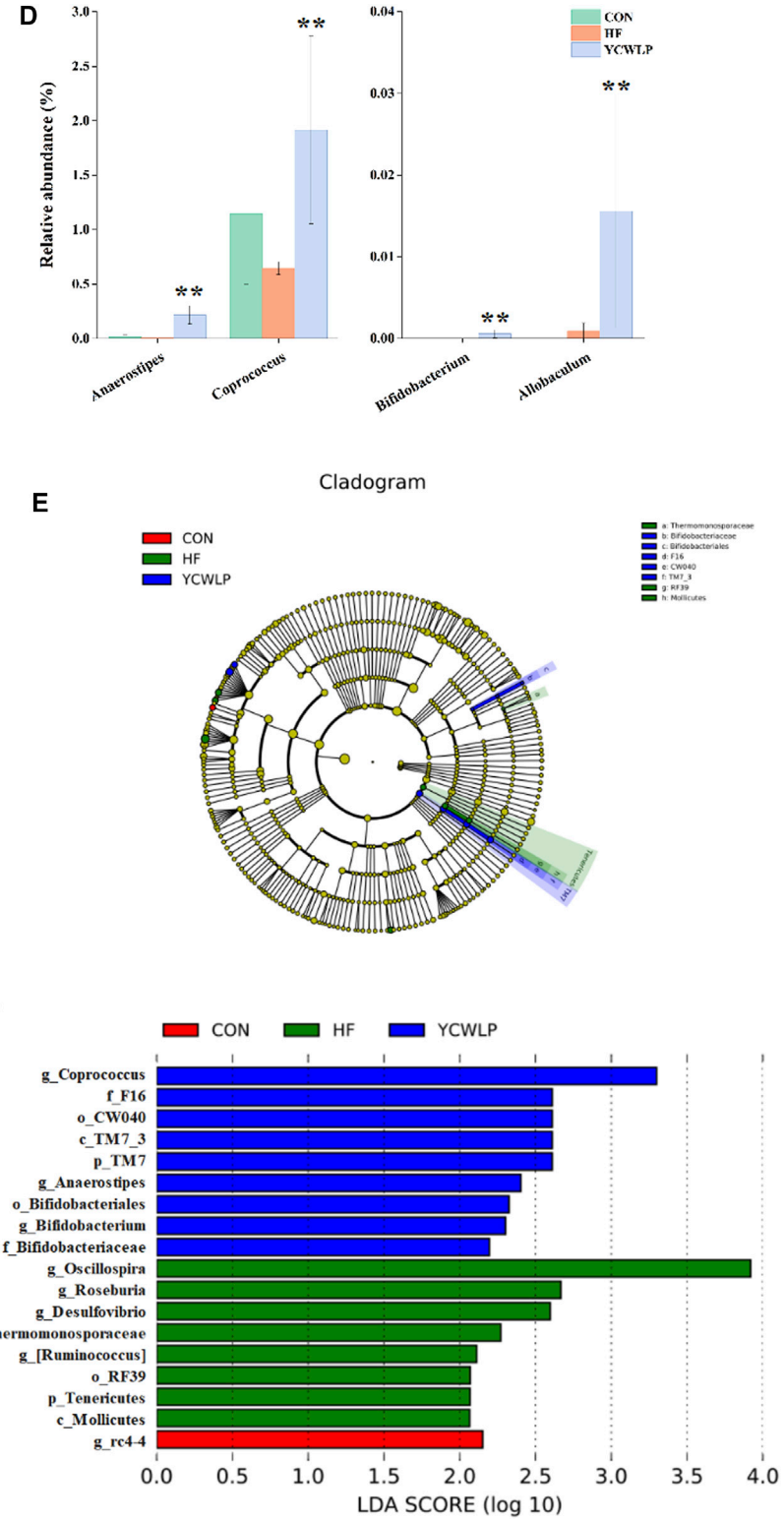

FIGURE 3 | Continued.

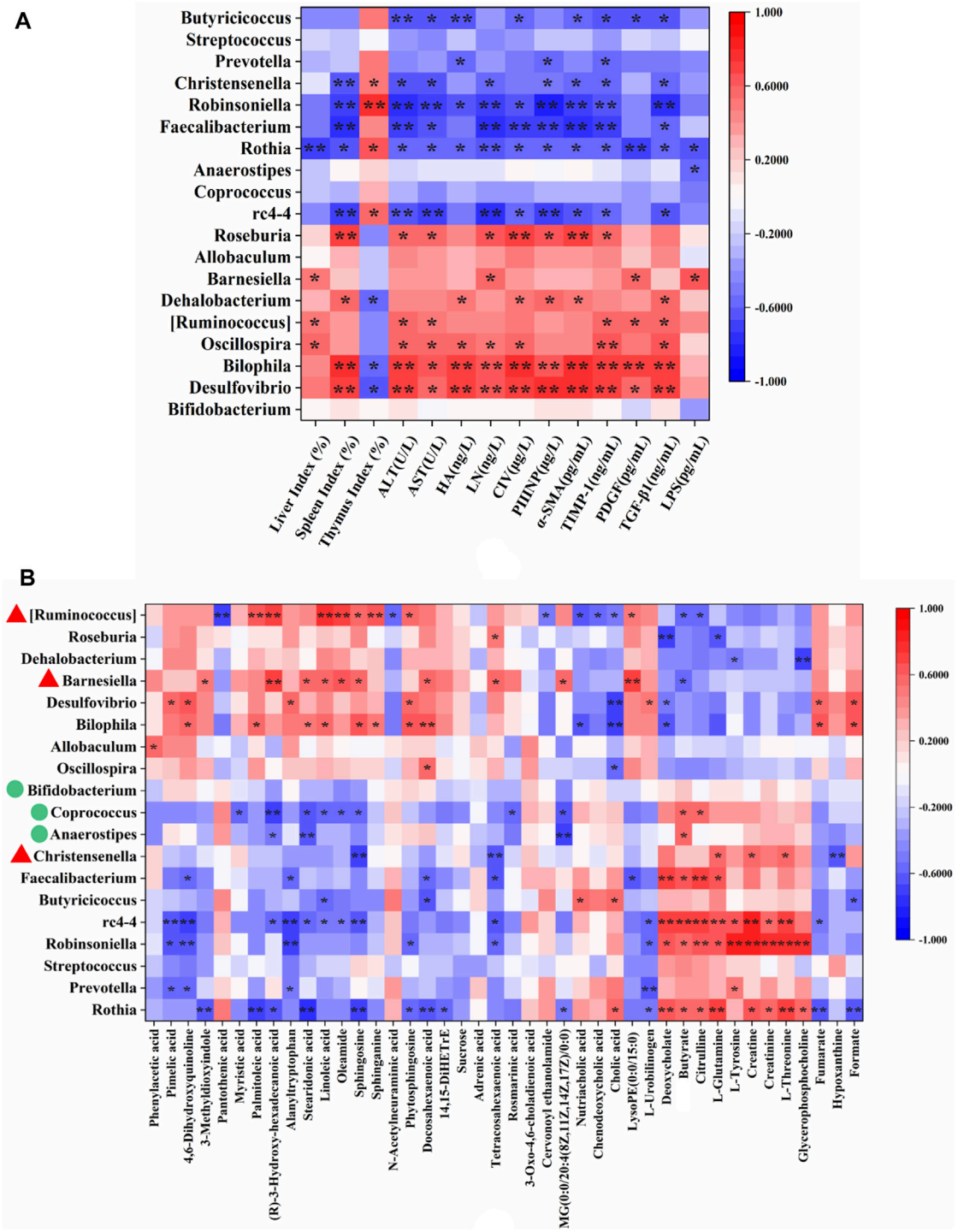

FIGURE 4 | Spearman's correlation analysis of HF-related pathological indices, key fecal metabolites and significantly changed genera. **(A)** Correlations between 19 significantly changed genera and 14 HF-related pathological indices; **(B)** Correlations between 19 significantly changed genera and 42 key fecal metabolites reversed by YCWLP treatment. $^{*}|r| > 0.5$ and p-value < 0.05; $^{**}|r| > 0.5$ and p-value < 0.01. The genera marked with red triangles in **(B)** represent the disordered HF-related genera reversed by YCWLP treatment. The genera marked with green circles in **(B)** represent the genera increased significantly after YCWLP treatment.

identified for *Desulfovibrio*, *Bilophila*, *Oscillospira* [*Ruminococcus*], *Dehalobaterium*, *Barnesiella* and *Roseburia,* while significant negative relationships were identified for *rc4-4*, *Rothia*, *Faecalibacterium*, *Robinsoniella*, *Christensenella* and *Butyricicoccus. Desulfovibrio* is a sulfate-reducing bacteria, which has been proved to promote the occurrence and development of HF (Chen, 2018). *Bilophila* is significantly associated with fatty liver disease caused by overfeeding. High-fat diet can increase its proportion in gut microbiota and increase the risk of inflammatory bowel disease and hepatobiliary disease (Jian et al., 2021). Moreover, both *Desulfovibrio* and *Bilophila* can produce LPS and promote inflammation (Wei et al., 2015; Song et al., 2017). Studies have shown that [*Ruminococcus*] is significantly positively correlated with the degree of HF (Boursier et al., 2016). In addition, the up-regulation of [*Ruminococcus*] can be used as the intestinal microbiological characteristics of the progress of non-alcoholic fatty liver disease (NAFLD) (Del Chierico et al., 2017). *Barnesiella* has been reported to be positively correlated with glucose and lipid metabolism disorders and dyslipidemia (Deng et al., 2020). Furthermore, *Barnesiella* was significantly enriched in hepatocellular carcinoma (HCC) patients, and its relative abundance gradually increased during the development of HCC (Jiang et al., 2020). The relative abundance of these pathogens increased significantly in HF rats, while the relative abundance of beneficial bacteria *Christensenella* and short-chain fatty acid producing bacteria *Butyricicoccus* and *Faecalibacterium* decreased significantly. The changes of these gut microbiota might promote the deterioration of HF.

YCWLP treatment could significantly restore the relative abundance of *Christensenella* [*Ruminococcus*] and *Barnesiella* in HF rats. Therefore, it can be considered that these three genera were responsible for the treatment of YCWLP. In addition, LEfSe analysis showed that *Bifidobacterium*, *Coprococcus* and *Anaerostipes* were the characteristic genera enriched in the YCWLP group (LDA >2). The relative abundance of these three genera in YCWLP-treated rats were much higher than those in the CON and HF groups, which might be the reason why they had no significant correlations with the HF phenotype. However, they might still play a key role in the treatment of HF with YCWLP. Interestingly, we also found that these three genera are closely related to the production of butyrate. *Coprococcus* and *Anaerostipes* belonging to Lachnospiraceae are butyrate-producing bacteria (Feng et al., 2018). The main metabolites of *Bifidobacterium* are acetic acid, lactic acid and formic acid. In the intestinal ecosystem, lactic acid and acetate are used to produce butyrate or propionate by *Firmicutes* (Scott et al., 2014). The results of this study also showed that the content of butyrate in feces increased significantly after YCWLP treatment (**Figure 5**), and *Coprococcus* and *Anaerostipes* were strongly positively correlated with butyrate (**Figure 4B**). Butyrate is an important energy source of intestinal epithelial cells, which can protect the intestinal barrier by stimulating tight junction and mucus formation (Usami et al., 2015). Butyrate can also inhibit the proliferation of pathogenic bacteria such as *Escherichia coli*, *Staphylococcus* and *Clostridium* by releasing H^+, and promote the growth and reproduction of beneficial bacteria *Lactobacillus* (Allen et al., 2018). Studies have shown that the decrease of Lachnospiraceae, which are characterized by butyrate production, may lead to an increase of colonic pH. This is believed to promote the production and absorption of ammonia, and resulting in hepatic encephalopathy (Woodhouse et al., 2018). In addition, butyrate can also regulate the immune response by affecting the production of inflammatory mediators, the migration and adhesion of immune cells and cell function (Correa et al., 2016). Therefore, the effect of YCWLP on increasing the production of butyrate is of great significance to improve HF.

Fecal non-targeted metabolomics showed that YCWLP could reverse 42 metabolites that were changed by CCl_4 in HF rats. Through metabolic pathway analysis, we found that YCWLP could significantly correct the disorder of three metabolic pathways, including arginine biosynthesis, sphingolipid metabolism and alanine, aspartate and glucose metabolism. The relationship between the potential metabolic pathways and their corresponding metabolites were shown in **Figure 6**. Intestinal flora affects host metabolism by transforming, absorbing and metabolizing exogenous substances (Li et al., 2019). The changes of metabolites reflect the alternations of gut microbiota to a certain extent. Therefore, in order to explore the mechanism of gut microbiota regulating the occurrence and development of HF and the treatment of YCWLP through affecting host metabolism, we conducted Spearman's correlation analysis on 42 key fecal metabolites and 19 intestinal microflora, which were related to the treatment of HF with YCWLP (**Figure 4B**).

Amino Acid Metabolism

Citrulline is the intermediate of the urea cycle, and the urea cycle is the main way to eliminate ammonia. Most of the ammonia in the human body is produced and absorbed in the gastrointestinal tract (Romero-Gomez et al., 2009). After absorption, most of the ammonia in the portal vein is detoxified through the urea cycle, and the rest is removed by glutamine synthetase in liver cells around the vein, which catalyzes the reaction of ammonia with glutamate to produce glutamine (Wright et al., 2011). In the condition of HF, the function of urea cycle is weakened, resulting in the accumulation of ammonia (Dabos et al., 2015). On the other hand, liver injury can lead to the dysfunction of glutamine synthetase, which can not effectively catalyze the combination of glutamate and ammonia, leading to the increase of blood ammonia. Clinical studies have shown that reduction of urea production and hyperammonemia are characteristic phenomena in patients with HF (Weissenborn et al., 2007). In this study, the levels of citrulline and glutamine in feces of rats with HF were significantly decreased, indicating that the urea cycle was weakened and the ammonia clearance pathway was blocked. After YCWLP intervention, the levels of citrulline and glutamine were significantly increased (**Figure 6B**), indicating YCWLP could improve the urea cycle, promote glutamine synthesis and reduce ammonia accumulation.

In addition, the small intestinal bacterial overgrowth and the damage of the intestinal mucosal barrier caused by HF will also lead to the increase of ammonia production, and a large amount of ammonia will be absorbed into the blood circulation, resulting

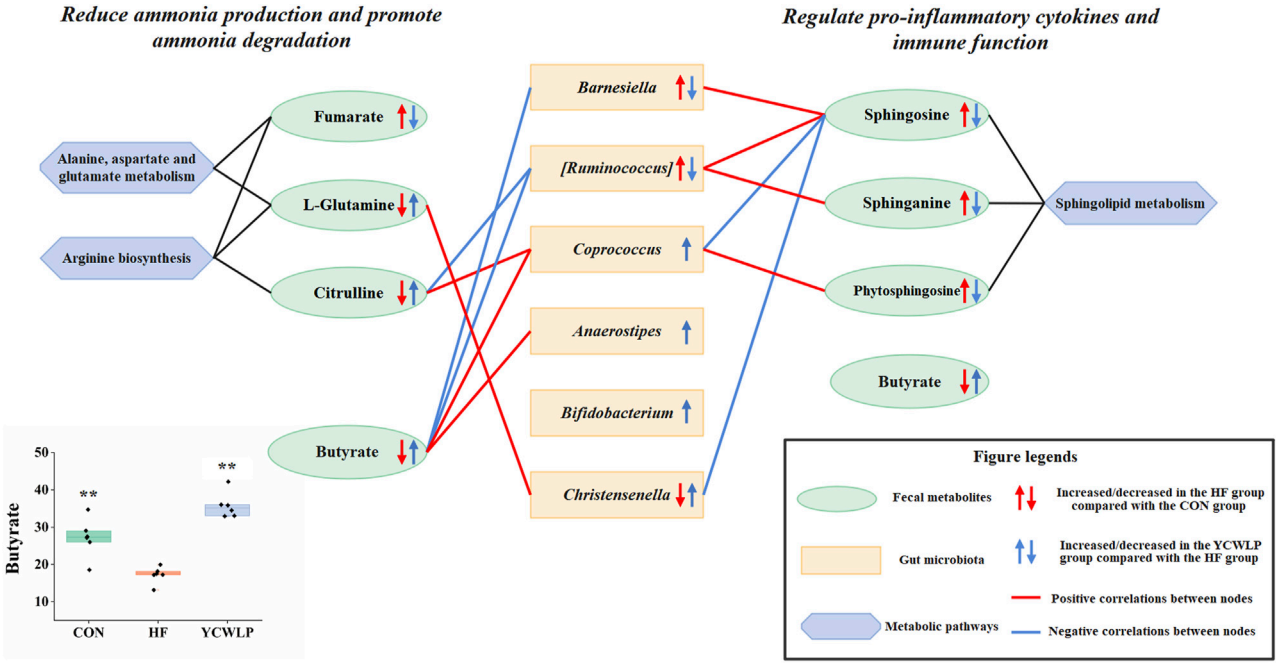

FIGURE 5 | Mechanism of YCWLP in the treatment of HF based on the interactions between gut microbiota and host metabolism. Significant difference compared with the HF group: * *p*-value < 0.05; ** *p*-value < 0.01.

in the accumulation of blood ammonia. The metagenomic experiment confirmed that the genes related to ammonia metabolism and amino acid transport in the gut microbiota of patients with HF were highly expressed (Qin et al., 2014). In this study, Spearman's correlation analysis showed that citrulline was negatively correlated with [*Ruminococcus*], and positively correlated with *Rothia*, *Robinsoniella*, *rc4-4*, *Faecalibacterium* and *Coprococcus*. Glutamine was positively correlated with *Rothia*, *Robinsoniella*, *Faecalibacterium*, *rc4-4* and *Christensenella*, and negatively correlated with *Roseburia*. Among these genera, YCWLP could significantly affect the relative abundance of [*Ruminococcus*], *Coprococcus* and *Christensenella*. In 16Sr RNA sequencing analysis [*Ruminococcus*] was the most critical genus in the treatment of HF with YCWLP, which was significantly enriched in HF rats. Ammonia is the necessary nitrogen source for the growth and reproduction of [*Ruminococcus*]. Therefore, we speculated that the accumulation of ammonia in the intestine of HF rats might be responsible for its enrichment. However, YCWLP treatment could significantly reduce the abundance of [*Ruminococcus*], which might be related to its effect of reducing ammonia accumulation. As mentioned before, *Coprococcus* was the characteristic genus of YCWLP-treated rats, which could reduce ammonia production and absorption by producing butyrate.

In summary, YCWLP could promote the production of butyrate to reduce the production and absorption of ammonia by improving the abundance of butyrate-producing bacteria. On the other hand, YCWLP could accelerate ammonia elimination by promoting urea cycle and glutamine synthesis.

Sphingolipid Metabolism

Sphingolipids (SLs), as a class of bioactive lipids, are the main structural components of the cell membrane (Kraft, 2017). SLs mainly include ceramide, sphingosine and sphingosine-1-phosphate, which participate in the occurrence and development of liver diseases by regulating cell proliferation and differentiation, gene expression and apoptosis (Ilan, 2019). Studies have shown that liver injury can lead to the disturbance of sphingosine metabolism and significant changes of the related substances (Acunha et al., 2018). In this study, the levels of sphingosine, sphinganine and phytosphingosine in the feces of HF rats were significantly increased (**Figure 6B**), indicating that the metabolism of sphingolipid was disordered. In the organism, sphingosine, sphinganine and phytosphingosine play an important role in ceramide production (**Figure 6A**). Ceramide has been proved to be implicated in inflammation, which can attenuate LPS response in macrophages and regulate T cell function (Ali et al., 2015). Inhibition of ceramide synthesis may affect pro-inflammatory cytokine signaling and immune cell chemotaxis to a certain extent, further aggravating the liver injury (Montefusco et al., 2018). YCWLP treatment could significantly restore the levels of sphingosine, sphinganine and phytosphingosine (**Figure 6B**), indicating that YCWLP could regulate the disorder of sphingosine metabolism in HF rats, and treat HF by regulating pro-inflammatory cytokines and immune function.

Spearman's correlation analysis showed that sphingosine was positively correlated with *Bilophila*, *Barnesiella* and [*Ruminococcus*], while negatively correlated with *Rothia*, *rc4-4*, *Christensenella* and *Coprococcus*. Sphinganine was positively

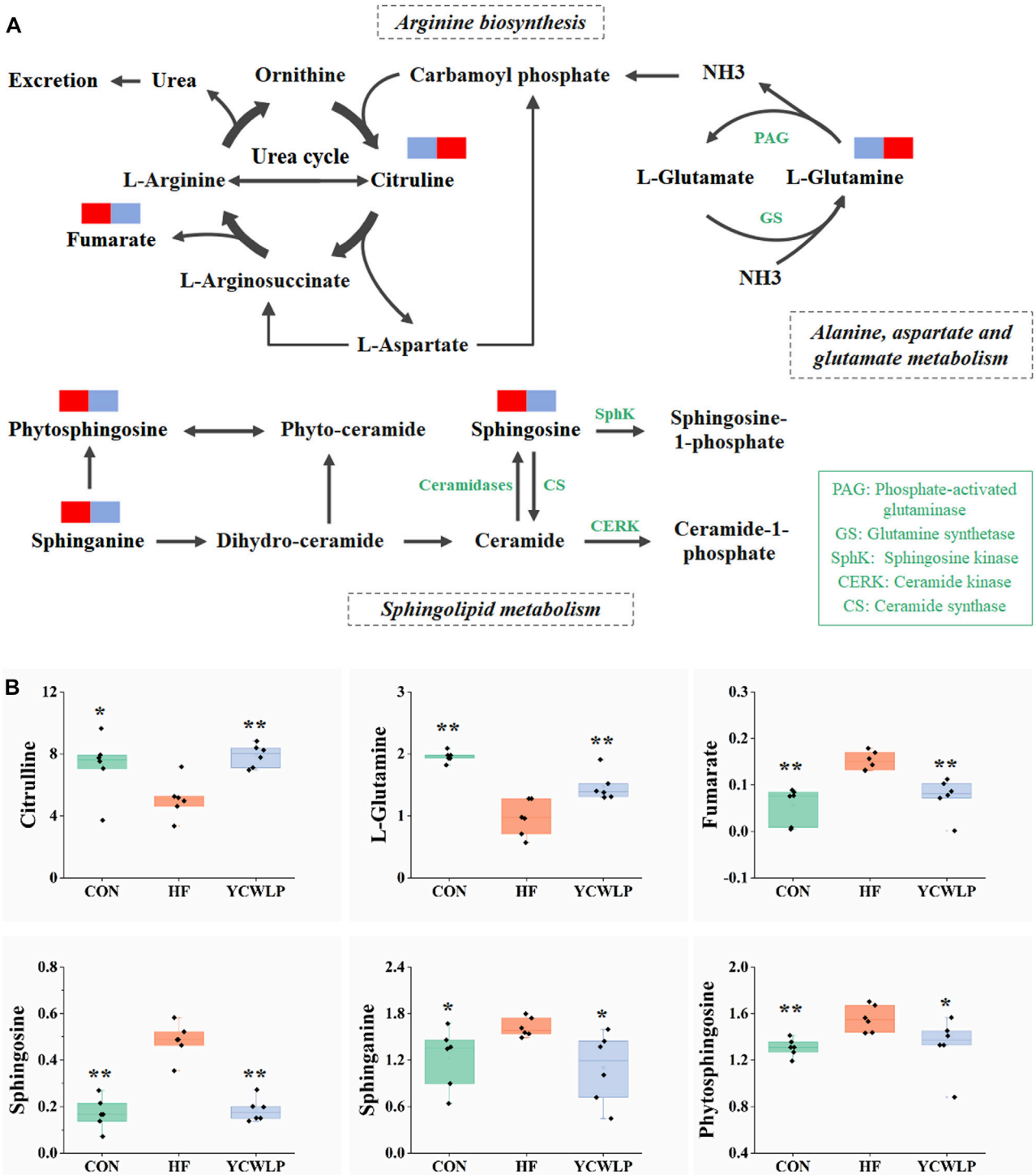

FIGURE 6 | Schematic of arginine biosynthesis, sphingolipid metabolism and alanine, aspartate and glutamate metabolism pathways **(A)** and the related metabolites **(B)**. The blue rectangles in **(A)** represent being significantly down-regulated, and the red rectangles represent being significantly up-regulated. Significant difference compared with the HF group: * p-value < 0.05; ** p-value < 0.01.

correlated with *Bilophila* and [*Ruminococcus*]. Phytosphingosine was positively correlated with *Bilophila*, *Desulfovibrio* and [*Ruminococcus*], while negatively correlated with *Rothia* and *Robinsoniella*. Given these correlations, it's likely the modulatory effects of YCWLP on sphingolipid metabolism might occur by affecting the relative abundances of *Barnesiella*, [*Ruminococcus*], *Christensenella*, *Coprococcus* and *Anaerostipes*.

CONCLUSION

In this study, an integrated method of 16S rRNA gene sequencing combined with ^{1}H NMR and UPLC-MS based metabolomics was performed to evaluate the effects of YCWLP on the gut microbiota and the interaction between gut microbiota and host metabolism in rats with CCl_4-induced HF. The therapeutic mechanisms of YCWLP on HF were likely linked to restoring the dysbiosis of *Barnesiella* [*Ruminococcus*] and *Christensenella*, increasing the relative abundance of *Bifidobacterium*, *Coprococcus* and *Anaerostipes* which closely related to butyrate production, and regulating the disorder of arginine biosynthesis, sphingolipid metabolism and alanine, aspartate and glutamate metabolism in HF rats (**Figure 5**). These regulatory effects suggested that YCWLP might treat HF by reducing ammonia production and promoting ammonia degradation, regulating pro-inflammatory cytokines and immune function. Moreover, we found that butyrate plays a pivotal role in the treatment of HF by YCWLP. Increasing the abundance of butyrate-producing bacteria might be an important therapeutic mechanism of YCWLP on HF. Our study focuses on the interaction mechanism between gut microbiota and host metabolisms, which provides new insights into the potential anti-fibrosis mechanism of YCWLP and lays a foundation for further development of YCWLP as a potential strategy in treating HF. However, although non-targeted metabolomics analysis covers a wide range of endogenous substances, it still has the weakness of low sensitivity and selectivity. Besides, 16S rRNA analysis lacks the ability to predict the function of gut microbiota. Therefore, the detailed modulatory effects of YCWLP on gut microbiota and fecal metabolism needs to be further investigated by metagenomics and targeted metabolomics.

DATA AVAILABILITY STATEMENT

The data generated in this article can be found in NCBI using accession PRJNA732726.

ETHICS STATEMENT

The animal study was reviewed and approved by the Medical Ethics Committee of Shenyang Pharmaceutical University.

AUTHOR CONTRIBUTIONS

YZ, XJ and TL designed and performed the study; YZ, MZ, XJ and QQ performed analysis and interpreted the data; YZ, MZ and TL drafted the manuscript; MZ and CZ revised the manuscript; CZ and MW supervised research and provided funding.

FUNDING

This work was supported by the National Natural Science Foundation of China (NSFC: 81973284).

SUPPLEMENTARY MATERIAL

The Supplementary Material for this article can be found online at: https://www.frontiersin.org/articles/10.3389/fphar.2021.713197/full#supplementary-material.

REFERENCES

Acunha, T., García-Cañas, V., Valdés, A., Cifuentes, A., and Simó, C. (2018). Metabolomics Study of Early Metabolic Changes in Hepatic HepaRG Cells in Response to Rosemary Diterpenes Exposure. *Analytica Chim. Acta* 1037, 140–151. doi:10.1016/j.aca.2017.12.006

Ali, M., Saroha, A., Pewzner-Jung, Y., and Futerman, A. H. (2015). LPS-mediated Septic Shock Is Augmented in Ceramide Synthase 2 Null Mice Due to Elevated Activity of TNFα-Converting Enzyme. *Febs Lett.* 589 (17), 2213–2217. doi:10.1016/j.febslet.2015.06.045

Allen, J. M., Mailing, L. J., Niemiro, G. M., Moore, R., Cook, M. D., White, B. A., et al. (2018). Exercise Alters Gut Microbiota Composition and Function in Lean and Obese Humans. *Med. Sci. Sport Exer.* 50 (4), 747–757. doi:10.1249/MSS.0000000000001495

Andruszkow, J., Hartleben, B., Schlué, J., Ritz, T., Knüchel, R., Hasan, A., et al. (2019). Staging der Leberfibrose bei Gallengangatresie. *Pathologe* 40 (1), 85–92. doi:10.1007/s00292-018-0558-z

Boursier, J., Mueller, O., Barret, M., Machado, M., Fizanne, L., Araujo-Perez, F., et al. (2016). The Severity of Nonalcoholic Fatty Liver Disease Is Associated with Gut Dysbiosis and Shift in the Metabolic Function of the Gut Microbiota. *Hepatology* 63 (3), 764–775. doi:10.1002/hep.28356

Chang, C.-J., Lin, C.-S., Lu, C.-C., Martel, J., Ko, Y.-F., Ojcius, D. M., et al. (2017). Correction: Corrigendum: Ganoderma Lucidum Reduces Obesity in Mice by Modulating the Composition of the Gut Microbiota. *Nat. Commun.* 8 (6), 16130. doi:10.1038/ncomms16130

Chen, B. (2012). Clinical Study of Yinchen Wuling Powder on Liver Function and Serum Indexes in Patients with Liver Fibrosis. *Shandong J. Tradit. Chin. Med.* 31 (03), 162–164. doi:10.16295/j.cnki.0257-358x.2012.03.028

Chen, H. D. (2018). "Study for the Correlation between Desulfovibrio and Liver Fibrosis," (China: Jiangnan University). Dissertation/Master's thesis.

Chen, R., Liao, C., Guo, Q., Wu, L., Zhang, L., and Wang, X. (2018). Combined Systems Pharmacology and Fecal Metabonomics to Study the Biomarkers and Therapeutic Mechanism of Type 2 Diabetic Nephropathy Treated with Astragalus and Leech. *RSC Adv.* 8, 27448–27463. doi:10.1039/c8ra04358b

Clarke, K. R. (1993). Non-parametric Multivariate Analyses of Changes in Community Structure. *Austral Ecol.* 18, 117–143. doi:10.1111/j.1442-9993.1993.tb00438.x

Corrêa-Oliveira, R., Fachi, J. L., Vieira, A., Sato, F. T., and Vinolo, M. A. (2016). Regulation of Immune Cell Function by Short-Chain Fatty Acids. *Clin. Transl Immunol.* 5, e73. doi:10.1038/cti.2016.17

Dabos, K. J., Parkinson, J. A., Sadler, I. H., Plevris, J. N., and Hayes, P. C. (2015). 1H Nuclear Magnetic Resonance Spectroscopy-Based Metabonomic Study in Patients with Cirrhosis and Hepatic Encephalopathy. *World J. Hepatol.* 7 (12), 1701–1707. doi:10.4254/wjh.v7.i12.1701

Del Chierico, F., Nobili, V., Vernocchi, P., Russo, A., De Stefanis, C., Gnani, D., et al. (2017). Gut Microbiota Profiling of Pediatric Nonalcoholic Fatty Liver Disease and Obese Patients Unveiled by an Integrated Meta-omics-based Approach. *Hepatology* 65 (2), 451–464. doi:10.1002/hep.28572

Deng, J., Guo, W., Guo, J., Li, Y., Zhou, W., Lv, W., et al. (2020). Regulatory Effects of a Grifola Frondosa Extract Rich in Pseudobaptigenin and Cyanidin-3-O-Xylosylrutinoside on Glycolipid Metabolism and the Gut Microbiota in High-Fat Diet-Fed Rats. *J. Funct. Foods* 75, 104230. doi:10.1016/j.jff.2020.104230

Dhiman, R. K., Rana, B., Agrawal, S., Garg, A., Chopra, M., Thumburu, K. K., et al. (2014). Probiotic VSL#3 Reduces Liver Disease Severity and Hospitalization in Patients With Cirrhosis: A Randomized, Controlled Trial. *Gastroenterology* 146, 1327–1337. doi:10.1053/j.gastro.2014.08.031

Feng, W., Ao, H., and Peng, C. (2018). Gut Microbiota, Short-Chain Fatty Acids, and Herbal Medicines. *Front. Pharmacol.* 9, 1354. doi:10.3389/fphar.2018.01354

Guo, J., and Friedman, S. L. (2010). Toll-like Receptor 4 Signaling in Liver Injury and Hepatic Fibrogenesis. *Fibrogenesis Tissue Repair* 3 (21). doi:10.1186/1755-1536-3-21

Ilan, Y. (2019). Immune Rebalancing by Oral Immunotherapy: A Novel Method for Getting the Immune System Back on Track. *J. Leukoc. Biol.* 105 (3), 463–472. doi:10.1002/JLB.5RU0718-276RR

Jian, C., Luukkonen, P., Sädevirta, S., Yki-Järvinen, H., and Salonen, A. (2021). Impact of Short-Term Overfeeding of Saturated or Unsaturated Fat or Sugars on the Gut Microbiota in Relation to Liver Fat in Obese and Overweight Adults. *Clin. Nutr.* 40 (1), 207–216. doi:10.1016/j.clnu.2020.05.008

Jiang, N., Song, X., Peng, Y. M., Wang, W. N., and Song, Z. (2020). Association of Disease Condition with Changes in Intestinal flora, and Plasma Endotoxin and Vascular Endothelial Growth Factor Levels in Patients with Liver Cancer. *Eur. Rev. Med. Pharmacol. Sci.* 24 (7), 3605–3613. doi:10.26355/eurrev_202004_20822

Kraft, M. L. (2017). Sphingolipid Organization in the Plasma Membrane and the Mechanisms that Influence it. *Front. Cel Dev. Biol.* 4, 154. doi:10.3389/fcell.2016.00154

Li, Q., Liu, F., Liu, J., Liao, S., and Zou, Y. (2019). Mulberry Leaf Polyphenols and Fiber Induce Synergistic Antiobesity and Display a Modulation Effect on Gut Microbiota and Metabolites. *Nutrients* 11 (5), 1017. doi:10.3390/nu11051017

Li, Z., Ni, M., Yu, H., Wang, L., Zhou, X., Chen, T., et al. (2020). Gut Microbiota and Liver Fibrosis: One Potential Biomarker for Predicting Liver Fibrosis. *Biomed. Res. Int.* 2020, 1–15. doi:10.1155/2020/3905130

Liu, X., Lv, M., Wang, Y., Zhao, D., Zhao, S., Li, S., et al. (2020). Deciphering the Compatibility Rules of Traditional Chinese Medicine Prescriptions Based on NMR Metabolomics: A Case Study of Xiaoyaosan. *J. Ethnopharmacol.* 254, 112726. doi:10.1016/j.jep.2020.112726

Liu, X. L., and Zhao, L. H. (2011). 50 Cases of Nonalcoholic Fatty Liver Treated with Yinchen Wuling Powder. *Shanxi J. Tradit. Chin. Med.* 32 (05), 520–521.

Ma, Q. (2020). The Therapeutic Effect of Yinchen Wuling Powder on Children with Acute Jaundice Hepatitis. *Chin. Pediatr. Integr. Tradit. West. Med.* 12 (03), 258–260.

Montefusco, D. J., Allegood, J. C., Spiegel, S., and Cowart, L. A. (2018). Non-alcoholic Fatty Liver Disease: Insights from Sphingolipidomics. *Biochem. Biophys. Res. Commun.* 504 (3), 608–616. doi:10.1016/j.bbrc.2018.05.078

Nicholson, J. K., Holmes, E., Kinross, J., Burcelin, R., Gibson, G., Jia, W., et al. (2012). Host-gut Microbiota Metabolic Interactions. *Science* 336 (6068), 1262–1267. doi:10.1126/science.1223813

Pinzani, M., and Rombouts, K. (2004). Liver Fibrosis: from the Bench to Clinical Targets. *Dig. Liver Dis.* 36 (4), 231–242. doi:10.1016/j.dld.2004.01.003

Qin, N., Yang, F., Li, A., Prifti, E., Chen, Y., Shao, L., et al. (2014). Alterations of the Human Gut Microbiome in Liver Cirrhosis. *Nature* 513 (7516), 59–64. doi:10.1038/nature13568

Romero-Gómez, M., Jover, M., Galán, J. J., and Ruiz, A. (2009). Gut Ammonia Production and its Modulation. *Metab. Brain Dis.* 24 (1), 147–157. doi:10.1007/s11011-008-9124-3

Santiago, G. T., Contreras, J. I. S., Camargo, M. E. M., and Vallejo, L. G. Z. (2019). NMR-based Metabonomic Approach Reveals Changes in the Urinary and Fecal Metabolome Caused by Resveratrol. *J. Pharm. Biomed. Anal.* 162 (5), 234–241. doi:10.1016/j.jpba.2018.09.025

Scott, K. P., Martin, J. C., Duncan, S. H., and Flint, H. J. (2014). Prebiotic Stimulation of Human Colonic Butyrate-Producing Bacteria and Bifidobacteria,*In Vitro*. *Fems. Microbiol. Ecol.* 87 (1), 30–40. doi:10.1111/1574-6941.12186

Seki, E., and Schnabl, B. (2012). Role of Innate Immunity and the Microbiota in Liver Fibrosis: Crosstalk between the Liver and Gut. *J. Physiol.* 590 (3), 447–458. doi:10.1113/jphysiol.2011.219691

Song, J. J., Tian, W. J., Kwok, L.-Y., Wang, Y. L., Shang, Y. N., Menghe, B., et al. (2017). Effects of microencapsulatedLactobacillus plantarumLIP-1 on the Gut Microbiota of Hyperlipidaemic Rats. *Br. J. Nutr.* 118 (7), 481–492. doi:10.1017/S0007114517002380

Usami, M., Miyoshi, M., and Yamashita, H. (2015). Gut Microbiota and Host Metabolism in Liver Cirrhosis. *World J. Hepatol.* 21 (41), 11597–11608. doi:10.3748/wjg.v21.i41.11597

Wahlström, A., Sayin, S. I., Marschall, H.-U., and Bäckhed, F. (2016). Intestinal Crosstalk between Bile Acids and Microbiota and its Impact on Host Metabolism. *Cel Metab.* 24 (1), 41–50. doi:10.1016/j.cmet.2016.05.005

Wei, Z. S., Augusto, L. A., Zhao, L. P., and Caroff, M. (2015). Desulfovibrio Desulfuricans Isolates from the Gut of a Single Individual: Structural and Biological Lipid A Characterization. *Febs. Lett.* 589 (1), 165–171. doi:10.1016/j.febslet.2014.11.04210.1016/j.febslet.2015.04.002

Weissenborn, K., Ahl, B., Fischer-Wasels, D., van den Hoff, J., Hecker, H., Burchert, W., et al. (2007). Correlations between Magnetic Resonance Spectroscopy Alterations and Cerebral Ammonia and Glucose Metabolism in Cirrhotic Patients with and without Hepatic Encephalopathy. *Gut* 56 (12), 1736–1742. doi:10.1136/gut.2006.110569

Williams, R. (2006). Global Challenges in Liver Disease. *Hepatology* 44 (3), 521–526. doi:10.1002/hep.21347

Woodhouse, C. A., Patel, V. C., Singanayagam, A., and Shawcross, D. L. (2018). Review Article: the Gut Microbiome as a Therapeutic Target in the Pathogenesis and Treatment of Chronic Liver Disease. *Aliment. Pharmacol. Ther.* 47 (2), 192–202. doi:10.1111/apt.14397

Wright, G., Noiret, L., Olde Damink, S. W. M., and Jalan, R. (2011). Interorgan Ammonia Metabolism in Liver Failure: the Basis of Current and Future Therapies. *Liver Int.* 31 (2), 163–175. doi:10.1111/j.1478-3231.2010.02302.x

Xu, J., Lian, F., Zhao, L., Zhao, Y., Chen, X., Zhang, X., et al. (2015). Structural Modulation of Gut Microbiota during Alleviation of Type 2 Diabetes with a Chinese Herbal Formula. *ISME J.* 9 (3), 552–562. doi:10.1038/ismej.2014.177

Yu, M., Jia, H.-M., Zhou, C., Yang, Y., Sun, L.-L., and Zou, Z.-M. (2017). Urinary and Fecal Metabonomics Study of the Protective Effect of Chaihu-Shu-Gan-San on Antibiotic-Induced Gut Microbiota Dysbiosis in Rats. *Sci. Rep.* 7 (1), 46551. doi:10.1038/srep46551

Zhang, Y., Zhao, M., Liu, Y., Liu, T., Zhao, C., and Wang, M. (2021). Investigation of the Therapeutic Effect of Yinchen Wuling Powder on CCl4-Induced Hepatic Fibrosis in Rats by 1H NMR and MS-based Metabolomics Analysis. *J. Pharm. Biomed. Anal.* 200, 114073. doi:10.1016/j.jpba.2021.114073

Zierer, J., Jackson, M. A., Kastenmüller, G., Mangino, M., Long, T., Telenti, A., et al. (2018). The Fecal Metabolome as a Functional Readout of the Gut Microbiome. *Nat. Genet.* 50 (6), 790–795. doi:10.1038/s41588-018-0135-7

Conflict of Interest: The authors declare that the research was conducted in the absence of any commercial or financial relationships that could be construed as a potential conflict of interest.

Publisher's Note: All claims expressed in this article are solely those of the authors and do not necessarily represent those of their affiliated organizations, or those of the publisher, the editors and the reviewers. Any product that may be evaluated in this article, or claim that may be made by its manufacturer, is not guaranteed or endorsed by the publisher.

frontiers in Pharmacology

ORIGINAL RESEARCH
published: 02 September 2021
doi: 10.3389/fphar.2021.695035

Efficacy of Zhuyu Pill Intervention in a Cholestasis Rat Model: Mutual Effects on Fecal Metabolism and Microbial Diversity

Han Yu[1], *Chao Liu*[1], *Fenghua Zhang*[1], *Jianfei Wang*[2], *Jun Han*[3], *Xin Zhou*[1], *Yueqiang Wen*[1]* *and Tao Shen*[1]*

[1]School of Basic Medicine, Chengdu University of Traditional Chinese Medicine, Chengdu, China, [2]Department of Nephrology, South of Guang'anmen Hospital, Beijing, China, [3]Department of Reader Service and Culture Education, Chengdu University of Traditional Chinese Medicine, Chengdu, China

Cholestasis is a clinical condition resulting from impaired bile flow. Currently, patients with cholestasis face several barriers in seeking diagnosis and treatment. Zhuyu Pill (ZYP) is an ancient classic formula of the Coptis-Evodia herb couples (CEHC), and has been used for cholestasis treatment in the clinic, however, its underlying biological activity in cholestasis remain to be clarified. In this study, an α-naphthyl-isothiocyanate (ANIT, 50 mg/kg)-induced rat model of cholestasis was treated with ZYP. Serum biochemical indices and histopathological evaluation was performed, together with the metabolomics analyses of feces and 16S rDNA sequencing of the fecal microbiota. We evaluated the anti-cholestatic activity of ZYP and investigated the mechanisms underlying its correlation with fecal microbiota and fecal metabolite regulation. The relationships between biochemical indices and changes in gene expression associated with liver injury, levels fecal metabolites, and composition of fecal microbiota were analyzed. The results showed that both high (1.2 g/kg) and low (0.6 g/kg) doses of ZYP could effectively improve biochemical parameters in the blood of cholestasis-induced rat models; the intervention effect of high dose ZYP was superior to that that of lower dose ZYP. Based on a metabolomics test of fecal samples, significantly altered metabolites in the ANIT and ZYP treatment group were identified. In total, 734 metabolites were differentially expressed, and whose biological functions were mainly associated with amino acid metabolism, steroid hormone biosynthesis, and bile secretion. In addition, sequencing of the 16S rDNA unit in fecal samples revealed that the ZYP could improve the fecal microbiota dysbiosis that ANIT had induced. Therefore, we conclude that ANIT altering of blood biochemical and metabolic profiles and of fecal microbiota could effectively be alleviated with ZYP treatment. This study contributes to the "TCM wisdom" applied in clinical diagnosis and treatment of cholestasis.

Keywords: cholestasis, zhuyu pill, fecal metabolism, fecal microbial diversity, mutual effects

OPEN ACCESS

Edited by:
Annabella Vitalone, Sapienza University of Rome, Italy

Reviewed by:
Pedro Miguel Rodrigues, Biodonostia Health Research Institute (IIS Biodonostia), Spain
Rachel McQuade, University of Melbourne, Australia

***Correspondence:**
Yueqiang Wen
wenyueqiang@cdutcm.edu.cn
Tao Shen
st@cdutcm.edu.cn

Specialty section:
This article was submitted to Gastrointestinal and Hepatic Pharmacology, a section of the journal Frontiers in Pharmacology

Received: *14 April 2021*
Accepted: *23 August 2021*
Published: *02 September 2021*

Citation:
Yu H, Liu C, Zhang F, Wang J, Han J, Zhou X, Wen Y and Shen T (2021) Efficacy of Zhuyu Pill Intervention in a Cholestasis Rat Model: Mutual Effects on Fecal Metabolism and Microbial Diversity. Front. Pharmacol. 12:695035. doi: 10.3389/fphar.2021.695035

Abbreviation: CEHC, Coptis-Evodia herb couple; TCM, Traditional Chinese medicine; ZYP, Zhuyu Pill; ZYP-, ZYP-low dose; ZYP+, ZYP-high dose.

INTRODUCTION

In recent years, changes in dietary habits and living environments, the incidence of liver diseases, and associated complications represent a major healthcare burden in China (Tang et al., 2017). Cholestasis, which can be caused by pre-existing medical conditions including infections, drug treatment, and metabolic or genetic disorders (Boyer, 2007), is classified as intrahepatic, involving mainly liver parenchymal cells, or extrahepatic, involving any excretory block outside of the liver (Chatterjee et al., 2020). A cross-sectional study of cholestasis in 1000 patients in China demonstrated that, the biochemical parameters in the blood of intrahepatic cholestasis, such as alkaline phosphatase (ALP) and γ-glutamyl transferase (γ-GT), were higher than the upper limit of normal, and the risk and severity of liver damage in these patients were markedly increased (Cheng et al., 2015). Due to the lack of timely treatment, liver cells, including portal myofibroblasts and hepatic stellate cells, are hyperactivated and cholestasis leads to fibrosis and even cirrhosis (Allen et al., 2011). Currently available therapeutic options of cholestasis are limited.

Bile acids such as ursodeoxycholic acid (UDCA) and chenodeoxycholic acid (CDCA) are used routinely for the dissolution of gallstones and have recently been proposed as treatment for chronic cholestatic liver disease (Crosignani et al., 1996; Beuers et al., 1998; Sasaki et al., 2001). However, approximately one-third of patients achieve little or no response to UDCA treatment (Itakura et al., 2004; Lane and Murray, 2017). Traditional Chinese medicine (TCM) has been used to treat liver and digestive disease in China since ancient times. *Coptidis rhizoma* (Coptis, Huanglian in Chinese) and *Evodiae fructus* (Evodia, Wuzhuyu in Chinese) is a well-known herbal combination usually used to treat liver and digestive diseases. *Zuojin Pill* (ZJP, usually in a mixture ratio 6:1, g/g) and *Zhuyu Pill* (ZYP, usually in mixture ratio 1:1, g/g) are the ancient classic formulas of the Coptis-Evodia herb couple (CEHC). To date, studies have shown that ZJP can influence the metabolism of venlafaxine (Cheng et al., 2011), the brain-gut axis, and cell proliferation, and its therapeutic effects in liver and stomach diseases have been reported (Wang et al., 2015; Guo et al., 2019). These results support the CEHC combination for the treatment of liver and digestive diseases. However, compared with ZJP, less attention has been paid to ZYP and the efficacy and effector mechanisms of ZYP remain to be examined.

TCM is a complex therapy involving multiple targets with synergistic or antagonistic interactions among its components. In contrast to the Western medicine notion of "one target, one drug," TCM is characterized by "multi-component, multi-target, and multi-pathway" activity; this concept of the holistic view is emphasized in the theory of TCM. Metabonomics is an important technique in systems biology (Kaddurah-Daouk et al., 2008). It is the study of the composition and variation of metabolic groups, and thereby reveals the overall metabolic response and dynamic changes induced under different conditions. Metabonomics has been used to study the organism as a whole, which is consistent with the holistic view of TCM and the concept of syndrome differentiation and treatment (Wang et al., 2017). Because the modernization of TCM is becoming necessary and urgent (Li et al., 2008), metabolomics represents a modern technology with a great potential toward understanding the efficacy and mechanism of TCM (Sun et al., 2012; Wang et al., 2020).

Intestinal microecology not only comprises the gut microbiota, but also numerous gut microbiota metabolites (Chen C. et al., 2019). Hence, the gut microbiota can be defined as a "metabolic organ" (Wei et al., 2020). Recent studies have shown that, bile acids (BAs) are host-derived and microbial-modified metabolites that regulate both the gut microbiome and host metabolism (Islam et al., 2011; Wahlstrom et al., 2016; Kemis et al., 2019). The fecal metabolome provides unique information on the metabolic interactions between the fecal microbiota, diet, and host. Combined with 16S next-generation-sequencing, the metabolome can provide a comprehensive phenotype of the host-microbiome interplay (Yang et al., 2019).

In this study, an animal model of cholestasis was induced using α-naphthylisothiocyanate (ANIT) (Hill et al., 1999) and the pharmacodynamic effects were evaluated by changes in serum biochemical indices, liver histopathology, liver inflammation, apoptosis, and gene expression associated with fibrosis. Differential metabolites levels were identified using liquid chromatography-mass spectrometry (LC-MS) with an untargeted metabolomics approach and the abundance of fecal microbiota was analyzed using 16S ribosomal RNA (16S rRNA). In addition, to characterizing the mechanisms of ZYP activity in regulating cholestasis, we aimed: *1*) to explore the effects of ZYP on improving liver function; *2*) to measure the composition of the fecal microbiota in order to identify differential metabolites induced of ZYP in cholestasis; and *3*) to correlate the results of untargeted metabolomics and the diversity of fecal microbes to better define the underlying biological mechanisms involved in the anticholestatic activity of ZYP. These findings will enhance our understanding of pathogenic mechanisms of cholestasis and will provide a new therapeutic option for the treatment of cholestasis.

MATERIALS AND METHODS

Reagents

ANIT was purchased from Sigma-Aldrich Co. (St. Louis, MO, United States). *Coptidis rhizoma* and *Evodiae fructus* were purchased from Beijing Tongrentang Science and Technology Development Co. Ltd (Beijing, China). Water, methanol, acetonitrile, and formic acid were purchased from the CNW Technologies GmbH (Düsseldorf, Germany). L,-2-chlorophenylalanine was from Shanghai Hengchuang Biotechnology Co., Ltd. (Shanghai, China). All chemicals and solvents were analytical or HPLC grade.

Preparation and Quality Control of ZYP

Zhuyu Pill was prepared as follows: *Coptidis rhizoma* (6 g), and *Evodiae fructus* (6 g) were weighed and placed in 120 ml of distilled water (1:10, w/v) for 6 h. These samples were then boiled twice, for 45 min each time.

TABLE 1 | The schematic diagram of the animal experimental design.

Group	week old	1–7 days	8–13 days	14 days	15–18 days	19 days
Control	7–8	acclimate	distilled water	Olive Oil	distilled water	Sacrifice
Model	7–8	acclimate	distilled water	50 mg/kg ANIT	distilled water	Sacrifice
ZYP–	7–8	acclimate	0.6 g/kg ZYP	50 mg/kg ANIT	0.6 g/kg ZYP	Sacrifice
ZYP+	7–8	acclimate	1.2 g/kg ZYP	50 mg/kg ANIT	1.2 g/kg ZYP	Sacrifice

To determine the active constituents, two main alkaloids (berberine and coptisine) in ZYP were analyzed by HPLC using the Agilent 1260 Infinity II (Agilent Technologies Inc., California, United States). The chromatographic separation was carried out with a Welch Ultimate XB-C18 Column (4.6 mm × 250 mm, 5 μm, Maryland, United States) at a column temperature of 30°C. The linear-gradient mobile phase consisted of mobile phase A (50 mM monopotassium phosphate+0.4% sodium heptane sulfonate, pH = 4) and mobile phase B (pure methanol). The gradient of the mobile phase was utilized (0–15 min, 95% A, 5% B; 15–40 min, 50% A, 50% B; 40–55 min, 30% A, 70% B, 55–60 min, 95% A, 5% B), and a flow rate of 1.0 ml/min was adopted. The detection wavelength was set as (0–44 min, 345 nm; 44–48 min, 226 nm; 48–60 min, 345 nm). The HPLC analysis showed that the contents of berberine and coptisine in ZYP were 33.2 and 13.4 mg/g, respectively.

Animals and Treatments

A total of 24 male Sprague-Dawley rats (7–8 wk old; weighing 260 ± 20 g) were obtained from Beijing HFK Bioscience Co., Ltd. (Beijing, China; certification no. SCXK-JING 2019-0008). All animals were allowed to acclimate for 1 wk prior to the experiments and were maintained at a constant temperature (25 ± 2°C) and 50% humidity with a 12-h/12-h light/dark cycle; all the rats had access to water and food *ad libitum*.

An overview of the experimental design is presented in **Table 1**. The animals were randomly divided into four groups of six rats each, including the control, model, ZYP-low dose (ZYP–) and ZYP-high dose (ZYP+) groups. The rats in the normal group served as the normal control and were given distilled water each day and treated with vehicle (olive oil) alone. The model group was treated with 50 mg/kg ANIT dissolved in an equal volume of olive oil by gavage (Chen et al., 2016). ZYP was given to the treatment groups at doses of 0.6 (ZYP–), 1.2 (ZYP+) g/kg body weight, respectively, six times before and four times after they were treated with 50 mg/kg ANIT by gavage. In this study, ZYP doses that were adopted were based on the maximum recommended clinical dose (MRCD, 12 g/60 kg/day).

ETHICS APPROVAL AND CONSENT TO PARTICIPATE

The study protocol was performed in strict accordance with the recommendations of the Guidelines for the Care and Use of Laboratory Animals of the Ministry of Science and Technology of China, and was approved by Ethics Committee of Chengdu University of Traditional Chinese Medicine (Chengdu, China). All efforts were made to minimize animal suffering.

Sample Collection, Liver Function, and Gene Expression Assays

The rats were provided with standard chow and water on completion of treatments. At least two fresh stools pellets were obtained from each rat after the last ZYP administration. Samples were placed in sterile conical tubes and immediately frozen at −80°C until further metabolic profiling and microbial community analysis, respectively.

According to pilot experiments, the rats were then fasted for 12 h, and were then euthanized 12 h after the last ZYP administration. Blood samples were collected from the inferior vena cava and the liver was excised from each rat immediately after sacrifice. The blood samples were collected and centrifuged at 3500 × g and 4°C for 15 min to obtain the serum. The serum total cholesterol (TC; cat. no. 105-000448-00), aspartate aminotransferase (AST; cat. no. 105-000443-00), alanine aminotransferase (ALT; cat. no. 105-000442-00), γ-glutamyl transpeptidase (γ-GT; cat. no. 105-000445-00), total bilirubin (TBIL; cat. no. 0041-30-53548) and total bile acid (TBA; cat. no. 105-000456-00) levels were detected using a fully automatic biochemical analyzer (BS-240VET), which together with all assay kits were purchased from Mindray Bio-medical Electronics Company (Mindray Bio-medical Electronics Company, Ltd, Shenzhen, China).

Total RNA of liver samples was extracted by mirVana™ RNA Isolation Kit (Cat. AM1561; Thermo Fisher Scientific, Waltham, MA, United States). The expression of tumour necrosis factor alpha (TNF-α), transforming growth factor beta 1 (TGF-β1), interleukin-10 (IL-10), metalloproteinase inhibitor 1 (TIMP-1), Glutamate cysteine ligase catalytic subunit (GCLC), Glutamate cysteine ligase regulatory subunit (GCLM), B-cell lymphoma 2 (BCL2) and BCL2 associated X (BAX) were detected by Quantitative Real-time PCR (qPCR). Quantification was performed using a two-step reaction process: reverse transcription (RT) and PCR. Each RT reaction (10 μl total) consisted of 0.5 μg of RNA, 2 μl of 5×TransScript All-in-one SuperMix for qPCR, and 0.5 μl of gDNA Remover. Reactions were performed in a GeneAmp® PCR System 9700 (Thermo Fisher Scientific) for 15 min at 42°C and then 5 s at 85°C. The RT reaction mix was then diluted 10× in nuclease-free water and held at −20°C.

Real-time PCR was performed using a LightCycler® 480 II Real-time PCR Instrument (Roche, Basel, Switzerland) with a

TABLE 2 | mRNA primer sequences.

Gene Symbol	Forward primer (5->3)	Reverse primer (5->3)	Product length (bp)	Tm (°C)
TNF-α	5′-CCCTGGTATGAGCCCATGTA-3′	5′-CGGACTCCGTGATGTCTAAGTA-3′	106	60
TGF-β1	5′-TACGTCAGACATTCGGGAAG-3′	5′-TACGTGTTGCTCCACAGTT-3′	97	60
IL-10	5′-CTTTAAGGGTTACTTGGGTTGC-3′	5′-TTTCTGGGCCATGGTTCTC-3′	95	60
TIMP-1	5′-GATATGTCCACAAGTCCCAGA-3′	5′-CAGTGATGTGCAAATTTCCG-3′	81	60
GCLC	5′-CCCTCTTCTTTCCAGACG-3′	5′-TGGCACATTGATGACAACC-3′	104	60
GCLM	5′-GTGTGATGCCACCAGATT-3′	5′-TTGCCTCAGAGAGCAGTTC-3′	93	60
BCL2	5′-GATTGTGGCCTTCTTTGAGT-3′	5′-CACAGAGCGATGTTGTCC-3′	90	60
BAX	5′-TGAGCTGACCTTGGAGCA-3′	5′-GTCCAGTTCATCGCCAAT-3′	85	60
ACTB	5′-GCGAGTACAACCTTCTTGC-3′	5′-TATCGTCATCCATGGCGAAC-3′	72	60

10 μl PCR reaction mixture that included 1 μl of cDNA, 5 μl of 2×PerfectStartTM Green qPCR SuperMix, 0.2 μl each of forward and reverse primers, and 3.6 μl of nuclease-free water. Reactions were incubated in a 384-well optical plate (Roche, Basel, Switzerland) at 94°C for 30 s, followed by 45 cycles of 94°C for 5 s and 60°C for 30 s. Each sample was analysed in triplicates. At the end of the PCR cycles, melting curve analysis was performed to validate the specific generation of the expected PCR product. The primer sequences were designed in the laboratory and synthesised by TsingKe Biotech based on the mRNA sequences obtained from the NCBI database (**Table 2**).

Histological Analysis of Liver Damage

Liver tissues were excised and fixed in 10% phosphate-buffered formalin. Fixed issues were cut into 1 × 1 × 0.3 cm sections. Sections were dehydrated in a gradient alcohol series, and embedded in paraffin wax blocks. The embedded wax blocks were cut into 4–5 μm thick slices. Following dewaxing slides in xylene, the slides were stained with hematoxylin and agitated for 30 s, rinsed in H_2O for 1 min, followed by staining with 1% eosin Y solution for 30 s with agitation, all at room temperature (20–25°C). Slides were examined under an Eclipse E100 microscope (NIKON, Tokyo, Japan). The degree of inflammation and necrosis were classified according to the Ishak Scoring System (Ishak et al., 1995; Goodman, 2007).

Sample Preparation for Metabolome Profiling

A 60 mg stool sample was accurately weighed and transferred to a 1.5-ml Eppendorf tube. Two small steel balls were added to the tube. A 20 μl volume of internal standard (2-chloro-l-phenylalanine in methanol, 0.3 mg/ml) and 600 μl extraction solvent with methanol/water (4/1, v/v) were added to each sample. Samples were stored at −20°C for 5 min and then ground at 60 Hz for 2 min, ultrasonicated at ambient temperature (25–28°C) for 10 min, stored at −20°C for 30 min. The extract was centrifuged at 9800 × g, 4°C for 10 min and then, a 300 μl sample of the supernatant in a brown and glass vial was dried in a freeze concentration centrifugal dryer. Next, 400 μl of a mixture of methanol and water (1/4, v/v) were added to each sample, and samples were vortexed for 30 s, ultrasonicated for 3 min, and then placed at −20°C for 2 h. Finally, samples were centrifuged at 9800 × g, at 4°C for 10 min and the supernatants (150 μl) from each tube were collected using crystal syringes, filtered through 0.22 μm microfilters, and transferred to LC vials. The vials were stored at −80°C until LC-MS analysis. QC samples were prepared by mixing aliquots of the all samples to form a pooled sample. All extraction reagents were precooled at −20°C before use.

LC-MS Analysis

A Dionex Ultimate 3000 RS UHPLC system fitted with Q-Exactive quadrupole-Orbitrap mass spectrometer equipped with heated electrospray ionization (ESI) source (Thermo Fisher Scientific) was used to analyze the metabolic profiles in both the ESI positive and ESI negative ion modes. An ACQUITY UPLC HSS T3 (100 mm × 2.1 mm, 1.8 μm) was employed in both positive and negative modes. The binary gradient elution system consisted of (A) water (containing 0.1% formic acid, v/v) and (B) acetonitrile (containing 0.1% formic acid, v/v) and separation was achieved using the following gradient: 5–20% B over 0–2 min, 20–60% B over 2–4 min, 60–100% B over 4–11 min, the composition was held at 100% B for 2 min, then 13–13.5 min, 100–5% B, and 13.5–14.5 min holding at 5% B. The flow rate was 0.35 ml/min and column temperature was 45°C. All the samples were kept at 4°C during the analysis. The injection volume was 2 μl.

The mass range was from m/z 100 to 1000. The resolution was set at 70,000 for the full MS scans and 17,500 for MS/MS scans. The collision energy was set at 10, 20, and 40 eV. The mass spectrometer operated as follows: spray voltage, 3800 V (+) and 3000 V (−); sheath gas flow rate, 35 arbitrary units; Aux gas flow rate, eight arbitrary units; capillary temperature, 320°C.

The QCs were injected at regular intervals (every four samples) throughout the analytical run to provide a set of data from which repeatability could be assessed. Raw sequence data of metabolomics have been uploaded to Metabolights (https://www.ebi.ac.uk/metabolights/) and are available through accession number (MTBLS2721).

Data Preprocessing and Statistical Analysis

The acquired LC-MS raw data were analyzed using the Progenesis QI software (version 2.3; Nonlinear Dynamics, Newcastle, United Kingdom), based on a self-built databases (the EMDB database, is specific for human and animals species, and was set up as an exclusive metabolite database containing data for over 3600 metabolites, including amino acids, lipids, nucleotides,

carbohydrates, vitamins and cofactors, and hormones. It also includes information on metabolite structure and mass spectrum data to address metabonomics biology). The following parameters were used: precursor tolerance was set 5 ppm, product tolerance was set 10 ppm, and retention time (RT) tolerance was set 0.02 min. Internal standard detection parameters were deselected for peak RT alignment, isotopic peaks were excluded for analysis, and the noise elimination level was set at 10.00, the minimum intensity was set to 15% of the base peak intensity. An Excel file was obtained containing three-dimensional data sets including m/z, peak RT, and peak intensities, and RT–m/z pairs were used as the identifier for each ion. The resulting matrix was further reduced by removing any peaks with missing value (ion intensity = 0) in more than 50% of the samples. Positive and negative data were combined data, which was then imported into R ropls package.

Principle component analysis (PCA) and Orthogonal partial least-squares-discriminant analyses (OPLS-DA) were carried out to visualize the metabolic alterations between experimental groups, after mean centering (Ctr) and Pareto variance (Par) scaling, respectively. The Hotelling's T2 region, shown as an ellipse in the score plots of the models, defined the 95% confidence interval (CI) of the modeled variation. Variable importance in the projection (VIP) ranked the overall contribution of each variable to the OPLS-DA model, and variables with VIP >1 were considered relevant for group discrimination. Default seven-round cross-validation and the 200 response permutation test were applied, with one-seventh of the samples excluded from the mathematical model in each round to avoid overfitting.

The differential metabolites were selected based on the combination of a statistically significant threshold of variable influence on projection (VIP) values obtained from the OPLS-DA model and p-values derived from a two-tailed Student's t test using the normalized peak areas, where metabolites with VIP > 1.0 and $p < 0.05$ were considered as differential metabolites.

DNA Extraction, Library Construction, and Sequencing

Total genomic DNA was extracted using DNA Extraction Kit following the manufacturer's instructions (Cat.12888; QIAGEN, Dusseldorf, Germany). The DNA concentration was verified with using the NanoDrop and by agarose gel electrophoresis. The DNA genome was used as template for PCR amplification with barcoded primers and Tks Gflex DNA Polymerase (R060B; TaKaRa Bio, Beijing, China). For bacterial diversity analysis, the V3–V4 variable region of the 16S rRNA gene was amplified using primers 343F and 798R (Nossa et al., 2010), using a commercial PCR kit (Cat. 51531; Qiagen).

Amplicon quality was visualized by gel electrophoresis, and amplicons were purified with AMPure XP beads (Cat. A63880; Agencourt), and amplified for another round of PCR. After a second purification with the AMPure XP beads, the final amplicon was quantified using Qubit dsDNA assay kit (Cat. Q32854; Thermo Fisher Scientific). Equal amounts of purified amplicon were pooled for subsequent sequencing based on Novaseq PE250. Raw sequence data were uploaded to the National Center for Biotechnology Information (NCBI) database (https://www.ncbi.nlm.nih.gov/) and are available through accession number (PRJNA720504).

Taxonomical Annotation

Raw sequencing data were exported in FASTQ format. Paired-end reads were then preprocessed using Trimmomatic software (Bolger et al., 2014) to detect and eliminate ambiguous bases (N). Further, low quality sequences were eliminated having an average quality score below 20 using sliding window trimming approach. After trimming, paired-end reads were assembled using FLASH software (version 34.0.0.118) (Reyon et al., 2012). Parameters of assembly were: 10 bp of minimal overlapping, 200 bp of maximum overlapping and a 20% maximum mismatch rate. Sequences were further filtered as follows: reads with ambiguous, homologous sequences or below 200 bp were abandoned; reads with 75% of bases above Q20 were retained; and, reads with chimera were detected and removed. These steps were achieved using QIIME software (version 1.8.0) (Caporaso et al., 2010b).

Clean reads were subjected to primer sequences removal and clustering to generate operational taxonomic units (OTUs) using Vsearch software (Version 2.4.2) (Rognes et al., 2016) with a 97% similarity cutoff. The representative read of each operational taxonomic unit (OTU) was selected using the QIIME package. All representative reads were annotated and blasted against Unite database (ITSs rDNA) using pynast (v0.1) (Caporaso et al., 2010a).

Statistical Analysis

Statistical analysis of serum biochemical indexes and gene expression was processed using Graphpad Prism, version v8 (GraphPad Software, Inc., San Diego, United States). All experiments were repeated at least six times and the obtained data are presented as the mean ± standard deviation. The Student's t-test was used for the analysis of statistical significance between two groups, and one-way analysis of variance followed by Tukey test was applied to analyze statistical significance across three groups or more. A p-value < 0.05 was considered to indicate a statistically significant difference.

RESULTS

Therapeutic Effects of ZYP on Serum Biochemistry, Liver Inflammation Markers, Cell Necrosis, Fibrosis Mediators, and Liver Histopathology

As shown in **Figure 1**, the cholestasis-induced rats exhibited a significant increase in serum ALT and AST levels, which were markedly reduced following treatment with high or low doses of ZYP. Similarly, the levels of TC, TBA, γ-GT, TBIL, the expression of TNF-α, TIMP-1, and the BAX/BCL-2 ratio were significantly increased in cholestasis-induced rats compared with the control

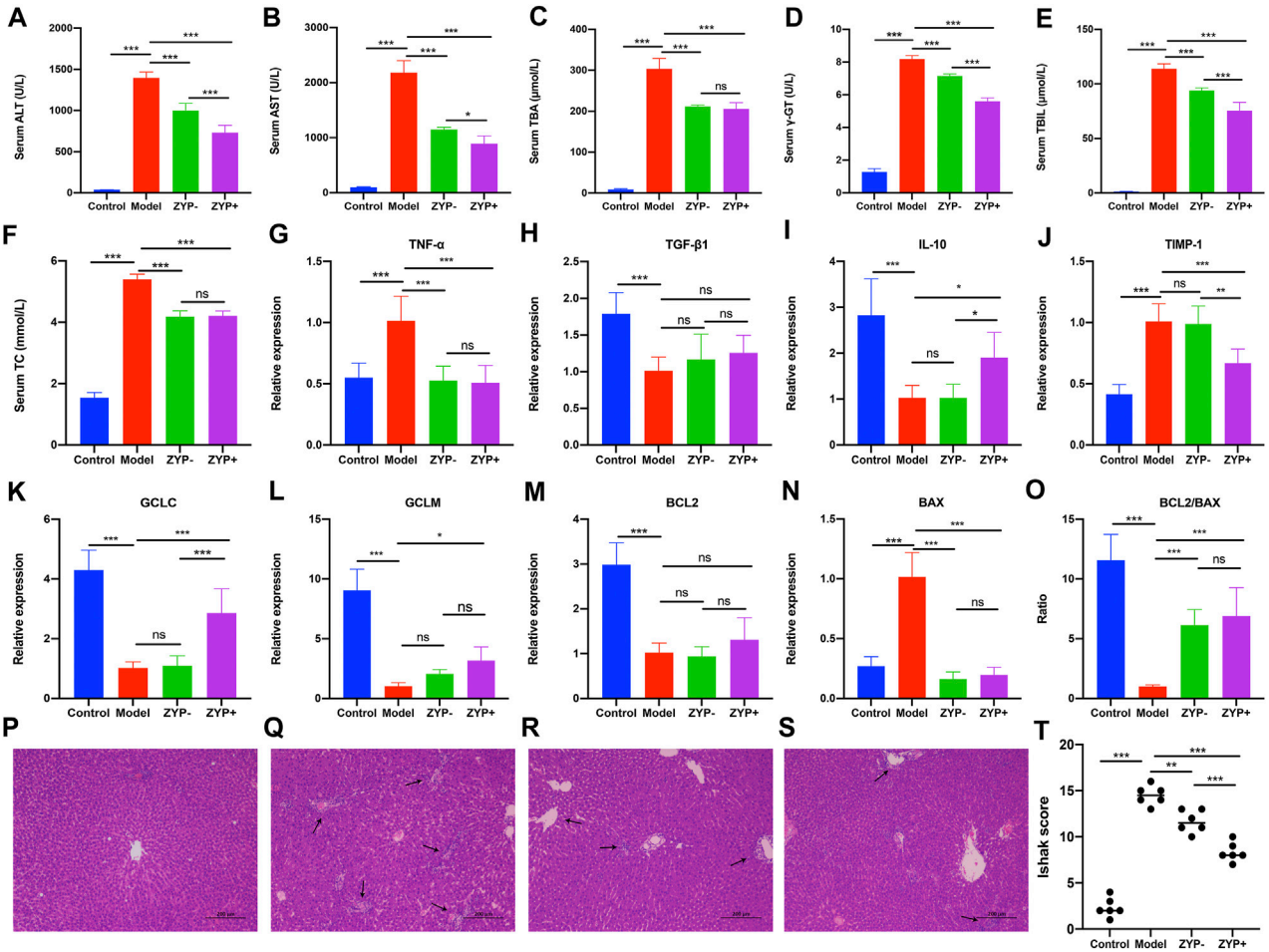

FIGURE 1 | Serum biochemistry, gene expression changes, and histopathological examination of livers evaluating liver injury in Control, Model, ZYP– and ZYP+ groups. **(A)** ALT; **(B)** γ-GT; **(C)** TC; **(D)** AST; **(E)** TBA; **(F)** TBIL; **(G)** TNF-α; **(H)** TGF-β1; **(I)** IL-10; **(J)** TIMP-1; **(K)** GCLC; **(L)** GCLM; **(M)** BCL2; **(N)** BAX; **(O)** BCL2/BAX. Histopathological examination of liver by HE staining at magnification ×100. **(P)** Control; **(Q)** Cholestasis Model; **(R)** ZYP–; **(S)** ZYP+. Arrows indicate the pathological loci. **(T)** Ishak score of hepatic inflammation and necrosis. $n = 6$, ***/**/*, $p < 0.001/p < 0.01/p < 0.05$; ns, no significant.

rats, and these changes were effectively alleviated following treatment with ZYP. In contrast, the expression of IL-10, GCLC and GCLM showed opposite results, while TGF-β1 showed no significant difference after ZYP intervention (**Figures 1A–O**). Representative photomicrographs of hematoxylin and eosin (HE)-stained liver tissue from control rats and the cholestasis rats with or without ZYP (0.6/1.2 g/kg) treatment are presented in **Figures 1P–S**. The Ishak scores are presented in **Figure 1T**. The morphology of liver lobules was normal in the control group, and the central veins and radiating hepatic cords were clearly visible. In contrast, rats with cholestasis exhibited significantly elevated inflammation and necrosis scores and significant changes in liver structure, including acute infiltration of polymorphonuclear neutrophils, nuclear deformation, and necrosis-induced inflammation. However, the cholestasis-induced rats treated with ZYP, especially the ZYP+ group, presented significantly reduced Ishak scores and exhibited only mild inflammatory infiltration of the central vein and portal area, and relatively milder bile duct epithelial damage.

Multivariate Statistical Analysis of LC-MS

PCA was used to compare the differences among all groups. As shown in **Figure 2**, a score plot allowed visualization of the observational clusters, which differed significantly between the control, model, ZYP–, ZYP+, and QC groups (**Figures 2A,C–E**). The results of the PCA indicated that multivariate statistical analysis was necessary to clarify the differences among the groups; therefore, OPLS-DA models were built to facilitate data interpretation.

OPLS-DA analysis was performed to obtain a deeper understanding of the differential metabolites, which were accountable for the intergroup separation. In this study, the control, model, ZYP–, and ZYP+ groups could be distinguished. The R^2X, R^2Y, and Q^2 (cum) of the model and control groups were 0.75, 0.997, and 0.953 respectively, as

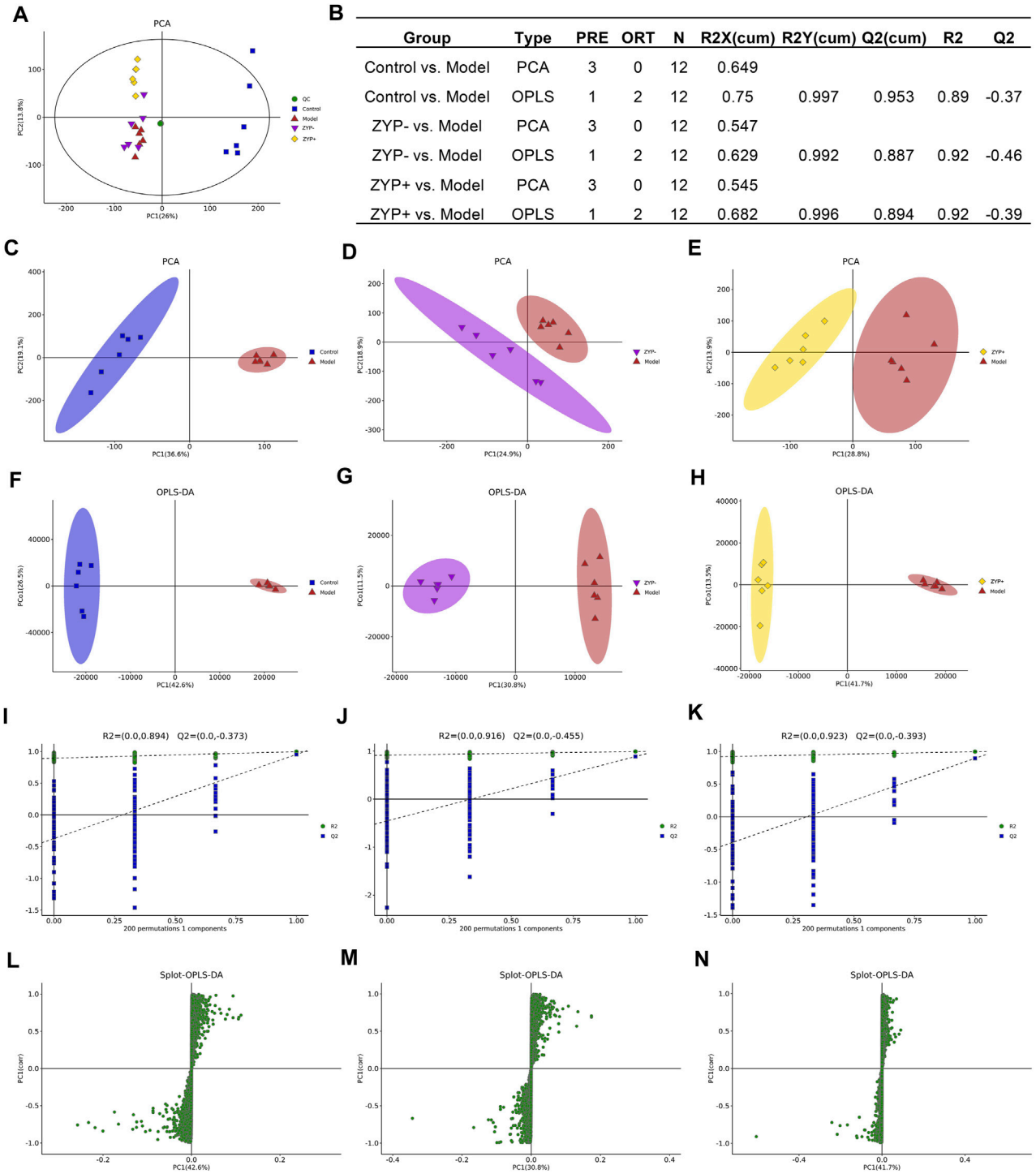

Group	Type	PRE	ORT	N	R2X(cum)	R2Y(cum)	Q2(cum)	R2	Q2
Control vs. Model	PCA	3	0	12	0.649				
Control vs. Model	OPLS	1	2	12	0.75	0.997	0.953	0.89	-0.37
ZYP- vs. Model	PCA	3	0	12	0.547				
ZYP- vs. Model	OPLS	1	2	12	0.629	0.992	0.887	0.92	-0.46
ZYP+ vs. Model	PCA	3	0	12	0.545				
ZYP+ vs. Model	OPLS	1	2	12	0.682	0.996	0.894	0.92	-0.39

FIGURE 2 | Multivariate statistical analysis of metabolic profiles derived from the Control, Model, ZYP–, and ZYP+ groups. **(A)** PCA score plot of the Control, Model (ANIT), ZYP–, ZYP+ and QC groups; **(B)** Parameters of PCA; **(C–E)** PCA of Model vs Control group, ZYP– vs Model and ZYP+ vs Model, respectively; **(F–H)** OPLS-DA of the Model vs Control group, ZYP– vs Model and ZYP+ vs Model, respectively; **(I–K)** 200-permutation test of the Model vs Control group, ZYP– vs Model and ZYP+ vs Model, respectively; **(L–N)** OPLS-DA score plot of the Model vs Control group, ZYP– vs Model and ZYP+ vs Model, respectively.

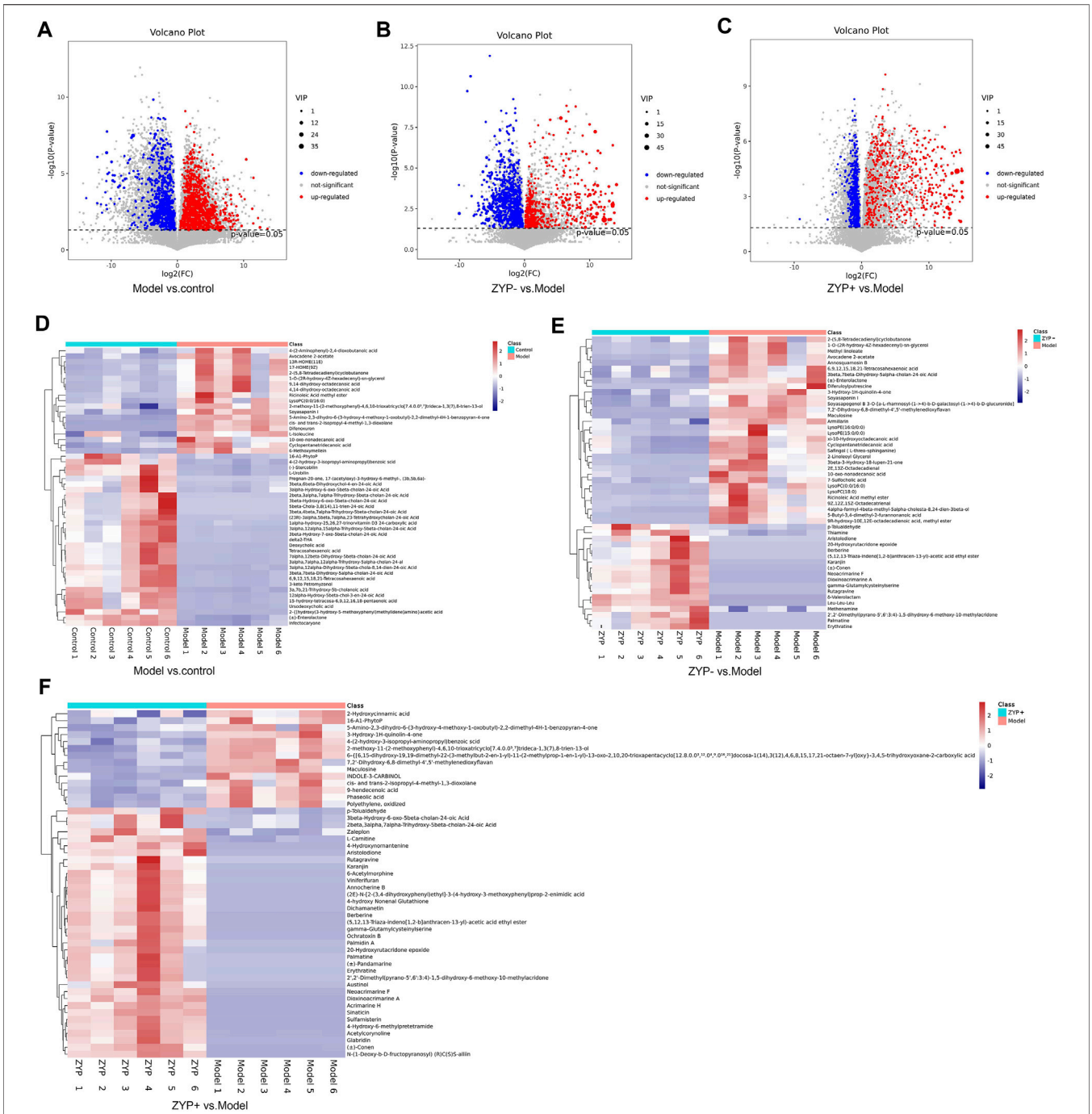

FIGURE 3 | Volcano plot and Heat map of the differential metabolites. **(A–C)** Volcano plot of Model vs Control groups, ZYP– vs Model and ZYP+ vs Model groups, respectively; **(D–F)** Heat map of Model vs Control groups, ZYP– vs Model and ZYP+ vs Model groups, respectively. Red, blue, and gray represent the upregulated, downregulated, and non-significant changes, respectively.

compared with the values of 0.682, 0.996, 0.894 (ZYP– vs control), and 0.684, 0.993, 0.866 (ZYP+ vs model), respectively, of the ZYP–/ZYP+ and model groups (**Figures 2F–H**). To prevent overfitting of the model, the quality of the model was examined by seven-cycle interactive verification and 200-response ranking test. These results indicated that these OPLS-DA were not overfit and indicated that the OPLS-DA achieved high separating capacity (**Figures 2I–K**). The OPLS-DA loading scatter plot identified several critical variables that were distant from the center of the loading plot, suggesting that these critical variables were important variables for clustering (**Figures 2L–N**).

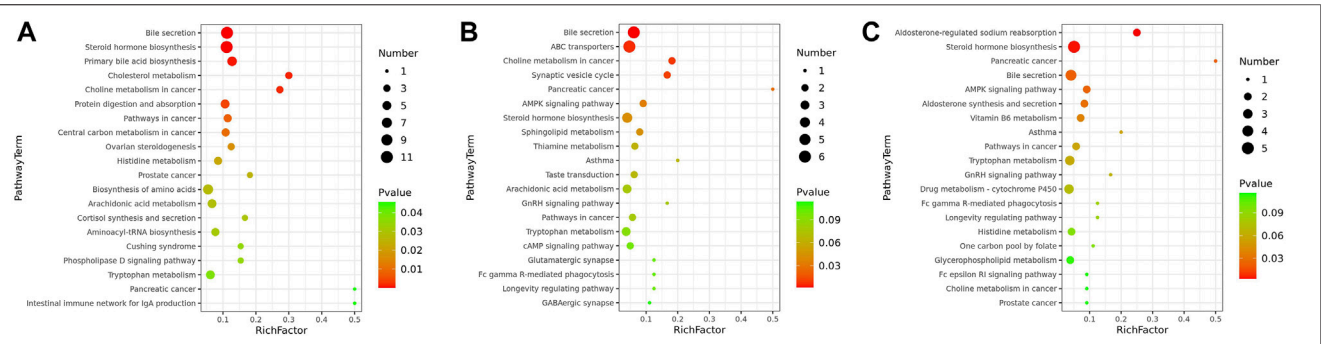

FIGURE 4 | Bubble diagrams of the control, cholestasis model, and ZYP treatment groups. **(A)** Model vs Control group; **(B)** ZYP– vs Model; **(C)** ZYP+ vs Model, respectively. The x-axis shows the Rich factor, the color of each circle indicates the *p*-value, and the size of each circle reflects the number of metabolites of each pathway.

Metabolite Identification and Pathway Analysis in ZYP-treated Rats With Cholestasis

Differential metabolite levels were determined based on VIP values > 1 and adjusted *p*-values < 0.05. We identified a total of 1090 metabolites that were significantly differentially expressed between the Model and Control groups, and 965 and 734 significantly differentially expressed metabolites between ZYP– and Model group, and the ZYP+ and Model groups, respectively (**Supplementary Data**).

Based on the results of the serum biochemistry and liver histological examination, the ZYP+ group (1.2 g/kg) exhibited better effects than the ZYP– group (0.6 g/kg). Additionally, the dose of the ZYP+ group is that commonly used in clinical practice; thus for the reasons described above, it is worthy to focus specifically on this group. In the ZYP+ vs Model comparison, the subclasses of differential metabolites analysis was associated with amino acids, peptides, and analogues (54 differential metabolites), fatty acids, and conjugates (37 differential metabolites), and flavonoids (37 differential metabolites). The number and trend of metabolites in different groups were presented in a volcano plot (**Figures 3A–C**), and the Top 50 differential metabolites between the Control, Model, ZYP+, and ZYP– groups were presented as a heatmap (**Figures 3D–F**).

To determine the functions of the differential metabolites, pathway analysis was carried out to further identify potentially enriched pathways ($p < 0.05$) associated with model alterations or ZYP treatment intervention. The results of the significant pathway terms emerging in the Kyoto Encyclopedia of Genes and Genomes (KEGG) analysis were mapped onto a bubble graph (**Figure 4**). Activation of eight pathways was identified, specifically bile secretion, steroid hormone biosynthesis, choline metabolism in cancer, pathways in cancer, histidine metabolism, prostate cancer, pancreatic cancer, and tryptophan metabolism when compared to the Model vs Control groups and ZYP+ vs Model groups. The above results suggested that ZYP participated in above biological process and signaling pathways and generated significant beneficial effects as intervention of cholestasis.

Fecal Microbiota Analysis

To explore whether the effects of the ZYP extract were associated with changes in the fecal microbiota, we analyzed the fecal flora composition of rats after ANIT-induced cholestasis or ZYP treatment.

The OTUs at the 97% similarity level were obtained using cluster tags, as is shown in the OTUs-Venn diagram (**Figure 5A**). In total, 140 OTUs were shared by the Control, Model, ZYP– and ZYP+ groups, the information regarding species, genus, family, order, class, phylum and kingdom level for each sample is shown in **Figure 5B**.

Alpha diversity is widely used for the analysis of microbial community diversity. Good's Diversity Index, the Shannon Diversity Index, and the species accumulation curves (SAC) of each group are shown in **Figures 6A–C**. The violin plots of the Good's diversity Index and the Shannon Diversity Index suggest that treatment with oral ZYP (low dose or high dose) had no significant effects on the alpha diversity of the fecal microbiota in cholestasis-induced rats. The amount of sequencing data was sufficient to reflect most microbial information in the samples.

Beta diversity analysis defines the extent of similarities and differences among microbial communities. The results of the Non-metric Multidimensional Scaling (NMDS), Principal Co-ordinates Analysis (PCoA, unweighted_unifrac), and PCA analyses are shown in **Figures 6D–F**. The data of the beta diversity analysis revealed distinct differences in Control, Model, ZYP–, and ZYP+ groups, illustrating that oral ZYP (either low or high doses) had a significant effect on the microbiota of cholestasis rats.

To evaluate the differences in microbial diversity, one-way ANOVA was applied to identify significant alterations in the composition of the host fecal microbiota at the genus and the phylum levels during infection (**Figures 7A,B**), the results show that cholestasis and ZYP influenced species abundances. To filter which bacteria differed between the experimental groups, we conducted a LEfSe (linear discriminant analysis coupled with

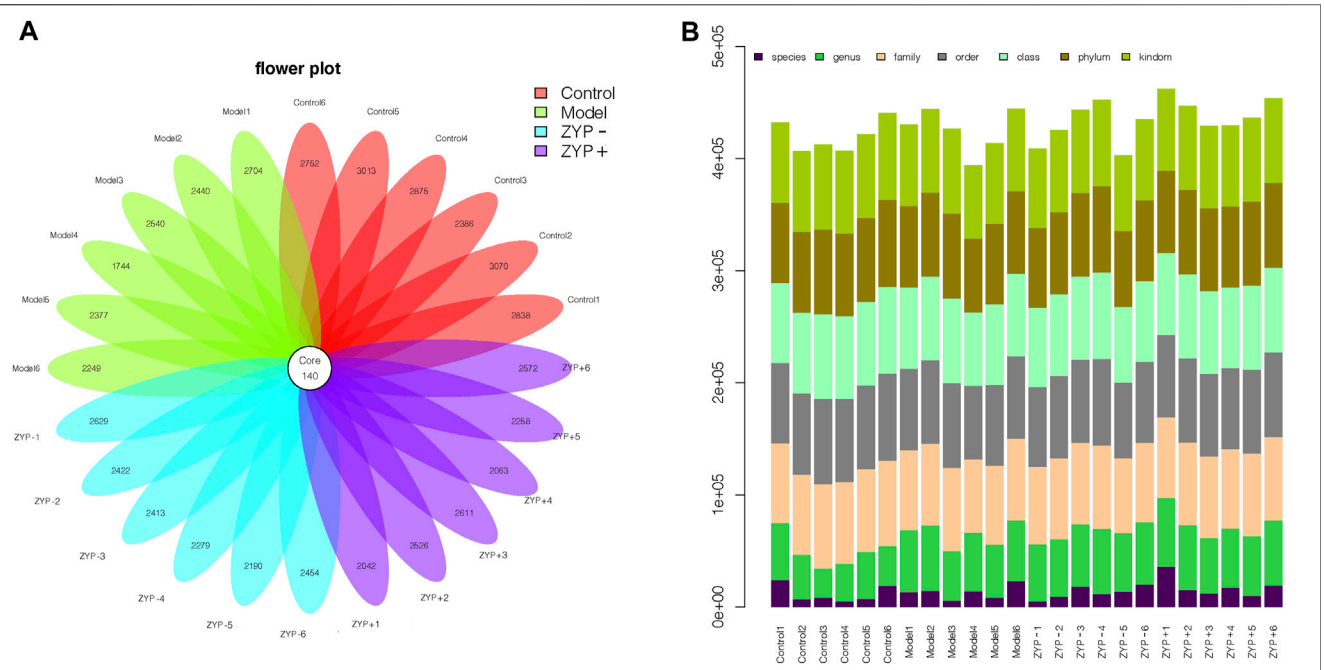

FIGURE 5 | OTUs classification results. **(A)** Operational Taxonomic Units (OTUs) based petal maps; **(B)** Comment situation of tags.

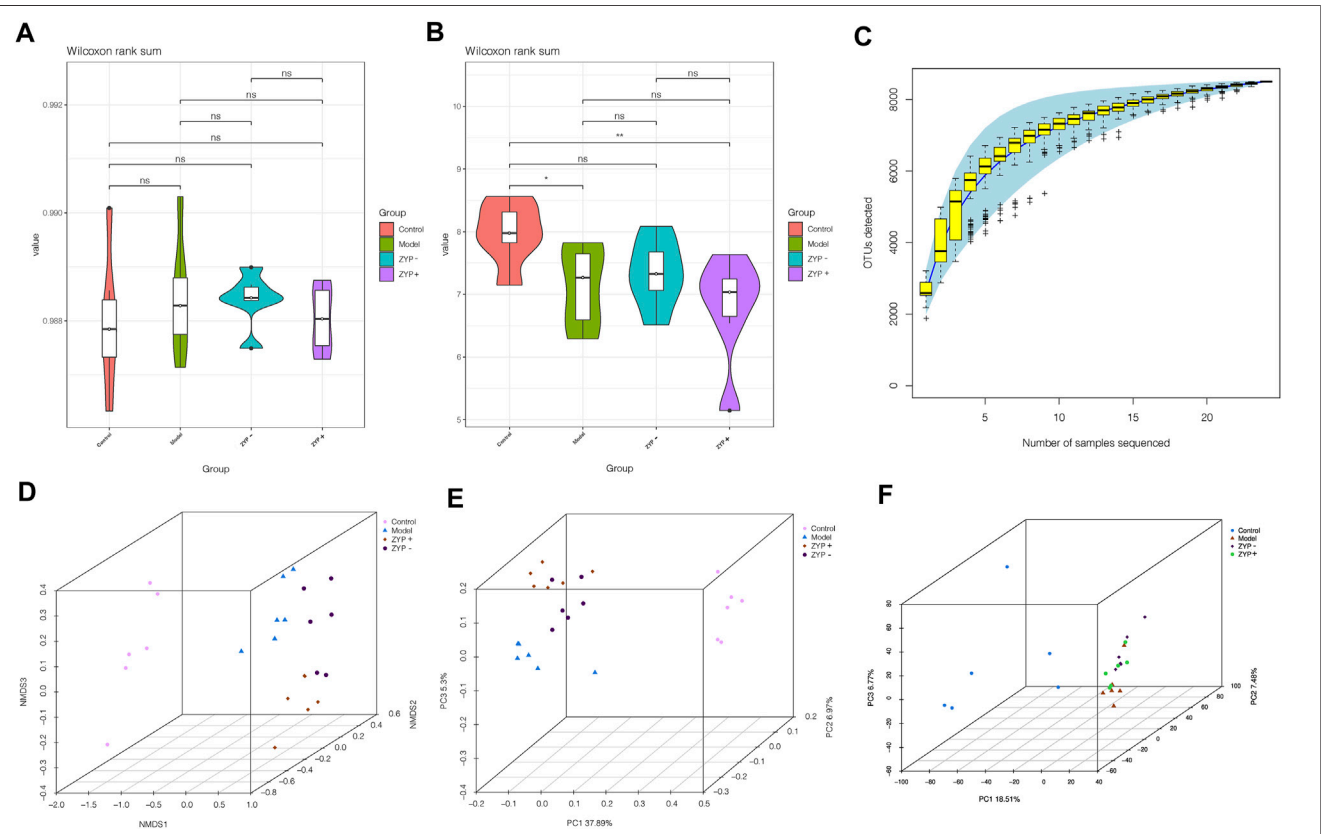

FIGURE 6 | Alpha and beta diversity analysis of the OTUs. **(A)** Good diversity analysis; **(B)** Shannon diversity analysis; **(C)** Curve of SAC; **(D)** NMDS analysis; **(E)** PCoA analysis; **(F)** PCA analysis.

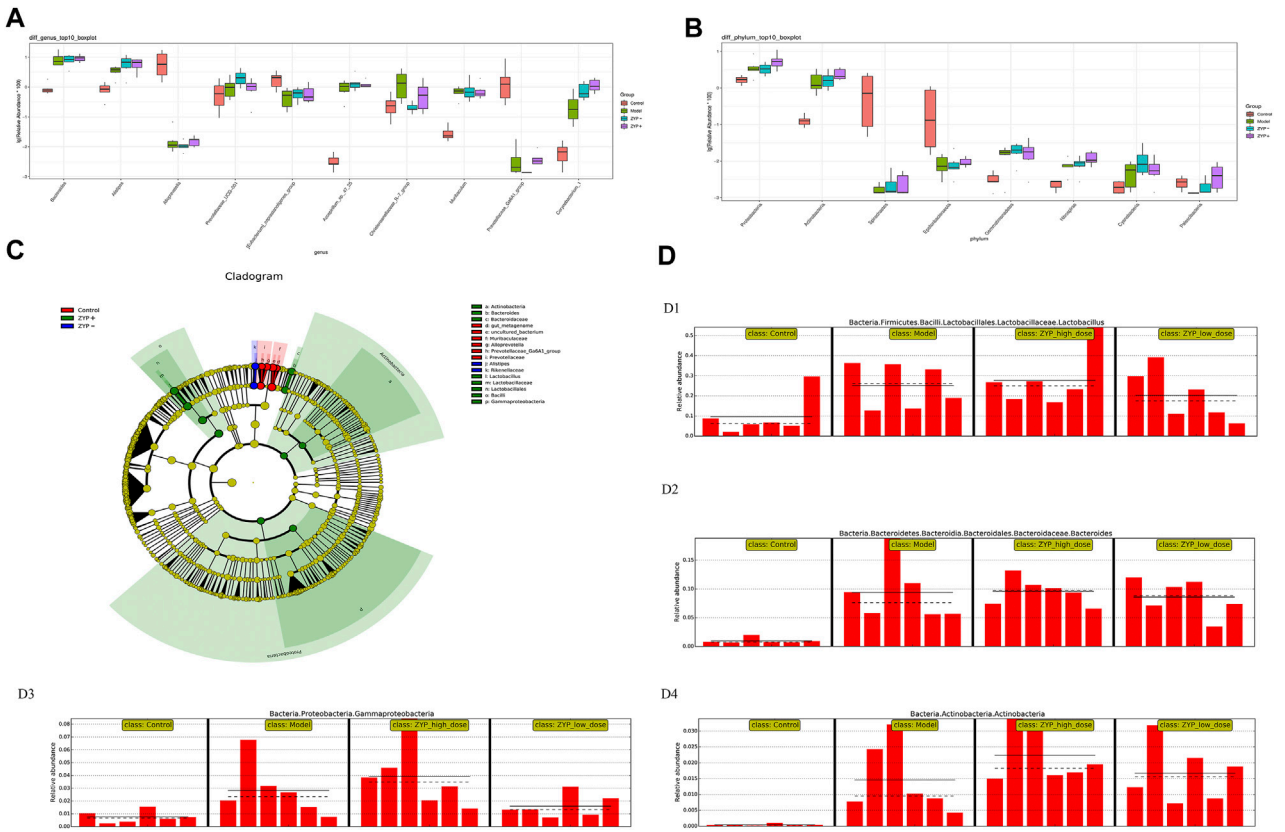

FIGURE 7 | Statistical analysis of microbial multivariate. **(A)** One-way ANOVA analysis of genus level; **(B)** One-way ANOVA analysis of phylum level; **(C)** Example diagram of annotated branches of different species; **(D)** Histogram of relative abundance. D1, *Lactobacillus*; D2, *Bacteroides*; D3, *Gammaproteobacteria*; D4, *Actinobacteria*. The solid line is the mean value of the relative abundance and the dashed line is the median value of relative abundance.

effect size measurements) analysis (**Figure 7C**). Overall, at the class and genus level, two classes and nine genera, specifically *Prevotellaceae_Ga6A1_group*, *uncultured_bacterium*, *Alloprevotella*, *gut_metagenome*, *Lactobacillus*, *Bacteroides*, *Gammaproteobacteria*, *Actinobacteria*, and *Alistipes*, were found to have significant differences. Of these, *Lactobacillus*, *Bacteroides*, *Gammaproteobacteria*, and *Actinobacteria* were the most representative bacteria in the ZYP+ treatment group. The above information is shown in **Figure 7D**.

Potential Relationships Between Biochemical Indexes, Fecal Metabolites, and Fecal Microbiota

To comprehensively analyze the relationships between biochemical indexes, fecal metabolites, and the genera of fecal microbiota, a correlation matrix was established calculating Spearman's correlation coefficient. As shown in **Figures 8A,B**, the pairwise correlation between the Model vs Control and the ZYP+ vs Model groups showed consistently strong correlations between intestinal microorganism and fecal metabolites. Furthermore, six biochemical indices, (ALT, AST, TBIL, TBA, TC, γ-GT) and eight genes (TNF-α, TGF-β1, IL-10, TIMP-1, GCLC, GCLM, BCL2, and BAX) exhibited positive or negative correlations with a variety of metabolites (**Figures 8C,D**). These relationships suggested that the biochemical indices, gene expression associated with liver injury, fecal metabolites, and fecal microbiota can influence each other.

DISCUSSION

Cholestasis is a widespread clinical liver disease which requires new therapeutic options. In clinical practice, ZYP is an effective combination medicine for cholestasis treatment. The purpose of this study was to determine the therapeutic effects of ZYP on cholestasis, and to elucidate the related mechanisms by metabolomics and intestinal flora profiling.

Serum liver enzymes (including ALT, AST, and γ-GT), TC, TBA, and TBIL are important indices of the clinical manifestations of cholestatic hepatitis (Bouchier and Pennington, 1978; Gomez Selgas et al., 2014; Wu et al., 2021). TNF-α, IL-10, TIMP-1, GCLC, GCLM, BCL2, and BAX are common indicators used to evaluate the inflammatory response, oxidative stress, apoptosis, and fibrosis (Yamazaki, 1994; Golbar et al., 2017; Strasser and Vaux, 2018). The results of the present study suggested that ZYP, especially high-doses of ZYP (1.2 g/kg/d) could represent a potential anti-

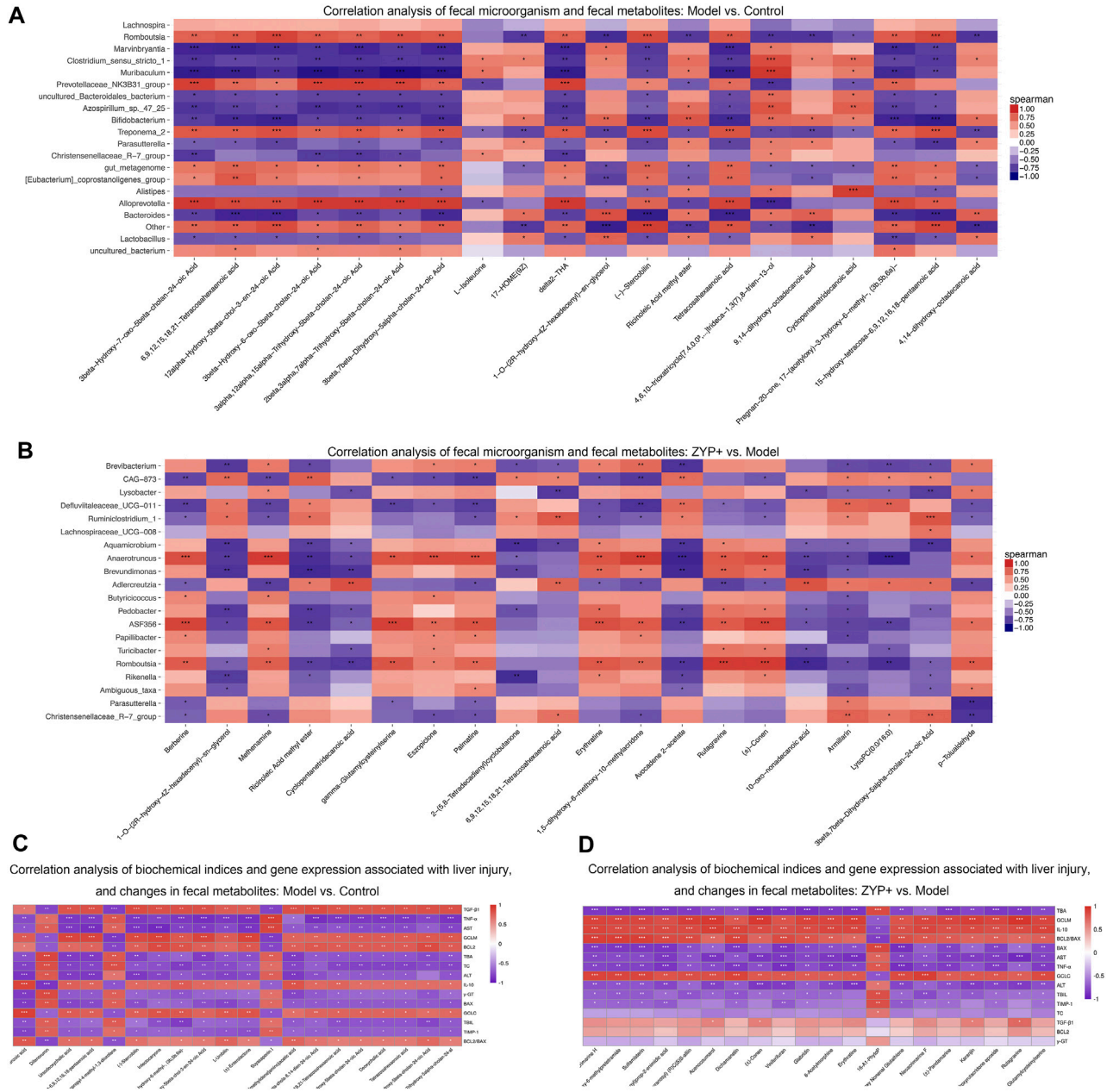

FIGURE 8 | Combined analysis of blood biochemistry, gene expression changes, fecal microorganism composition, and fecal metabolism variables in liver injury. Correlation analysis of fecal microorganism and fecal metabolites **(A)** Cholestasis model vs Control; **(B)** ZYP+ vs Untreated Cholestasis model. Correlation analysis of biochemical indices and gene expression associated with liver injury, and changes in fecal metabolites **(C)** Cholestasis model vs Control; **(D)** ZYP+ vs Untreated Cholestasis model. *$p < 0.05$, **$p < 0.01$, ***$p < 0.001$. The correlation matrices were obtained from the cloud platform of Shanghai OE Biotech, Inc. (https://cloud.oebiotech.cn/task/).

inflammatory, antioxidant, anti-fibrosis and anti-apoptosis effects. Furthermore, a clear improvement in liver damage was observed following ZYP treatment. Overall, these results indicated that ZYP could represent a potential therapeutic drug with protective effects against ANIT-induced cholestasis or following liver injury.

The diversity of fecal bacteria is associated with alterations and of the gut microbiome, and is often correlated with metabolism and immunity in patients with primary biliary cirrhosis (Lv et al., 2016; Wang et al., 2019). To explore the relevant fecal bacteria associated with ZYP treatment and cholestasis, we used 16S microbiome sequencing, which provides a measure of relative but not absolute bacterial abundance. In this study, we determined that *Lactobacillus*, *Bacteroides*, *Gammaproteobacteria*, and *Actinobacteria* were the most representative bacteria in the ZYP+ group (**Figure 7**). Thus,

we hypothesized two possible explanations for the diversity observed in the Model and ZYP+ groups. First, most of the representative bacteria in the ZYP+ group, which may contribute to higher diversity, were beneficial bacteria, and were enhanced in the cholestasis Model group, such as *Lactobacillus*, *Bacteroidetes*, and *Actinobacteria*. Of these, bacteria of the *Lactobacillus* genus have been shown to increase resistance against environmental stresses, and are sensitive or weakly tolerant to acidic environments and bile acid.

Bacteroidetes and *Lactobacillus* express bile salt hydrolase (BSH) and are involved in the metabolism of bile (Han et al., 2017; Chen et al., 2020). *Actinobacteria* has been implicated in the modulation of gut permeability, the immune system, metabolism, and the gut-brain axis (Binda et al., 2018). Further, *Bacteroidetes* and *Lactobacillus* may be associated with elevated levels of bile acids, and the enhanced expression of *Actinobacteria* may be associated with immune-inflammatory and autoimmune response by inducing regulatory T-cells (O'Mahony et al., 2008; Lyons et al., 2010). High doses of ZYP enhance the expression of the above bacteria, which indicated an improvement in the expression of BSH or T cell activity; thus, the promotion of bile metabolism may partly explain the interventional mechanism of ZYP in cholestasis. Second, *Gammaproteobacteria*, a class of pathogenic bacteria, may exhibit detrimental potential and cause abnormal inflammatory activation (Williams et al., 2010), however, it also considered as survival tool for bacteria in the environment (Vazquez-Rosas-Landa et al., 2017). In this study, ZYP enhanced the expression of *Gammaproteobacteria*, which allows us to speculate that bacteria–bacteria interactions may play a role in the interventional mechanism of ZYP in cholestasis. However, the detailed mechanisms involved remain to be further explored.

Untargeted metabolomics may contribute to provide evidence that fecal microbiota metabolites infer host-microbiome co-metabolic effects (Griffiths et al., 2010), and may help further explain the potential mechanisms of ZYP in cholestasis, The metabolomes of fecal samples were analyzed *via* an untargeted LC-MS-based metabolomics approach. We identified 1090, 965, and 734 metabolites as differential metabolites between the Model vs Control, ZYP− vs Model, and ZYP+ vs Model group comparisons, respectively. To explore the underlying biological mechanisms and relationships involved in the differential production of these metabolites, we applied KEGG pathway analysis. As a result, eight pathways, namely bile secretion, steroid hormone biosynthesis, choline metabolism in cancer, pathways in cancer, histidine metabolism, prostate cancer, pancreatic cancer, and tryptophan metabolism were enriched when compared to metabolites generated by the Model vs Control and ZYP+ vs Model groups. Among these metabolic pathways, bile secretion plays a vital role in the health of an organism and blockage of bile secretion leads to cholestasis (Jia et al., 2020).

Recent studies have shown that steroid hormone biosynthesis involves the coordinate activity of several members of the cytochrome P450 superfamily of monooxygenases and is associated with fatty-acid degradation (Li et al., 2012; Zhao et al., 2019). Histidine metabolism and tryptophan metabolism also undergo amino acid metabolism. Previous studies have confirmed that amino acid metabolism has a clear correlation with cholestasis, as amino acids are the main precursors of glutathione biosynthesis (Yu et al., 2018; Li et al., 2019). Further, amino acid metabolism interferes with cholestasis by affecting glutathione synthesis and thus produces antioxidant stress, which is supported by other study showing that γ-GT catabolizes biliary glutathione and expands the pool of amino acid precursors required for conjugation (glycine directly and taurine through cysteine oxidation) (Chen MF. et al., 2019). However, in our study, correlation analysis between metabolomics and γ-GT showed that there was no significant correlation between the two in the ZYP+ vs model groups (**Figure 8D**); thus, the detailed mechanisms remain to be further explored. Altogether, the above findings suggest that perturbation of these metabolic pathways may act to improve metabolic activity, which ultimately explains the beneficial effects on cholestasis by ZYP intervention. In addition, the pathways in cancer, prostate cancer, pancreatic cancer, and choline metabolism in cancer were perturbed when comparing the Model vs Control groups and ZYP+ vs Model groups, which indicated that ZYP may also be promising as a potential anticancer agent.

To comprehensively analyze the relationships between biochemical indices, changes in the inflammatory response, apoptosis, and gene expression associated with fibrosis, fecal metabolites, and the impact on the genera of fecal microbiota, a correlation matrix was established using Spearman's correlation coefficient analysis. Our findings confirmed a mutual effect between the biochemical indices, gene expression associated with liver injury, fecal metabolites, and fecal microbial genera, which suggested an underlying reciprocal relationship among these factors.

CONCLUSION

In summary, the results of the present study demonstrated that ZYP exerts significant anti-cholestatic effects through a synergistic effect on fecal metabolism and fecal microbes. We also revealed that the altered fecal microbial composition achieved following ZYP treatment was marked by an increase of beneficial bacteria (*Bacteroidetes*, *Lactobacillus* and *Actinobacteria*) and pathogenic bacteria (*Gammaproteobacteria*) compared with the Model group, bacteria–bacteria interactions may play a role in the interventional mechanism of ZYP in cholestasis. In addition, oral administration of high-doses of ZYP also exerted a significant influence on fecal metabolomics against cholestasis in the rat, which might be associated with amino acid metabolism, steroid hormone biosynthesis, and bile secretion. These findings highlight that ZYP, an ancient classic formulation of Coptis-Evodia herb couple, may prevent cholestasis. Future research will improve the understanding of ZYP's mechanisms and the pharmacological rationale underlying its therapeutic application.

DATA AVAILABILITY STATEMENT

The datasets presented in this study can be found in online repositories. The names of the repository/repositories and

accession number(s) can be found below: NCBI [accession: PRJNA720504]; Metabolights [accession: MTBLS2721].

ETHICS STATEMENT

The animal study was reviewed and approved by Ethics Committee of Chengdu University of Traditional Chinese Medicine.

AUTHOR CONTRIBUTIONS

TS and YW conceived and designed the study. HY acquired, analyzed, interpreted the data, and prepared the manuscript. CL was responsible for handling the animals and obtaining tissue specimens. FZ, JW, JH, and XZ performed statistical analyses. All authors have read and approved the final version of this manuscript.

FUNDING

The current work was supported by the China Postdoctoral Science Foundation (no. 2020M683641XB), "Xinglin Scholar" discipline talents Research Enhancement Programme of Chengdu University of Traditional Chinese Medicine (no. BSH2019020), National Natural Science Foundation Project of China (no. 81973743), Science and Technology Department Project of Sichuan Province (no. 20MZGC0241) and Social Science 13th Five-Year Plan Project of Sichuan Province (no. SC18KP029).

ACKNOWLEDGMENTS

The authors would like to thank the staff of the Experimental Center of Integrated Chinese and Western Medicine of Chengdu University of Traditional Chinese Medicine (Chengdu, China), Shanghai OE Biotech, Inc. (Shanghai, China), and Doctors Zongying Xu, Zhili Zheng and Dingnan Wang for their technical support.

SUPPLEMENTARY MATERIAL

The Supplementary Material for this article can be found online at: https://www.frontiersin.org/articles/10.3389/fphar.2021.695035/full#supplementary-material

REFERENCES

Allen, K., Jaeschke, H., and Copple, B. L. (2011). Bile Acids Induce Inflammatory Genes in Hepatocytes: A Novel Mechanism of Inflammation During Obstructive Cholestasis. *Am. J. Pathol.* 178 (1), 175–186. doi:10.1016/j.ajpath.2010.11.026

Beuers, U., Boyer, J. L., and Paumgartner, G. (1998). Ursodeoxycholic Acid in Cholestasis: Potential Mechanisms of Action and Therapeutic Applications. *Hepatology* 28 (6), 1449–1453. doi:10.1002/hep.510280601

Binda, C., Lopetuso, L. R., Rizzatti, G., Gibiino, G., Cennamo, V., and Gasbarrini, A. (2018). Actinobacteria: A Relevant Minority for the Maintenance of Gut Homeostasis. *Dig. Liver Dis.* 50 (5), 421–428. doi:10.1016/j.dld.2018.02.012

Bolger, A. M., Lohse, M., and Usadel, B. (2014). Trimmomatic: A Flexible Trimmer for Illumina Sequence Data. *Bioinformatics* 30 (15), 2114–2120. doi:10.1093/bioinformatics/btu170

Bouchier, I. A., and Pennington, C. R. (1978). Serum Bile Acids in Hepatobiliary Disease. *Gut* 19 (6), 492–496. doi:10.1136/gut.19.6.492

Boyer, J. L. (2007). New Perspectives for the Treatment of Cholestasis: Lessons from Basic Science Applied Clinically. *J. Hepatol.* 46 (3), 365–371. doi:10.1016/j.jhep.2006.12.001

Caporaso, J. G., Bittinger, K., Bushman, F. D., DeSantis, T. Z., Andersen, G. L., and Knight, R. (2010a). PyNAST: A Flexible Tool for Aligning Sequences to a Template Alignment. *Bioinformatics* 26 (2), 266–267. doi:10.1093/bioinformatics/btp636

Caporaso, J. G., Kuczynski, J., Stombaugh, J., Bittinger, K., Bushman, F. D., Costello, E. K., et al. (2010b). QIIME Allows Analysis of High-Throughput Community Sequencing Data. *Nat. Methods* 7 (5), 335–336. doi:10.1038/nmeth.f.303

Chatterjee, A., Mukherjee, S., Basu, B., Roy, D., Basu, R., Ghosh, H., et al. (2020). Insight into the Distinctive Paradigm of Human Cytomegalovirus Associated Intrahepatic and Extrahepatic Cholestasis in Neonates. *Sci. Rep.* 10 (1), 15861. doi:10.1038/s41598-020-73009-z

Chen, Z., Zhu, Y., Zhao, Y., Ma, X., Niu, M., Wang, J., et al. (2016). Serum Metabolomic Profiling in a Rat Model Reveals Protective Function of Paeoniflorin Against ANIT Induced Cholestasis. *Phytother Res.* 30 (4), 654–662. doi:10.1002/ptr.5575

Chen, C., Yin, Q., Wu, H., Cheng, L., Kwon, J. I., Jin, J., et al. (2019a). Different Effects of Premature Infant Formula and Breast Milk on Intestinal Microecological Development in Premature Infants. *Front. Microbiol.* 10, 3020. doi:10.3389/fmicb.2019.03020

Chen, M. F., Gong, F., Zhang, Y. Y., Li, C., Zhou, C., Hong, P., et al. (2019b). Preventive Effect of YGDEY from Tilapia Fish Skin Gelatin Hydrolysates Against Alcohol-Induced Damage in HepG2 Cells Through ROS-Mediated Signaling Pathways. *Nutrients* 11 (2), 392. doi:10.3390/nu11020392

Chen, X., Wu, Y., Hu, Y., Zhang, Y., and Wang, S. (2020). Lactobacillus Rhamnosus GG Reduces β-conglycinin-Allergy-Induced Apoptotic Cells by Regulating Bacteroides and Bile Secretion Pathway in Intestinal Contents of BALB/c Mice. *Nutrients* 13 (1), 55. doi:10.3390/nu13010055

Cheng, D. H., Zhao, Y. L., and Yang, H. B. (2011). Effect of Zuojin Pill and Fanzuojin Pill on the Growth Metabolism of Enterobacteria by Microcalorimetry. *Zhongguo Zhong Xi Yi Jie He Za Zhi* 31 (2), 209–212. doi:10.1088/1009-0630/13/1/25

Cheng, J., Wang, J., Zhang, W., Yang, X., and Cao, Y. (2015). A Cross-Sectional Study on Intrahepatic Cholestasis Indicators of Viral Hepatitis Patients. *J. Hepatol.* 62 (Suppl. 2), S538. doi:10.1016/S0168-8278(15)30798-4

Crosignani, A., Setchell, K. D., Invernizzi, P., Larghi, A., Rodrigues, C. M., and Podda, M. (1996). Clinical Pharmacokinetics of Therapeutic Bile Acids. *Clin. Pharmacokinet.* 30 (5), 333–358. doi:10.2165/00003088-199630050-00002

Golbar, H. M., Izawa, T., Bondoc, A., Wijesundera, K. K., Tennakoon, A. H., Kuwamura, M., et al. (2017). Attenuation of Alpha-Naphthylisothiocyanate (ANIT)-induced Biliary Fibrosis by Depletion of Hepatic Macrophages in Rats. *Exp. Toxicol. Pathol.* 69 (4), 221–230. doi:10.1016/j.etp.2017.01.005

Gómez Selgas, A., Bexfield, N., Scase, T. J., Holmes, M. A., and Watson, P. (2014). Total Serum Bilirubin as a Negative Prognostic Factor in Idiopathic Canine Chronic Hepatitis. *J. Vet. Diagn. Invest.* 26 (2), 246–251. doi:10.1177/1040638713520602

Goodman, Z. D. (2007). Grading and Staging Systems for Inflammation and Fibrosis in Chronic Liver Diseases. *J. Hepatol.* 47 (4), 598–607. doi:10.1016/j.jhep.2007.07.006

Griffiths, W. J., Koal, T., Wang, Y., Kohl, M., Enot, D. P., and Deigner, H. P. (2010). Targeted Metabolomics for Biomarker Discovery. *Angew. Chem. Int. Ed. Engl.* 49 (32), 5426–5445. doi:10.1002/anie.200905579

Guo, W., Huang, J., Wang, N., Tan, H. Y., Cheung, F., Chen, F., et al. (2019). Integrating Network Pharmacology and Pharmacological Evaluation for Deciphering the Action Mechanism of Herbal Formula Zuojin Pill in Suppressing Hepatocellular Carcinoma. *Front. Pharmacol.* 10, 1185. doi:10.3389/fphar.2019.01185

Han, K., Bose, S., Wang, J. H., Lim, S. K., Chin, Y. W., Kim, Y. M., et al. (2017). In Vivo Therapeutic Effect of Combination Treatment with Metformin and Scutellaria Baicalensis on Maintaining Bile Acid Homeostasis. *PLoS One* 12 (9), e0182467. doi:10.1371/journal.pone.0182467

Hill, D. A., Jean, P. A., and Roth, R. A. (1999). Bile Duct Epithelial Cells Exposed to Alpha-Naphthylisothiocyanate Produce a Factor that Causes Neutrophil-dependent Hepatocellular Injury In Vitro. *Toxicol. Sci.* 47 (1), 118–125. doi:10.1093/toxsci/47.1.118

Ishak, K., Baptista, A., Bianchi, L., Callea, F., De Groote, J., Gudat, F., et al. (1995). Histological Grading and Staging of Chronic Hepatitis. *J. Hepatol.* 22 (6), 696–699. doi:10.1016/0168-8278(95)80226-6

Islam, K. B., Fukiya, S., Hagio, M., Fujii, N., Ishizuka, S., Ooka, T., et al. (2011). Bile Acid Is a Host Factor that Regulates the Composition of the Cecal Microbiota in Rats. *Gastroenterology* 141 (5), 1773–1781. doi:10.1053/j.gastro.2011.07.046

Itakura, J., Izumi, N., Nishimura, Y., Inoue, K., Ueda, K., Nakanishi, H., et al. (2004). Prospective Randomized Crossover Trial of Combination Therapy with Bezafibrate and UDCA for Primary Biliary Cirrhosis. *Hepatol. Res.* 29 (4), 216–222. doi:10.1016/j.hepres.2004.04.001

Jia, Z., Cheng, Y., Jiang, X., Zhang, C., Wang, G., Xu, J., et al. (2020). 3D Culture System for Liver Tissue Mimicking Hepatic Plates for Improvement of Human Hepatocyte (C3A) Function and Polarity. *Biomed. Res. Int.* 2020, 6354183. doi:10.1155/2020/6354183

Kaddurah-Daouk, R., Kristal, B. S., and Weinshilboum, R. M. (2008). Metabolomics: A Global Biochemical Approach to Drug Response and Disease. *Annu. Rev. Pharmacol. Toxicol.* 48, 653–683. doi:10.1146/annurev.pharmtox.48.113006.094715

Kemis, J. H., Linke, V., Barrett, K. L., Boehm, F. J., Traeger, L. L., Keller, M. P., et al. (2019). Genetic Determinants of Gut Microbiota Composition and Bile Acid Profiles in Mice. *Plos Genet.* 15 (8), e1008073. doi:10.1371/journal.pgen.1008073

Lane, E., and Murray, K. F. (2017). Neonatal Cholestasis. *Pediatr. Clin. North. Am.* 64 (3), 621–639. doi:10.1016/j.pcl.2017.01.006

Li, W. F., Jiang, J. G., and Chen, J. (2008). Chinese Medicine and its Modernization Demands. *Arch. Med. Res.* 39 (2), 246–251. doi:10.1016/j.arcmed.2007.09.011

Li, D., Dammer, E. B., and Sewer, M. B. (2012). Resveratrol Stimulates Cortisol Biosynthesis by Activating SIRT-dependent Deacetylation of P450scc. *Endocrinology* 153 (7), 3258–3268. doi:10.1210/en.2011-2088

Li, Y., Yu, H., Xu, Z., Shi, S., Wang, D., Shi, X., et al. (2019). Melatonin Ameliorates ANIT-induced C-holestasis by A-ctivating Nrf2 through a PI3K/Akt-dependent P-athway in R-ats. *Mol. Med. Rep.* 19 (2), 1185–1193. doi:10.3892/mmr.2018.9746

Lv, L. X., Fang, D. Q., Shi, D., Chen, D. Y., Yan, R., Zhu, Y. X., et al. (2016). Alterations and Correlations of the Gut Microbiome, Metabolism and Immunity in Patients with Primary Biliary Cirrhosis. *Environ. Microbiol.* 18 (7), 2272–2286. doi:10.1111/1462-2920.13401

Lyons, A., O'Mahony, D., O'Brien, F., MacSharry, J., Sheil, B., Ceddia, M., et al. (2010). Bacterial Strain-specific Induction of Foxp3+ T Regulatory Cells Is Protective in Murine Allergy Models. *Clin. Exp. Allergy* 40 (5), 811–819. doi:10.1111/j.1365-2222.2009.03437.x

Nossa, C. W., Oberdorf, W. E., Yang, L., Aas, J. A., Paster, B. J., Desantis, T. Z., et al. (2010). Design of 16S rRNA Gene Primers for 454 Pyrosequencing of the Human Foregut Microbiome. *World J. Gastroenterol.* 16 (33), 4135–4144. doi:10.3748/wjg.v16.i33.4135

O'Mahony, C., Scully, P., O'Mahony, D., Murphy, S., O'Brien, F., Lyons, A., et al. (2008). Commensal-induced Regulatory T Cells Mediate Protection Against Pathogen-Stimulated NF-kappaB Activation. *Plos Pathog.* 4 (8), e1000112. doi:10.1371/journal.ppat.1000112

Reyon, D., Tsai, S. Q., Khayter, C., Foden, J. A., Sander, J. D., and Joung, J. K. (2012). FLASH Assembly of TALENs for High-Throughput Genome Editing. *Nat. Biotechnol.* 30 (5), 460–465. doi:10.1038/nbt.2170

Rognes, T., Flouri, T., Nichols, B., Quince, C., and Mahé, F. (2016). VSEARCH: A Versatile Open Source Tool for Metagenomics. *PeerJ* 4, e2584. doi:10.7717/peerj.2584

Sasaki, M., Maeda, A., Sakamoto, K., and Fujimura, A. (2001). Effect of Bile Acids on Absorption of Nitrendipine in Healthy Subjects. *Br. J. Clin. Pharmacol.* 52 (6), 699–701. doi:10.1046/j.0306-5251.2001.01489.x

Strasser, A., and Vaux, D. L. (2018). Viewing BCL2 and Cell Death Control from an Evolutionary Perspective. *Cell Death Differ.* 25 (1), 13–20. doi:10.1038/cdd.2017.145

Sun, H., Zhang, A., and Wang, X. (2012). Potential Role of Metabolomic Approaches for Chinese Medicine Syndromes and Herbal Medicine. *Phytother Res.* 26 (10), 1466–1471. doi:10.1002/ptr.4613

Tang, L., Liu, H., Wu, Y., Li, M., Li, W., Jiang, M., et al. (2017). Sevoflurane May Be More Beneficial Than Propofol in Patients Receiving Endoscopic Variceal Ligation and Endoscopic Variceal Sclerotherapy: A Randomized, Double-Blind Study. *Exp. Ther. Med.* 14 (4), 3145–3152. doi:10.3892/etm.2017.4919

Vázquez-Rosas-Landa, M., Ponce-Soto, G. Y., Eguiarte, L. E., and Souza, V. (2017). Comparative Genomics of Free-Living Gammaproteobacteria: Pathogenesis-Related Genes or Interaction-Related Genes? *Pathog. Dis.* 75 (5), ftx059. doi:10.1093/femspd/ftx059

Wahlström, A., Sayin, S. I., Marschall, H. U., and Bäckhed, F. (2016). Intestinal Crosstalk Between Bile Acids and Microbiota and its Impact on Host Metabolism. *Cell Metab.* 24 (1), 41–50. doi:10.1016/j.cmet.2016.05.005

Wang, J., Zhang, T., Zhu, L., Ma, C., and Wang, S. (2015). Anti-ulcerogenic Effect of Zuojin Pill against Ethanol-Induced Acute Gastric Lesion in Animal Models. *J. Ethnopharmacol* 173, 459–467. doi:10.1016/j.jep.2015.04.017

Wang, M., Chen, L., Liu, D., Chen, H., Tang, D. D., and Zhao, Y. Y. (2017). Metabolomics Highlights Pharmacological Bioactivity and Biochemical Mechanism of Traditional Chinese Medicine. *Chem. Biol. Interact* 273, 133–141. doi:10.1016/j.cbi.2017.06.011

Wang, Y., Gao, X., Zhang, X., Xiao, Y., Huang, J., Yu, D., et al. (2019). Gut Microbiota Dysbiosis Is Associated with Altered Bile Acid Metabolism in Infantile Cholestasis. *mSystems* 4 (6), e00463-19. doi:10.1128/mSystems.00463-19

Wang, T., Xu, Y., Chen, Q., Zheng, W., Wang, J., Zeng, H., et al. (2020). Metabolomics Analysis of Laparoscopic Surgery Combined with Wuda Granule to Promote Rapid Recovery of Patients with Colorectal Cancer Using UPLC/Q-TOF-MS/MS. *Evid. Based Complement. Alternat Med.* 2020, 5068268. doi:10.1155/2020/5068268

Wei, M., Huang, F., Zhao, L., Zhang, Y., Yang, W., Wang, S., et al. (2020). A Dysregulated Bile Acid-Gut Microbiota Axis Contributes to Obesity Susceptibility. *EBioMedicine* 55, 102766. doi:10.1016/j.ebiom.2020.102766

Williams, K. P., Gillespie, J. J., Sobral, B. W., Nordberg, E. K., Snyder, E. E., Shallom, J. M., et al. (2010). Phylogeny of Gammaproteobacteria. *J. Bacteriol.* 192 (9), 2305–2314. doi:10.1128/JB.01480-09

Wu, P., Gao, W., Su, M., Nice, E. C., Zhang, W., Lin, J., et al. (2021). Adaptive Mechanisms of Tumor Therapy Resistance Driven by Tumor Microenvironment. *Front Cel. Dev. Biol.* 9, 641469. doi:10.3389/fcell.2021.641469

Yamazaki, M. (1994). TNF-alpha. *Gan To Kagaku Ryoho* 21 (15), 2679–2687.

Yang, Y., Yin, Y., Chen, X., Chen, C., Xia, Y., Qi, H., et al. (2019). Evaluating Different Extraction Solvents for GC-MS Based Metabolomic Analysis of the Fecal Metabolome of Adult and Baby Giant Pandas. *Sci. Rep.* 9 (1), 12017. doi:10.1038/s41598-019-48453-1

Yu, H., Li, Y., Xu, Z., Wang, D., Shi, S., Deng, H., et al. (2018). Identification of Potential Biomarkers in Cholestasis and the Therapeutic Effect of Melatonin by Metabolomics, Multivariate Data and Pathway Analyses. *Int. J. Mol. Med.* 42 (5), 2515–2526. doi:10.3892/ijmm.2018.3859

Zhao, X., Chen, S., Tan, Z., Wang, Y., Zhang, F., Yang, T., et al. (2019). Transcriptome Analysis of Landrace Pig Subcutaneous Preadipocytes During Adipogenic Differentiation. *Genes (Basel)* 10 (7), 552. doi:10.3390/genes10070552

Conflict of Interest: The authors declare that the research was conducted in the absence of any commercial or financial relationships that could be construed as a potential conflict of interest.

Publisher's Note: All claims expressed in this article are solely those of the authors and do not necessarily represent those of their affiliated organizations, or those of the publisher, the editors and the reviewers. Any product that may be evaluated in this article, or claim that may be made by its manufacturer, is not guaranteed or endorsed by the publisher.

frontiers in Pharmacology

ORIGINAL RESEARCH
published: 21 September 2021
doi: 10.3389/fphar.2021.727636

Study on the Hepatoprotection of *Schisandra chinensis* Caulis Polysaccharides in Nonalcoholic Fatty Liver Disease in Rats Based on Metabolomics

*Yanbo Feng, Han Li, Cong Chen, Hao Lin, Guangyu Xu, He Li, Chunmei Wang, Jianguang Chen and Jinghui Sun**

College of Pharmacy, Beihua University, Jilin, China

OPEN ACCESS

Edited by:
Silvia Di Giacomo, Sapienza University of Rome, Italy

Reviewed by:
Sara De Martin, University of Padua, Italy
Ana Cristina Jacobowski, Federal University of Mato Grosso do Sul, Brazil

***Correspondence:**
Jinghui Sun
sunjinghui2008@126.com

Specialty section:
This article was submitted to Gastrointestinal and Hepatic Pharmacology, a section of the journal Frontiers in Pharmacology.

Received: *19 June 2021*
Accepted: *19 August 2021*
Published: *21 September 2021*

Citation:
Feng Y, Li H, Chen C, Lin H, Xu G, Li H, Wang C, Chen J and Sun J (2021) Study on the Hepatoprotection of Schisandra chinensis *Caulis Polysaccharides in Nonalcoholic Fatty Liver Disease in Rats Based on Metabolomics. Front. Pharmacol. 12:727636. doi: 10.3389/fphar.2021.727636*

The aim of this study was to investigate the hepatoprotection of *Schisandra chinensis* Caulis polysaccharides (SCPs) in the nonalcoholic fatty liver disease (NAFLD) induced by high-fat diet (HFD) in rats. A total of 30 Wistar rats were randomly divided into the control group (CON), model group (MOD), and *Schisandra chinensis* caulis polysaccharide (SCP) group. Except for those in the CON group, the other rats were fed with high-fat diet for 4 weeks to establish an NAFLD model. From the 5th week, rats in the SCP group were given SCP solution (100 mg kg^{-1}) by gavage for 6 weeks, and those in the CON and MOD groups were given an equal volume of distilled water in the same way. Aspartate aminotransferase (AST), alanine aminotransferase (ALT), triglyceride (TG), total cholesterol (TC), low-density lipoprotein cholesterol (LDL-C), high-density lipoprotein cholesterol (HDL-C) levels in serum, the malondialdehyde (MDA) level, glutathione peroxidase (GSH-Px), and superoxide dismutase (SOD) activities in the liver tissue were detected. The small molecular metabolites in the blood of rats were determined by the metabolomics method of ultra-high-performance liquid chromatography-quadrupole/electrostatic field orbitrap high-resolution mass spectrometry (UHPLC-Q-Orbitrap-MS/MS) combined with multivariate analysis. The enrichment analysis and pathway analysis of the different metabolites were carried out. The therapeutic mechanism of SCP in NAFLD rats was verified by western blot. The results showed that the levels of AST, ALT, TG, TC, and LDL-C in the serum of rats in the SCP group were significantly lower, and the levels of HDL-C were significantly higher than those in the MOD group. The screening and analysis of the metabolic pathways showed that SCP could alleviate the development of NAFLD by regulating the expression of UDP-glucose pyrophosphorylase (UGP2), UDP-glucose 6-dehydrogenase (UGDH), acetyl CoA carboxylase (ACC), and fatty acid synthase (FAS) in the liver of NAFLD rats. This study may provide a theoretical basis for the development and utilization of SCP.

Keywords: *Schisandra chinensis* Caulis, polysaccharides, nonalcoholic fatty liver disease, metabolomics, UGP2, UGDH

INTRODUCTION

Nonalcoholic fatty liver disease (NAFLD) refers to the accumulation of fat in the liver without excessive drinking or other known liver diseases and gradually evolved into nonalcoholic steatohepatitis, liver cirrhosis, and hepatocellular carcinoma (Abdelmoneim et al., 2021). With the improvement of people's living standards, excessive intake of sugar and high-fat and high-calorie diets can easily lead to increased blood lipids and fatty liver disease. In recent years, the prevalence of NAFLD in the world has been on the rise (Schön, 2021), so it is of great significance to study the body changes under the conditions of nonalcoholic fatty liver disease.

Schisandra chinensis, the dry and mature fruit of a *Magnoliaceae* plant *Schisandra chinensis* (Turcz.) Baill., is widely used because of its significant hepatoprotection, hypolipidemia, and antioxidation (Chen et al., 2019; Zhu et al., 2019; Yan et al., 2020). However, other parts of *Schisandra chinensis*, such as caulis, have not been utilized. According to statistics, nearly 1,000 tons of *Schisandra chinensis* caulis are pruned and discarded every year only in Northeast China where *Schisandra chinensis* is planted, resulting in a waste of resources (Mocan et al., 2016). Studies have shown that the components in the dried caulis of *Schisandra chinensis* are similar to those in its fruit, with a significant hypolipidemic effect (Zheng et al., 2014; Li et al., 2018). Therefore, it is speculated that *Schisandra chinensis* fruit and *Schisandra chinensis* caulis have the same protective effect against fatty liver injury, but the specific mechanism is not clear.

All the effects of exogenous substances, pathophysiological changes, or genetic variation will be reflected in various biological pathways, which will interfere with the steady-state balance of endogenous metabolites to change the concentration and proportion of various substances in endogenous metabolites, and at the same time, the metabolites will interact with upstream genes and proteins to feed back it them the upstream life activity network, revealing the life activity picture of the body at the overall level (Bjerrum et al., 2017; Li et al., 2021). Metabolomics is to study the regulation and response of organisms to the changes of internal and external environments from the perspective of the system so as to expand the research of the disease mechanism from the internal differences of organisms to the interaction between organisms and their environment, making the research more systematic, dynamic, and accurate (Bjerrum and Nielsen, 2019). Therefore, in this study, a large number of endogenous metabolites in the blood of NAFLD rats were detected qualitatively and quantitatively before and after the administration of the *Schisandra chinensis* caulis polysaccharide (SCP) by the metabolomics method based on UHPLC-Q-Orbitrap-MS/MS combined with multivariate analysis, and its specific mechanism was further explored.

MATERIALS AND METHODS

Chemicals and Reagents

Dried *Schisandra chinensis* caulis (Ji'an *Schisandra Chinensis* Planting Base in Jilin Province, Jilin, China); ALT, AST, TG, TC, HDL-C, LDL-C, MDA, GSH-Px, and SOD test kits (Nanjing Jiancheng Bioengineering Research Institute, Nanjing, China; batch number: 20191212, 20191212, 20191214, 20191212, 20191214, 20191212, 20210721, 20210721, and 20210721, respectively); and UGP-2, UGDH, FAS, and ACC antibodies (Wuhan Abclonal, Wuhan, China) were the chemicals and reagents.

Extraction and Determination of the *Schisandra chinensis* Caulis Polysaccharide

The dried *Schisandra chinensis* caulis was ground into powders, and then, the powders were immersed in 10 times the volume of distilled water at room temperature overnight. The next day, the mixture was boiled at 100°C for 3 h to obtain the water extraction, then the water extraction was concentrated at 80°C by rotary evaporation, and 95% ethanol was added to the supernatant. Finally, the ethanol concentration was adjusted to 75%, and then, the mixture was precipitated at room temperature overnight. The precipitate was collected by centrifuging it at 20°C for 15 min, then washed with 95% ethanol and anhydrous ethanol one time, and freeze-dried to obtain the powdery SCP.

The total carbohydrate content of SCP was determined by the phenol sulfuric acid method with glucose as the standard. The monosaccharide composition and molecular weight distribution of SCP were determined by high-performance liquid chromatography (HPLC).

Animal Grouping and Administration

Male Wistar rats, weighing 250–300 g, were provided by Changchun Yisi Experimental Animal Technology Co., Ltd. (Changchun, China), and the certificate number was SCXK (Ji) 2019-0007. The rats were reared in separate cages in a sterile feeding room at a temperature of 18–23°C and in a humidity of 40–60%. The standard feed and the high-fat feed for experimental rats were provided by Changchun Yisi Experimental Animal Technology Co., Ltd. (Changchun, China). The high-fat diet contained lard (15%), sucrose (20%), cholesterol (1.2%), sodium cholate (0.2%), casein (10%), calcium hydrogen phosphate (0.6%), and basic diet (53%). Animal experiments were approved by the Experimental Animal Ethics Committee of Beihua University (Jilin, China), and all the experimental procedures were performed in accordance with the Guide for the Care and Use of Laboratory Animals.

A total of 30 rats were randomly divided into the control group (CON), model group (MOD), and *Schisandra chinensis* caulis polysaccharide (SCP) group. Except for those in the CON group, all rats were fed with the high-fat diet for 4 weeks. Then, rats in the SCP group were given 100 mg kg^{-1} SCP solution for 6 weeks by gavage from the 5th week, and those in the CON and MOD groups were given an equal volume of distilled water in the same way. Rats in all groups were given standard diet from the 5th week to the 10th week. Blood samples of all the rats were collected from the abdominal aorta of anesthetized rats by the intraperitoneal injection of 25% urethane (100 mg kg^{-1}) on the 11th week. The blood samples were left standing at room temperature for 1 h and then centrifuged at 3,000 r min^{-1} to separate the serum, and the

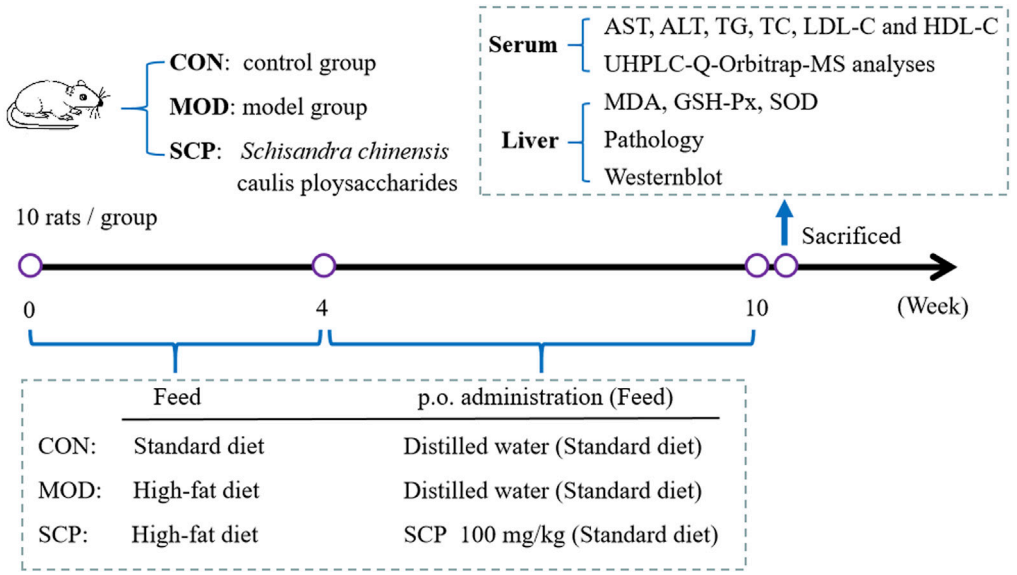

FIGURE 1 | Grouping and administration of rats and experimental processes.

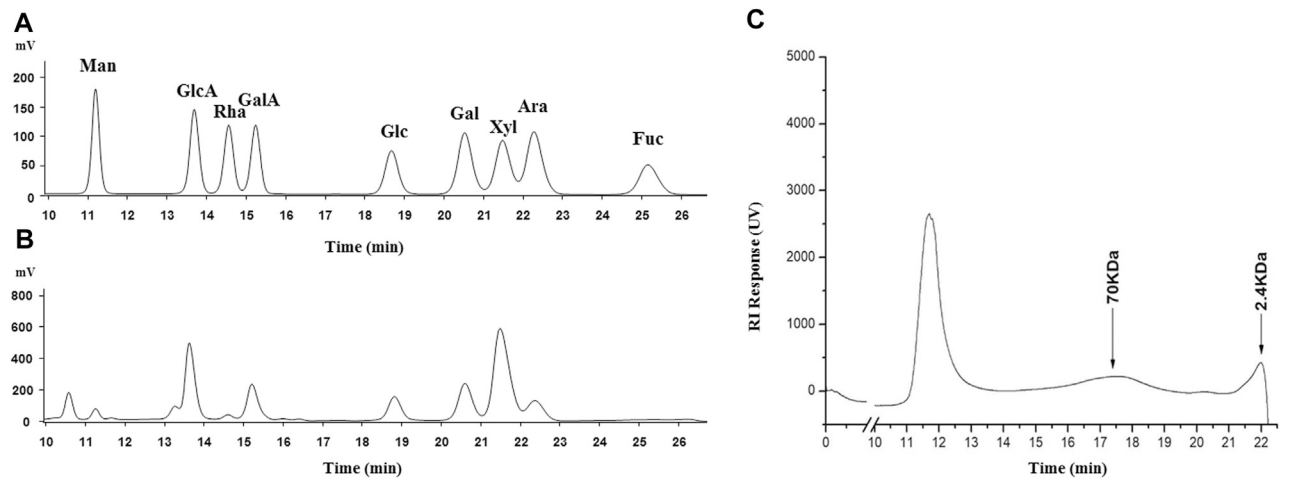

FIGURE 2 | HPLC spectrograms of monosaccharide composition in SCP (**A**: reference; **B**: SCP) and molecular weight distribution of SCP **(C)**. Man, mannose; GlcA, glucuronic acid; Rha, rhamnose; GalA, galacturonic acid; Glc, glucose; Gal, galactose; Xyl, xylose; Ara, arabinose; Fuc, fructose.

serum samples were stored at −20°C for standby. The hepatic tissue was washed with cold saline and divided into three parts: the first part was fixed with 10% neutral formaldehyde for histopathological examination, the second part was prepared into homogenates for the detection of antioxidant indexes, and the third part was preserved at −80°C for western blot analysis. The grouping and administration of rats and experimental processes are shown in **Figure 1**.

TABLE 1 | Chemical properties of SCP.

Monosaccharide composition (mol%)								
Man	GlcA	Rha	GalA	Glc	Gal	Xyl	Ara	Fuc
2.80	18.78	2.05	10.60	9.03	13.03	34.23	8.22	1.25

Man, mannose; GlcA, glucuronic acid; Rha, rhamnose; GalA, galacturonic acid; Glc, glucose; Gal, galactose; Xyl, xylose; Ara, arabinose; Fuc, fructose.

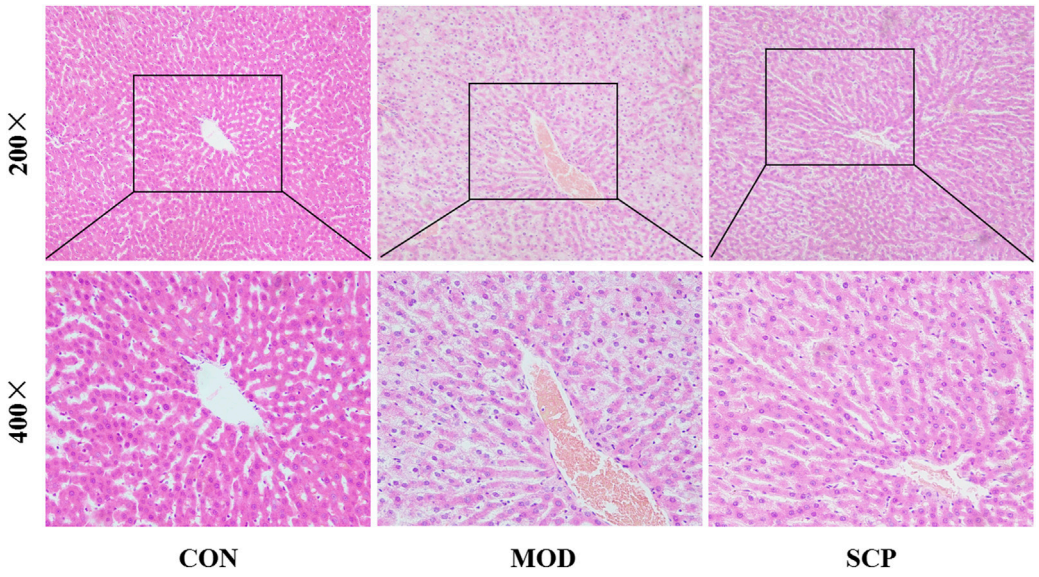

FIGURE 3 | Effects of SCP on histomorphological changes in the live tissue of mice.

Histomorphological Observation

The liver of rats was separated, the redundant tissue and fascia attached on the surface of liver were stripped, and the liver tissue was fixed with 10% formalin solution at room temperature for 24 h. The liver tissue was routinely sliced (5 μm thick), and the slices were embedded in paraffin and stained with Hematoxylin-eosin at room temperature for 10 min. Pathological changes of the liver tissue were observed under a light microscope (magnification:×200, ×400).

Determination of Biochemical Indexes

The levels of serum aspartate aminotransferase (AST), alanine aminotransferase (ALT), triglyceride (TG), total cholesterol (TC), low-density lipoprotein cholesterol (LDL-C), high-density lipoprotein cholesterol (HDL-C), liver malondialdehyde (MDA), glutathione peroxidase (GSH-Px), and superoxide dismutase (SOD) were detected by following the instructions of the test kits.

Metabolomic Analysis

One hundred μl of the serum was added with 400 μl of methanol. The serum–methanol solution was mixed using a vortex oscillator for 20 s and then centrifuged at 12,000 rpm and 4°C for 5 min to obtain the supernatant. The supernatant was evaporated to dryness with nitrogen, and its volume was fixed to 1 ml with methanol for use.

An Ultimate 3000 ultra-high-performance liquid chromatography (UHPLC) system (Thermo, San Jose, CA, United States) was used for the separation, in which the chromatographic column was a Supelco C18 column (3.0 × 50 mm, 2.7 μm; Sigma-Aldrich, United States), the column temperature was 35°C, and acetonitrile and water with 0.1% formic acid were used as mobile phases A and B, respectively; the gradient elution procedures were as follows: 65% B (0–5 min), 65–45% B (5–10 min), 45–15% B (10–20 min), 15–10% B (20–25 min), and 10–65% B (25–30 min); the flow rate was 0.3 ml/min; and the injection volume was 10 μl. The UHPLC system was connected with a mass spectrometer.

Q-Orbitrap-MS/MS (Thermo, San Jose, CA, United States) was used for the determination by mass spectrometry, in which the positive ion mode and negative ion mode were set. The electrospray ionization (ESI) source conditions were as follows: the sheath gas flow was 35 Arb, the auxiliary gas flow rate was 10 Arb, and the sweep gas flow was 1 Arb. The S-Lens RF was 50%, the capillary voltage was set to +4.0 kV, the capillary temperature was 340°C, and the mass scanning range was *m/z* 100–1,500 Da. LC-MS data were extracted, filtered, and normalized using Thermo software Xcalibur (version 4.3) to obtain the molecular weight, retention time, and absorption peak area of the compounds in each sample.

SIMCA 14.1 software (Umetrics, Kinelon, NJ, United States) was used for the multivariate data analysis, and potential marker compounds with importance of variables (VIP) >1 were screened by using principal component analysis (PCA), orthogonal partial least square discriminant analysis (OPLS-DA), and s-plot score analysis. The molecular weight, retention time, and MS/MS fragmentation ion characteristics of the different compounds were compared by using Xcalibur (version 4.3), and the structures were identified and elucidated in HMDB and KEGG databases. Finally, the selected endogenous compounds were input into the Metabo Analyst system to identify potential metabolic pathways related to the different compounds.

Western Blot Analysis

Fifty mg of the liver tissue was added with the lysis buffer for the lysis on ice for 1 h, and the lysate was centrifuged at

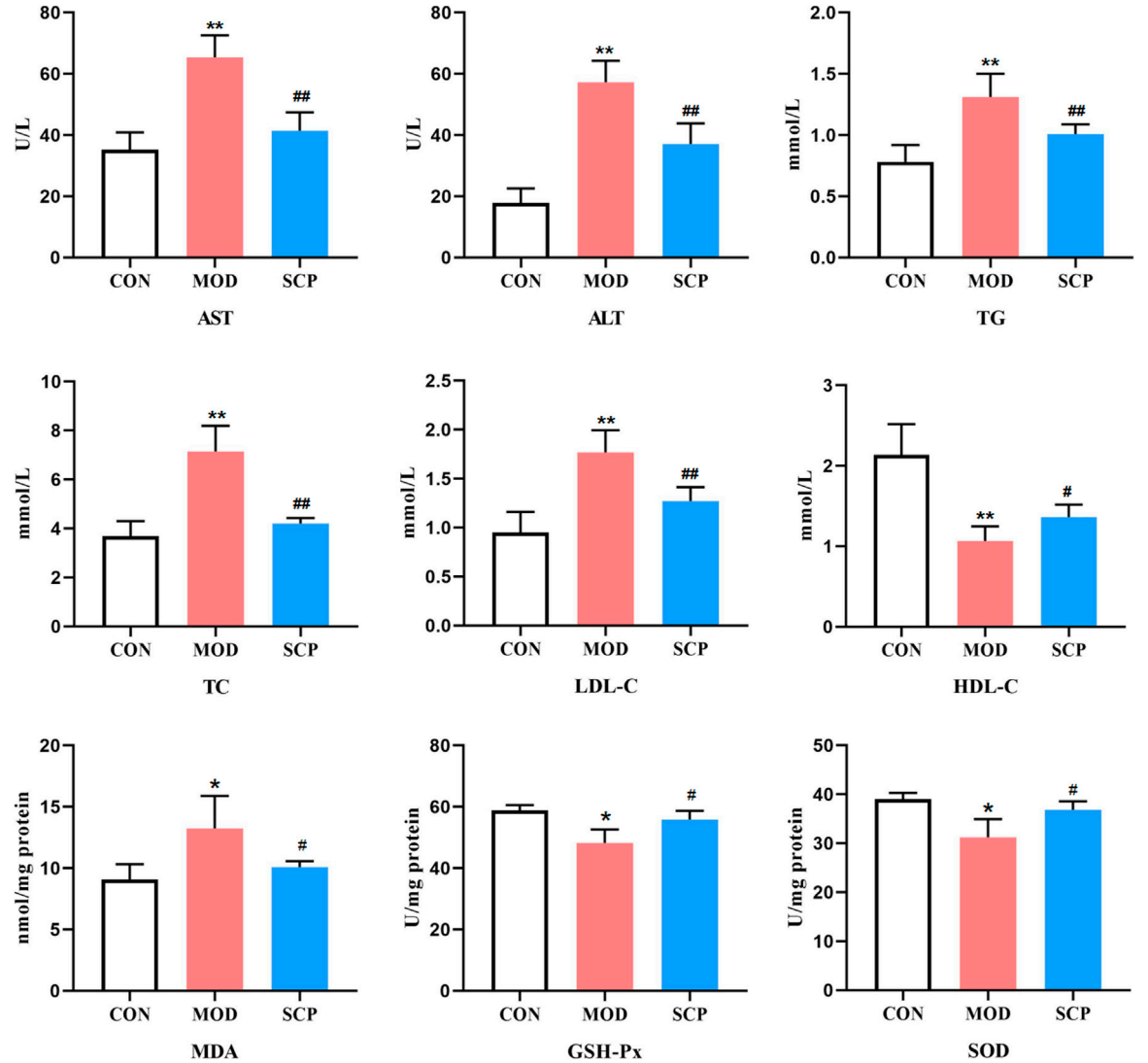

FIGURE 4 | Effects of SCP on the AST, ALT, TG, TC, LDL-C, and HDL-C levels in serum, the MDA level, and GSH-Px and SOD activities in the liver tissue. All the values were expressed as means ± standard deviation; compared with the CON group, $^{*}p < 0.05$, $^{**}p < 0.01$; compared with the MOD group, $^{\#}p < 0.05$, $^{\#\#}p < 0.01$.

12,000 rpm for 5 min. Then, the supernatant was taken and the protein content in it was determined by bicinchoninic acid, and the supernatant was stored at −20°C for use. The proteins were separated by sodium dodecyl sulfate-polyacrylamide gel electrophoresis and transferred onto poly(vinylidene difluoride) membranes (2 h). Tris-buffered saline with Tween 20 (TBST) containing 5% skimmed milk powder was added onto the membranes for blocking (1.5 h), and then, the blocking solution was discarded and the membranes were washed with TBST three times, with 10 min each time. The primary antibodies UGP2 (1:1,000), UGDH (1:1,000), FAS (1:1,000), and ACC (1:1,000) were added onto the membranes, and the membranes were incubated at 4°C overnight. Then, the membranes were washed with TBST three times, with 10 min each time. The membranes were incubated with the secondary antibody at room temperature for 1 h, and then, the enhanced chemiluminescence solution ECL was added onto the membranes for development after they were washed with TBST in the same way and photographed with a gel imager. GAPDH was used as the internal reference, and the gray value of each band was measured with Image J image analysis software. The ratio of each gray value to the gray value of GAPDH was the relative expression of proteins.

Statistical Analysis

Statistical analysis was performed using SPSS software (Windows version 19.0; IBM Corp., Armonk, NY, United States). One-way ANOVA was used for the comparison between groups. It was considered that $p < 0.05$ indicated a statistically significant difference.

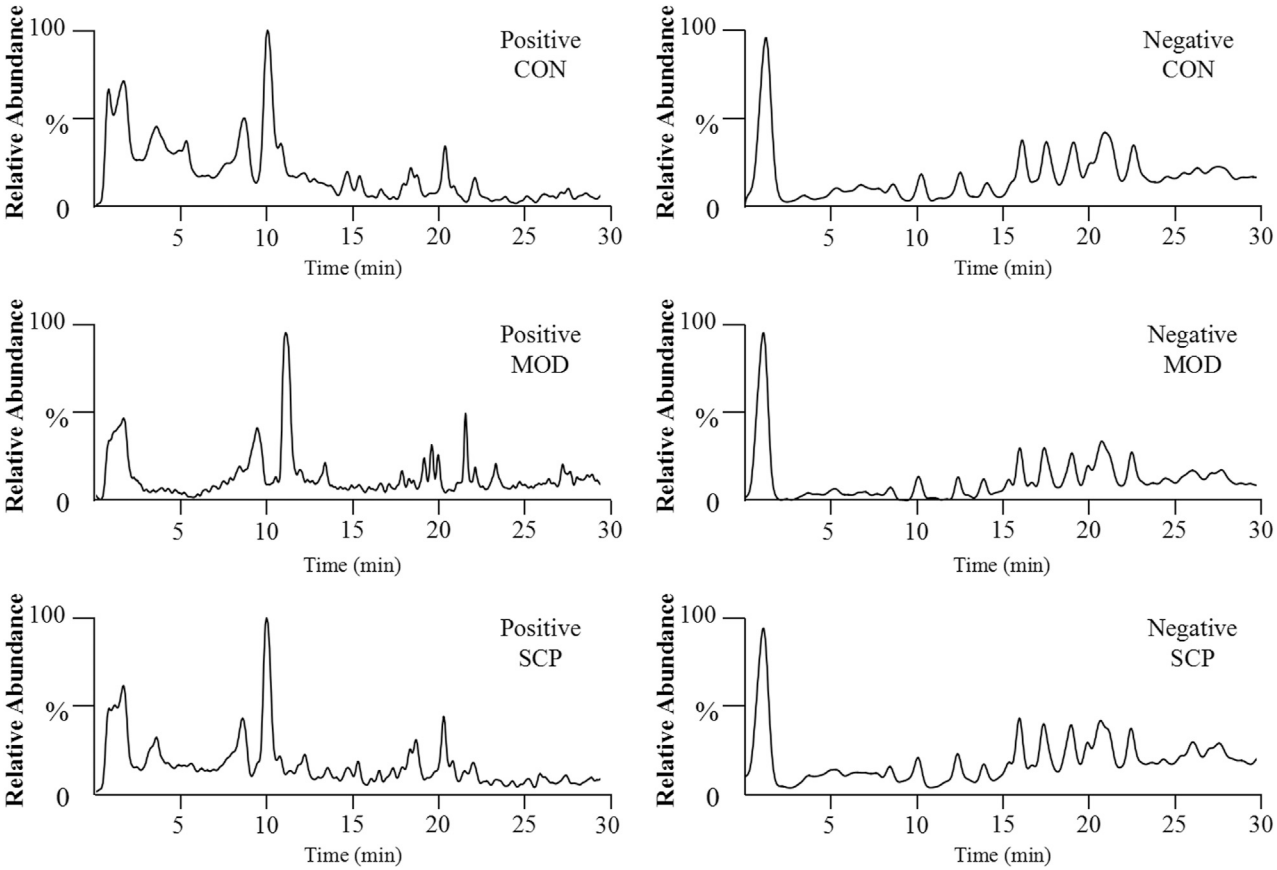

FIGURE 5 | BPI chromatograms of serum samples obtained from the negative and positive ion UHPLC-Q-Orbitrap-MS analyses.

RESULTS

Polysaccharide Content in *Schisandra chinensis* Caulis

After the water extraction, alcohol precipitation, and drying, 53.4 g of SCP was obtained from 1 kg of the dried *Schisandra chinensis* caulis, with a yield of 5.34%. The total carbohydrate content of SCP was 32.7%. As shown in **Figure 2**, the molecular weight of SCP was mainly from two fragments (peaks 2 and 3), and the relative molecular weight was 70 and 2.4 kDa, respectively. The monosaccharide contents in SCP are shown in **Table 1**.

Histomorphological Observation

In the CON group, the liver tissue structure of rats was normal and the lobule structure was clear. In the MOD group, the fatty degeneration of the hepatocyte tissue of rats was obvious, accompanied with the local punctate necrosis of hepatocytes, indicating that HFD could cause a severe liver injury in rats. Compared with the MOD group, the fatty degeneration of hepatocytes in the SCP group was alleviated, the blood sinus cavity returned to normal, and the local necrosis was alleviated, indicating that SPC should have a protective effect against NAFLD caused by HFD (**Figure 3**).

Effects of *Schisandra chinensis* Caulis Polysaccharides on Biochemical Indexes of Nonalcoholic Fatty Liver Disease Rats

Compared with those in the CON group, the levels of AST, ALT, TG, TC, and LDL-C in serum and MDA in the liver were significantly increased ($p < 0.05$, $p < 0.01$), while those of HDL-C in serum and GSH-Px and SOD in the liver were significantly decreased ($p < 0.05$, $p < 0.01$) in the MOD group; compared with those in the MOD group, the levels of AST, ALT, TG, TC, and LDL-C in serum and MDA in the liver were significantly decreased ($p < 0.05$, $p < 0.01$), and those of HDL-C in serum and GSH-Px and SOD in the liver were significantly increased ($p < 0.05$) in the SCP group (**Figure 4**).

Metabonomic Analysis

Figure 5 shows the base peak intensity (BPI) chromatograms of representative samples in the positive and negative ion modes. Based on the UHPLC-Q-Qrbitrap-MS/MS data, the potential metabolites in the serum samples of rats in the CON, MOD, and SCP groups were analyzed by PCA. PCA, a commonly used unsupervised multivariate data analysis method, is considered to reduce the number of dimensions with a minimum information loss and show the characteristics of each sample. As shown in the PCA score plots (**Figures 6A,B**), the scattering points of samples

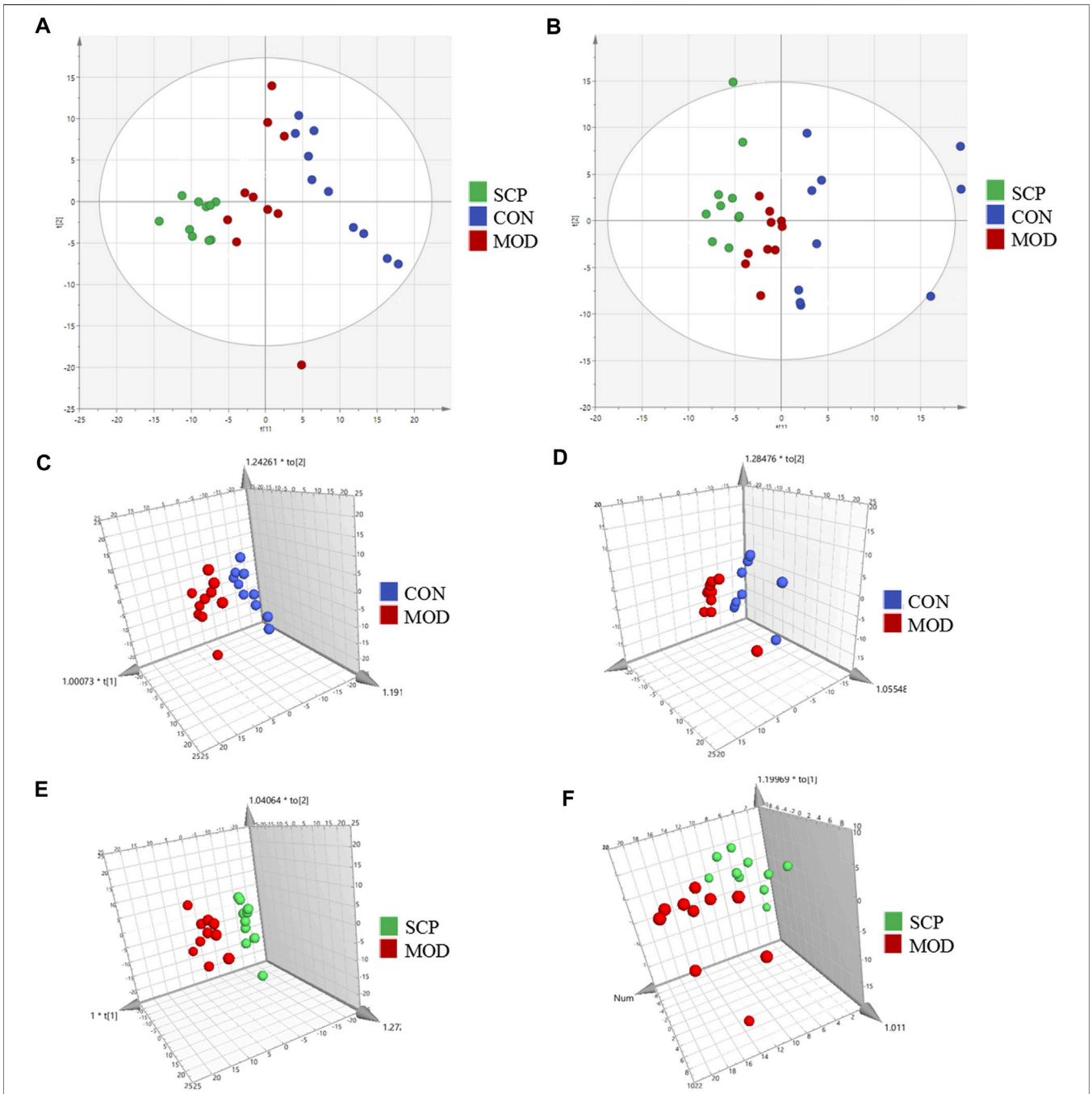

FIGURE 6 | PCA score plots of the CON, MOD, and SCP groups in the positive mode **(A)** and negative mode **(B)**; OPLS-DA score plots of the CON and MOD groups in the positive mode **(C)** and negative mode **(D)**; OPLS-DA score plots of the MOD and SCP groups in the positive mode **(E)** and negative mode **(F)**.

in the CON, MOD, and SCP groups showed an obvious separation in the positive and negative ion modes. Then, supervised OPLS discriminant analysis was used to maximize the difference of metabolites among the three groups and detect metabolites in biological samples. The metabolites in the blood of rats in the different groups were well separated, with obvious differences, indicating that HFD and SCP may induce significant changes in related components (**Figures 6C–F**).

The validity of the model was verified by 100 iterations of the permutation test. The R^2 (cumulative) and Q^2 (cumulative) values of all permutations on the left were lower than those of the original point on the right, and the intercept of the blue regression line of the R^2 point was negative, indicating that the original model was valid (**Figures 7A,B**). Further S-plot analysis was performed, and compounds with an evaluation parameter of VIP > 1 were regarded as potential biomarkers

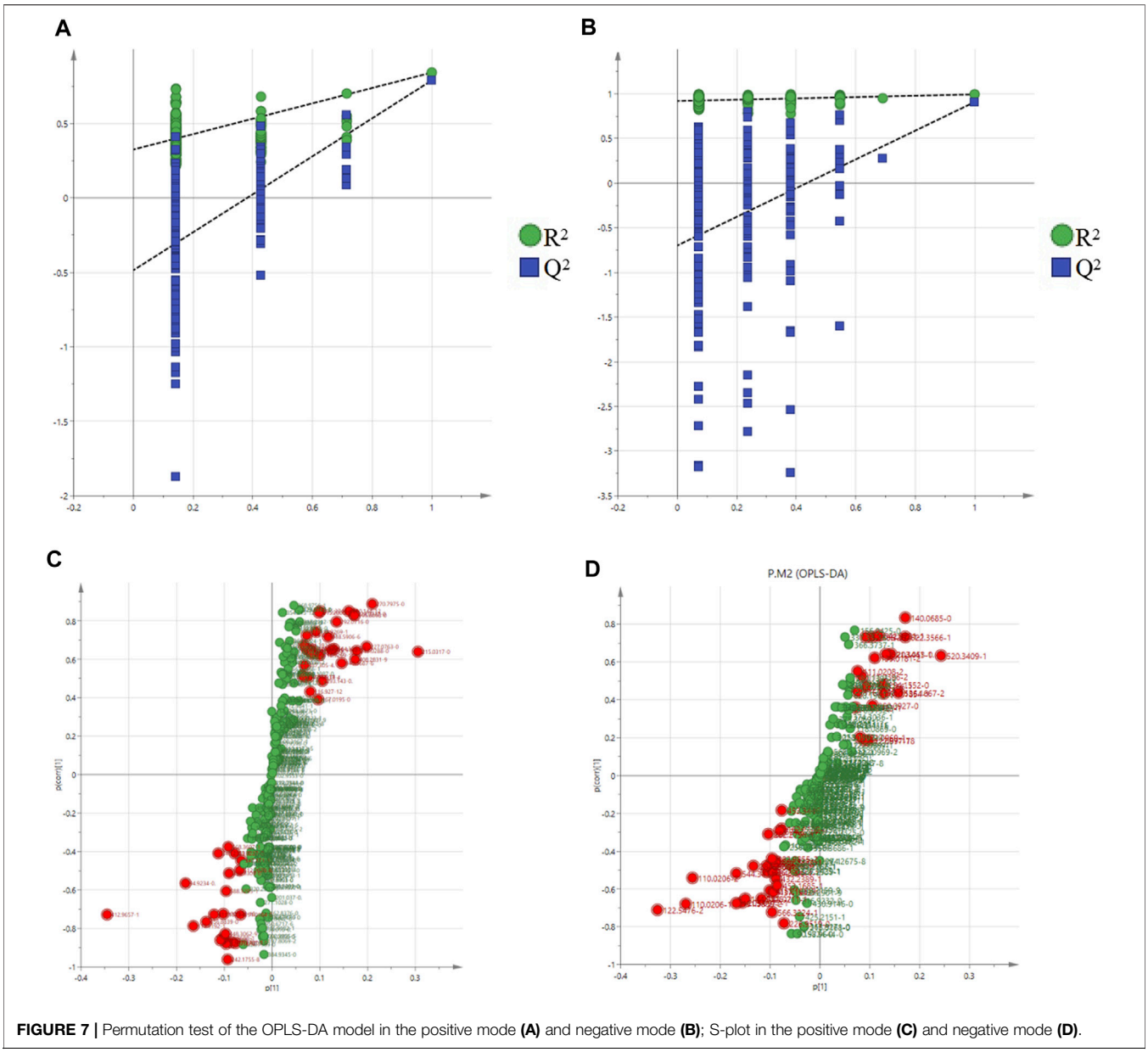

FIGURE 7 | Permutation test of the OPLS-DA model in the positive mode **(A)** and negative mode **(B)**; S-plot in the positive mode **(C)** and negative mode **(D)**.

based on the VIP in the projection of the OPLS-DA model (**Figures 7C,D**).

The accurate molecular mass and fragmentation ion characteristics (quality error <5 ppm) of the different metabolites were aligned with those in the human metabolism database (HMDB), lipidomics Gateway, and KEGG and PubChem databases, and 13 different metabolites among the groups were screened out (**Table 2**). The clustering analysis showed that compared with those in the CON group, the contents of citric acid, fumaric acid, proline, α-ketopentadic acid, sabouramide succinic acid, and acetylphosphate in the MOD group were significantly increased but significantly decreased after the intervention of SCP. Compared with those in the CON group, the contents of D-glucuronic acid, nicotinic acid, and butyric acid in the MOD group were significantly decreased, while those in the SCP group were significantly increased (**Figure 8A**). The pathway enrichment analysis of these 13 different metabolites showed that the metabolic differences were mainly in the metabolism of ascorbic acid and uronic acid, the mutual transformation of pentose and glucuronide, the metabolism of nicotinic acid and nicotinamide, the tricarboxylic acid cycle, the metabolism of butyric acid, and the metabolism of inositol phosphate (**Figure 8B**).

Metabolomic Validation

The analysis of the function and pathway enrichment was performed with metaboanalysis network tools, and the obtained pathways were further aligned through the KEGG database to find UDP-glucose pyrophosphorylase (UGP2),

TABLE 2 | Information of different metabolites among groups.

Mode	Time	*m/z*	Formula	VIP	Compound name	Trend		Related pathway
						C-M	M-S	
N	0.68	193.0351	$C_6H_{10}O_7$	2.74	D-Glucuronic acid	↓	↑	Ascorbate and aldarate metabolism
	18.47	114.0562	$C_5H_9NO_2$	2.62	Proline	↑	↓	Arginine and proline metabolism
	21.71	205.0514	$C_{11}H_{10}O_4$	1.72	Citropten	↑	↓	TCA cycle
	0.75	291.0587	$C_9H_{16}N_4O_7$	1.67	Canavaninosuccinate	↑	↓	TCA cycle
	15.57	115.0029	$C_4H_4O_4$	1.47	Fumaric acid	↑	↓	TCA cycle
	0.73	87.0469	$C_4H_8O_2$	1.25	Butyric acid	↓	↑	Butanoate metabolism
	4.63	485.1904	$C_{18}H_{34}N_2O_{13}$	1.10	Glucosylgalactosyl hydroxylysine	↑	↓	Amino acid metabolism
	8.51	510.1124	$C_{17}H_{29}N_4O_8P_2S$	1.07	3-Methyl-1-hydroxybutyl-ThPP	↑	↓	Valine, leucine, and isoleucine degradation
P	21.33	147.0299	$C_5H_6O_5$	2.05	α-Ketoglutaric acid	↑	↓	TCA cycle
	21.53	140.9932	$C_2H_5O_5P$	1.52	Acetylphosphate	↑	↓	Pyruvate metabolism
	13.44	508.9845	$C_{10}H_{15}N_4O_{14}P_3$	1.46	Inosine triphosphate	↑	↓	Purine metabolism
	16.15	124.0969	$C_6H_5NO_2$	1.34	Nicotinic acid	↓	↑	Nicotinate and nicotinamide metabolism
	21.46	184.0257	$C_4H_9NO_5S$	1.32	L-Homocysteic acid	↓	↑	Aminoacyl-tRNA biosynthesis

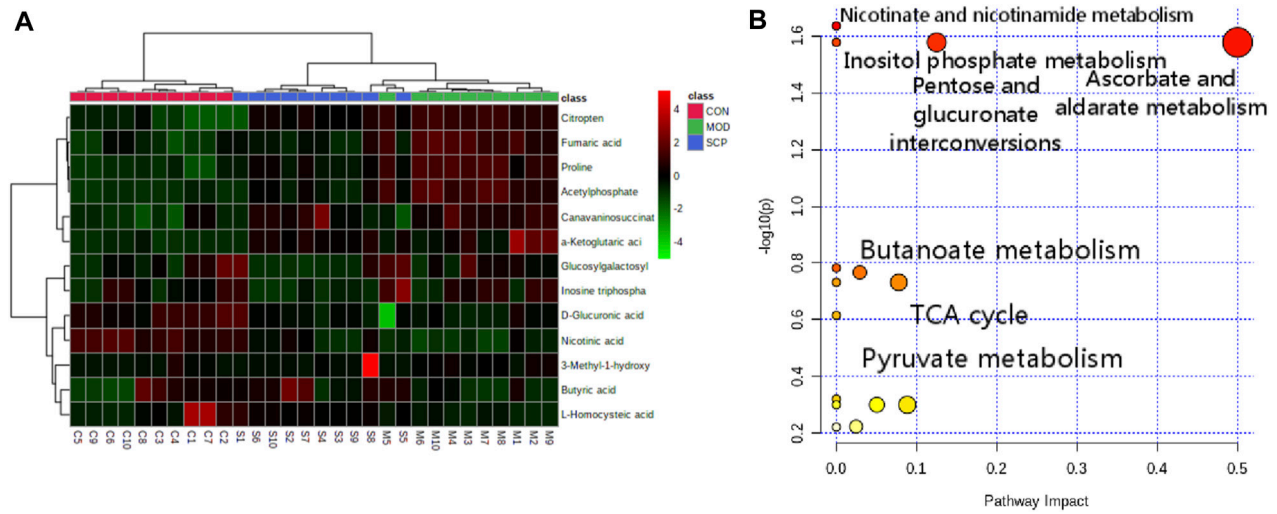

FIGURE 8 | Heat map of potential biomarker changes **(A)** and pathways in SCP-treated rats **(B)**.

UDP glucose 6-dehydrogenase (UGDH), acetyl CoA carboxylase (ACC), and fatty acid synthase (FAS) related to the metabolic pathways. Then, western blot was used to detect their expressions in the liver tissue of rats.

As shown in **Figure 9**, compared with those in the CON group, the levels of UGP2 and UGDH in the liver tissue of rats were significantly decreased ($p < 0.01$), and those of FAS and ACC were significantly increased ($p < 0.01$) in the MOD group; compared with those in the MOD group, the levels of UGP2 and UGDH in the liver tissue of rats were significantly increased ($p < 0.01$), and those of FAS and ACC were significantly decreased ($p < 0.01$) in the SCP group.

DISCUSSION

NAFLD is one of the most important causes of liver diseases, with a global prevalence rate of about 25% (Araújo et al., 2018), and may become the most important inducing cause of advanced liver diseases such as hepatocellular carcinoma in the next few decades (Younossi et al., 2017). At present, it is widely believed that the pathogenesis of NAFLD mainly includes insulin resistance, glucose metabolism disorder, metabolic syndrome, and the abnormal lipid metabolism (Cobbina and Akhlaghi, 2017; Goedeke et al., 2018). In this study, UHPLC-Q-Orbitrap-MS/MS, a metabonomics-based method, was used to study the endogenous metabolites of small molecules in the serum of NAFLD rats after the intervention of SCP.

The enrichment analysis of metabolic pathways showed that the pathways most related to the different metabolites mainly included the metabolism of ascorbic acid and uronic acid and the transformation of pentose and glucuronic acid. These two metabolic pathways are involved in the production of D-glucose-1-phosphate, UDP-glucose, D-glucuronic acid, and pyruvate from the downstream D-glucose after the intake of sugar and nutrients by organisms. It has been reported that one of

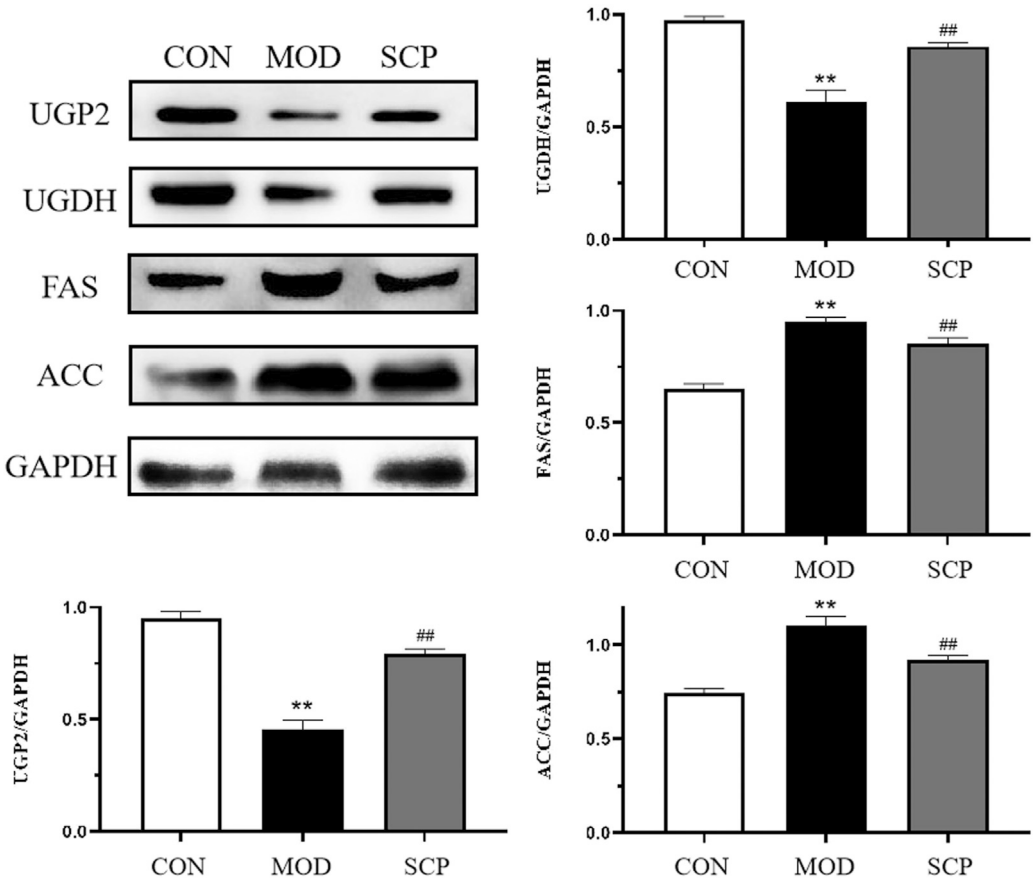

FIGURE 9 | Effects of SCP on the expression of UGP2, UGDH, FAS, ACC, and GAPDH proteins in the liver tissue. All the values were expressed as means ± standard deviation. Compared with the CON group, $^{*}p < 0.05$, $^{**}p < 0.01$; compared with the MOD group, $^{\#}p < 0.05$, $^{\#\#}p < 0.01$.

the causes of NAFLD is insulin resistance, characterized by the decreased utilization of glucose (Chen et al., 2016; Gastaldelli, 2017; Watt et al., 2019). In this study, the content of D-glucuronide in the serum of NAFLD rats was significantly lower than that in the CON group, indicating the abnormality of these two related metabolic pathways and the possibility of insulin resistance occurrence, while the content of D-glucuronide in the serum of NAFLD rats in the SCP group was increased, indicating that SCP may play a therapeutic role in NAFLD by regulating the D-glucuronide-related metabolic pathway. In order to verify this hypothesis, we first searched for the two pathways in the KEGG database, and it was found that both UGP2 and UGDH participated in the above metabolic process by participating in the mutual transformation of D-glucose 1-phosphate and UDP-glucose to produce D-glucuronic acid. It has been pointed out that UGP2, a key enzyme in glycogen biosynthesis (Looft et al., 2000; Mohammad et al., 2012), has been demonstrated to be related to the occurrence and development of a variety of cancers (Tan et al., 2014; Wang et al., 2018; Zeng et al., 2019), including hepatocellular carcinoma (HCC) (Zhou et al., 2012). Then, the expression levels of UGP2 and UGDH in the liver tissue of rats were detected by western blot. Compared with those in the CON group, the expression levels of UGP2 and UGDH in the liver tissue of rats in the MOD group were significantly decreased, confirming our hypothesis that NAFLD could cause the abnormality in the metabolism of ascorbic acid and uronic acid as well as the transformation pathway of pentose and glucuronic acid and reduce the body's utilization of glucose, resulting in gluconeogenesis; compared with those in the MOD group, the expression levels of UGP2 and UGDH in the liver tissue of rats in the SCP group increased, indicating that SCP could play a hepatoprotective role in NAFLD rats by regulating the metabolism of ascorbic acid and uronic acid as well as the transformation pathway of pentose and glucuronic acid.

Pyruvate is produced from the diet ingested by the body through the metabolism. Acetylphosphate and nicotinic acid are found to be involved in the metabolism of pyruvate and nicotinamide among the differential metabolites. Both these metabolites can affect the production of pyruvate. In particular, nicotinic acid can treat dyslipidemia and cardiovascular diseases by affecting the metabolism of lipids (Meyers et al., 2004), help to change the abnormal fat accumulation (Ganji et al., 2004), and reduce the content of plasma triglycerides (Ganji et al., 2014). In NAFLD rats, the relative content of nicotinic acid decreased sharply, while the

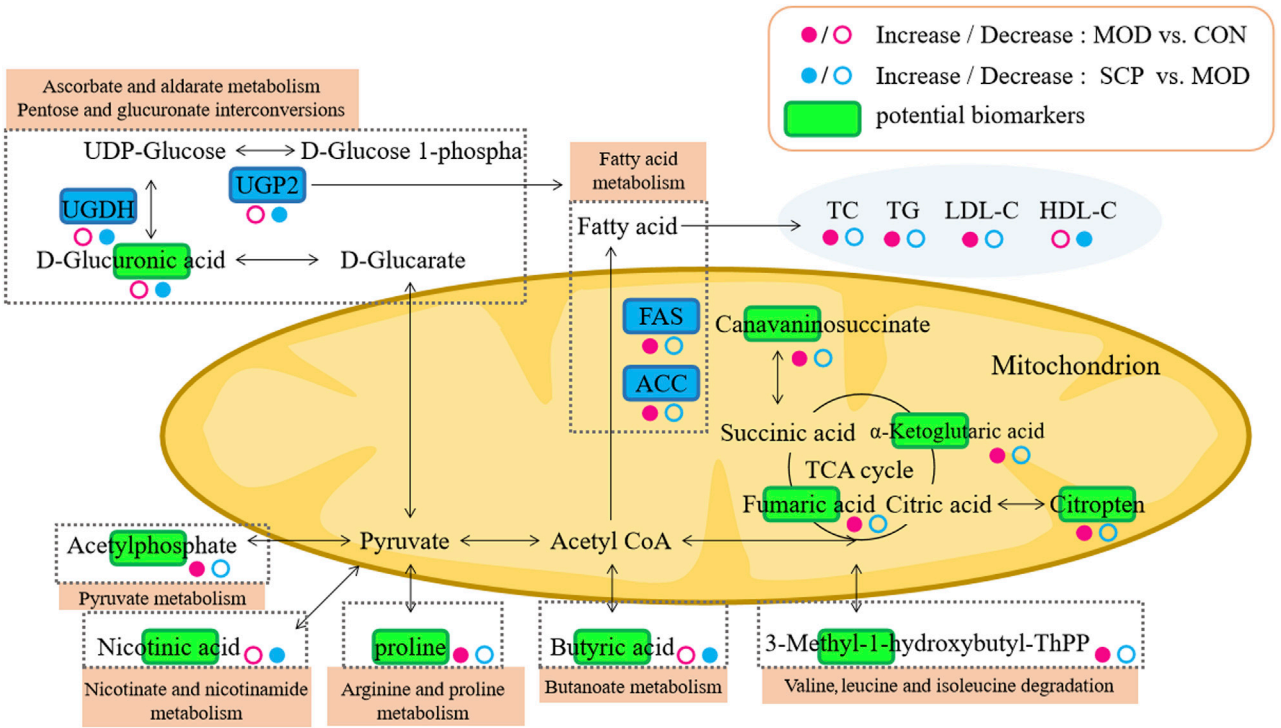

FIGURE 10 | Proposed metabolic pathways regulated by SCP in NAFLD.

relative content of acetylphosphate increased sharply, suggesting that the abnormality in the metabolism of both pyruvate and nicotinic acid could occur in NAFLD, and nicotinic acid could not normally inhibit the excessive production of pyruvate by regulating the lipid metabolism, increasing the content of free fatty acids in the body. Moreover, free fatty acids are accumulated in the liver due to insulin resistance, leading to steatosis in the liver (Mccommis and Finck, 2019), which can eventually evolve into NAFLD. In the SCP group, the relative level of nicotinic acid increased and the level of acetylphosphate decreased, indicating that SCP can also play a hepatoprotective role in NAFLD rats by regulating the metabolism of pyruvate and nicotinic acid.

A lower relative expression of butyric acid was also found in NAFLD rats. Butyric acid, a short-chain fatty acid, is produced by the fermentation of resistant starch, dietary fiber, and other low-digestibility polysaccharides by microorganisms in the distal intestine and colon (Kau et al., 2011). It has been found that butyric acid can affect the occurrence and development of NAFLD by reducing inflammatory response, inhibiting insulin resistance, and weakening oxidative stress of liver mitochondria (Baumann et al., 2020). Compared with that in the MOD group, the expression level of butyric acid was increased in the SCP group, indicating that SCP may alleviate NAFLD by regulating the metabolism of butyric acid.

Mitochondria are vulnerable to various damage factors such as oxides due to their high sensitivity, leading to the occurrence of a fatty liver (Horvath and Daum, 2013). High-fat diet can induce endoplasmic reticulum stress and then cause the lipid deposition in hepatocytes and the occurrence of a fatty liver (Zhang et al., 2019). It is found that ACC and FAS play an important role in the development and treatment of NAFLD. ACC catalyzes the irreversible carboxylation of acetyl coenzyme A in mitochondria to produce malonyl coenzyme A. FAS then condenses acetyl coenzyme A and malonyl coenzyme A to generate long-chain fatty acids, resulting in the fat accumulation (Kohjima et al., 2007; Kwan et al., 2015). Butyrate and pyruvate are also involved in the metabolic pathway of acetyl CoA. In addition, it has been reported that the low expression of UGP2 is significantly correlated with the fatty acid metabolism and related to fatty acid metabolic enzymes such as FAS, so it is speculated that UGP2 may play an important role in the occurrence and development of liver diseases by regulating the metabolism of fatty acid (Hu et al., 2020). The results showed that compared with those in the CON group, the levels of ACC and FAS in the MOD group were significantly increased, indicating that the low expression of UGP2 could cause the disorder of the fatty acid metabolism to cause or develop NAFLD; compared with those in the MOD group, the levels of ACC and FAS in the SCP group were significantly decreased, indicating that SCP could alleviate the disorder of the fatty acid metabolism by regulating UGP2 to regulate ACC and FAS so as to promote the decomposition and metabolism of fat, reduce the accumulation of fat in the liver of NAFLD rats, reverse the intrahepatic steatosis of NAFLD rats, and facilitate the recovery of the liver morphology, structure, and function.

Pyruvate enters mitochondria for oxidative decarboxylation to form acetyl coenzyme A and finally enters the tricarboxylic

acid cycle. α-Ketoglutarate, a product of oxidative deamination of glutamic acid, can participate in the tricarboxylic acid cycle with citric acid and fumaric acid together, indicating that it is an important intermediate. In this study, compared with those in the CON group, the levels of D-glucose in the serum of rats were decreased, while those of α-ketoglutarate, citric acid, and fumaric acid were increased in the MOD group, indicating that the tricarboxylic acid cycle should be inhibited and the utilization rate of glucose should be reduced, which may also be a manifestation of insulin resistance. Oxidative stress is one of the pathogenic mechanisms of NAFLD, and Kupffer cells are the main effectors responsible for the generation of reactive oxygen species (ROS), which consequently affect hepatic stellate cells (HSCs) and hepatocytes. ROS-activated HSCs undergo a phenotypic switch and deposit an excessive amount of the extracellular matrix that alters the normal liver architecture and negatively affects the liver function. Additionally, ROS stimulate necrosis and apoptosis of hepatocytes, which causes liver injury and leads to the progression of end-stage liver disease (Luangmonkong et al., 2018; Farzanegi et al., 2019). Oxidative stress can also inhibit the tricarboxylic acid cycle to cause the accumulation and increase of the above substances in the body (Langley et al., 2020). The lower levels of α-ketoglutarate, citric acid, and fumaric acid in the serum of rats in the SCP group than those in the MOD group suggest that SCP may treat NAFLD by inhibiting oxidative stress, and the results of MDA, GSH-Px, and SOD detection also confirm this. The mechanism pathways regulated by SCP in NAFLD are summarized in **Figure 10**.

The early diagnosis of liver steatosis lacks specific and sensitive biomarkers, and the biomarkers change significantly only in severe liver injury, so it is necessary to find more sensitive biomarkers (Chen et al., 2014). In recent years, with the continuous development of metabolomics, a large number of studies have reported the biomarkers of NAFLD, such as fatty acid amides, phosphatidylcholine, amino acids, and so forth (Caussy et al., 2019; Kim, 2021). The integration of metabolomics data and clinical information will be hopeful to discover the individual molecular characteristics in patients with NAFLD, and thereby, the patients at a risk of occurrence and progression of NAFLD will be found between patient subgroups. Our study will provide a datum support for the discovery of NAFLD biomarkers and lay a theoretical foundation for the further development and utilization of SCP.

CONCLUSIONS

Effects of SCP on plasma metabolites of NAFLD rats were studied by the metabolomics method based on UHPLC-Q-Orbitrap-MS/MS combined with multivariate analysis. A total of 13 differential metabolites were identified. The enrichment analysis found that the pathways through which SCP could play a therapeutic role in NAFLD mainly include the metabolism of ascorbic acid and uronic acid, the mutual transformation of pentose and glucuronide, the metabolism of nicotinic acid and nicotinamide, the tricarboxylic acid cycle, the metabolism of butyric acid, and the metabolism of inositol phosphate. The mechanism through which SCP could play a therapeutic role in NAFLD was confirmed by detecting the expression of the key targets in these metabolic pathways, including UGP2, UGDH, ACC, and FAS proteins. This study may provide some potential targets for the application of SCP in the treatment of NAFLD. In order to in-depth clarify the therapeutic mechanism of SCP, both *in vitro* studies on searching for immortalized cell lines and *in vivo* studies with genetic mouse models lacking the expression of the target genes should be carried out in the future.

DATA AVAILABILITY STATEMENT

The datasets presented in this study can be found in online repositories. The names of the repository/repositories and accession number(s) can be found below: MetaboLights, MTBLS3194, https://www.ebi.ac.uk/metabolights/MTBLS3194/descriptors.

ETHICS STATEMENT

The animal study was reviewed and approved by the Experimental Animal Ethics Committee of Beihua University.

AUTHOR CONTRIBUTIONS

YF, GX, and JS contributed to the conception and design of the study; YF and Han L carried out the metabolomics analysis; YF, Han L, and CC were involved in the determination of SCP; Han L, CC, and Hao L participated in the animal experiments and data collection; He L and CW performed the statistical analysis; GX, JC, and JS wrote the manuscript. All authors read and approved the submitted version.

FUNDING

This work was supported by the National Natural Science Foundation of China (No. 81973371), the Natural Science Foundation of Jilin Province (No 20200404022YY), and the TCM science and technology project of Jilin Province (No. 2020119).

SUPPLEMENTARY MATERIAL

The Supplementary Material for this article can be found online at: https://www.frontiersin.org/articles/10.3389/fphar.2021.727636/full#supplementary-material

REFERENCES

Abdelmoneim, D., El-Adl, M., El-Sayed, G., and El-Sherbini, E. S. (2021). Protective Effect of Fenofibrate Against High-Fat-High-Fructose Diet Induced Non-Obese NAFLD in Rats. *Fundam. Clin. Pharmacol.* 35, 379–388. doi:10.1111/fcp.12597

Araújo, A. R., Rosso, N., Bedogni, G., Tiribelli, C., and Bellentani, S. (2018). Global Epidemiology of Non-alcoholic Fatty Liver Disease/non-Alcoholic Steatohepatitis: What We Need in the Future. *Liver Int.* 38 (Suppl. 1), 47–51. doi:10.1111/liv.13643

Baumann, A., Jin, C. J., Brandt, A., Sellmann, C., Nier, A., Burkard, M., et al. (2020). Oral Supplementation of Sodium Butyrate Attenuates the Progression of Non-alcoholic Steatohepatitis. *Nutrients* 12, 951. doi:10.3390/nu12040951

Bjerrum, J. T., and Nielsen, O. H. (2019). Metabonomics in Gastroenterology and Hepatology. *Int. J. Mol. Sci.* 20, 3638. doi:10.3390/ijms20153638

Bjerrum, J. T., Steenholdt, C., Ainsworth, M., Nielsen, O. H., Reed, M. A., Atkins, K., et al. (2017). Metabonomics Uncovers a Reversible Proatherogenic Lipid Profile during Infliximab Therapy of Inflammatory Bowel Disease. *BMC Med.* 15, 184. doi:10.1186/s12916-017-0949-7

Caussy, C., Ajmera, V. H., Puri, P., Hsu, C. L., Bassirian, S., Mgdsyan, M., et al. (2019). Serum Metabolites Detect the Presence of Advanced Fibrosis in Derivation and Validation Cohorts of Patients with Non-alcoholic Fatty Liver Disease. *Gut* 68, 1884–1892. doi:10.1136/gutjnl-2018-317584

Chen, H., Miao, H., Feng, Y. L., Zhao, Y. Y., and Lin, R. C. (2014). Metabolomics in Dyslipidemia. *Adv. Clin. Chem.* 66, 101–119. doi:10.1016/b978-0-12-801401-1.00004-9

Chen, X., Tang, R., Liu, T., Dai, W., Liu, Q., Gong, G., et al. (2019). Physicochemical Properties, Antioxidant Activity and Immunological Effects *In Vitro* of Polysaccharides from *Schisandra sphenanthera* and *Schisandra chinensis*. *Int. J. Biol. Macromol* 131, 744–751. doi:10.1016/j.ijbiomac.2019.03.129

Chen, Y., Li, C., Liu, L., Guo, F., Li, S., Huang, L., et al. (2016). Serum Metabonomics of NAFLD Plus T2DM Based on Liquid Chromatography-Mass Spectrometry. *Clin. Biochem.* 49, 962–966. doi:10.1016/j.clinbiochem.2016.05.016

Cobbina, E., and Akhlaghi, F. (2017). Non-Alcoholic Fatty Liver Disease (NAFLD) - Pathogenesis, Classification, and Effect on Drug Metabolizing Enzymes and Transporters. *Drug Metab. Rev.* 49, 197–211. doi:10.1080/03602532.2017.1293683

Farzanegi, P., Dana, A., Ebrahimpoor, Z., Asadi, M., and Azarbayjani, M. A. (2019). Mechanisms of Beneficial Effects of Exercise Training on Non-alcoholic Fatty Liver Disease (NAFLD): Roles of Oxidative Stress and Inflammation. *Eur. J. Sport Sci.* 19, 994–1003. doi:10.1080/17461391.2019.1571114

Ganji, S. H., Kukes, G. D., Lambrecht, N., Kashyap, M. L., and Kamanna, V. S. (2014). Therapeutic Role of Niacin in the Prevention and Regression of Hepatic Steatosis in Rat Model of Nonalcoholic Fatty Liver Disease. *Am. J. Physiol. Gastrointest. Liver Physiol.* 306, G320–G327. doi:10.1152/ajpgi.00181.2013

Ganji, S. H., Tavintharan, S., Zhu, D., Xing, Y., Kamanna, V. S., and Kashyap, M. L. (2004). Niacin Noncompetitively Inhibits DGAT2 but Not DGAT1 Activity in HepG2 Cells. *J. Lipid Res.* 45, 1835–1845. doi:10.1194/jlr.M300403-JLR200

Gastaldelli, A. (2017). Insulin Resistance and Reduced Metabolic Flexibility: Cause or Consequence of NAFLD? *Clin. Sci.* 131, 2701–2704. doi:10.1042/CS20170987

Goedeke, L., Bates, J., Vatner, D. F., Perry, R. J., Wang, T., Ramirez, R., et al. (2018). Acetyl-CoA Carboxylase Inhibition Reverses NAFLD and Hepatic Insulin Resistance but Promotes Hypertriglyceridemia in Rodents. *Hepatology* 68, 2197–2211. doi:10.1002/hep.30097

Horvath, S. E., and Daum, G. (2013). Lipids of Mitochondria. *Prog. Lipid Res.* 52, 590–614. doi:10.1016/j.plipres.2013.07.002

Hu, Q., Shen, S., Li, J., Liu, L., Liu, X., Zhang, Y., et al. (2020). Low UGP2 Expression is Associated with Tumour Progression and Predicts Poor Prognosis in Hepatocellular Carcinoma. *Dis. Markers* 2020, 3231273. doi:10.1155/2020/3231273

Kau, A. L., Ahern, P. P., Griffin, N. W., Goodman, A. L., and Gordon, J. I. (2011). Human Nutrition, the Gut Microbiome and the Immune System. *Nature* 474, 327–336. doi:10.1038/nature10213

Kim, H. Y. (2021). Recent Advances in NAFLD Metabolomics. *Clin. Mol. Hepatol.* [Epub ahead of print]. doi:10.3350/cmh.2021.0127

Kohjima, M., Enjoji, M., Higuchi, N., Kato, M., Kotoh, K., Yoshimoto, T., et al. (2007). Re-evaluation of Fatty Acid Metabolism-Related Gene Expression in Nonalcoholic Fatty Liver Disease. *Int. J. Mol. Med.* 20, 351–358. doi:10.3892/ijmm.20.3.351

Kwan, H. Y., Niu, X., Dai, W., Tong, T., Chao, X., Su, T., et al. (2015). Lipidomic-based Investigation into the Regulatory Effect of Schisandrin B on Palmitic Acid Level in Non-alcoholic Steatotic Livers. *Sci. Rep.* 5, 9114. doi:10.1038/srep09114

Langley, M. R., Yoon, H., Kim, H. N., Choi, C. I., Simon, W., Kleppe, L., et al. (2020). High Fat Diet Consumption Results in Mitochondrial Dysfunction, Oxidative Stress, and Oligodendrocyte Loss in the central Nervous System. *Biochim. Biophys. Acta Mol. Basis Dis.* 1866, 165630. doi:10.1016/j.bbadis.2019.165630

Li, X., Sun, J., Chen, Z., Jiang, J., and Jackson, A. (2021). Metabolite Profile and Genes/proteins Expression in β-citraturin Biosynthesis during Fruit Ripening in Chinese Raspberry (Rubus Chingii Hu). *Plant Physiol. Biochem.* 163, 76–86. doi:10.1016/j.plaphy.2021.03.022

Li, Y. Z., Wang, Z., Ma, Z. N., Li, Q., Ren, K., and Li, W. (2018). Effect of Extract from the Stems of Schisandra Chinensis on High Fat Diet-Induced Obesity in Mice. *J. Chin. Pharmaceutival.* 53, 518–525. doi:10.11669/cpj.2018.07.008

Looft, C., Paul, S., Thomsen, P. D., Yerle, M., Brenig, B., and Kalm, E. (2000). Isolation and Assignment of the UDP-Glucose Pyrophosphorylase Gene (UGP2) to Porcine Chromosome 3q21-->q22 by FISH and by Analysis of Somatic Cell and Radiation Hybrid Panels. *Cytogenet. Cel Genet* 89, 154–155. doi:10.1159/000015599

Luangmonkong, T., Suriguga, S., Mutsaers, H. A. M., Groothuis, G. M. M., Olinga, P., and Boersema, M. (2018). Targeting Oxidative Stress for the Treatment of Liver Fibrosis. *Rev. Physiol. Biochem. Pharmacol.* 175, 71–102. doi:10.1007/112_2018_10

Mccommis, K. S., and Finck, B. N. (2019). Treating Hepatic Steatosis and Fibrosis by Modulating Mitochondrial Pyruvate Metabolism. *Cell Mol. Gastroenterol. Hepatol.* 7, 275–284. doi:10.1016/j.jcmgh.2018.09.017

Meyers, C. D., Kamanna, V. S., and Kashyap, M. L. (2004). Niacin Therapy in Atherosclerosis. *Curr. Opin. Lipidol.* 15, 659–665. doi:10.1097/00041433-200412000-00006

Mocan, A., Schafberg, M., Crișan, G., and Rohn, S. (2016). Determination of Lignans and Phenolic Components of *Schisandra chinensis* (Turcz.) Baill. Using HPLC-ESI-ToF-MS and HPLC-Online TEAC: Contribution of Individual Components to Overall Antioxidant Activity and Comparison with Traditional Antioxidant Assays. *J. Funct. Foods* 24, 579–594. doi:10.1016/j.jff.2016.05.007

Mohammad, M. A., Hadsell, D. L., and Haymond, M. W. (2012). Gene Regulation of UDP-Galactose Synthesis and Transport: Potential Rate-Limiting Processes in Initiation of Milk Production in Humans. *Am. J. Physiol. Endocrinol. Metab.* 303, E365–E376. doi:10.1152/ajpendo.00175.2012

Schön, M. P. (2021). Psoriasis and Non-alcoholic Fatty Liver Disease. *J. Dtsch. Dermatol. Ges.* 19, 503–504. doi:10.1111/ddg.14469

Tan, G. S., Lim, K. H., Tan, H. T., Khoo, M. L., Tan, S. H., Toh, H. C., et al. (2014). Novel Proteomic Biomarker Panel for Prediction of Aggressive Metastatic Hepatocellular Carcinoma Relapse in Surgically Resectable Patients. *J. Proteome Res.* 13, 4833–4846. doi:10.1021/pr500229n

Wang, L., Xiong, L., Wu, Z., Miao, X., Liu, Z., Li, D., et al. (2018). Expression of UGP2 and CFL1 Expression Levels in Benign and Malignant Pancreatic Lesions and Their Clinicopathological Significance. *World J. Surg. Oncol.* 16, 11. doi:10.1186/s12957-018-1316-7

Watt, M. J., Miotto, P. M., De Nardo, W., and Montgomery, M. K. (2019). The Liver as an Endocrine Organ-Linking NAFLD and Insulin Resistance. *Endocr. Rev.* 40, 1367–1393. doi:10.1210/er.2019-00034

Yan, C., Guo, H., Ding, Q., Shao, Y., Kang, D., Yu, T., et al. (2020). Multiomics Profiling Reveals Protective Function of Schisandra Lignans against Acetaminophen-Induced Hepatotoxicity. *Drug Metab. Dispos* 48, 1092–1103. doi:10.1124/dmd.120.000083

Younossi, Z., Anstee, Q. M., Marietti, M., Hardy, T., Henry, L., Eslam, M., et al. (2017). Global Burden of NAFLD and NASH: Trends, Predictions, Risk Factors and Prevention. *Nat. Rev. Gastroenterol. Hepatol.* 15, 11–20. doi:10.1038/nrgastro.2017.109

Zeng, C., Xing, W., and Liu, Y. (2019). Identification of UGP2 as a Progression Marker that Promotes Cell Growth and Motility in Human Glioma. *J. Cell. Biochem.* 120, 12489–12499. doi:10.1002/jcb.28515

Zhang, L., Qi, Y., ALuo, Z., Liu, S., Zhang, Z., and Zhou, L. (2019). Betaine Increases Mitochondrial Content and Improves Hepatic Lipid Metabolism. *Food Funct.* 10, 216–223. doi:10.1039/c8fo02004c

Zheng, L. S., Du, S. S., and Cai, Q. (2014). [Study on Chemical Constituents from Schisandra Chinensis Stem]. *Zhong Yao Cai* 37, 1803–1806. doi:10.13863/j.issn1001-4454.2014.10.025

Zhou, L., Wang, Q., Yin, P., Xing, W., Wu, Z., Chen, S., et al. (2012). Serum Metabolomics Reveals the Deregulation of Fatty Acids Metabolism in Hepatocellular Carcinoma and Chronic Liver Diseases. *Anal. Bioanal. Chem.* 403, 203–213. doi:10.1007/s00216-012-5782-4

Zhu, P., Li, J., Fu, X., and Yu, Z. (2019). Schisandra Fruits for the Management of Drug-Induced Liver Injury in China: A Review. *Phytomedicine* 59, 152760. doi:10.1016/j.phymed.2018.11.020

Conflict of Interest: The authors declare that the research was conducted in the absence of any commercial or financial relationships that could be construed as a potential conflict of interest.

Publisher's Note: All claims expressed in this article are solely those of the authors and do not necessarily represent those of their affiliated organizations, or those of the publisher, the editors and the reviewers. Any product that may be evaluated in this article, or claim that may be made by its manufacturer, is not guaranteed or endorsed by the publisher.

frontiers in Pharmacology

ORIGINAL RESEARCH
published: 22 September 2021
doi: 10.3389/fphar.2021.747010

An Integrative Pharmacology Based Analysis of Refined Liuweiwuling Against Liver Injury: A Novel Component Combination and Hepaprotective Mechanism

Yuan Gao[1†], Wei Shi[2,3†], Hongyu Yao[2†], Yongqiang Ai[2,3], Ruisheng Li[4], Zhilei Wang[2,3], Tingting Liu[2,3], Wenzhang Dai[2,3], Xiaohe Xiao[2,3], Jun Zhao[2], Ming Niu[5]* and Zhaofang Bai[2,3]**

[1]School of Traditional Chinese Medicine, Capital Medical University, Beijing, China, [2]Senior Department of Hepatology, The Fifth Medical Center of PLA General Hospital, Beijing, China, [3]China Military Institute of Chinese Materia, The Fifth Medical Center of PLA General Hospital, Beijing, China, [4]Department of Infectious Disease Medicine, The Fifth Medical Center of PLA General Hospital, Beijing, China, [5]Department of Poisoning Treatment, The Fifth Medical Center of PLA General Hospital, Beijing, China

OPEN ACCESS

Edited by:
Silvia Di Giacomo,
Sapienza University of Rome, Italy

Reviewed by:
XinZhou Yang,
South-Central University for Nationalities, China
Duygu Ağagündüz,
Gazi University, Turkey

***Correspondence:**
Jun Zhao
zhj68@263.net
Ming Niu
nmbright@163.com
Zhaofang Bai
baizf2008@hotmail.com

†These authors have contributed equally to this work

Specialty section:
This article was submitted to Gastrointestinal and Hepatic Pharmacology, a section of the journal Frontiers in Pharmacology

Received: 25 July 2021
Accepted: 08 September 2021
Published: 22 September 2021

Citation:
Gao Y, Shi W, Yao H, Ai Y, Li R, Wang Z, Liu T, Dai W, Xiao X, Zhao J, Niu M and Bai Z (2021) An Integrative Pharmacology Based Analysis of Refined Liuweiwuling Against Liver Injury: A Novel Component Combination and Hepaprotective Mechanism. Front. Pharmacol. 12:747010. doi: 10.3389/fphar.2021.747010

Liver disease is a major cause of illness and death worldwide. In China, liver diseases, primarily alcoholic and nonalcoholic fatty liver disease, and viral hepatitis, affect approximately 300 million people, resulting in a major impact on the global burden of liver diseases. The use of Liuweiwuling (LWWL), a traditional Chinese medicine formula, approved by the Chinese Food and Drug Administration for decreasing aminotransferase levels induced by different liver diseases. Our previous study indicated a part of the material basis and mechanisms of LWWL in the treatment of hepatic fibrosis. However, knowledge of the materials and molecular mechanisms of LWWL in the treatment of liver diseases remains limited. Using pharmacokinetic and network pharmacology methods, this study demonstrated that the active components of LWWL were involved in the treatment mechanism against liver diseases and exerted anti-apoptosis and anti-inflammatory effects. Furthermore, esculetin, luteolin, schisandrin A and schisandrin B may play an important role by exerting anti-inflammatory and hepatoprotective effects *in vitro*. Esculeti and luteolin dose-dependently inhibited H_2O_2-induced cell apoptosis, and luteolin also inhibited the NF-κB signaling pathway in bone marrow-derived macrophages. schisandrin A and B inhibited the release of ROS in acetaminophen (APAP)-induced acute liver injury *in vitro*. Moreover, LWWL active ingredients protect against APAP-induced acute liver injury in mice. The four active ingredients may inhibit oxidative stress or inflammation to exert hepatoprotective effect. In conclusion, our results showed that the novel component combination of LWWL can protect against APAP-induced acute liver injury by inhibiting cell apoptosis and exerting anti-inflammatory effects.

Abbreviations: APAP, Acetaminophen; ALT, Alanine aminotransferase; AST, Aspartate aminotransferase; BMDMs, Bone marrow-derived macrophages; CFDA, Chinese Food and Drug Administration; DMEM, Dulbecco's modified Eagle medium; FBS, fetal bovine serum; HSCs, Hepatic stellate cells; LWWL, Liuweiwuling; LPS, lipopolysaccharide; TCM, traditional Chinese medicine.

Keywords: hepatoprotective effect, liuweiwuling, network pharmacology, component combination, antiapoptosis, anti-inflammation

INTRODUCTION

Liver diseases lead to severe public health problems owing to their high prevalence worldwide and poor long-term clinical outcomes, including cirrhosis and hepatocellular carcinoma (Wang et al., 2014). Different types of liver diseases, including chronic hepatitis B virus infection, alcoholic liver disease, nonalcoholic fatty liver disease, autoimmune liver disease, and drug-induced liver disease, potentially threaten a large proportion of the global population. In China, approximately 300 million people are affected by liver diseases, which has a major impact on the global burden of liver diseases (Cui and Jia, 2013; Zhang et al., 2016; Sarin et al., 2020).

In China, many patients with liver diseases opt for traditional Chinese medicine (TCM) as an alternative or complementary therapy. In China, the use of Liuweiwuling (LWWL), a TCM compound, has been approved by the Chinese State Food and Drug Administration (CFDA) for decreasing aminotransferase levels induced by different liver diseases (Xin et al., 2009; Du and Jaeschke, 2016; Branch of Hepatobiliary Diseases, CMCA, 2020). LWWL is constituted by the following six traditional Chinese herbs: Schisandrae chinensis fructus, Fructus Ligustri Lucidi, Forsythiae fructus, Curcumae rhizoma, Perennial sow thistle, and Ganoderma spore. In particular, clinical studies have confirmed that LWWL has definite therapeutic effects on liver fibrosis (Wang et al., 2018; Li et al., 2020). The dysregulated inflammatory responses, oxidative stress and cell live/death have been widely documented as primarily involved mechanisms underlying liver diseases (Zhang and Schuppan, 2014; Li et al., 2019). Emerging evidence suggests that TCM directly regulates the production of inflammatory cytokines and chemokines to improve inflammation and liver injury. (Wang C. et al., 2016). Our previous study indicated that LWWL could attenuate hepatic fibrosis via the modulation of TGF-β1 and NF-κB signaling pathways in rat models, based on bile duct ligation (BDL)- and CCl4-induced hepatic fibrosis (Liu et al., 2018a; Liu et al., 2018b). However, it is still unclear whether the underlying mechanisms and core signaling pathways mediate the multi-linked and multi-targeted effects of LWWL against liver diseases.

Integrative pharmacology can focus on predicting potential targets, pathways, and consequences and may provide clues for designing subsequent drug studies. This study used an integrative pharmacology approach to understand the systemic, liver disease-related, and molecular effects of LWWL. Our experimental results largely validated the mechanism of action of LWWL, as predicted by the integrative pharmacology analysis.

MATERIALS AND METHODS

Reagents and Antibodies

Dimethyl sulfoxide and ultrapure lipopolysaccharide (LPS) were purchased from Sigma-Aldrich (Munich, Germany). Apigenin, esculetin, gomisin N, schisanhenol, schisandrin A, schisandrin B, anwulignan, schisantherin A, schisantherin B, specnuezhenide, schisandrin, luteolin, quinic acid, curcumenol, and acetaminophen (APAP) were obtained from MCE (New Jersey, NJ, United States). Anti-mouse-IL-1β, anti-mouse-NLRP3, and anti-mouse-ASC antibodies were purchased from Santa Cruz Biotechnology (Beijing, China). Anti-mouse-caspase-1 p45, anti-mouse-pro-IL-1β, and anti-GAPDH antibodies were purchased from Proteintech (Chicago, IL, United States). MitoSOX was purchased from Invitrogen (Carlsbad, CA, United States).

Preparation and Analysis of LWWL by LC-MS/MS

The formula of LWWL per dose is listed in **Supplementary Table S1**. Briefly, the LWWL was accurately measured 1 g in a 25 ml volumetric flask and then dissolved in methanol solution. The sample was kept at 40°C for 1 h after it was sonicated for 5min. Subsequently, the LWWL extraction was centrifuged at 4°C, 12,000 rpm for 15 min, and then the supernatant was filtered with 0.22 μm filter membrane. Finally, the sample filtrate solution was used to UHPLC analysis. To verify the metabolite components in LWWL, chromatographic analysis was performed using a Triple TOF 5600- quadrupole-LC/MS system (SCIEX Technologies, United States). The SHISEIDO CAPCELL PAK ADME column (2.1 mml.D*150 mm, 4.6 um) was performed in LC-MS/MS analysis. The flow rate was set at 0.4 ml/min and the sample injection volume was 5 μL. The mobile phase conditions were as follows: mobile phase A was 0.1% formic acid in water, and the mobile phase B was acetonitrile. The multistep linear elution gradient program was as follows: 0 → 0.5 min, 90 → 60% A; 0.5 → 4.0 min, 60 → 10% A; 4 → 9.0 min, 10 → 10% A; 9.0 → 12.01 min, 10 → 90% A; 12.01→ 15 min, 90 → 90% A. Then, A quality control sample was employed to optimize the UHPLC-Q-TOF/MS conditions. MS was performed using Triple TOF 5600-quadrupole-LC/MS with an electrospray ionization source in both positive and negative modes. The electrospray source parameters were fixed as follows: MS data were gathered in the full scan mode from m/z 50–1,250 with a scan rate of 1 spectra/s. The electrospray capillary voltage was 5.5 kV in the negative mode and 5.0 kV in the positive mode. The atomization temperature of the ion source was set to 550°C. The nebulizer pressure was set to 50 psi (GS1) and 50 psi (GS2). Air curtain gas at 35 psi and cluster voltage DP at 80 V.

Animals

Male Sprague–Dawley rats (weight: 180–220 g) and male C57BL/6 mice (6–8-weeks old) were purchased from SPF Biotechnology Co., Ltd. (Beijing, China). All animals were maintained under 12-h light/dark conditions at 22–24°C with unrestricted access to food and water for the duration of the experiment. All animal

experiments in this study were conducted according to the guidelines for care and use of laboratory animals, and the study protocol was approved by the Animal Ethics Committee of the Fifth Medical Centre, Chinese People's Liberation Army (PLA) General Hospital (animal ethics committee approval number: IACUC-2017-003).

Human Samples and Study Design

The study protocol was approved by the Medical Ethics Committee of the Fifth Medical Center, General Hospital of PLA (No.2015180D), registered at ClinicalTrials.gov. All volunteers in this study were self-reported as Han Chinese and provided written informed consent. Blood samples were collected from each volunteer who studied or worked at the Fifth Medical Center, General Hospital of PLA (Beijing, China). According to the overall study design, all healthy volunteers took LWWL three times per day according to the specification for 2 consecutive days, and they were prohibited from smoking and consuming alcohol, tea, and coffee drinks.

Sample Preparation

Rat plasma, urine, liver tissue homogenate, and human plasma (500 μL) were added to acetonitrile (1,500 μL). The protein was precipitated by shaking for 1 min on a shaker. Centrifugation was performed at 13,000 rpm for 10 min. The supernatant was dried at 45°C under nitrogen. Further, 100 μL methanol:water (V/v = 1: 1) was used to redissolve the samples, and 5 μL of the sample was injected for analysis.

Network Construction and Analysis

The components detected in the blood samples from volunteers and the blood, urine, and tissue samples from animals were obtained by their CAS numbers from the open online databases TCM-SP and Chemspider. The putative targets of these compounds were predicted by PharmMapper (http://59.78.96.61/pharmmapper/) with a fit score greater than 3.0 and Z-score greater than 0. Multiple targets associated with liver diseases were collected by keyword-based searches in the Online Mendelian Inheritance in Man database; the disease names and keywords were related to the Medical Subject Headings database from the NIH and the U.S. National Library of Medicine. All collected targets were converted into UniProt IDs, and protein–protein interactions between them were screened from the Database of Interacting Proteins. Thereafter, the components and their putative targets, liver disease-related targets, and interactive proteins were combined to construct a compound–target–disease network, and Cytoscape V3.7.2 was applied to visualize and analyze the network. The topological features of each node in the network were calculated using Network Analyzer in the Cytoscape software, and the most probable disease targets on which LWWL components or their metabolites might act were screened with three topologic parameters ("Degree," "Betweenness centrality," and "Closeness centrality"). Only hubnodes ("Degree" greater than 2-fold of the median value) with higher "Betweenness centrality" and "Closeness centrality" (above the median value) values were identified as candidate targets of LWWL. All candidate targets were supplied to the Database for Annotation, Visualization and Integrated Discovery for Gene Ontology (GO) and pathway analysis, and only the results with Bonferroni adjustment *p*-values less than 0.01 were used for further analysis.

Cell Culture

Bone marrow-derived macrophages (BMDMs) were isolated from the femoral bone marrow of 10-week-old female C57BL/6 mice and cultured in Dulbecco's modified Eagle medium (DMEM) supplemented with 10% fetal bovine serum (FBS), 1% penicillin/streptomycin (P/S), and 50 ng/ml murine macrophage colony-stimulating factor. L02 and HepaG2 cells were grown in DMEM supplemented with 10% FBS and 1% P/S. All cells were cultured in a humidified 5% (v/v) CO_2 atmosphere at 37°C.

Cell Viability Assay

L02 cells were seeded at 8.5×10^4 cells/well onto 96-well plates overnight. The cells were incubated at 37°C, followed by treatment with the active components of LWWL (apigenin, esculetin, gomisin N, schisanhenol, schisandrin A, schisandrin B, anwulignan, schisantherin A, schisantherin B, specnuezhenide, schisandrin, luteolin, quinic acid, and curcumenol) for 24 h. Thereafter, the medium was replaced with DMEM containing CCK-8 solution for 30 min. The optical density was determined at a wavelength of 450 nm.

NF-κB Signing Pathway Activation

BMDMs were seeded at 5×10^5 cells/well onto 24-well plates overnight and then treated with apigenin, esculetin, gomisin N, schisanhenol, schisandrin A, schisandrin B, anwulignan, schisantherin A, schisantherin B, specnuezhenide, schisandrin, luteolin, quinic acid, and curcumenol for 4 h. BMDMs were then stimulated with LPS (50 ng/ml) for 1 h. The proteins were then analyzed by immunoblotting.

H_2O_2-Induced Hepatocyte Injury *in vitro*

L02 cells were seeded at 8.5×10^4 cells/well onto 24-well plates overnight. The next day, the medium was replaced with DMEM containing apigenin, esculetin, gomisin N, schisanhenol, schisandrin A, schisandrin B, anwulignan, schisantherin A, schisantherin B, specnuezhenide, schisandrin, luteolin, quinic acid, and curcumenol; cells were incubated for 1 h and then stimulated with H_2O_2 for 12 h. The cell supernatants were collected, digested, and rinsed with phosphate-buffered saline. An Annexin V-FITC Apoptosis Detection Kit (BD, New York, United States) was used to detect the apoptosis of L02 cells by flow cytometry.

APAP-Induced Hepatocyte Injury *in vitro*

HepaG2 cells were seeded at 0.25×10^5 cells/well onto 24-well plates overnight. The following day, the medium was replaced with DMEM containing apigenin, esculetin, gomisin N, schisanhenol, schisandrin A, schisandrin B, anwulignan, schisantherin A, schisantherin B, specnuezhenide, schisandrin, luteolin, quinic acid, and curcumenol; cells were incubated for 1 h

and then stimulated with APAP (20 mM) for 12 h. The cell supernatants were collected, digested, rinsed with Hank's balanced salt solution, and stained with 4 μM MitoSOX red mitochondrial superoxide indicator (Invitrogen) at 37°C for 15 min. Thereafter, the cells were washed again with Hanks' balanced salt solution and assayed by flow cytometry using a BD FACSCanto™ II cell analyzer (Franklin Lakes, NJ, United States) (Liu et al., 2021).

Western Blotting

Protein extraction and western blotting assays on cell culture supernatant and whole cell lysis were performed as described previously (Gao et al., 2021).

Enzyme-Linked Immunosorbent Assay

ELISA measurements of mouse IL-1β, TNF-α, and IL-6 (Dakewe, Beijing, China) levels were performed in accordance with the manufacturer's instructions.

Serum Biochemistry

Serum ALT, AST, DBIL, and TBA levels were determined using a commercially available assay kit (Nanjing Jiancheng Bioengineering Institute, Nanjing, China) according to the manufacturer's instructions.

Animal Experiments

After 7 days of adaptive breeding, mice were randomly divided into the following seven groups (n = 6): control group, APAP group (300 mg/kg), APAP + SA (schisandrin A [159.78 mg/kg]), APAP + SB (schisandrin B [162.43 mg/kg]), APAP + E (esculetin [0.93 mg/kg]), APAP + L (luteolin [8.56 mg/kg]) and APAP + SSEL group (schisandrin A [159.78 mg/kg] + schisandrin B [162.43 mg/kg] + esculetin [0.93 mg/kg] + luteolin [8.56 mg/kg]). schisandrin A, schisandrin B, esculetin, and luteolin were injected into the mice for 6 consecutive days. The normal and APAP groups were treated with the vehicle in the same manner. One hour after the final administration of schisandrin A, schisandrin B, esculetin, and luteolin, mice (except those in the control group) were administered APAP via a single intraperitoneal injection. After 12 h, the mice were euthanized, and blood samples were collected.

Statistical Analyses

Prism 6 and SPSS statistics (version 21.0) were used for statistical analysis. All experimental data are expressed as mean ± standard deviation. A two-tailed unpaired Student's t-test was used to evaluate significant differences between the two groups. Statistical significance was set at $p < 0.05$.

RESULTS

Identification of the Active Components of LWWL in Rats and Humans

Firstly, we analysis the active components of LWWL by LC-MS/MS. As shown in **Supplementary Figure S1** and **Supplementary Table S1**, a total of 20 active compounds were confirmed in LWWL. To examine the effective components of LWWL *in vivo*, we used UPLC/Q-TOF-MS for qualitatively analyzing the active components of LWWL in rats and humans. Rats were gavaged with LWWL (6.4 g/kg) for 2 consecutive days. After the last administration, the blood was collected from the orbital vein at 1, 2, 4, 8, 12, and 24 h. Thereafter, the serum was fully mixed after centrifugation (**Supplementary Figure S2A**). We also detected active components in the liver of the rats (**Supplementary Figure S2B**). During the animal gavage, the urine of rats was collected in a metabolic cage (**Supplementary Figure S3**). Subsequently, we used UPLC/Q-TOF-MS to analyze the active components of LWWL in the human body. Volunteers took LWWL for 2 consecutive days (three tablets at a time, three times per day). After the last dose, one of the volunteer's blood was collected from the vein at 1, 2 h, the other one of the volunteers' blood was collected from the vein at 4, 8 h, the last volunteers' blood was collected from the vein at 12, 24 h, and the serum was then completely mixed after centrifugation (**Supplementary Figure S4**). Overall, as a result, apigenin, esculetin, gomisin N, schisanhenol, schisandrin A, schisandrin B, anwulignan, schisantherin A, schisantherin B, specnuezhenide, schisandrin, luteolin, quinic acid, and curcumenol were identified according to the described chromatographic conditions.

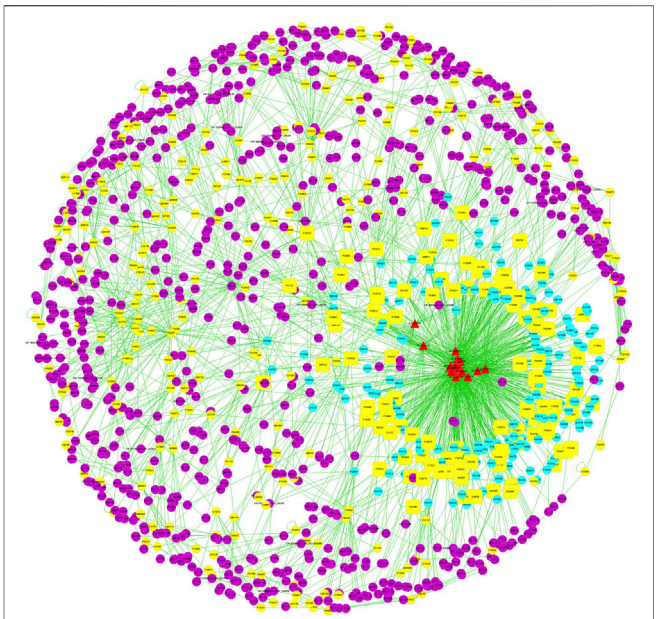

FIGURE 1 | Prediction of the effective targets of LWWL with network pharmacology.

Prediction of the Effective Targets of LWWL With Network Pharmacology

In total, 18 compounds of LWWL, 289 drug targets, 358 liver disease-related targets, and 785 interactive proteins were

TABLE 1 | The targets related liver diseases.

No	Uniprot IDs	Degree	Closeness Centrality	Betweenness Centrality	Direct target
1	P10275	43	0.276	0.108	Direct
2	P06213	24	0.293	0.059	Direct
3	P00533	23	0.269	0.049	Direct
4	P03372	23	0.263	0.033	Direct
5	P04150	21	0.267	0.025	Direct
6	P15056	19	0.262	0.025	Direct
7	P19793	19	0.250	0.019	Direct
8	P11362	18	0.252	0.024	Direct
9	P35968	15	0.262	0.016	Direct
10	Q02750	15	0.257	0.009	Direct
11	P12931	14	0.263	0.026	Direct
12	P31749	14	0.263	0.022	Direct
13	P01112	14	0.243	0.017	Direct
14	P00519	12	0.269	0.017	Direct
15	P02679	12	0.253	0.002	Direct
16	P49841	10	0.278	0.043	Direct
17	P13501	10	0.234	0.037	Direct
18	P08069	10	0.226	0.014	Direct
19	P35221	10	0.249	0.011	Direct
20	P20339	10	0.255	0.009	Direct
21	P55055	10	0.241	0.008	Direct
22	P22830	10	0.268	0.003	Direct
23	Q06187	10	0.236	0.002	Direct
24	P08581	9	0.252	0.006	Direct
25	P11766	9	0.266	0.002	Direct
26	P04637	60	0.285	0.147	Indirect
27	P06400	33	0.236	0.053	Indirect
28	P38398	30	0.250	0.049	Indirect
29	Q00653	28	0.220	0.017	Indirect
30	Q9Y6K9	22	0.244	0.029	Indirect
31	P35222	22	0.226	0.024	Indirect
32	P19838	21	0.221	0.013	Indirect
33	Q04206	19	0.235	0.034	Indirect
34	P01106	19	0.255	0.028	Indirect
35	Q07812	15	0.247	0.015	Indirect
36	O14920	15	0.240	0.012	Indirect
37	P05412	13	0.248	0.019	Indirect
38	Q96EB6	12	0.225	0.016	Indirect
39	Q16665	12	0.207	0.014	Indirect
40	P15692	12	0.211	0.007	Indirect
41	P09874	11	0.236	0.030	Indirect
42	P25445	11	0.229	0.017	Indirect
43	O00255	11	0.215	0.006	Indirect
44	Q09472	10	0.247	0.018	Indirect
45	O75581	10	0.224	0.011	Indirect
46	Q13315	9	0.237	0.014	Indirect
47	P27986	9	0.235	0.007	Indirect
48	Q07820	9	0.226	0.006	Indirect

screened, and the network relationships between compounds and disease targets are shown in **Figure 1**. The topological parameters of disease nodes in the network, such as degree, betweenness centrality, and closeness centrality, were analyzed. The median values of degree, betweenness centrality, and closeness centrality were 4, 0.002, and 0.206, respectively. The hub node (>2-fold of the median degree values) with a higher betweenness centrality and closeness centrality values (more than the median values) were identified as the candidate targets of LWWL in liver diseases. As a result, 48 liver disease-related targets were identified (**Table 1**).

The results of GO analysis of the screened targets of LWWL are shown in **Figure 2A–D**. The potential targets of LWWL were mainly distributed in the cellular components of the nucleus, cytosol, cytoplasm, nucleoplasm, and mitochondria. These targets could bind and activate transcription factors, DNA, proteins, and kinases, which are mainly involved in biological processes to regulate RNA or DNA transcription, apoptotic process, ERK1 and ERK2 cascade, protein autophosphorylation, and MAPK cascade. Based on the pathway enrichment analysis, we also found that LWWL could influence many inflammation-related pathways, including the PI3K-Akt, TNF-α, MAPK, and Toll-like receptor signaling pathways. Finally, these pathways could influence the NF-κB signaling pathway. In addition, we found that the apoptosis and HIF-1 signaling pathways were influenced by LWWL. In conclusion, network pharmacology showed that the anti-inflammatory and anti-apoptotic effects of LWWL may be involved in the treatment of liver diseases.

Effects of Active Components of LWWL on the Cell Viability

The effect of the active constituents of LWWL on L02 cells was tested using the CCK-8 assay. Our results showed that apigenin, esculetin, schisandrin A, schisandrin B, schisantherin A, schisandrin B, specnuezhenide, schisandrin, quinic acid, and curcumenol were not toxic to L02 cells, even at concentrations up to 160 μmol/L. However, our results also showed that after exposure to gomisin N, schisanhenol, anwulignan, or luteolin for 24 h, the half-maximal inhibitory concentration (IC50) of L02 cells was 89, 122, 68, and 123 μmol/L, respectively. However, they did not affect cell viability at low concentrations (**Figure 3**). Thus, according to our results, 0–40 μmol/L active components of LWWL were selected for the next test.

Luteolin Inhibits NF-κB Signaling Pathway

The NF-κB signaling pathway is primarily responsible for regulating the production of pro-inflammatory and pro-fibrotic cytokines and can upregulate the production of IL-1β and TNF-α(Sun, 2017). To identify the active components of LWWL that could influence the NF-κB signaling pathway, we tested the expression of TNF-α and, IL-6 and the expression of proteins related to the NF-κB signaling pathway. Our results showed that only luteolin inhibited the NF-κB signaling pathway (**Figures 4A–C**). To further determine the inhibitory effect of luteolin on the NF-κB signaling pathway and whether luteolin inhibited the NF-κB signaling pathway at a wide range of concentrations, BMDMs were first treated with luteolin at 0, 10, 20, and 40 μmol/L for 1 h and then stimulated with LPS for 4 h. **Figures 4D–F** shows that luteolin dose-dependently inhibited pro-IL-1β and NLRP3 production in cell lysates and the production of TNF-α and IL-6 in culture supernatants by

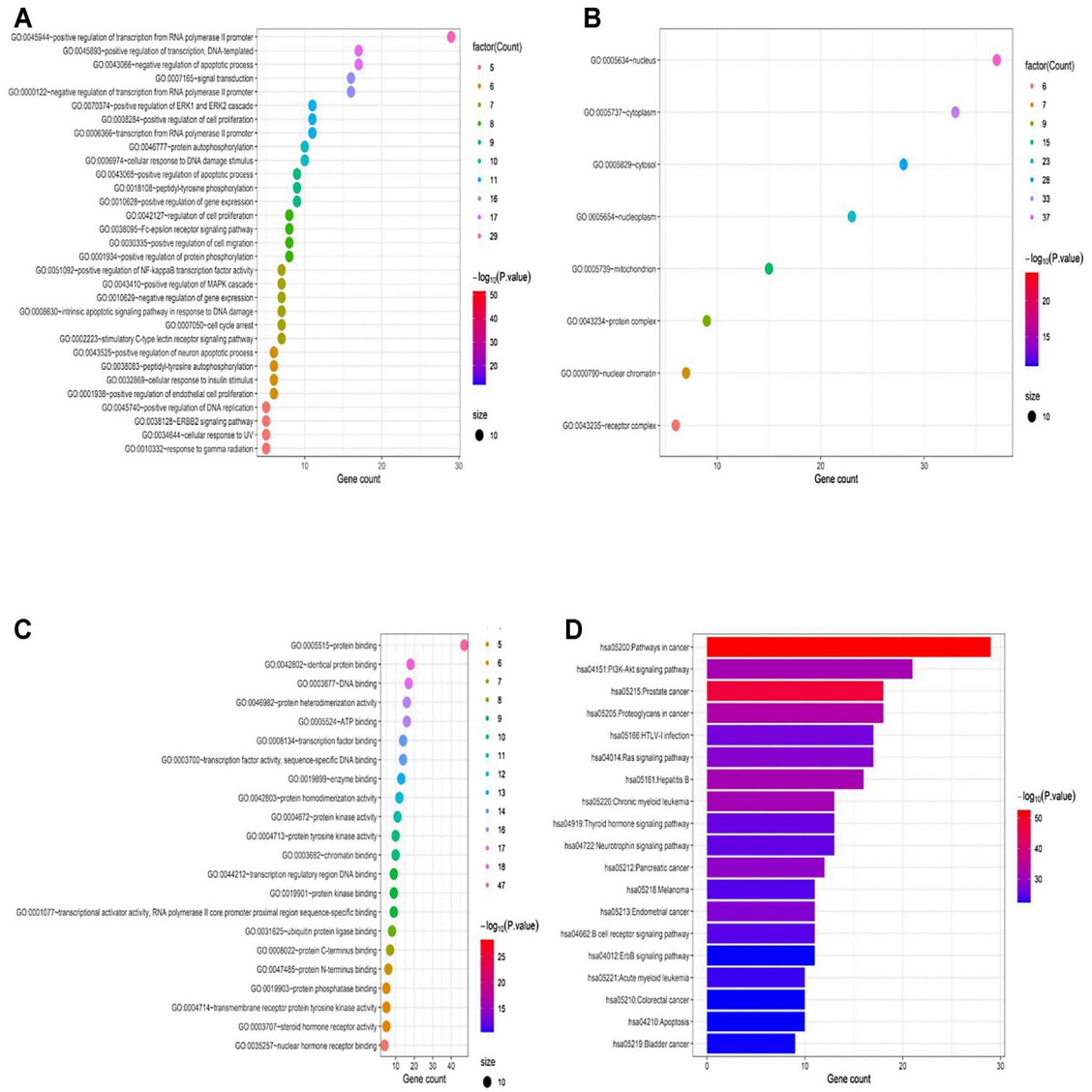

FIGURE 2 | Compound–target interaction network and preliminary gene ontology (GO) analysis of drug targets. **(A)** the potential targets of LWWL mainly distributed in the cellular component, **(B)** the potential targets of LWWL can bind and activate molecular function, **(C)** the potential targets engaged in the biological process, and **(D)** KEGG pathway analysis of LWWL.

ELISA assay kit. Taken together, these results demonstrate that luteolin inhibits the NF-κB signaling pathway in BMDMs *in vitro*.

Luteolin and Esculetin Suppress H_2O_2-Induced Apoptosis

Furthermore, the protective effects of the active constituents of LWWL on hepatocytes were examined using the Annexin V-FITC Apoptosis Detection Kit. We selected a typical hydrogen peroxide (H_2O_2)-induced cell apoptosis model. The results demonstrated that luteolin and esculetin treatment significantly inhibited H_2O_2-induced apoptosis of L02 cells. Thereafter, we treated H_2O_2-induced apoptosis of L02 cells with different concentrations of esculetin or luteolin. The results showed that esculetin and luteolin could dose-dependently inhibit H_2O_2-induced cell apoptosis at 5, 10, and 20 μmol/L, and esculetin and luteolin could also inhibit the total apoptotic cells, early apoptotic cells, and late apoptotic cells (**Figure 5**). These results indicated that esculetin and luteolin could protect against hepatocyte injury.

Schisandrin A And Schisandrin B Inhibit The Release Of Reactive Oxygen Species

Oxidative stress and mitochondrial dysfunction play important roles in the pathogenesis of APAP-induced acute liver injury (Miele et al., 2007). Therefore, we examined the effect of active components of LWWL on the production of ROS induced by

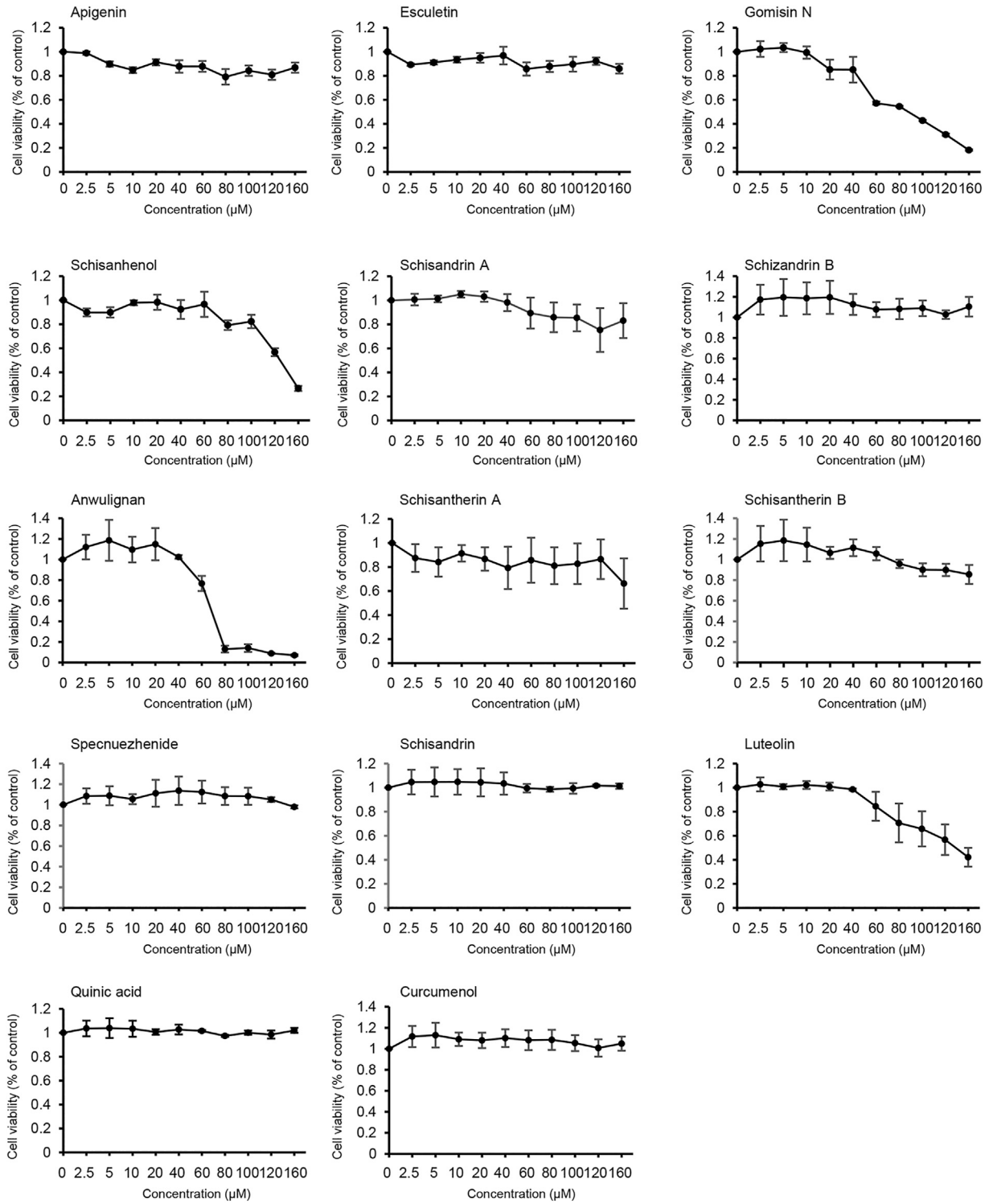

FIGURE 3 | Effects of the active components of LWWL on cell viability. The viability of L02 cells treated with the active components of LWWL for 24 h was determined. Data are presented as mean ± SD using biological samples.

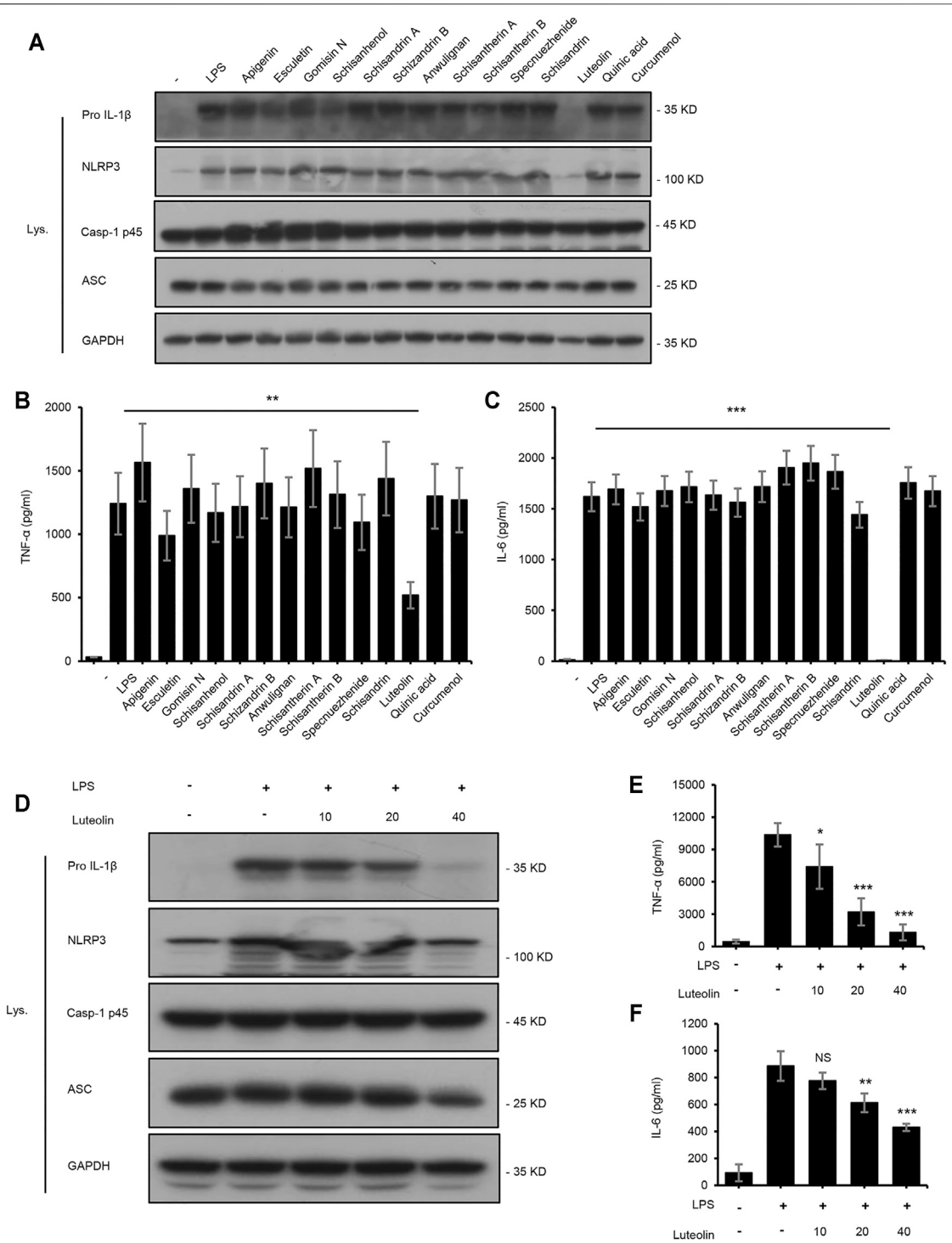

FIGURE 4 | Luteolin inhibits the NF-κB signaling pathway. **(A)** Western blotting of pro IL-1β, NLRP3, Casp-1 p45, ASC, and GAPDH in BMDMs treated with apigenin, esculetin, gomisin N, schisanhenol, schisandrin A, schisandrin B, anwulignan, schisantherin A, schisandrin B, specnuezhenide, schisandrin, luteolin, quinic acid, and curcumenol (40 μM) for 4 h and then stimulated with LPS (50 ng/ml) for 1 h. **(B,C)** ELISA of TNF-α **(B)** and IL-6 **(C)** in SN from samples described in A. **(D)** Western blotting of pro IL-1β, NLRP3, Casp-1 p45, ASC, and GAPDH in BMDMs treated with luteolin for 4 h and then stimulated with LPS (50 ng/ml) for 1 h. **(E,F)** ELISA of TNF-α **(E)** and IL-6 **(F)** in SN from samples described in D. GAPDH served as a loading control. Data are represented as the mean ± SD using biological samples.

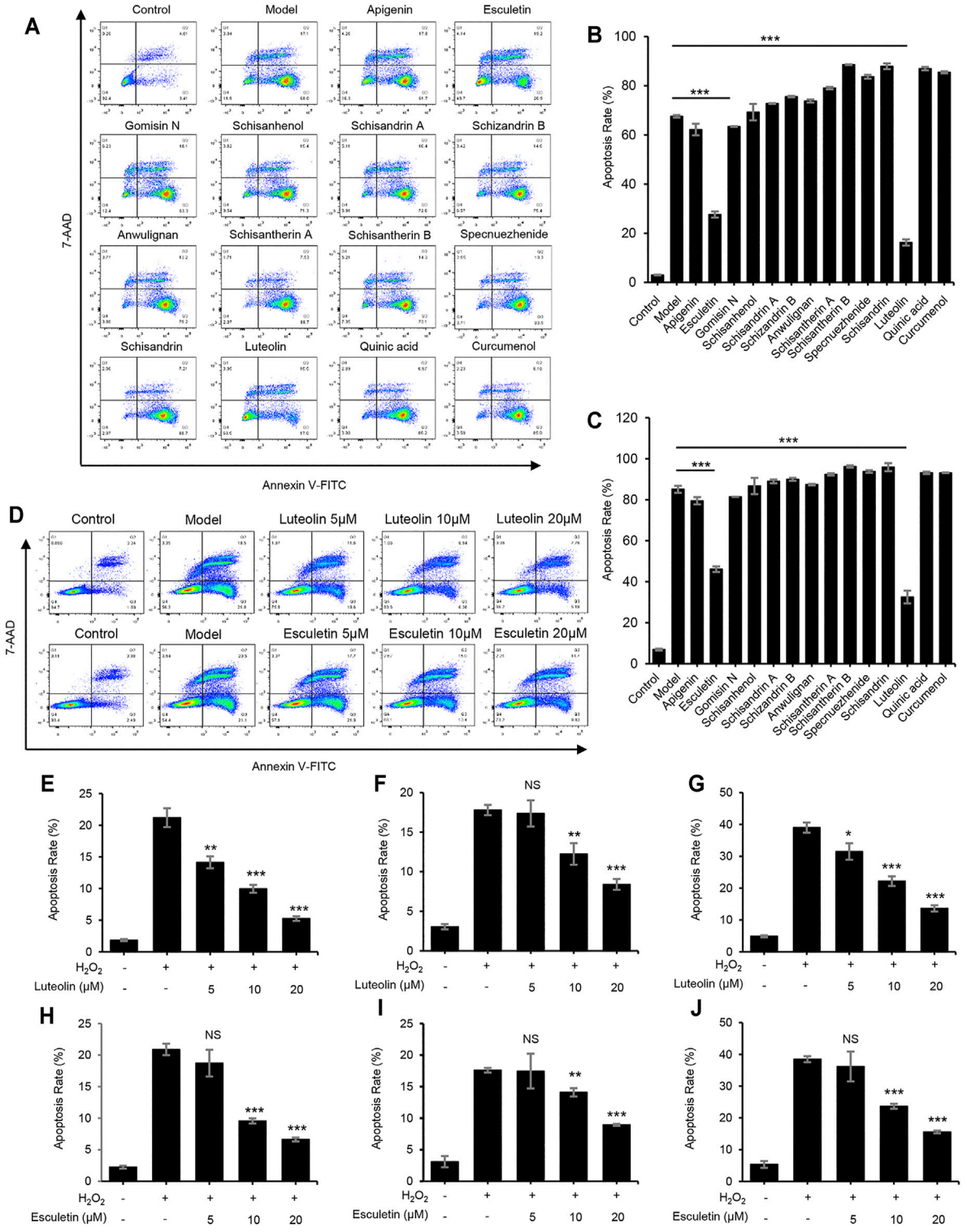

FIGURE 5 | Luteolin and esculetin suppress H_2O_2-induced apoptosis. **(A)** Apoptosis of L02 cells treated with apigenin, esculetin, gomisin N, schisanhenol, schisandrin A, schisandrin B, anwulignan, schisantherin A, schisantherin B, specnuezhenide, schisandrin, luteolin, quinic acid, and curcumenol (40 μM) and then exposed to APAP, as detected by flow cytometry. **(B)** The percentage of early apoptotic cells from samples described in A. **(C)** The percentage of total apoptotic cells from samples described in A. **(D)** Apoptosis of L02 cells treated with esculetin or luteolin (5, 10, and 20 μM) and then exposed to APAP, as detected by flow cytometry. **(E–G)** The percentage of early apoptotic cells **(E)**, late apoptotic cells **(F)**, and total apoptotic cells **(G)** treated with luteolin (5, 10, and 20 μM). **(H–J)** The percentage of early apoptotic cells **(H)**, late apoptotic cells **(I)**, and total apoptotic cells **(J)** treated with esculetin (5, 10, and 20 μM). Data are represented as the mean ± SD using biological samples. The significance of the differences was analyzed using unpaired Student's t-test: **p < 0.05, **p < 0.01, ***p < 0.001* vs. the control, NS, not significant.

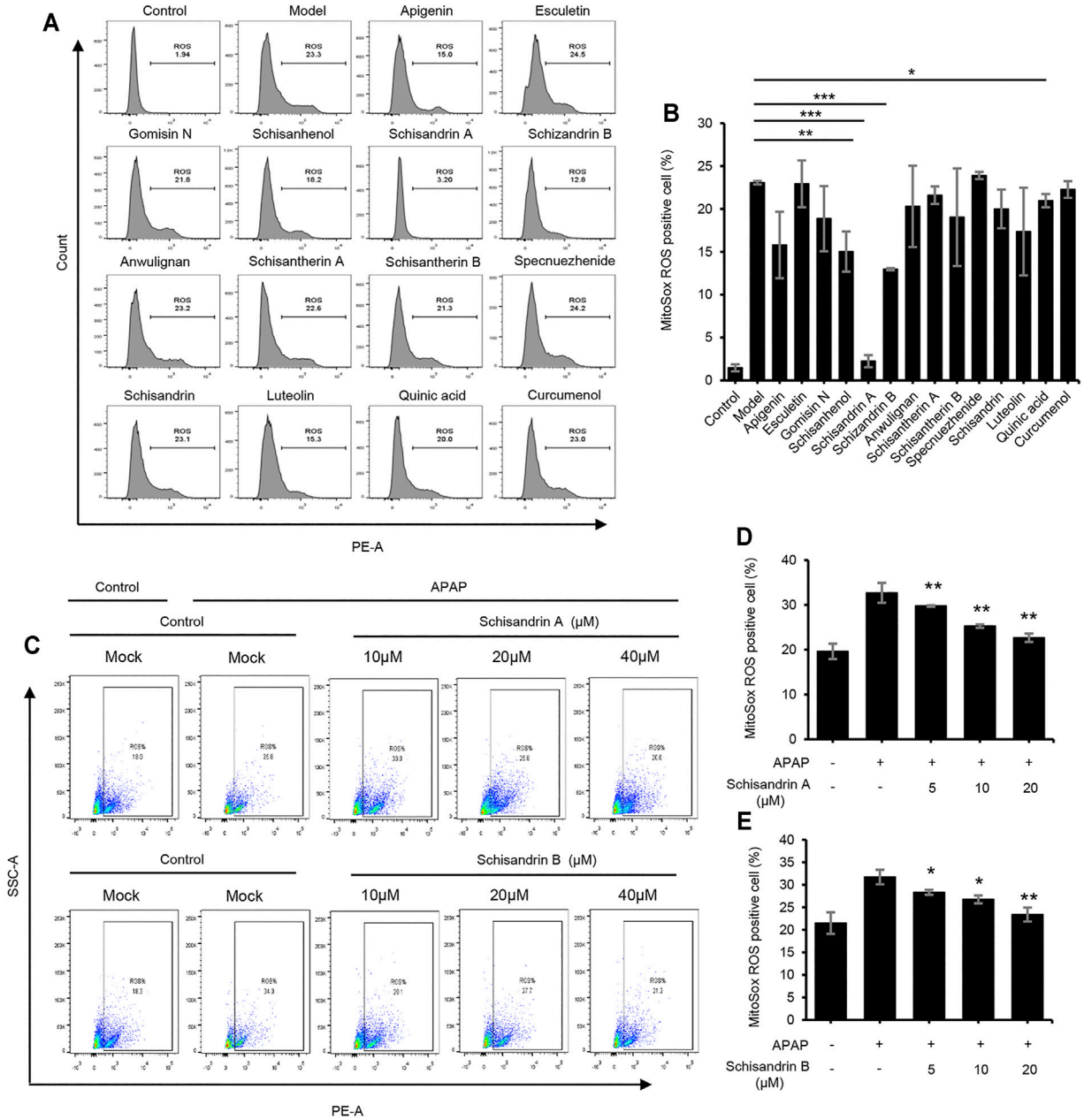

FIGURE 6 | Schisandrin A and schisandrin B inhibit the release of ROS. **(A)** HepaG2 cells were treated with apigenin, esculetin, gomisin N, schisanhenol, schisandrin A, schisandrin B, anwulignan, schisantherin A, schisantherin B, specnuezhenide, schisandrin, luteolin, quinic acid, and curcumenol (40 μM) before being stimulated with APAP. HepaG2 were loaded with MitoSOX red mitochondrial superoxide indicator (Ex/Em: 510/580 nm). After staining and washing, flow cytometry was conducted to test mtROS production. **(B)** Percentage of ROS-positive cells in HepaG2 cells from samples described in A. **(C)** The production of mtROS was detected by flow cytometry in HepaG2 cells treated with schisandrin A or schisandrin B (10, 20, and 40 μM). **(D,E)** Percentage of ROS-positive cells in HepaG2 cells pretreated with schisandrin A **(D)** or schisandrin B **(E)** (10, 20, and 40 μM) and then stimulated with APAP, followed by staining with MitoSox. Data are represented as the mean ± SD using biological samples. The significance of the differences was analyzed using unpaired Student's t-test: *$p < 0.05$, **$p < 0.01$, ***$p < 0.001$ vs. the control, NS, not significant.

APAP *in vitro*. Our results showed that several active components, especially schisandrin A and schisandrin B, could inhibit the release of ROS after APAP treatment (**Figures 6A,B**). As shown in **Figures 6C–E**, schisandrin A and schisandrin B dose-dependently inhibited the production of mitochondrial ROS. Therefore, schisandrin A and schisandrin B exert protective effects against liver injury by inhibiting the release of ROS *in vitro*.

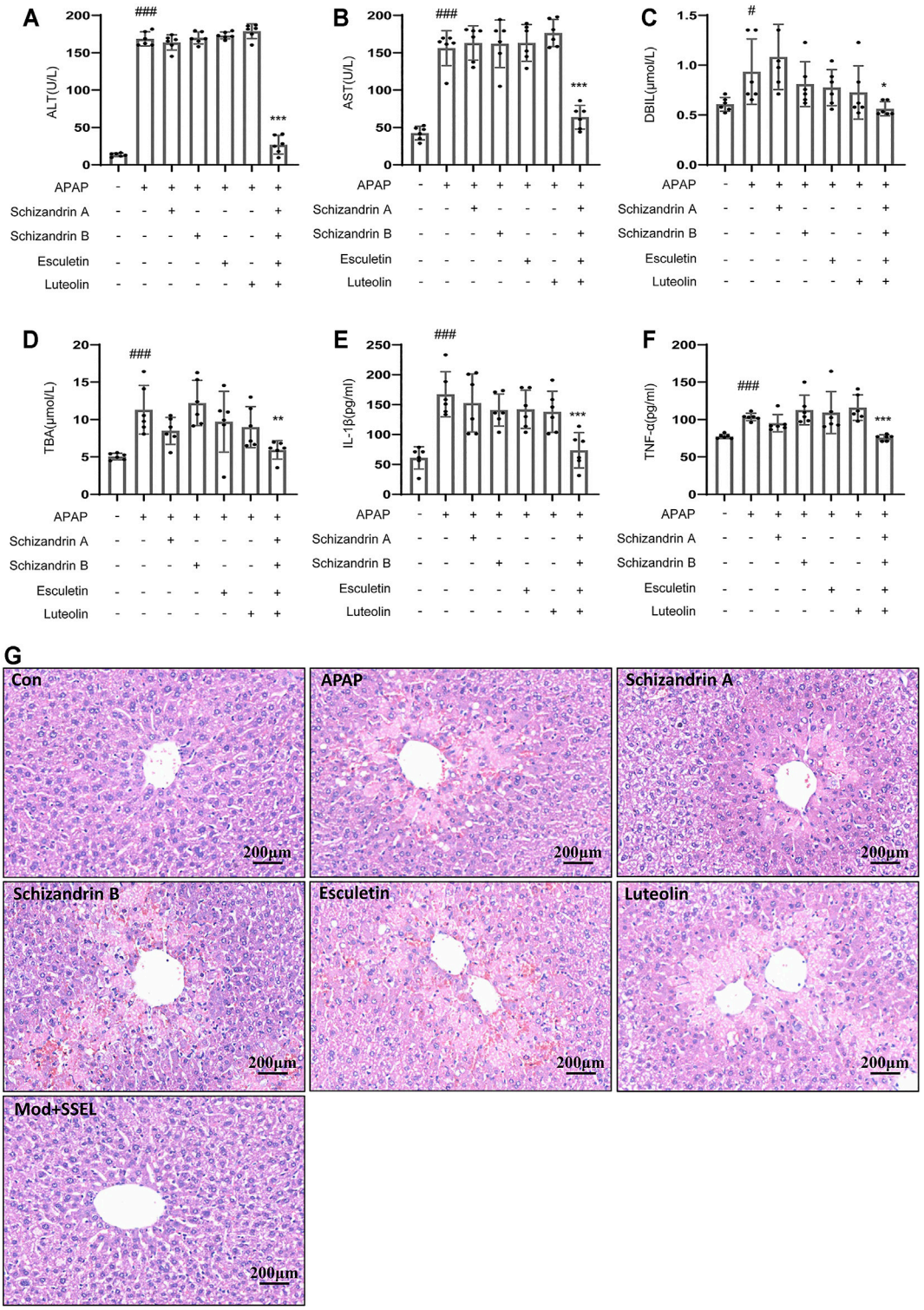

FIGURE 7 | Combination of LWWL active ingredients protect against APAP-induced acute liver injury *in vivo*. **(A–G)** Eight-week-old C57BL/6 male mice were administered with a vehicle, schisandrin A, schisandrin B, esculetin, and luteolin every day by gavage for 7 days. Further, 1 h after the final gavage of schisandrin A, schisandrin B, esculetin and luteolin, mice in all groups (except the control group) were administered with APAP (300 mg/kg) by a single intraperitoneal injection. **(A–D)** Serum levels of ALT**(A)**, AST**(B)**, DBIL **(C)** and TBA **(D)**. **(E,F)** ELISA of IL-1β **(E)** and TNF-α **(F)**. **(G)** H&E staining. The significance of the differences was analyzed using unpaired Student's t-test: #$p < 0.05$, ##$p < 0.01$, ###$p < 0.001$ vs. control group; *$p < 0.05$, **$p < 0.01$, ***$p < 0.001$ vs. the APAP group, NS, not significant.

Combination of LWWL Active Ingredients Protect APAP-Induced Acute Liver Injury *in vivo*

To test whether the combination of LWWL active ingredients (schisandrin A, schisandrin B, esculetin and luteolin) protects against acute liver injury *in vivo*, we chose APAP to induce acute liver injury. **Figures 7A–D** showed that the serum levels of ALT, AST, DBIL, and TBA in the APAP-treated group were higher than those in the control group. schisandrin A, schisandrin B, esculetin and luteolin respectively treatment have no effect on APAP-induced acute liver injury. But the combination of schisandrin A, schisandrin B, esculetin and luteolin prevented the increase in serum ALT and AST levels compared with those in the APAP group. Consistent with the results of ALT and AST, treatment with the combination of schisandrin A, schisandrin B, esculetin and luteolin attenuated the expression of DBIL and TBA compared with that in the APAP group. We also detected that the combination of schisandrin A, schisandrin B, esculetin and luteolin influenced the production of IL-1β and TNF-α (**Figures 7E,F**). As expected, the combination of schisandrin A, schisandrin B, esculetin and luteolin treatment significantly decreased the production of IL-1β and TNF-α *in vivo*. Moreover, histopathologic studies showed that the combination of LWWL active ingredients treatment definitely alleviated the liver failure with reduced hepatocyte necrosis and liver cell degeneration (**Figure 7G**). Collectively, these results suggest that the four LWWL active ingredients play an important role in the regulation of hepatoprotective activity.

DISCUSSION

At present, TCM has been confirmed to have significant therapeutic efficacy for complex diseases by exerting pharmacological effects in a multi-component and multi-target manner (Wang et al., 2018). Some Chinese patent medicines, such as LWWL and San-Cao granule, have been used clinically to treat liver diseases for many years (Wei et al., 2016). However, unclear active medicinal ingredients and mechanisms of Chinese patent medicine restrict the widespread use of TCM.

In China, LWWL, a Chinese medicine formula, is widely used to treat liver injury induced by chronic hepatitis B (Lei et al., 2015). Previous clinical and experimental studies showed that LWWL inhibits liver injury and reverses the progression of hepatic fibrosis (Liu et al., 2018a; Liu et al., 2018b). Hepatocyte injury, a primary inducer of hepatic fibrosis, can increase inflammation and activation of hepatic stellate cells (HSCs) (Ai et al., 2021). Thus, reversal of hepatocyte injury is an important way to prevent and treat hepatic fibrosis (Lee et al., 2015). Our previous studies indicated that LWWL could significantly suppress HSC activation and reverse histological fibrosis and liver injury (Liu et al., 2018b). In addition, LWWL regulates the expression of inflammatory cytokines by inhibiting the activation of NF-κB p65 and phosphorylation of IκBα (Liu et al., 2018a).

In this study, we designed an integrated strategy to explore and identify the components of LWWL by integrating network pharmacology with systems biology. We successfully employed this strategy to demonstrate the preventive effect and elementary mechanisms of LWWL against inflammatory diseases of the liver.

We used UPLC/Q-TOF-MS to analyze the active components of LWWL *in vivo*. As a result, apigenin, esculetin, gomisin N, schisanhenol, schisandrin A, schisandrin B, anwulignan, schisantherin A, schisandrin B, specnuezhenide, schisandrin, luteolin, quinic acid, and curcumin were identified. Thereafter, we predicted the effective targets of LWWL with network pharmacology. According to network pharmacology, LWWL can be used to treat liver diseases owing to its anti-inflammatory and anti-apoptotic functions.

NF-κB is one of the most important transcription factors and plays a role in the expression of pro-inflammatory genes, such as cytokines, chemokines, and adhesion molecules (Oeckinghaus and Ghosh, 2009; Aziz et al., 2018). NF-κB and upstream kinase cascades are known to have promotional roles in inflammation (Reuter et al., 2010). Inhibition of cellular inflammation has been considered a promising approach to lower the risk of inflammation-driven diseases (Rakariyatham et al., 2018). Luteolin is an abundant flavone found in LWWL, and *in vitro* and *in vivo* experiments have revealed its anti-inflammatory activity. Luteolin exerts its anti-inflammatory effects by altering the NF-κB signaling pathway (Aziz et al., 2018). In addition, cytokine regulation is crucial because cytokines are key modulators of both acute and chronic inflammation (Turner et al., 2014; Aziz et al., 2018). Moreover, luteolin significantly attenuates TNF-α-induced intracellular ROS generation (Xia et al., 2014). As expected, luteolin is an anti-inflammatory active component of LWWL and exerts its anti-inflammatory effects by inhibiting NF-κB signaling and regulating inflammatory mediators such as IL-6 and TNF-α.

Apoptosis is a biochemical process strictly controlled by an organism to scavenge dead cells through natural physiological methods (Chen et al., 2017). ROS are normal metabolites of various redox reactions in cells (Kalyanaraman et al., 2018; Gao et al., 2019). Hydrogen peroxide, the major ROS contributor in cells, is an intermediate product of oxidative metabolism in the body, affecting the structure and function of nucleic acids, membrane phospholipids, or proteins, resulting in cell damage and death (Pessayre et al., 2002). It is commonly used to evaluate antioxidant capacity, particularly for evaluating ROS scavenging capacity in cells (Wang L. et al., 2016). This study investigated whether the 14 active constituents of LWWL exert protective effects against H_2O_2-induced oxidative damages; we found that esculetin and luteolin could dose-dependently inhibit H_2O_2-induced cell apoptosis. Therefore, esculetin and luteolin are both anti-apoptosis active components of LWWL.

Some studies indicated that mitochondrial dysfunction and altered mitochondrial ROS levels affect signaling pathways, contributing to liver fibrogenesis, inflammation, and innate immune responses to viral infections (Pessayre et al., 2002; Gao and Bataller, 2011; Tell et al., 2013; Koliaki et al., 2015; Vacca et al., 2015). *Schisandra chinensis* is a commonly used traditional herbal medicine and nutritive food in many countries (Szopa et al., 2017) and has pharmacological effects in stimulating immune response and anti-inflammatory effects (Chen et al., 2019; Zhu et al., 2019). Several studies identified that the whole extract and bioactive lignans of *Schisandra chinensis* protect

against liver injuries induced by hepatotoxins such as acetaminophen or carbon tetrachloride (Bi et al., 2013; Jiang et al., 2015; Fan et al., 2019). schisandrin A and schisandrin B are both the bioactive lignans isolated from *Schisandra chinensis*, which exerts hepatoprotection against liver damage (Leong et al., 2016; Zeng et al., 2017). This study also demonstrated that schisandrin A and schisandrin B could reduce APAP-induced ROS production.

In APAP-induced liver injury, oxidative stress accumulation and inflammatory responses can result in massive hepatocyte necrosis or liver failure (Paul et al., 2016). Some studies have indicated that APAP could increase the levels of lipid peroxidation products that are associated with oxidative stress, resulting in cell death or the destruction of cellular components (Li et al., 2015). After APAP overdose, cell necrosis can lead to the release of local damage-associated molecular patterns (DAMPs), which cause the transcriptional activation of inflammatory cytokines in macrophages (Williams et al., 2011; Kubes and Mehal, 2012; McGill et al., 2012; Woolbright and Jaeschke, 2017; Chao et al., 2018). Some active components of LWWL especially schisandrin A and schisandrin B could reduce the production of ROS, according to our results. Moreover, luteolin and esculetin suppressed H_2O_2-induced apoptosis, and luteolin, one of the active components of LWWL, could also inhibit the NF-κB signaling pathway. One of the intriguing findings in our study was that the combination of luteolin, esculetin, schisandrin A and schisandrin B decreased the serum levels of ALT, AST, DBIL, and TBA, and the combination of active ingredients significantly decreased the production of IL-1β and TNF-α. These data suggest that the combination of LWWL active ingredients could effectively protect against APAP-induced liver injury.

This study provides a better understanding of the pharmacological effects of LWWL from the perspective of its bioactive ingredients. The development of TCM formulae as a complementary and alternative therapy for liver inflammation is extremely urgent. Therefore, further development and incorporation of many disciplines (such as biochemistry, molecular biology, and bioinformatics) are necessary to elucidate the curative and biological mechanisms of TCM. The strategy proposed in this study provides a new method to identify modern indications for TCM with notable clinical efficacy using an integrated approach.

CONCLUSIONS

In this study, we show that luteolin could inhibit the NF-κB signaling pathway in BMDMs, Esculeti and luteolin also dose-dependently suppressed H_2O_2-induced cell apoptosis, schisandrin A and schisandrin B inhibited the release of ROS in APAP-induced acute liver injury *in vitro*. Moreover, the combination of the four active ingredients could protect against APAP-induced acute liver injury *in vivo*. Our study indicated that combination therapy with four compounds (esculetin, luteolin, schisandrin A, and schisandrin B) inhibiting oxidative stress or inflammation exhibit better a hepatoprotective effect. In conclusion, our data demonstrate that the combination of esculetin, luteolin, schisandrin A, and schisandrin B protects liver injury by targeting different pathways, the anti-inflammatory effects of the combination of the four on liver injury is superior to that of esculetin, luteolin, schisandrin A, or schisandrin B alone. The combination of LWWL active ingredients could be applied as a potential therapy to protect or treat liver diseases in a clinical setting, but we also recognize that LWWL, as a TCM, has some limitations in its wide application in the world.

DATA AVAILABILITY STATEMENT

The original contributions presented in the study are included in the article/**Supplementary Material**, further inquiries can be directed to the corresponding authors.

ETHICS STATEMENT

The studies involving human participants were reviewed and approved by The study protocol was approved by the Medical Ethics Committee of the Fifth Medical Center, General Hospital of PLA (NO.2017056D), registered at ClinicalTrials.gov. The patients/participants provided their written informed consent to participate in this study. The animal study was reviewed and approved by the All animal experiments in this study were conducted according to the guidelines for care and use of laboratory animals, and the study protocol was approved by the Animal Ethics Committee of the Fifth Medical Centre, Chinese People's Liberation Army (PLA) General Hospital (animal ethics committee approval number: IACUC-2017-003).

AUTHOR CONTRIBUTIONS

ZB and MN supervised the project. ZB acquired the funding for this study. MN and JZ designed the experiments. YG and WS performed most of the experiments. HY performed the mechanistic studies and analyzed the data. RL and YA analyzed the immunohistochemistry data. ZW, TL, and WD analyzed the data of mice experiments.

FUNDING

This work was supported by National Science and Technology Major Project "Key New Drug Creation and Manufacturing Program" & (2017ZX09301022), National Natural Science Foundation of China (81930110), and Beijing Nova Program (Z181100006218001).

SUPPLEMENTARY MATERIAL

The Supplementary Material for this article can be found online at: https://www.frontiersin.org/articles/10.3389/fphar.2021.747010/full#supplementary-material

REFERENCES

Ai, Y., Shi, W., Zuo, X., Sun, X., Chen, Y., Wang, Z., et al. (2021). The Combination of Schisandrol B and Wedelolactone Synergistically Reverses Hepatic Fibrosis via Modulating Multiple Signaling Pathways in Mice. *Front. Pharmacol.* 12, 655531. doi:10.3389/fphar.2021.655531

Aziz, N., Kim, M. Y., and Cho, J. Y. (2018). Anti-inflammatory Effects of Luteolin: A Review of *In Vitro*, *In Vivo*, and In Silico Studies. *J. Ethnopharmacol* 225, 342–358. doi:10.1016/j.jep.2018.05.019

Bi, H., Li, F., Krausz, K. W., Qu, A., Johnson, C. H., and Gonzalez, F. J. (2013). Targeted Metabolomics of Serum Acylcarnitines Evaluates Hepatoprotective Effect of Wuzhi Tablet (Schisandra Sphenanthera Extract) against Acute Acetaminophen Toxicity. *Evid. Based Complement. Alternat Med.* 2013, 985257. doi:10.1155/2013/985257

Branch of Hepatobiliary Diseases, CMCA (2020). Expert Consensus on Clinical Application of Liuweiwuling Tablets in the Treatment of Chronic Hepatitis B. *Chin. J. Integrated Traditional West. Med. Liver Dis.* 30 (05), 482–485. doi:10.3969/j.issn.1005-0264.2020.05.034

Chao, X., Wang, H., Jaeschke, H., and Ding, W. X. (2018). Role and Mechanisms of Autophagy in Acetaminophen-Induced Liver Injury. *Liver Int.* 38 (8), 1363–1374. doi:10.1111/liv.13866

Chen, X. X., Lam, K. H., Chen, Q. X., Leung, G. P., Tang, S. C. W., Sze, S. C., et al. (2017). Ficus Virens Proanthocyanidins Induced Apoptosis in Breast Cancer Cells Concomitantly Ameliorated 5-fluorouracil Induced Intestinal Mucositis in Rats. *Food Chem. Toxicol.* 110, 49–61. doi:10.1016/j.fct.2017.10.017

Chen, Z., Liu, F., Zheng, N., Guo, M., Bao, L., Zhan, Y., et al. (2019). Wuzhi Capsule (Schisandra Sphenanthera Extract) Attenuates Liver Steatosis and Inflammation during Non-alcoholic Fatty Liver Disease Development. *Biomed. Pharmacother.* 110, 285–293. doi:10.1016/j.biopha.2018.11.069

Cui, Y., and Jia, J. (2013). Update on Epidemiology of Hepatitis B and C in China. *J. Gastroenterol. Hepatol.* 28 Suppl 1 (Suppl. 1), 7–10. doi:10.1111/jgh.12220

Du, K., and Jaeschke, H. (2016). Liuweiwuling Tablets Protect against Acetaminophen Hepatotoxicity: What Is the Protective Mechanism? *World J. Gastroenterol.* 22 (11), 3302–3304. doi:10.3748/wjg.v22.i11.3302

Fan, S., Liu, C., Jiang, Y., Gao, Y., Chen, Y., Fu, K., et al. (2019). Lignans from Schisandra Sphenanthera Protect against Lithocholic Acid-Induced Cholestasis by Pregnane X Receptor Activation in Mice. *J. Ethnopharmacol* 245, 112103. doi:10.1016/j.jep.2019.112103

Gao, B., and Bataller, R. (2011). Alcoholic Liver Disease: Pathogenesis and New Therapeutic Targets. *Gastroenterology* 141 (5), 1572–1585. doi:10.1053/j.gastro.2011.09.002

Gao, X., Wang, C., Chen, Z., Chen, Y., Santhanam, R. K., Xue, Z., et al. (2019). Effects of N-Trans-Feruloyltyramine Isolated from Laba Garlic on Antioxidant, Cytotoxic Activities and H_2O_2-Induced Oxidative Damage in HepG2 and L02 cells. *Food Chem. Toxicol.* 130, 130–141. doi:10.1016/j.fct.2019.05.021

Gao, Y., Xu, G., Ma, L., Shi, W., Wang, Z., Zhan, X., et al. (2021). Icariside I Specifically Facilitates ATP or Nigericin-Induced NLRP3 Inflammasome Activation and Causes Idiosyncratic Hepatotoxicity. *Cell Commun Signal* 19 (1), 13. doi:10.1186/s12964-020-00647-1

Jiang, Y., Fan, X., Wang, Y., Tan, H., Chen, P., Zeng, H., et al. (2015). Hepatoprotective Effects of Six Schisandra Lignans on Acetaminophen-Induced Liver Injury Are Partially Associated with the Inhibition of CYP-Mediated Bioactivation. *Chem. Biol. Interact* 231, 83–89. doi:10.1016/j.cbi.2015.02.022

Kalyanaraman, B., Cheng, G., Hardy, M., Ouari, O., Bennett, B., and Zielonka, J. (2018). Teaching the Basics of Reactive Oxygen Species and Their Relevance to Cancer Biology: Mitochondrial Reactive Oxygen Species Detection, Redox Signaling, and Targeted Therapies. *Redox Biol.* 15, 347–362. doi:10.1016/j.redox.2017.12.012

Koliaki, C., Szendroedi, J., Kaul, K., Jelenik, T., Nowotny, P., Jankowiak, F., et al. (2015). Adaptation of Hepatic Mitochondrial Function in Humans with Non-alcoholic Fatty Liver Is Lost in Steatohepatitis. *Cell Metab* 21 (5), 739–746. doi:10.1016/j.cmet.2015.04.004

Kubes, P., and Mehal, W. Z. (2012). Sterile Inflammation in the Liver. *Gastroenterology* 143 (5), 1158–1172. doi:10.1053/j.gastro.2012.09.008

Lee, Y. A., Wallace, M. C., and Friedman, S. L. (2015). Pathobiology of Liver Fibrosis: a Translational success story. *Gut* 64 (5), 830–841. doi:10.1136/gutjnl-2014-306842

Lei, Y. C., Li, W., and Luo, P. (2015). Liuweiwuling Tablets Attenuate Acetaminophen-Induced Acute Liver Injury and Promote Liver Regeneration in Mice. *World J. Gastroenterol.* 21 (26), 8089–8095. doi:10.3748/wjg.v21.i26.8089

Leong, P. K., Wong, H. S., Chen, J., Chan, W. M., Leung, H. Y., and Ko, K. M. (2016). Differential Action between Schisandrin A and Schisandrin B in Eliciting an Anti-inflammatory Action: The Depletion of Reduced Glutathione and the Induction of an Antioxidant Response. *PLoS One* 11 (5), e0155879. doi:10.1371/journal.pone.0155879

Li, D., Zhu, M., Zhou, C., and Liu, X. (2020). Effect of Liuweiwuling Tablet on Biochemical and Virological Parameters, and Quality of Life in Patients with Hepatitis B Virus-Related Cirrhosis: A Protocol for a Systematic Review and Meta-Analysis. *Medicine (Baltimore)* 99 (37), e22065. doi:10.1097/md.0000000000022065

Li, X., Sun, R., and Liu, R. (2019). Natural Products in Licorice for the Therapy of Liver Diseases: Progress and Future Opportunities. *Pharmacol. Res.* 144, 210–226. doi:10.1016/j.phrs.2019.04.025

Li, Y. Y., Huang, S. S., Lee, M. M., Deng, J. S., and Huang, G. J. (2015). Anti-inflammatory Activities of Cardamonin from Alpinia Katsumadai through Heme Oxygenase-1 Induction and Inhibition of NF-Kb and MAPK Signaling Pathway in the Carrageenan-Induced Paw Edema. *Int. Immunopharmacol* 25 (2), 332–339. doi:10.1016/j.intimp.2015.02.002

Liu, H., Dong, F., Li, G., Niu, M., Zhang, C., Han, Y., et al. (2018a). Liuweiwuling Tablets Attenuate BDL-Induced Hepatic Fibrosis via Modulation of TGF-β/Smad and NF-Kb Signaling Pathways. *J. Ethnopharmacol* 210, 232–241. doi:10.1016/j.jep.2017.08.029

Liu, H., Zhan, X., Xu, G., Wang, Z., Li, R., Wang, Y., et al. (2021). Cryptotanshinone Specifically Suppresses NLRP3 Inflammasome Activation and Protects against Inflammasome-Mediated Diseases. *Pharmacol. Res.* 164, 105384. doi:10.1016/j.phrs.2020.105384

Liu, H., Zhang, Z., Hu, H., Zhang, C., Niu, M., Li, R., et al. (2018b). Protective Effects of Liuweiwuling Tablets on Carbon Tetrachloride-Induced Hepatic Fibrosis in Rats. *BMC Complement. Altern. Med.* 18 (1), 212. doi:10.1186/s12906-018-2276-8

McGill, M. R., Sharpe, M. R., Williams, C. D., Taha, M., Curry, S. C., and Jaeschke, H. (2012). The Mechanism Underlying Acetaminophen-Induced Hepatotoxicity in Humans and Mice Involves Mitochondrial Damage and Nuclear DNA Fragmentation. *J. Clin. Invest.* 122 (4), 1574–1583. doi:10.1172/jci59755

Miele, L., Forgione, A., Gasbarrini, G., and Grieco, A. (2007). Noninvasive Assessment of Fibrosis in Non-alcoholic Fatty Liver Disease (NAFLD) and Non-alcoholic Steatohepatitis (NASH). *Transl Res.* 149 (3), 114–125. doi:10.1016/j.trsl.2006.11.011

Oeckinghaus, A., and Ghosh, S. (2009). The NF-kappaB Family of Transcription Factors and its Regulation. *Cold Spring Harb Perspect. Biol.* 1 (4), a000034. doi:10.1101/cshperspect.a000034

Paul, S., Islam, M. A., Tanvir, E. M., Ahmed, R., Das, S., Rumpa, N. E., et al. (2016). Satkara (Citrus Macroptera) Fruit Protects against Acetaminophen-Induced Hepatorenal Toxicity in Rats. *Evid. Based Complement. Alternat Med.* 2016, 9470954. doi:10.1155/2016/9470954

Pessayre, D., Mansouri, A., and Fromenty, B. (2002). Nonalcoholic Steatosis and Steatohepatitis. V. Mitochondrial Dysfunction in Steatohepatitis. *Am. J. Physiol. Gastrointest. Liver Physiol.* 282 (2), G193–G199. doi:10.1152/ajpgi.00426.2001

Rakariyatham, K., Wu, X., Tang, Z., Han, Y., Wang, Q., and Xiao, H. (2018). Synergism between Luteolin and Sulforaphane in Anti-inflammation. *Food Funct.* 9 (10), 5115–5123. doi:10.1039/c8fo01352g

Reuter, S., Gupta, S. C., Chaturvedi, M. M., and Aggarwal, B. B. (2010). Oxidative Stress, Inflammation, and Cancer: How Are They Linked? *Free Radic. Biol. Med.* 49 (11), 1603–1616. doi:10.1016/j.freeradbiomed.2010.09.006

Sarin, S. K., Kumar, M., Eslam, M., George, J., Al Mahtab, M., Akbar, S. M. F., et al. (2020). Liver Diseases in the Asia-Pacific Region: a Lancet Gastroenterology & Hepatology Commission. *Lancet Gastroenterol. Hepatol.* 5 (2), 167–228. doi:10.1016/s2468-1253(19)30342-5

Sun, S. C. (2017). The Non-canonical NF-Kb Pathway in Immunity and Inflammation. *Nat. Rev. Immunol.* 17 (9), 545–558. doi:10.1038/nri.2017.52

Szopa, A., Ekiert, R., and Ekiert, H. (2017). Current Knowledge of Schisandra Chinensis (Turcz.) Baill. (Chinese magnolia Vine) as a Medicinal Plant Species: a Review on the Bioactive Components, Pharmacological Properties, Analytical

and Biotechnological Studies. *Phytochem. Rev.* 16 (2), 195–218. doi:10.1007/s11101-016-9470-4

Tell, G., Vascotto, C., and Tiribelli, C. (2013). Alterations in the Redox State and Liver Damage: Hints from the EASL Basic School of Hepatology. *J. Hepatol.* 58 (2), 365–374. doi:10.1016/j.jhep.2012.09.018

Turner, M. D., Nedjai, B., Hurst, T., and Pennington, D. J. (2014). Cytokines and Chemokines: At the Crossroads of Cell Signalling and Inflammatory Disease. *Biochim. Biophys. Acta* 1843 (11), 2563–2582. doi:10.1016/j.bbamcr.2014.05.014

Vacca, M., Allison, M., Griffin, J. L., and Vidal-Puig, A. (2015). Fatty Acid and Glucose Sensors in Hepatic Lipid Metabolism: Implications in NAFLD. *Semin. Liver Dis.* 35 (3), 250–261. doi:10.1055/s-0035-1562945

Wang, C., Duan, X., Sun, X., Liu, Z., Sun, P., Yang, X., et al. (2016a). Protective Effects of Glycyrrhizic Acid from Edible Botanical glycyrrhiza Glabra against Non-alcoholic Steatohepatitis in Mice. *Food Funct.* 7 (9), 3716–3723. doi:10.1039/c6fo00773b

Wang, F. S., Fan, J. G., Zhang, Z., Gao, B., and Wang, H. Y. (2014). The Global burden of Liver Disease: the Major Impact of China. *Hepatology* 60 (6), 2099–2108. doi:10.1002/hep.27406

Wang, J. B., Cui, H. R., Wang, R. L., Zhang, C. E., Niu, M., Bai, Z. F., et al. (2018). A Systems Pharmacology-Oriented Discovery of a New Therapeutic Use of the TCM Formula Liuweiwuling for Liver Failure. *Sci. Rep.* 8 (1), 5645. doi:10.1038/s41598-018-21515-6

Wang, L., Ding, L., Yu, Z., Zhang, T., Ma, S., and Liu, J. (2016b). Intracellular ROS Scavenging and Antioxidant Enzyme Regulating Capacities of Corn Gluten Meal-Derived Antioxidant Peptides in HepG2 Cells. *Food Res. Int.* 90, 33–41. doi:10.1016/j.foodres.2016.10.023

Wei, S., Niu, M., Wang, J., Wang, J., Su, H., Luo, S., et al. (2016). A Network Pharmacology Approach to Discover Active Compounds and Action Mechanisms of San-Cao Granule for Treatment of Liver Fibrosis. *Drug Des. Devel Ther.* 10, 733–743. doi:10.2147/dddt.s96964

Williams, C. D., Antoine, D. J., Shaw, P. J., Benson, C., Farhood, A., Williams, D. P., et al. (2011). Role of the Nalp3 Inflammasome in Acetaminophen-Induced Sterile Inflammation and Liver Injury. *Toxicol. Appl. Pharmacol.* 252 (3), 289–297. doi:10.1016/j.taap.2011.03.001

Woolbright, B. L., and Jaeschke, H. (2017). Role of the Inflammasome in Acetaminophen-Induced Liver Injury and Acute Liver Failure. *J. Hepatol.* 66 (4), 836–848. doi:10.1016/j.jhep.2016.11.017

Xia, F., Wang, C., Jin, Y., Liu, Q., Meng, Q., Liu, K., et al. (2014). Luteolin Protects HUVECs from TNF-α-Induced Oxidative Stress and Inflammation via its Effects on the Nox4/ROS-NF-Kb and MAPK Pathways. *J. Atheroscler. Thromb.* 21 (8), 768–783. doi:10.5551/jat.23697

Xin, S., Han, J., Ding, J., Chen, J., Wang, R., Li, X., et al. (2009). The Clinical Study of Liuweiwuling Tablet on Patients with Chronic Hepatitis B. *Chin. J. Integrated Traditional West. Med. Liver Dis.* 19 (01), 7–9. doi:10.3969/j.issn.1005-0264.2009.01.003

Zeng, H., Jiang, Y., Chen, P., Fan, X., Li, D., Liu, A., et al. (2017). Schisandrol B Protects against Cholestatic Liver Injury through Pregnane X Receptors. *Br. J. Pharmacol.* 174 (8), 672–688. doi:10.1111/bph.13729

Zhang, L., and Schuppan, D. (2014). Traditional Chinese Medicine (TCM) for Fibrotic Liver Disease: hope and Hype. *J. Hepatol.* 61 (1), 166–168. doi:10.1016/j.jhep.2014.03.009

Zhang, S., Ma, Q., Liang, S., Xiao, H., Zhuang, G., Zou, Y., et al. (2016). Annual Economic burden of Hepatitis B Virus-Related Diseases Among Hospitalized Patients in Twelve Cities in China. *J. Viral Hepat.* 23 (3), 202–210. doi:10.1111/jvh.12482

Zhu, P., Li, J., Fu, X., and Yu, Z. (2019). Schisandra Fruits for the Management of Drug-Induced Liver Injury in China: A Review. *Phytomedicine* 59, 152760. doi:10.1016/j.phymed.2018.11.020

Conflict of Interest: The authors declare that the research was conducted in the absence of any commercial or financial relationships that could be construed as a potential conflict of interest.

Publisher's Note: All claims expressed in this article are solely those of the authors and do not necessarily represent those of their affiliated organizations, or those of the publisher, the editors and the reviewers. Any product that may be evaluated in this article, or claim that may be made by its manufacturer, is not guaranteed or endorsed by the publisher.

frontiers in Pharmacology

MINI REVIEW
published: 29 October 2021
doi: 10.3389/fphar.2021.780330

Curcuma longa Hepatotoxicity: A Baseless Accusation. Cases Assessed for Causality Using RUCAM Method

Gianmarco Stati[1]*, *Francesco Rossi*[2,3], *Silvia Sancilio*[1], *Mariangela Basile*[1] and *Roberta Di Pietro*[1]

[1]Department of Medicine and Ageing Sciences, G. d'Annunzio University of Chieti-Pescara, Chieti, Italy, [2]Department of Molecular Sciences and Nanosystems, Ca' Foscari University, Venice, Italy, [3]Biophysics Group, Department of Physics and Astronomy, University College London, London, United Kingdom

OPEN ACCESS

Edited by:
Silvia Di Giacomo,
Sapienza University of Rome, Italy

Reviewed by:
Sadaf Jahan,
Majmaah University, Saudi Arabia
Rolf Teschke,
Hospital Hanau, Germany

***Correspondence:**
Gianmarco Stati
statigianmarco@gmail.com

Specialty section:
This article was submitted to Gastrointestinal and Hepatic Pharmacology, a section of the journal Frontiers in Pharmacology

Received: 20 September 2021
Accepted: 18 October 2021
Published: 29 October 2021

Citation:
Stati G, Rossi F, Sancilio S, Basile M and Di Pietro R (2021) Curcuma longa Hepatotoxicity: A Baseless Accusation. Cases Assessed for Causality Using RUCAM Method. Front. Pharmacol. 12:780330. doi: 10.3389/fphar.2021.780330

Curcuma longa is a perennial herb that belongs to the Zingiberaceae family. To date, literature includes more than 11.000 scientific articles describing all its beneficial properties. In the last 3 decades various surveys by the U.S. Food and Drug Administration (FDA) concluded that curcumin, the most active ingredient of the drug, is a "generally safe" compound with strong anti-oxidant effects. *Curcuma longa* was introduced in the daily diet by ayurvedic teachers due to its beneficial effects on health. Nonetheless, recently several reports, from the various global surveillance systems on the safety of plant products, pointed out cases of hepatotoxicity linked to consumption of food supplements containing powdered extract and preparations of *Curcuma longa*. The latest trend is the use of *Curcuma longa* as a weight-loss product in combination with piperine, which is used to increase its very low systemic bioavailability. Indeed, only 20 mg piperine, one of the alkaloids found in black pepper (*Piper nigrum*), assumed at the same time with 2 g curcumin increased 20-fold serum curcumin bioavailability. This combination of natural products is now present in several weight loss supplements containing *Curcuma longa*. The enhanced drug bioavailability caused by piperine is due to its potent inhibition of drug metabolism, being able to inhibit human P-glycoprotein and CYP3A4, while it interferes with UDP-glucose dehydrogenase and glucuronidation activities in liver. While only few cases of hepatotoxicity, assessed using Roussel Uclaf Causality Assessment Method (RUCAM) method, from prolonged intake of piperine and curcumin have been reported, it would be reasonable to speculate that the suspected toxicity of *Curcuma longa* could be due to the concomitant presence of piperine itself. Hence, not only there is the need of more basic research to understand the etiopathology of curcumin-related hepatotoxicity and of the combination curcumin-piperine, but human trials will be necessary to settle this dispute.

Keywords: *Curcuma longa*, curcumin, piperine, food supplement, hepatotoxicity, bioavailability enhancer, RUCAM

INTRODUCTION

The aim of this short review is to trigger a more critical evaluation of scientific evidence existing in literature on potential hepatotoxicity of *Curcuma longa*. The revision of sources would be against the latest trend that blames this famous spice widely used for centuries. *Curcuma longa* has been used throughout human history for various purposes due to its wide range of biological activity (Sharifi-Rad et al., 2020). Curcumin was found to be the primary active component of the extract from the rhizome, known as turmeric. Curcumin is the ingredient responsible for the effects of turmeric as a drug in its long history of use in traditional Asian medicine for a wide variety of disorders.

The Compendium of Sushruta, the foundational text of Ayurveda dating to 250 BCE (Joshi et al., 2017), recommends an ointment containing turmeric, *Curcuma longa* powdered, to relieve the effects of poisoned food. It is not surprising, therefore, that curcumin is currently sold as a dietary supplement and that numerous clinical trials are ongoing to evaluate curcumin activity. In the last decade a large number of reports have been published on the beneficial effects of curcumin (Barchitta et al., 2019) and it has been repeatedly claimed that this natural product is efficient and safe for the prevention and treatment of several diseases (Abd El-Hack et al., 2021). Moreover, curcumin has been widely studied for its antioxidant, anti-inflammatory, and wound-healing effects (Menon and Sudheer, 2007; Shirban et al., 2021). This natural polyphenol is considered by some authors as a "wonder drug of life" (Gera et al., 2017) and it is categorized as a "generally recognized as safe" (GRAS) material, with a stable metabolism and low toxicity (Nelson et al., 2017).

Over recent years, food supplements containing *Curcuma longa* have been widely used by an increasing number of consumers and there is accumulating evidence that curcumin may not be so effective and safe. A number of reports have been issued that described the cases of highly probable drug-induced autoimmune hepatitis (DIAIH) ascribed to ingestion of *Curcuma longa* dietary supplement (Philips et al., 2020). That is, in contrast with the use, since ancient times, of *Curcuma longa*, as hepatoprotective (Rahmani et al., 2016; Tung et al., 2017; Peng et al., 2018) and for the treatment of digestive tract problems (Gera et al., 2017). Furthermore, in literature it is reported that curcumin may prevent oxidative stress-related liver disorder causing a series of metabolic reactions as i) decreasing the levels of alanine transaminase (ALT), aspartase transaminase (AST), and alkaline phosphatase (ALP). ii) It increases the expression of glutathione-S-transferase (GST), glutathione reductase (GR), glutathione peroxidase (GPx), superoxide dismutase (SOD) and catalase (CAT) while further iii) reducing NO production and inhibiting ROS formation (Farzaei et al., 2018).

The most common substance associated with *Curcuma longa* in its use as food supplement is piperine from *Piper nigrum L.* Black pepper (*Piper nigrum L.*) is the most used specie of pepper and it has found a worldwide use as a spice. Its history of use in traditional medicine is thousands of years old, being mentioned in Ayurvedic medicine treaties and in traditional Chinese medicine as early as the 250 BCE (Stojanović-Radić et al., 2019). The peculiar flavour of the *piper* family fruits, and its main pharmacological activity is given by piperine, a molecule of the alkaloid family. Between all the varieties of Piperaceae, *Piper Nigrum L.* contains the largest amount of piperine with certain cultivar reaching the 9% in weight of piperine content (Gorgani et al., 2017). Piperine structure consists of a benzodioxol ring connected to a chain with conjugated double bonds, which on the other extremity is attached to a piperidine moiety throughout a carbonylamide bond (Koul et al., 2000). The presence of a benzodioxol moiety in proximity with a conjugated system is a common feature of many bioactive molecules as psychoactive drugs (Almalki et al., 2020) and molecules able to inhibit the cytochrome P450 (Koul et al., 2000).

Piperine in particular plays a large role in traditional medicine for the treatment of flu-like symptoms and to increase appetite (Stojanović-Radić et al., 2019). In the last decade, a number of works have tested the medical properties of piperine as antioxidant (Vijayakumar et al., 2004), its effect on lipid metabolism (Du et al., 2020) and its anticancer capability (de Almeida et al., 2020). While the most important property of piperine, which is gaining the attention of the scientific community, is its ability to increase the bioavailability of drugs and other active molecules extracted by plants (Gorgani et al., 2017; Lee et al., 2018; Stojanović-Radić et al., 2019).

Piperine, as a component of black pepper, has been demonstrated to have a limited or no toxicity when assumed as a spice (≈ 1 pg/kg per day). The European Food Safety Authority identified 5 mg/kg per day as the no observed adverse effects level (NOAEL) (Bolognesi et al., 2015; Burdock, 2016). On the metabolic level, piperine has been shown to have fundamental effects on p-glycoprotein and many enzyme systems, leading to enhancement of the absorption and bioavailability of several therapeutic drugs. Piperine's bioavailability enhancing property is also partly attributed to increased absorption as a result of its effect on the ultrastructure of intestinal brush border (Meghwal and Goswami, 2013).

INFLUENCE OF PIPERINE ON CURCUMIN BIOAVAILABILITY

Curcumin is a lipophilic polyphenol that is, nearly insoluble in water, with an oral bioavailability lower than 2%. The molecule of curcumin, 1,7-bis(4-hydroxy-3- methoxyphenyl)-1,6-heptadiene-3,5-dione (diferuloylmethane), when orally administrated, is quite stable in the acidic pH of the stomach (Wang et al., 1997), but it undergoes extensive first pass metabolism, is conjugated in the liver, and excreted in the feces. The main metabolites of this process are identified in curcumin glucuronide and curcumin sulfate (Ireson et al., 2001).

Its bioavailability can be enhanced by increasing its absorption and decreasing its metabolic clearance. The co-administration of curcumin with naturally occurring UDP-glucuronyl transferase (UGT) inhibitors, like piperine, improves curcumin bioavailability compared to curcumin alone (Shoba et al., 2007). Curcumin given alone at 2 g/kg achieves a very low serum concentration over a period of 4 h while the co-administration of curcumin in the

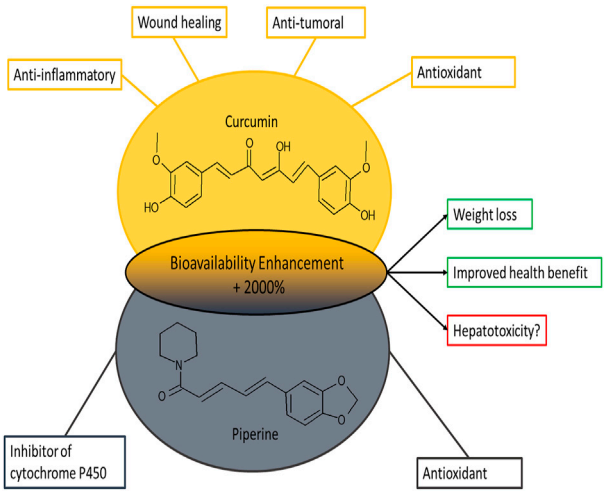

FIGURE 1 | Representation of the chemical structures of curcumin and piperine and their main biological effects.

presence of 20 mg/kg of piperine increases its serum concentration for a short period of 1–2 h post drug intake (Chen et al., 2017). Piperine strongly influences a number of enzymatic biotransforming reactions in hepatic tissue, both *in vitro* and *in vivo* (Atal et al., 1985), acting as a non-specific inhibitor of drug metabolism which does not discriminate among the different forms of the cytochrome P_{450} (Dalvi and Dalvi, 1991).

In particular, piperine strongly inhibits hepatic microsomal aryl hydrocarbon hydroxylase (AHH) and UGT (Atal et al., 1985), leading to a significantly decreased clearance of the co-administered substance and a plasma half-life significantly increased. The overall increase in the bioavailability of curcumin by piperine is of the 2000% (Shoba et al., 2007) (**Figure 1**).

Consuming turmeric and piperine separately is overall safe and it is even associated to a protective effect on cardiovascular mortality (Hashemian et al., 2019).

DISCUSSION

In recent years, numerous risk warnings related to products of natural origin have emerged. In particular, a series of reports on the possible hepatotoxicity of *Curcuma longa*, connected with the use of dietary supplements, have been published (Crijns et al., 2002; Costa et al., 2018; Lukefahr et al., 2018; Imam et al., 2019; Luber et al., 2019; Abdallah et al., 2020; Lee et al., 2020; Suhail et al., 2020; Lombardi et al., 2021). In the present article we have considered only reports who have applied Roussel Uclaf Causality Assessment Method (RUCAM) for causality assessment (Benichou et al., 1993; Danan and Benichou, 1993; Danan and Teschke, 2016), since the weaknesses of LiverTox database approach include a case selection merely based on published case number and not on a strong causality assessment method such as RUCAM (Teschke and Danan, 2021). It is nowadays the suitable method applied in 81,856 DILI and HILI cases worldwide, according to (Teschke and Danan, 2020). The considered cases were judged as probable, supporting the causal relationship to the use of *Curcuma longa* containing supplements and herb-induced liver injury (HILI).

These reports have already caused a level of response from the regulatory bodies, for example, the European Medicine Agency (EMA) has revised its guideline in the September 25, 2018 excluding the use of *Curcuma longa* supplements in case of obstruction of the bile duct, cholangitis, liver disease, gallstones, and any other biliary diseases (European Medicines Agency, 2018). A change of the policy was a consequence of this report requiring from the January 1, 2020 to add a specific warning on the label of food supplements containing curcumin, aimed at discouraging their use by people with liver disease, alterations in biliary function or with gallstones and, in case of concomitant drug intake, aimed at inviting them to consult the doctor (Ministero della Salute, 2019).

CONCLUSION

The overall limited number of cases worldwide, and the few toxicity studies available together with the preliminary determinations of regulatory organs seems to exclude the possibility of an intrinsic toxicity of curcumin. At the same time no solid evidence exists that the combination of curcumin and piperine could be the cause of hepatotoxicity. This seems to exonerate the spice which for millennia has been considered a panacea for all illnesses, indicating that the supposed *Curcuma longa*-related hepatotoxicity would be a baseless accusation. Overall, these type of food supplements should get the same level of attention from regulatory organs that is, given to drugs. Ideally, all the toxicity cases should be evaluated using a comparable method, as the updated RUCAM, and made available to the scientific community. For the specific case of curcumin, the number of cases reported is still too limited for definitive answer and only a more extensive clinical trial in presence of bioavailability enhancers could definitively settle this dispute.

AUTHOR CONTRIBUTIONS

GS wrote and conceptualized the paper. FR contributed in the writing and editing of the manuscript. SS and MB contributed to the literature search. RD contributed to vital revising.

REFERENCES

Abd El-Hack, M. E., El-Saadony, M. T., Swelum, A. A., Arif, M., Abo Ghanima, M. M., Shukry, M., et al. (2021). Curcumin, the Active Substance of Turmeric: its Effects on Health and Ways to Improve its Bioavailability. *J. Sci. Food Agric.* 101, 5747–5762. doi:10.1002/jsfa.11372

Abdallah, M. A., Abdalla, A., Ellithi, M., Abdalla, A. O., Cunningham, A. G., Yeddi, A., et al. (2020). Turmeric-Associated Liver Injury. *Am. J. Ther.* 27, e642–e645. doi:10.1097/MJT.0000000000001025

Almalki, A. J., Clark, C. R., Abiedalla, Y., and DeRuiter, J. (2020). GC-MS Analysis of Methylenedioxybenzyl Analogues of the Serotonin Receptor Agonists 25X-NBOMe Drugs. *Forensic Chem.* 21, 100284. doi:10.1016/J.FORC.2020.100284

Atal, C. K., Dubey, R. K., and Singh, J. (1985). Biochemical Basis of Enhanced Drug Bioavailability by Piperine: Evidence that Piperine Is a Potent Inhibitor of Drug Metabolism. *J. Pharmacol. Exp. Ther.* 232, 258–262. Available at: http://www.ncbi.nlm.nih.gov/pubmed/3917507 (Accessed September 17, 2021).

Barchitta, M., Maugeri, A., Favara, G., Magnano San Lio, R., Evola, G., Agodi, A., et al. (2019). Nutrition and Wound Healing: An Overview Focusing on the Beneficial Effects of Curcumin. *Int. J. Mol. Sci.* 20, 1119. doi:10.3390/ijms20051119

Benichou, C., Danan, G., and Flahault, A. (1993). Causality Assessment of Adverse Reactions to Drugs--II. An Original Model for Validation of Drug Causality Assessment Methods: Case Reports with Positive Rechallenge. *J. Clin. Epidemiol.* 46, 1331–1336. doi:10.1016/0895-4356(93)90102-7

Bolognesi, C., Castle, L., Cravedi, J.-P., Engel, K.-H., Fowler, P., Franz, R., et al. (2015). Scientific Opinion on Flavouring Group Evaluation 86, Revision 2 (FGE.86Rev2): Consideration of Aliphatic and Arylalkyl Amines and Amides Evaluated by JECFA (65th Meeting). *EFSA J.* 13, 3998. doi:10.2903/j.efsa.2015.3998

Burdock, G. A. (2016). *Fenaroli's Handbook of Flavor Ingredients*. Boca Ratón, FL: CRC Press. doi:10.1201/9781439847503

Chen, Z., Sun, D., Bi, X., Zeng, X., Luo, W., Cai, D., et al. (2017). Pharmacokinetic Based Study on "lagged Stimulation" of Curcumae Longae Rhizoma - Piper Nigrum Couplet in Their Main Active Components' Metabolism Using UPLC-MS-MS. *Phytomedicine* 27, 15–22. doi:10.1016/j.phymed.2017.01.012

Costa, M. L., Rodrigues, J. A., Azevedo, J., Vasconcelos, V., Eiras, E., and Campos, M. G. (2018). Hepatotoxicity Induced by Paclitaxel Interaction with Turmeric in Association with a Microcystin from a Contaminated Dietary Supplement. *Toxicon* 150, 207–211. doi:10.1016/j.toxicon.2018.05.022

Crijns, A. P. G., de Smet, P. A. G. M., van den Heuvel, M., Schot, B. W., and Haagsma, E. B. (2002). Acute Hepatitis after Use of a Herbal Preparation with Greater Celandine (Chelidonium Majus), *Ned. Tijdschr. Geneeskd.*, 146, 124–128. Available at: https://europepmc.org/article/med/11826672 (Accessed October 11, 2021).

Dalvi, R. R., and Dalvi, P. S. (1991). Comparison of the Effects of Piperine Administered Intragastrically and Intraperitoneally on the Liver and Liver Mixed-Function Oxidases in Rats. *Drug Metabol. Drug Interact.* 9, 23–30. doi:10.1515/DMDI.1991.9.1.23

Danan, G., and Benichou, C. (1993). Causality Assessment of Adverse Reactions to Drugs--I. A Novel Method Based on the Conclusions of International Consensus Meetings: Application to Drug-Induced Liver Injuries. *J. Clin. Epidemiol.* 46, 1323–1330. doi:10.1016/0895-4356(93)90101-6

Danan, G., and Teschke, R. (2016). RUCAM in Drug and Herb Induced Liver Injury: the Update. *Int. J. Mol. Sci.* 17 (1), 14. doi:10.3390/ijms17010014

de Almeida, G. C., Oliveira, L. F. S., Predes, D., Fokoue, H. H., Kuster, R. M., Oliveira, F. L., et al. (2020). Piperine Suppresses the Wnt/β-Catenin Pathway and Has Anti-cancer Effects on Colorectal Cancer Cells. *Sci. Rep.* 10, 11681. doi:10.1038/s41598-020-68574-2

Du, Y., Chen, Y., Fu, X., Gu, J., Sun, Y., Zhang, Z., et al. (2020). Effects of Piperine on Lipid Metabolism in High-Fat Diet Induced Obese Mice. *J. Funct. Foods* 71, 104011. doi:10.1016/J.JFF.2020.104011

European Medicines Agency (2018). European Union Herbal Monograph on Curcuma Longa L., Rhizoma Final. *Comm. Herb. Med. Prod.* 44, 1–7. Available at: https://www.ema.europa.eu/en/documents/herbal-monograph/final-european-union-herbal-monograph-curcuma-longa-l-rhizoma-revision-1_en.pdf.

Farzaei, M. H., Zobeiri, M., Parvizi, F., El-Senduny, F. F., Marmouzi, I., Coy-Barrera, E., et al. (2018). Curcumin in Liver Diseases: A Systematic Review of the Cellular Mechanisms of Oxidative Stress and Clinical Perspective. *Nutrients* 10, 855. doi:10.3390/nu10070855

Gera, M., Sharma, N., Ghosh, M., Huynh, D. L., Lee, S. J., Min, T., et al. (2017). Nanoformulations of Curcumin: an Emerging Paradigm for Improved Remedial Application. *Oncotarget* 8, 66680–66698. Available at:www.impactjournals.com/oncotarget/. doi:10.18632/oncotarget.19164

Gorgani, L., Mohammadi, M., Najafpour, G. D., and Nikzad, M. (2017). Piperine-The Bioactive Compound of Black Pepper: From Isolation to Medicinal Formulations. *Compr. Rev. Food Sci. Food Saf.* 16, 124–140. doi:10.1111/1541-4337.12246

Hashemian, M., Poustchi, H., Murphy, G., Etemadi, A., Kamangar, F., Pourshams, A., et al. (2019). Turmeric, Pepper, Cinnamon, and Saffron Consumption and Mortality. *Jaha* 8. doi:10.1161/JAHA.119.012240

Imam, Z., Khasawneh, M., Jomaa, D., Iftikhar, H., and Sayedahmad, Z. (20192019). Drug Induced Liver Injury Attributed to a Curcumin Supplement. *Case Rep. Gastrointest. Med.* 2019, 6029403–6029404. doi:10.1155/2019/6029403

Ireson, C., Orr, S., Jones, D. J., Verschoyle, R., Lim, C. K., Luo, J. L., et al. (2001). Characterization of Metabolites of the Chemopreventive Agent Curcumin in Human and Rat Hepatocytes and in the Rat *In Vivo*, and Evaluation of Their Ability to Inhibit Phorbol Ester-Induced Prostaglandin E2 Production. *Cancer Res.* 61, 1058–1064.

Joshi, V. K., Joshi, A., and Dhiman, K. S. (2017). The Ayurvedic Pharmacopoeia of India, Development and Perspectives. *J. Ethnopharmacol.* 197, 32–38. doi:10.1016/J.JEP.2016.07.030

Koul, S., Koul, J. L., Taneja, S. C., Dhar, K. L., Jamwal, D. S., Singh, K., et al. (2000). Structure-activity Relationship of Piperine and its Synthetic Analogues for Their Inhibitory Potentials of Rat Hepatic Microsomal Constitutive and Inducible Cytochrome P450 Activities. *Bioorg. Med. Chem.* 8, 251–268. doi:10.1016/S0968-0896(99)00273-4

Lee, B. S., Bhatia, T., Chaya, C. T., Wen, R., Taira, M. T., and Lim, B. S. (2020). Autoimmune Hepatitis Associated with Turmeric Consumption. *ACG Case Rep. J.* 7, e00320. doi:10.14309/crj.0000000000000320

Lee, S. H., Kim, H. Y., Back, S. Y., and Han, H. K. (2018). Piperine-mediated Drug Interactions and Formulation Strategy for Piperine: Recent Advances and Future Perspectives. *Expert Opin. Drug Metab. Toxicol.* 14, 43–57. doi:10.1080/17425255.2018.1418854

Lombardi, N., Crescioli, G., Maggini, V., Ippoliti, I., Menniti-Ippolito, F., Gallo, E., et al. (2021). Acute Liver Injury Following Turmeric Use in Tuscany: An Analysis of the Italian Phytovigilance Database and Systematic Review of Case Reports. *Br. J. Clin. Pharmacol.* 87, 741–753. doi:10.1111/bcp.14460

Luber, R. P., Rentsch, C., Lontos, S., Pope, J. D., Aung, A. K., Schneider, H. G., et al. (2019). Turmeric Induced Liver Injury: A Report of Two Cases. *Case Rep. Hepatol* 2019, 6741213–6741214. doi:10.1155/2019/6741213

Lukefahr, A. L., McEvoy, S., Alfafara, C., and Funk, J. L. (2018). Drug-induced Autoimmune Hepatitis Associated with Turmeric Dietary Supplement Use. *BMJ Case Rep.* 2018, 1–7. doi:10.1136/bcr-2018-224611

Meghwal, M., and Goswami, T. K. (2013). *Piper Nigrum* and Piperine: An Update. *Phytother Res.* 27, 1121–1130. doi:10.1002/PTR.4972

Menon, V. P., and Sudheer, A. R. (2007). "Antioxidant and Anti-inflammatory Properties of Curcumin," in *The Molecular Targets and Therapeutic Uses of Curcumin in Health and Disease* (Boston, MA: Springer US), 105–125. doi:10.1007/978-0-387-46401-5_3

Ministero della Salute (2019). *Food Supplements Containing Extract and Derivatives of* Curcuma Longa. Available at: https://www.salute.gov.it/portale/news/p3_2_1_1_1.jsp?lingua=italiano&menu=notizie&p=dalministero&id=3842 (Accessed September 17, 2021).

Nelson, K. M., Dahlin, J. L., Bisson, J., Graham, J., Pauli, G. F., and Walters, M. A. (2017). The Essential Medicinal Chemistry of Curcumin. *J. Med. Chem.* 60, 1620–1637. doi:10.1021/acs.jmedchem.6b00975

Peng, X., Dai, C., Liu, Q., Li, J., and Qiu, J. (2018). Curcumin Attenuates on Carbon Tetrachloride-Induced Acute Liver Injury in Mice via Modulation of the Nrf2/HO-1 and TGF-β1/Smad3 Pathway. *Molecules* 23, 215. doi:10.3390/molecules23010215

Philips, C. A., Ahamed, R., Rajesh, S., George, T., Mohanan, M., and Augustine, P. (2020). Comprehensive Review of Hepatotoxicity Associated with Traditional Indian Ayurvedic Herbs. *World J. Hepatol.* 12, 574–595. doi:10.4254/WJH.V12.I9.574

Rahmani, S., Asgary, S., Askari, G., Keshvari, M., Hatamipour, M., Feizi, A., et al. (2016). Treatment of Non-alcoholic Fatty Liver Disease with Curcumin: A Randomized Placebo-Controlled Trial. *Phytother Res.* 30, 1540–1548. doi:10.1002/PTR.5659

Sharifi-Rad, J., Rayess, Y. E., Rizk, A. A., Rizk, C., Zgheib, R., Zam, W., et al. (2020). Turmeric and its Major Compound Curcumin on Health: Bioactive Effects and Safety Profiles for Food, Pharmaceutical, Biotechnological and Medicinal Applications. *Front. Pharmacol.* 11, 01021–01023. doi:10.3389/fphar.2020.01021

Shirban, F., Gharibpour, F., Ehteshami, A., Bagherniya, M., Sathyapalan, T., and Sahebkar, A. (2021). The Effects of Curcumin in the Treatment of Gingivitis: A Systematic Review of Clinical Trials. *Adv. Exp. Med. Biol.*, 1291, 179–211. doi:10.1007/978-3-030-56153-6_11

Shoba, G., Joy, D., Joseph, T., Majeed, M., Rajendran, R., and Srinivas, P. S. (2007). Influence of Piperine on the Pharmacokinetics of Curcumin in Animals and Human Volunteers. *Planta Med.* 64, 353–356. doi:10.1055/S-2006-957450

Stojanović-Radić, Z., Pejčić, M., Dimitrijević, M., Aleksić, A., V. Anil Kumar, N., Salehi, B., et al. (2019). Piperine-A Major Principle of Black Pepper: A Review of its Bioactivity and Studies. *Appl. Sci.* 9, 4270. doi:10.3390/app9204270

Suhail, F. K., Masood, U., Sharma, A., John, S., and Dhamoon, A. (2020). Turmeric Supplement Induced Hepatotoxicity: a Rare Complication of a Poorly Regulated Substance. *Clin. Toxicol. (Phila)* 58, 216–217. doi:10.1080/15563650.2019.1632882

Teschke, R., and Danan, G. (2021). Idiosyncratic Drug-Induced Liver Injury (DILI) and Herb-Induced Liver Injury (HILI): Diagnostic Algorithm Based on the Quantitative Roussel Uclaf Causality Assessment Method (RUCAM). *Diagnostics (Basel)* 11, 458. doi:10.3390/diagnostics11030458

Teschke, R., and Danan, G. (2020). Worldwide Use of RUCAM for Causality Assessment in 81,856 Idiosyncratic DILI and 14,029 HILI Cases Published 1993-Mid 2020: A Comprehensive Analysis. *Medicines (Basel)* 7, 62. doi:10.3390/medicines7100062

Tung, B. T., Hai, N. T., and Son, P. K. (2017). Hepatoprotective Effect of Phytosome Curcumin against Paracetamol-Induced Liver Toxicity in Mice. *Braz. J. Pharm. Sci.* 53, 1–13. doi:10.1590/s2175-97902017000116136

Vijayakumar, R. S., Surya, D., and Nalini, N. (2004). Antioxidant Efficacy of Black Pepper (Piper Nigrum L.) and Piperine in Rats with High Fat Diet Induced Oxidative Stress. *Redox Rep.* 9, 105–110. doi:10.1179/135100004225004742

Wang, Y. J., Pan, M. H., Cheng, A. L., Lin, L. I., Ho, Y. S., Hsieh, C. Y., et al. (1997). Stability of Curcumin in Buffer Solutions and Characterization of its Degradation Products. *J. Pharm. Biomed. Anal.* 15, 1867–1876. doi:10.1016/S0731-7085(96)02024-9

Conflict of Interest: The authors declare that the research was conducted in the absence of any commercial or financial relationships that could be construed as a potential conflict of interest.

Publisher's Note: All claims expressed in this article are solely those of the authors and do not necessarily represent those of their affiliated organizations, or those of the publisher, the editors and the reviewers. Any product that may be evaluated in this article, or claim that may be made by its manufacturer, is not guaranteed or endorsed by the publisher.

frontiers in Pharmacology

REVIEW
published: 04 November 2021
doi: 10.3389/fphar.2021.771459

The Potential Application of Chinese Medicine in Liver Diseases: A New Opportunity

Ke Fu†, *Cheng Wang*†, *Cheng Ma*†, *Honglin Zhou and Yunxia Li**

State Key Laboratory of Southwestern Chinese Medicine Resources, Key Laboratory of Standardization for Chinese Herbal Medicine, Ministry of Education, School of Pharmacy, Chengdu University of Traditional Chinese Medicine, Chengdu, China

Liver diseases have been a common challenge for people all over the world, which threatens the quality of life and safety of hundreds of millions of patients. China is a major country with liver diseases. Metabolic associated fatty liver disease, hepatitis B virus and alcoholic liver disease are the three most common liver diseases in our country, and the number of patients with liver cancer is increasing. Therefore, finding effective drugs to treat liver disease has become an urgent task. Chinese medicine (CM) has the advantages of low cost, high safety, and various biological activities, which is an important factor for the prevention and treatment of liver diseases. This review systematically summarizes the potential of CM in the treatment of liver diseases, showing that CM can alleviate liver diseases by regulating lipid metabolism, bile acid metabolism, immune function, and gut microbiota, as well as exerting anti-liver injury, anti-oxidation, and anti-hepatitis virus effects. Among them, Keap1/Nrf2, TGF-β/SMADS, p38 MAPK, NF-κB/IκBα, NF-κB-NLRP3, PI3K/Akt, TLR4-MyD88-NF-κB and IL-6/STAT3 signaling pathways are mainly involved. In conclusion, CM is very likely to be a potential candidate for liver disease treatment based on modern phytochemistry, pharmacology, and genomeproteomics, which needs more clinical trials to further clarify its importance in the treatment of liver diseases.

Keywords: liver diseases, natural agents, toxicity, clinical trials, potential application, Chinese medicine

OPEN ACCESS

Edited by:
Annabella Vitalone, Sapienza University of Rome, Italy

Reviewed by:
Luis Enrique Gomez-Quiroz, Autonomous Metropolitan University, Mexico
Maitane Asensio, University of Salamanca, Spain

****Correspondence:***
Yunxia Li
lyxtgyxcdutcm@163.com

†*These authors have contributed equally to this work*

Specialty section:
This article was submitted to Gastrointestinal and Hepatic Pharmacology, a section of the journal Frontiers in Pharmacology

Received: *06 September 2021*
Accepted: *19 October 2021*
Published: *04 November 2021*

Citation:
Fu K, Wang C, Ma C, Zhou H and Li Y (2021) The Potential Application of Chinese Medicine in Liver Diseases: A New Opportunity. Front. Pharmacol. 12:771459. doi: 10.3389/fphar.2021.771459

INTRODUCTION

Chinese medicine (CM) is an effective drug treatment system with a history of thousands of years. It is used for disease prevention, treatment and diagnosis. CM is characterized by individualized adjustment of multiple components and multiple targets, which makes the body change from an abnormal state to a normal state (Wang et al., 2018). It has made an indelible contribution to human health and is considered

Abbreviations: ALD, alcoholic liver disease; AMPK, adenine monophosphate activated protein kinase; ARE, antioxidant responsive element; BAs, bile acids; CM, Chinese medicine; CYP, cytochrome P450; FL, fatty liver; FSE, Forsythiae Fructuse water extract; GSH, glutathione; HBV, hepatitis B virus; HCC, hepatocellular carcinoma; HCV, hepatitis C virus; HSCs, hepatic stellate cells; IL-1β, interleukin-1β; IL-6, interleukin-6; KCs, kupffer cells; LC, liver cirrhosis; LSECs, liver sinusoidal endothelial cells; MAFLD, metabolic associated fatty liver disease; NAFL, non-alcoholic fatty liver; NASH, non-alcoholic steatohepatitis; NF-κB, nuclear factor kappa-B; NK, natural killer; Nrf2, nuclear factor-erythroid 2-related factor 2; ROS, reactive oxygen species; RSM, Radix Salvia Miltiorrhiza; SOD, superoxide dismutase; TC, total cholesterol; TG, triglyceride; TGF-β, transforming growth factor-β; TNF-α, tumor necrosis factor-α.

a potential natural source of therapeutic drugs (Hesketh and Zhu, 1997; Chan and Ng, 2020). For example, Tu won the 2015 Nobel Prize for discovering and developing artemisinin in *Artemisia annua* Linn. It is a clear example to prove the therapeutic potential of CM and is of great significance to the continued development of the field (Tu, 2016). Besides, this field has huge and undeveloped resources. Screening and providing effective monomer chemicals are important means of CM to promote the development of medicine in the world (Wang et al., 2018).

Liver diseases are serious diseases threatening the whole human health, mainly including metabolic associated fatty liver disease (MAFLD), alcoholic liver disease (ALD), chronic viral hepatitis (e.g., hepatitis B virus (HBV) and hepatitis C virus (HCV) infections), autoimmune hepatitis, hepatic schistosomiasis, drug-induced liver injury, liver cirrhosis (LC), hepatocellular carcinoma (HCC), and so on (Li, Q. et al., 2018; Wang et al., 2014). China has the highest incidence of liver diseases in the world, and about 300,000–400,000 people die from various liver diseases each year. According to the data, MAFLD, HBV and ALD are the three most common liver diseases in China, with the incidence of 49.3, 22.9 and 14.8% respectively (Wang et al., 2014).

At present, CM has shown significant efficacy in the treatment of liver diseases, such as *Rheum palmatum* L. (Jin et al., 2005; Yang et al., 2012; Neyrinck et al., 2017), *Silybum marianum* (L.) Gaertn. (Alaca et al., 2017; Jindal et al., 2019), and *Sophora flavescens* Ait. (Yang et al., 2018; Yim et al., 2019). Furthermore, liver diseases are various, and the course of each disease is also different. Fortunately, CM can effectively treat a variety of liver diseases, and it has played an important role in the prevention and treatment of liver diseases. For example, *Zingiber officinale* and *Glycyrrhiza uralensis* Fischer can effectively treat ALD and MAFLD (Jung et al., 2016; Kandeil et al., 2019), and *Rhizoma Coptidis* can be used in the treatment of hepatitis virus (Hung et al., 2018). For more serious liver diseases, such as liver cirrhosis and liver cancer, *Salvia offificinalis* L. and *Portulaca oleracea* L. have shown good effects (Guoyin et al., 2017; Jiang, Y. et al., 2017). Besides, according to relevant records, the variety of CM commonly used in the treatment of liver diseases is up to 90 kinds (Wu, 2001). It can be seen that the resources of CM for the treatment of liver diseases are rich and valuable, which is worthy of further research and development.

In this review, we collected relevant literature in recent 6 years (2015–2020) through CNKI, PubMed, ScienceDirect and Google academic, and analyzed the application, toxicology and clinical data of CM and their related compounds, aiming to dig out more CM with potential biological activities for liver diseases, and promote their application value in the treatment of liver diseases, further providing relevant reference for the clinical application CM.

CHARACTERISTICS OF SEVERAL IMPORTANT LIVER DISEASES

The Three Most Common Liver Diseases in China

MAFLD

MAFLD is a clinical syndrome characterized by hepatocyte steatosis and increased lipid deposition with the exception of alcohol and other clear liver-damaging factors (Mantovani et al., 2019). It is associated with obesity, insulin resistance, type 2 diabetes mellitus, hypertension, hyperlipidemia, and metabolic syndrome (Younossi, 2019). MAFLD is a broad umbrella term for a range of liver disorders, from non-alcoholic fatty liver (NAFL) to non-alcoholic steatohepatitis (NASH). It is called NAFL if it is only steatosis (fatty liver) and NASH if there is severe inflammation and liver cell damage (steatohepatitis). The course of MAFLD is complex and variable, which can lead to cirrhosis and liver cancer in severe cases (Friedman et al., 2018).

The pathogenesis of MAFLD mainly includes abnormal lipid metabolism, oxidative stress, inflammasome activation, insulin resistance, mitochondrial dysfunction, and genetic determinants (Buzzetti et al., 2016). Abnormal lipid metabolism in hepatocytes is the initial factor for MAFLD. When the number of fatty acids entering the liver is greater than their oxidation and secretion, the lipid accumulates in the liver, resulting in hepatic lipid deposition (Onyekwere et al., 2015), which leads directly to MAFLD. Furthermore, excessive lipid deposition further aggravates tissue damage by promoting the production of reactive oxygen species (ROS) and a series of pathological changes, such as the peroxidation of cells themselves, the release of pro-inflammatory factors and the infiltration of inflammatory cells, damaged hepatocytes activate the nuclear factor kappa-B (NF-κB) pathway, thus inducing the production of proinflammatory cytokine tumor necrosis factor-α (TNF-α) and interleukin-1β/-6 (IL-1β, IL-6) (Buzzetti et al., 2016; Xiao et al., 2020). These inflammatory factors can not only induce the activation of astrocytes and the remodeling of cell matrix, but also accelerate the progression of the disease by promoting insulin resistance. In addition, MAFLD is strongly associated with gut microbes, some of which carry genes that ferment dietary sugars into ethanol. When released into the bloodstream, they will increase oxidative stress and inflammation in the liver. In the liver, alcohol dehydrogenase metabolizes ethanol into toxic acetaldehyde, which forms adducts with proteins and other molecules in the cell because of its electrophilic properties, resulting in the loss of hepatocyte structure and function (Kolodziejczyk et al., 2019).

HBV Infection

HBV, a part of the *Hepadnaviridae* family, consists of nucleocapsid, envelope, and three complete membrane proteins (Seitz et al., 2007), which is a partially double-stranded and non-cytopathic DNA virus. The virus replicates the DNA by reverse transcription of the pre-RNA genome and has many serological markers such as HBsAg and anti-HBs, HBeAg and anti-HBe, and anti-HBc IgM and IgG (Trépo et al., 2014; Hu and Liu, 2017). HBV is the most common chronic virus in the world. Infected cells produce covalently closed circular DNA intermediates and integrated sequences that act as transcription templates for viral proteins (Fanning et al., 2019). HBV is transmitted through a number of routes, but mainly in the form of blood and body fluids, including perinatal and mother-to-child transmission, as well as sexual and extraintestinal patterns (Yuen et al., 2018).

At present, vaccination is still the most effective tool to prevent HBV infection, but there are also other therapeutic approaches, such as antiviral drugs that directly act on virus replication (interferon) and immune modulators (including reverse-transcriptase inhibitors, primarily a nucleoside or nucleotide analogue) (Yuen et al., 2018). These treatments can effectively inhibit HBV replication, but the disadvantages are the long-term medication and side effects. In addition, HBV infection can lead to chronic hepatitis and a series of complications, and studies have shown that HBV may persist in the body even after the infected person has fully recovered (Rehermann et al., 1996; Shi and Zheng, 2020). If immunosuppression-mediated host immune control is weakened, or several therapies and drugs have a direct effect on HBV replication, HBV may be reactivated (Shi and Zheng, 2020). Therefore, it is urgent to find a more effective HBV therapy to ensure the health of all human beings.

ALD

ALD refers to hepatocyte necrosis and destruction of normal liver function under the action of ethanol for a long time, which is a series of liver diseases including fatty liver, alcoholic hepatitis, cirrhosis, and its complications (such as ascites, portal hypertension-related bleeding, hepatic encephalopathy, and HCC) (Singal et al., 2018). The disease initially presents as alcoholic fatty liver disease, then gradually develops into alcoholic cirrhosis, even extensive hepatocyte necrosis, eventually inducing liver failure (Penny, 2013; Hu et al., 2019).

Sustained large quantity of alcohol stimulation is the primary factor of ALD. The pathogenesis is complicated and varied, mainly related to genetics, oxidative stress, hepatic steatosis, hepatic inflammation, and so on (2018). There is some evidence that aldehyde dehydrogenase2*2 and alcohol dehydrogenase 1B*3 alleles are closely related to alcoholic liver disease, and they can have some kind of chemical reaction with alcohol to achieve rapid metabolism (Agrawal and Bierut, 2012; Dodge et al., 2014); transmembrane 6 superfamily member 2 gene mutation can lead to the accumulation of liver fat, so that the disease will develop into a bad situation (2018); patatinlike phospholipase domain-containing protein 3, which mediates triglyceride hydrolysis in adipocytes, is closely related to lipid metabolism in the liver, but the mechanism of how it affects ALD is unclear (Salameh et al., 2015; BasuRay et al., 2017). At the same time, membrane-bound O-acetyltransferase domain-containing protein 7 is also an important genetic material related to ALD, but its mechanism is not clear (2018).

Oxidative stress plays a crucial role in the pathogenesis of ALD. In biological systems, free radicals include oxygen free radicals and nitrogen free radicals, among which oxygen free radicals and non-free radicals such as hypochlorite and ozone are called ROS. Under normal circumstances, the body contains antioxidants (such as superoxide dismutase (SOD), catalase, glutathione (GSH), glutathione peroxidase, glutathione transferase, heme oxygenase bilirubin etc.) and ROS in a state of balance, which are not harmful to the human body (Li et al., 2015). But in the case of long-term alcohol abuse, the reduction in the level or activity of antioxidants in the body causes oxidative stress. Alcohol may also increase the level of ROS. For example, ROS and nicotinamide adenine dinucleotide (NADH) are produced when ethanol is oxidized to acetaldehyde by alcohol dehydrogenase in the liver. Acetaldehyde is oxidized to acetic acid in mitochondria, which stimulates the body to produce large amounts of ROS (Li et al., 2014). NADH also interferes with the mitochondrial electron transport system and promotes ROS production (Ceni et al., 2014). Alcohol can also activate the NAD (P) H oxidase in hepatocytes, leading to an increase in the production of superoxide (Kalyanaraman, 2013). There is also evidence that another important pathophysiological mechanism of ALD is the interaction between endotoxin and Kupffer cells (KCs). Long-term high alcohol intake can induce low levels of intestinal endotoxemia, and increase intestinal permeability, causing Gram-negative bacteria to enter the hepatic portal circulation to suppress immune function (Mello et al., 2008; Gao and Liu, 2016). KCs recognize and clear gut-derived endotoxins, and promote oxidative stress and inflammatory response through their interaction (Yang and Wei, 2017).

Other Liver Diseases

HCV Infection

Hepatitis C is an infectious disease caused by HCV. HCV is an RNA virus, 45–65 nm in diameter, encapsulated in a lipid bilayer, belonging to the *Flaviviridae* family (Manns et al., 2017). HCV enters its target cells by a variety of host factors, including CD81, low-density lipoprotein receptor, dendritic cell-specific ICAM-grabbing non-integrin, claudin-1, and occludin. Among the different types of liver diseases, HCV is unique in requiring liver specific microRNA-122 replication (Luna et al., 2015). In addition, the genotypes of HCV are very rich. By the culture, analysis and identification of HCV strains isolated from all parts of the world, seven major HCV genotypes were found, namely 1–7 (Manns et al., 2017). Genotype 1 is the most prevalent in the world, including 83.4 million cases (46.2% of all HCV cases), about a third of which are in East Asia. Genotype 3 ranks second in the world (54.3 million, 30.1%), genotype 2, 4 and 6 account for 22.8% of all cases, and genotype 5 accounts for less than 1% of the remaining cases (Messina et al., 2015).

HCV transmission is most commonly associated with direct percutaneous exposure to blood *via* blood transfusions, health-care-related injections, and injecting drug use (Spearman et al., 2019). Alcohol is also a common cofactor for HCV infection, and alcohol use is more strongly associated with the progression of liver fibrosis (Poynard et al., 1997). Secondly, HCV infection can induce the abnormal expression of two host microRNAs (miR-208b and miR-499a-5p) encoded by myosin genes in hepatocytes. MiR-208b and miR-499a-5p inhibit type I IFN signal transduction in infected hepatocytes by directly down-regulating type I IFN receptor expression (Jarret et al., 2016). In addition, chronic HCV infection can also lead to liver fibrosis, cirrhosis, hepatocellular carcinoma and other serious complications.

LC

LC is a pathological stage characterized by diffuse fibrosis, pseudolobules formation, and intrahepatic and extrahepatic

vascular proliferation (He and Liu, 2021). It is one of the main causes of death in patients with liver diseases all over the world, and also the final result of the development of a variety of acute and chronic liver diseases. LC shows symptoms such as portal hypertension and liver dysfunction. At present, the diagnosis of LC mainly depends on the imaging of irregular nodular liver by ultrasound, CT or MRI and the evaluation of liver synthesis function. In clinical practices, LC is considered as an end-stage manifestation of liver pathology with a high mortality without liver transplantation treatment (Tsochatzis et al., 2014; Zhou et al., 2014). But liver transplantation requires a lot of ligands and money, which is not an easy thing to solve, so CM has become a more effective approach.

The pathological pathway of LC is very complicated, but the research has shown that it is closely related to the expression of some cells on the wall of hepatic sinus. Hepatic sinus walls are composed of three kinds of non-parenchymal cells (liver sinusoidal endothelial cells (LSECs), KCs and hepatic stellate cells (HSCs)), which are involved in the development of LC (Zhou et al., 2014). In non-diseased liver, HSCs are located in the subendothelial space of Disse and are primarily involved in the storage of retinoic acid, but HSC is activated in the area of liver injury (Friedman, 1993; Hernandez-Gea and Friedman, 2011). In this activated phenotype, HSC is the main source of collagen and non-collagen matrix proteins in fibrosis. Related studies have shown that LSECs can secrete the cytokine IL-33 to activate HSCs and promote fibrosis (Marvie et al., 2010). Secondly, the exfoliation and capillarization of LSECs were proved to be the main contributing factors of liver dysfunction in cirrhosis (Yokomori et al., 2012). Finally, KCs can mediate liver inflammation to aggravate liver damage and fibrosis (López-Navarrete et al., 2011). Cytokines such as platelet-derived growth factor, transforming growth factor-β (TGF-β), TNF-α, and Interferon also play a crucial role in the pathogenesis of liver fibrosis and cirrhosis (Zhou et al., 2014). It is worth mentioning that if a patient has been diagnosed with ALD, concomitant chronic hepatitis B or C infection will directly aggravate the liver injury, leading to more frequent and rapid occurrence of cirrhosis (Poynard et al., 1997).

HCC

HCC is the most common form of liver cancer, accounting for 90% of the total cases of liver cancer. Among the various chronic liver diseases, HCC is the final stage of the disease in some patients with LC. About 80% of HCC patients have the pathological basis of LC, and the rate of HCC in patients with cirrhosis disease base in the short-term can be 5–30% (El-Serag, 2012). HBV and HCV are major risk factors for the development of HCC (Llovet et al., 2021). Others include exposure to aflatoxin, excessive drinking, smoking, diabetes, and knowledge of other risk factors such as MAFLD has been gradually recognized (Forner et al., 2012; Forner et al., 2018). The high incidence of HCC is concentrated in developing countries such as China, mainly due to chronic HBV infection (Jemal et al., 2011). Until now, there has been no nationwide cancer screening in China. Once a patient develops HCC, not only does the patient face tremendous pain from radiation therapy, but the improvement in survival rates is very limited, if more potential anti-cancer drugs can be tapped from the CM system, it will be beneficial to HCC patients.

Figure 1 is a map of the major pathogenesis of some important liver diseases.

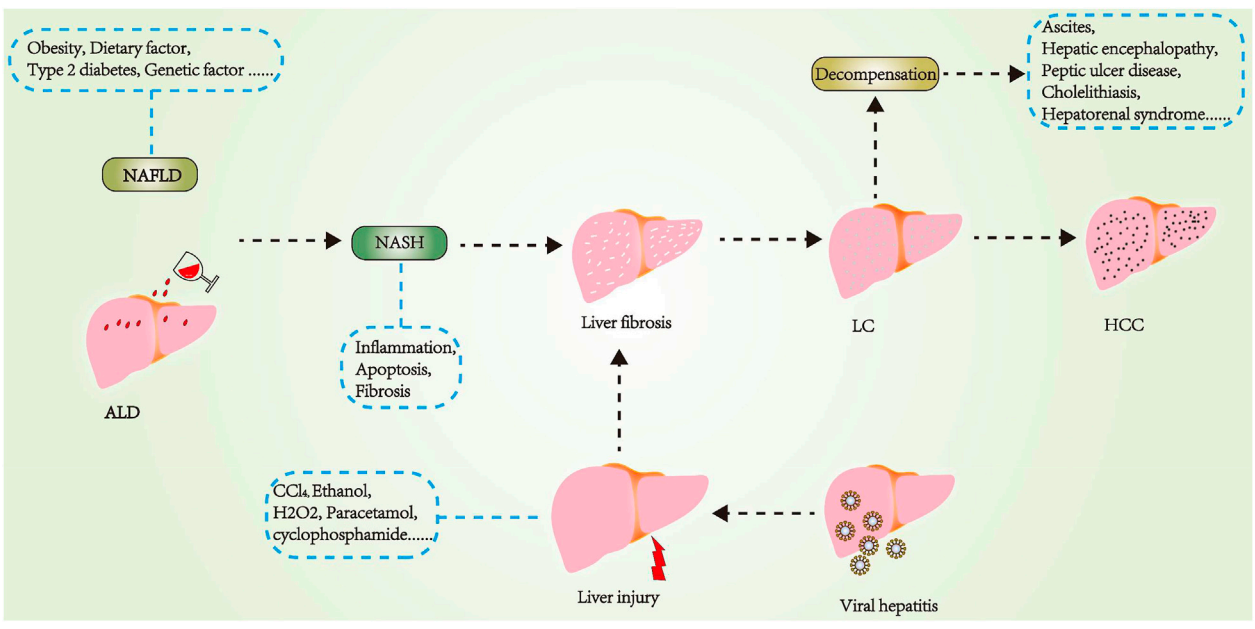

FIGURE 1 | Main pathogenesis of important liver diseases.

Pharmacological Effects of CM for Management of Liver Disease

There are abundant varieties of natural CM resources in China, which is worthy of further development and utilization. For example, **Figure 2** only shows the distribution of some CM for liver disease in the main producing area (also named "Daodi" producing area). Among them, many of the common CM have shown anti-liver disease activity, *see* **Table 1**. In addition, the pharmacological effects of CM on liver disease are summarized in **Figure 3**.

Regulating Lipid Metabolism

Lipid uptake, esterification, oxidation, and fatty acid secretion all occur in hepatocytes. These processes are regulated by hormones, nuclear receptors, and transcription factors to maintain liver lipid homeostasis (Nguyen et al., 2008). If the balance of liver lipid metabolism is destroyed, the lipid will accumulate abnormally in the liver. Excessive lipid accumulation will lead to liver steatosis, insulin resistance and the development of fatty liver disease, and even induce oxidative stress, causing inflammation, cytotoxicity and aggravating liver injury. Therefore, maintaining normal lipid metabolism is an important function of the liver (Ding, H.-R. et al., 2018; Li, X. et al., 2019).

Many CMs have shown good effects in regulating lipid metabolism, such as *Radix Bupleuri*, *Pericarpium Citri Reticulatae*, *Rhubarb*, *Polygonum Multiflorum*, *Coptis Chinensis*, *Artemisia Annua*, *Flos Lonicera* and *Radix Sophorae Tonkinensis*. The results showed that the serum high-density lipoprotein cholesterol (HDL-C), TC and low-density lipoprotein cholesterol (LDL-C) levels of c57BL/6 mice were reduced by Citrus reticulata Blanco peel extract. The author further revealed that 0.2 and 0.5% of the extract could effectively prevent the micro fatty degeneration and excessive accumulation of lipid droplets in the liver (Ke et al., 2020). *Rheum Palmatum* L. can continuously reduce the accumulation of excess fat and the expression of lipogenic genes in the liver of male Sprague-Dawley rats induced by a high-fat diet. Concomitantly, increased phosphorylation of adenine monophosphate activated protein kinase (AMPK) and acetyl-CoA carboxylaze was observed (Yang,

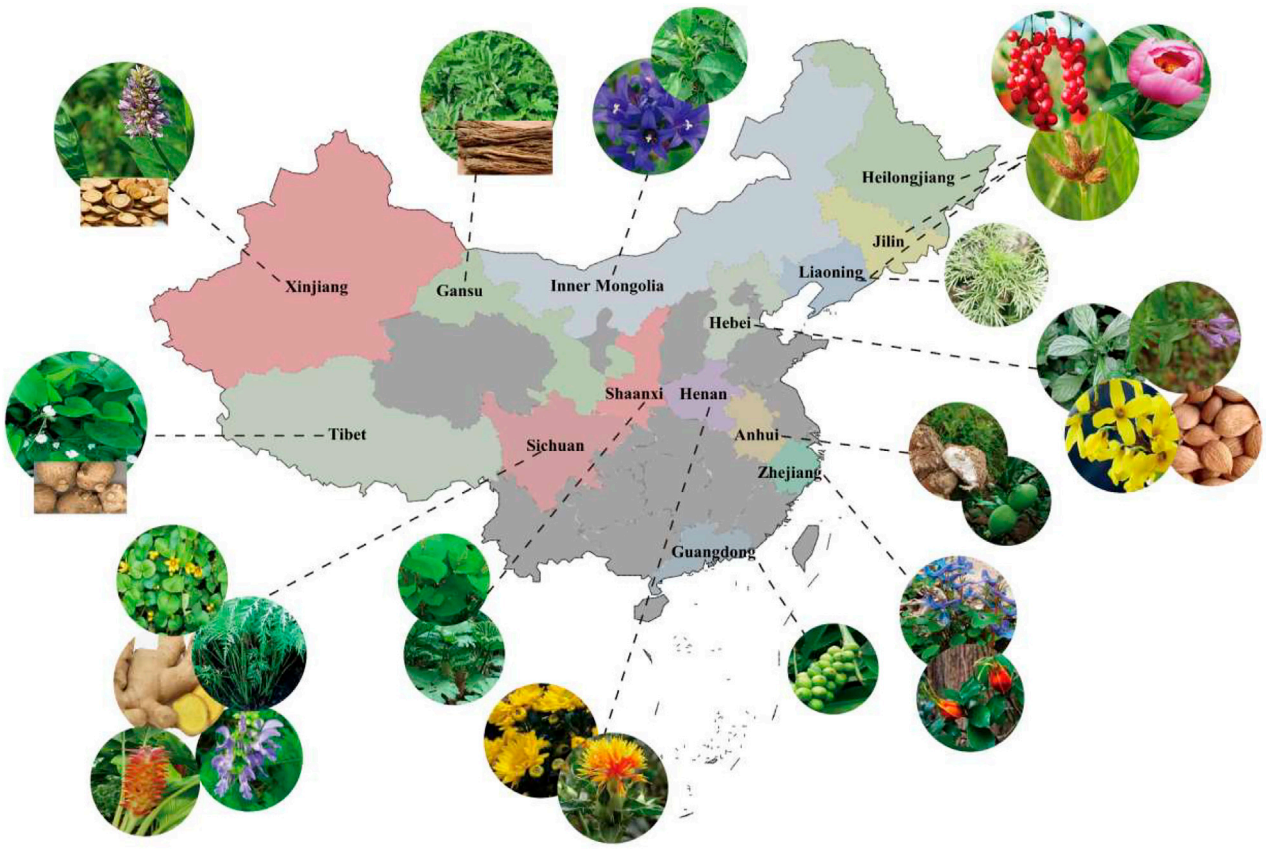

FIGURE 2 | Distribution of some Chinese medicine for liver diseases in main producing areas (also named "Daodi" producing area). Shaanxi: *Rheum palmatum* L., *Polygonum cuspidatum* Sieb.et Zucc.; Sichuan: *Salvia miltiorrhiza* Bunge., *Zingiber officinale* Rosc., *Ligusticum chuanxiong* Hort., *Curcuma wenyujin* Y. H. Chen et C. Ling, *Lysimachia christinae* Hance; Gansu: *Angelica sinensis* (Oliv.) Diels; Tibet: *Alisma orientalis* (Sam.) Juzep.; Hebei: *Prunus persica* (L.) Batsch, *Forsythia suspensa* (Thunb.) Vahl, *Isatis indigotica* Fort., *Scutellaria baicalensis* Georgi; Henan: *Carthamus tinctorius* L., *Chrysanthemum morifolium* Ramat.; Zhejiang: *Gardenia jasminoides* Ellis, *Corydalis yanhusuo* W. T. Wang; Liaoning: *Artemisia scoparia* Waldst. et Kit.; Guangdong: *Alpinia oxyphylla* Miq.; Anhui: *Chaenomeles speciosa* (Sweet) Nakai, *Poria cocos* (Schw.) Wolf; Xinjiang: *Glycyrrhiza uralensis* Fisch.; Inner Mongolia: *Gentiana scabra* Bunge, *Isatis indigotica* Fort.; Dongbei (Heilongjiang, Jilin, Liaoning): *Schisandra chinensis* (Turcz.) Baill., *Paeonia lactiflora* Pall., *Sparganium stoloniferum* Buch-Ham.

TABLE 1 | Some of the Chinese medicine used for the treatment of liver diseases are described in the standard and their biological activities.

No	Latin name	English name	Family	Used part	Types of liver diseases that can be treated recorded in the standard	Reported biological activities associated with liver diseases
1	*Rheum palmatum* L *Rheum offcinale* Baill *Rheum tan*guticum Maxim.ex Balf	Rhei Radix et Rhizoma	Polygonaceae	Root and rhizome	Damp-heat jaundice[a]; Acute infectious hepatitis[b]	Regulating gut microbiota Neyrinck et al. (2017), protective effect on high fat diet-induced hepatosteatosis, α-naphthylisothiocyanate induced liver injury and diethylnitrosamine (DENA)-induced hepatocellular carcinoma El-Saied et al. (2018); Yang et al. (2012); Yang et al. (2016a), anti-hepatic fibrosis Jin et al. (2005)
2	*Angelica sinensis* (Oliv.) Diels	Radix Angelicae Sinensis	Apiaceae	Root	Blood deficiency and chlorosis[a]; Syndrome of blood deficiency[c]	Anti-inflammatory, anti-oxidative stress Mo et al. (2018)
3	*Silybum marianum* (L.) Gaertn	Herba Silybi	Asteraceae	Whole grass and achene	Fruit and extract for liver disease and jaundice[d]; Fatty liver, chronic hepatitis, cirrhosis[c]; Acute or chronic hepatitis, liver cirrhosis, fatty liver, metabolic toxic liver injury[b]	Protective effect on liver injury caused by cholestasis Alaca et al. (2017), protective effect against hepatotoxicity caused by deltamethrin Jindal et al. (2019), anti-oxidative stress Egresi et al. (2020); Zhu.et al. (2018a), regulating lipid metabolism Feng et al. (2019)
4	*Artemisia scoparia* Waldst. et Kit *Artemisia capillaris* Thunb	Herba Artemisiae Scopariae	Asteraceae	Aboveground part	Infectious icteric hepatitis[a,d]	Anti-hepatocellular carcinoma Jang et al. (2017); Jung et al. (2018); Kim et al. (2018); Yan et al. (2018)
5	*Gentiana scabra* Bunge	Gentianae Radix et Rhizoma	Gentianaceae	Root and rhizome	Liver channel is hot and jaundice[d]; Damp-heat jaundice, head distension and headache caused by liver and gallbladder excess fire[c]	Anti-hepatic fibrosis Qu et al. (2015), protective effect on liver injury caused by B19-NS1 Sheu et al. (2017)
6	*Bupleurum chinense* DC.	Radix Bupleuri	Apiaceae	Root	Chest pain, irregular menstruation[a,c,d]	Protective effect on liver injury caused by acetaminophen and D-galactosamine/lipopolysaccharide Wang et al. (2019a); Zou et al. (2018), anti-oxidative, anti-inflammatory Jia et al. (2019), enhancing immune function Zou et al. (2019)
7	*Polygonum cuspidatum* Sieb. et Zucc	Rhizoma Polygoni Cuspidati	Polygonaceae	Root and rhizome	Damp-heat jaundice, amenorrhea in women[a,c,d]	regulating lipid metabolism, anti-oxidative stress, alleviating insulin resistance Kim. et al. (2020a); Zhao. et al. (2019a)
8	*Atractylodes macrocephala* Koidz	Rhizoma Atractylodis Macrocephalae	Asteraceae	Rhizome	Jaundice[d]	Anti-acute liver injury Han et al. (2016)
9	*Scutellaria baicalensis* Georgi	Radix Scutellariae	Labiatae	Root	Jaundice[a]; Headache due to liver fire, swelling and pain due to red eyes, damp-heat jaundice[c]	Relieving endoplasmic reticulum stress Dong et al. (2016), anti-hepatocellular carcinoma Wang. et al. (2020a), anti-oxidative stress, anti-inflammatory Park et al. (2017), anti-hepatic fibrosis Pan et al. (2015a)
10	*Curcuma longa* L	Rhizoma Curcumae Longae	Zingiberaceae	Rhizome	Amenorrhea of women[a]; Women with blood stasis and amenorrhea[d]; Women have dysmenorrhea and amenorrhea[c]	Relieving endoplasmic reticulum stress Kim et al. (2017a), anti-oxidative stress, anti-inflammatory, protective effect on liver injury caused by CCl_4, ethanol and methotrexate Lee. et al. (2017a); Moghadam et al. (2015); Uchio et al. (2017)
11	*Ligusticum chuanxiong* Hort	Rhizoma Chuanxiong	Apiaceae	Rhizome	Irregular menstruation, dysmenorrhea, chest pain[b,c,d]	Anti-hepatocellular carcinoma (Hu et al. 2015), protective effect against D-galactose-induced liver and kidney injury (Mo et al. 2017)

(Continued on following page)

TABLE 1 | (*Continued*) Some of the Chinese medicine used for the treatment of liver diseases are described in the standard and their biological activities.

No	Latin name	English name	Family	Used part	Types of liver diseases that can be treated recorded in the standard	Reported biological activities associated with liver diseases
12	*Glycyrrhiza uralensis* Fisch *Glycyrrhiza inflata* Bat *Glycyrrhiza glabra* L	Radix Glycyrrhizae	Leguminosae	Root	Hepatitis[b]	Hepatoprotective activities against CCl4/alcohol -induced liver injury Jung et al. (2016); Lin et al. (2017), anti-oxidative stress Cao et al. (2017)
13	*Prunus persica* (L.) Batsch *Prunus davidiana* (Carr.) Franch	Semen Persicae	Rosaceae	Mature seed	Amenorrhea, dysmenorrhea[a,c,d]	Anti-hepatocellular carcinoma Shen et al. (2017), protective effect on liver injury caused by CCl_4 Rehman et al. (2021), anti-oxidative stress, anti-inflammatory Kim. et al. (2017b); Lee et al. (2008)
14	*Sophora flavescens* Ait	Radix Sophorae Flavescentis	Leguminosae	Root	Jaundice[a,c,d]	Anti-hepatitis B virus Yang et al. (2018)
15	*Sophora tonkinensis* Gapnep	Radix Sophorae Tonkinensis	Leguminosae	Root and rhizome	Jaundice[b,d]	regulating lipid metabolism, anti-oxidative stress, anti-inflammatory Zhao et al. (2020)
16	*Salvia miltiorrhiza* Bunge	Radix Salviae Miltiorrhizae	Labiatae	Root and rhizome	Irregular menstruation, amenorrhea and dysmenorrhea[b,c,d]; Hepatosplenomegaly[b]	Protective effect on liver injury caused by paracetamol and lipopolysaccharide Gao et al. (2015); Zhou et al. (2015), anti-hepatocellular carcinoma Jiang et al. (2017b), anti-hepatic fibrosis Peng et al. (2018)
17	*Aloe barbadensis* Miller *Aloe ferox* Miller	Aloe	Liliaceae	The liquid concentrate of plant leaves	Liver heat[a]; Liver fire, headache, red eyes, convulsion[c]; Liver meridian excess heat, dizziness, headache, tinnitus, irritability, constipation[b]	Hepatoprotective effect against cartap- and malathion induced toxicityGupta et al. (2019), anti-inflammatory and anti-oxidant Klaikeaw et al. (2020)
18	*Coptis chinensis* Franch *Coptis deltoidea* C. Y. Cheng et Hsiao *Coptis teeta* Wall	Rhizoma Coptidis	Ranunculaceae	Rhizome	Liver fire, red eyes, jaundice, disharmony between liver and stomach[a]; Liver fire, red eyes, swelling and pain[c]	Anti-hepatocellular carcinoma Auyeung and Ko. (2009); Lin et al. (2004); Ma et al. (2018a), anti-hepatitis C virus Hung et al. (2018), protective effect on liver injury caused by CCl_4 Ma. et al. (2018b)
19	*Paeonia lactiflora* Pall	Radix Paeoniae Alba	Ranunculaceae	Root	Hypochondriac pain, blood deficiency and chlorosis, Irregular menstruation[a]; Chest and abdomen rib pain, irregular menstruation[b,d]	Improving liver function, anti-inflammatory and anti-oxidant Wang. et al. (2020b)
20	*Paeonia lactiflora* Pall *Paeonia veitchii* Lynch	Radix Paeoniae Rubra	Ranunculaceae	Root	Eye red swelling and pain, liver depression, hypochondriac pain, amenorrhea and dysmenorrhea[a,c]	Protective effect on liver injury caused by cholestasis Ma et al. (2018a); Ma et al. (2015)
21	*Isatis indigotica* Fort	Folium Isatidis	Brassicaceae	leaf	Jaundice[a,c]; Jaundice, acute infectious hepatitis[d]; Acute hepatitis[b]	Enhancing the endogenous antioxidant system Ding and Zhu (2020)
22	*Isatis indigotica* Fort	Radix Isatidis	Brassicaceae	Root	Acute and chronic hepatitis[d]; Hepatitis[c]	Alleviating insulin resistance Li et al. (2019b)
23	*Lycium barbarum* L	Fructus Lycii	Solanaceae	fruit	The eyes are not clear[a]; Yin deficiency of liver and kidney, dizziness[c,d]	Protective effect against paracetamol-induced acute hepatotoxicity Gündüz et al. (2015), anti-hepatocellular carcinoma Ceccarini et al. (2016), Regulating the immune system Tan et al. (2019)

[a]*Cited from "Chinese Pharmacopoeia."*
[b]*Cited from "Zhong Yao Da Ci Dian".*
[c]*Cited from "Zhong Hua Ben Cao".*
[d]*Cited from "Quan Guo Zhong Cao Yao Hui Bian".*
(Note: doctor of traditional Chinese medicine holds that the liver stores blood and the liver is a sea of blood).

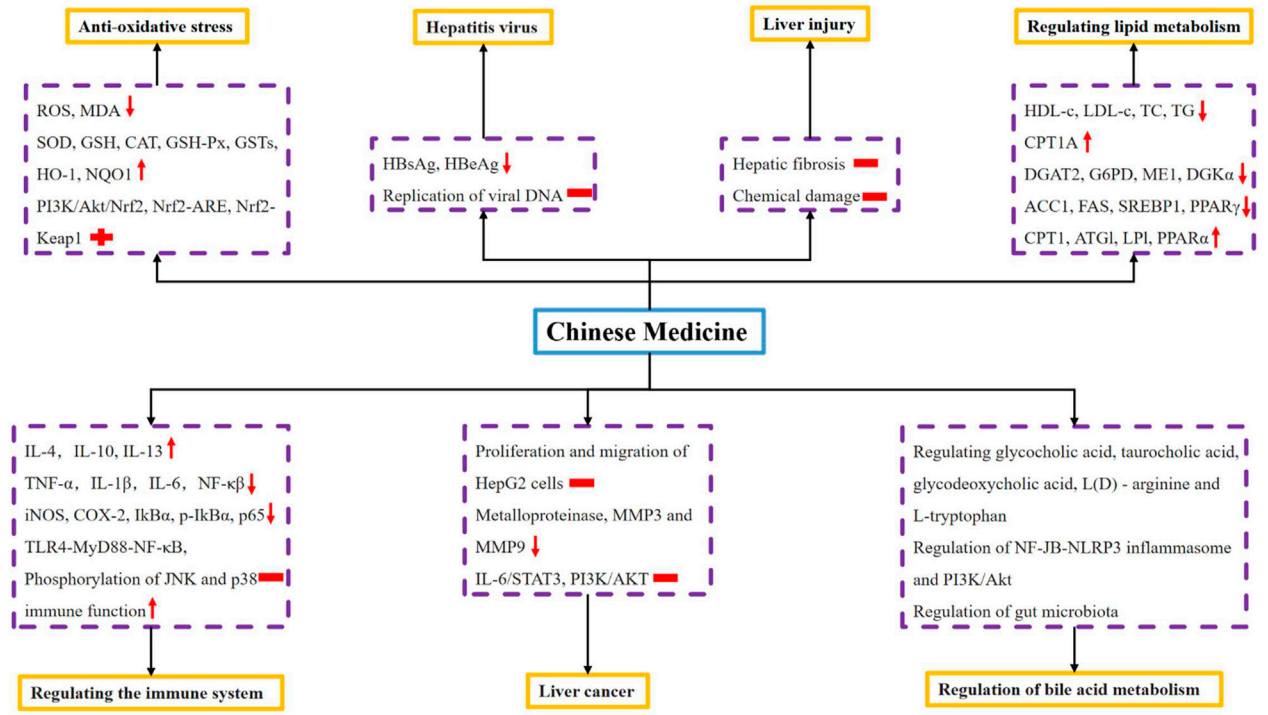

FIGURE 3 | Pharmacological effects of Chinese medicine on liver diseases.

M. et al., 2016). In addition, *Sophorae Tonkinensis* water extract and *Polygonum Multiflorum* Thunb. extract alleviate nonalcoholic liver disease by enhancing hepatic carnitine palmitoyltransferase 1A activity to promote fatty acids β-oxidation, and regulating the protein response to lipid metabolism and expression in the liver to reduce lipid accumulation (Jung et al., 2020; Zhao et al., 2020).

It is worth mentioning that relevant studies of hepatic lipid metabolism were also conducted in fish. Addition of 200–400 mg/kg *Radix Bupleuri* extract to the daily diet of hybrid grouper fish can reduce the expression of lipogenesis-related genes, such as diacylgycerol acyltransferase 2, glucose-6-phosphate dehydrogenase, malic enzyme 1 and diacylglycerol kinase alpha (Zou et al., 2019). Lonicera japonica extract can effectively reduce the levels of LDL-C, triglyceride (TG) and total cholesterol (TC) in the serum of grass carp as well as the expression of lipogenic genes acc1, fas, SREBP1 and PPARγ, and increase the expression of liposoluble genes CPT1, ATGL, LPL and PPARα (Meng et al., 2019).

Liver Injury

Liver Fibrosis

Liver fibrosis belongs to chronic liver injury, mainly manifested as the accumulation of extracellular matrix (Tsuchida and Friedman, 2017), which is a dynamic process. Hepatocytes, activated hepatic stellate cells, endothelial cells, immune cells, and macrophages all participate in its establishment and regression (Campana and Iredale, 2017). Liver fibrosis is a pathological insult mainly caused by chronic liver disease (viral infection, alcoholic liver disease, NASH, etc). If not treated in time, it will continue to deteriorate and eventually progress to cirrhosis and even liver cancer.

The TGF-β/Smads pathway plays an important role in the regulation of liver fibrosis. In the background of liver fibrosis, Smad3 and Smad4 are pro-fibrosis, while Smad2 and Smad7 are anti-fibrosis (Xu et al., 2016). Meanwhile, TGF-β is also activated by the deposits in the fibrous extracellular matrix, and expressed and released from a variety of cells (Dewidar et al., 2019). The evidence has shown that *Forsythiae Fructuse* water extract (FSE), *Curcuma Wenyujin*, and *Zingiber Officinale* can effectively inhibit the development of liver fibrosis through the TGF-β/Smads signaling pathway (Hasan et al., 2016; Hu et al., 2020a; Xie et al., 2020).

Radix Salvia Miltiorrhiza (RSM) is the dry root and rhizome of Labiatae plant *Salvia Miltiorrhiza* Bunge, whose main functions include removing blood stasis, relieving pain, activating blood circulation, clearing the heart, and removing trouble (Commission, 2015). It is widely used in the treatment of liver fibrosis in clinic, but the specific mechanisms are not clear. The recent study of Yuan et al. showed that RSM improved liver fibrosis by increasing the activity of natural killer (NK) cells as well as the effects of NKG2D and NKp46 on NK cells, and inhibiting the activation of HSCs *in vivo* and *in vitro* (Peng et al., 2018). Another study showed that the mixture of RSM extract

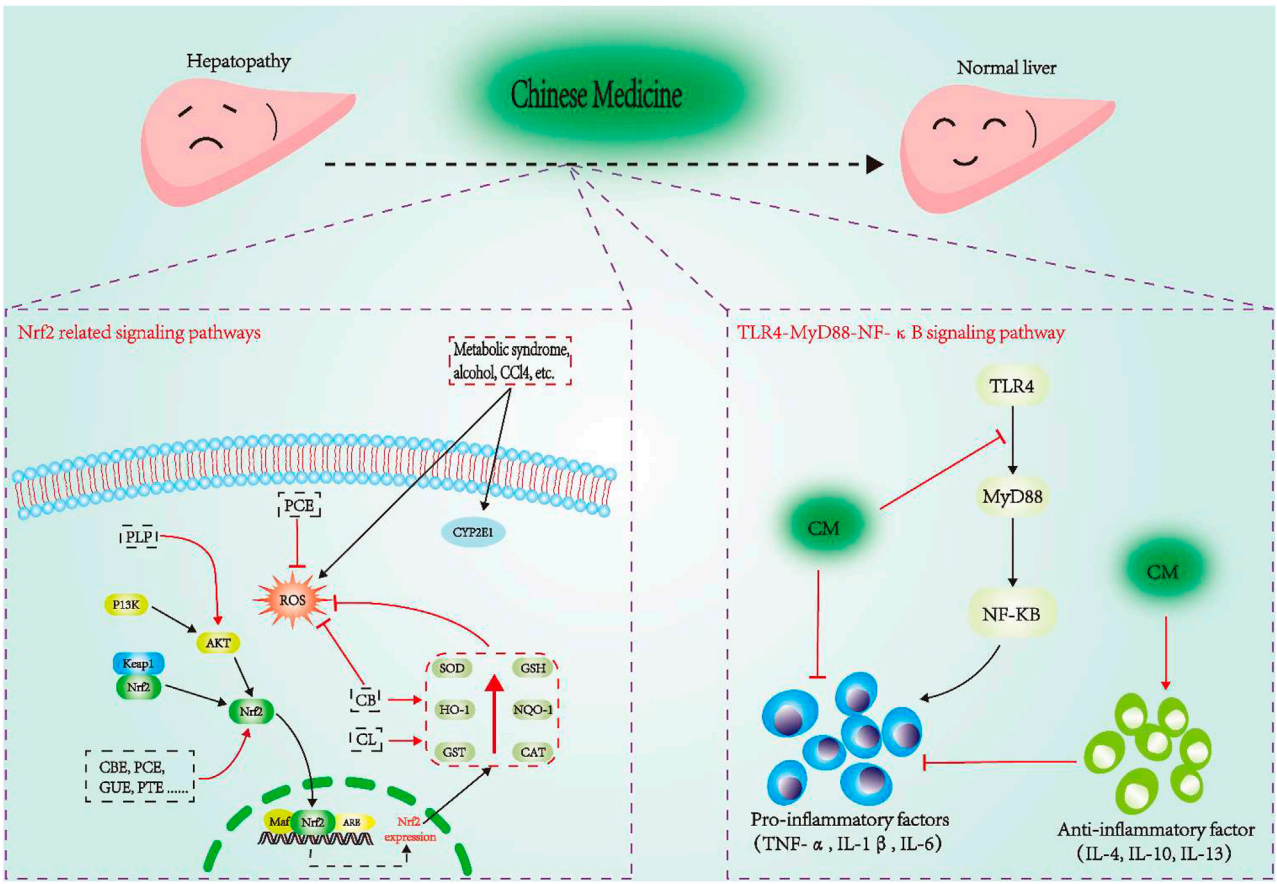

FIGURE 4 | Some CM treat liver disease through Nrf2 and TLR4-MyD88-NF-κB signaling pathway. CBE, Citrus reticulata Blanco peel extract; GUE, Glycyrrhiza uralensis ethanol extract; PTE, Polygonum multiflorum Thunb. ethanolic extract; PLP, Paeonia lactiflflora Pall.; CL, Curcuma longa; CB, Calculus bovis; PCE, Polygonum cuspidatum extract.

and *Astragalus Membranaceus* extract at a ratio of 1:1 could regulate the expression of TGF-β1 and Cyclin D1 to improve liver fibrosis and the liver functions, especially having a good effect on reducing the cyclin D1 expression (Cao et al., 2020). In addition, many CM have anti-fibrosis activities. For example, *Gentiana Scabra* bage inhibits fibrosis by reducing the expression of hepatic type I and type III collagen proteins in rats (Qu et al., 2015). *Ginkgo biloba* is also a common CM mainly used in coronary heart disease, angina pectoris, and hyperlipidemia (Commission, 2015). Wang et al. found that *Ginkgo biloba* extract could improve liver fibrosis by inhibiting inflammation, HSC activation, and hepatocyte apoptosis, which may be related to the p38MAPK, NF-κB/IκBα, and Bcl-2/Bax signaling pathway (Wang et al., 2015).

Chemical Liver Injury

Chemical liver injury is mainly caused by alcohol, toxic chemicals, and drugs. As we all know, the liver has dual blood supply of hepatic artery and hepatic vein, which is the main detoxification organ of human body. The liver plays a core role in biotransformation and excretion of foreign compounds, so it is the main target of the adverse reactions of drugs and other heterologous organisms (Holt and Ju, 2010). Secondly, the liver is the initial contact site of alcohol, chemical toxic substances, and the oral drugs absorbed through the intestine, so it is vulnerable to chemical damage. At the same time, electrophilic compounds and free radicals are the intermediate products of many chemical substances after liver metabolism. These substances may change the structure and function of cell macromolecules, and even lead to the occurrence of liver cancer (Gu and Manautou, 2012).

At present, a variety of CM are widely used for chemical injuries. Both *Schisandra Sphenanthera* extract and *Polygonatum Sibiricum* water extract can regulate alcoholic liver injury in mice through the nuclear factor-erythroid 2-related factor 2 (Nrf2)-antioxidant responsive element (ARE) signaling pathway (Wang, G. et al., 2021; Zeng et al., 2017). The liver damage caused by CCl4 can be alleviated by *Curcuma longa* L. extract and *Prunus persica* Seeds Extract, which is mainly related to inhibiting liver oxidative stress, and increasing the Nrf2 and NQO-1 levels, as well as reducing type III collagen mRNA expression (Lee, G.-H. et al., 2017; Rehman et al., 2021). In addition, *Hedyotis Diffusa* water extract, *Ligusticum Chuanxiong* Hort, and *Panax ginseng* can also be used to respectively relieve the chemical damage caused by

hydrogen peroxide and D-galactose (Gao et al., 2016; Mo et al., 2017). It is worth mentioning that a large number of CM can also alleviate drug-induced liver injuries. Paracetamol (acetaminophen) is a commonly used drug in clinic, which is mainly used for cold-induced fever, headache, joint pain, neuralgia, migraine, dysmenorrhea, and so on. *Lycium Barbarum* extract can significantly improve paracetamol-induced apoptosis to protect the liver from chemical damage (Gündüz et al., 2015), and *Isatidis Folium* can enhance the endogenous antioxidant system and reduce paracetamol-induced liver damage in mice (Ding and Zhu, 2020). Ahmed et al. also found that *Panax ginseng* could be used as a hepatoprotective agent, which prevented cyclophosphamide (with immunosuppressive and anti-cancer potential)-induced liver injury by reducing the expression of TNF-α, IL-1β and Caspase3 genes, as well as increasing the BCL-2 gene expression, and its liver-protective effect is better than vitamin E (Abdelfattah-Hassan et al., 2019).

Anti-oxidative Stress

Oxidative stress is the main influencing factor of the pathogenesis of ALD and MAFLD. It has been briefly discussed in the previous content. When the level or activity of antioxidants in the human body is reduced, oxidative stress will occur. Due to the stimulation of external factors (such as alcohol), the body will produce a large amount of active oxygen, which is the key to the development of fatty liver into steatohepatitis. GSH is an endogenous antioxidant, which is widely present in animals. Excessive oxidative stress can cause GSH consumption and lead to the accumulation of ROS (Li, X. et al., 2019). In addition, cytochrome P4502E1 (CYP2E1) plays a key role in the generation of ROS, which is also induced by alcohol (Leung and Nieto, 2013). *Calculus bovis* is a commonly used CM for fever, faintness, stroke and phlegm. The evidence showed that *calculus bovis* could inhibit oxidative stress in hepatocytes by reducing ROS and increasing SOD content, thereby achieving the liver-protective effect on mice with nonalcoholic fatty liver. And *curcuma longa* hot water extract and *zingiber officinale* hydroalcoholic extract can reduce the level of GSH to protect the liver.

Nrf2 is an important redox-sensitive transcription factor, and controls the basic and induced expression of a series of antioxidant response element-dependent genes, which is beneficial to improve the body's oxidative stress state, thus regulating the physiological and pathological consequences under oxidant exposure (Ma, 2013). Under normal physiological conditions, Nrf2 is locked in the cytoplasm by Keap1. But when the cells are attacked by ROS or electrophiles, Nrf2 will dissociate from Keap1 and quickly translocate into the nucleus, first forming a heterodimer with the small Maf protein, and then combining with the ARE, which finally transcribes and activates the expression of the antioxidant enzyme genes regulated by Nrf2 (Ho et al., 2012; Heiss et al., 2013). In addition, the signal pathways related to Nrf2 (such as Nrf2-Keap1 and Nrf2-ARE) in the oxidative stress system have been widely recognized, especially the Nrf2-Keap1 pathway, which is an anti-stress mechanism inherited from our ancestors, as well as a defense system to maintain the homeostasis of the cells (Buendia et al., 2016; Bellezza et al., 2018). As reported, *Polygonum Cuspidatum* extract could reduce oxidative stress by targeting the Keap1/Nrf2 pathway, and down-regulate the levels of sterol regulatory element bending protein 1, fatty acid synthase, and stearoyl coenzyme alpha desaturase-1 to prevent hepatic lipid accumulation in fructose-fed rats (Zhao, X.-J. et al., 2019). *Paeonia Lactiflora* Pall. (PLP) can increase the expression of AKt, Nrf2, HO-1, NQO1 and GCLC, and activate the PI3K/Akt/Nrf2 pathway to enhance the antioxidant system, thereby reducing ANIT-induced liver tissue damage (Ma et al., 2015). In addition, *Citrus Reticulata* Blanco peel extract, Glycyrrhiza Uralensis ethanol extract, and *Polygonum Multiflorum* Thunb. ethanolic extract can directly activate the Nrf2 to regulate the redox state of liver injury (Cao et al., 2017; Ke et al., 2020; Lin, E.-Y. et al., 2018). The details are showed in **Figure 4**.

REGULATION OF BILE ACID METABOLISM

Bile acids (BAs) are important components of bile, which have the functions of regulating metabolism, endocrine and immune (Chávez-Talavera et al., 2017). The liver is the site of bile acid synthesis. The primary bile acids, such as cholic acid and chenodeoxycholic acid, combine with glycine or taurine to form bound BAs, which are secreted into bile canaliculus through the transport proteins such as bile salt export pump and multidrug resistance associated protein 2, and are temporarily stored in the gallbladder and released through the bile duct. When BAs and other components of bile are discharged into the intestine together, they can promote the emulsification and absorption of dietary fat, cholesterol, and fat-soluble vitamins. About 90–95% of BAs are reabsorbed in the ileum through apical sodium-dependent bile acid transporter and ileal bile acid transporter (IBAT), and the remaining 5–10% of BAs are excreted in feces (Li and Chiang, 2014; Tripathi et al., 2018). BAs are the important physiological basis involved in the regulation of liver function and disease states. According to the data, the metabolism and inflammation related to obesity, type 2 diabetes, dyslipidemia, and MAFLD are all regulated by BAs (Chávez-Talavera et al., 2017). Therefore, BAs' normal synthesis, transportation and excretion are vital factors for the homeostasis.

Cholestasis means that the bile cannot flow from the liver to the duodenum, and its flow is decreased, which is characterized by the excessive accumulation of bile acids and other toxic compounds (Crocenzi et al., 2012). Excessive accumulation of bile acids in the liver may cause liver damage, liver fibrosis, and eventually liver failure and biliary cirrhosis (Padda et al., 2011). The study has shown that PLP can regulate glycocholic acid, taurocholic acid, glycodeoxycholic acid, L (D)-arginine, and L-tryptophan, and these metabolites are related to bile acid secretion and amino acid metabolism, which is concluded that bile acid metabolism may be involved in the therapeutic effects of PLP on cholestasis (Ma et al., 2016). Ma et al. further demonstrated that PLP could alleviate cholestasis by regulating the NF-κB-NLRP3 inflammasome and the PI3K/Akt-dependent

pathways (Ma, X. et al., 2018; Ma et al., 2015). Another study showed that the ethanol extract of *Schisandra Chinensis* could significantly protect the mice from intrahepatic cholestasis induced by cholic acid (Zeng et al., 2016). In addition, *Schisandra Chinensis* extract can also enhance the excretion of bile acids from the serum and liver to the intestine and feces, and adjust the intestinal microorganisms disturbed by the external factors to achieve the protective effects on liver injury caused by cholestasis (Li, D.-S. et al., 2020).

REGULATING THE IMMUNE SYSTEM

Inhibition of Inflammatory Response

Inflammation is the basis of a variety of physiological and pathological processes, mainly induced by infection and tissue damage (Medzhitov, 2008). When natural antioxidants are out of balance, the free radicals produced by different organisms and environments can further lead to various inflammation-related diseases (Arulselvan et al., 2016). As we all know, there are many kinds of cytokines involved in the inflammatory response. For example, TNF-α, IL-1β, and IL-6 play a pro-inflammatory role, by contrary, TGF-β, IL-4, IL-10, and IL-13 can inhibit the occurrence and progress of inflammation. There is evidence that the inflammatory mechanisms of the liver are essential for maintaining the homeostasis of the tissues and organs. When the inflammatory mechanisms are out of balance, the hepatic pathological process will be drived, such as chronic infection, autoimmunity, and malignant tumor (Robinson et al., 2016). FSE, *Gentianae Macrophyllae* extract, and *Aloe vera* can reduce inflammatory liver injury by reducing the serum concentration of TNF-α, IL-1β, IL-6, NF-κB, and other cytokines (Zhao et al., 2017; Cui et al., 2019; Hu et al., 2020a; Klaikeaw et al., 2020). Moreover, *Radix Bupleuri* extract and *Schisandra Sphenanthera* extract can directly inhibit the mRNA expression of TNF-α, IL-1β, and IL-6 to protect the liver (Chen et al., 2019; Jia et al., 2019). In addition, *Angelica Sinensis* Supercritical Fluid CO2 Extract can significantly inhibit D-galactose-mediated expression of inflammatory cytokines, such as iNOS, COX-2, IKBα, *p*-IκBα, and p65, protecting the liver and kidney tissues (Mo et al., 2018).

Toll-like receptor4 (TLR4)-myeloid differentiation factor 88 (MyD88)-NF-κB signaling pathway is a key pathway in the physiologic and biochemical reactions of diseases. It widely exists in various tissues and cells, which is one of the important signaling pathways that mediate the expression of inflammatory factors (Wu et al., 2017). As one of the important pathways associated with inflammatory response and hepatic fibrosis, its activation can lead to the release of downstream inflammatory factors and induce the production of TNF-α, IL-1β, and IL-6. Hu et al. found that FSE could improve the inflammatory state of liver fibrosis through the TLR4-MyD88-NF-κB pathway (Hu et al., 2020a). Jia et al. found that RBE could inhibit TLR4-MyD88-NF-κB signaling pathway to reduce H_2O_2-induced liver inflammation in tilapia (Jia et al., 2019). Another study showed that GME could also attenuate ALD by inhibiting the phosphorylation of JNK and p38 to inhibit the initiation of inflammation (Cui et al., 2019).

The molecular mechanisms of the CM alleviating liver diseases through inflammatory pathways are shown in **Figure 4**.

Enhancing Immune Function

Zou et al. found that adding 200–800 mg/kg RBE to the diet of hybrid grouper could effectively reduce the serum ALP, ALT, AST, and LDH contents. In addition, it could down-regulate the expression of apoptosis-related genes (caspase-9), and up-regulate the antioxidant genes (CAT) and immune-related genes (MHC2, IKKα, and TGF-β1) (Zou et al., 2019). Tan et al. reported that dietary supplementation of *Lycium barbarum* extract (0.50–2.00 g/kg) could effectively increase IL-10 and TGF-β1 mRNA levels in the liver of HFD-fed hybrid grouper (Tan et al., 2019). In addition, *Ginkgo biloba* extract not only improves the hepatic antioxidant status of HFD-fed hybrid grouper, and maintains normal liver histology and preserves liver function, but also up-regulates the expression of immune-related genes (MHC2 and TLR3) (Tan et al., 2018).

Hepatitis Virus

Some CM have inhibitory effects on hepatitis virus and can assist the treatment of patients with viral hepatitis. Some studies have shown that most of the terpenoids isolated from *Flos Lonicerae* can inhibit the secretion of HBsAg and HBeAg, as well as the DNA replication of HBV (Ge et al., 2019). In addition, Yang et al. found that the methanolic extract of *Rhizoma Coptidis* could block the attachment of HCV and the entry/fusion with host cells, which effectively inhibited the infection of pseudoparticles of HCV in Huh-7.5 cells, and hindered the infection of several HCV genotypes (Hung et al., 2018).

Liver Cancer

Currently, Western medicine and therapies are the main treatment strategies for liver cancer, but the overall prognosis of liver cancer patients is still very poor. Under such circumstances, it is extremely urgent to find a better method for the treatment of liver cancer. CM contains abundant treatment resources and has been used for the prevention of liver cancer for thousands of years. In modern China, CM has also been proven to be an effective method for the treatment of liver cancer. However, the theory of CM prevention and treatment of liver cancer is more widely accepted in China than abroad (Liao et al., 2020). According to relevant data, most CM can show anti-liver cancer effects. Ethanol extract of root of *Prunus Persica* can significantly inhibit the migration of liver cancer HepG2 cells and the expression of extracellular matrix metalloproteinases, MMP3 and MMP9. It is worth mentioning that it can also inhibit tumor growth in nude mice *in vivo* (Shen et al., 2017). *Artemisia capillaris* extract can inhibit the growth, migration and invasion of Huh7 and HepG2 liver cancer cells. This inhibitory effect is closely related to blocking the PI3K/AKT signaling pathway (Yan, Honghua et al., 2018). Jiang et al. further found that the anti-liver cancer effect of *Artemisia capillaris* extract is also related to the inhibition of the IL-6/STAT3 signal axis (Jang et al., 2017). Futhermore, Zheng et al. found

TABLE 2 | Summary of polysaccharides and glycosides with significant anti-liver disease activity.

Compounds	Source	The species investigated	Dose	Mechanisms	References
Polysaccharides					
PRAM2	*Rhizoma Atractylodis Macrocephalae*	Male ICR mice	50, 100, 200 mg/kg	Inhibition of NOS activity and NO level and its reduction of the production of free radicals	Han et al. (2016)
Radix isatidis polysaccharide	*Radix isatidis*	3T3-L1 preadipocytes	25, 50, 100 μg/ml	Improvement of the glucose metabolism, lipid metabolism and oxidative stress	Li, et al. (2019c)
		Male Wistar rats	25, 50, 100 mg/kg		
Salvia miltiorrhiza polysaccharide	*Salvia miltiorrhiza*	Chickens	0.5, 1, 2 g/L	Down-regulation of the contents of ALT, AST, and MDA, and up-regulation of the contents of GSH and CYP450	Han et al. (2019)
		Chicken hepatocytes	100, 200, 500 μg/ml		
Angelica sinensis polysaccharide	*Angelica sinensis*	L02 cells	200, 400, 800 μg/ml	Through regulating lipid metabolism, anti-inflammation, anti-oxidation and inhibiting HSC activation	Ma et al. (2020); Wang et al. (2016); Wang. et al. (2020c)
		ICR male mice	100, 300, 500 mg/kg		
		Male Balb/c mice	1.5, 6 mg/kg		
		Murine splenocytes	5, 25,125 μg/ml		
		Male C57BL/6J mice	200 mg/kg		
		Primary splenocytes	50, 100, 200 μg/ml		
Codonopsis pilosula polysaccharide	*Codonopsis pilosula*	Female ICR mice	100, 150, 200 mg/kg	Through antioxidant effect	Liu et al. (2015)
Poria cocos polysaccharide	*Poria cocos*	Male Kunming mice	200, 400 mg/kg	By suppressing cell death, reducing hepatocellular inflammatory stress and apoptosis, and Hsp90 bioactivity	Wu et al. (2018c); Wu. et al. (2019b)
		AML12 cells	20, 40 g/L		
Lycium barbarum polysaccharide	*Lycium barbarum*	L02 cells	24 μg/ml	By reversing oxidative injury, inflammatory response and TLRs/NF-κB signaling pathway expression	Gan. et al. (2018b); Wei et al. (2020)
		Male wistar rats	400, 800, 1600 mg/kg		
Astragalus membranaceus-Polysaccharide	*Astragalus membranaceus*	HFSTZ Mice	500 mg/kg	Through improving peripheral metabolic stress, activating hepatic insulin signaling	Huang et al. (2016); Huang et al. (2017); Sun et al. (2019)
		C57BL/6 mice	800 mg/kg		
		HCC cells	0.1, 0.5, 1 mg/ml		
SFP-100	*Sophora flavescens*	Female Balb/c mice	500 mg/kg	By decreasing hepatocytes apoptosis, inhibit the infiltration of neutrophils and macrophages into liver	Yang et al., (2018)
		L02 cells	10, 50, 250 μg/ml		
		HepG2.2.15 cells	50, 100, 250, 500 μg/ml		
Codonopsis lanceolata polysaccharide	*Codonopsis lanceolata*	Male C57BL/6 mice	100 mg/kg	Through activating anti-oxidative signaling pathway	Zhang, et al. (2020a)
STRP	*Sophora tonkinensis*	Male ICR mice	50, 100, 200 mg/kg	By inhibiting MDA, ROS generation and increasing liver GSH, GPx, T-SOD, CAT levels	Cai et al. (2018); Shan et al. (2019)
Schisandra chinensis Polysaccharide	*Schisandra chinensis*	Mice	200, 400, 800 mg/kg	Regulation of Nrf2/antioxidant response element and TLR4/NF-κB signaling pathways	Shan et al. (2019)
Schisandra chinensis acidic polysaccharide	*Schisandra chinensis*	Male ICR mice	5, 10, 20 mg/kg	By inhibiting the expression of CYP2E1 protein and then alleviating oxidative stress injury	Yuan et al. (2018)
		HepG2 cells	3.12, 6.25, 12.5 μg/ml		
GBLP	*Ginkgo biloba*	Male Wistar rats	100, 200, 400 mg/kg	By attenuating IR, preserving liver function, enhancing antioxidant defense system, and reducing lipid peroxidation	Yan et al. (2015)
Paeoniae radix alba polysaccharides	*Paeoniae radix alba*	Male Kunming mice	0.2, 0.4, 0.8 g/kg	Inhibition of the NF-κB signaling pathway	Wang et al. (2020b)
Glycosides					
Chrysophanol 8-O-glucoside	*Rheum palmatum*	LX-2 cells	1, 5, 20 μg/ml	Regulation of the STAT3 signaling pathway	Park et al. (2020)
Sennoside A	*Rheum officinale Baill*	HepG2 cells	25, 50, 100 μM	Down-regulation of KRT7 and KRT81, and inhibition of the AKT and ERK pathways	Le et al. (2020); Zhu et al. (2020)
		SMMC-7721 cells	25, 50, 100 μM		
		Male C57BL/6J mice	15, 30, 60 mg/kg		
		HSC-T6 cells	10 μM		
Astragaloside IV	*Astragalus membranaceus*	SMMC-7721 cells	80 μg/ml	Inhibition of lncRNA-ATB, MRP2, PTP1B and anti-apoptotic signaling, and improvement insulin resistance	Li et al. (2018g); Qu et al. (2020); Su et al. (2020); Zhou et al. (2021)
		Huh-7 cells	80 μg/ml		
		HepG2 cells	0.4, 4, 40 μM		
		H22 cells	0.4, 4, 40 μM		
		Male BALB/c mice	50 mg/kg		

(Continued on following page)

TABLE 2 | (*Continued*) Summary of polysaccharides and glycosides with significant anti-liver disease activity.

Compounds	Source	The species investigated	Dose	Mechanisms	References
		HepG2 cells	6.4, 12.8, 25.6, 51.2, 102.4 μM		
		SK-Hep1 cells	200, 400 μM		
		Hep3B cells	200, 400 μM		
Amarogentin	*Swertia* and *Gentiana* roots	HSCs	0.01, 0.1, 1 mg/ml	By anti-oxidative properties and suppressing the mitogen-activated protein kinase signaling pathway	Zhang et al. (2017)
		Male C57BL/6 mice	25, 50, 100 mg/kg		
Amygdalin	*Armeniaca semen*	Female BALB/c mice	4, 8 mg/kg	regulation of the NLRP3, NF-κB, Nrf2/NQO1, PI3K/AKT and JAK2/STAT3 signaling pathways	Tang et al. (2019); Wang et al. (2021a); Yang et al. (2019a)
		HepG2 cells	80 μM		
		Male Sprague–Dawley rats	0.5, 1, 1.5, 3 mg/kg		
		LX-2 cells	1.25, 2.5, 5 mg/ml		
Forsythiaside A	*Forsythia suspensa*	Male BALB/c mice	15, 30, 60 mg/kg	Through modulating the remolding of extracellular matrix, PI3K/AKT and Nrf2 signaling pathway, and inhibition of NF-κB activation	Gong et al. (2021); Pan, et al. (2015a)
		Transgenic zebrafish	25, 50, 100 μM		
Gentiopicroside	*Gentiana manshurica Kitagawa*	Male Sprague–Dawley rats	20 mg/kg	Improvement of mitochondrial dysfunction and activation of LKB1/AMPK signaling	Li, et al. (2018e); Yang et al. (2020a); Zhang et al. (2021)
		Male C57BL/6 mice	40, 80 mg/kg		
		HepG2 cells	100 μM		
		RAW 264.7 macrophages	25, 50, 100 μM		
Paeoniflorin	*Paeonia lactiflora*	Male Sprague-Dawley rats	10, 20, 40, 80, 200 mg/kg	By activating LKB1/AMPK and AKT pathways, and inhibiting HMGB1-TLR4 signaling pathway and HIF-1α expression	Li, et al. (2018d); Xie et al. (2018); Zhao et al. (2014)
		Male C57BL/6 mice	100 mg/kg		
Swertiamarin	*Gentiana manshurica* Kitag	HSCs cells	2.4, 6, 15 μM	By suppressing angiotensin II–angiotensin type 1 receptor–extracellular signal-regulated kinase signaling	Li et al., (2016)
		MaleWistar rats	15, 20 mg/kg		
Nodakenin	*Angelica biserrata*	Male ICR mice	10, 30 mg/kg	By regulating apoptosis-related mitochondrial proteins	Lim et al. (2021)
Geniposide	*Gardenia jasminoides frui*	HepG2 cells	65, 130, 260 μmol/L	Regulation of Nrf2/AMPK/mTOR signaling pathways	Shen et al. (2020)
		Male wild-type mice	50, 75, 100 mg/kg		

that oral administration of *portulaca oleracea* extract to male AKR mice for seven consecutive days could contribute to the treatment of liver cancer. The results showed that the serum levels of IL-6, IL-1β, TNF-α and MDA in mice decreased after 7 days of treatment, while the activity of SOD increased. The pathological changes of the liver were significantly alleviated. Meanwhile, *portulaca oleracea* extract could effectively inhibit PI3K, Akt, mTOR, NF-κB and IκBα, and up regulate the expression of Nrf2 and HO-1. These effects are attributed to the protective effect of *Portulaca oleracea* extract on liver cancer by regulating PI3K/Akt/mTOR and Nrf2/HO-1/NF-κB pathway (Guoyin et al., 2017).

In addition, some CM can also achieve protection against liver cancer through various other effects. For examples, *Astragalus membranaceus* and *Curcuma wenyujin* promote the normalization of blood vessels in liver tumor endothelial cells by increasing the expression of CD34 and reducing the expression of HIF1a (Zang et al., 2019). *Artemisia capillaris* leaves can achieve pro-apoptotic effects on liver cancer cells by reducing the expression of XIAP and the release of cytochrome C through mitochondrial membrane potential (Kim et al., 2018). Besides, *Ligustrum lucidum* Ait. fruit extract can induce apoptosis and cell senescence of human liver cancer cell Bel-7402 by up-regulating p21. All in all, there are abundant resources of CM against liver cancer, which are worthy of our further development and utilization.

Other Anti-liver Disease Mechanisms

A large number of studies have shown that the occurrence of liver diseases is also closely related to endoplasmic reticulum stress and insulin resistance. *Scutellaria baicalensis* Georgi extract can regulate the endoplasmic reticulum stress and protect the liver by reducing the expression of glucose-related protein 78 (Dong et al., 2016). HFD increased the expression of adipose-derived carbohydrate response element binding protein and endoplasmic reticulum stress genes CHOP, x-box binding protein 1, and glucose regulated protein 78 in male wistar rats, and *Ginger*

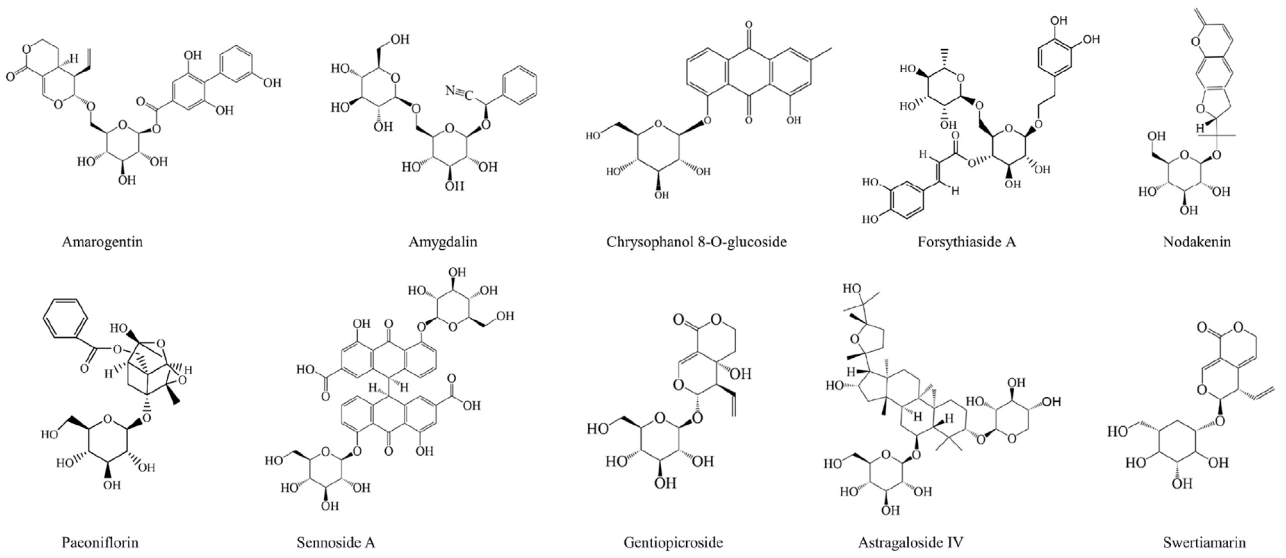

FIGURE 5 | The chemical structures of glycosides showing anti-hepatopathy activity.

extract could restore these changes to normal state (Kandeil et al., 2019). Jung et al. reported that *Polygonum multiflfluorum* thunb. reduced nonalcoholic steatosis and insulin resistance by regulating the expression of the proteins on lipid metabolism and glucose transport in the liver (Jung et al., 2020).

Recently, the evidence has shown that gut microbiota play an important role in metabolism, immune system, and so on. The changes of gut microbiota and their function can promote the development of acute and chronic liver diseases. In addition, the destruction of intestinal barrier can make microorganisms transfer to the blood, and continuously cause inflammatory reaction, thus promoting liver injury, hepatic fibrosis, cirrhosis, and carcinogenic transformation (Shen et al., 2018; Chopyk and Grakoui, 2020). *Rhubarb* extract can promote some intestinal bacteria (such as *Akkermansia muciniphila* and *Parabacteroides goldsteinii*.) to participate in the intestinal barrier function, and alleviate liver inflammation caused by acute alcohol intake (Neyrinck et al., 2017). In addition, *Schisandra chinensis* bee pollen could inhibit the expression of LXR-α, SREBP-1c, and FAS genes, and regulate the structure of intestinal microflora in obese mice, so as to achieve the protective effect on MAFLD (Cheng et al., 2019).

NATURAL AGENTS FROM CM FOR LIVER DISEASE TREATMENT

Polysaccharides and Glycosides

Polysaccharide is one of the active components of CM. The polysaccharides in CM have a wide range of biological activities in enhancing immunity, antiviral, anti-inflammation, anti-oxidation, and anti-tumor (Chen et al., 2016). *Ginkgo biloba* leaf polysaccharides and *Astragalus* polysaccharides can effectively inhibit liver steatosis (Yan et al., 2015; Huang et al., 2017). The polysaccharides from roots of *Sophora flavescens* can significantly inhibit the HBsAg and HBeAg secretion of HepG2.2.15 cells, and have good anti-HBV activity (Yang et al., 2018). In addition, the polysaccharides extracted from many CM have obvious protective effects on acute liver injury, such as *Rhizoma Atractylodis Macrocephalae* polysaccharides (Han et al., 2016), *Angelica sinensis* polysaccharides (Wang, K. et al., 2020), *Poria Cocos* polysaccharides (Wu, K. et al., 2018), *Lycium barbarum* polysaccharides (Wei et al., 2020), and *Schizandra chinensis* acidic polysaccharides (Yuan et al., 2018). Wang et al. reported that *Paeoniae Radix Alba* polysaccharides inhibited the NF-κB signaling pathway (including the liver infiltration of inflammatory CD^{4+} and CD^{8+} cells, and the overexpression of inflammatory cytokines IL-2, IL-6, and IL-10) to inhibit the immune inflammatory response in experimental autoimmune hepatitis mice (Wang, S. et al., 2020). Finally, it is also important that APS is the main active component extracted from *Astragalus*, which has been proved to have a significant inhibitory effect on many types of human solid tumors. A recent study showed that APS could reduce the activity of hepatoma cells and induce the apoptosis of HCC cells in a concentration-dependent manner. The study further showed that the results might be related to inhibiting the expression of Notch 1 in HCC cells (Huang et al., 2016).

Glycosides are a class of compounds formed by linking the sugar or sugar derivative with another non-sugar substance through the terminal carbon atom of the sugar. The studies have shown that most glycosides have good hepatoprotective effects on liver, such as amygdalin, amarogentin, and forsythiaside A (Pan, C.-W. et al., 2015; Tang et al., 2019; Zhang et al., 2017). Chrysophanol 8-o-glucoside, extracted from *Rheum palmatum*, can significantly inhibit the gene expression of α-SMA and collagen I, and inhibit the phosphorylation of STAT3 by inhibiting the nuclear

TABLE 3 | Summary of phenols and flavonoids with significant anti-liver disease activity.

Compounds	Source	The species investigated	Dose	Mechanisms	References
Phenols					
Resveratrol	*Polygonum cuspidatum*	Male C57BL/6J mice	60 mg/kg	Through improving insulin sensitivity and glucose levels	Hajighasem et al. (2018); Zhao et al. (2019a)
		HepG2 cells	20, 50, 100 μM		
		Male Wistar rats	25 mg/kg		
Salvianolic acid B	*Salvia miltiorrhiza*	Male Kunming mice	15, 30 mg/kg	Inhibition of MAPK-mediated P-Smad2/3L signaling	Wu et al. (2019b)
		HSC-T6 cells	25, 50, 100 μM		
		LX-2 cells	25, 50, 100 μM		
Salvianolic Acid C	*Salvia miltiorrhiza*	Male ICR mice	5, 10, 20 mg/kg	By attenuating inflammation, oxidative stress, and apoptosis through inhibition of the Keap1/Nrf2/HO-1 signaling	Wu, et al. (2019c)
Polydatin	*Polygonum cuspidatum*	Male Sprague-Dawley rats	7.5, 15, 30 mg/kg	Through increasing miR-200a to regulate Keap1/Nrf2 pathway, and restoring the antioxidant balance as well as the MMP/TIMP balance	Koneru et al. (2017); Zhao, et al. (2018a)
		BRL-3A cells	10, 20, 40 μM		
		HepG2 cells	10, 20, 40 μM		
		Male C57BL/6 mice	50, 100 mg/kg		
Curcumin	*Curcumin longa*	Pregnant NMRI mice	10 mg/kg	By suppression of oxidative stress-related inflammation *via* PI3K/AKT and NF-kB related signaling	Barandeh et al. (2019); Lee et al. (2017b); Zhong et al. (2016)
		Male Sprague-Dawley rats	200 mg/kg		
		Male C57BL/6 mice	20, 40, 80 mg/kg		
		HSCs	0.5, 1, 2 μM		
Chlorogenic acid	*Oriental Wormwood*	Female Sprague-Dawley rats	50 mg/kg	Inhibition of oxidative stress, JNK pathway and miR-21-Regulated TGF-β1/Smad7 signaling pathway	Shi et al. (2016); Yang et al. (2017)
		Male Sprague-Dawley rats	15, 30, 60 mg/kg		
		HSCs	12.5, 25, 50 mg/ml		
		LX2 cells	20, 40, 80 μg/ml		
Lithospermic acid	*Salvia miltiorrhiza*	Huh-7 cells	5, 10, 20, 40 μg/ml	Reduction of free radicals, restoration of liver functions and inhibition of caspase activity associated with apoptosis	Chan and Ho (2015)
		Male BALB/c mice	50, 100 mg/kg		
Flavonoids					
Hesperidin	*Citrus*	Male Wistar rats	200 mg/kg	Inhibition of free radicals, NF-κB activation and PI3K/Akt pathway, and activation of the Akt pathway	Li et al. (2020b); Mo'men et al. (2019); Pérez-Vargas et al. (2014)
		Male C57BL/6J mice	100, 200, 400 mg/kg		
		Hepatocytes	10, 20 ng/ml		
Licochalcone A	*Licorice Glycyrrhiza*	$Nrf2^{-/-}$ C57BL/6 mice	50, 100 mg/kg	Up-regulation of the Nrf2 antioxidant and sirt-1/AMPK pathway	Liou et al. (2019); Lv et al. (2018)
		HepG2 cells	1.5, 3, 3.7, 6, 12 μM		
		Male C57BL/6 mice	5, 10 mg/kg		
Licochalcone B	*Licorice Glycyrrhiza*	HepG2 cells	40, 80, 120 μM	Inhibition of Caspase 8 and Caspase 9 proteins	Wang et al. (2019b)
Wogonin	*Scutellaria radix*	Male C57BL/6 mice	10, 20, 40 mg/kg	Regulation of hepatic stellate cell activation and apoptosis	Du et al. (2019)
		HSC-T6 cells	1.25 μg/ml		
		LX-2 cells	20 μg/ml		
Quercetin	*Radix Bupleuri*	Male C57BL/6J mice	0.05% (wt/wt)	By ameliorating inflammation, oxidative stress, and lipid metabolism, and modulating intestinal microbiota imbalance and related gut-liver axis activation	Li et al. (2018b); Porras et al. (2017); Yang et al. (2019a); Zhu et al. (2018a)
		Male BALB/c mice	50 mg/kg		
		Raw 264.7 cells	50 μM		
		Male db/db mice	100 mg/kg		
		Male Sprague-Dawley rats	100 mg/kg		

(Continued on following page)

TABLE 3 | (*Continued*) Summary of phenols and flavonoids with significant anti-liver disease activity.

Compounds	Source	The species investigated	Dose	Mechanisms	References
		HepG2 cells	100 μM		
Baicalin	*Scutellariae radix*	Male C57BL/6 mice	15, 30, 60 mg/kg	By regulating the ERK signaling pathway, TLR4-Mediated NF-κB pathway and miR-3595/ACSL4 axis	Cheng et al. (2017); Liao et al. (2017); Wu et al. (2018a)
		HSC-T6 cells	50, 100, 150 μM		
		Young chicken	50, 100, 200 mg/kg		
Baicalein	*Scutellariae radix*	BEL-7402 cells	5, 10 μg/ml	By activating apoptosis and ameliorating P-glycoprotein activity	Li. et al. (2018a)
		BEL-7402/5-FU cells	5, 10 μg/ml		
Rutin	*Forsythia suspensa*	Male db/db mice	60, 120 mg/kg	By interfering with oxidative stress, inflammation and apoptosis, and facilitating signal transduction and activated state of insulin IRS-2/PI3K/Akt/GSK-3β signal pathway	D'Atanasio et al. (2018); Elsawy et al. (2019); Liang et al. (2018); Liu et al. (2017)
		HepG2 cells	8, 16, 32, 64 μg/ml		
		Male albino rats	70 mg/kg		
		Male Sprague Dawley rats	50, 100 mg/kg		
		Male C57BL/6 mice	200 mg/kg		
Calycosin	*Radix astragali*	Male C57BL/6 mice	12.5, 25, 50 mg/kg	By activating farnesoid X receptor	Duan et al. (2017)
Silybin	*Silybum marianum*	Male C57BL/6 mice	105 mg/kg	By reducing oxidative damage to mitochondria, proteins, lipids, and involvement with the NF-κB pathway	Goh et al. (2020); Ou et al. (2018)
		LO2 cells	25, 50 μM		
Isorhamnetin	/	Male C57BL/6J mice	50 mg/kg	By inhibiting *de novo* lipogenic pathway, by inhibiting TGF-β/Smad signaling and relieving oxidative stress, inhibiting Extracellular Matrix Formation *via* the TGF-β1/Smad3 and TGF-β1/p38 MAPK Pathways (*via* inhibition of TGF-β1-mediated Smad3 and p38 MAPK signaling pathways.)	Ganbold et al. (2019); Liu et al. (2019a); Yang et al. (2016b)
		LX-2 cells	25, 50, 100 μM		
		HepG2 cells	25, 50, 100 μM		
		Male ICR mice	10, 30 mg/kg		
Oroxylin A	*Scutellaria baicalensis*	Male ICR mice	30 mg/kg	Inhibition of hypoxia inducible factor 1alpha, and activation PKM1/HNF4 alpha	Jin et al. (2018); Wei et al. (2017)
		LO2 cells	10, 20, 40 μM		
		HepG2 cells	6, 8, 10 μM		
		SMMC-7721 cells	15, 20, 25 μM		
		C57BL/6J mice	75 mg/kg		

translocation of p-STAT3, thus alleviating fibrosis and achieving liver protection (Park et al., 2020). What's more, Gentiopicroside not only protects alcoholic liver disease by improving lipid metabolism imbalance and mitochondrial dysfunction caused by alcohol (Yang, H.-X. et al., 2020; Zhang et al., 2021), but also treats alcoholic liver cancer by regulating the activation of P2x7R-NLRP3 inflammasome (Li, Xia et al., 2018). It is worth mentioning that astragaloside IV can inhibit hepatoma cells by inhibiting multidrug resistance-associated protein 2, and long noncoding RNA ATB (Li, Y. et al., 2018; Qu et al., 2020).

The specific information of polysaccharides and glycosides is shown in **Table 2**. In addition, the chemical structures of the glycosides with therapeutic effects on liver diseases are shown in **Figure 5**.

Phenols and Flavonoids

Phenolic compounds are composed of the aromatic rings with one or more hydroxyl groups. They play an important role on oxidative stress in the human by maintaining the balance between oxidants and antioxidants, which are divided into phenolic acids, flavonoids, coumarins, and tannins (Van Hung, 2016). A large number of phenolic compounds in CM have obvious antioxidant capacity, which can reduce the oxidative damage of the liver, such as Lithospermic acid, Chlorogenic acid, Curcumin, Polydatin, and Salvianolic acid C (Chan and Ho, 2015; Koneru et al., 2017; Shi et al., 2016; Wu, C.-T. et al., 2019; Zhong et al., 2016). Yang et al. further found that Chlorogenic acid could reduce the expression of α-SMA, collagen I in the liver tissue and serum TGF-β1 by increasing the mRNA and protein expression of Smad7 and MMP-9, thus alleviating liver fibrosis (Wu, C. et al., 2019). The studies have shown that Curcumin and Polydatin can inhibit lipid accumulation by regulating endoplasmic reticulum stress and the Keap1/Nrf2 pathway (Lee, H.-Y. et al., 2017; Zhao, X.-J. et al., 2018). In addition, Yan et al. demonstrated that Chlorogenic acid could improve liver injury and insulin resistance by inactivating the JNK pathway and inhibiting the autophagy in MAFLD rats (Yan, Hua et al., 2018).

Flavonoids, a part of phenolic compounds, also have significant hepatoprotective effects. For example, Isorhamnetin suppresses the TGF-β/Smad pathway and reduces oxidative stress to alleviate hepatic fibrosis (Yang,

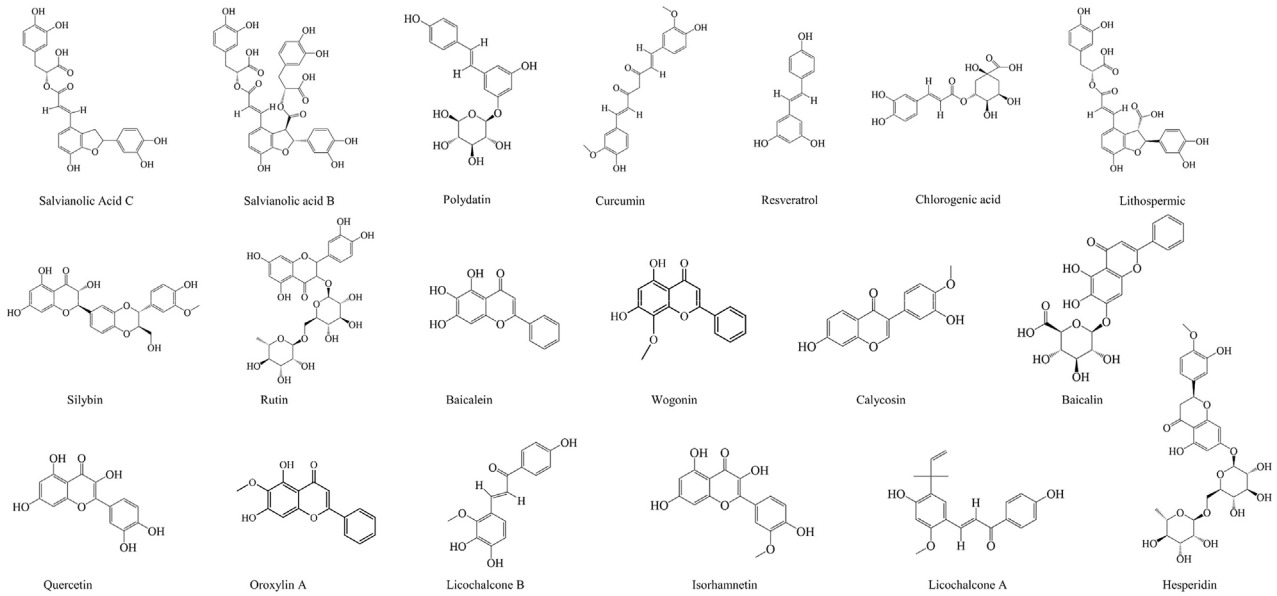

FIGURE 6 | The chemical structures of phenols and flavonoids showing anti-hepatopathy activity.

J.H. et al., 2016), and Wogonin reduces hepatic fibrosis by regulating the activation and apoptosis of HSCs (Du et al., 2019). Quercetin can effectively alleviate MAFLD, which depends on its regulation of intestinal microbiota imbalance and related gut-liver axis activation (Porras et al., 2017). Hesperidin and Oxylin A have significant anti-hepatoma activity (Mo'men et al., 2019; Wei et al., 2017). In addition, Licochalcone A can increase the expression of antioxidant enzymes by reducing the apoptosis, mitochondrial dysfunction, and reactive oxygen production stimulated by tert butyl peroxide and Acetaminophen, thus protecting APAP-induced hepatotoxicity, which is largely dependent on the antioxidant Nrf2 pathway (Lv et al., 2018). What's more, rutin has a good protective effect on various acute liver injury induced by carbon tetrachloride, lipopolysaccharide, and mercury chloride (Caglayan et al., 2019; Elsawy et al., 2019; Rakshit et al., 2021).

Bacalin, a kind of flavonoid extracted from *Scutellaria baicalensis*, has significant biological activity, which is widely used in the treatment of liver diseases. The study has shown that bacalin suppresses the production of IL-1β, IL-6, and TNF-α, as well as regulates the TLR4 expression and inhibits the NF-κB activation, protecting the inflammation of chicken's liver induced by LPS through the negative regulation of inflammatory medium (Cheng et al., 2017). Another study showed that the inhibition of the proliferation, apoptosis, invasion, migration, and activation of HSCs induced by platelet derived growth factor-BB through mir-3595/acsl4 axis is one of the mechanisms of bacalin in anti-hepatic fibrosis (Wu, X. et al., 2018).

The specific information of the phenols and flavonoids is shown in **Table 3**, and the chemical structures of the phenols and flavonoids are shown in **Figure 6**.

Terpenoids

Terpenoids (isoprenoids) are the most abundant chemical compounds in plants (Tholl, 2015), which has a wide range of biological activities, such as anti-inflammation (Kim, T. et al., 2020), anti-depressant (Agatonovic-Kustrin et al., 2020), anti-cancer (Ateba et al., 2018), and so on. Many studies have shown that terpenoids are also widely used in the treatment of liver diseases. Leucodin is a sesquiterpene lactone isolated from *Artemisia capillaris*, which can inhibit the inflammatory response of macrophages, and P2x7R-NLRP3-mediated lipid accumulation in hepatocytes (Shang et al., 2018). Saikosaponin-d is an active component isolated from *Radix Bupleuri*, which can inhibit the COX2 expression through the p-STAT3/C/EBPβ signaling pathway in HCC (Ren et al., 2019). Oleanolic acid (OA) is a kind of triterpenoid widely existing in fruits, vegetables, and herbs. It is liver-specific and can selectively inhibit adipogenesis (Lin, Y.-N. et al., 2018). In addition, OA can regulate antioxidant status, and induce mitochondria-mediated apoptosis and regulate inflammation, which effectively inhibits 7,12-Dimethylbenz[a]anthracene-induced liver cancer (Hosny et al., 2021).

Rhizoma Alismatis is a kind of common CM, which is often used in clinic for adverse urination, edema, diarrhea, and so on. Modern studies have shown that many compounds extracted from *Rhizoma Alismatis* have hepatoprotective effects. For example, Alisol A 24-acetate, a natural triterpene extracted from *Rhizoma Alismatis*, can improve NASH by inhibiting oxidative stress, and stimulating autophagy through the AMPK/mTOR signaling pathway (Wu, C. et al., 2018). Meng et al. found that Alisol A 23-acetate could also improve NASH in the mice, which was achieved by the activation of X-like receptor (Meng et al., 2017). Futhermore, Meng et al. found that Alisol A 23-acetate

activated FXR to induced the phosphorylation of STAT3 and the expression of its target genes, Bcl-xl and SOCS3. And it reduced the expression of the liver uptake transporter NTCP, and bile acid synthases CYP7A1 and Cyp8b1, as well as increased the expression of the outflow transporters BSEP and MRP2, reducing the hepatic bile acid deposition, which achieved the protective effect on CCl_4-induced hepatotoxicity in the mice (Meng et al., 2015).

The specific information of the terpenoids in the treatment of liver diseases is shown in **Table 4**, and the chemical structures of the terpenoids with therapeutic effects on liver diseases are shown in **Figure 7**.

Alkaloids

Alkaloids are an important class of natural products, which have a wide range of biological activities, and have been used in folk medicine for many years (Stöckigt et al., 2011). We are surprised to find that alkaloids play an important role in the treatment of liver diseases. Matrine and Oxymatrine are the main active substances extracted from the roots of *Sophora flavescens*, and are widely used (Yuan et al., 2010). They have significant biological activities against MAFLD, liver injury, and liver cancer (Gao et al., 2018; Shi et al., 2020; Wei et al., 2018; Xu et al., 2018; Zhang, H. et al., 2020). Ligustrazine is an alkaloid extracted from *Ligusticum chuanxiong*. It not only activates Nrf2 to inhibit hepatic steatosis, but also induces the apoptosis and autophagy of hepatoma cells to exert an anti-hepatoma effect (Cao et al., 2015; Lu et al., 2017). And coptisine exerts an anti-hepatoma effect by activating the 67 kDa laminin receptor/cGMP signal to induce the apoptosis of human hepatoma cells, and the proliferation and migration of HCC cells (Chai et al., 2018a; Zhou et al., 2018).

The specific information of various alkaloids in the treatment of liver diseases is shown in **Table 5**. In addition, the chemical structure formulas are shown in **Figure 8**.

Other Bioactive Ingredients

In addition to the above compounds, many compounds have the activities of anti-liver diseases, including phenylpropanoids (such as simple phenylpropanoids, coumarins, and lignans), anthraquinones, and volatile oils. Some lignans extracted from CM have been proved to have the effects on improving liver diseases. For example, Gomisin N extracted from *Schisandra chinensis* not only has protective effects on endoplasmic reticulum stress-induced hepatic steatosis, but also alleviates the liver injury caused by ethanol by improving lipid metabolism and oxidative stress (Jang et al., 2016; Nagappan et al., 2018). Futhermore, Arctigenin can inhibit the proliferation of HepG2 cells and block the autophagy cells that lead to the accumulation of sequestosome 1/p62, so as to achieve the therapeutic effects on liver cancer. It will become a new drug for the autophagy research and cancer chemoprevention. It is worth noting that many anthraquinones in *Rhubarb* have good activities of anti-liver diseases, including chrysophanol, emodin, rhein, and aloe emodin (Bai et al., 2020; Dong et al., 2017; Kuo et al., 2020; Li, Y. et al., 2019). Cryptotanshinone, the main anthraquinone extracted from *Salvia miltiorrhiza* Bunge, can protect liver by activating the AMPK/SIRT1 and Nrf2, and inhibiting CYP2E1 to inhibit adipogenesis, oxidative stress, and inflammation (Nagappan et al., 2019). Other bioactive components against liver diseases are shown in **Table 6**. In addition, the related chemical structures are also shown in **Figure 9**.

Toxicity

After the above discussion, it is not difficult to find the important position of CM in the treatment of liver diseases. As we all know, CM is a relatively safe class of drugs, but we can't ignore its toxic and side effects on the liver when we use CM to treat liver diseases. The studies have found that some CM show certain hepatotoxicity. For example, *Rhubarb* extract had a certain protective effect on the rats with chronic renal failure, but the incidence of mild hepatotoxicity was also observed in normal rats (Wang et al., 2009). *Ginkgo biloba* extract induced DNA damage by inhibiting the topoisomerase II activity in human hepatocytes (Zhang et al., 2015). Interestingly, the hepatotoxicity of some CM comes from their own hydrolysates. For example, after the intragastric administration of *Sophora flavescens* extract to the rats, kurarinone glucosides was hydrolyzed into Kurarinone in liver cells, which eventually led to the lipid accumulation and liver injury through a series of actions (Jiang, P. et al., 2017). In addition, the use of herbal products is also a crucial cause of acute liver injury. It has been reported that a 68-year-old woman suffered from acute liver injury caused by aloe, after stopping taking aloe, her liver functions returned to normal levels (Parlati et al., 2017). It is worth noting that the first case of autoimmune hepatitis caused by turmeric supplements has been reported (Lukefahr et al., 2018).

The dosage of CM is often closely related to hepatotoxicity. In order to study the hepatotoxicity of *Cortex Dictamni*, fan et al. used its water extract and alcohol extract to carry out the toxicity experiments *in vivo* and *in vitro*. The results showed that high dose of water extract and alcohol extract significantly increased the levels of ALT and AST, absolute and relative liver weight, and the liver-to-brain ratio, and the histological examination of the liver showed the cell enlargement and nuclear contraction. *In vitro* cell experiment also showed that water extract and alcohol extract reduced the cell viability in a dose-dependent manner (Fan et al., 2018). A single oral dose of 60 g/kg *Cortex Dictamni* ethanol extract for 24 h resulted in severe hepatocyte necrosis in mice, and the induced liver injury showed a dose and time-dependent manner (Huang et al., 2020). Saikosaponins, a major bioactive component extracted from *Radix Bupleuri*, enhances the CYP2E1 expression in a dose and time-dependent manner, and induces oxidative stress *in vivo* and *in vitro*, leading to liver injury in mice (Li et al., 2017). In another study, the rats were fed with 300, 1250 and 2500 mg kg^{-1}·D^{-1} *Radix Scutellariae Baicalensis* ethanol extract for 26 weeks. It was found that the liver tissues of the rats in the high-dose group showed some inflammatory changes mainly characterized by leukocyte infiltration. In addition, there were also some changes in the levels of glucose, electrolyte, and lipid (Yi et al., 2018). It can be seen that the hepatotoxicity of many CM are closely related to the dosage.

TABLE 4 | Summary of terpenoids with significant anti-liver disease activity.

Compounds	Source	The species investigated	Dose	Mechanisms	References
Betulinic acid	*Betula pubescens*	Male C57BL/6J mice	15, 30, 60, 150 mg/kg	Through the YY1/FAS, MAPK/ERK and PI3K/AKT/mTOR signaling pathway	Liu et al. (2019b); Liu et al. (2019c); Mu et al. (2020)
		SMMC-7721 cells	2.5, 5, 10, 20, 40 μM		
		HepG2 cells	2.5, 5, 10, 20, 40 μM		
Saikosaponin-d	*Radix Bupleuri*	SMMC-7721 cells	2.5, 5, 10 μg/L	Through SENP5- Dependent Inhibition of Gli1 SUMOylation Under Hypoxia, and p-STAT3/C/EBPβ signaling	Ren et al. (2019); Zhang et al. (2019)
		HepG2 cells	2.5, 5, 10 μg/L		
Cycloastragenol	*Astragali Radix*	HepG2 cells	12, 25, 50 μM	By activating farnesoid X receptor signaling	Gu et al. (2017)
		Female C57BL/6 mice	100 mg/100 g diet		
Limonin	Citrus fruit and plants	Male Wistar rats	100 mg/kg	By activating Nrf2 antioxidative pathway and inhibiting NF-κB inflammatory response and TLR-signaling pathway	Mahmoud et al. (2014); Yang et al. (2020b)
		L-02 cells	10, 25, 50 μM		
		Male C57BL/6 mice	40, 80 mg/kg		
Oleanolic acid	*Forsythia suspensa*	Male Swiss albino mice	75 mg/kg	Through induction of mitochondrial-mediated apoptosis and autophagy, and inhibition of Liver X Receptor Alpha and Pregnane X Receptor	Hosny et al. (2021)
		EAC cells	9.32 μM		
		HepG2 cells	10, 20, 32.58, 27.56 μM		
		SMMC-7721 cells	10, 30, 60 μmol/L		
Ginsenoside Rg1	*Panax ginseng*	Male C57BL/6 mice	15, 30, 60 mg/kg	By activating Nrf2 signaling pathway	Ning et al. (2018)
Ursolic acid	*Forsythia suspensa*	C57BL/6 mice	40 mg/kg	Through RhoA-related signaling pathways, and inhibition of interactive NOX4/ROS, RhoA/R and CASP3	Gan et al. (2018a); Ma et al. (2021); Wan et al. (2019); Wan et al. (2020)
		HepG2 cells	10 μM		
		Male Kunming mice	20, 40, 80 mg/kg		
		Sprague–Dawley rats	40 mg/kg		
Alisol A	*Rhizoma Alismatis*	C57BL/6 mice	100 mg/kg	Through the AMPK/ACC/SREBP-1c pathway	Ho et al. (2019)
Alisol B 23-acetate	*Rhizoma Alismatis*	Male C57BL/6 mice	10, 15, 20, 30, 40, 60 mg/kg	Regulation of the FXR and STAT3 signaling pathway	Meng et al. (2015); Meng et al. (2017)
Leucodin	*Artemisia capillaris*	HepG2 cells	1, 5 μM	Through the P2x7 receptor pathway	Shang et al. (2018)

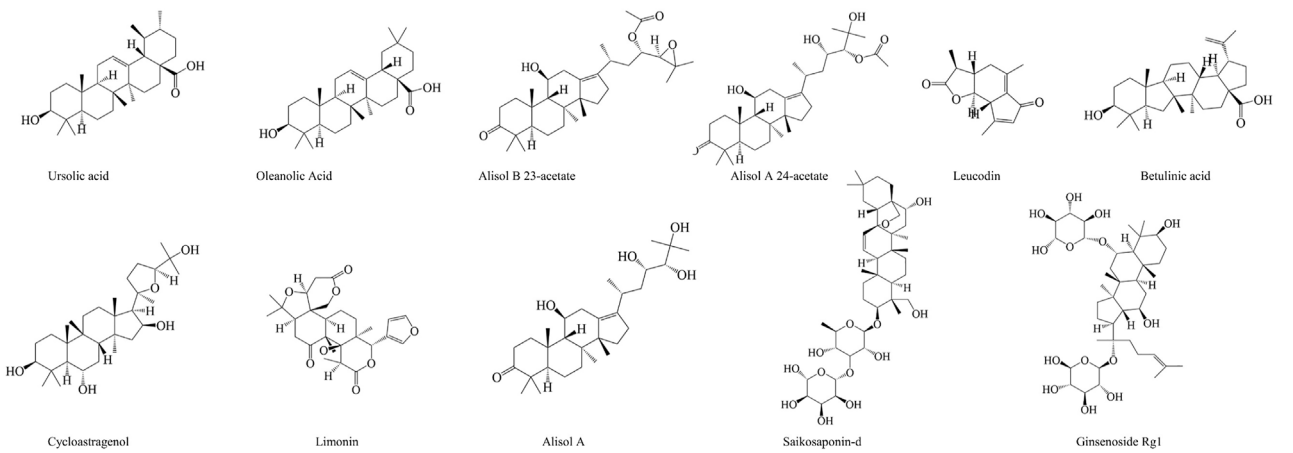

FIGURE 7 | The chemical structures of terpenoids showing anti-hepatopathy activity.

In addition, the abuse of CM without the guidance of doctors is also the source of toxic reactions. Because traditional Chinese medical science thinks that "toxicity" refers to the biases of drugs, the toxic components of CM are often the effective components for treating diseases. The key to judging whether CM is toxic or non-toxic is to see whether it is used according to

TABLE 5 | Summary of alkaloids with significant anti-liver disease activity.

Compounds	Source	The species investigated	Dose	Mechanisms	References
Tetramethylpyrazine	*Ligusticum chuanxiong Hort*	Male Sprague-Dawley rats Human HCC HepG2 cells Male BALB/c nude mice Male ICR mice Human LO2 hepatocytes	50, 100, 200 mg/kg 50, 100, 200 μM 50, 100, 150 mg/kg 100 mg/kg 20 μM	Through PDGF-bR/NLRP3/caspase1 pathway to reduce liver inflammation, and exerts antitumor effects by inducing apoptosis and autophagy in hepatocellular carcinoma, and inhibition of hepatic steatosis by activating the Nrf2 signaling pathway	Cao et al. (2015); Lu et al. (2017); Wu et al. (2015)
Coptisine	*Rhizoma Coptidis*	Kunming mice HepG2 cells L02 cells SMMC7721 cells Male BALB/c nude mice HepG2 cells Huh7 cells	37.5, 150 mg/kg 12.5, 25, 50, 100 μg/ml 25 μg/ml 12.5, 25, 50, 100 μM 150 mg/kg 25 μg/ml 25 μg/ml	Through up-regulating expression of miR-122, and activating 67-kDa laminin receptor/cGMP signaling	Chai et al. (2018a); Chai et al. (2018b); Zhou et al. (2018)
Matrine	*Sophora flavescens*, *Sophora subprostrata*	Male C57BL/6J mice L02 cells HepG2 cells Huh7 cells	0.5, 2.5, 10 mg/kg 200, 400, 800 μM 1, 5 nM 1, 5 nM	Regulation of SERCA pathway, and inhibition of mitophagy, PINK1/Parkin pathways and Notch signaling pathway	Gao et al. (2018); Wei et al. (2018)
Betaine	*Lycium chinensis*	Male Sprague-Dawley rats Male C57BL/6 mice	20 g/kg 1.5% (w/v)	Regulation of oxidative stress, inflammation, apoptosis, autophagy and Akt/mTOR signaling	Abu Ahmad et al. (2019); Veskovic et al. (2019)
Berberine	*Rhizoma Coptidis*	Male C57BL/6 mice MIHA cells HepG2 cells	2, 5 mg/kg 10, 20, 100 μM 10, 20 μM	Inhibition of oxidative stress, hepatocyte necrosis, inflammatory response, and AKT-mTOR-S6K signaling pathway	Li. et al. (2018a); Zhao et al. (2018b)
Oxymatrine	*Sophora alopecuroides*	Male Sprague-Dawley rats BMDMs HSC-T6 cells Male C57BL/6 mice Wistar male rats	30, 60, 120 mg/kg 1.0 mg/ml 250, 500, 1000 μg/ml 120 mg/kg 80 mg/kg	Activation of Nrf2/HO-1, regulation of miR-182, and modulation of TLR4-dependent inflammatory and TGF-β1 signaling pathways	Xu et al. (2018); Zhang et al. (2020b); Zhao et al. (2016)
Levo-tetrahydropalmatine	*Corydalis yanhusuo*	Male C57 mice LX-2 cells Male Balb/c mice	20, 40 mg/kg 34.01 μmol/L 20, 40 mg/kg	Modulation of PPARγ/NF-κB, TGF-β1/Smad and TRAF6/JNK signaling pathway	Yu et al. (2021); Yu et al. (2018)

the syndrome. As long as the treatment is besed on the syndrome, toxic drugs are also safe. If the treatment is not for the syndrome, non-toxic drugs may be harmful. It is worth noting that there are also some CM products considered non-toxic or low toxic, which have obvious toxicological effects on different organs in animal and human models (Liu, R. et al., 2020). So it is a great problem to control the toxic and non-toxic boundaries reasonably, and every traditional medical scholar should make efforts to do so.

Clinical Trials

Most drugs for anti-liver diseases used in clinic are CM compounds, and less clinical research and application involve only one CM or one compound. **Table 7** shows some CM (excluding CM compounds) used in the clinical treatment of liver diseases. The purpose is to improve the richness of clinical medication, so that more CM with potential and significant therapeutic effects can be noticed.

Single extract or chemical component of CM showed good activity of anti-liver diseases in clinical research. *Artemisia annua* L. extract can improve the liver function in the patients with mild to moderate nonalcoholic liver dysfunction, and no obvious adverse reactions were observed in all subjects (Han et al., 2020). Futhermore, *Portulaca oleracea* extract can improve liver enzyme, blood lipid, and blood glucose in the patients with MAFLD (Darvish

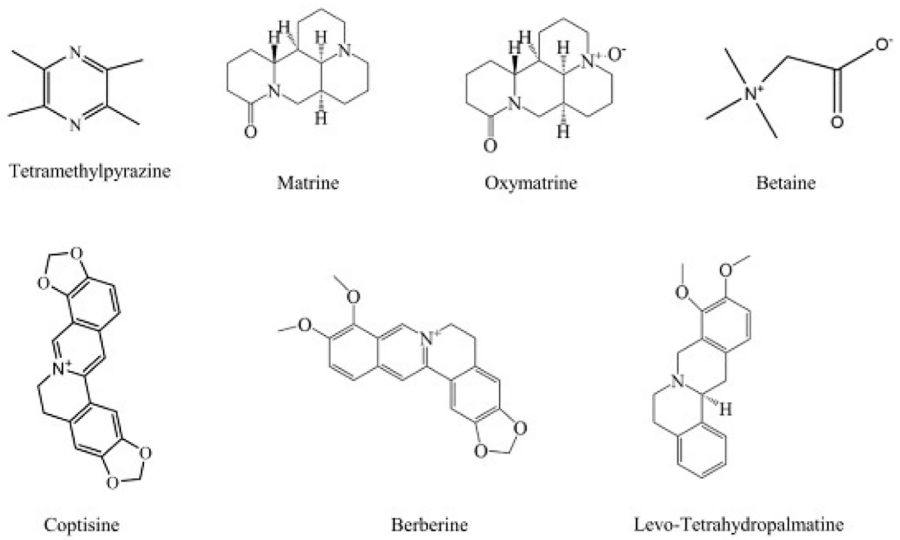

FIGURE 8 | The chemical structures of alkaloids showing anti-hepatopathy activity.

Damavandi et al., 2021). It is worth noting that *Carcuma longa* has a wide range of clinical applications, with a large number of clinical data, suggesting its position in the clinical treatment of liver diseases. To assess the effect of *Carcuma longa* on MAFLD, 92 MAFLD patients aged 20–60 years were enrolled in a 12-week study. The results showed that *Carcuma longa* supplement was very useful in controlling MAFLD-related risk factors (Darvish Damavandi et al., 2021). Curcumin, the main active component of *Curcuma longa*, can increase the serum inflammatory cytokine levels in the patients with MAFLD, which may be partly dependent on the anti-steatosis effect (Saberi-Karimian et al., 2020). In addition, curcumin can improve the quality of life of the patients with liver cirrhosis (Nouri-Vaskeh et al., 2020a). Although the clinical application of *Curcuma longa* has surpassed other CM against liver diseases, it still fails to solve the problem of its optimal dosage, and the molecular mechanisms on treating liver diseases is unclear. More importantly, in view of the widespread use of *Curcuma longa*, we need larger, more impartial and high-quality controlled randomized trials to conduct a deeper evaluation.

In the future, more clinical experiments should be studied, which makes more CM into clinical application, and even go to the international stage. There are still many deficiencies in the current clinical research. First, the dosage is single and the sample size is small, which is not good for screening the best treatment dose. Secondly, the existing clinical experiments mainly focus on the study of MAFLD, but there are many kinds of liver diseases. In the future, the research can be expanded to make more patients with liver diseases benefit from CM. Finally, the mechanisms of many CM (especially CM compounds) used in the treatment of liver diseases are not clear. We should further explore the mechanism of action of CM, making its fuzzy mechanism clearer and letting more people accept it.

CONCLUSION AND PERSPECTIVES

In conclusion, CM can prevent and treat liver diseases through many ways, including regulating lipid metabolism, anti-liver injury (such as CCl_4, H_2O_2, alcohol, and drug damage), anti-oxidant stress (including reducing ROS, increasing SOD, GSH and CAT content, and regulating Nrf2 and other related pathways), regulating bile acid metabolism (including regulating the excreted and ingested receptors), regulating the immune system, anti-hepatitis virus, and anti-liver cancer. In terms of the current situation, a large number of studies have proved the potential of CM in the treatment of liver diseases. However, the resources of CM are huge, and it is probably known that the effective CM for liver diseases are only one corner of the iceberg. More tasks need the joint efforts of all traditional medicine scholars. In addition, a large part of the current research has not only been focused on the study of efficacy, but also the expression level of genes and proteins. But it is not enough, and more new methods should be explored, such as using multi-group analysis (metabolomics, proteomics), so as to promote the progress of CM in the treatment of liver diseases.

It is worth noting that there is also relevant evidence that the new technology of CM combined with other preparations can greatly enhance the therapeutic effects on liver diseases. For example, due to the characteristics of unstable chemical

TABLE 6 | Summary of other bioactive ingredients with significant anti-liver disease activity.

Compounds	Source	The species investigated	Dose	Mechanisms	References
Phenylpropanoids					
Ferulic Acid	*Angelica sinensis*	Male Swiss albino mice Male ApoE$^{-/-}$ mice Male Wistar rats LX-2 cells	50, 100 mg/kg 30 mg/kg 10, 25, 50 mg/kg 5, 15, 30 μM	Upregulation of Nrf2/HO-1 signaling, and inhibition of TGF-β/smad signaling pathway, and modulation of the gut microbiota composition	Ma et al. (2019); Mahmoud et al. (2020); Mu et al. (2018); Roghani et al. (2020)
Phillygenin	*Forsythia suspensa*	LX2 cells	12.5, 25, 50 μM	Through TLR4/MyD88/NF-κB signaling pathway	Hu et al. (2020b)
Arctigenin	*Arctium lappa*	HepG2 cells MCF-7 cells	10 μM 10 μM	Through autophagy inhibition in hepatocellular carcinoma cells	Okubo et al. (2020)
Imperatorin	*Angelica dahurica*	Male C57BL/6 mice Hepatocytes	50, 100 mg/kg 5, 10 μM	By stimulating the SIRT1-FXR pathway	Gao et al. (2020)
Pinoresinol	*Forsythiae Fructus*	Male ICR mice	25, 50, 100, 200 mg/kg	Through inhibition of NF-κB and AP-1	Kim et al. (2010)
Schisandrol B	*Schisandra sphenanthera*	Male C57BL/6 mice	12.5, 50, 200 mg/kg	Inhibition of CYP-mediated bioactivation and regulation of liver regeneration	Jiang et al. (2015)
Schisantherin A	*Schisandra sphenanthera*	Male C57BL/6 mice	25, 50, 100, 200, 400, 800 mg/kg	Inhibition of mitogen-activated protein kinase pathway	Zheng et al. (2017)
Schisandrin B	*Schisandra sphenanthera*	Male Wistar rats HSC-T6 cells	25, 50 mg/kg 5, 10, 30 μM	Regulation of Nrf2-ARE and TGF-β/smad signaling pathways	Chen et al. (2017)
Gomisin N	*Schisandra sphenanthera*	Male C57BL/6N mice HepG2 cells C57BL/6 mice	5, 20 mg/kg 10, 50, 100 μM 1, 30 mg/kg	Through ameliorating lipid metabolism, oxidative Stress and ER stress	Nagappan et al. (2018); Yun et al. (2017)
Scoparone	*Artemisia capillaris*	AML12 cells RAW264.7 cells Male C57BL/6 J mice	200 mM 25, 50, 100, 200 mM 20, 40, 80 mg/kg	By regulating the ROS/P38/Nrf2 axis, PI3K/AKT/mTOR pathway, and TLR4/NF-κB signaling pathway	Liu et al. (2020b)
Anthraquinones					
Chrysophanol	*Rheum palmatum*	HSC-T6 cells	30 mM	By regulating endoplasmic reticulum stress and ferroptosis	Kuo et al. (2020)
Emodin	*Rheum palmatum*	Male BALB/c nude mice HepG2 cells SK-Hep-1 cells Male C57B/6 mice Male Sprague-Dawley rats RAW264.7 cells Male Balb/c mice SMMC-7721 cells	15, 25, 30, 50, 60 mg/kg 3, 10, 30, 100 μM 30 μM 10, 30 mg/kg 10, 20, 40 mg/kg 15, 30, 60 μg/ml 20, 40, 80 mg/kg 25, 50, 100 μM	By regulating VEGFR2, miR-34a, AMPK with Hippo/Yap signalling pathway, MAPK, PI3K/AKT signaling pathways, and inhibiting the TLR4 signaling pathway and epithelial-mesenchymal transition and transforming growth factor-β1	Bai et al. (2020); Ding et al. (2018a); Lee et al. (2020); Lin et al. (2016); Liu et al. (2018)
Rhein	*Polygonum multiflorum*	Male Sprague-Dawley rats L02 cells	10, 30, 1000 mg/kg 25, 50, 100 μM	Through regulating the Fas death pathway and the mitochondrial pathway, and promoting bile acid transport and reduce bile acid accumulation	Li et al. (2019c); Xian et al. (2020)
Aloe-emodin	*Rheum palmatum*	HepG2 cells Male and female Kunming mouse HL-7702 cells	1, 15, 30 μM 0.8, 1.6 g/kg 5, 10, 20, 40 μM	Regulation of the Fas death pathway and the mitochondrial pathway, and inhibition of multidrug resistance protein 2	Dong et al. (2017); Liu et al. (2020b)
Cryptotanshinone	*Salvia miltiorrhiza*	Male C57BL/6 mice HepG2 cells AML-12 cells	20, 40 mg/kg 2.5, 5 μM 2.5, 5 μM	Inhibition of MAPKs phosphorylation regulated by TAK1, and activation of AMPK/SIRT1 and Nrf2 signaling pathways	Jin et al. (2014); Nagappan et al. (2019)
Volatile oil					
Z-ligustilide and n-Butylidenephthalide	*Angelica tenuissima*	MaleC57BL/6mice HepG2 cells	10, 50 mg/kg 10, 50, 100 μg/ml	Inhibition of fatty acid uptake and esterification	Lee et al. (2019)
Butylidenephthalide	*Angelica sinensis*	HSC-T6 cells Male Wistar rats	15, 25, 35 μg/ml 15, 80 mg/kg	Reduction of EMT, decreasing inflammatory reaction, and liver cell proliferation	Chuang et al. (2016)
Ligustilide	*Angelica sinensis*	Male Sprague-Dawley	10, 20, 40 mg/kg	Promotion of phosphorylation of Nrf2 and AMPKa1	Guo et al. (2021)

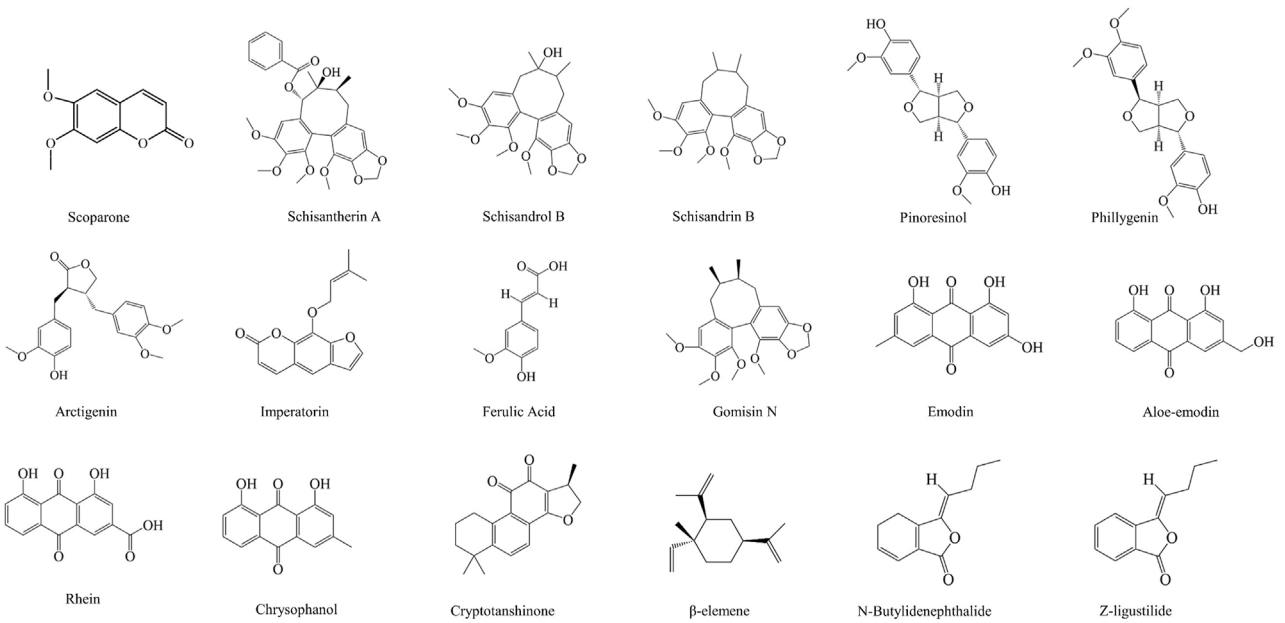

FIGURE 9 | The related chemical structures of other anti-hepatopathy bioactive components.

structure, low bioavailability, easy oxidation, and UV degradation, the toxic effect of curcumin on hepatoma cells is limited. Therefore, Kong et al. used curcumin loaded mesoporous silica nanoparticles, and found that the complex had better antioxidant activity than curcumin alone, as well as significantly enhanced the cytotoxic effect on hepatoma cells (Kong et al., 2019). Another study showed that curcumin liposome had a greater inhibitory effect on the growth and apoptosis of cancer cells (Feng et al., 2017). But these studies are still very few, which should be increased later.

This paper lists and elaborates the active ingredients of some CM against liver diseases, such as polysaccharides, glycosides, phenols, flavonoids, terpenoids, alkaloids, etc. We found the research on the mechanism of action of each ingredient was relatively single, and CM showed the joint action of multi-component and multi-target in the treatment of liver diseases. Therefore, screening more effective components and studying their molecular mechanisms should be greatly strengthened. For example, recent studies have shown that iron is essential for life, but excessive iron may be cytotoxic, which may lead to cell death and some diseases (Bogdan et al., 2016; Nakamura et al., 2019). In addition, in the previous discussion, we also know that the gut microbiota plays an important role in the treatment of liver diseases. Therefore, it is suggested that we can refer to these relevant mechanisms in the future research of CM on treating liver diseases.

CM, including Tibetan medicine, has shown good effects of anti-liver diseases (Li, Qi et al., 2018; Fu et al., 2020), which is indispensable in the treatment of liver diseases. This paper is a comprehensive review of CM and the related compounds, toxicology, and clinical research, which is aimed to provide scientific and effective references for the treatment of liver diseases, and to better use and develop the treasure of CM.

AUTHOR CONTRIBUTIONS

KF and YL designed this article and established the structure. CW, CM, and HZ assisted in data collection and form establishment. YL helped to revise the manuscript.

FUNDING

The study was supported by National Natural Science Foundation of China (No: 81891012, 81630101, and U19A2010), Sichuan Science and Technology Program (2021JDRC0041).

TABLE 7 | Some Chinese medicine are used to treat liver diseases in clinic.

CM or its compounds	disease	Subject	Study design	Treatment groups	Length	Clinical outcome	References
Turmeric supplementation (Combined use of chicory seeds)	MAFLD	92 patients (aged 20–60 years)	Double-blind, randomized, controlled clinical trial	Control group: placebo Experimental group: turmeric supplementation (3 g/d, TUR); Chicory seed supplementation (9 g/d, CHI); Turmeric and chicory seed supplementation (3 g/d, TUR + CHI)	12 weeks	Significantly decreased serum alkaline phosphatase and increased serum HDL-C	Ghaffari et al. (2019)
Curcuminoids supplementation	MAFLD	55 patients	Double-blind, randomized, placebo-controlled trial	Control group: placebo capsules Experimental group: 500 mg curcuminoids (plus 5 mg piperine to increase intestinal absorption)	8 weeks	Improved the severity of MAFLD; serum concentrations of TNF-α, MCP-1 and EGF were improved	Saberi-Karimian et al. (2020)
Curcumin (amorphous dispersion formulation)	MAFLD	80 cases	Randomized double-blind placebo-controlled trial	Control group: placebo Experimental group: 500 mg/day equivalent to 70 mg curcumin	8 weeks	The liver fat content, biochemical parameters and anthropometry were significantly improved in patients with MAFLD	Rahmani et al. (2016)
Curcumin supplementation	LC	70 patients (aged 20–70 years)	Randomized, double-blind, placebo-controlled trial	Control group: placebo Experimental group: 1000 mg/day curcumin	3 months	MELD(i), MELD, MELD-Na and Child-Pugh scores decreased significantly	Nouri-Vaskeh et al. (2020b)
Curcumin	LC	70 cases (aged 20–70 years)	Randomized double-masked placebo-controlled trial	Control group: placebo Experimental group: 1000 mg/day curcumin	12 weeks	The total score and most of the CLDQ, physical and mental health scores and most of the SF-36 areas were significantly improved, and the LDSI2.0 domain was significantly decreased	Nouri-Vaskeh et al. (2020a)
Resveratrol	MAFLD	60 subjects	Double-blind, randomized, placebo-controlled trial	Control group: placebo Experimental group: 150 mg resveratrol twice daily	3 months	Significantly reduced aspartate aminotransferase (AST), glucose, LDL-C, total cholesterol; reduced the levels of tumour necrosis factor-alpha, cytokeratin 18 and fifibroblast growth factor 21	Chen et al. (2015)
Portulaca oleracea L. hydroalcohoic extract	MAFLD	74 patients	Randomized, double-blind clinical trial	Control group: placebo capsules Experimental group: 300 mg purslane extract	12 weeks	The levels of alanine aminotransferase (ALT), aspartate transaminase, γ-glutamyltransferase, fasting blood glucose, insulin resistance, triglyceride and LDL-C were significantly reduced	Darvish Damavandi et al. (2021)
Portulaca oleracea L. seeds	MAFLD	Sixty eligible individuals (12 men and 48 women)	Randomized controlled clinical trial	Control group: low-calorie diet Experimental group: 10 g/day of purslane seeds and low-calorie diet	8 weeks	Reduced fasting blood glucose, total cholesterol, and LDL-C	Gheflati et al. (2019)
Hesperidin (Combined use of flaxseed)	MAFLD	One hundred eligible patients	Randomized, controlled, clinical trial	Control group: lifestyle modification program Experimental group: lifestyle modification program with 30 g whole flaxseed powder; lifestyle modification program with 1 g hesperidin	12 weeks	The levels of ALT, insulin resistance, insulin sensitivity index, fasting blood glucose and fatty liver index decreased significantly	Yari et al. (2021)

(Continued on following page)

TABLE 7 | (*Continued*) Some Chinese medicine are used to treat liver diseases in clinic.

CM or its compounds	disease	Subject	Study design	Treatment groups	Length	Clinical outcome	References
				supplementation; lifestyle modification program with combination of 30 g flaxseed and 1 g hesperidin			
Artemisia annua L. Extract	Nonalcoholic liver dysfunction	79 subjects	Randomized, double-Blind, placebo-controlled	Control group: placebo Experimental group: powdered-water extract of *Artemisia annua*	4 weeks	Levels of AST and ALT were significantly reduced, and scores on the multidimensional fatigue scale were reduced, significantly enhancing liver function and health	Han et al. (2020)
Silymarin	NASH	78 patients	Randomized, double-blind, placebo controlled trial	Control group: placebo Experimental group: proprietary standardized silymarin preparation 420 mg or 700 mg	12 months	After 48 weeks of treatment, the MAFLD activity score (NAS) decreased by at least two points, fibrosis stage improved, baseline changes, serum ALT and AST decreased	Navarro et al. (2019)
Silymarin	NASH	99 patients	Randomized, double-blind, placebo-controlled trial	Control group: placebo Experimental group: Silymarin (three times daily)	48 weeks	The fibrosis was reduced and the ratio of AST to platelet index was also significantly decreased	Wah Kheong et al. (2017)

REFERENCES

Abdelfattah-Hassan, A., Shalaby, S. I., Khater, S. I., El-Shetry, E. S., Abd El Fadil, H., and Elsayed, S. A. (2019). Panax Ginseng Is superior to Vitamin E as a Hepatoprotector Against Cyclophosphamide-Induced Liver Damage. *Complement. Ther. Med.* 46, 95–102. doi:10.1016/j.ctim.2019.08.005

Abu Ahmad, N., Raizman, M., Weizmann, N., Wasek, B., Arning, E., Bottiglieri, T., et al. (2019). Betaine Attenuates Pathology by Stimulating Lipid Oxidation in Liver and Regulating Phospholipid Metabolism in Brain of Methionine-Choline-Deficient Rats. *FASEB J.* 33 (8), 9334–9349. doi:10.1096/fj.201802683R

Agatonovic-Kustrin, S., Kustrin, E., Gegechkori, V., and Morton, D. W. (2020). Anxiolytic Terpenoids and Aromatherapy for Anxiety and Depression. *Adv. Exp. Med. Biol.* 1260, 283–296. doi:10.1007/978-3-030-42667-5_11

Agrawal, A., and Bierut, L. J. (2012). Identifying Genetic Variation for Alcohol Dependence. *Alcohol. Res.* 34 (3), 274–281.

Alaca, N., Özbeyli, D., Uslu, S., Şahin, H. H., Yiğittürk, G., Kurtel, H., et al. (2017). Treatment with Milk Thistle Extract (Silybum marianum), Ursodeoxycholic Acid, or Their Combination Attenuates Cholestatic Liver Injury in Rats: Role of the Hepatic Stem Cells. *Turk J. Gastroenterol.* 28 (6), 476–484. doi:10.5152/tjg.2017.16742

Arulselvan, P., Fard, M. T., Tan, W. S., Gothai, S., Fakurazi, S., Norhaizan, M. E., et al. (2016). Role of Antioxidants and Natural Products in Inflammation. *Oxid Med. Cel Longev* 2016, 5276130. doi:10.1155/2016/5276130

Ateba, S. B., Mvondo, M. A., Ngeu, S. T., Tchoumtchoua, J., Awounfack, C. F., Njamen, D., et al. (2018). Natural Terpenoids Against Female Breast Cancer: A 5-year Recent Research. *Curr. Med. Chem.* 25 (27), 3162–3213. doi:10.2174/0929867325666180214110932

Auyeung, K. K., and Ko, J. K. (2009). Coptis Chinensis Inhibits Hepatocellular Carcinoma Cell Growth Through Nonsteroidal Anti-inflammatory Drug-Activated Gene Activation. *Int. J. Mol. Med.* 24 (4), 571–577. doi:10.3892/ijmm_00000267

Bai, J., Wu, J., Tang, R., Sun, C., Ji, J., Yin, Z., et al. (2020). Emodin, A Natural Anthraquinone, Suppresses Liver Cancer In Vitro and In Vivo by Regulating VEGFR2 and miR-34a. *Invest. New Drugs* 38 (2), 229–245. doi:10.1007/s10637-019-00777-5

Barandeh, B., Amini Mahabadi, J., Azadbakht, M., Gheibi Hayat, S. M., and Amini, A. (2019). The Protective Effects of Curcumin on Cytotoxic and Teratogenic Activity of Retinoic Acid in Mouse Embryonic Liver. *J. Cel Biochem* 120 (12), 19371–19376. doi:10.1002/jcb.28934

BasuRay, S., Smagris, E., Cohen, J. C., and Hobbs, H. H. (2017). The PNPLA3 Variant Associated with Fatty Liver Disease (I148M) Accumulates on Lipid Droplets by Evading Ubiquitylation. *Hepatology* 66 (4), 1111–1124. doi:10.1002/hep.29273

Bellezza, I., Giambanco, I., Minelli, A., and Donato, R. (2018). Nrf2-Keap1 Signaling in Oxidative and Reductive Stress. *Biochim. Biophys. Acta Mol. Cel Res* 1865 (5), 721–733. doi:10.1016/j.bbamcr.2018.02.010

Bogdan, A. R., Miyazawa, M., Hashimoto, K., and Tsuji, Y. (2016). Regulators of Iron Homeostasis: New Players in Metabolism, Cell Death, and Disease. *Trends Biochem. Sci.* 41 (3), 274–286. doi:10.1016/j.tibs.2015.11.012

Buendia, I., Michalska, P., Navarro, E., Gameiro, I., Egea, J., and León, R. (2016). Nrf2-ARE Pathway: An Emerging Target Against Oxidative Stress and Neuroinflammation in Neurodegenerative Diseases. *Pharmacol. Ther.* 157, 84–104. doi:10.1016/j.pharmthera.2015.11.003

Buzzetti, E., Pinzani, M., and Tsochatzis, E. A. (2016). The Multiple-Hit Pathogenesis of Non-alcoholic Fatty Liver Disease (NAFLD). *Metabolism* 65 (8), 1038–1048. doi:10.1016/j.metabol.2015.12.012

Caglayan, C., Kandemir, F. M., Darendelioğlu, E., Yıldırım, S., Kucukler, S., and Dortbudak, M. B. (2019). Rutin Ameliorates Mercuric Chloride-Induced Hepatotoxicity in Rats via Interfering with Oxidative Stress, Inflammation and Apoptosis. *J. Trace Elem. Med. Biol.* 56, 60–68. doi:10.1016/j.jtemb.2019.07.011

Cai, L., Zou, S., Liang, D., and Luan, L. (2018). Structural Characterization, Antioxidant and Hepatoprotective Activities of Polysaccharides from Sophorae Tonkinensis Radix. *Carbohydr. Polym.* 184, 354–365. doi:10.1016/j.carbpol.2017.12.083

Campana, L., and Iredale, J. P. (2017). Regression of Liver Fibrosis. *Semin. Liver Dis.* 37 (1), 1–10. doi:10.1055/s-0036-1597816

Cao, J., Miao, Q., Miao, S., Bi, L., Zhang, S., Yang, Q., et al. (2015). Tetramethylpyrazine (TMP) Exerts Antitumor Effects by Inducing Apoptosis and Autophagy in Hepatocellular Carcinoma. *Int. Immunopharmacol* 26 (1), 212–220. doi:10.1016/j.intimp.2015.03.028

Cao, L. J., Hou, Z. Y., Li, H. D., Zhang, B. K., Fang, P. F., Xiang, D. X., et al. (2017). The Ethanol Extract of Licorice (Glycyrrhiza Uralensis) Protects Against Triptolide-Induced Oxidative Stress Through Activation of Nrf2. *Evid. Based Complement. Alternat Med.* 2017, 2752389. doi:10.1155/2017/2752389

Cao, T., Lu, Y., Zhu, M., Cheng, J., Ye, B., Fang, N., et al. (2020). Effects of Salvia Miltiorrhiza and Radix Astragali on the TGF-β/Smad/Wnt Pathway and the Pathological Process of Liver Fibrosis in Rats. *Cel Mol Biol (Noisy-le-grand)* 66 (6), 46–51. doi:10.14715/cmb/2020.66.6.9

Ceccarini, M. R., Vannini, S., Cataldi, S., Moretti, M., Villarini, M., Fioretti, B., et al. (2016). In Vitro Protective Effects of Lycium Barbarum Berries Cultivated in Umbria (Italy) on Human Hepatocellular Carcinoma Cells. *Biomed. Res. Int.* 2016, 7529521. doi:10.1155/2016/7529521

Ceni, E., Mello, T., and Galli, A. (2014). Pathogenesis of Alcoholic Liver Disease: Role of Oxidative Metabolism. *World J. Gastroenterol.* 20 (47), 17756–17772. doi:10.3748/wjg.v20.i47.17756

Chai, F. N., Ma, W. Y., Zhang, J., Xu, H. S., Li, Y. F., Zhou, Q. D., et al. (2018a). Coptisine from Rhizoma Coptidis Exerts an Anti-cancer Effect on Hepatocellular Carcinoma by Up-Regulating miR-122. *Biomed. Pharmacother.* 103, 1002–1011. doi:10.1016/j.biopha.2018.04.052

Chai, F. N., Zhang, J., Xiang, H. M., Xu, H. S., Li, Y. F., Ma, W. Y., et al. (2018b). Protective Effect of Coptisine from Rhizoma Coptidis on LPS/D-GalN-induced Acute Liver Failure in Mice Through Up-Regulating Expression of miR-122. *Biomed. Pharmacother.* 98, 180–190. doi:10.1016/j.biopha.2017.11.133

Chan, H. H. L., and Ng, T. (2020). Traditional Chinese Medicine (TCM) and Allergic Diseases. *Curr. Allergy Asthma Rep.* 20 (11), 67. doi:10.1007/s11882-020-00959-9

Chan, K. W., and Ho, W. S. (2015). Anti-oxidative and Hepatoprotective Effects of Lithospermic Acid Against Carbon Tetrachloride-Induced Liver Oxidative Damage In Vitro and In Vivo. *Oncol. Rep.* 34 (2), 673–680. doi:10.3892/or.2015.4068

Chávez-Talavera, O., Tailleux, A., Lefebvre, P., and Staels, B. (2017). Bile Acid Control of Metabolism and Inflammation in Obesity, Type 2 Diabetes, Dyslipidemia, and Nonalcoholic Fatty Liver Disease. *Gastroenterology* 152 (7), 1679–1694.e3. doi:10.1053/j.gastro.2017.01.055

Chen, Q., Zhang, H., Cao, Y., Li, Y., Sun, S., Zhang, J., et al. (2017). Schisandrin B Attenuates CCl4-Induced Liver Fibrosis in Rats by Regulation of Nrf2-ARE and TGF-β/Smad Signaling Pathways. *Drug Des. Devel Ther.* 11, 2179–2191. doi:10.2147/DDDT.S137507

Chen, S., Zhao, X., Ran, L., Wan, J., Wang, X., Qin, Y., et al. (2015). Resveratrol Improves Insulin Resistance, Glucose and Lipid Metabolism in Patients with Non-alcoholic Fatty Liver Disease: a Randomized Controlled Trial. *Dig. Liver Dis.* 47 (3), 226–232. doi:10.1016/j.dld.2014.11.015

Chen, Y., Yao, F., Ming, K., Wang, D., Hu, Y., and Liu, J. (2016). Polysaccharides from Traditional Chinese Medicines: Extraction, Purification, Modification, and Biological Activity. *Molecules* 21 (12), 1705. doi:10.3390/molecules21121705

Chen, Z., Liu, F., Zheng, N., Guo, M., Bao, L., Zhan, Y., et al. (2019). Wuzhi Capsule (Schisandra Sphenanthera Extract) Attenuates Liver Steatosis and Inflammation During Non-alcoholic Fatty Liver Disease Development. *Biomed. Pharmacother.* 110, 285–293. doi:10.1016/j.biopha.2018.11.069

Cheng, N., Chen, S., Liu, X., Zhao, H., and Cao, W. (2019). Impact of SchisandraChinensis Bee Pollen on Nonalcoholic Fatty Liver Disease and Gut Microbiota in HighFat Diet Induced Obese Mice. *Nutrients* 11 (2), 346. doi:10.3390/nu11020346

Cheng, P., Wang, T., Li, W., Muhammad, I., Wang, H., Sun, X., et al. (2017). Baicalin Alleviates Lipopolysaccharide-Induced Liver Inflammation in Chicken by Suppressing TLR4-Mediated NF-Kb Pathway. *Front. Pharmacol.* 8, 547. doi:10.3389/fphar.2017.00547

Chopyk, D. M., and Grakoui, A. (2020). Contribution of the Intestinal Microbiome and Gut Barrier to Hepatic Disorders. *Gastroenterology* 159 (3), 849–863. doi:10.1053/j.gastro.2020.04.077

Chuang, H. M., Su, H. L., Li, C., Lin, S. Z., Yen, S. Y., Huang, M. H., et al. (2016). The Role of Butylidenephthalide in Targeting the Microenvironment Which Contributes to Liver Fibrosis Amelioration. *Front. Pharmacol.* 7, 112. doi:10.3389/fphar.2016.00112

Commission, C.P. (2015). *Pharmacopoeia of the People's republic of China*. Beijing: China medical science and technology press.

Crocenzi, F. A., Zucchetti, A. E., Boaglio, A. C., Barosso, I. R., Sanchez Pozzi, E. J., Mottino, A. D., et al. (2012). Localization Status of Hepatocellular Transporters in Cholestasis. *Front. Biosci. (Landmark Ed.* 17, 1201–1218. doi:10.2741/3981

Cui, Y., Jiang, L., Shao, Y., Mei, L., and Tao, Y. (2019). Anti-alcohol Liver Disease Effect of Gentianae Macrophyllae Extract Through MAPK/JNK/p38 Pathway. *J. Pharm. Pharmacol.* 71 (2), 240–250. doi:10.1111/jphp.13027

D'Atanasio, E., Trombetta, B., Bonito, M., Finocchio, A., Di Vito, G., Seghizzi, M., et al. (2018). The Peopling of the Last Green Sahara Revealed by High-Coverage Resequencing of Trans-saharan Patrilineages. *Genome Biol.* 19 (1), 20. doi:10.1186/s13059-018-1393-5

Darvish Damavandi, R., Shidfar, F., Najafi, M., Janani, L., Masoodi, M., Akbari-Fakhrabadi, M., et al. (2021). Effect of Portulaca Oleracea (Purslane) Extract on Liver Enzymes, Lipid Profile, and Glycemic Status in Nonalcoholic Fatty Liver Disease: A Randomized, Double-Blind Clinical Trial. *Phytother Res.* 35 (6), 3145–3156. doi:10.1002/ptr.6972

Dewidar, B., Meyer, C., Dooley, S., and Meindl-Beinker, A. N. (2019). TGF-β in Hepatic Stellate Cell Activation and Liver Fibrogenesis-Updated 2019. *Cells* 8 (11), 1419. doi:10.3390/cells8111419

Ding, C. H., and Zhu, H. (2020). Isatidis Folium Alleviates Acetaminophen-Induced Liver Injury in Mice by Enhancing the Endogenous Antioxidant System. *Environ. Toxicol.* 35 (11), 1251–1259. doi:10.1002/tox.22990

Ding, H. R., Wang, J. L., Ren, H. Z., and Shi, X. L. (2018a). Lipometabolism and Glycometabolism in Liver Diseases. *Biomed. Res. Int.* 2018, 1287127. doi:10.1155/2018/1287127

Ding, Y., Liu, P., Chen, Z. L., Zhang, S. J., Wang, Y. Q., Cai, X., et al. (2018b). Emodin Attenuates Lipopolysaccharide-Induced Acute Liver Injury via Inhibiting the TLR4 Signaling Pathway In Vitro and In Vivo. *Front. Pharmacol.* 9, 962. doi:10.3389/fphar.2018.00962

Dodge, N. C., Jacobson, J. L., and Jacobson, S. W. (2014). Protective Effects of the Alcohol Dehydrogenase-Adh1b*3 Allele on Attention and Behavior Problems in Adolescents Exposed to Alcohol During Pregnancy. *Neurotoxicol Teratol* 41, 43–50. doi:10.1016/j.ntt.2013.11.003

Dong, Q., Chu, F., Wu, C., Huo, Q., Gan, H., Li, X., et al. (2016). Scutellaria Baicalensis Georgi Extract Protects Against Alcohol Induced Acute Liver Injury in Mice and Affects the Mechanism of ER Stress. *Mol. Med. Rep.* 13 (4), 3052–3062. doi:10.3892/mmr.2016.4941

Dong, X., Fu, J., Yin, X., Yang, C., and Ni, J. (2017). Aloe-emodin Induces Apoptosis in Human Liver HL-7702 Cells Through Fas Death Pathway and the Mitochondrial Pathway by Generating Reactive Oxygen Species. *Phytother Res.* 31 (6), 927–936. doi:10.1002/ptr.5820

Du, X. S., Li, H. D., Yang, X. J., Li, J. J., Xu, J. J., Chen, Y., et al. (2019). Wogonin Attenuates Liver Fibrosis via Regulating Hepatic Stellate Cell Activation and Apoptosis. *Int. Immunopharmacol* 75, 105671. doi:10.1016/j.intimp.2019.05.056

Duan, X., Meng, Q., Wang, C., Liu, Z., Liu, Q., Sun, H., et al. (2017). Calycosin Attenuates Triglyceride Accumulation and Hepatic Fibrosis in Murine Model of Non-alcoholic Steatohepatitis via Activating Farnesoid X Receptor. *Phytomedicine* 25, 83–92. doi:10.1016/j.phymed.2016.12.006

Egresi, A., Süle, K., Szentmihályi, K., Blázovics, A., Fehér, E., Hagymási, K., et al. (2020). Impact of Milk Thistle (Silybum marianum) on the Mycotoxin Caused Redox-Homeostasis Imbalance of Ducks Liver. *Toxicon* 187, 181–187. doi:10.1016/j.toxicon.2020.09.002

El-Saied, M. A., Sobeh, M., Abdo, W., Badr, O. M., Youssif, L. T., Elsayed, I. H., et al. (2018). Rheum Palmatum Root Extract Inhibits Hepatocellular Carcinoma in Rats Treated with Diethylnitrosamine. *J. Pharm. Pharmacol.* 70 (6), 821–829. doi:10.1111/jphp.12899

El-Serag, H. B. (2012). Epidemiology of Viral Hepatitis and Hepatocellular Carcinoma. *Gastroenterology* 142 (6), 1264–e1. doi:10.1053/j.gastro.2011.12.061

Elsawy, H., Badr, G. M., Sedky, A., Abdallah, B. M., Alzahrani, A. M., and Abdel-Moneim, A. M. (2019). Rutin Ameliorates Carbon Tetrachloride (CCl4)-Induced Hepatorenal Toxicity and Hypogonadism in Male Rats. *PeerJ* 7, e7011. doi:10.7717/peerj.7011

Fan, Q., Zhao, B., Wang, C., Zhang, J., Wu, J., Wang, T., et al. (2018). Subchronic Toxicity Studies of Cortex Dictamni Extracts in Mice and its Potential Hepatotoxicity Mechanisms In Vitro. *Molecules* 23 (10), 2486. doi:10.3390/molecules23102486

Fanning, G. C., Zoulim, F., Hou, J., and Bertoletti, A. (2019). Therapeutic Strategies for Hepatitis B Virus Infection: Towards a Cure. *Nat. Rev. Drug Discov.* 18 (11), 827–844. doi:10.1038/s41573-019-0037-0

Feng, R., Chen, J. H., Liu, C. H., Xia, F. B., Xiao, Z., Zhang, X., et al. (2019). A Combination of Pueraria Lobata and Silybum marianum Protects Against Alcoholic Liver Disease in Mice. *Phytomedicine* 58, 152824. doi:10.1016/j.phymed.2019.152824

Feng, T., Wei, Y., Lee, R. J., and Zhao, L. (2017). Liposomal Curcumin and its Application in Cancer. *Int. J. Nanomedicine* 12, 6027–6044. doi:10.2147/IJN.S132434

Forner, A., Llovet, J. M., and Bruix, J. (2012). Hepatocellular Carcinoma. *Lancet* 379 (9822), 1245–1255. doi:10.1016/S0140-6736(11)61347-0

Forner, A., Reig, M., and Bruix, J. (2018). Hepatocellular Carcinoma. *Lancet* 391 (10127), 1301–1314. doi:10.1016/S0140-6736(18)30010-2

Friedman, S. L., Neuschwander-Tetri, B. A., Rinella, M., and Sanyal, A. J. (2018). Mechanisms of NAFLD Development and Therapeutic Strategies. *Nat. Med.* 24 (7), 908–922. doi:10.1038/s41591-018-0104-9

Friedman, S. L. (1993). Seminars in Medicine of the Beth Israel Hospital, Boston. The Cellular Basis of Hepatic Fibrosis. Mechanisms and Treatment Strategies. *N. Engl. J. Med.* 328 (25), 1828–1835. doi:10.1056/NEJM199306243282508

Fu, K., Xu, M., Zhou, Y., Li, X., Wang, Z., Liu, X., et al. (2020). The Status Quo and Way Forwards on the Development of Tibetan Medicine and the Pharmacological Research of Tibetan Materia Medica. *Pharmacol. Res.* 155, 104688. doi:10.1016/j.phrs.2020.104688

Gan, D., Zhang, W., Huang, C., Chen, J., He, W., Wang, A., et al. (2018a). Ursolic Acid Ameliorates CCl4-Induced Liver Fibrosis Through the NOXs/ROS Pathway. *J. Cel Physiol* 233 (10), 6799–6813. doi:10.1002/jcp.26541

Gan, F., Liu, Q., Liu, Y., Huang, D., Pan, C., Song, S., et al. (2018b). Lycium Barbarum Polysaccharides Improve CCl4-Induced Liver Fibrosis, Inflammatory Response and TLRs/NF-kB Signaling Pathway Expression in Wistar Rats. *Life Sci.* 192, 205–212. doi:10.1016/j.lfs.2017.11.047

Ganbold, M., Owada, Y., Ozawa, Y., Shimamoto, Y., Ferdousi, F., Tominaga, K., et al. (2019). Isorhamnetin Alleviates Steatosis and Fibrosis in Mice with Nonalcoholic Steatohepatitis. *Sci. Rep.* 9 (1), 16210. doi:10.1038/s41598-019-52736-y

Gao, L. N., Yan, K., Cui, Y. L., Fan, G. W., and Wang, Y. F. (2015). Protective Effect of Salvia Miltiorrhiza and Carthamus tinctorius Extract Against Lipopolysaccharide-Induced Liver Injury. *World J. Gastroenterol.* 21 (30), 9079–9092. doi:10.3748/wjg.v21.i30.9079

Gao, X., Guo, S., Zhang, S., Liu, A., Shi, L., and Zhang, Y. (2018). Matrine Attenuates Endoplasmic Reticulum Stress and Mitochondrion Dysfunction in Nonalcoholic Fatty Liver Disease by Regulating SERCA Pathway. *J. Transl Med.* 16 (1), 319. doi:10.1186/s12967-018-1685-2

Gao, X., Li, C., Tang, Y. L., Zhang, H., and Chan, S. W. (2016). Effect of Hedyotis Diffusa Water Extract on Protecting Human Hepatocyte Cells (LO2) from H2O2-Induced Cytotoxicity. *Pharm. Biol.* 54 (7), 1148–1155. doi:10.3109/13880209.2015.1056310

Gao, X., and Liu, L. (2016). Research Progress on Epidemiology and Pathogenesis of Alcoholic Liver Disease. *Chin. J. Gastroenterol. Imaging* 6 (02), 62–65.

Gao, Z., Zhang, J., Wei, L., Yang, X., Zhang, Y., Cheng, B., et al. (2020). The Protective Effects of Imperatorin on Acetaminophen Overdose-Induced Acute Liver Injury. *Oxid Med. Cel Longev* 2020, 8026838. doi:10.1155/2020/8026838

Ge, L., Xiao, L., Wan, H., Li, J., Lv, K., Peng, S., et al. (2019). Chemical Constituents from *Lonicera japonica* Flower Buds and Their Anti-hepatoma and Anti-HBV Activities. *Bioorg. Chem.* 92, 103198. doi:10.1016/j.bioorg.2019.103198

Ghaffari, A., Rafraf, M., Navekar, R., Sepehri, B., Asghari-Jafarabadi, M., and Ghavami, S. M. (2019). Turmeric and Chicory Seed Have Beneficial Effects on Obesity Markers and Lipid Profile in Non-alcoholic Fatty Liver Disease (NAFLD). *Int. J. Vitam Nutr. Res.* 89 (5-6), 293–302. doi:10.1024/0300-9831/a000568

Gheflati, A., Adelnia, E., and Nadjarzadeh, A. (2019). The Clinical Effects of Purslane (Portulaca Oleracea) Seeds on Metabolic Profiles in Patients with Nonalcoholic Fatty Liver Disease: A Randomized Controlled Clinical Trial. *Phytother Res.* 33 (5), 1501–1509. doi:10.1002/ptr.6342

Goh, Z. H., Tee, J. K., and Ho, H. K. (2020). An Evaluation of the In Vitro Roles and Mechanisms of Silibinin in Reducing Pyrazinamide- and Isoniazid-Induced Hepatocellular Damage. *Int. J. Mol. Sci.* 21 (10), 3714. doi:10.3390/ijms21103714

Gong, L., Zhou, H., Wang, C., He, L., Guo, C., Peng, C., et al. (2021). Hepatoprotective Effect of Forsythiaside a Against Acetaminophen-Induced Liver Injury in Zebrafish: Coupling Network Pharmacology with Biochemical Pharmacology. *J. Ethnopharmacol* 271, 113890. doi:10.1016/j.jep.2021.113890

Gu, M., Zhang, S., Zhao, Y., Huang, J., Wang, Y., Li, Y., et al. (2017). Cycloastragenol Improves Hepatic Steatosis by Activating Farnesoid X Receptor Signalling. *Pharmacol. Res.* 121, 22–32. doi:10.1016/j.phrs.2017.04.021

Gu, X., and Manautou, J. E. (2012). Molecular Mechanisms Underlying Chemical Liver Injury. *Expert Rev. Mol. Med.* 14, e4. doi:10.1017/S1462399411002110

Gündüz, E., Dursun, R., Zengin, Y., İçer, M., Durgun, H. M., Kanıcı, A., et al. (2015). Lycium Barbarum Extract Provides Effective protection Against Paracetamol-Induced Acute Hepatotoxicity in Rats. *Int. J. Clin. Exp. Med.* 8 (5), 7898–7905.

Guo, S., Wang, G., and Yang, Z. (2021). Ligustilide Alleviates the Insulin Resistance, Lipid Accumulation, and Pathological Injury with Elevated Phosphorylated AMPK Level in Rats with Diabetes Mellitus. *J. Recept Signal. Transduct Res.* 41 (1), 85–92. doi:10.1080/10799893.2020.1789877

Guoyin, Z., Hao, P., Min, L., Wei, G., Zhe, C., and Changquan, L. (20172017). Antihepatocarcinoma Effect of Portulaca Oleracea L. In Mice by PI3K/Akt/mTOR and Nrf2/HO-1/nf-Kb Pathway. *Evid. Based Complement. Alternat Med.* 2017, 8231358. doi:10.1155/2017/8231358

Gupta, V. K., Siddiqi, N. J., Ojha, A. K., and Sharma, B. (2019). Hepatoprotective Effect of Aloe Vera Against Cartap- and Malathion-Induced Toxicity in Wistar Rats. *J. Cel Physiol* 234 (10), 18329–18343. doi:10.1002/jcp.28466

Hajighasem, A., Farzanegi, P., Mazaheri, Z., Naghizadeh, M., and Salehi, G. (2018). Effects of Resveratrol, Exercises and Their Combination on Farnesoid X Receptor, Liver X Receptor and Sirtuin 1 Gene Expression and Apoptosis in the Liver of Elderly Rats with Nonalcoholic Fatty Liver. *PeerJ* 6, e5522. doi:10.7717/peerj.5522

Han, B., Gao, Y., Wang, Y., Wang, L., Shang, Z., Wang, S., et al. (2016). Protective Effect of a Polysaccharide from Rhizoma Atractylodis Macrocephalae on Acute Liver Injury in Mice. *Int. J. Biol. Macromol* 87, 85–91. doi:10.1016/j.ijbiomac.2016.01.086

Han, B., Kim, S. M., Nam, G. E., Kim, S. H., Park, S. J., Park, Y. K., et al. (2020). A Randomized, Double-Blind, Placebo-Controlled, Multi-Centered Clinical Study to Evaluate the Efficacy and Safety of Artemisia Annua L. Extract for Improvement of Liver Function. *Clin. Nutr. Res.* 9 (4), 258–270. doi:10.7762/cnr.2020.9.4.258

Han, C., Wei, Y., Wang, X., Ba, C., and Shi, W. (2019). Protective Effect of Salvia Miltiorrhiza Polysaccharides on Liver Injury in Chickens. *Poult. Sci.* 98 (9), 3496–3503. doi:10.3382/ps/pez153

Hasan, I. H., El-Desouky, M. A., Hozayen, W. G., and Abd el Aziz, G. M. (2016). Protective Effect of Zingiber Officinale Against CCl4-Induced Liver Fibrosis Is Mediated Through Downregulating the TGF-β1/Smad3 and NF-κb/iκb Pathways. *Pharmacology* 97 (1-2), 1–9. doi:10.1159/000441229

He, Y., and Liu, Y. (2021). Research Progress of Intestinal Bacterial Overgrowth in Patients with Liver Cirrhosis. *J. integrated Chin. West. Med. Liver Dis.* 31 (03), 286–288.

Heiss, E. H., Schachner, D., Zimmermann, K., and Dirsch, V. M. (2013). Glucose Availability Is a Decisive Factor for Nrf2-Mediated Gene Expression. *Redox Biol.* 1, 359–365. doi:10.1016/j.redox.2013.06.001

Hernandez-Gea, V., and Friedman, S. L. (2011). Pathogenesis of Liver Fibrosis. *Annu. Rev. Pathol.* 6, 425–456. doi:10.1146/annurev-pathol-011110-130246

Hesketh, T., and Zhu, W. X. (1997). Health in China. Traditional Chinese Medicine: One Country, Two Systems. *BMJ* 315 (7100), 115–117. doi:10.1136/bmj.315.7100.115

Ho, C., Gao, Y., Zheng, D., Liu, Y., Shan, S., Fang, B., et al. (2019). Alisol A Attenuates High-Fat-Diet-Induced Obesity and Metabolic Disorders via the AMPK/ACC/SREBP-1c Pathway. *J. Cel Mol Med* 23 (8), 5108–5118. doi:10.1111/jcmm.14380

Ho, C. Y., Cheng, Y. T., Chau, C. F., and Yen, G. C. (2012). Effect of Diallyl Sulfide on In Vitro and In Vivo Nrf2-Mediated Pulmonic Antioxidant Enzyme Expression via Activation ERK/p38 Signaling Pathway. *J. Agric. Food Chem.* 60 (1), 100–107. doi:10.1021/jf203800d

Holt, M., and Ju, C. (2010). "Drug-induced Liver Injury," in *Handb Exp Pharmacol.* Editor J. E. Barrett (New York, NY: Springer), 196.

Hosny, S., Sahyon, H., Youssef, M., and Negm, A. (2021). Oleanolic Acid Suppressed DMBA-Induced Liver Carcinogenesis Through Induction of Mitochondrial-Mediated Apoptosis and Autophagy. *Nutr. Cancer* 73 (6), 968–982. doi:10.1080/01635581.2020.1776887

Hu, B., Gongji, G., Ta, N., and Wuli, J. (2019). Research Progress of Alcoholic Liver Disease. *J. inner mongolia Univ. nationalities* 34 (06), 535–538.

Hu, J., and Liu, K. (2017). Complete and Incomplete Hepatitis B Virus Particles: Formation, Function, and Application. *Viruses* 9 (3), 56. doi:10.3390/v9030056

Hu, N., Guo, C., Dai, X., Wang, C., Gong, L., Yu, L., et al. (2020a). Forsythiae Fructuse Water Extract Attenuates Liver Fibrosis via TLR4/MyD88/NF-Kb and TGF-B/smads Signaling Pathways. *J. Ethnopharmacol* 262, 113275. doi:10.1016/j.jep.2020.113275

Hu, N., Wang, C., Dai, X., Zhou, M., Gong, L., Yu, L., et al. (2020b). Phillygenin Inhibits LPS-Induced Activation and Inflammation of LX2 Cells by TLR4/MyD88/NF-Kb Signaling Pathway. *J. Ethnopharmacol* 248, 112361. doi:10.1016/j.jep.2019.112361

Hu, Y., Bi, X., Zhao, P., Zheng, H., and Huang, X. (2015). Cytotoxic Activities, SAR and Anti-invasion Effects of Butylphthalide Derivatives on Human Hepatocellular Carcinoma SMMC7721 Cells. *Molecules* 20 (11), 20312–20319. doi:10.3390/molecules201119699

Huang, L., Li, Y., Pan, H., Lu, Y., Zhou, X., and Shi, F. (2020). Cortex Dictamni-Induced Liver Injury in Mice: The Role of P450-Mediated Metabolic Activation of Furanoids. *Toxicol. Lett.* 330, 41–52. doi:10.1016/j.toxlet.2020.05.004

Huang, W. H., Liao, W. R., and Sun, R. X. (2016). Astragalus Polysaccharide Induces the Apoptosis of Human Hepatocellular Carcinoma Cells by Decreasing the Expression of Notch1. *Int. J. Mol. Med.* 38 (2), 551–557. doi:10.3892/ijmm.2016.2632

Huang, Y. C., Tsay, H. J., Lu, M. K., Lin, C. H., Yeh, C. W., Liu, H. K., et al. (2017). Astragalus Membranaceus-Polysaccharides Ameliorates Obesity, Hepatic Steatosis, Neuroinflammation and Cognition Impairment without Affecting Amyloid Deposition in Metabolically Stressed APPswe/PS1dE9 Mice. *Int. J. Mol. Sci.* 18 (12), 2746. doi:10.3390/ijms18122746

Hung, T. C., Jassey, A., Lin, C. J., Liu, C. H., Lin, C. C., Yen, M. H., et al. (2018). Methanolic Extract of Rhizoma Coptidis Inhibits the Early Viral Entry Steps of Hepatitis C Virus Infection. *Viruses* 10 (12), 669. doi:10.3390/v10120669

Jang, E., Kim, S. Y., Lee, N. R., Yi, C. M., Hong, D. R., Lee, W. S., et al. (2017). Evaluation of Antitumor Activity of Artemisia Capillaris Extract Against Hepatocellular Carcinoma Through the Inhibition of IL-6/STAT3 Signaling Axis. *Oncol. Rep.* 37 (1), 526–532. doi:10.3892/or.2016.5283

Jang, M. K., Yun, Y. R., Kim, S. H., Kim, J. H., and Jung, M. H. (2016). Protective Effect of Gomisin N Against Endoplasmic Reticulum Stress-Induced Hepatic Steatosis. *Biol. Pharm. Bull.* 39 (5), 832–838. doi:10.1248/bpb.b15-01020

Jarret, A., McFarland, A. P., Horner, S. M., Kell, A., Schwerk, J., Hong, M., et al. (2016). Hepatitis-C-virus-induced microRNAs Dampen Interferon-Mediated Antiviral Signaling. *Nat. Med.* 22 (12), 1475–1481. doi:10.1038/nm.4211

Jemal, A., Bray, F., Center, M. M., Ferlay, J., Ward, E., and Forman, D. (2011). Global Cancer Statistics. *CA Cancer J. Clin.* 61 (2), 69–90. doi:10.3322/caac.20107

Jia, R., Gu, Z., He, Q., Du, J., Cao, L., Jeney, G., et al. (2019). Anti-oxidative, Anti-inflammatory and Hepatoprotective Effects of Radix Bupleuri Extract Against Oxidative Damage in Tilapia (*Oreochromis niloticus*) via Nrf2 and TLRs Signaling Pathway. *Fish. Shellfish Immunol.* 93, 395–405. doi:10.1016/j.fsi.2019.07.080

Jiang, P., Zhang, X., Huang, Y., Cheng, N., and Ma, Y. (2017a). Hepatotoxicity Induced by Sophora Flavescens and Hepatic Accumulation of Kurarinone, a Major Hepatotoxic Constituent of Sophora Flavescens in Rats. *Molecules* 22 (11), 1809. doi:10.3390/molecules22111809

Jiang, Y., Fan, X., Wang, Y., Chen, P., Zeng, H., Tan, H., et al. (2015). Schisandrol B Protects Against Acetaminophen-Induced Hepatotoxicity by Inhibition of CYP-Mediated Bioactivation and Regulation of Liver Regeneration. *Toxicol. Sci.* 143 (1), 107–115. doi:10.1093/toxsci/kfu216

Jiang, Y., Zhang, L., and Rupasinghe, H. P. (2017b). Antiproliferative Effects of Extracts from Salvia Officinalis L. And Saliva Miltiorrhiza Bunge on Hepatocellular Carcinoma Cells. *Biomed. Pharmacother.* 85, 57–67. doi:10.1016/j.biopha.2016.11.113

Jin, H., Lian, N., Bian, M., Zhang, C., Chen, X., Shao, J., et al. (2018). Oroxylin A Prevents Alcohol-Induced Hepatic Steatosis Through Inhibition of Hypoxia Inducible Factor 1alpha. *Chem. Biol. Interact* 285, 14–20. doi:10.1016/j.cbi.2018.02.025

Jin, H., Sakaida, I., Tsuchiya, M., and Okita, K. (2005). Herbal Medicine Rhei Rhizome Prevents Liver Fibrosis in Rat Liver Cirrhosis Induced by a Choline-Deficient L-Amino Acid-Defined Diet. *Life Sci.* 76 (24), 2805–2816. doi:10.1016/j.lfs.2004.09.041

Jin, Q., Jiang, S., Wu, Y. L., Bai, T., Yang, Y., Jin, X., et al. (2014). Hepatoprotective Effect of Cryptotanshinone from Salvia Miltiorrhiza in D-Galactosamine/lipopolysaccharide-Induced Fulminant Hepatic Failure. *Phytomedicine* 21 (2), 141–147. doi:10.1016/j.phymed.2013.07.016

Jindal, R., Sinha, R., and Brar, P. (2019). Evaluating the Protective Efficacy of Silybum marianum Against Deltamethrin Induced Hepatotoxicity in Piscine Model. *Environ. Toxicol. Pharmacol.* 66, 62–68. doi:10.1016/j.etap.2018.12.014

Jung, J. C., Lee, Y. H., Kim, S. H., Kim, K. J., Kim, K. M., Oh, S., et al. (2016). Hepatoprotective Effect of Licorice, the Root of Glycyrrhiza Uralensis Fischer, in Alcohol-Induced Fatty Liver Disease. *BMC Complement. Altern. Med.* 16, 19. doi:10.1186/s12906-016-0997-0

Jung, K. H., Rumman, M., Yan, H., Cheon, M. J., Choi, J. G., Jin, X., et al. (2018). An Ethyl Acetate Fraction of Artemisia Capillaris (ACE-63) Induced Apoptosis and Anti-angiogenesis via Inhibition of PI3K/AKT Signaling in Hepatocellular Carcinoma. *Phytother Res.* 32 (10), 2034–2046. doi:10.1002/ptr.6135

Jung, S., Son, H., Hwang, C. E., Cho, K. M., Park, S. W., Kim, H., et al. (2020). The Root of Polygonum Multiflorum Thunb. Alleviates Non-alcoholic Steatosis and Insulin Resistance in High Fat Diet-Fed Mice. *Nutrients* 12 (8), 2353. doi:10.3390/nu12082353

Kalyanaraman, B. (2013). Teaching the Basics of Redox Biology to Medical and Graduate Students: Oxidants, Antioxidants and Disease Mechanisms. *Redox Biol.* 1, 244–257. doi:10.1016/j.redox.2013.01.014

Kandeil, M. A., Hashem, R. M., Mahmoud, M. O., Hetta, M. H., and Tohamy, M. A. (2019). Zingiber Officinale Extract and omega-3 Fatty Acids Ameliorate Endoplasmic Reticulum Stress in a Nonalcoholic Fatty Liver Rat Model. *J. Food Biochem.* 43 (12), e13076. doi:10.1111/jfbc.13076

Ke, Z., Zhao, Y., Tan, S., Chen, H., Li, Y., Zhou, Z., et al. (2020). Citrus Reticulata Blanco Peel Extract Ameliorates Hepatic Steatosis, Oxidative Stress and Inflammation in HF and MCD Diet-Induced NASH C57BL/6 J Mice. *J. Nutr. Biochem.* 83, 108426. doi:10.1016/j.jnutbio.2020.108426

Kim, H. G., Lee, S. B., Lee, J. S., Kim, W. Y., Choi, S. H., and Son, C. G. (2017a). Artemisia Iwayomogi Plus Curcuma Longa Synergistically Ameliorates Nonalcoholic Steatohepatitis in HepG2 Cells. *Evid. Based Complement. Alternat Med.* 2017, 4390636. doi:10.1155/2017/4390636

Kim, H. J., Park, K. K., Chung, W. Y., Lee, S. K., and Kim, K. R. (2017b). Protective Effect of White-fleshed Peach (Prunus Persica (L.) Batsch) on Chronic Nicotine-Induced Toxicity. *J. Cancer Prev.* 22 (1), 22–32. doi:10.15430/JCP.2017.22.1.22

Kim, H. Y., Kim, J. K., Choi, J. H., Jung, J. Y., Oh, W. Y., Kim, D. C., et al. (2010). Hepatoprotective Effect of Pinoresinol on Carbon Tetrachloride-Induced Hepatic Damage in Mice. *J. Pharmacol. Sci.* 112 (1), 105–112. doi:10.1254/jphs.09234fp

Kim, J., Jung, K. H., Yan, H. H., Cheon, M. J., Kang, S., Jin, X., et al. (2018). Artemisia Capillaris Leaves Inhibit Cell Proliferation and Induce Apoptosis in Hepatocellular Carcinoma. *BMC Complement. Altern. Med.* 18 (1), 147. doi:10.1186/s12906-018-2217-6

Kim, J., Kim, C. S., Jo, K., Lee, I. S., Kim, J. H., and Kim, J. S. (2020a). POCU1b, the n-Butanol Soluble Fraction of Polygoni Cuspidati Rhizoma et Radix, Attenuates Obesity, Non-Alcoholic Fatty Liver, and Insulin Resistance via Inhibitions of Pancreatic Lipase, cAMP-Dependent PDE Activity, AMPK Activation, and SOCS-3 Suppression. *Nutrients* 12 (12), 3612. doi:10.3390/nu12123612

Kim, T., Song, B., Cho, K. S., and Lee, I. S. (2020b). Therapeutic Potential of Volatile Terpenes and Terpenoids from Forests for Inflammatory Diseases. *Int. J. Mol. Sci.* 21 (6), 2187. doi:10.3390/ijms21062187

Klaikeaw, N., Wongphoom, J., Werawatganon, D., Chayanupatkul, M., and Siriviriyakul, P. (2020). Anti-inflammatory and Anti-oxidant Effects of Aloe Vera in Rats with Non-alcoholic Steatohepatitis. *World J. Hepatol.* 12 (7), 363–377. doi:10.4254/wjh.v12.i7.363

Kolodziejczyk, A. A., Zheng, D., Shibolet, O., and Elinav, E. (2019). The Role of the Microbiome in NAFLD and NASH. *EMBO Mol. Med.* 11 (2), e9302. doi:10.15252/emmm.201809302

Koneru, M., Sahu, B. D., Gudem, S., Kuncha, M., Ravuri, H. G., Kumar, J. M., et al. (2017). Polydatin Alleviates Alcohol-Induced Acute Liver Injury in Mice: Relevance of Matrix Metalloproteinases (MMPs) and Hepatic Antioxidants. *Phytomedicine* 27, 23–32. doi:10.1016/j.phymed.2017.01.013

Kong, Z. L., Kuo, H. P., Johnson, A., Wu, L. C., and Chang, K. L. B. (2019). Curcumin-Loaded Mesoporous Silica Nanoparticles Markedly Enhanced Cytotoxicity in Hepatocellular Carcinoma Cells. *Int. J. Mol. Sci.* 20 (12), 2918. doi:10.3390/ijms20122918

Kuo, C. Y., Chiu, V., Hsieh, P. C., Huang, C. Y., Huang, S. J., Tzeng, I. S., et al. (2020). Chrysophanol Attenuates Hepatitis B Virus X Protein-Induced Hepatic Stellate Cell Fibrosis by Regulating Endoplasmic Reticulum Stress and Ferroptosis. *J. Pharmacol. Sci.* 144 (3), 172–182. doi:10.1016/j.jphs.2020.07.014

Le, J., Fu, Y., Han, Q., Ma, Y., Ji, H., Wei, X., et al. (2020). Transcriptome Analysis of the Inhibitory Effect of Sennoside A on the Metastasis of Hepatocellular Carcinoma Cells. *Front. Pharmacol.* 11, 566099. doi:10.3389/fphar.2020.566099

Lee, C. K., Park, K. K., Hwang, J. K., Lee, S. K., and Chung, W. Y. (2008). The Pericarp Extract of Prunus Persica Attenuates Chemotherapy-Induced Acute Nephrotoxicity and Hepatotoxicity in Mice. *J. Med. Food* 11 (2), 302–306. doi:10.1089/jmf.2007.545

Lee, E. H., Baek, S. Y., Park, J. Y., and Kim, Y. W. (2020). Emodin in Rheum Undulatum Inhibits Oxidative Stress in the Liver via AMPK with Hippo/Yap Signalling Pathway. *Pharm. Biol.* 58 (1), 333–341. doi:10.1080/13880209.2020.1750658

Lee, G. H., Lee, H. Y., Choi, M. K., Chung, H. W., Kim, S. W., and Chae, H. J. (2017a). Protective Effect of Curcuma Longa L. Extract on CCl4-Induced Acute Hepatic Stress. *BMC Res. Notes* 10 (1), 77. doi:10.1186/s13104-017-2409-z

Lee, H. Y., Kim, S. W., Lee, G. H., Choi, M. K., Chung, H. W., Lee, Y. C., et al. (2017b). Curcumin and Curcuma Longa L. Extract Ameliorate Lipid Accumulation Through the Regulation of the Endoplasmic Reticulum Redox and ER Stress. *Sci. Rep.* 7 (1), 6513. doi:10.1038/s41598-017-06872-y

Lee, W., Koo, H. R., Choi, Y. J., Choi, J. G., Oh, M. S., Jin, X., et al. (2019). Z-ligustilide and N-Butylidenephthalide Isolated from the Aerial Parts of Angelica Tenuissima Inhibit Lipid Accumulation In Vitro and In Vivo. *Planta Med.* 85 (9-10), 719–728. doi:10.1055/a-0901-1307

Leung, T. M., and Nieto, N. (2013). CYP2E1 and Oxidant Stress in Alcoholic and Non-alcoholic Fatty Liver Disease. *J. Hepatol.* 58 (2), 395–398. doi:10.1016/j.jhep.2012.08.018

Li, C. H., Tang, S. C., Wong, C. H., Wang, Y., Jiang, J. D., and Chen, Y. (2018a). Berberine Induces miR-373 Expression in Hepatocytes to Inactivate Hepatic Steatosis Associated AKT-S6 Kinase Pathway. *Eur. J. Pharmacol.* 825, 107–118. doi:10.1016/j.ejphar.2018.02.035

Li, D. S., Huang, Q. F., Guan, L. H., Zhang, H. Z., Li, X., Fu, K. L., et al. (2020a). Targeted Bile Acids and Gut Microbiome Profiles Reveal the Hepato-Protective Effect of WZ Tablet (Schisandra Sphenanthera Extract) Against LCA-Induced Cholestasis. *Chin. J. Nat. Med.* 18 (3), 211–218. doi:10.1016/S1875-5364(20)30023-6

Li, J., Duan, B., Guo, Y., Zhou, R., Sun, J., Bie, B., et al. (2018b). Baicalein Sensitizes Hepatocellular Carcinoma Cells to 5-FU and Epirubicin by Activating Apoptosis and Ameliorating P-Glycoprotein Activity. *Biomed. Pharmacother.* 98, 806–812. doi:10.1016/j.biopha.2018.01.002

Li, J. P., Yuan, Y., Zhang, W. Y., Jiang, Z., Hu, T. J., Feng, Y. T., et al. (2019a). Effect of Radix Isatidis Polysaccharide on Alleviating Insulin Resistance in Type 2 Diabetes Mellitus Cells and Rats. *J. Pharm. Pharmacol.* 71 (2), 220–229. doi:10.1111/jphp.13023

Li, J., Zhang, L., Gao, H., Song, X., and Wu, X. (2014). Progress in Pathogenesis and Treatment of Alcoholic Cirrhosis. *Med. innovation China* 11 (35), 147–149.

Li, Q., Li, H. J., Xu, T., Du, H., Huan Gang, C. L., Fan, G., et al. (2018c). Natural Medicines Used in the Traditional Tibetan Medical System for the Treatment of Liver Diseases. *Front. Pharmacol.* 9, 29. doi:10.3389/fphar.2018.00029

Li, S., Qin, Q., Luo, D., Pan, W., Wei, Y., Xu, Y., et al. (2020b). Hesperidin Ameliorates Liver Ischemia/reperfusion Injury via Activation of the Akt Pathway. *Mol. Med. Rep.* 22 (6), 4519–4530. doi:10.3892/mmr.2020.11561

Li, S., Tan, H. Y., Wang, N., Zhang, Z. J., Lao, L., Wong, C. W., et al. (2015). The Role of Oxidative Stress and Antioxidants in Liver Diseases. *Int. J. Mol. Sci.* 16 (11), 26087–26124. doi:10.3390/ijms161125942

Li, S., Wang, Q., Tao, Y., and Liu, C. (2016). Swertiamarin Attenuates Experimental Rat Hepatic Fibrosis by Suppressing Angiotensin II-Angiotensin Type 1 Receptor-Extracellular Signal-Regulated Kinase Signaling. *J. Pharmacol. Exp. Ther.* 359 (2), 247–255. doi:10.1124/jpet.116.234179

Li, T., and Chiang, J. Y. (2014). Bile Acid Signaling in Metabolic Disease and Drug Therapy. *Pharmacol. Rev.* 66 (4), 948–983. doi:10.1124/pr.113.008201

Li, X., Jin, Q., Yao, Q., Xu, B., Li, L., Zhang, S., et al. (2018d). The Flavonoid Quercetin Ameliorates Liver Inflammation and Fibrosis by Regulating Hepatic Macrophages Activation and Polarization in Mice. *Front. Pharmacol.* 9, 72. doi:10.3389/fphar.2018.00072

Li, X., Li, X., Lu, J., Huang, Y., Lv, L., Luan, Y., et al. (2017). Saikosaponins Induced Hepatotoxicity in Mice via Lipid Metabolism Dysregulation and Oxidative Stress: A Proteomic Study. *BMC Complement. Altern. Med.* 17 (1), 219. doi:10.1186/s12906-017-1733-0

Li, X., Sun, R., and Liu, R. (2019b). Natural Products in Licorice for the Therapy of Liver Diseases: Progress and Future Opportunities. *Pharmacol. Res.* 144, 210–226. doi:10.1016/j.phrs.2019.04.025

Li, X., Zhang, Y., Jin, Q., Xia, K. L., Jiang, M., Cui, B. W., et al. (2018e). Liver Kinase B1/AMP-Activated Protein Kinase-Mediated Regulation by Gentiopicroside Ameliorates P2X7 Receptor-dependent Alcoholic Hepatosteatosis. *Br. J. Pharmacol.* 175 (9), 1451–1470. doi:10.1111/bph.14145

Li, Y., Shen, F., Bao, Y., Chen, D., and Lu, H. (2019c). Apoptotic Effects of Rhein Through the Mitochondrial Pathways, Two Death Receptor Pathways, and Reducing Autophagy in Human Liver L02 Cells. *Environ. Toxicol.* 34 (12), 1292–1302. doi:10.1002/tox.22830

Li, Y., Ye, Y., and Chen, H. (2018g). Astragaloside IV Inhibits Cell Migration and Viability of Hepatocellular Carcinoma Cells via Suppressing Long Noncoding RNA ATB. *Biomed. Pharmacother.* 99, 134–141. doi:10.1016/j.biopha.2017.12.108

Li, Y. C., Qiao, J. Y., Wang, B. Y., Bai, M., Shen, J. D., and Cheng, Y. X. (2018f). Paeoniflorin Ameliorates Fructose-Induced Insulin Resistance and Hepatic Steatosis by Activating LKB1/AMPK and AKT Pathways. *Nutrients* 10 (8), 1024. doi:10.3390/nu10081024

Liang, W., Zhang, D., Kang, J., Meng, X., Yang, J., Yang, L., et al. (2018). Protective Effects of Rutin on Liver Injury in Type 2 Diabetic Db/db Mice. *Biomed. Pharmacother.* 107, 721–728. doi:10.1016/j.biopha.2018.08.046

Liao, C. C., Day, Y. J., Lee, H. C., Liou, J. T., Chou, A. H., and Liu, F. C. (2017). ERK Signaling Pathway Plays a Key Role in Baicalin Protection Against Acetaminophen-Induced Liver Injury. *Am. J. Chin. Med.* 45 (1), 105–121. doi:10.1142/S0192415X17500082

Liao, X., Bu, Y., and Jia, Q. (2020). Traditional Chinese Medicine as Supportive Care for the Management of Liver Cancer: Past, Present, and Future. *Genes Dis.* 7 (3), 370–379. doi:10.1016/j.gendis.2019.10.016

Lim, J. Y., Lee, J. H., Yun, D. H., Lee, Y. M., and Kim, D. K. (2021). Inhibitory Effects of Nodakenin on Inflammation and Cell Death in Lipopolysaccharide-Induced Liver Injury Mice. *Phytomedicine* 81, 153411. doi:10.1016/j.phymed.2020.153411

Lin, C. C., Ng, L. T., Hsu, F. F., Shieh, D. E., and Chiang, L. C. (2004). Cytotoxic Effects of Coptis Chinensis and Epimedium Sagittatum Extracts and Their Major Constituents (Berberine, Coptisine and Icariin) on Hepatoma and Leukaemia Cell Growth. *Clin. Exp. Pharmacol. Physiol.* 31 (1-2), 65–69. doi:10.1111/j.1440-1681.2004.03951.x

Lin, E. Y., Chagnaadorj, A., Huang, S. J., Wang, C. C., Chiang, Y. H., and Cheng, C. W. (2018a2018). Hepatoprotective Activity of the Ethanolic Extract of Polygonum Multiflorum Thunb. Against Oxidative Stress-Induced Liver Injury. *Evid. Based Complement. Alternat Med.* 2018, 4130307. doi:10.1155/2018/4130307

Lin, W., Zhong, M., Yin, H., Chen, Y., Cao, Q., Wang, C., et al. (2016). Emodin Induces Hepatocellular Carcinoma Cell Apoptosis Through MAPK and PI3K/AKT Signaling Pathways In Vitro and In Vivo. *Oncol. Rep.* 36 (2), 961–967. doi:10.3892/or.2016.4861

Lin, Y., Kuang, Y., Li, K., Wang, S., Ji, S., Chen, K., et al. (2017). Nrf2 Activators from Glycyrrhiza Inflata and Their Hepatoprotective Activities Against CCl4-Induced Liver Injury in Mice. *Bioorg. Med. Chem.* 25 (20), 5522–5530. doi:10.1016/j.bmc.2017.08.018

Lin, Y. N., Chang, H. Y., Wang, C. C. N., Chu, F. Y., Shen, H. Y., Chen, C. J., et al. (2018b). Oleanolic Acid Inhibits Liver X Receptor Alpha and Pregnane X Receptor to Attenuate Ligand-Induced Lipogenesis. *J. Agric. Food Chem.* 66 (42), 10964–10976. doi:10.1021/acs.jafc.8b03372

Liou, C. J., Lee, Y. K., Ting, N. C., Chen, Y. L., Shen, S. C., Wu, S. J., et al. (2019). Protective Effects of Licochalcone A Ameliorates Obesity and Non-alcoholic Fatty Liver Disease via Promotion of the Sirt-1/AMPK Pathway in Mice Fed a High-Fat Diet. *Cells* 8 (5), 447. doi:10.3390/cells8050447

Liu, B., Deng, X., Jiang, Q., Li, G., Zhang, J., Zhang, N., et al. (2020a). Scoparone Improves Hepatic Inflammation and Autophagy in Mice with Nonalcoholic Steatohepatitis by Regulating the ROS/P38/Nrf2 axis and PI3K/AKT/mTOR Pathway in Macrophages. *Biomed. Pharmacother.* 125, 109895. doi:10.1016/j.biopha.2020.109895

Liu, C., Chen, J., Li, E., Fan, Q., Wang, D., Li, P., et al. (2015). The Comparison of Antioxidative and Hepatoprotective Activities of Codonopsis Pilosula Polysaccharide (CP) and Sulfated CP. *Int. Immunopharmacol* 24 (2), 299–305. doi:10.1016/j.intimp.2014.12.023

Liu, D. M., Yang, D., Zhou, C. Y., Wu, J. S., Zhang, G. L., Wang, P., et al. (2020b). Aloe-emodin Induces Hepatotoxicity by the Inhibition of Multidrug Resistance Protein 2. *Phytomedicine* 68, 153148. doi:10.1016/j.phymed.2019.153148

Liu, F., Zhang, J., Qian, J., Wu, G., and Ma, Z. (2018). Emodin Alleviates CCl4-induced L-iver F-ibrosis by S-uppressing E-pithelial-mesenchymal T-ransition and T-ransforming G-rowth F-actor-β1 in R-ats. *Mol. Med. Rep.* 18 (3), 3262–3270. doi:10.3892/mmr.2018.9324

Liu, N., Feng, J., Lu, X., Yao, Z., Liu, Q., Lv, Y., et al. (2019a). Isorhamnetin Inhibits Liver Fibrosis by Reducing Autophagy and Inhibiting Extracellular Matrix Formation via the TGF-β1/Smad3 and TGF-B1/p38 MAPK Pathways. *Mediators Inflamm.* 2019, 6175091. doi:10.1155/2019/6175091

Liu, Q., Pan, R., Ding, L., Zhang, F., Hu, L., Ding, B., et al. (2017). Rutin Exhibits Hepatoprotective Effects in a Mouse Model of Non-alcoholic Fatty Liver Disease by Reducing Hepatic Lipid Levels and Mitigating Lipid-Induced Oxidative Injuries. *Int. Immunopharmacol* 49, 132–141. doi:10.1016/j.intimp.2017.05.026

Liu, R., Li, X., Huang, N., Fan, M., and Sun, R. (2020c). Toxicity of Traditional Chinese Medicine Herbal and Mineral Products. *Adv. Pharmacol.* 87, 301–346. doi:10.1016/bs.apha.2019.08.001

Liu, W., Li, S., Qu, Z., Luo, Y., Chen, R., Wei, S., et al. (2019b). Betulinic Acid Induces Autophagy-Mediated Apoptosis Through Suppression of the PI3K/AKT/mTOR Signaling Pathway and Inhibits Hepatocellular Carcinoma. *Am. J. Transl Res.* 11 (11), 6952–6964.

Liu, Y., Bi, Y., Mo, C., Zeng, T., Huang, S., Gao, L., et al. (2019c). Betulinic Acid Attenuates Liver Fibrosis by Inducing Autophagy via the Mitogen-Activated Protein Kinase/extracellular Signal-Regulated Kinase Pathway. *J. Nat. Med.* 73 (1), 179–189. doi:10.1007/s11418-018-1262-2

Llovet, J. M., Kelley, R. K., Villanueva, A., Singal, A. G., Pikarsky, E., Roayaie, S., et al. (2021). Hepatocellular Carcinoma. *Nat. Rev. Dis. Primers* 7 (1), 6. doi:10.1038/s41572-020-00240-3

López-Navarrete, G., Ramos-Martínez, E., Suárez-Álvarez, K., Aguirre-García, J., Ledezma-Soto, Y., León-Cabrera, S., et al. (2011). Th2-associated Alternative Kupffer Cell Activation Promotes Liver Fibrosis Without Inducing Local Inflammation. *Int. J. Biol. Sci.* 7 (9), 1273–1286. doi:10.7150/ijbs.7.1273

Lu, C., Xu, W., Shao, J., Zhang, F., Chen, A., and Zheng, S. (2017). Nrf2 Activation Is Required for Ligustrazine to Inhibit Hepatic Steatosis in Alcohol-Preferring Mice and Hepatocytes. *Toxicol. Sci.* 155 (2), 432–443. doi:10.1093/toxsci/kfw228

Lukefahr, A. L., McEvoy, S., Alfafara, C., and Funk, J. L. (2018). Drug-induced Autoimmune Hepatitis Associated with Turmeric Dietary Supplement Use. *BMJ Case Rep.* 2018, bcr2018224611. doi:10.1136/bcr-2018-224611

Luna, J. M., Scheel, T. K., Danino, T., Shaw, K. S., Mele, A., Fak, J. J., et al. (2015). Hepatitis C Virus RNA Functionally Sequesters miR-122. *Cell* 160 (6), 1099–1110. doi:10.1016/j.cell.2015.02.025

Lv, H., Xiao, Q., Zhou, J., Feng, H., Liu, G., and Ci, X. (2018). Licochalcone A Upregulates Nrf2 Antioxidant Pathway and Thereby Alleviates Acetaminophen-Induced Hepatotoxicity. *Front. Pharmacol.* 9, 147. doi:10.3389/fphar.2018.00147

Ma, B. X., Meng, X. S., Tong, J., Ge, L. L., Zhou, G., and Wang, Y. W. (2018a). Protective Effects of Coptis Chinensis Inflorescence Extract and Linarin Against Carbon Tetrachloride-Induced Damage in HepG2 Cells Through the MAPK/Keap1-Nrf2 Pathway. *Food Funct.* 9 (4), 2353–2361. doi:10.1039/c8fo00078f

Ma, P., Sun, C., Li, W., Deng, W., Adu-Frimpong, M., Yu, J., et al. (2020). Extraction and Structural Analysis of Angelica Sinensis Polysaccharide with Low Molecular Weight and its Lipid-Lowering Effect on Nonalcoholic Fatty Liver Disease. *Food Sci. Nutr.* 8 (7), 3212–3224. doi:10.1002/fsn3.1581

Ma, Q. (2013). Role of Nrf2 in Oxidative Stress and Toxicity. *Annu. Rev. Pharmacol. Toxicol.* 53, 401–426. doi:10.1146/annurev-pharmtox-011112-140320

Ma, X., Chi, Y. H., Niu, M., Zhu, Y., Zhao, Y. L., Chen, Z., et al. (2016). Metabolomics Coupled with Multivariate Data and Pathway Analysis on Potential Biomarkers in Cholestasis and Intervention Effect of Paeonia Lactiflora Pall. *Front. Pharmacol.* 7, 14. doi:10.3389/fphar.2016.00014

Ma, X., Wen, J. X., Gao, S. J., He, X., Li, P. Y., Yang, Y. X., et al. (2018b). Paeonia Lactiflora Pall. Regulates the NF-Kb-NLRP3 Inflammasome Pathway to Alleviate Cholestasis in Rats. *J. Pharm. Pharmacol.* 70 (12), 1675–1687. doi:10.1111/jphp.13008

Ma, X., Zhao, Y. L., Zhu, Y., Chen, Z., Wang, J. B., Li, R. Y., et al. (2015). Paeonia Lactiflora Pall. Protects Against ANIT-Induced Cholestasis by Activating Nrf2 via PI3K/Akt Signaling Pathway. *Drug Des. Devel Ther.* 9, 5061–5074. doi:10.2147/DDDT.S90030

Ma, X. Y., Zhang, M., Fang, G., Cheng, C. J., Wang, M. K., Han, Y. M., et al. (2021). Ursolic Acid Reduces Hepatocellular Apoptosis and Alleviates Alcohol-Induced Liver Injury via Irreversible Inhibition of CASP3 In Vivo. *Acta Pharmacol. Sin* 42 (7), 1101–1110. doi:10.1038/s41401-020-00534-y

Ma, Y., Chen, K., Lv, L., Wu, S., and Guo, Z. (2019). Ferulic Acid Ameliorates Nonalcoholic Fatty Liver Disease and Modulates the Gut Microbiota Composition in High-Fat Diet Fed ApoE-/- Mice. *Biomed. Pharmacother.* 113, 108753. doi:10.1016/j.biopha.2019.108753

Mahmoud, A. M., Hussein, O. E., Hozayen, W. G., Bin-Jumah, M., and Abd El-Twab, S. M. (2020). Ferulic Acid Prevents Oxidative Stress, Inflammation, and Liver Injury via Upregulation of Nrf2/HO-1 Signaling in Methotrexate-Induced Rats. *Environ. Sci. Pollut. Res. Int.* 27 (8), 7910–7921. doi:10.1007/s11356-019-07532-6

Mahmoud, M. F., Gamal, S., and El-Fayoumi, H. M. (2014). Limonin Attenuates Hepatocellular Injury Following Liver Ischemia and Reperfusion in Rats via Toll-like Receptor Dependent Pathway. *Eur. J. Pharmacol.* 740, 676–682. doi:10.1016/j.ejphar.2014.06.010

Manns, M. P., Buti, M., Gane, E., Pawlotsky, J. M., Razavi, H., Terrault, N., et al. (2017). Hepatitis C Virus Infection. *Nat. Rev. Dis. Primers* 3, 17006. doi:10.1038/nrdp.2017.6

Mantovani, A., Gatti, D., Zoppini, G., Lippi, G., Bonora, E., Byrne, C. D., et al. (2019). Association Between Nonalcoholic Fatty Liver Disease and Reduced Bone Mineral Density in Children: A Meta-Analysis. *Hepatology* 70 (3), 812–823. doi:10.1002/hep.30538

Marvie, P., Lisbonne, M., L'Helgoualc'h, A., Rauch, M., Turlin, B., Preisser, L., et al. (2010). Interleukin-33 Overexpression Is Associated with Liver Fibrosis in Mice and Humans. *J. Cel Mol Med* 14 (6B), 1726–1739. doi:10.1111/j.1582-4934.2009.00801.x

Medzhitov, R. (2008). Origin and Physiological Roles of Inflammation. *Nature* 454 (7203), 428–435. doi:10.1038/nature07201

Mello, T., Ceni, E., Surrenti, C., and Galli, A. (2008). Alcohol Induced Hepatic Fibrosis: Role of Acetaldehyde. *Mol. Aspects Med.* 29 (1-2), 17–21. doi:10.1016/j.mam.2007.10.001

Meng, Q., Chen, X., Wang, C., Liu, Q., Sun, H., Sun, P., et al. (2015). Protective Effects of Alisol B 23-acetate from Edible Botanical Rhizoma Alismatis Against Carbon Tetrachloride-Induced Hepatotoxicity in Mice. *Food Funct.* 6 (4), 1241–1250. doi:10.1039/c5fo00082c

Meng, Q., Duan, X. P., Wang, C. Y., Liu, Z. H., Sun, P. Y., Huo, X. K., et al. (2017). Alisol B 23-acetate Protects Against Non-alcoholic Steatohepatitis in Mice via Farnesoid X Receptor Activation. *Acta Pharmacol. Sin* 38 (1), 69–79. doi:10.1038/aps.2016.119

Meng, X. L., Zhu, Z. X., Lu, R. H., Li, S., Hu, W. P., Qin, C. B., et al. (2019). Regulation of Growth Performance and Lipid Metabolism in Juvenile Grass Carp (Ctenopharyngodon Idella) with Honeysuckle (*Lonicera japonica*) Extract. *Fish. Physiol. Biochem.* 45 (5), 1563–1573. doi:10.1007/s10695-019-00644-3

Messina, J. P., Humphreys, I., Flaxman, A., Brown, A., Cooke, G. S., Pybus, O. G., et al. (2015). Global Distribution and Prevalence of Hepatitis C Virus Genotypes. *Hepatology* 61 (1), 77–87. doi:10.1002/hep.27259

Mo, Z. Z., Lin, Z. X., Su, Z. R., Zheng, L., Li, H. L., Xie, J. H., et al. (2018). Angelica Sinensis Supercritical Fluid CO2 Extract Attenuates D-Galactose-Induced Liver and Kidney Impairment in Mice by Suppressing Oxidative Stress and Inflammation. *J. Med. Food* 21 (9), 887–898. doi:10.1089/jmf.2017.4061

Mo, Z. Z., Liu, Y. H., Li, C. L., Xu, L. Q., Wen, L. L., Xian, Y. F., et al. (2017). Protective Effect of SFE-CO2 of Ligusticum Chuanxiong Hort Against D-Galactose-Induced Injury in the Mouse Liver and Kidney. *Rejuvenation Res.* 20 (3), 231–243. doi:10.1089/rej.2016.1870

Mo'men, Y. S., Hussein, R. M., and Kandeil, M. A. (2019). Involvement of PI3K/Akt Pathway in the Protective Effect of Hesperidin Against a Chemically Induced Liver Cancer in Rats. *J. Biochem. Mol. Toxicol.* 33 (6), e22305. doi:10.1002/jbt.22305

Moghadam, A. R., Tutunchi, S., Namvaran-Abbas-Abad, A., Yazdi, M., Bonyadi, F., Mohajeri, D., et al. (2015). Pre-administration of Turmeric Prevents Methotrexate-Induced Liver Toxicity and Oxidative Stress. *BMC Complement. Altern. Med.* 15, 246. doi:10.1186/s12906-015-0773-6

Mu, M., Zuo, S., Wu, R. M., Deng, K. S., Lu, S., Zhu, J. J., et al. (2018). Ferulic Acid Attenuates Liver Fibrosis and Hepatic Stellate Cell Activation via Inhibition of TGF-β/Smad Signaling Pathway. *Drug Des. Devel Ther.* 12, 4107–4115. doi:10.2147/DDDT.S186726

Mu, Q., Wang, H., Tong, L., Fang, Q., Xiang, M., Han, L., et al. (2020). Betulinic Acid Improves Nonalcoholic Fatty Liver Disease Through YY1/FAS Signaling Pathway. *FASEB J.* 34 (9), 13033–13048. doi:10.1096/fj.202000546R

Nagappan, A., Jung, D. Y., Kim, J. H., Lee, H., and Jung, M. H. (2018). Gomisin N Alleviates Ethanol-Induced Liver Injury Through Ameliorating Lipid Metabolism and Oxidative Stress. *Int. J. Mol. Sci.* 19 (9), 2601. doi:10.3390/ijms19092601

Nagappan, A., Kim, J. H., Jung, D. Y., and Jung, M. H. (2019). Cryptotanshinone from the Salvia Miltiorrhiza Bunge Attenuates Ethanol-Induced Liver Injury by Activation of AMPK/SIRT1 and Nrf2 Signaling Pathways. *Int. J. Mol. Sci.* 21 (1), 265. doi:10.3390/ijms21010265

Nakamura, T., Naguro, I., and Ichijo, H. (2019). Iron Homeostasis and Iron-Regulated ROS in Cell Death, Senescence and Human Diseases. *Biochim. Biophys. Acta Gen. Subj* 1863 (9), 1398–1409. doi:10.1016/j.bbagen.2019.06.010

Navarro, V. J., Belle, S. H., D'Amato, M., Adfhal, N., Brunt, E. M., Fried, M. W., et al. (2019). Silymarin in Non-cirrhotics with Non-alcoholic Steatohepatitis: A Randomized, Double-Blind, Placebo Controlled Trial. *PLoS One* 14 (9), e0221683. doi:10.1371/journal.pone.0221683

Neyrinck, A. M., Etxeberria, U., Taminiau, B., Daube, G., Van Hul, M., Everard, A., et al. (2017). Rhubarb Extract Prevents Hepatic Inflammation Induced by Acute Alcohol Intake, an Effect Related to the Modulation of the Gut Microbiota. *Mol. Nutr. Food Res.* 61 (1), 1–12. doi:10.1002/mnfr.201500899

Nguyen, P., Leray, V., Diez, M., Serisier, S., Le Bloc'h, J., Siliart, B., et al. (2008). Liver Lipid Metabolism. *J. Anim. Physiol. Anim. Nutr. (Berl)* 92 (3), 272–283. doi:10.1111/j.1439-0396.2007.00752.x

Ning, C., Gao, X., Wang, C., Huo, X., Liu, Z., Sun, H., et al. (2018). Hepatoprotective Effect of Ginsenoside Rg1 from Panax Ginseng on Carbon Tetrachloride-Induced Acute Liver Injury by Activating Nrf2 Signaling Pathway in Mice. *Environ. Toxicol.* 33 (10), 1050–1060. doi:10.1002/tox.22616

Nouri-Vaskeh, M., Afshan, H., Malek Mahdavi, A., Alizadeh, L., Fan, X., and Zarei, M. (2020a). Curcumin Ameliorates Health-Related Quality of Life in Patients with Liver Cirrhosis: A Randomized, Double-Blind Placebo-Controlled Trial. *Complement. Ther. Med.* 49, 102351. doi:10.1016/j.ctim.2020.102351

Nouri-Vaskeh, M., Malek Mahdavi, A., Afshan, H., Alizadeh, L., and Zarei, M. (2020b). Effect of Curcumin Supplementation on Disease Severity in Patients with Liver Cirrhosis: A Randomized Controlled Trial. *Phytother Res.* 34 (6), 1446–1454. doi:10.1002/ptr.6620

Okubo, S., Ohta, T., Shoyama, Y., and Uto, T. (2020). Arctigenin Suppresses Cell Proliferation via Autophagy Inhibition in Hepatocellular Carcinoma Cells. *J. Nat. Med.* 74 (3), 525–532. doi:10.1007/s11418-020-01396-8

Onyekwere, C. A., Ogbera, A. O., Samaila, A. A., Balogun, B. O., and Abdulkareem, F. B. (2015). Nonalcoholic Fatty Liver Disease: Synopsis of Current Developments. *Niger. J. Clin. Pract.* 18 (6), 703–712. doi:10.4103/1119-3077.163288

Ou, Q., Weng, Y., Wang, S., Zhao, Y., Zhang, F., Zhou, J., et al. (2018). Silybin Alleviates Hepatic Steatosis and Fibrosis in NASH Mice by Inhibiting Oxidative Stress and Involvement with the Nf-Kb Pathway. *Dig. Dis. Sci.* 63 (12), 3398–3408. doi:10.1007/s10620-018-5268-0

Padda, M. S., Sanchez, M., Akhtar, A. J., and Boyer, J. L. (2011). Drug-induced Cholestasis. *Hepatology* 53 (4), 1377–1387. doi:10.1002/hep.24229

Pan, C. W., Zhou, G. Y., Chen, W. L., Zhuge, L., Jin, L. X., Zheng, Y., et al. (2015a). Protective Effect of Forsythiaside A on Lipopolysaccharide/d-Galactosamine-Induced Liver Injury. *Int. Immunopharmacol* 26 (1), 80–85. doi:10.1016/j.intimp.2015.03.009

Pan, T. L., Wang, P. W., Huang, C. H., Leu, Y. L., Wu, T. H., Wu, Y. R., et al. (2015b). Herbal Formula, Scutellariae Radix and Rhei Rhizoma Attenuate Dimethylnitrosamine-Induced Liver Fibrosis in a Rat Model. *Sci. Rep.* 5, 11734. doi:10.1038/srep11734

Park, C. H., Shin, M. R., An, B. K., Joh, H. W., Lee, J. C., Roh, S. S., et al. (2017). Heat-Processed Scutellariae Radix Protects Hepatic Inflammation through the Amelioration of Oxidative Stress in Lipopolysaccharide-Induced Mice. *Am. J. Chin. Med.* 45 (6), 1233–1252. doi:10.1142/S0192415X17500689

Park, Y. J., Lee, K. H., Jeon, M. S., Lee, Y. H., Ko, Y. J., Pang, C., et al. (2020). Hepatoprotective Potency of Chrysophanol 8-O-Glucoside from Rheum Palmatum L. Against Hepatic Fibrosis via Regulation of the STAT3 Signaling Pathway. *Int. J. Mol. Sci.* 21 (23), 9044. doi:10.3390/ijms21239044

Parlati, L., Voican, C. S., Perlemuter, K., and Perlemuter, G. (2017). Aloe Vera-Induced Acute Liver Injury: A Case Report and Literature Review. *Clin. Res. Hepatol. Gastroenterol.* 41 (4), e39–e42. doi:10.1016/j.clinre.2016.10.002

Peng, Y., Yang, T., Huang, K., Shen, L., Tao, Y., and Liu, C. (2018). Salvia Miltiorrhiza Ameliorates Liver Fibrosis by Activating Hepatic Natural Killer Cells In Vivo and In Vitro. *Front. Pharmacol.* 9, 762. doi:10.3389/fphar.2018.00762

Penny, S. M. (2013). Alcoholic Liver Disease. *Radiol. Technol.* 84 (6), 577–585.

Pérez-Vargas, J. E., Zarco, N., Shibayama, M., Segovia, J., Tsutsumi, V., and Muriel, P. (2014). Hesperidin Prevents Liver Fibrosis in Rats by Decreasing the Expression of Nuclear Factor-Kb, Transforming Growth Factor-β and Connective Tissue Growth Factor. *Pharmacology* 94 (1-2), 80–89. doi:10.1159/000366206

Porras, D., Nistal, E., Martínez-Flórez, S., Pisonero-Vaquero, S., Olcoz, J. L., Jover, R., et al. (2017). Protective Effect of Quercetin on High-Fat Diet-Induced Non-alcoholic Fatty Liver Disease in Mice Is Mediated by Modulating Intestinal Microbiota Imbalance and Related Gut-Liver Axis Activation. *Free Radic. Biol. Med.* 102, 188–202. doi:10.1016/j.freeradbiomed.2016.11.037

Poynard, T., Bedossa, P., and Opolon, P. (1997). Natural History of Liver Fibrosis Progression in Patients with Chronic Hepatitis C. The OBSVIRC, METAVIR, CLINIVIR, and DOSVIRC Groups. *Lancet* 349 (9055), 825–832. doi:10.1016/s0140-6736(96)07642-8

Qu, X., Gao, H., Zhai, J., Sun, J., Tao, L., Zhang, Y., et al. (2020). Astragaloside IV Enhances Cisplatin Chemosensitivity in Hepatocellular Carcinoma by Suppressing MRP2. *Eur. J. Pharm. Sci.* 148, 105325. doi:10.1016/j.ejps.2020.105325

Qu, Z. X., Li, F., Ma, C. D., Liu, J., Li, S. D., and Wang, W. L. (2015). Effects of gentiana Scabra Bage on Expression of Hepatic Type I, III Collagen Proteins in Paragonimus Skrjabini Rats with Liver Fibrosis. *Asian Pac. J. Trop. Med.* 8 (1), 60–63. doi:10.1016/S1995-7645(14)60188-7

Rahmani, S., Asgary, S., Askari, G., Keshvari, M., Hatamipour, M., Feizi, A., et al. (2016). Treatment of Non-alcoholic Fatty Liver Disease with Curcumin: A Randomized Placebo-Controlled Trial. *Phytother Res.* 30 (9), 1540–1548. doi:10.1002/ptr.5659

Rakshit, S., Shukla, P., Verma, A., Kumar Nirala, S., and Bhadauria, M. (2021). Protective Role of Rutin Against Combined Exposure to Lipopolysaccharide and D-Galactosamine-Induced Dysfunctions in Liver, Kidney, and Brain: Hematological, Biochemical, and Histological Evidences. *J. Food Biochem.* 45 (2), e13605. doi:10.1111/jfbc.13605

Rehermann, B., Ferrari, C., Pasquinelli, C., and Chisari, F. V. (1996). The Hepatitis B Virus Persists for Decades after Patients' Recovery from Acute Viral Hepatitis Despite Active Maintenance of a Cytotoxic T-Lymphocyte Response. *Nat. Med.* 2 (10), 1104–1108. doi:10.1038/nm1096-1104

Rehman, S., Nazar, R., Butt, A. M., Ijaz, B., Tasawar, N., Sheikh, A. K., et al. (2021). Phytochemical Screening and Protective Effects of Prunus Persica Seeds Extract on Carbon Tetrachloride-Induced Hepatic Injury in Rats. *Curr. Pharm. Biotechnol.* doi:10.2174/1389201022666210203142138

Ren, M., McGowan, E., Li, Y., Zhu, X., Lu, X., Zhu, Z., et al. (2019). Saikosaponin-d Suppresses COX2 Through p-STAT3/C/EBPβ Signaling Pathway in Liver Cancer: A Novel Mechanism of Action. *Front. Pharmacol.* 10, 623. doi:10.3389/fphar.2019.00623

Robinson, M. W., Harmon, C., and O'Farrelly, C. (2016). Liver Immunology and its Role in Inflammation and Homeostasis. *Cell Mol Immunol* 13 (3), 267–276. doi:10.1038/cmi.2016.3

Roghani, M., Kalantari, H., Khodayar, M. J., Khorsandi, L., Kalantar, M., Goudarzi, M., et al. (2020). Alleviation of Liver Dysfunction, Oxidative Stress and Inflammation Underlies the Protective Effect of Ferulic Acid in Methotrexate-Induced Hepatotoxicity. *Drug Des. Devel Ther.* 14, 1933–1941. doi:10.2147/DDDT.S237107

Saberi-Karimian, M., Keshvari, M., Ghayour-Mobarhan, M., Salehizadeh, L., Rahmani, S., Behnam, B., et al. (2020). Effects of Curcuminoids on Inflammatory Status in Patients with Non-alcoholic Fatty Liver Disease: A Randomized Controlled Trial. *Complement. Ther. Med.* 49, 102322. doi:10.1016/j.ctim.2020.102322

Salameh, H., Raff, E., Erwin, A., Seth, D., Nischalke, H. D., Falleti, E., et al. (2015). PNPLA3 Gene Polymorphism Is Associated with Predisposition to and Severity of Alcoholic Liver Disease. *Am. J. Gastroenterol.* 110 (6), 846–856. doi:10.1038/ajg.2015.137

Seitz, S., Urban, S., Antoni, C., and Böttcher, B. (2007). Cryo-electron Microscopy of Hepatitis B Virions Reveals Variability in Envelope Capsid Interactions. *EMBO J.* 26 (18), 4160–4167. doi:10.1038/sj.emboj.7601841

Shan, Y., Jiang, B., Yu, J., Wang, J., Wang, X., Li, H., et al. (2019). Protective Effect of Schisandra Chinensis Polysaccharides Against the Immunological Liver Injury in Mice Based on Nrf2/ARE and TLR4/NF-Kb Signaling Pathway. *J. Med. Food* 22 (9), 885–895. doi:10.1089/jmf.2018.4377

Shang, Y., Li, X. F., Jin, M. J., Li, Y., Wu, Y. L., Jin, Q., et al. (2018). Leucodin Attenuates Inflammatory Response in Macrophages and Lipid Accumulation in Steatotic Hepatocytes via P2x7 Receptor Pathway: A Potential Role in Alcoholic Liver Disease. *Biomed. Pharmacother.* 107, 374–381. doi:10.1016/j.biopha.2018.08.009

Shen, B., Feng, H., Cheng, J., Li, Z., Jin, M., Zhao, L., et al. (2020). Geniposide Alleviates Non-alcohol Fatty Liver Disease via Regulating Nrf2/AMPK/mTOR Signalling Pathways. *J. Cel Mol Med* 24 (9), 5097–5108. doi:10.1111/jcmm.15139

Shen, H., Wang, H., Wang, L., Wang, L., Zhu, M., Ming, Y., et al. (2017). Ethanol Extract of Root of Prunus Persica Inhibited the Growth of Liver Cancer Cell HepG2 by Inducing Cell Cycle Arrest and Migration Suppression. *Evid. Based Complement. Alternat Med.* 2017, 8231936. doi:10.1155/2017/8231936

Shen, T. D., Pyrsopoulos, N., and Rustgi, V. K. (2018). Microbiota and the Liver. *Liver Transpl.* 24 (4), 539–550. doi:10.1002/lt.25008

Sheu, M. J., Chiu, C. C., Yang, D. J., Hsu, T. C., and Tzang, B. S. (2017). The Root Extract of Gentiana Macrophylla Pall. Alleviates B19-NS1-Exacerbated Liver Injuries in NZB/W F1 Mice. *J. Med. Food* 20 (1), 56–64. doi:10.1089/jmf.2016.3817

Shi, H., Shi, A., Dong, L., Lu, X., Wang, Y., Zhao, J., et al. (2016). Chlorogenic Acid Protects Against Liver Fibrosis In Vivo and In Vitro Through Inhibition of Oxidative Stress. *Clin. Nutr.* 35 (6), 1366–1373. doi:10.1016/j.clnu.2016.03.002

Shi, J., Han, G., Wang, J., Han, X., Zhao, M., Duan, X., et al. (2020). Matrine Promotes Hepatic Oval Cells Differentiation into Hepatocytes and Alleviates Liver Injury by Suppression of Notch Signalling Pathway. *Life Sci.* 261, 118354. doi:10.1016/j.lfs.2020.118354

Shi, Y., and Zheng, M. (2020). Hepatitis B Virus Persistence and Reactivation. *BMJ* 370, m2200. doi:10.1136/bmj.m2200

Singal, A. K., Bataller, R., Ahn, J., Kamath, P. S., and Shah, V. H. (2018). ACG Clinical Guideline: Alcoholic Liver Disease. *Am. J. Gastroenterol.* 113 (2), 175–194. doi:10.1038/ajg.2017.469

Spearman, C. W., Dusheiko, G. M., Hellard, M., and Sonderup, M. (2019). Hepatitis C. *Lancet* 394 (10207), 1451–1466. doi:10.1016/S0140-6736(19)32320-7

Stöckigt, J., Antonchick, A. P., Wu, F., and Waldmann, H. (2011). The Pictet-Spengler Reaction in Nature and in Organic Chemistry. *Angew. Chem. Int. Ed. Engl.* 50 (37), 8538–8564. doi:10.1002/anie.201008071

Su, C. M., Wang, H. C., Hsu, F. T., Lu, C. H., Lai, C. K., Chung, J. G., et al. (2020). Astragaloside IV Induces Apoptosis, G1-phase Arrest and Inhibits Anti-apoptotic Signaling in Hepatocellular Carcinoma. *In Vivo* 34 (2), 631–638. doi:10.21873/invivo.11817

Sun, J., Liu, Y., Yu, J., Wu, J., Gao, W., Ran, L., et al. (2019). APS Could Potentially Activate Hepatic Insulin Signaling in HFD-Induced IR Mice. *J. Mol. Endocrinol.* 63 (1), 77–91. doi:10.1530/JME-19-0035

Tan, X., Sun, Z., Liu, Q., Ye, H., Zou, C., Ye, C., et al. (2018). Effects of Dietary Ginkgo Biloba Leaf Extract on Growth Performance, Plasma Biochemical Parameters, Fish Composition, Immune Responses, Liver Histology, and Immune and Apoptosis-Related Genes Expression of Hybrid Grouper (Epinephelus Lanceolatus♂ × Epinephelus Fuscoguttatus♀) Fed High Lipid Diets. *Fish. Shellfish Immunol.* 72, 399–409. doi:10.1016/j.fsi.2017.10.022

Tan, X., Sun, Z., Ye, C., and Lin, H. (2019). The Effects of Dietary Lycium Barbarum Extract on Growth Performance, Liver Health and Immune Related Genes Expression in Hybrid Grouper (Epinephelus Lanceolatus♂ × E. Fuscoguttatus♀) Fed High Lipid Diets. *Fish. Shellfish Immunol.* 87, 847–852. doi:10.1016/j.fsi.2019.02.016

Tang, F., Fan, K., Wang, K., and Bian, C. (2019). Amygdalin Attenuates Acute Liver Injury Induced by D-Galactosamine and Lipopolysaccharide by Regulating the NLRP3, NF-Kb and Nrf2/NQO1 Signalling Pathways. *Biomed. Pharmacother.* 111, 527–536. doi:10.1016/j.biopha.2018.12.096

Tholl, D. (2015). Biosynthesis and Biological Functions of Terpenoids in Plants. *Adv. Biochem. Eng. Biotechnol.* 148, 63–106. doi:10.1007/10_2014_295

Trépo, C., Chan, H. L., and Lok, A. (2014). Hepatitis B Virus Infection. *Lancet* 384 (9959), 2053–2063. doi:10.1016/S0140-6736(14)60220-8

Tripathi, A., Debelius, J., Brenner, D. A., Karin, M., Loomba, R., Schnabl, B., et al. (2018). The Gut-Liver Axis and the Intersection with the Microbiome. *Nat. Rev. Gastroenterol. Hepatol.* 15 (7), 397–411. doi:10.1038/s41575-018-0011-z

Tsochatzis, E. A., Bosch, J., and Burroughs, A. K. (2014). Liver Cirrhosis. *Lancet* 383 (9930), 1749–1761. doi:10.1016/S0140-6736(14)60121-5

Tsuchida, T., and Friedman, S. L. (2017). Mechanisms of Hepatic Stellate Cell Activation. *Nat. Rev. Gastroenterol. Hepatol.* 14 (7), 397–411. doi:10.1038/nrgastro.2017.38

Tu, Y. (2016). Artemisinin-A Gift from Traditional Chinese Medicine to the World (Nobel Lecture). *Angew. Chem. Int. Ed. Engl.* 55 (35), 10210–10226. doi:10.1002/anie.201601967

Uchio, R., Higashi, Y., Kohama, Y., Kawasaki, K., Hirao, T., Muroyama, K., et al. (2017). A Hot Water Extract of Turmeric (Curcuma Longa) Suppresses Acute Ethanol-Induced Liver Injury in Mice by Inhibiting Hepatic Oxidative Stress and Inflammatory Cytokine Production. *J. Nutr. Sci.* 6, e3. doi:10.1017/jns.2016.43

Van Hung, P. (2016). Phenolic Compounds of Cereals and Their Antioxidant Capacity. *Crit. Rev. Food Sci. Nutr.* 56 (1), 25–35. doi:10.1080/10408398.2012.708909

Veskovic, M., Mladenovic, D., Milenkovic, M., Tosic, J., Borozan, S., Gopcevic, K., et al. (2019). Betaine Modulates Oxidative Stress, Inflammation, Apoptosis, Autophagy, and Akt/mTOR Signaling in Methionine-Choline Deficiency-Induced Fatty Liver Disease. *Eur. J. Pharmacol.* 848, 39–48. doi:10.1016/j.ejphar.2019.01.043

Wah Kheong, C., Nik Mustapha, N. R., and Mahadeva, S. (2017). A Randomized Trial of Silymarin for the Treatment of Nonalcoholic Steatohepatitis. *Clin. Gastroenterol. Hepatol.* 15 (12), 1940–1949.e8. doi:10.1016/j.cgh.2017.04.016

Wan, S., Luo, F., Huang, C., Liu, C., Luo, Q., and Zhu, X. (2020). Ursolic Acid Reverses Liver Fibrosis by Inhibiting Interactive NOX4/ROS and RhoA/ROCK1 Signalling Pathways. *Aging (Albany NY)* 12 (11), 10614–10632. doi:10.18632/aging.103282

Wan, S. Z., Liu, C., Huang, C. K., Luo, F. Y., and Zhu, X. (2019). Ursolic Acid Improves Intestinal Damage and Bacterial Dysbiosis in Liver Fibrosis Mice. *Front. Pharmacol.* 10, 1321. doi:10.3389/fphar.2019.01321

Wang, F. S., Fan, J. G., Zhang, Z., Gao, B., and Wang, H. Y. (2014). The Global Burden of Liver Disease: The Major Impact of China. *Hepatology* 60 (6), 2099–2108. doi:10.1002/hep.27406

Wang, G., Fu, Y., Li, J., Li, Y., Zhao, Q., Hu, A., et al. (2021a). Aqueous Extract of Polygonatum Sibiricum Ameliorates Ethanol-Induced Mice Liver Injury via Regulation of the Nrf2/ARE Pathway. *J. Food Biochem.* 45 (1), e13537. doi:10.1111/jfbc.13537

Wang, J., Liao, A. M., Thakur, K., Zhang, J. G., Huang, J. H., and Wei, Z. J. (2019a). Licochalcone B Extracted from Glycyrrhiza Uralensis Fisch Induces Apoptotic Effects in Human Hepatoma Cell HepG2. *J. Agric. Food Chem.* 67 (12), 3341–3353. doi:10.1021/acs.jafc.9b00324

Wang, J., Wong, Y. K., and Liao, F. (2018). What Has Traditional Chinese Medicine Delivered for Modern Medicine? *Expert Rev. Mol. Med.* 20, e4. doi:10.1017/erm.2018.3

Wang, J., Zhao, Y., Xiao, X., Li, H., Zhao, H., Zhang, P., et al. (2009). Assessment of the Renal protection and Hepatotoxicity of Rhubarb Extract in Rats. *J. Ethnopharmacol* 124 (1), 18–25. doi:10.1016/j.jep.2009.04.018

Wang, K., Song, Z., Wang, H., Li, Q., Cui, Z., and Zhang, Y. (2016). Angelica Sinensis Polysaccharide Attenuates Concanavalin A-Induced Liver Injury in Mice. *Int. Immunopharmacol* 31, 140–148. doi:10.1016/j.intimp.2015.12.021

Wang, K., Wang, J., Song, M., Wang, H., Xia, N., and Zhang, Y. (2020a). Angelica Sinensis Polysaccharide Attenuates CCl4-Induced Liver Fibrosis via the IL-22/STAT3 Pathway. *Int. J. Biol. Macromol* 162, 273–283. doi:10.1016/j.ijbiomac.2020.06.166

Wang, Q., Liang, Y., Peng, C., and Jiang, P. (2020b). Network Pharmacology-Based Study on the Mechanism of Scutellariae Radix for Hepatocellular Carcinoma Treatment. *Evid. Based Complement. Alternat Med.* 2020, 8897918. doi:10.1155/2020/8897918

Wang, R., Zhang, D., Tang, D., Sun, K., Peng, J., Zhu, W., et al. (2021b). Amygdalin Inhibits TGFβ1-Induced Activation of Hepatic Stellate Cells (HSCs) In Vitro and CCl4-Induced Hepatic Fibrosis in Rats In Vivo. *Int. Immunopharmacol* 90, 107151. doi:10.1016/j.intimp.2020.107151

Wang, S., Xu, J., Wang, C., Li, J., Wang, Q., Kuang, H., et al. (2020c). Paeoniae Radix alba Polysaccharides Obtained via Optimized Extraction Treat Experimental Autoimmune Hepatitis Effectively. *Int. J. Biol. Macromol* 164, 1554–1564. doi:10.1016/j.ijbiomac.2020.07.214

Wang, Y., Wang, R., Wang, Y., Peng, R., Wu, Y., and Yuan, Y. (2015). Ginkgo Biloba Extract Mitigates Liver Fibrosis and Apoptosis by Regulating P38 MAPK, NF-Kb/ικbα, and Bcl-2/Bax Signaling. *Drug Des. Devel Ther.* 9, 6303–6317. doi:10.2147/DDDT.S93732

Wang, Y. X., Du, Y., Liu, X. F., Yang, F. X., Wu, X., Tan, L., et al. (2019b). A Hepatoprotection Study of Radix Bupleuri on Acetaminophen-Induced Liver Injury Based on CYP450 Inhibition. *Chin. J. Nat. Med.* 17 (7), 517–524. doi:10.1016/S1875-5364(19)30073-1

Wei, J., Zhang, L., Liu, J., Pei, D., Wang, N., Wang, H., et al. (2020). Protective Effect of Lycium Barbarum Polysaccharide on Ethanol-Induced Injury in Human Hepatocyte and its Mechanism. *J. Food Biochem.*, e13412. doi:10.1111/jfbc.13412

Wei, L., Dai, Y., Zhou, Y., He, Z., Yao, J., Zhao, L., et al. (2017). Oroxylin A Activates PKM1/HNF4 Alpha to Induce Hepatoma Differentiation and Block Cancer Progression. *Cell Death Dis* 8 (7), e2944. doi:10.1038/cddis.2017.335

Wei, R., Cao, J., and Yao, S. (2018). Matrine Promotes Liver Cancer Cell Apoptosis by Inhibiting Mitophagy and PINK1/Parkin Pathways. *Cell Stress Chaperones* 23 (6), 1295–1309. doi:10.1007/s12192-018-0937-7

Wu, C., Chen, W., Ding, H., Li, D., Wen, G., Zhang, C., et al. (2019b). Salvianolic Acid B Exerts Anti-liver Fibrosis Effects via Inhibition of MAPK-Mediated Phospho-Smad2/3 at Linker Regions In Vivo and In Vitro. *Life Sci.* 239, 116881. doi:10.1016/j.lfs.2019.116881

Wu, C., Jing, M., Yang, L., Jin, L., Ding, Y., Lu, J., et al. (2018a). Alisol A 24-acetate Ameliorates Nonalcoholic Steatohepatitis by Inhibiting Oxidative Stress and Stimulating Autophagy through the AMPK/mTOR Pathway. *Chem. Biol. Interact* 291, 111–119. doi:10.1016/j.cbi.2018.06.005

Wu, C. T., Deng, J. S., Huang, W. C., Shieh, P. C., Chung, M. I., and Huang, G. J. (2019a). Salvianolic Acid C Against Acetaminophen-Induced Acute Liver Injury by Attenuating Inflammation, Oxidative Stress, and Apoptosis through Inhibition of the Keap1/Nrf2/HO-1 Signaling. *Oxid Med. Cel Longev* 2019, 9056845. doi:10.1155/2019/9056845

Wu, K., Fan, J., Huang, X., Wu, X., and Guo, C. (2018b). Hepatoprotective Effects Exerted by Poria Cocos Polysaccharides Against Acetaminophen-Induced Liver Injury in Mice. *Int. J. Biol. Macromol* 114, 137–142. doi:10.1016/j.ijbiomac.2018.03.107

Wu, K., Guo, C., Yang, B., Wu, X., and Wang, W. (2019c). Antihepatotoxic Benefits of Poria Cocos Polysaccharides on Acetaminophen-Lesioned Livers In Vivo and In Vitro. *J. Cel Biochem* 120 (5), 7482–7488. doi:10.1002/jcb.28022

Wu, Q. (2001). *Traditional Chinese Medicine for Liver Disease*. Beijing: China medical science and technology press.

Wu, X., Zhang, F., Xiong, X., Lu, C., Lian, N., Lu, Y., et al. (2015). Tetramethylpyrazine Reduces Inflammation in Liver Fibrosis and Inhibits Inflammatory Cytokine Expression in Hepatic Stellate Cells by Modulating NLRP3 Inflammasome Pathway. *IUBMB Life* 67 (4), 312–321. doi:10.1002/iub.1348

Wu, X., Zhi, F., Lun, W., Deng, Q., and Zhang, W. (2018c). Baicalin Inhibits PDGF-BB-Induced Hepatic Stellate Cell Proliferation, Apoptosis, Invasion, Migration and Activation via the miR-3595/ACSL4 axis. *Int. J. Mol. Med.* 41 (4), 1992–2002. doi:10.3892/ijmm.2018.3427

Wu, Z., Meng, X., Hu, J., Ding, Y., and Peng, Y. (2017). Research Progress on the Relationship between TLR4-MyD88-NF-kB Signaling Pathway and Hepatitis Liver Fibrosis Liver Cancer axis. *Int. J. Pharm. Res.* 44 (05), 396–401.

Xian, Z., Tian, J., Wang, L., Zhang, Y., Han, J., Deng, N., et al. (2020). Effects of Rhein on Bile Acid Homeostasis in Rats. *Biomed. Res. Int.* 2020, 8827955. doi:10.1155/2020/8827955

Xiao, Y., Kim, M., and Lazar, M. A. (2020). Nuclear Receptors and Transcriptional Regulation in Non-alcoholic Fatty Liver Disease. *Mol. Metab.* 50, 101119. doi:10.1016/j.molmet.2020.101119

Xie, H., Su, D., Zhang, J., Ji, D., Mao, J., Hao, M., et al. (2020). Raw and Vinegar Processed Curcuma Wenyujin Regulates Hepatic Fibrosis via Bloking TGF-β/Smad Signaling Pathways and Up-Regulation of MMP-2/TIMP-1 Ratio. *J. Ethnopharmacol* 246, 111768. doi:10.1016/j.jep.2019.01.045

Xie, T., Li, K., Gong, X., Jiang, R., Huang, W., Chen, X., et al. (2018). Paeoniflorin Protects Against Liver Ischemia/reperfusion Injury in Mice via Inhibiting HMGB1-TLR4 Signaling Pathway. *Phytother Res.* 32 (11), 2247–2255. doi:10.1002/ptr.6161

Xu, F., Liu, C., Zhou, D., and Zhang, L. (2016). TGF-β/SMAD Pathway and its Regulation in Hepatic Fibrosis. *J. Histochem. Cytochem.* 64 (3), 157–167. doi:10.1369/0022155415627681

Xu, J., Li, C., Li, Z., Yang, C., Lei, L., Ren, W., et al. (2018). Protective Effects of Oxymatrine Against lipopolysaccharide/D-galactosamine-induced A-cute L-iver F-ailure through O-xidative D-amage, via A-ctivation of Nrf2/HO-1 and M-odulation of I-nflammatory TLR4-signaling P-athways. *Mol. Med. Rep.* 17 (1), 1907–1912. doi:10.3892/mmr.2017.8060

Yan, H., Gao, Y. Q., Zhang, Y., Wang, H., Liu, G. S., and Lei, J. Y. (2018). Chlorogenic Acid Alleviates Autophagy and Insulin Resistance by Suppressing JNK Pathway in a Rat Model of Nonalcoholic Fatty Liver Disease. *J. Biosci.* 43 (2), 287–294. doi:10.1007/s12038-018-9746-5

Yan, H., Jung, K. H., Kim, J., Rumman, M., Oh, M. S., and Hong, S. S. (2018). Artemisia Capillaris Extract AC68 Induces Apoptosis of Hepatocellular Carcinoma by Blocking the PI3K/AKT Pathway. *Biomed. Pharmacother.* 98, 134–141. doi:10.1016/j.biopha.2017.12.043

Yan, Z., Fan, R., Yin, S., Zhao, X., Liu, J., Li, L., et al. (2015). Protective Effects of Ginkgo Biloba Leaf Polysaccharide on Nonalcoholic Fatty Liver Disease and its Mechanisms. *Int. J. Biol. Macromol* 80, 573–580. doi:10.1016/j.ijbiomac.2015.05.054

Yang, F., Luo, L., Zhu, Z. D., Zhou, X., Wang, Y., Xue, J., et al. (2017). Chlorogenic Acid Inhibits Liver Fibrosis by Blocking the miR-21-Regulated TGF-β1/Smad7 Signaling Pathway In Vitro and In Vivo. *Front. Pharmacol.* 8, 929. doi:10.3389/fphar.2017.00929

Yang, F., Xu, Y., Xiong, A., He, Y., Yang, L., Wan, Y. J., et al. (2012). Evaluation of the Protective Effect of Rhei Radix et Rhizoma Against α-naphthylisothiocyanate Induced Liver Injury Based on Metabolic Profile of Bile Acids. *J. Ethnopharmacol* 144 (3), 599–604. doi:10.1016/j.jep.2012.09.049

Yang, G., and Wei, W. (2017). Research Progress on Immune Mechanism of Alcoholic Liver Disease and Prevention and Treatment of Traditional Chinese Medicine. *J. southwest Med. Univ.* 40 (03), 319–321.

Yang, H., Yang, T., Heng, C., Zhou, Y., Jiang, Z., Qian, X., et al. (2019a). Quercetin Improves Nonalcoholic Fatty Liver by Ameliorating Inflammation, Oxidative Stress, and Lipid Metabolism in Db/db Mice. *Phytother Res.* 33 (12), 3140–3152. doi:10.1002/ptr.6486

Yang, H., Zhou, Z., He, L., Ma, H., Qu, W., Yin, J., et al. (2018). Hepatoprotective and Inhibiting HBV Effects of Polysaccharides from Roots of Sophora Flavescens. *Int. J. Biol. Macromol* 108, 744–752. doi:10.1016/j.ijbiomac.2017.10.171

Yang, H. X., Shang, Y., Jin, Q., Wu, Y. L., Liu, J., Qiao, C. Y., et al. (2020a). Gentiopicroside Ameliorates the Progression from Hepatic Steatosis to Fibrosis Induced by Chronic Alcohol Intake. *Biomol. Ther. (Seoul)* 28 (4), 320–327. doi:10.4062/biomolther.2020.008

Yang, J. H., Kim, S. C., Kim, K. M., Jang, C. H., Cho, S. S., Kim, S. J., et al. (2016a). Isorhamnetin Attenuates Liver Fibrosis by Inhibiting TGF-β/Smad Signaling and Relieving Oxidative Stress. *Eur. J. Pharmacol.* 783, 92–102. doi:10.1016/j.ejphar.2016.04.042

Yang, M., Li, X., Zeng, X., Ou, Z., Xue, M., Gao, D., et al. (2016b). Rheum Palmatum L. Attenuates High Fat Diet-Induced Hepatosteatosis by Activating AMP-Activated Protein Kinase. *Am. J. Chin. Med.* 44 (3), 551–564. doi:10.1142/S0192415X16500300

Yang, R., Song, C., Chen, J., Zhou, L., Jiang, X., Cao, X., et al. (2020b). Limonin Ameliorates Acetaminophen-Induced Hepatotoxicity by Activating Nrf2 Antioxidative Pathway and Inhibiting NF-Kb Inflammatory Response via Upregulating Sirt1. *Phytomedicine* 69, 153211. doi:10.1016/j.phymed.2020.153211

Yang, Y., Zhao, J., Song, X., Li, L., Li, F., Shang, J., et al. (2019b). Amygdalin Reduces Lipopolysaccharide-Induced Chronic Liver Injury in Rats by Down-Regulating PI3K/AKT, JAK2/STAT3 and NF-Kb Signalling Pathways. *Artif. Cell Nanomed Biotechnol* 47 (1), 2688–2697. doi:10.1080/21691401.2019.1634084

Yari, Z., Cheraghpour, M., Alavian, S. M., Hedayati, M., Eini-Zinab, H., and Hekmatdoost, A. (2021). The Efficacy of Flaxseed and Hesperidin on Non-alcoholic Fatty Liver Disease: An Open-Labeled Randomized Controlled Trial. *Eur. J. Clin. Nutr.* 75 (1), 99–111. doi:10.1038/s41430-020-0679-3

Yi, Y., Zhao, Y., Li, C., Zhang, Y., Bin, Y., Yuan, Y., et al. (2018). Potential Chronic Liver Toxicity in Rats Orally Administered an Ethanol Extract of Huangqin (Radix Scutellariae Baicalensis). *J. Tradit Chin. Med.* 38 (2), 242–256.

Yim, D., Kim, M. J., Shin, Y., Lee, S. J., Shin, J. G., and Kim, D. H. (2019). Inhibition of Cytochrome P450 Activities by Sophora Flavescens Extract and its Prenylated Flavonoids in Human Liver Microsomes. *Evid. Based Complement. Alternat Med.* 2019, 2673769. doi:10.1155/2019/2673769

Yokomori, H., Oda, M., Yoshimura, K., and Hibi, T. (2012). Recent Advances in Liver Sinusoidal Endothelial Ultrastructure and Fine Structure Immunocytochemistry. *Micron* 43 (2-3), 129–134. doi:10.1016/j.micron.2011.08.002

Younossi, Z. M. (2019). Non-alcoholic Fatty Liver Disease - A Global Public Health Perspective. *J. Hepatol.* 70 (3), 531–544. doi:10.1016/j.jhep.2018.10.033

Yu, Q., Liu, T., Li, S., Feng, J., Wu, L., Wang, W., et al. (20182018). The Protective Effects of Levo-Tetrahydropalmatine on ConA-Induced Liver Injury Are via TRAF6/JNK Signaling. *Mediators Inflamm.* 2018, 4032484. doi:10.1155/2018/4032484

Yu, Q., Cheng, P., Wu, J., and Guo, C. (2021). Pparγ/NF-Kb and TGF-β1/Smad Pathway Are Involved in the Anti-fibrotic Effects of Levo-Tetrahydropalmatine on Liver Fibrosis. *J. Cel Mol Med* 25 (3), 1645–1660. doi:10.1111/jcmm.16267

Yuan, F., Chen, J., Wu, W. J., Chen, S. Z., Wang, X. D., Su, Z., et al. (2010). Effects of Matrine and Oxymatrine on Catalytic Activity of Cytochrome P450s in Rats. *Basic Clin. Pharmacol. Toxicol.* 107 (5), 906–913. doi:10.1111/j.1742-7843.2010.00596.x

Yuan, R., Tao, X., Liang, S., Pan, Y., He, L., Sun, J., et al. (2018). Protective Effect of Acidic Polysaccharide from Schisandra Chinensis on Acute Ethanol-Induced Liver Injury through Reducing CYP2E1-dependent Oxidative Stress. *Biomed. Pharmacother.* 99, 537–542. doi:10.1016/j.biopha.2018.01.079

Yuen, M. F., Chen, D. S., Dusheiko, G. M., Janssen, H. L. A., Lau, D. T. Y., Locarnini, S. A., et al. (2018). Hepatitis B Virus Infection. *Nat. Rev. Dis. Primers* 4, 18035. doi:10.1038/nrdp.2018.35

Yun, Y. R., Kim, J. H., Kim, J. H., and Jung, M. H. (2017). Protective Effects of Gomisin N Against Hepatic Steatosis Through AMPK Activation. *Biochem. Biophys. Res. Commun.* 482 (4), 1095–1101. doi:10.1016/j.bbrc.2016.11.164

Zang, W., Bian, H., Huang, X., Yin, G., Zhang, C., Han, L. I., et al. (2019). Traditional Chinese Medicine (TCM) Astragalus Membranaceus and Curcuma Wenyujin Promote Vascular Normalization in Tumor-Derived Endothelial Cells of Human Hepatocellular Carcinoma. *Anticancer Res.* 39 (6), 2739–2747. doi:10.21873/anticanres.13400

Zeng, H., Li, D., Qin, X., Chen, P., Tan, H., Zeng, X., et al. (2016). Hepatoprotective Effects of Schisandra Sphenanthera Extract Against Lithocholic Acid-Induced Cholestasis in Male Mice Are Associated with Activation of the Pregnane X Receptor Pathway and Promotion of Liver Regeneration. *Drug Metab. Dispos* 44 (3), 337–342. doi:10.1124/dmd.115.066969

Zeng, X., Li, X., Xu, C., Jiang, F., Mo, Y., Fan, X., et al. (2017). Schisandra Sphenanthera Extract (Wuzhi Tablet) Protects Against Chronic-Binge and Acute Alcohol-Induced Liver Injury by Regulating the NRF2-ARE Pathway in Mice. *Acta Pharm. Sin B* 7 (5), 583–592. doi:10.1016/j.apsb.2017.04.002

Zhang, C. Y., Jiang, Z. M., Ma, X. F., Li, Y., Liu, X. Z., Li, L. L., et al. (2019). Saikosaponin-d Inhibits the Hepatoma Cells and Enhances Chemosensitivity through SENP5-dependent Inhibition of Gli1 SUMOylation Under Hypoxia. *Front. Pharmacol.* 10, 1039. doi:10.3389/fphar.2019.01039

Zhang, H., Yang, L., Wang, Y., Huang, W., Li, Y., Chen, S., et al. (2020a). Oxymatrine Alleviated Hepatic Lipid Metabolism via Regulating miR-182 in Non-alcoholic Fatty Liver Disease. *Life Sci.* 257, 118090. doi:10.1016/j.lfs.2020.118090

Zhang, Y., Wang, H., Zhang, L., Yuan, Y., and Yu, D. (2020b). Codonopsis Lanceolata Polysaccharide CLPS Alleviates High Fat/high Sucrose Diet-Induced Insulin Resistance via Anti-oxidative Stress. *Int. J. Biol. Macromol* 145, 944–949. doi:10.1016/j.ijbiomac.2019.09.185

Zhang, Y., Yang, X., Wang, S., Song, S., and Yang, X. (2021). Gentiopicroside Prevents Alcoholic Liver Damage by Improving Mitochondrial Dysfunction in the Rat Model. *Phytother Res.* 35 (4), 2230–2251. doi:10.1002/ptr.6981

Zhang, Y., Zhao, H., Li, H., Cao, W., Wang, F., Zhang, T., et al. (2017). Protective Effects of Amarogentin Against Carbon Tetrachloride-Induced Liver Fibrosis in Mice. *Molecules* 22 (5). doi:10.3390/molecules22050754

Zhang, Z., Chen, S., Mei, H., Xuan, J., Guo, X., Couch, L., et al. (2015). Ginkgo Biloba Leaf Extract Induces DNA Damage by Inhibiting Topoisomerase II Activity in Human Hepatic Cells. *Sci. Rep.* 5, 14633. doi:10.1038/srep14633

Zhao, H., Zhang, Y., Shu, L., Song, G., and Ma, H. (2019a). Resveratrol Reduces Liver Endoplasmic Reticulum Stress and Improves Insulin Sensitivity In Vivo and In Vitro. *Drug Des. Devel Ther.* 13, 1473–1485. doi:10.2147/DDDT.S203833

Zhao, H. W., Zhang, Z. F., Chai, X., Li, G. Q., Cui, H. R., Wang, H. B., et al. (2016). Oxymatrine Attenuates CCl4-Induced Hepatic Fibrosis via Modulation of TLR4-dependent Inflammatory and TGF-B1 Signaling Pathways. *Int. Immunopharmacol* 36, 249–255. doi:10.1016/j.intimp.2016.04.040

Zhao, P., Piao, X., Pan, L., Zeng, Z., Li, Q., Xu, X., et al. (2017). Forsythia Suspensa Extract Attenuates Lipopolysaccharide-Induced Inflammatory Liver Injury in Rats via Promoting Antioxidant Defense Mechanisms. *Anim. Sci. J.* 88 (6), 873–881. doi:10.1111/asj.12717

Zhao, Q., Wei, M., Zhang, S., Huang, Z., Lu, B., and Ji, L. (2020). The Water Extract of Sophorae tonkinensis Radix et Rhizoma Alleviates Non-alcoholic Fatty Liver Disease and Its Mechanism. *Phytomedicine* 77, 153270. doi:10.1016/j.phymed.2020.153270

Zhao, X. J., Chen, L., Zhao, Y., Pan, Y., Yang, Y. Z., Sun, Y., et al. (2019b). Polygonum Cuspidatum Extract Attenuates Fructose-Induced Liver Lipid Accumulation through Inhibiting Keap1 and Activating Nrf2 Antioxidant Pathway. *Phytomedicine* 63, 152986. doi:10.1016/j.phymed.2019.152986

Zhao, X. J., Yu, H. W., Yang, Y. Z., Wu, W. Y., Chen, T. Y., Jia, K. K., et al. (2018a). Polydatin Prevents Fructose-Induced Liver Inflammation and Lipid Deposition through Increasing miR-200a to Regulate Keap1/Nrf2 Pathway. *Redox Biol.* 18, 124–137. doi:10.1016/j.redox.2018.07.002

Zhao, Y., Ma, X., Wang, J., Zhu, Y., Li, R., Wang, J., et al. (2014). Paeoniflorin Alleviates Liver Fibrosis by Inhibiting HIF-1α Through mTOR-dependent Pathway. *Fitoterapia* 99, 318–327. doi:10.1016/j.fitote.2014.10.009

Zhao, Z., Wei, Q., Hua, W., Liu, Y., Liu, X., and Zhu, Y. (2018b). Hepatoprotective Effects of Berberine on Acetaminophen-Induced Hepatotoxicity in Mice. *Biomed. Pharmacother.* 103, 1319–1326. doi:10.1016/j.biopha.2018.04.175

Zheng, N., Liu, F., Lu, H., Zhan, Y., Zhang, M., Guo, W., et al. (2017). Schisantherin A Protects Against Liver Ischemia-Reperfusion Injury via Inhibition of Mitogen-Activated Protein Kinase Pathway. *Int. Immunopharmacol* 47, 28–37. doi:10.1016/j.intimp.2017.03.019

Zhong, W., Qian, K., Xiong, J., Ma, K., Wang, A., and Zou, Y. (2016). Curcumin Alleviates Lipopolysaccharide Induced Sepsis and Liver Failure by Suppression of Oxidative Stress-Related Inflammation via PI3K/AKT and NF-Kb Related Signaling. *Biomed. Pharmacother.* 83, 302–313. doi:10.1016/j.biopha.2016.06.036

Zhou, L., Yang, F., Li, G., Huang, J., Liu, Y., Zhang, Q., et al. (2018). Coptisine Induces Apoptosis in Human Hepatoma Cells Through Activating 67-kDa Laminin Receptor/cGMP Signaling. *Front. Pharmacol.* 9, 517. doi:10.3389/fphar.2018.00517

Zhou, W. C., Zhang, Q. B., and Qiao, L. (2014). Pathogenesis of Liver Cirrhosis. *World J. Gastroenterol.* 20 (23), 7312–7324. doi:10.3748/wjg.v20.i23.7312

Zhou, X., Cheung, C. M., Yang, J. M., Or, P. M., Lee, W. Y., and Yeung, J. H. (2015). Danshen (Salvia Miltiorrhiza) Water Extract Inhibits Paracetamol-Induced Toxicity in Primary Rat Hepatocytes via Reducing CYP2E1 Activity and Oxidative Stress. *J. Pharm. Pharmacol.* 67 (7), 980–989. doi:10.1111/jphp.12381

Zhou, X., Wang, L. L., Tang, W. J., and Tang, B. (2021). Astragaloside IV Inhibits Protein Tyrosine Phosphatase 1B and Improves Insulin Resistance in Insulin-Resistant HepG2 Cells and Triglyceride Accumulation in Oleic Acid (OA)-treated HepG2 Cells. *J. Ethnopharmacol* 268, 113556. doi:10.1016/j.jep.2020.113556

Zhu, H., He, C., Zhao, H., Jiang, W., Xu, S., Li, J., et al. (2020). Sennoside A Prevents Liver Fibrosis by Binding DNMT1 and Suppressing DNMT1-Mediated PTEN Hypermethylation in HSC Activation and Proliferation. *FASEB J.* 34 (11), 14558–14571. doi:10.1096/fj.202000494RR

Zhu, S. Y., Jiang, N., Yang, J., Tu, J., Zhou, Y., Xiao, X., et al. (2018a). Silybum marianum Oil Attenuates Hepatic Steatosis and Oxidative Stress in High Fat Diet-Fed Mice. *Biomed. Pharmacother.* 100, 191–197. doi:10.1016/j.biopha.2018.01.144

Zhu, X., Xiong, T., Liu, P., Guo, X., Xiao, L., Zhou, F., et al. (2018b). Quercetin Ameliorates HFD-Induced NAFLD by Promoting Hepatic VLDL Assembly and Lipophagy via the IRE1a/XBP1s Pathway. *Food Chem. Toxicol.* 114, 52–60. doi:10.1016/j.fct.2018.02.019

Zou, C., Su, N., Wu, J., Xu, M., Sun, Z., Liu, Q., et al. (2019). Dietary Radix Bupleuri Extracts Improves Hepatic Lipid Accumulation and Immune Response of Hybrid Grouper (Epinephelus Lanceolatus♂ × Epinephelus Fuscoguttatus♀). *Fish. Shellfish Immunol.* 88, 496–507. doi:10.1016/j.fsi.2019.02.052

Zou, C., Tan, X., Ye, H., Sun, Z., Chen, S., Liu, Q., et al. (2018). The Hepatoprotective Effects of Radix Bupleuri Extracts Against D-Galactosamine/lipopolysaccharide Induced Liver Injury in Hybrid Grouper (Epinephelus Lanceolatus♂ × Epinephelus Fuscoguttatus♀). *Fish. Shellfish Immunol.* 83, 8–17. doi:10.1016/j.fsi.2018.08.047

Conflict of Interest: The authors declare that the research was conducted in the absence of any commercial or financial relationships that could be construed as a potential conflict of interest.

Publisher's Note: All claims expressed in this article are solely those of the authors and do not necessarily represent those of their affiliated organizations, or those of the publisher, the editors and the reviewers. Any product that may be evaluated in this article, or claim that may be made by its manufacturer, is not guaranteed or endorsed by the publisher.

frontiers in Pharmacology

ORIGINAL RESEARCH
published: 23 November 2021
doi: 10.3389/fphar.2021.726199

Anticholesterolemic Activity of Three Vegetal Extracts (Artichoke, Caigua, and Fenugreek) and Their Unique Blend

Jessica Frigerio[1,2], *Erik Tedesco*[3], *Federico Benetti*[3], *Violetta Insolia*[4], *Giovanna Nicotra*[4], *Valerio Mezzasalma*[1], *Stefania Pagliari*[2], *Massimo Labra*[2] *and Luca Campone*[2]*

[1]FEM2-Ambiente, Milano, Italy, [2]Zooplantlab, Department of Biotechnology and Biosciences, University of Milano-Bicocca, Milano, Italy, [3]ECSIN-European Center for the Sustainable Impact of Nanotechnology, ECAMRICERT SRL, Padova, Italy, [4]EPO Srl, Milano, Italy

OPEN ACCESS

Edited by:
Silvia Di Giacomo,
Sapienza University of Rome, Italy

Reviewed by:
Yanwen Wang,
National Research Council Canada (NRC-CNRC), Canada
Ginpreet Kaur,
SVKM's Narsee Monjee Institute of Management Studies, India

***Correspondence:**
Luca Campone
luca.campone@unimib.it

Specialty section:
This article was submitted to Gastrointestinal and Hepatic Pharmacology, a section of the journal Frontiers in Pharmacology

Received: *16 June 2021*
Accepted: *18 October 2021*
Published: *23 November 2021*

Citation:
Frigerio J, Tedesco E, Benetti F, Insolia V, Nicotra G, Mezzasalma V, Pagliari S, Labra M and Campone L (2021) Anticholesterolemic Activity of Three Vegetal Extracts (Artichoke, Caigua, and Fenugreek) and Their Unique Blend. Front. Pharmacol. 12:726199. doi: 10.3389/fphar.2021.726199

Hepatic-related diseases, in particular hyperlipidemia and hypercholesterolemia, are a thorn on the side of the national health institutes around the globe. Indeed, liver lipid and cholesterol dysregulation could lead to atherosclerotic plaque formation and cardiovascular diseases. Currently, statin administration and monacolin K consumption are the main therapies proposed to counter this alarming connection, but relevant side effects are known. To overcome this issue, safe nutraceutical formulations and/or vegetal extracts, endowed with anticholesterolemic activity, could be instrumental in hypercholesterolemia prevention and treatment. In the present work, the anticholesterolemic efficacy of three vegetal extracts used in traditional medicine (artichoke, caigua, and fenugreek), their unique blend (ACFB), and the monacolin K-containing red yeast extract (RYR), was investigated with an *in vitro* approach based on hepatic cell line HepG2. The impact on cholesterol of the three extracts, their blend, and RYR were investigated by determining hepatocyte total and free cholesterol and bile acids biosynthesis. According to our results, the anticholesterolemic activity of the vegetal extracts was confirmed, and a novel choleretic activity of caigua extract was evidenced. ACFB showed to be safer than RYR while showing a similar effect on total and free cholesterol and bile acids synthesis compared to it. The anticholesterolemic activity of the blend was obtained with lower vegetal extract concentrations compared with the single vegetal extract, potentially indicating an additive effect between the extracts. In conclusion, the vegetal extracts and their blend, ACFB, are safe and are endowed with anticholesterolemic activity, potentially providing complementary therapies to the statin-based ones for hyperlipidemia and hypercholesterolemia-related complications.

Keywords: anticholesterolemic activity, caigua, fenugreek, artichoke, botanicals, hepatic disease, choleretic activity

INTRODUCTION

The liver is considered one of the most active organs in the human body (Ozougwu and Eyo, 2014). Indeed, the liver is a multifunctional organ, dealing with the regulation of many critical processes, such as bile secretion, metabolic detoxification, etc., and it is the mastermind behind nutrient metabolism and waste metabolites excretion. As such, it is not surprising that liver disease accounts for approximately 2 million deaths per year, equivalent to about 3.5% of all deaths worldwide (Rinella and Charlton, 2016; Asrani et al., 2019). In parallel with alcohol consumption, the progressive accumulation of fat in the liver (i.e., liver steatosis) is one of the main processes responsible for the onset and development of liver diseases. The liver is responsible for lipid homeostasis, regulating their absorption, distribution, and storage, β-oxidation, and lipogenesis (Ponziani et al., 2015; Pei et al., 2020). Among lipids in which homeostasis is regulated by the liver, cholesterol is undoubtedly one of the most important. Indeed, other than being a structural building block for all cell membranes (Liscum and Underwood, 1995; Simons and Ikonen, 2000; Grouleff et al., 2015), cholesterol is a cell signaling and neuronal conduction modulator (Orth and Bellosta, 2012; Sheng et al., 2012; Jin et al., 2019; Dai et al., 2021), and precursor to several relevant biomolecules such as steroid hormones, vitamin D, and bile acids (Russell, 2009). Cholesterol could be synthetized (*de novo* biosynthesis) by virtually all nucleated cells through the mevalonate pathway, a complex biochemical pathway mainly regulated by the activity of the HMG-CoA reductase (HMGCR), the primary rate-limiting enzyme in cholesterol biosynthesis. Beyond *de novo* cholesterol biosynthesis, responsible for two-thirds of the body cholesterol, cholesterol is also absorbed at the intestinal epithelium level, through a process known as exogenous pathway, involving several key proteins, such as the cholesterol transporter NPC1L1, the clathrin adaptor NUMB, and the adaptor protein LIMA1 (Altmann et al., 2004; Li et al., 2014; Afonso et al., 2018; Y-Y et al., 2018). Once within the cell, cholesterol is dynamically transported to the destined membranes for structural and functional needs (Morgan et al., 2016; Luo et al., 2019; Qi et al., 2020). However, when its absorption and/or *de novo* synthesis exceeds the cellular demand, cholesterol is either exported outside the cell by specific transporters, the ATP-binding cassette (ABC) transporters, or converted to cholesteryl esters by A:cholesterol acyltransferases (ACATs) and then stored in lipid droplets or secreted in the bloodstream via lipoproteins (Chang et al., 2006; Wang et al., 2017). However, while virtually all nucleated cells possess the molecular machinery to synthesize cholesterol (Arnold and Kwiterovich, 2003), only the liver, and in particular the hepatocytes, has the ability to eliminate cholesterol via bile secretion or its conversion into bile acids, with the latter now recognized as fundamental modulators of lipid, glucose, and energy metabolism through the activation of specific receptors (Russell, 2003; De Aguiar Vallim et al., 2013; Li and Chiang, 2015; Chiang and Ferrell, 2019). As such, the liver is the principal site for cholesterol homeostasis, mainly via biosynthesis, uptake through low-density lipoprotein receptors, lipoprotein release in the blood, storage by esterification and degradation, and conversion into bile acids (Weber et al., 2004). Liver failure in regulating cholesterol homeostasis, leading to hypercholesterolemia, is known to be a key point in cardiovascular disease development, such as coronary artery diseases (CAD), linked with the progressive accumulation of cholesterol at the atherosclerotic plaque level (Wider et al., 2016). Currently, statins (i.e. atorvastatin, fluvastatin, etc.) are the most widely prescribed drugs to lower plasma and hepatic cholesterol levels (Tiwari and Pathak, 2011) and, in response to the increased hypercholesterolemia population incidence, their use (and abuse) has grown exponentially. A clear example of this uncontrolled use is represented by monacolin K, the major representative of monacolins, natural statins present in *Monascus purpureus* Went (red yeast) extract (Nannoni et al., 2015). Despite their undeniable efficacy, some concerns were raised regarding statin- and monacolin-based therapy safety (Adhyaru and Jacobson, 2018). Regarding this topic, the European Food Safety Authority (EFSA) has recently published a scientific opinion on monacolin k safety, indicating that a dietary intake that does not give rise to concerns about harmful effects to health was not identified, for both the general population and vulnerable subgroups of the population (Younes et al., 2018). Regarding hypercholesterolemia problems, nutraceutical formulations have received considerable interest due to their nutritional, safety, and efficacy features. Indeed, the application of natural products, in particular, plant extracts, for cholesterol-related diseases, due mainly to fat-rich diet, is well rooted in the history of many populations. For example, the Mediterranean population reduced hypercholesterolemia-related conditions with the assumption of artichoke (*Cynara scolymus* L.) leaves or their extracts (Shimoda et al., 2003; Heidarian et al., 2011; Mohamed Abdel Magied et al., 2016), traditionally used as a diuretic and choleretic as well as for jaundice and liver insufficiency treatment (Wider et al., 2016). To the same end, the Brazilian population consumes caigua (*Cyclanthera pedata* Schrad.), an herbaceous vine better known as "maxixe do reino." While its consumption is still very limited, recent studies have highlighted its potential use for hypercholesterolemia treatment, since it effectively lowers serum cholesterol level by regulating low- and high-density lipoproteins (LDL and HDL) (Gonzales et al., 1995; Montoro et al., 2001). In India and China (Asia), the side effects of a cholesterol-rich diet are traditionally dealt with the consumption of *Trigonella foenum-graecum* L. (fenugreek), an annual plant of the Fabaceae family. Fenugreek has been traditionally used for hypercholesterolemia, diabetes, coughs, congestion, bronchitis, fever, and high blood pressure (Basch et al., 2003; Vyas et al., 2008). The aim of the present work is to screen these novel vegetal extracts as single and uniquely blended in a novel nutraceutical formulation (artichoke caigua fenugreek blend; ACFB) for their anticholesterolemic activity at the hepatic level, as potential monacolin K substitute in hypercholesterolemia treatment. While *in vivo* studies remain the more reliable approach to investigate the effect of novel substances on liver metabolism, they are challenging due to the use of proxy measurements (e.g., the use of stable isotope tracers) and

limited availability of liver biopsies (Steenbergen et al., 2013; Green et al., 2015). As such, for a preliminary screening of vegetal extracts and formulation efficacy and safety, an *in vitro* approach is usually preferred. For *in vitro* cellular studies, primary human hepatocytes are considered the best choice, but they present availability issues, interdonor variability, and a limited timeframe in which they remain differentiated (Steenbergen et al., 2013; Green et al., 2015). As a result, proliferating human hepatoma cell models, such as HepG2 cells, are the most widely used option. The human hepatoblastoma-derived cell line HepG2 is endowed with many functions attributed to a normal human hepatocyte. Indeed, this cell line secretes different plasma proteins (Knowles et al., 1980), including apolipoproteins, among which apoB-100 is the sole apoB species secreted by the human liver. Furthermore, HepG2 cells can synthesize and secrete lipoproteins, ranging from very low-density lipoprotein (VLDL) to high-density lipoprotein (HDL) (Rash et al., 1981; Zannis et al., 1981; Tam et al., 1985). Of the hepato-specific functions, these cells retain the ability to express the major regulatory enzymes of hepatic, plasma, and biliary cholesterol metabolism and are reported to synthesize and secrete bile acids including chenodeoxycholate and cholate (Everson and Polokoff, 1986). These activities respond in a manner consistent with what is known about human cholesterol metabolism *in vivo*, at least at a qualitative level. Moreover, HepG2 express receptors for insulin and transferrin (Ciechanover et al., 1983), estrogen (Tam et al., 1985), and LDL (Havekes et al., 1983; Dashti et al., 1984; Wu et al., 1984; Hoeg et al., 1985), and bind HDL (Hoeg et al., 1985), showing a close resemblance to primary hepatocyte receptor pool. Finally, HepG2 has a hepatocyte-like differentiated plasma membrane including a bile canalicular region, closely resembling primary hepatocyte morphology (Geuze et al., 1983).

The botanical identification of the three plant species was performed by DNA barcoding analysis, whereas the chemical characterization of the major constituent was performed by ultraperformance liquid chromatography coupled with quadrupole time of flight tandem mass spectrometry (UHPLC/QTof-MS). Moreover, in the present study, the anticholesterolemic and bile acid synthesis-promoting activity of ACFB is compared with two well-known anticholesterolemic substances, atorvastatin and *M. purpureus* extract.

MATERIALS AND METHODS

Materials

The Plant Genomic DNA Extract Mini Kit was purchased from Fisher Molecular Biology (Rome, Italy). The Qubit dsDNA HS Assay Kit was purchased from Invitrogen (Carlsbad, CA, USA). The PCR Mix Plus was purchased from A&A Biotechnology (Gdansk, Poland). HepG2 cell line (ATCC® HB-8065™) was purchased from ATCC (Manassas, VA, USA). Dulbecco's modified Eagle medium (DMEM) with GlutaMAX was purchased from Thermo Fisher Scientific (Waltham, MA, USA). Phosphate-buffered saline (PBS), penicillin–streptomycin mix, dimethyl sulfoxide (DMSO), and Cholesterol Quantitation Kit were purchased from Sigma-Aldrich (St. Louis, MO, USA). Fetal bovine serum (FBS) was purchased from Euroclone (Milan, Italy). CellTiter 96® AQueous One Solution Cell Proliferation Assay (MTS) was purchased from Promega (Madison, WI, USA). The Total Bile Acid Assay Kit (Fluorometric) was purchased from Cell Biolabs San Diego, CA, USA). OriginLab software was purchase from OriginLab Corporation (Northampton, MA, USA).

Methods

The determination of anticholesterolemic activity with an *in vitro* hepatic model, based on HepG2 cells, was performed on five samples, wherein each commercial name is reported in SI1: three vegetal extracts (*C. scolymus*, *C. pedata*, and *T. foenum-graecum*) and two formulations, *M. purpureus* extract (red yeast rice), 5% monacolin K (RYR), and ACFB. The latter formulation, known commercially as Omeolipid, is a polyextract of *C. scolymus*, *C. pedata*, and *T. foenum-graecum*, originating from the three vegetal simultaneous extraction (**Supplementary Table S1**).

Species identification by DNA barcoding

Sample collection and DNA extraction

Analyzed samples *Cyclanthera pedata*, *Trigonella foenum-graecum*, and *Cynara scolymus* were provided by EPO Srl. Among those provided as *Cyclanthera pedata*, one sample (DB690) came from some fresh fruits collected in Val Camonica (Italy) in November 2020. In order to analyze each batch representatively, five samples for each batch were collected. Fifty milligrams of dried plants were treated for DNA extraction by using the Plant Genomic DNA Extraction Mini Kit, following the manufacturer instructions. DNA for each sample was checked for concentration by using a Qubit 4.0 Fluorometer and Qubit dsDNA HS Assay Kit.

PCR condition, DNA sequencing, and species identification

The most suitable DNA barcode region for each species was chosen after an assessment of interspecific variability. Since *T. foenum-graecum* has high intraspecific variability, the gene *rbcL*, coding for the RuBisCO, was chosen as the most effective marker. For the species *C. pedata* and *C. scolymus*, the intergenic spacer *psbA-trnH* was chosen, due to its high power of discrimination. The primers used for DNA amplification are described in **Supplementary Table S2**. PCR amplification was carried out using PCR Mix Plus. The mix reaction is composed of 12.5 µl of PCR Mix Plus, 1 µl of each primer (10 µM), 7.5 µl of sterile water, and 3 µl of genomic DNA (30–50 ng). PCR cycles consisted of an initial denaturation step (7 min at 94°C), followed by 35 cycles of denaturation (45 s at 94°C), annealing (30 s at 50°C for rbcL and 53°C for psbA-trnH), and extension (1 min at 72°C), and a final extension step at 72°C for 7 min. Amplicon presence was assessed by electrophoresis on 1.5% agarose gel. Purified amplification products were bidirectionally sequenced by Eurofins Genomics. The 3′ and 5′ terminal portions of each sequence were clipped to generate consensus sequences for each sample. All sequences were manually edited, the primer was removed, and after pairwise alignment, the obtained sequences were identified by a standard comparison approach against a GenBank database with Basic Local Alignment Search Tool (BLAST) (https://blast.ncbi.nlm.

nih.gov/). Each barcode sequence was taxonomically assigned to the plant species with the nearest matches (maximum identity >99% and query coverage of 100%) according to Galimberti and colleagues (Galimberti et al., 2016).

UHPLC-DAD-HRMS/MS profiles of ACFB

The identification of compounds in the extracts was carried out using using a Waters ACQUITY UPLC system coupled with a Waters Xevo G2-XS QTof Mass Spectrometer (Waters Corp., Milford, MA, USA). All analytes were separated on a Kinetex Biphenyl (100 mm × 2.1 mm, 2.6 μm). The mobile phases were both MS grade H_2O (A) and CH_3CN (B), both containing 0.1% formic acid (HCOOH), with gradient elution as follows: 0–2.0 min, 5–10% B; 2.0–17.0 min, 10–35% B; 17.0–18.0 min, 35%–95%, after each run of 5 min of wash (98% B), and 5 min of equilibration was performed before the next sample injection. Elution was performed at a flow rate of 400 μl min^{-1}, and the injection volume was 10 μl. The column temperature was set to 30°C. UV spectra were acquired in the range of 210–400 nm, and two wavelengths, 280 and 330 nm, were employed for the detection of target analytes. The Xevo G2-XS QTof Mass Spectrometer equipped with an ESI source, was used in negative and positive ionization modes to acquire full-scan MS, and the spectra were recorded in the range of m/z 100–1,000. The source parameters were as follows: electrospray capillary voltage 2.5 kV, source temperature 150°C, and desolvation temperature 500°C. The cone and desolvation gas flows were 10 and 1,000 L/h, respectively. A scan time of 0.5 s was employed. The cone voltage was set to 60 V, and ramping collision energies ranged from 6 to 30 V to produce abundant product ions before detection at the Tof. The mass spectrometer was calibrated with 0.5 M sodium formate, and leucine-enkephalin (100 pg/μl) was used as LockMass (m/z 554.2615, 2 kV ionization voltage), which was infused simultaneously with the flow of column at 10 μl/min and acquired for 1 s each 10 s. The base peak chromatograms (BPI) were acquired at low (6) and high (30) energy from which the peak identification was performed. From the low-energy spectra, the molecular ion mass [M – H]– was obtained from which the elementary composition was calculated (mass error <5 ppm), while from the high-energy spectra, the fragmentation pattern was obtained, and the information was used for the identification. Phenolic compounds were characterized according to the corresponding spectral characteristics (UV and MS spectra [M – H]–), accurate mass, characteristic fragmentation, and consulted different databases (PubChem, ChemSpider, and KEGG). The MassLynx software (version 4.2) was used for instrument control, data acquisition, and data processing.

HepG2 cell culture

The human epithelial hepatocellular carcinoma HepG2 cells (passage 90–95) were maintained in HepG2 cell culture medium (HepG2 CCM) (DMEM + GlutaMAX medium supplemented with 10% FBS and 1% penicillin–Streptomycin mix). The cells were grown in a controlled atmosphere incubator (85% relative humidity, 5% CO_2, and 37°C). HepG2 cells were seeded at 20,000 cell/cm^2, and the medium changed every other day. Cells were subcultivated by trypsinization every 4 days, when 80%–90% confluent.

Solubilization of vegetal extracts, ACFB, and red yeast rice

The three vegetal extracts were resuspended in water up to a concentration of 750 mg/ml for *C. scolymus* and *C. pedate* extracts and 400 mg/ml for *T. foenum-graecum* extract. ACFB was easily resuspended in water to a concentration of 300 mg/ml, while RYR shown to be sparingly soluble in the same solvent. To improve the solubilization of monacolin K, RYR was resuspended in DMSO to a concentration of 200 mg/ml. This stock was further diluted in HepG2 culture medium to a concentration of 100 mg/ml, vortexed, centrifuged to pellet insoluble material, and finally, the resultant supernatant was collected. Monacolin K concentration in the supernatant was determined by HPLC (high-performance liquid chromatography). Since the concentration of extracted monacolin K was low (0.08 μg/ml), we tried to improve monacolin K solubilization with different solvents (i.e., ethanol and methanol), following the indications provided by the work of Singgih and colleagues (Singgih et al., 2014). Briefly, RYR was resuspended in methanol and ethanol, agitated with a shaker for 2 h at RT, and the supernatant was collected following centrifugation. At the end of the solubilization process, a spectrophotometric analysis of the obtained supernatants was performed, and the solubilization efficiency was evaluated by comparing their absorption at 240 nm (absorption peak for monacolin K) with that resulting from DMSO-based solubilization. Considering the different solvents in which the vegetal extracts of the ACFB and the RYR were resuspended, preliminary experiments were conducted to rule out any solvent-dependent effect on the considered endpoints (i.e., bile acids synthesis and cholesterol metabolism).

Cell viability assay on human hepatic cell line

To evaluate the impact of artichoke, caigua, and fenugreek extracts on HepG2 cells, and to determine their higher, non-toxic concentration, a dose–response curve experiment on HepG2 cells was performed. Briefly, HepG2 cells were seeded on 96-multiwell plates and left to adhere and propagate for 24 h. Following incubation, HepG2 cells were treated with increasing concentrations of caigua extract (from 0 to 75 mg/ml), fenugreek extract (from 0 to 40 mg/ml), and artichoke extract (from 0 to 75 mg/ml) for 48 h, corresponding to the duration of anticholesterolemic activity experiments. At the end of the incubation time, treated HepG2 cells were carefully washed with PBS, and their viability was determined by MTS assay, according to the instruction of the manufacturer. The same approach was applied to ACFB (from 0 to 10 mg/ml), RYR (from 0 to 2 mg/ml), and atorvastatin (positive control; from 0 to 9. 1 μg/ml), a statin medication used to treat abnormal lipid levels and to prevent cardiovascular disease in those at high risk (Lennernäs, 2003). Viability results were expressed as a percentage (%) compared with the negative control (HepG2 CCM-treated cells). Obtained results were fitted with OriginLab, and the EC50 (half-maximal effective concentration) value was calculated.

Anticholesterolemic activity evaluation

The specific anticholesterolemic activity at the hepatic level of the three vegetal extracts, ACFB, RYR, and atorvastatin was evaluated in a human hepatic cell line (HepG2). Briefly, HepG2 cells were seeded in six multiwell plates and were made to adhere and proliferate for 24 h. At the end of the incubation, HepG2 were exposed, for 48 h in controlled conditions, to the highest, non-toxic concentration of the three vegetal extracts, ACFB, and RYR, according to the dose–response results. For the positive control atorvastatin, a concentration comparable with that available in literature was applied (Han et al., 2017). At the end of the treatment, the hepatic cells were thoroughly washed with prewarmed PBS and processed for the determination of bile acids and the different forms of cholesterol.

1.2.6.1 Hepatic cholesterol biosynthesis evaluation

The anticholesterolemic activity of ACFB and RYR was evaluated by determining the total, free, and esterified cholesterol fractions following treatment (Guo et al., 2017). The different fractions were assessed with a commercial kit, Cholesterol Quantitation Kit, following the instructions of the producer. Briefly, at the end of the treatment with the three vegetal extracts, ACFB, RYR, and atorvastatin, treated HepG2 were collected by trypsinization, pelleted by centrifugation, and extracted with chloroform:isopropanol:IGEPAL® CA-630 (7:11:0.1 ratio) in a microhomogenizer. Then samples were centrifuged at 13,000 × *g* for 10 min to pellet insoluble material and the organic phase transferred to a new tube and air dried at 50°C to remove chloroform. To remove any residual organic solvent, samples were put under a vacuum for 30 min. Obtained dried lipids were resuspended in an appropriate buffer and sonicated until the mixture was homogenous. The different cholesterol fractions were measured with a coupled enzymatic reaction, which ensures the direct proportionality between the produced fluorescence (excitation wavelength 535 nm; emission wavelength 587 nm) and the concentration of the different cholesterol forms. Fluorescence readings were performed with a multiwell plate reader (Synergy4, Biotek). The results for total, free, and esterified cholesterol were normalized on sample protein concentration and expressed as a percentage (%) compared with the negative control (untreated hepatic cells).

Determination of bile acid production

The production of bile acids by the HepG2 cells, following treatment with vegetal extracts, ACFB, RYR, and atorvastatin, was evaluated with a fluorimetric assay (total bile acid assay) (Shao et al., 2016). Briefly, at the end of the treatment (48 h), cells were thoroughly washed with cold PBS before lysis, which was performed by sonication in cold PBS. Then lysates were centrifuged at 10,000 × *g* for 10 min at 4°C, and obtained supernatants were assayed for the presence of bile acids. Bile acid determination is based on the production of a fluorescent substrate (resorufin; excitation wavelength 560 nm and emission wavelength 590 nm) in their presence, due to the coupled activity of two enzymes. As for the cholesterol, obtained results were normalized on the protein concentration and expressed as a percentage (%) compared with the negative control (untreated hepatic cells).

Statistical analysis

Results were statistically analyzed by t-test, using OriginLab software (OriginLab Corporation, Northampton, MA, USA). Experiments were performed in triplicate, and results were presented as average ± standard deviation. For ACFB UHPLC-DAD-HRMS/MS profiles statistical analysis, analysis of variance (ANOVA) was used to compare the means, while Turkey's test was used to assess the statistically significant differences among treatments. A p-value of ≤0.05 was considered significant.

RESULTS

DNA barcoding results

DNA barcoding approach is a widely used molecular-based identification system based on the analysis of the variability within a standard region of the genome. An ideal DNA barcode requires high taxonomic coverage and high resolution (Hebert et al., 2003). As a general principle, a DNA barcode region should have a high interspecific and low intraspecific variability. Good DNA quality (i.e., A260/A230 and A260/A280 within the range 1.8–2.2) and extraction yield (i.e., 20–40 ng/μl) were obtained for all the analyzed samples. Each barcode sequence was taxonomically assigned by using BLASTn analysis to the plant species with the nearest matches (maximum identity >99% and query coverage of 100%). All the samples returned 100% maximum identity (with 100% query coverage). As shown in **Supplementary Table S3**, the results of DNA barcoding confirmed the declared species for all the samples, a fundamental step to obtain the suitable phytocomplexes for ACPB regarding the sample DB690. The results confirmed that the fruit known as "milione" or "miliun" is effectively *Cyclanthera pedata*, demonstrating, for the first time, to the best of our knowledge, that caigua is also grown in Val Camonica (Lombardy, Italy). This finding could positively impact the agriculture of this mountainous area, leading to a more sustainable supply chain for its use as food and in food supplements.

UHPLC-ESI-HRMS untarget analysis of ACFB

In order to verify the content of active substances within the blended extract (ACFB), the UHPLC-ESI-HRMS analysis was carried out. Initially, to obtain a good chromatographic separation and improve ionization of compounds, mobile phase composition, columns, and elution gradient were optimized. UHPLC profiles were acquired with UV (280–330 nm) and by HRMS. The MS data both in positive and negative ionization modes were acquired to obtain a fully and complementary structural information, and each metabolite was fragmentated to allow a deep structural elucidation. The metabolite identification was carried out by using UV spectra, HRMS data (accurate mass, isotopic distribution, and MS/MS characteristic fragmentation pathway), and literature databases. Finally, the tentatively identified compounds were confirmed with the standard whenever available. UHPLC-UV

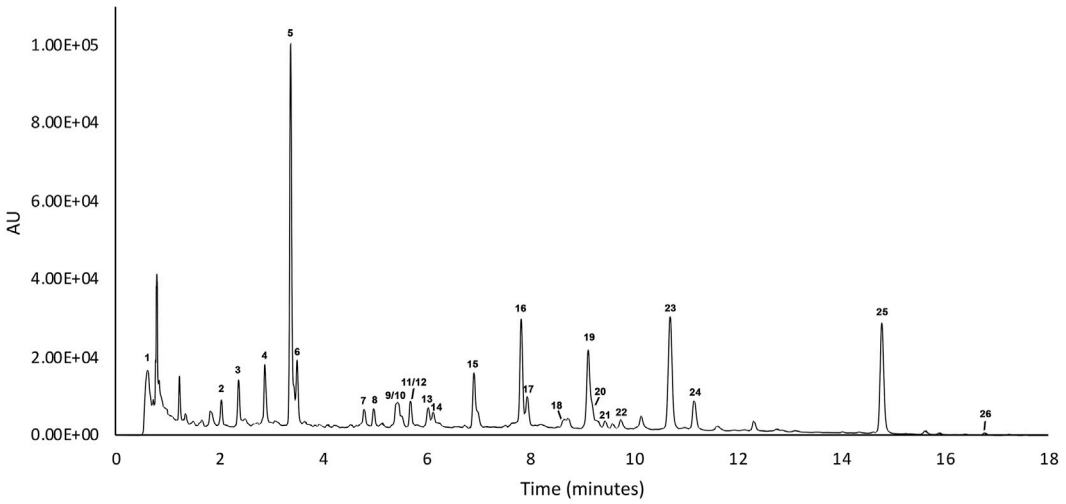

FIGURE 1 | UV chromatograms of ACFB sample recorded at 280 nm.

chromatograms of ACFB at 280 nm are given in **Figure 1** and in **Table 1** reports the list of the 255 identified phytochemicals numbered according to elution order. The UHPLC-UV-HRMS/MS analysis allowed the identification of 266 metabolites belonging mainly to two different classes: flavone and quinic acid (**Table 1**). The flavones were detected in the extracts in both C and O glycosidic form. Ten flavone C-glucosides (7, 8, 10–15, 23–25) were detected, and the fragmentation pathway that was observed in their MS2 spectra confirmed the structure of the identified compounds (Farag et al., 2013; Celano et al., 2019). These flavone c-glucosides in their (−) MS2 spectra produced a characteristic fragmentation pathway, showing successive or simultaneous losses of the glycosylic group (60, 90, and 120 Da) corresponding to [M−H-pentose] and/or [M−H-hexose], respectively. Four flavone O-glucosides detected were putatively identified as glycoside derivatives of apigenin and luteolin, respectively, based on molecular formulae, product ions, literature data, and comparison with reference standards (16). Another class of detected compounds belong to the quinic acid compounds, in particular, mono- and di-caffeoylquinic acids. With regard to mono-caffeoylquinic acid, four compounds were detected (21, 3, 5, 64) showing the same [M−H]− at m/z 352.0880 in accordance with the molecular formula C16H17O9−. In their (−) MS2 spectra, the fragmentation ion at m/z 191 was produced, which represents a quinic acid, resulting from neutral loss of caffeic acid (Sanchez-Rabaneda et al., 2003; Moglia et al., 2008). On the basis of these data, these compounds have been assigned as mono-caffeoylquinic acid and its isomers. In addition, compounds 97, 187, 198, 221, with the same precursor ion at m/z 515.1194 and identical molecular formula C25H23O10− in their (−) MS2 spectra showed the typical fragmentation pathway of di-caffeoylquinic acid isomer (Sanchez-Rabaneda et al., 2003; Moglia et al., 2008). Finally, the latter identified compound, not visible in the chromatogram UV at 280 nm but clearly visible only in positive mode, is the alkaloid trigonelline (1). The alkaloid trigonelline show [M + H]+ at m/z 138.0551 in accordance with the molecular formula $C_7H_8NO_2^+$, and in the (+) MS2 spectra the fragmentation ion at m/z 92 and 94 was produced, in accordance with literature data (Oldoni et al., 2019).

Cytotoxicity evaluation of the three vegetal extracts, ACFB, and red yeast rice

Before exploring the potential anticholesterolemic activity of the three vegetal extracts, ACFB, atorvastatin, and RYR, their impact on HepG2 cell viability was evaluated by dose–response toxicological analysis, considering 48 as relevant exposure times. As shown in **Figure 2**, a significant reduction in HepG2 cell viability is observed following exposure to a concentration starting from 2,500 μg/ml for artichoke (**Figure 2A**), 10,000 μg/ml for caigua (**Figure 2B**), and 250 μg/ml for fenugreek (**Figure 2C**). As such, the artichoke extract is the more cytotoxic among those tested, as indicated by its lower EC50 (**Table 2**), while caigua showed to be the safest one. The vegetal extracts blend, ACFB, significantly lowered HepG2 viability starting from 1,000 μg/ml (about 20% viability reduction) (**Figure 2D**). However, a significant effect on hepatic cell morphology was highlighted even at lower concentrations (750 μg/ml) (**Supplementary Figure S1**). No adverse effect on HepG2 cell viability was observed for atorvastatin at all tested concentrations (**Figure 2E**).

The cytotoxicity of RYR solubilized in DMSO, ethanol, and methanol was also tested. As evidenced by dose–response curves reported in **Figure 3**, RYR solubilized with methanol significantly affected HepG2 cell viability at lower concentrations compared with RYR solubilized in ethanol (100 versus 500 μg/ml) (**Figures 3A, B**). No adverse effect on hepatic *in vitro* model viability was observed up to 1,000 μg/ml when RYR is solubilized in DMSO (**Figure 3C**). As confirmed by EC50 values reported in **Table 2**, RYR solubilized in DMSO is less cytotoxic, while RYR in methanol showed the highest toxicity (i.e., lowest EC50). As

TABLE 1 | List of compounds deteced following UHPLC-ESI-HRMS untarget analysis of ACFB.

N°	Rt (min)	[M – H]–	[M + H]+	Formula	Δ ppm[a]	MS/MS[b]	Name	Class	Ref
1	0,61	/	138,0551	C7H8NO2	–2.9	92/94	Trigonelline	Alkaloid	Oldoni et al. (2019)
2	2.03	353.0880	355.1079	C16H17O9	2.0	191	Mono-caffeoylquinic acid isomer	Quinic acid	Abu-Reidah et al. (2013)
3	2.36	353.0880	355.1079	C16H17O9	2.0	191	Mono-caffeoylquinic acid isomer	Quinic acid	Abu-Reidah et al. (2013)
4	2.88	433.0511	435.0626	/	/	415/387/258/215/191/161	Unknown	/	/
5	3.36	353.0880	355.1079	C16H17O9	2.0	191	Mono-caffeoylquinic acid isomer	Quinic acid	Abu-Reidah et al. (2013)
6	3.49	353.0880	355.1079	C16H17O9	2.0	191	Mono-caffeoylquinic acid isomer	Quinic acid	Abu-Reidah et al. (2013)
7	4.78	593.1523	595.1665	C27H29O15	2.9	503/473/383/353	Apigenin 6.8-di C-hexoside (vicenin2) isomer	Flavone-C-glycoside	M.A. Farag et al. (2014)
8	4.97	593.1523	595.1665	C27H29O15	2.9	503/473/383/353	Apigenin 6.8-di C-hexoside (vicenin2) isomer	Flavone-C-glycoside	M.A. Farag et al. (2014)
9	5.36	515.1194	/	C25H23O12	0.8	353/179/173/191	Di-caffeoylqyuinic acid isomer	Quinic acid	Abu-Reidah et al. (2013)
10	5.4	563.1385	565.1635	C26H27O14	–2.8	503/473/443/383/353	Apigenin-6-C-hexoside-8-C-pentoside (vicenin 3) isomer	Flavone-C-glycoside	M.A. Farag et al. (2014)
11	5.68	447.0918	449.1126	C21H19O11	–2.0	357/327	Luteolin-6-C-glucoside (isoorietin)	Flavone-C-glycoside	M.A. Farag et al. (2014)
12	5.68	447.0918	449.1126	C21H19O11	–2.0	357/327	Luteolin-8-C-glucoside(orientin) isomer	Flavone-C-glycoside	M.A. Farag et al. (2014)/Orsini et al. (2019)
13	6.02	563.1385	565.1635	C26H27O14	–2.8	503/473/443/383/353	Apigenin-6-C-hexoside-8-C-pentoside (vicenin 3) isomer	Flavone-C-glycoside	M.A. Farag et al. (2014)
14	6.12	447.0918	449.1126	C21H19O11	–2.0	357/327	Luteolin-8-C-glucoside(orientin) isomer	Flavone-C-glycoside	M.A. Farag et al. (2014)/Orsini et al. (2019)
15	6.9	431.0998	433.1181	C21H19O10	4.6	311/341/283	Apigenin-6-C-glucoside (isovitexin)	Flavone-C-glycoside	Orsini et al. (2019)
16	7.82	447.0943	449.1126	C21H19O11	3.6	285	Luteolin-7-O-glucoside (cynaroside)	Flavone-O-glycoside	Abu-Reidah et al. (2013)
17	7.93	461.0706	463.0952	C21H17O12	–3.0	285	Luteolin-7-O-glucuronide	Flavone-O-glycoside	Abu-Reidah et al. (2013)
18	8.55	515.1194	/	C25H23O12	0.8	353/179/173/191	Di-caffeoylqyuinic acid isomer	Quinic acid	Abu-Reidah et al. (2013)
19	9.11	515.1194	/	C25H23O12	0.8	353/179/173/191	Di-caffeoylqyuinic acid isomer	Quinic acid	Abu-Reidah et al. (2013)
20	9.17	431.0976	433.1181	C21H19O10	–0.5	269	Apigenin-7-O-glucoside (cosmoside) I	Flavone-O-glycoside	Abu-Reidah et al. (2013)
21	9.44	445.0766	447.098	C21H17O11	–1.1	269	Apigenin-7-O-glucoronide I	Flavone-O-glycoside	Abu-Reidah et al. (2013)
22	9.74	515.1194	/	C25H23O12	0.8	353/179/173/191	Di-caffeoylqyuinic acid isomer	Quinic acid	Abu-Reidah et al. (2013)
23	10.69	399.1156	401.1355	C21H19O8	–1.3	325/295/267	Chrysin 6-C-fucopyranoside	Flavone-C-glycoside	Orsini et al. (2019)
24	11.16	415.1027	417.1251	C21H19O9	–0.5	325/295/267	Chrysin derivative	Flavone-C-glycoside	Orsini et al. (2019)
25	14.78	399.1156	401.1295	C21H19O8	–1.3	325/295/267	Chrysin 6-C-fucopyranoside	Flavone-C-glycoside	Orsini et al. (2019)
26	16.8	441.1200	443.1355	C23H21O9	3.2	381/337/307/295	Chrysin derivative	Flavone	Orsini et al. (2019)

for ACFB, morphological alteration of HepG2 cells was observed down to 500 µg/ml for DMSO-solubilized RYR (data not shown). In the light of the obtained results, the anticholesterolemic activity assessment was performed at 1,000, 7,500, and 100 µg/ml for artichoke, caigua, and fenugreek extracts, respectively. To ensure a better comparison, ACFB and RYR were solubilized in DMSO and tested at the same concentration (250 µg/ml).

Effect of vegetal extracts, ACFB, and red yeast rice on bile acid biosynthesis

One of the main mechanisms by which the liver regulates the overall cholesterol level is via choleresis. Choleresis is a complex biochemical process leading to the production of bile, an iso-osmotic electrolyte solution that is formed in the liver as a product of its secretory function. It mainly consists of

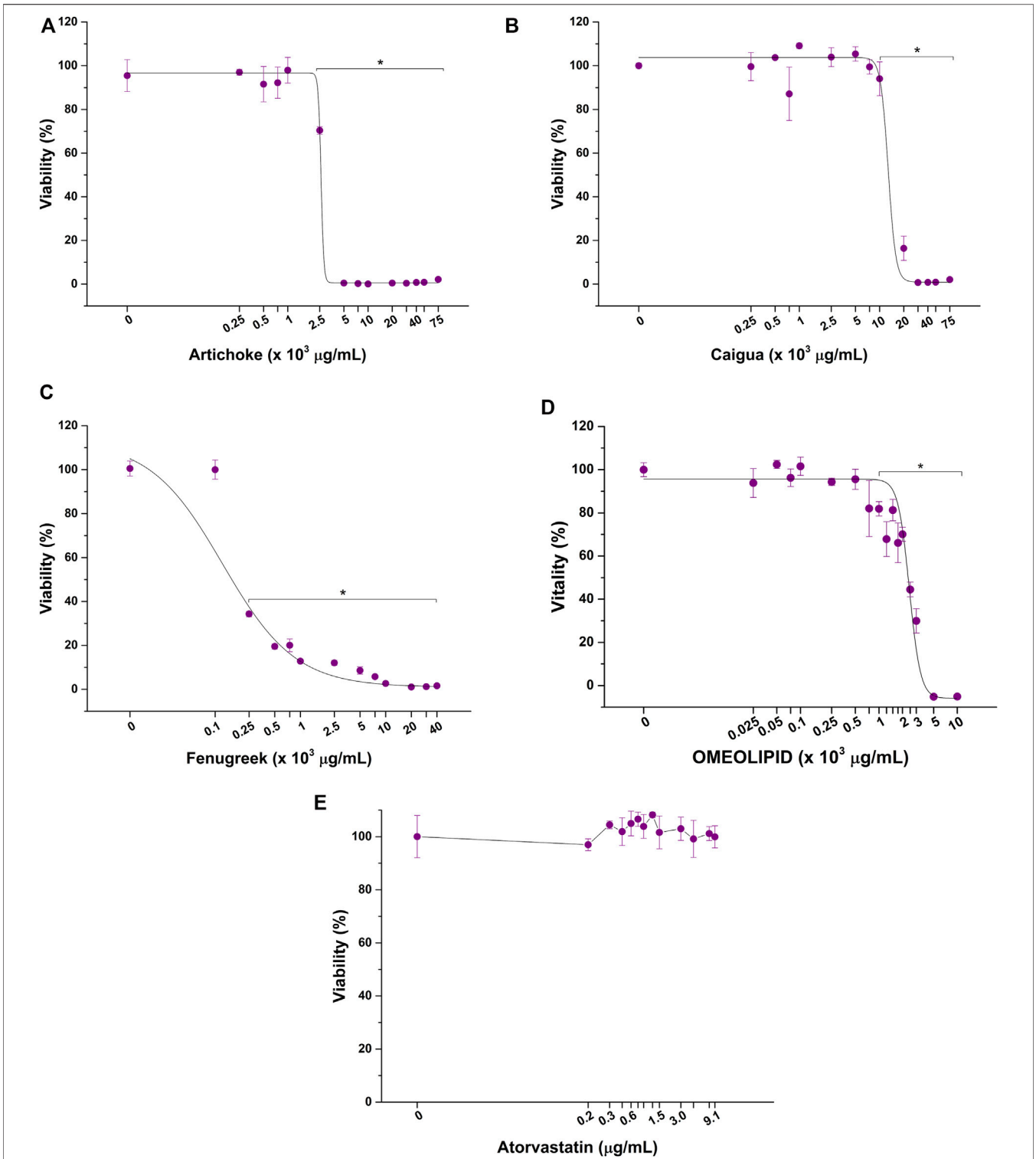

FIGURE 2 | Cytotoxic effect of artichoke **(A)**, caigua **(B)**, fenugreek **(C)**, ACFB, **(D),** and atorvastatin **(E)** on hepatic *in vitro* model viability following 48 h of exposure. *$p < 0.05$.

suspended or dissolved organic and inorganic substances in water (Vovkun et al., 2018). Bile is enriched with bile acids (BAs), which are generated from cholesterol processed at the hepatic level. This represents a key step in general cholesterol homeostasis (i.e., excretion pathway) and a potential target for hypercholesterolemia treatment (Forker, 1977; Goldstein and

TABLE 2 | EC50 values of the vegetal extracts, their blend (ACFB), and RYR solubilized in different solvents (ethanol, methanol, and DMSO).

Treatment	EC50 (μg/ml)
Artichoke extract	2,763.9 ± 299.8
Caigua extract	12,790.9 ± 4,418.2
Fenugreek extract	139.5 ± 49.8
ACFB	2,435.7 ± 93.6
Red yeast rice(RYR) (ethanol)	424.0 ± 7.0
RYR (methanol)	238.0 ± 14.0
RYR [dimethyl sulfoxide (DMSO)]	>2,000
Atorvastatin	>9.1

Note. The results are reported as mean ± standard deviation.

Brown, 1990). The potential ability of the vegetal extracts and their blend, ACFB, to increase the cholesterol-to-bile acid conversion was therefore investigated. As shown in **Figure 4** and **Supplementary Table S4**, the three vegetal extracts significantly increase the production of bile acids in the *in vitro* hepatic model. With about a 17% increase, caigua showed to be the best choleresis-inducing extract. Artichoke and fenugreek extracts increase bile acid production by 9% and 13%, respectively. Atorvastatin increased bile acid production by about 10%, confirming its bile acid synthesis-stimulating activity (Parker et al., 2013; Schonewille et al., 2016). No impact of the different solvents on bile acid biosynthesis was observed (data not shown).

The choleretic-stimulating activity of ACFB and RYR was tested at 100 and 250 μg/ml. Both formulations significantly increased bile acid synthesis in the *in vitro* hepatic model in a concentration-independent manner (about 7% for ACFB and 5% for RYR) (**Figure 5**; **Supplementary Table S5**). Noteworthy, the increase in bile acids induced by ACFB was achieved with lower vegetal extract concentrations than the single extracts, indicating an additive effect between them. As for the vegetal extracts, no difference in bile acid biosynthesis between different solvents was highlighted (data not shown).

Impact of vegetal extracts, ACFB, and red yeast rice on hepatic cholesterol biosynthesis

Cholesterol is both synthesized by cells and introduced with food. The liver is the principal site for cholesterol homeostasis maintenance via a plethora of mechanisms, such as biosynthesis, uptake through low-density lipoprotein receptors (LDLr), lipoprotein release in the blood, storage by esterification, and degradation and conversion into bile acids (Weber et al., 2004). Independently from its origin (biosynthesis or food intake), the hepatic cholesterol pool can be enzymatically esterified by AcylCoA-cholesterol acyltransferase and incorporated into very-low-density lipoproteins (VLDL), which are then secreted into the bloodstream for transport to the peripheral tissues (Bays et al., 2008), or excreted as free cholesterol or cholesterol-derived bile acids into the bile and eliminated through the feces (Ikonen, 2006). Consequently, effective treatment for hypercholesterolemia could reduce

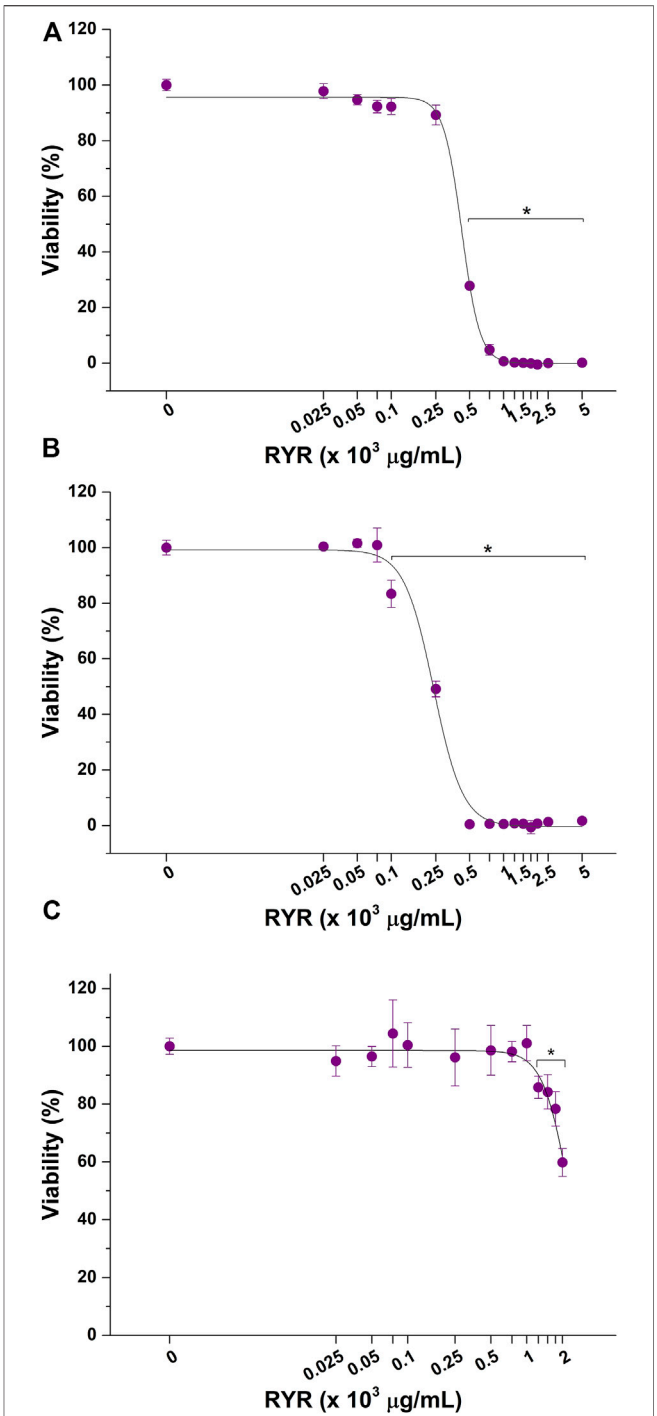

FIGURE 3 | Cytotoxic effect of red yeast rice (RYR) solubilized in ethanol **(A)**, methanol **(B)**, and dimethyl sulfoxide (DMSO) **(C)** on hepatic *in vitro* model viability following 48 h of exposure. *$p < 0.05$.

cholesterol by lowering total cholesterol and/or increasing free cholesterol hepatic content. The latter represents the main form of cholesterol released through bile (Mayes and Botham, 2003; de Boer et al., 2018). Among the tested vegetal extracts, only caigua significantly reduced the total cholesterol content in HepG2 cells

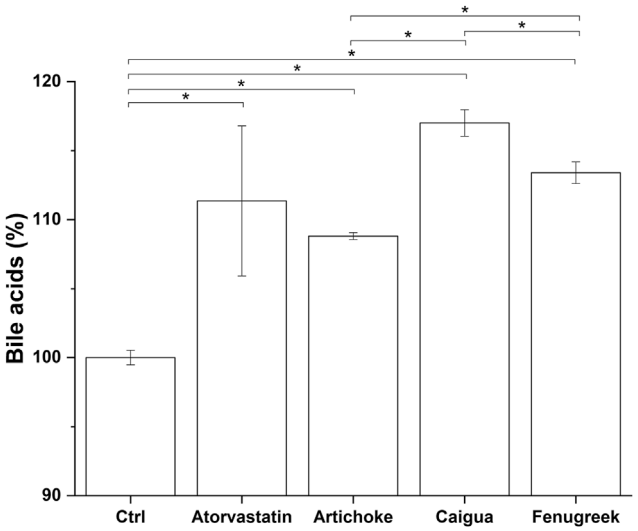

FIGURE 4 | Bile acid production following treatment of hepatic *in vitro* model with atorvastatin (positive control) and the highest, no-toxic concentration of artichoke, caigua, and fenugreek extracts. Monacolin K concentration is indicated between brackets; *$p < 0.05$.

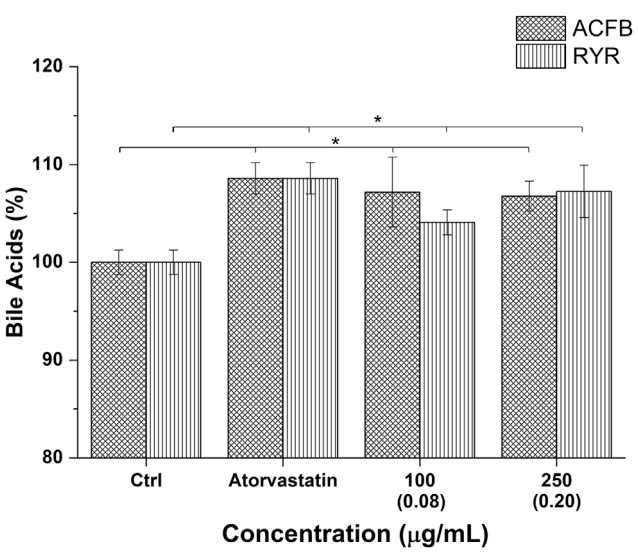

FIGURE 5 | Bile acid production following treatment of hepatic *in vitro* model with atorvastatin (positive control) and different concentrations of ACFB and RIR. Monacolin K concentration is indicated between brackets; *$p < 0.05$.

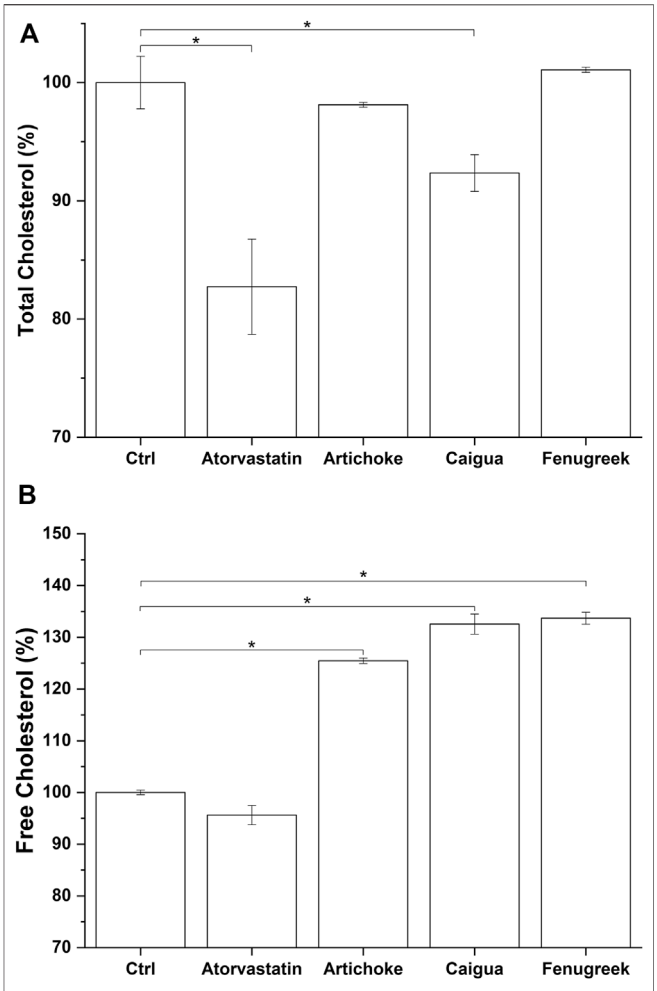

FIGURE 6 | Total cholesterol **(A)** and free cholesterol **(B)** biosynthesis by the hepatic *in vitro* model following 48 h of treatment with atorvastatin and different concentrations of the three vegetal extracts. Monacolin K concentration is indicated between brackets (The result for 100 μg/ml of RICE KOLIN solubilized in ethanol is not shown since it is not statistically different from that at 50 μg/ml). *$p < 0.05$.

(8% reduction) (**Figure 6A** and **Supplementary Table S6**), while all the three extracts are effective in increasing free cholesterol production (about 25%, 33%, and 34% for artichoke, caigua, and fenugreek extracts, respectively) (**Figure 6B**; **Supplementary Table S6**). As expected, no effect on free cholesterol was observed exposing *in vitro* hepatic model to atorvastatin, while total cholesterol was significantly reduced by about 18% (**Figures 6A,B**; **Supplementary Table S6**).

The impact on cholesterol metabolism was also tested for ACFB and RYR. Due to poor monacolin K solubilization in DMSO, as confirmed by HPLC analysis (0.08 μg/ml), no effect on cholesterol metabolism was observed (data not shown). Therefore, total and free cholesterol content was measured after treating cells with ethanolic-solubilized rice red extract. Indeed, monacolin K concentration in ethanol is 10 times higher compared with DMSO (**Supplementary Table S7**). The vegetal extract blend, ACFB, and RYR were tested, respectively, at 100 and 250 μg/ml and 25, 50, and 100 μg/ml. As shown in **Figure 7A** and **Supplementary Table S7**, ACFB induces a concentration-independent decrease in total cholesterol (about 20% reduction), while RYR significantly reduces total cholesterol starting from 50 μg/ml, equivalent to a monacolin K concentration of 0.2 μg/ml. No significant effect was observed for RYR at 25 μg/ml. The same behavior was observed for free cholesterol (**Figure 7B**; **Supplementary Table S7**). ACFB increases free cholesterol synthesis in HepG2 cells in a concentration-independent way

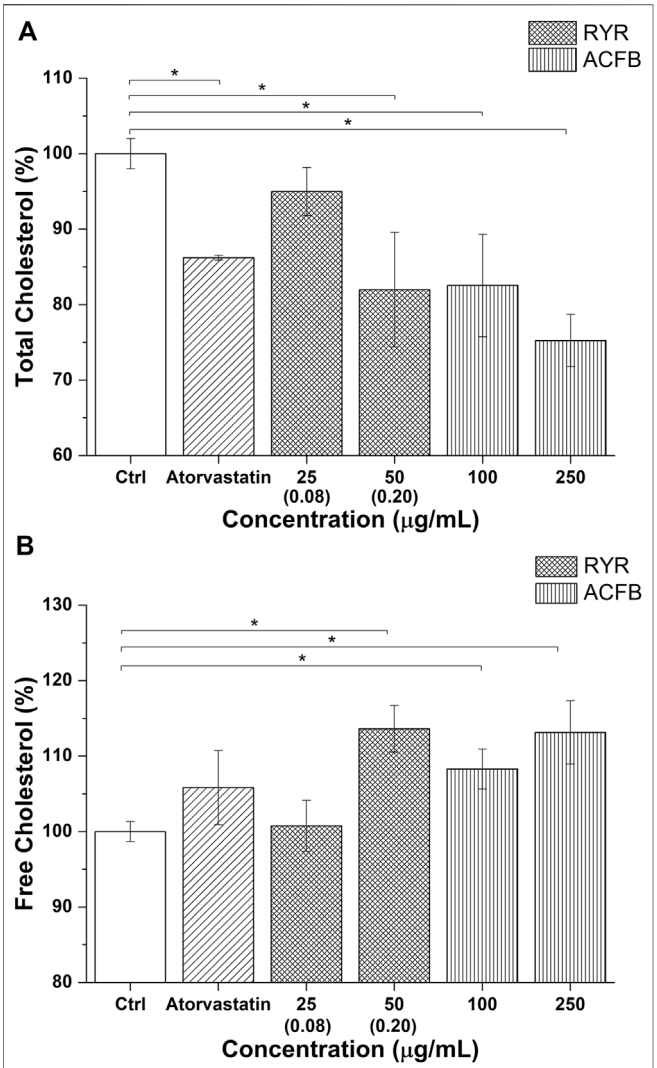

FIGURE 7 | Total cholesterol **(A)** and free cholesterol biosynthesis **(B)** by the hepatic *in vitro* model following 48 h of treatment with atorvastatin and different concentrations of ACFB and RYR formulation. Monacolin K concentration is indicated between brackets (The result for 100 μg/ml of RICE KOLIN solubilized in ethanol is not shown since it is not statistically different from that at 50 μg/ml). *$p < 0.05$.

(about 11% increase), while an effect of ethanol-solubilized RYR was highlighted starting from 50 μg/ml. HepG2 cholesterol biosynthesis was not affected following exposure to different solvents (data not shown). As for bile acid synthesis, a possible additive effect between the three vegetal extracts on cholesterol metabolism was highlighted, since significant results were achieved by ACFB with lower vegetal extract concentrations compared with the single vegetal extract.

DISCUSSION

In the last decades, the research for vegetal extracts endowed with anticholesterolemic activity, but without the statin long-term side effects has catalyzed the efforts of nutraceutical and food supplement industries, in particular, toward novel vegetal extracts used in traditional medicine. Artichoke, caigua, and fenugreek are known to possess antilipidemic and anticholesterolemic effects, and have been used in traditional medicine for the treatment of high lipid and high cholesterol diet-related metabolic diseases (Gonzales et al., 1995; Basch et al., 2003; Shimoda et al., 2003; Vyas et al., 2008; Heidarian et al., 2011; Mohamed Abdel Magied et al., 2016). To the best of our knowledge, this is the first study to investigate anticholesterolemic activity of a novel formulation, ACFB, obtained from the unique blend of these extracts. Our results indicate that ACFB significantly enhances, with a holistic approach, hepatic functionality and cholesterol elimination, by reducing total cholesterol synthesis while improving bile acid and free cholesterol production, as determined by total cholesterol, free cholesterol, and bile acids assays. Indeed, when blended together, the three extracts showed to be more effective than RYR in promoting hepatocyte cholesterol lowering, through a reduction in cholesterol synthesis and its conversion in bile acids (i.e., choleresis promotion). It is also important to underline that such effectiveness in hepatocyte cholesterol lowering was obtained with lower quantities of the extracts, compared with the ones necessary when the extracts were tested individually, indicating a potential additive effect between the extracts themselves. Moreover, to the best of our knowledge, this is the first work to highlight a significant procholeretic activity of caigua, as evidenced by the marked increase in HepG2 bile acid production following exposure to caigua extract. Furthermore, caigua showed to be the extract endowed with the best anticholesterolemic activity, since it shows a significantly higher reduction in total cholesterol and increase in bile acid biosynthesis, while retaining a similar effect on free cholesterol production compared with the other vegetal extracts. Taken together, the experimental findings of the present study primarily confirm the anticholesterolemic efficacy of artichoke, caigua, and fenugreek extract and highlight their increased effectiveness when combined in a unique blend, as in ACFB formulation, suggesting a potential use of this extract to complement or substitute statins. Indeed, while being the main drug for hypercholesterolemia and hyperlipemia treatment, statin-based therapies raised some concerns due to their uncontrolled use and the growing body of evidences highlighting their side effects (Argov, 2015; Pinal-Fernandez et al., 2018; Irvine, 2020). A stark example of statin abuse comes from monacolin K, a natural statin known as lovastatin, extracted from the red yeast *Monascus purpureus* Went. Indeed, despite its efficacy, an alarm was raised by EFSA in the form of a published scientific opinion, since an unharmful dietary intake was not found, for both the general population and vulnerable subgroups of the population (Younes et al., 2018). As such, anticholesterolemic therapies based on novel and safer vegetal extracts and their blends are required to assist or replace statins. Although our results from *in vitro* experiments cannot be directly extrapolated to antilipidemic and

anticholesterolemic clinical effects, such studies will assist in screening novel vegetal extracts and blends for their safety and anticholesterolemic efficacy, while starting to elucidate the mechanism through which cholesterol is lowered. To elucidate the molecular targets of these vegetal extracts and their blend, and to investigate other mechanisms responsible for cholesterol homeostasis, more detailed *in vitro* studies will be needed. In parallel to that, an *in vivo* approach will be instrumental in defining the bioavailability of the extracts and their blend and, as a consequence, their anticholesterolemic and antilipidemic efficacy. Finally, DNA barcoding analysis was an efficient tool in uniquely identifying the species of all plants used in this study. DNA testing of raw plants, used as a preliminary analysis, is necessary to select the correct species and, consequently, to obtain the suitable phytocomplexes for the ACFB. To the best of our knowledge, it was demonstrated, for the first time that caigua was also grown in Val Camonica (Lombardy, Italy) under the vernacular name of "milione" or "miliun." This finding could positively impact on the local agriculture in mountain areas and may lead to a more sustainable supply chain for its use in food and food supplements.

In conclusion, our results suggest that combining active ingredients coming from traditional herbal medicine, such as artichoke, caigua and fenugreek, in a unique blend like ACFB, could enhance their curative effects, potentially providing complementary therapies to the statin-based ones for hyperlipidemia and hypercholesterolemia-related complications.

DATA AVAILABILITY STATEMENT

The raw data supporting the conclusion of this article will be made available by the authors, without undue reservation.

AUTHOR CONTRIBUTIONS

ET, FB, ML, and LC conceptualized the study. FB, JF, VM, and LC performed the data curation. ET, JF, VI, GN, and SP performed the formal analysis. ET, JF, VM, and SP was in charge of the investigation. ET, FB, VI, ML, and LC supervised the study. ET, FB, VI, ML, LC, and GN wrote the original draft.

FUNDING

This work was supported by Regione Lombardia in the framework of the Program "Accordi per la ricerca e l'innovazione" under the project "Food Social Sensor Network Food NET," grant number: E47F17000020009. The funder had no role in the study design, data collection and analysis, decision to publish, or preparation of the manuscript. FEM2-Ambiente s.r.l. provided support in the form of a salary for authors VM and JF, but did not play a role in study design, data collection and analysis, the decision to publish, or preparation of the manuscript and only provided financial support in the form of research materials.

ACKNOWLEDGMENTS

Caigua samples from Val Camonica were kindly provided by Ge.S.Di.Mont., Research Centre of Università degli Studi di Milano (Edolo—BS).

SUPPLEMENTARY MATERIAL

The Supplementary Material for this article can be found online at: https://www.frontiersin.org/articles/10.3389/fphar.2021.726199/full#supplementary-material

REFERENCES

Abu-Reidah, I. M., Arráez-Román, D., Segura-Carretero, A., Fernández-Gutiȳrrez, A., and Knowles, B. B. (2013). Extensive characterisation of bioactive phenolic constituents from globe artichoke (*Cynara scolymus* L.) by HPLC-DAD-ESI-QTOF-MS. *Food Chem.* 141 (3), 2269–2277.

Adhyaru, B. B., and Jacobson, T. A. (2018). Safety and Efficacy of Statin Therapy. *Nat. Rev. Cardiol.* 15, 757–769. doi:10.1038/s41569-018-0098-5

Afonso, M. S., Machado, R. M., Lavrador, M. S., Quintao, E. C. R., Moore, K. J., and Lottenberg, A. M. (2018). Molecular Pathways Underlying Cholesterol Homeostasis. *Nutrients* 10, 1–18. doi:10.3390/nu10060760

Altmann, S. W., Davis, H. R., Zhu, L. J., Yao, X., Hoos, L. M., Tetzloff, G., et al. (2004). Niemann-Pick C1 like 1 Protein Is Critical for Intestinal Cholesterol Absorption. *Science* 303, 1201–1204. doi:10.1126/science.1093131

Argov, Z. (2015). Statins and the Neuromuscular System: a Neurologist's Perspective. *Eur. J. Neurol.* 22, 31–36. doi:10.1111/ene.12604

Arnold, D. R., and Kwiterovich, P. O. (2003). CHOLESTEROL | Absorption, Function, and Metabolism. *Encycl. Food Sci. Nutr.*, 1226–1237. doi:10.1016/b0-12-227055-x/00225-x

Asrani, S. K., Devarbhavi, H., Eaton, J., and Kamath, P. S. (2019). Burden of Liver Diseases in the World. *J. Hepatol.* 70, 151–171. doi:10.1016/j.jhep.2018.09.014

Basch, E., Ulbricht, C., Kuo, G., Szapary, P., and Smith, M. (2003). Therapeutic Applications of Fenugreek. *Altern. Med. Rev.* 8, 20–27.

Bays, H. E., Neff, D., Tomassini, J. E., and Tershakovec, A. M. (2008). Ezetimibe: Cholesterol Lowering and beyond. *Expert Rev. Cardiovasc. Ther.* 6, 447–470. doi:10.1586/14779072.6.4.447

Celano, R., Campone, L., Pagano, I., Carabetta, S., Di Sanzo, R., Rastrelli, L., et al. (2019). Characterisation of Nutraceutical Compounds from Different Parts of Particular Species of Citrus Sinensis 'Ovale Calabrese' by UHPLC-UV-ESI-HRMS. *Nat. Prod. Res.* 33, 244–251. doi:10.1080/14786419.2018.1443102

Chang, T. Y., Chang, C. C., Ohgami, N., and Yamauchi, Y. (2006). Cholesterol Sensing, Trafficking, and Esterification. *Annu. Rev. Cel Dev. Biol.* 22, 129–157. doi:10.1146/annurev.cellbio.22.010305.104656

Chiang, J. Y. L., and Ferrell, J. M. (2019). Bile Acids as Metabolic Regulators and Nutrient Sensors. *Annu. Rev. Nutr.* 39, 175–200. doi:10.1146/annurev-nutr-082018-124344

Ciechanover, A., Schwartz, A. L., and Lodish, H. F. (1983). The Asialoglycoprotein Receptor Internalizes and Recycles Independently of the Transferrin and Insulin Receptors. *Cell* 32, 267–275. doi:10.1016/0092-8674(83)90517-2

Dai, L., Zou, L., Meng, L., Qiang, G., Yan, M., and Zhang, Z. (2021). Cholesterol Metabolism in Neurodegenerative Diseases: Molecular Mechanisms and Therapeutic Targets. *Mol. Neurobiol.* 58, 2183–2201. doi:10.1007/s12035-020-02232-6

Dashti, N., Wolfbauer, G., Koren, E., Knowles, B., and Alaupovic, P. (1984). Catabolism of Human Low Density Lipoproteins by Human Hepatoma Cell

Line HepG2. *Biochim. Biophys. Acta* 794, 373–384. doi:10.1016/0005-2760(84)90003-1

De Aguiar Vallim, T. Q., Tarling, E. J., and Edwards, P. A. (2013). Pleiotropic Roles of Bile Acids in Metabolism. *Cell Metab* 17, 657–669. doi:10.1016/j.cmet.2013.03.013

de Boer, J. F., Kuipers, F., and Groen, A. K. (2018). Cholesterol Transport Revisited: A New Turbo Mechanism to Drive Cholesterol Excretion. *Trends Endocrinol. Metab.* 29, 123–133. doi:10.1016/j.tem.2017.11.006

Everson, G. T., and Polokoff, M. A. (1986). HepG2. A Human Hepatoblastoma Cell Line Exhibiting Defects in Bile Acid Synthesis and Conjugation. *J. Biol. Chem.* 261, 2197–2201. doi:10.1016/s0021-9258(17)35917-3

Farag, M. A., El-Ahmady, S. H., Elian, F. S., and Wessjohann, L. A. (2013). Metabolomics Driven Analysis of Artichoke Leaf and its Commercial Products via UHPLC-Q-TOF-MS and Chemometrics. *Phytochemistry* 95, 177–187. doi:10.1016/j.phytochem.2013.07.003

Forker, E. L. (1977). Mechanisms of Hepatic Bile Formation. *Annu. Rev. Physiol.* 39, 323–347. doi:10.1146/annurev.ph.39.030177.001543

Galimberti, A., Spinelli, S., Bruno, A., Mezzasalma, V., De Mattia, F., Cortis, P., et al. (2016). Evaluating the Efficacy of Restoration Plantings through DNA Barcoding of Frugivorous Bird Diets. *Conserv. Biol.* 30, 763–773. doi:10.1111/cobi.12687

Geuze, H. J., Slot, J. W., Strous, G. J., and Schwartz, A. L. (1983). The Pathway of the Asialoglycoprotein-Ligand during Receptor-Mediated Endocytosis: a Morphological Study with Colloidal Gold/ligand in the Human Hepatoma Cell Line, Hep G2. *Eur. J. Cel Biol.* 32, 38–44. doi:10.1016/0092-8674(83)90518-4

Goldstein, J. L., and Brown, M. S. (1990). Regulation of the Mevalonate Pathway. *Nature* 343, 425–430. doi:10.1038/343425a0

Gonzales, G. F., Góñez, C., and Villena, A. (1995). Serum Lipid and Lipoprotein Levels in Postmenopausal Women: Short-Course Effect of Caigua. *Menopause* 2, 225–234. doi:10.1097/00042192-199502040-00007

Green, C. J., Johnson, D., Amin, H. D., Sivathondan, P., Silva, M. A., Wang, L. M., et al. (2015). Characterization of Lipid Metabolism in a Novel Immortalized Human Hepatocyte Cell Line. *Am. J. Physiol. Endocrinol. Metab.* 309, E511–E522. doi:10.1152/ajpendo.00594.2014

Grouleff, J., Irudayam, S. J., Skeby, K. K., and Schiøtt, B. (2015). The Influence of Cholesterol on Membrane Protein Structure, Function, and Dynamics Studied by Molecular Dynamics Simulations. *Biochim. Biophys. Acta* 1848, 1783–1795. doi:10.1016/j.bbamem.2015.03.029

Guo, J., Gao, Y., Cao, X., Zhang, J., and Chen, W. (2017). Cholesterol-lowing Effect of Taurine in HepG2 Cell. *Lipids Health Dis.* 16, 56–57. doi:10.1186/s12944-017-0444-3

Han, J. S., Sung, J. H., and Lee, S. K. (2017). Inhibition of Cholesterol Synthesis in HepG2 Cells by GINST-Decreasing HMG-CoA Reductase Expression via AMP-Activated Protein Kinase. *J. Food Sci.* 82, 2700–2705. doi:10.1111/1750-3841.13828

Havekes, L., Van Hinsbergh, V., Kempen, H. J., and Emeis, J. (1983). The Metabolism *In Vitro* of Human Low-Density Lipoprotein by the Human Hepatoma Cell Line Hep G2. *Biochem. J.* 214, 951–958. doi:10.1042/bj2140951

Hebert, P. D., Cywinska, A., Ball, S. L., and DeWaard, J. R. (2003). Biological Identifications through DNA Barcodes. *Proc. Biol. Sci.* 270, 313–321. doi:10.1098/rspb.2002.2218

Heidarian, E., Jafari-Dehkordi, E., and Seidkhani-Nahal, A. (2011). Beneficial Effects of Artichoke on Liver Phosphatidate Phosphohydrolase and Plasma Lipids in Rats Fed by Lipogenic Diet. *Int. J. Phytomedicine* 3, 285–293. doi:10.5138/ijpm.v3i2.196

Hoeg, J. M., Demosky, S. J., Edge, S. B., Gregg, R. E., Osborne, J. C., and Brewer, H. B. (1985). Characterization of a Human Hepatic Receptor for High Density Lipoproteins. *Arteriosclerosis* 5, 228–237. doi:10.1161/01.atv.5.3.228

Ikonen, E. (2006). Mechanisms for Cellular Cholesterol Transport: Defects and Human Disease. *Physiol. Rev.* 86, 1237–1261. doi:10.1152/physrev.00022.2005

Irvine, N. J. (2020). Anti-HMGCR Myopathy: A Rare and Serious Side Effect of Statins. *J. Am. Board Fam. Med.* 33, 785–788. doi:10.3122/JABFM.2020.05.190450

Jin, U., Park, S. J., and Park, S. M. (2019). Cholesterol Metabolism in the Brain and its Association with Parkinson's Disease. *Exp. Neurobiol.* 28, 554–567. doi:10.5607/en.2019.28.5.554

Knowles, B. B., Howe, C. C., and Aden, D. P. (1980). Human Hepatocellular Carcinoma Cell Lines Secrete the Major Plasma Proteins and Hepatitis B Surface Antigen. *Science* 209, 497–499. doi:10.1126/science.6248960

Lennernäs, H. (2003). Clinical Pharmacokinetics of Atorvastatin. *Clin. Pharmacokinet.* 42, 1141–1160. doi:10.2165/00003088-200342130-00005

Li, P. S., Fu, Z. Y., Zhang, Y. Y., Zhang, J. H., Xu, C. Q., Ma, Y. T., et al. (2014). The Clathrin Adaptor Numb Regulates Intestinal Cholesterol Absorption through Dynamic Interaction with NPC1L1. *Nat. Med.* 20, 80–86. doi:10.1038/nm.3417

Li, T., and Chiang, J. Y. (2015). Bile Acids as Metabolic Regulators. *Curr. Opin. Gastroenterol.* 31, 159–165. doi:10.1097/MOG.0000000000000156

Liscum, L., and Underwood, K. W. (1995). Intracellular Cholesterol Transport and Compartmentation. *J. Biol. Chem.* 270, 15443–15446. doi:10.1074/jbc.270.26.15443

Luo, J., Jiang, L. Y., Yang, H., and Song, B. L. (2019). Intracellular Cholesterol Transport by Sterol Transfer Proteins at Membrane Contact Sites. *Trends Biochem. Sci.* 44, 273–292. doi:10.1016/j.tibs.2018.10.001

Mayes, P. A., and Botham, K. M. (2003). *Cholesterol synthesis, transport and excretion. a LANGE medical book*, 8641.

Moglia, A., Lanteri, S., Comino, C., Acquadro, A., De Vos, R., and Beekwilder, J. (2008). Stress-induced Biosynthesis of Dicaffeoylquinic Acids in globe Artichoke. *J. Agric. Food Chem.* 56, 8641–8649. doi:10.1021/jf801653w

MohamedAbdelMagied, M., DinHussien, S. E. L., MohamedZaki, S., and MohamedSaid, R. E. L. (2016). Artichoke (Cynara Scolymus L.) Leaves and Heads Extracts as Hypoglycemic and Hypocholesterolemic in Rats. *J. Food Nutr. Res.* 4, 60–68. doi:10.12691/jfnr-4-1-10

Montoro, P., Carbone, V., De Simone, F., Pizza, C., and De Tommasi, N. (2001). Studies on the Constituents of Cyclanthera Pedata Fruits: Isolation and Structure Elucidation of New Flavonoid Glycosides and Their Antioxidant Activity. *J. Agric. Food Chem.* 49, 5156–5160. doi:10.1021/jf010318q

Morgan, A. E., Mooney, K. M., Wilkinson, S. J., Pickles, N. A., and Mc Auley, M. T. (2016). Cholesterol Metabolism: A Review of How Ageing Disrupts the Biological Mechanisms Responsible for its Regulation. *Ageing Res. Rev.* 27, 108–124. doi:10.1016/j.arr.2016.03.008

Nannoni, G., Alì, A., and Di Pierro, F. (2015). Development of a New Highly Standardized and Granulated Extract from Monascus purpureus with a High Content of Monacolin K and KA and Free of Inactive Secondary Monacolins and Citrinin. *Nutrafoods* 14, 197–205. doi:10.1007/s13749-015-0047-4

Oldoni, T. L. C., Merlin, N., Karling, M., Carpes, S. T., Alencar, S. M., Morales, R. G. F., et al. (2019). Bioguided Extraction of Phenolic Compounds and UHPLC-ESI-Q-TOF-MS/MS Characterization of Extracts of Moringa Oleifera Leaves Collected in Brazil. *Food Res. Int.* 125, 108647. doi:10.1016/j.foodres.2019.108647

Orsini, F., Vovk, I., Glavnik, V., Jug, U., Corradini, D., and Beekwilder, J. (2019). HPTLC, HPTLC-MS/MS and HPTLC-DPPH methods for analyses of flavonoids and their antioxidant activity in Cyclanthera pedata leaves, fruits and dietary supplement. *J. Liq. Chromatogr. Related Technol.* 42 (9-10), 290–301. doi:10.1021/jf801653w

Orth, M., and Bellosta, S. (2012). Cholesterol: Its Regulation and Role in central Nervous System Disorders. *Cholesterol* 2012, 1–19. doi:10.1155/2012/292598

Ozougwu, J. C., and Eyo, J. E. (2014). Hepatoprotective Effects of Allium cepa (Onion) Extracts against Paracetamol-Induced Liver Damage in Rats. *Afr. J. Biotechnol.* 13, 2679–2688. doi:10.5897/ajb2014.13815

Parker, R. A., Garcia, R., Ryan, C. S., Liu, X., Shipkova, P., Livanov, V., et al. (2013). Bile Acid and Sterol Metabolism with Combined HMG-CoA Reductase and PCSK9 Suppression. *J. Lipid Res.* 54, 2400–2409. doi:10.1194/jlr.M038331

Pei, K., Gui, T., Kan, D., Feng, H., Jin, Y., Yang, Y., et al. (2020). Review Article an Overview of Lipid Metabolism and Nonalcoholic Fatty Liver Disease. *Biomed. Res. Int.* 2020, 4020249. doi:10.1155/2020/4020249

Pinal-Fernandez, I., Casal-Dominguez, M., and Mammen, A. L. (2018). Statins: Pros and Cons. *Med. Clin. (Barc)* 150, 398–402. doi:10.1016/j.medcli.2017.11.030.Statins

Ponziani, F. R., Pecere, S., Gasbarrini, A., and Ojetti, V. (2015). Physiology and Pathophysiology of Liver Lipid Metabolism. *Expert Rev. Gastroenterol. Hepatol.* 9, 1055–1067. doi:10.1586/17474124.2015.1056156

Qi, X., Zhang, Y., Guo, H., Hai, Y., Luo, Y., and Yue, T. (2020). Mechanism and Intervention Measures of Iron Side Effects on the Intestine. *Crit. Rev. Food Sci. Nutr.* 60, 2113–2125. doi:10.1080/10408398.2019.1630599

Rash, J. M., Rothblat, G. H., and Sparks, C. E. (1981). Lipoprotein Apolipoprotein Synthesis by Human Hepatoma Cells in Culture. *Biochim. Biophys. Acta* 666, 294–298. doi:10.1016/0005-2760(81)90120-X

Rinella, M., and Charlton, M. (2016). The Globalization of Nonalcoholic Fatty Liver Disease: Prevalence and Impact on World Health. *Hepatology* 64, 19–22. doi:10.1002/hep.28524

Russell, D. W. (2009). Fifty Years of Advances in Bile Acid Synthesis and Metabolism. *J. Lipid Res.* 50 Suppl, S120–S125. doi:10.1194/jlr.R800026-JLR200

Russell, D. W. (2003). The Enzymes, Regulation, and Genetics of Bile Acid Synthesis. *Annu. Rev. Biochem.* 72, 137–174. doi:10.1146/annurev.biochem.72.121801.161712

Sánchez-Rabaneda, F., Jáuregui, O., Lamuela-Raventós, R. M., Bastida, J., Viladomat, F., and Codina, C. (2003). Identification of Phenolic Compounds in Artichoke Waste by High-Performance Liquid Chromatography-Tandem Mass Spectrometry. *J. Chromatogr. A.* 1008, 57–72. doi:10.1016/s0021-9673(03)00964-6

Schonewille, M., De Boer, J. F., Mele, L., Wolters, H., Bloks, V. W., Wolters, J. C., et al. (2016). Statins Increase Hepatic Cholesterol Synthesis and Stimulate Fecal Cholesterol Elimination in Mice. *J. Lipid Res.* 57, 1455–1464. doi:10.1194/jlr.M067488

Shao, D., Wang, Y., Huang, Q., Shi, J., Yang, H., Pan, Z., et al. (2016). Cholesterol-Lowering Effects and Mechanisms in View of Bile Acid Pathway of Resveratrol and Resveratrol Glucuronides. *J. Food Sci.* 81, H2841–H2848. doi:10.1111/1750-3841.13528

Sheng, R., Chen, Y., Yung Gee, H., Stec, E., Melowic, H. R., Blatner, N. R., et al. (2012). Cholesterol Modulates Cell Signaling and Protein Networking by Specifically Interacting with PDZ Domain-Containing Scaffold Proteins. *Nat. Commun.* 3, 1249. doi:10.1038/ncomms2221

Shimoda, H., Ninomiya, K., Nishida, N., Yoshino, T., Morikawa, T., Matsuda, H., et al. (2003). Anti-hyperlipidemic Sesquiterpenes and New Sesquiterpene Glycosides from the Leaves of Artichoke (Cynara Scolymus L.): Structure Requirement and Mode of Action. *Bioorg. Med. Chem. Lett.* 13, 223–228. doi:10.1016/S0960-894X(02)00889-2

Simons, K., and Ikonen, E. (2000). How Cells Handle Cholesterol. *Science* 290, 1721–1726. doi:10.1126/science.290.5497.1721

Singgih, M., Saraswaty, V., Ratnaningrum, D., Priatni, S., and Damayanti, S. (2014). The Influence of Temperature and Ethanol Concentration in Monacolin K Extraction from Monascus Fermented Rice. *Proced. Chem.* 9, 242–247. doi:10.1016/j.proche.2014.05.029

Steenbergen, R. H., Joyce, M. A., Thomas, B. S., Jones, D., Law, J., Russell, R., et al. (2013). Human Serum Leads to Differentiation of Human Hepatoma Cells, Restoration of Very-Low-Density Lipoprotein Secretion, and a 1000-fold Increase in HCV Japanese Fulminant Hepatitis Type 1 Titers. *Hepatology* 58, 1907–1917. doi:10.1002/hep.26566

Tam, S. P., Archer, T. K., and Deeley, R. G. (1985). Effects of Estrogen on Apolipoprotein Secretion by the Human Hepatocarcinoma Cell Line, HepG2. *J. Biol. Chem.* 260, 1670–1675. doi:10.1016/s0021-9258(18)89646-6

Tiwari, R., and Pathak, K. (2011). Statins Therapy: A Review on Conventional and Novel Formulation Approaches. *J. Pharm. Pharmacol.* 63, 983–998. doi:10.1111/j.2042-7158.2011.01273.x

Vovkun, T., Yanchuk, P., Shtanova, L., Veselskiy, S., Filimonova, N., Shalamay, A., et al. (2018). Water-soluble Quercetin Modulates the Choleresis and Bile Lipid Ratio in Rats. *Gen. Physiol. Biophys.* 37, 111–120. doi:10.4149/gpb_2017015

Vyas, S., Agrawal, R. P., Solanki, P., and Trivedi, P. (2008). Analgesic and Anti-inflammatory Activities of Trigonella Foenum-Graecum (Seed) Extract. *Acta Pol. Pharm.* 65, 473–476.

Wang, Y. J., Bian, Y., Luo, J., Lu, M., Xiong, Y., Guo, S. Y., et al. (2017). Cholesterol and Fatty Acids Regulate Cysteine Ubiquitylation of ACAT2 through Competitive Oxidation. *Nat. Cel Biol.* 19, 808–819. doi:10.1038/ncb3551

Weber, L. W., Boll, M., and Stampfl, A. (2004). Maintaining Cholesterol Homeostasis: Sterol Regulatory Element-Binding Proteins. *World J. Gastroenterol.* 10, 3081–3087. doi:10.3748/wjg.v10.i21.3081

Wider, B., Pittler, M. H., Thompson-Coon, J., and Ernst, E. (2016). Artichoke Leaf Extract for Treating Hypercholesterolaemia. *Cochrane Database Syst. Rev.*, 28 (3), CD003335. doi:10.1002/14651858.CD003335.pub4

Wu, G. Y., Wu, C. H., Rifici, V. A., and Stockert, R. J. (1984). Activity and Regulation of Low Density Lipoprotein Receptors in a Human Hepatoblastoma Cell Line. *Hepatology* 4, 1190–1194. doi:10.1002/hep.1840040615

Y-Y, Z., Z-Y, F., J, W., W, Q., G, B., et al. (2018). A LIMA1 Variant Promotes Low Plasma LDL Cholesterol and Decreases Intestinal Cholesterol Absorption. *Espe* 1092, 1087–1092. doi:10.1530/ey.15.12.15

Younes, M., Younes, M., Aggett, P., Aguilar, F., Crebelli, R., Dusemund, B., et al. (2018). Scientific Opinion on the Safety of Monacolins in Red Yeast rice. *EFSA J.* 16, e05368. doi:10.2903/j.efsa.2018.5368

Zannis, V. I., Breslow, J. L., SanGiacomo, T. R., Aden, D. P., and Knowles, B. B. (1981). Characterization of the Major Apolipoproteins Secreted by Two Human Hepatoma Cell Lines. *Biochemistry* 20, 7089–7096. doi:10.1021/bi00528a006

Conflict of Interest: The authors VI and GN were employed by EPO Srl. Authors JF and VM were employed by FEM2-Ambiente.

The remaining authors declare that the research was conducted in the absence of any commercial or financial relationships that could be construed as a potential conflict of interest.

Publisher's Note: All claims expressed in this article are solely those of the authors and do not necessarily represent those of their affiliated organizations, or those of the publisher, the editors, and the reviewers. Any product that may be evaluated in this article, or claim that may be made by its manufacturer, is not guaranteed or endorsed by the publisher.

frontiers in Pharmacology

ORIGINAL RESEARCH
published: 26 November 2021
doi: 10.3389/fphar.2021.694607

Hepatoprotective Potential of Pomegranate in Curbing the Incidence of Acute Liver Injury by Alleviating Oxidative Stress and Inflammatory Response

Hamid Ali[1], Azra Jahan[2], Samrana Samrana[3], Abid Ali[3], Safdar Ali[4], Nurul Kabir[5], Amjad Ali[6], Riaz Ullah[7], Ramzi A. Mothana[7], Bibi Nazia Murtaza[8] and Muhammad Kalim[9]*

[1]Department of Biosciences, COMSATS University, Islamabad, Pakistan, [2]Department of Zoology, Abdul Wali Khan University, Mardan, Pakistan, [3]College of Agriculture and Biotechnology, Zhejiang University, Hangzhou, China, [4]Department of Physics, University of Swabi-Anbar, Mardan, Pakistan, [5]Faculty of Science, Institute of Biological Sciences, University of Malaya, Kuala Lumpur, Malaysia, [6]Faculty of Biological Sciences, Department of Biochemistry, Quaid-i-Azam University, Islamabad, Pakistan, [7]Department of Pharmacognosy, College of Pharmacy, King Saud University, Riyadh, Saudi Arabia, [8]Department of Zoology, Abbottabad University of Science and Technology, Abbottabad, Pakistan, [9]Cancer Research Institute, Houston Methodist Hospital, Houston, TX, United States

OPEN ACCESS

Edited by:
Antonella Di Sotto, Sapienza University of Rome, Italy

Reviewed by:
Sheikh Raisuddin, Jamia Hamdard University, India
Claudio Ferrante, University of Studies G. d'Annunzio Chieti and Pescara, Italy

***Correspondence:**
Hamid Ali
hamidpcmd@yahoo.com

Specialty section:
This article was submitted to Gastrointestinal and Hepatic Pharmacology, a section of the journal Frontiers in Pharmacology

Received: *13 April 2021*
Accepted: *30 September 2021*
Published: *26 November 2021*

Citation:
Ali H, Jahan A, Samrana S, Ali A, Ali S, Kabir N, Ali A, Ullah R, Mothana RA, Murtaza BN and Kalim M (2021) Hepatoprotective Potential of Pomegranate in Curbing the Incidence of Acute Liver Injury by Alleviating Oxidative Stress and Inflammatory Response. Front. Pharmacol. 12:694607. doi: 10.3389/fphar.2021.694607

Hepatitis is an inflammatory disease of the liver and is considered one of the leading causes of death worldwide. Due to its scavenging activity, *Punica granatum* may be used for the treatment and prevention of liver diseases. The current study investigated the protective mechanism underlying the effects of pomegranate against a rat model of carbon tetrachloride–induced liver injury. Intraperitoneal injection of CCl_4 resulted in liver inflammation, oxidative stress, and accumulation of lipid in hepatocytes. CCl_4 induced a downregulation of superoxide dismutase (SOD), glutathione (GSH), and melonaldehyde (MDA). Pomegranate protection was assessed in terms of biochemical parameters, histopathology, and immunohistochemistry. Promegranate administration decreased inflammation, elevated serum enzymes and ROS production, and countered the debilitating effects caused by CCl_4. In addition, CCl_4-induced histological changes were absent in the crude pomegranate extract group, which also enhanced the scavenging activity of reactive oxygen species by enhancing the antioxidant defense mechanism as confirmed by detecting MDA, SOD, and GSH expressions. The migration of $CD68^+$ macrophages was halted at the injured area of the central vein and the number of macrophages was reduced to the normal control by the crude extract compared to the positive control silymarin group. Likewise, protective effects of ethylacetate and the aqueous fraction of the crude extract were also observed. However, the butanol and *n*-hexane fractions displayed increased levels of ALT, AST, and ALP as compared to silymarin. About 25% damage to hepatocytes was observed in the butanol and *n*-hexane group by histopathological examination, which is a little better compared to the CCl_4-treated group. The crude extract and its ethyl acetate and aqueous fractions may be accountable for the hepatoprotective potential of *Punica granatum*, which was further

confirmed by *in vivo* experiments. Together, these findings confirm that pomegranate exerts hepatoprotective activity against CCl_4-induced oxidative stress and liver damage.

Keywords: pomegranate, hepatotoxicity, histology, oxidative stress, Kupffer cells, iNOS

INTRODUCTION

Liver diseases are one of the most serious health issues in the world. The liver is concerned with metabolism and detoxification of exogenous substances such as drugs, toxic chemicals, and viruses and hence is very prone to injury (Moore et al., 2010; Moore et al., 2013). Toxic chemicals are the most serious cause of liver injury, mediated by the free radical–induced oxidative stress (Rechnagel et al., 1973). Carbon tetrachloride (CCl_4) is one of the toxic xenobiotics widely used in animal models to induce oxidative stress–mediated hepatitis (Pierce et al., 1987), resulting in apoptosis, inflammation, and fibrosis (Wong et al., 1998). The main mechanism through which CCl_4 induces hepatotoxicity is the generation of free radicals (Qureshi et al., 2009). CCl_4 is metabolized by the cytochrome P450 enzymes to a highly reactive trichloromethyl (CCl_3^-) free radical which reacts with free oxygen to form the trichloromethyl peroxy radical (CCl_3OO^-). The free radical sequentially attacks the hepatocyte cell membrane, leading to lipid peroxidation and cell death. The damaged hepatocytes are linked with elevated serum levels of ALT, AST, and ALP and depletion of CAT, GSH, and SOD activities (Chen et al., 2017). In addition, CCl_4 intoxication triggers the production of proinflammatory cytokines such as TNF-α, TGF-β, and IL-6, stimulating inflammatory cell recruitment at the site of injury (Sun et al., 2001).

Naturally, the body's non-enzymatic or enzymatic antioxidant defenses can inhibit the injurious effects of toxic agents through free radical scavenging activity or by modulation of the inflammatory response (Percival, 1998; Domitrovic et al., 2009). However, when free radical generation overwhelms the antioxidants, oxidative damage of the hepatic cells follows (Bandyopadhyay et al., 2002). It has been reported that intake of a nonspecific antioxidant-rich diet is often linked with the risk of developing different liver diseases due to their uncertain formulation and unknown mechanism of action. Therefore, effective antioxidants and anti-inflammatory remedies with a clear mechanism of action and no side effects are urgently required for the treatment of liver diseases (Praneetha et al., 2019).

The modern pharmaceutical industry is still struggling to design reliable hepatoprotective drugs. Therefore, a large number of traditional remedies can be suggested as alternatives for the treatment of liver ailments. Many plant species have been used traditionally for the treatment of liver disorders around the globe such as *Verbena litoralis, V. montevidensis* (Vestena et al., 2019), *Boerhaavia diffusa* (Olaleye et al., 2010), *Annona squamosa*, *Cymbopogon citratus* (Rajeshkumar et al., 2015), *Silybum marianum* (AI Jarallah et al., 2013), *Fumaria indica* (Rathi et al., 2008), and *Punica granatum* (Stowe, 2011). These plants contain a wide range of bioactive constituents such as steroids, terpenoids, phenols, and flavonoids, exhibiting hepatoprotective activities.

The pomegranate (*Punica granatum*), commonly known as anar, a deciduous tree belonging to the Punicaceae family, is found all over Pakistan. In the holy book (Al-Qur'an) of the Muslims, it is mentioned as the fruit of "Adan" (Heaven). The pomegranate is one of the healthiest fruits on this planet (Malik et al., 2005). All of its parts contain beneficial compounds, and hence, it is consumed in many disease conditions globally. The flowers of the pomegranate have significant hepatoprotective and anti-inflammatory potential (Kaur et al., 2006; Stowe, 2011) and may also control glucose levels (Huang et al., 2005). The nephro-protective potential of the pomegranate has been credited to its seed oil (Bouroshaki et al., 2010). Recent studies have suggested that pomegranate (PG) derivatives abate chemical-induced skin, breast, lung, and colon cancer (Adhami et al., 2009). Fruit and fruit extracts of PG have been used for the last decade, as anticipatory and antioxidant agents against several life-threatening diseases such as type 2 diabetes (Banihani et al., 2013), cancer (Orgil et al., 2014), and cardiovascular diseases (Al-Jarallah et al., 2013; Hamoud et al., 2014). Nutraceutical properties of the PG fruit are not only restricted to the comestible part (arils) but also to the nonedible parts (peel and seed) which may appear to be useless, but actually contain higher amounts of medicinally and nutritionally significant phytochemicals than the comestible part (Abid et al., 2017). The PG peel (PP), constituting nearly 50% of the weight of the fruit, is characterized by different types of high–molecular weight antioxidant compounds present in it that have attracted many researchers to further explore its beneficial aspects (Hong et al., 2015).

PP and PPx (pomegranate peel extract) have been reported for substantial hepato-protection by attenuating inflammatory responses (Bchoual et al., 2011; El-Rashedy et al., 2011). Particularly, a rich variety of PG phenolic compounds such as flavonoids, phenolic acids (Soliman and Selim, 2012; Singh et al., 2017), and tannins has been reported for the hepatoprotective activity against fatty liver disorder (El-Rashedy et al., 2011). Among these compounds, flavonoids are the ones which have a considerable variety of activities such as anti-inflammatory, antidiabetic, anti-allergic, antiplatelet, anti-mutagenic, and antioxidant activities (Xiao, 2017; Khan et al., 2018).

Taking into account the above points, this work was designed to investigate the hepatoprotective, free radical–quenching, and anti-inflammatory activities of PPx and its fractions in Wistar rats, thereby providing scientific contribution for the incorporation of herbal remedies with modern medicine.

MATERIALS AND METHODS

Plant Material

Ripe and healthy pomegranate fruits were collected from the northern parts of Khyber Pakhtunkhwa and authenticated by the

taxonomist Dr. Muhammad Ilyas at the Department of Botany, University of Swabi, Pakistan, with the voucher number (PG/HA-1), deposited in the herbarium.

Extract Preparation

Pomegranate fruits were collected, washed thoroughly with tap water, and then peeled. The peels were shade-dried for one month. The dried peels were powdered in an electric grinder. The accurately weighed powdered sample (1 kg)/was mixed in 2 L of methanol to yield 100 g extract (Met-PPx). After removal of the solvent, the concentrated methanolic extract was suspended in water for further solubilization to get the aqueous fraction (15 g). Then *n*-hexane was added to the mixture to remove the fatty material, and the defatted fraction was then dissolved in ethylacetate and butanol to finally yield *n*-hexane (12 g), ethylacetate (25 g), and butanol (9 g) fractions, respectively. The extract and fractions were kept at 4°C until further use. The extract preparation scheme is given below in **Figure 1**.

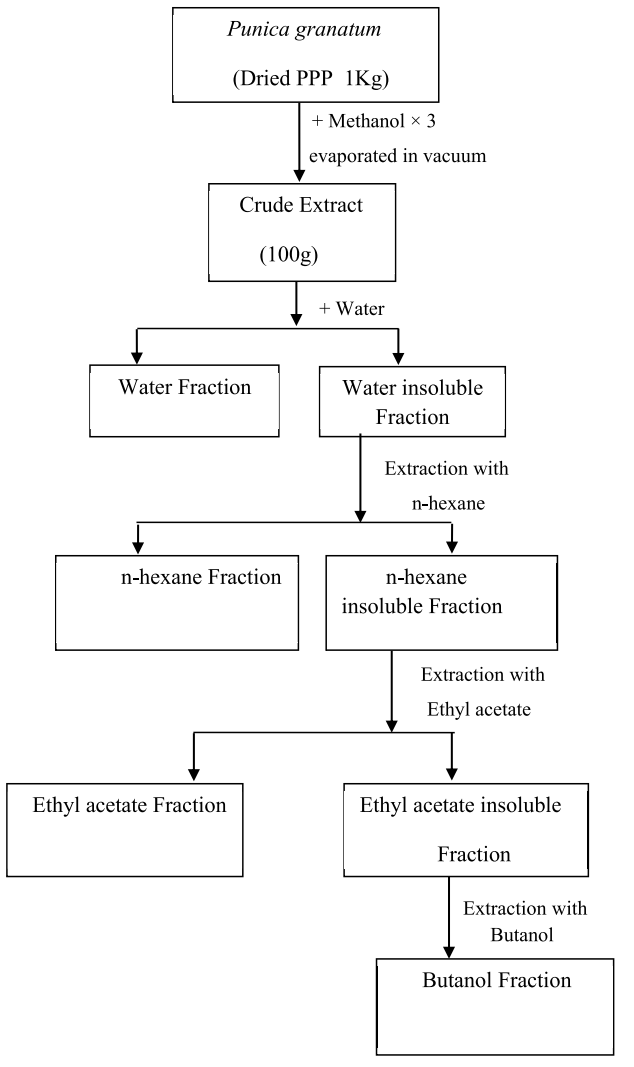

FIGURE 1 | Preparation of extracts from *Punica granatum* peel powder (PPP).

Animals

Male Wistar rats (150–180 g) were housed in individual cages for a week at ambient temperature under 12-h light/dark cycles, with access to chow and tap water *ad libitum* according to standard laboratory protocol. All animals received humane care, and all protocols concerning the animals were in agreement with the guidelines approved by the Institutional Ethics Committee approval letter (CUI/Bio/ERB/4-21/19) of COMSATS University, Islamabad.

CCl_4-Induced Acute Hepatotoxicity

Acute hepatotoxicity studies were performed using male Wistar rats. The experimental protocol for the current study was based on previous studies (Ali et al., 2014). All the experimental animals were divided into different groups, and six rats were included in each group as described here: Group 1 (normal control) were injected with vehicle only (1 ml/kg body weight olive oil), Group 2 (hepatotoxicity group) were treated with i.p. injection of CCl_4 (1 ml/kg) with 1:1 olive oil, Group 3 (positive control) were injected intraperitoneally with CCl_4 (1 ml/kg) with 1:1 olive oil and also administered orally with silymarin (100 mg/kg) 3 days before treatment and 2 days after treatment, and Groups 4–8 were treated with i.p. injection of CCl_4 (1 ml/kg) with 1:1 olive oil but also received methanolic extract, aqueous, *n*-hexane, ethyl acetate, and butanol fractions, respectively, at a dose of 100 mg/kg body weight for 3 days before treatment and 2 days after treatment.

Blood Biochemistry

All experimental animals were terminated 48 h after the administration of CCl_4 under sodium pentothal anesthesia. From animals, the blood was collected by cardiac puncture using a 5-ml sterile syringe and with a slight possible pressure to avoid hemolysis. Blood was centrifuged for 15 min at 2000 rpm to extract serum. The serum was used for the determination of liver damage by analyzing biological parameters (ALT, AST, and ALP) using a dry chemistry analyzer (Roche Diagnostics, Mannheim, Germany).

Oxidative Stress Markers

For identification of oxidative stress, the livers were excised and homogenized (Polytron homogenizer) in 50 mM phosphate buffer saline with a pH value of 7.4 (Kinematica, Lucerne, Switzerland). The homogenates were centrifuged at 15 000 g for 20 min at 4°C using a Beckman L7-65 Ultracentrifuge (Beckman, Fullerton, United States), and the supernatants were used to determine the Cu/Zn SOD activity, MDA, and GSH content. The quantification of protein in liver tissues was assessed using Bradford's method (Bradford, 1976). The activity of Cu/Zn SOD was measured at 550 nm by the reduction in cytochrome c by superoxide radicals using a UV–VIS spectrophotometer (Domitrović et al., 2011). Similarly, the MDA and GSH

TABLE 1 | Lesion scoring of liver tissue obtained after treatment under different conditions.

Groups	Control	CCl_4	CCl_4+silymarin	MeOH	H_2O	EtOAc	Butanol	*n*-hexane
Hepatocellular necrosis	0.00	12.91 ± 0.02[a]	8.12 ± 0.01[a]	2.91 ± 0.11[b]	1.72 ± 0.31[b]	0.10 ± 0.12[b]	9.32 ± 0.06[a]	7.23 ± 0.03[a]
Hepatocellular hypertrophy	0.00	7.2 ± 0.1[a]	5.3 ± 0.3[a]	3.01 ± 0.21[b]	1.11 ± 0.52[b]	0.02 ± 0.52[b]	6.4 ± 0.1[a]	5.8 ± 0.11[a]
Fatty degeneration	0.00	4.21 ± 0.32[a]	2.32 ± 0.11[a]	0.13 ± 0.31[b]	0.21 ± 0.13[b]	0.14 ± 0.21[b]	3.12 ± 0.12[a]	4.32 ± 0.31[a]
Congestion of RBC	0.00	4.1 ± 0.5[a]	3.5 ± 0.2[a]	1.6 ± 0.1[b]	1.2 ± 0.3[b]	0.1 ± 0.2[b]	3.1 ± 0.3[a]	5.2 ± 0.2[a]
Inflammatory cell infiltration	0.00	12.6 ± 0.12[a]	7.4 ± 0.21[a]	1.5 ± 0.12[b]	0.7 ± 0.23[b]	0.3 ± 0.12[b]	9.5 ± 0.11[a]	8.3 ± 0.21[a]
Pyknosis	0.00	6.7 ± 0.25[a]	1.45 ± 0.14[a]	0.35 ± 0.13[b]	0.13 ± 0.21[b]	0.23 ± 0.42[b]	3.6 ± 0.13[a]	2.7 ± 0.11[a]

Treatment effect of pomegranate extract and its fractions on the inflammation scores of liver tissues following CCl_4-induced hepatotoxicity. The values are means ± SD (n = *10), and data were analyzed by one-way ANOVA, followed by Tukey's* post hoc *test for multiple comparisons.*

[a]*Indicates significant from the control group.*

[b]*Denotes significant from the CCl_4 group.*

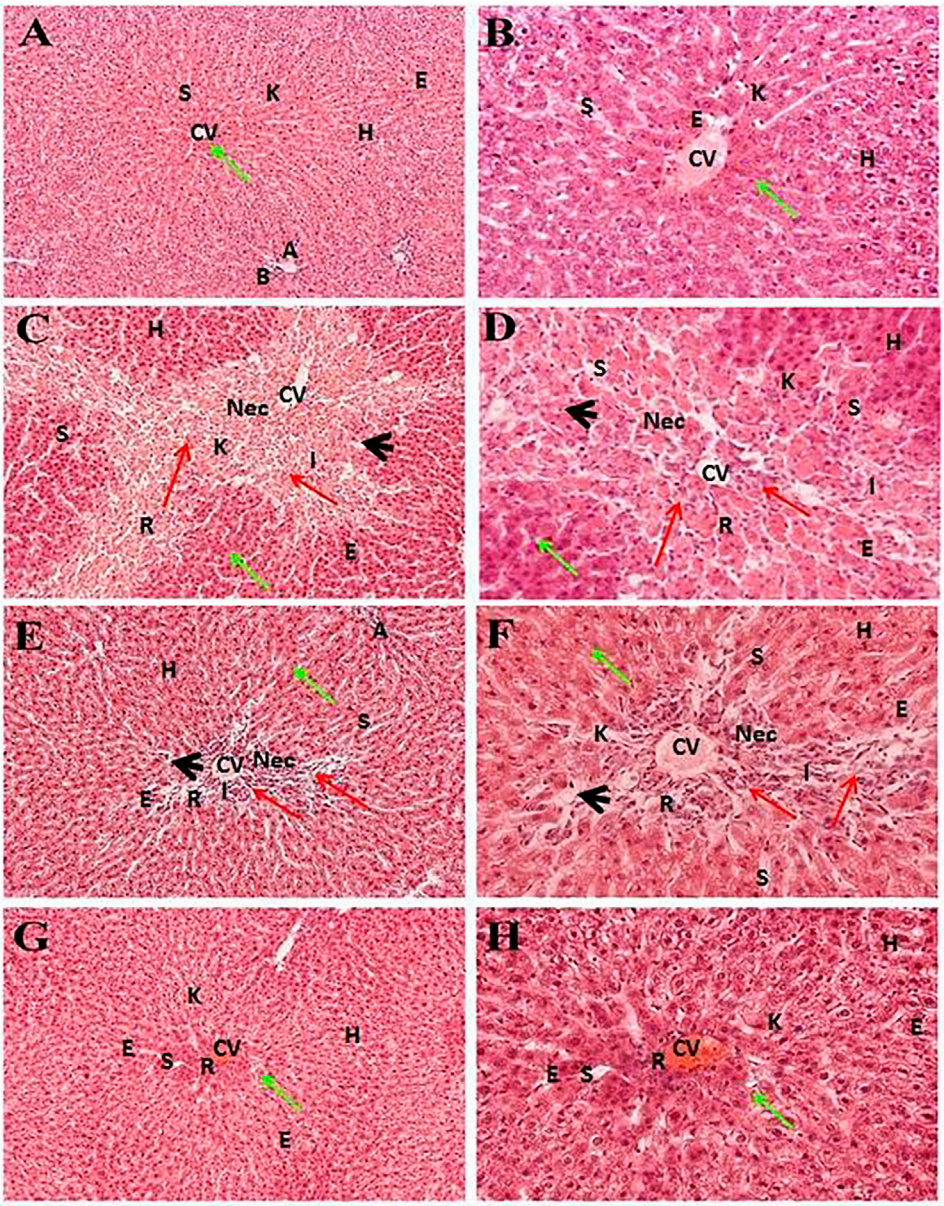

FIGURE 2 | Hepatoprotective potential of Met-PPX. Histological examination of the liver displays a typical (green arrows) central vein in the control group (normal, **(A, B)**); damaged areas (red arrows) after CCl_4 intoxication (CCl_4, **(C, D)**); silymarin protection (CCl_4+silymarin **(E, F)**); healing by methanolic extract (CCl_4+ Met-PPx, **(G, H)**). CCl_4+ Met-PPx represented better protection than standard silymarin. Scale bar is 250 and 25 μm, shown in **(G, H)**. CV, central vein; H, hepatocytes; S, sinusoidal spaces; E, endothelial cells; Nec, necrosis; A, artery; R, congestion of RBC; I, infiltration of inflammatory cells; arrowhead, pyknosis; K, Kupffer cells.

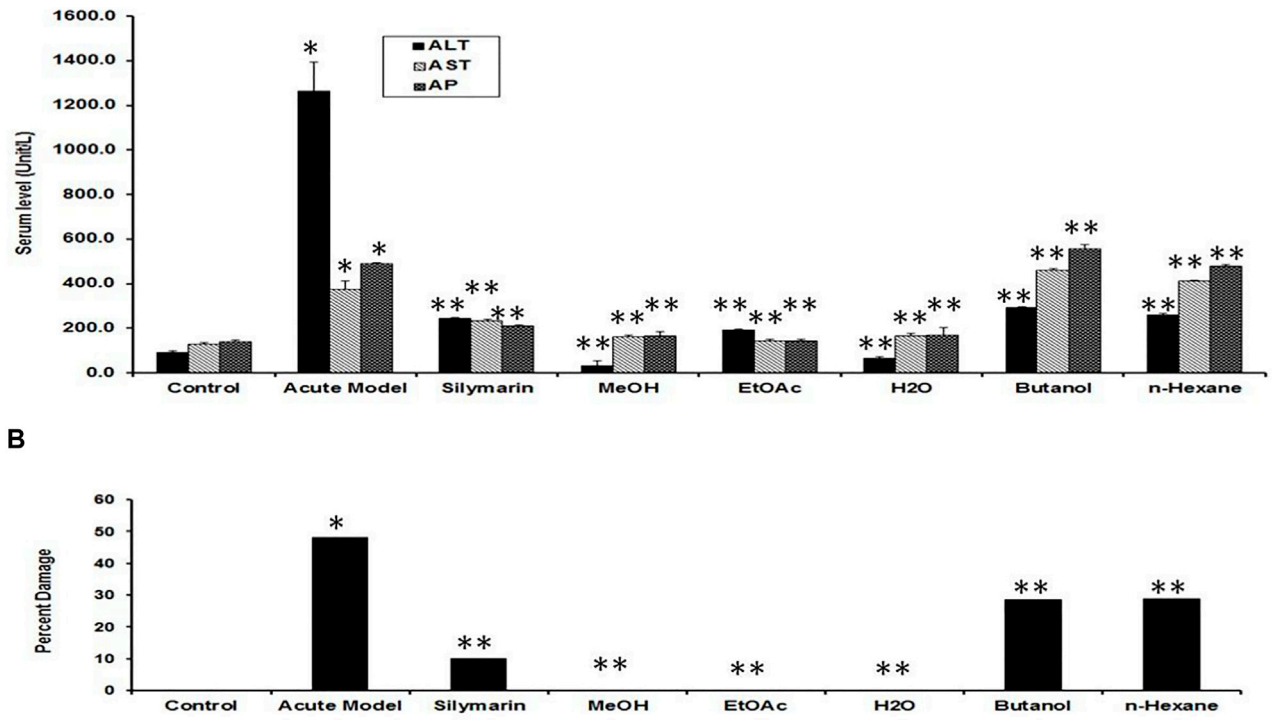

FIGURE 3 | Quantification of the effects of *Punica granatum* peel extract on CCl_4-induced hepatotoxicity. **(A)** Serum levels of ALT, AST, and ALP act as indicators of hepatic injury. We expressed the data as the mean ± SD where $^*p < 0.05$, when the groups was compared to the normal control; $^{**}p < 0.001$, when compared to the CCl_4 group. MeOH extract, EtOAc, and H_2O fractions showed ample protection against CCl_4 liver injury ($^{**}p < 0.001$) compared to CCl_4+silymarin ($^{**}p < 0.001$). Other fractions (butanol and *n*-hexane) did not show considerable outcomes. **(B)** Percent hepatic damage under various conditions as evaluated by histology. Note that the silymarin group shows some damage (~10%), whereas Met-PPx (MeOH), EtOAc, and aqueous (H_2O) fractions indicated no damage (0%). Effect of PPx on oxidative stress markers.

contents were determined according to a reported study (Anderson, 1985). The supernatant was deproteinized with 1.2 M metaphosphoric acid and centrifugation at 4500 g for 8 min (Rotina 420R, Andreas Hettich GmbH, Tuttlingen, Germany). Consequently, 700 µL of 0.3 mM NADPH in phosphate buffer saline and 25 µL of the deproteinized sample along with water and 100 µL of 6 mM DTNB were thoroughly mixed in a cuvette to get a final volume of 1.0 ml. Finally, 10 µL of glutathione reductase (50U ml^{-1}) was added to the mixture, and absorbance was observed for 30 min at 405 nm. From the series of dilution of stock solution of glutathione, their content was identified from the standard curve.

Histopathological Study of the Liver

After dissection, the liver was identified in the right upper quadrant and sliced up. The liver was kept in formalin for histopathological examination. Formalin-fixed liver tissues were desiccated through a series of graded alcohol, followed by their entrenchment in paraffin, and cut into 6-µm-thick sections. The liver sections were transferred onto the slides, dewaxed, and rehydrated through xylene and graded alcohol in the reverse sequence from dehydration. The deparaffinized tissues were stained with hematoxylin–eosin (H&E) and examined under a bright field microscope. The necrotic area of each group was measured in at least 30 different tissue sections of the liver using NIS-elements software from Nikon, Japan, and was expressed as the percentage of the entire area of the section.

Immunostaining

The previously dewaxed and rehydrated liver sections (6 µm thick) were used for immunohistochemical assessment. All selected liver sections were incubated with blocking solution in phosphate buffered solution (PBS, Roti-immunoblock, Carl Roth, Karlsruhe, Germany) for 25 min at normal temperature. Subsequently, these tissues were incubated with primary monoclonal antibody for CD68 (clone ED1, abcam) and iNOS (ab3523) at dilution (1:100) for 45 min at 37°C. The liver tissues were thoroughly washed with PBS and incubated with secondary antibodies, FITC/Texas Red-conjugated goat anti-mouse IgG (1:

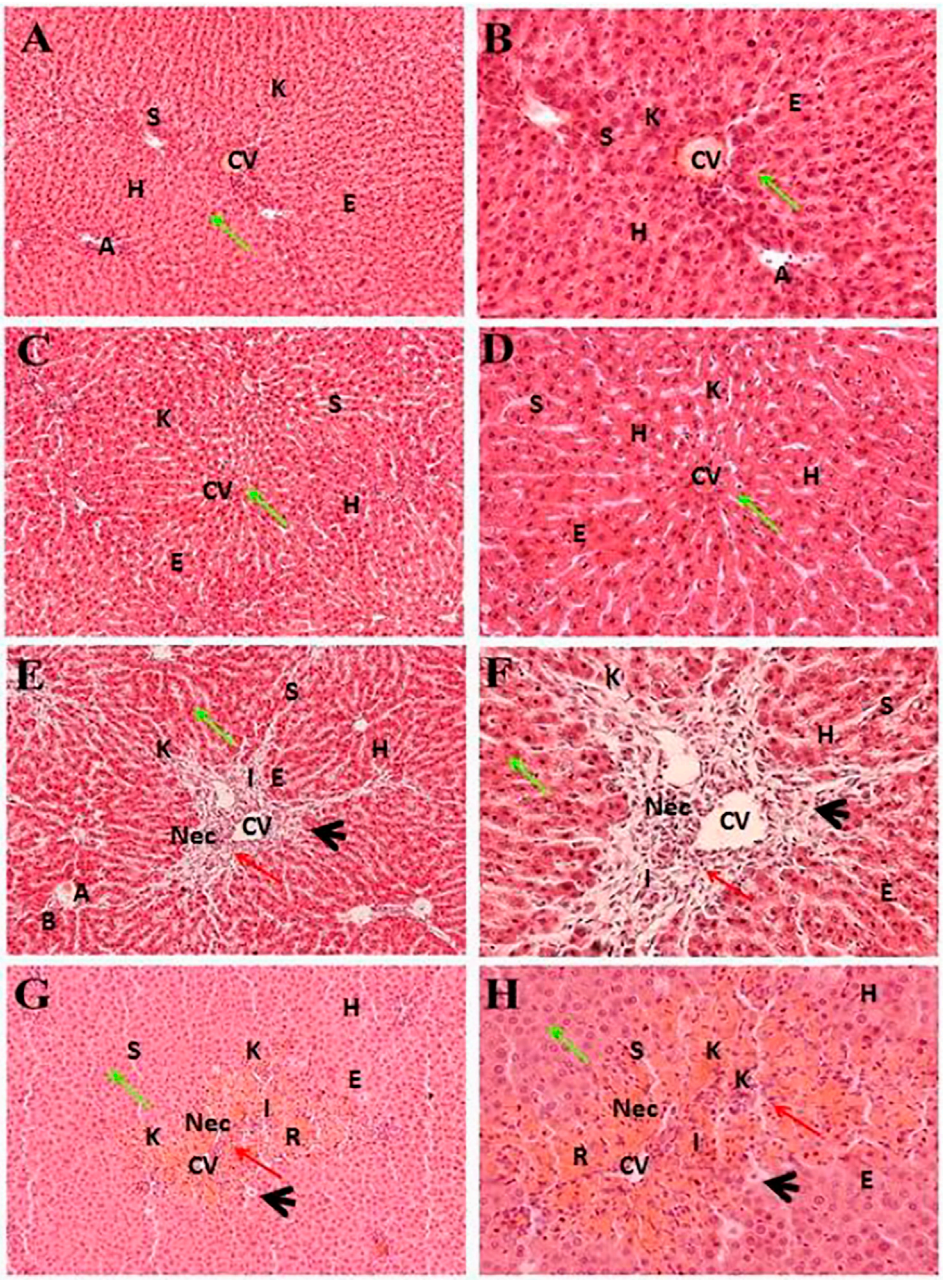

FIGURE 4 | Hepatoprotective potential of different fractions of Met-PPx. Liver histopathology of the ethyl acetate fraction (CCl_4+EtOAc, **(A, B)**) showing normal histology with a prominent central vein. Similar results were seen for the aqueous fraction (CCl_4+H_2O, **(C, D)**). However, the butanol (CCl_4+Butanol, **(E, F)**) and *n*-hexane (CCl_4+ *n*-hexane, **(G, H)**) fraction groups showed damage to the hepatic architecture (red arrows). CV, central vein; H, hepatocytes; S, sinusoidal spaces; E, endothelial cells; Nec, necrosis; A, artery; R, congestion of RBC; I, infiltration of inflammatory cells; arrowhead, pyknosis; K, Kupffer cells.

100), for 40 min. After briefly rinsing twice with PBS, the nuclei were stained with DAPI for around a minute and then rinsed with PBS and mounted in mounting media. The immunostained tissues were analyzed by fluorescence microscopy, and their images were acquired using a Nikon DXM 1200 C camera using image analysis software AR 3.0 (Nikon, Japan). All the acquiesced images were processed using Adobe Photoshop software. The number of Kupffer cells was counted in different portions surrounding the injured area from their elongated nuclei stained with DAPI using NIS-elements software.

Data Analysis

Results are expressed as mean ± SD. Total variation present in a set of data was estimated by one-way analysis of variance

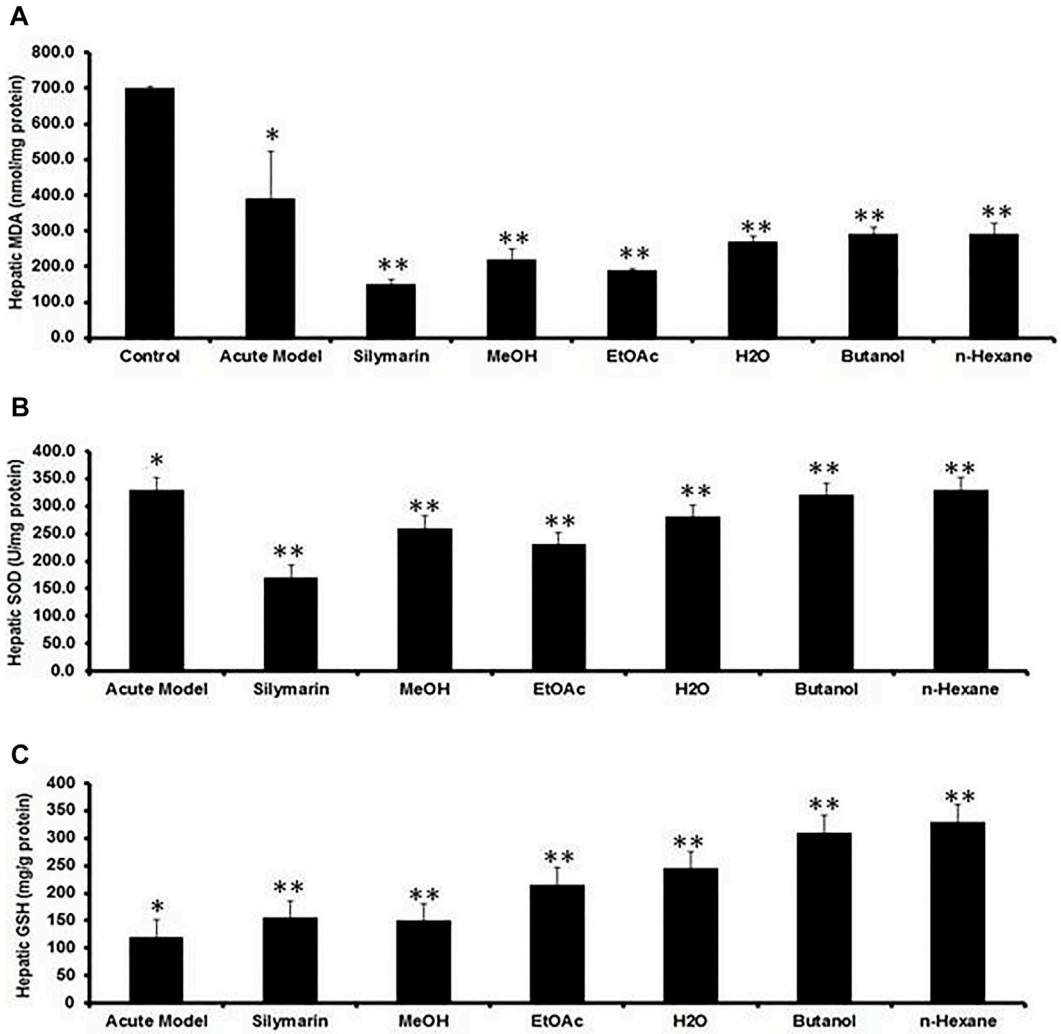

FIGURE 5 | Quantification of the effects of *P. granatum* extract and fractions on antioxidant activity. **(A)** MDA, **(B)** SOD, and **(C)** GSH levels act as liver damage indicators under several conditions. The data were expressed as the mean ± SD where *$p < 0.05$, when compared to the normal control while MeOH extract and EtOAc and H_2O fractions revealed best protection compared to CCl_4 (**$p < 0.001$) and silymarin (**$p < 0.001$) treatment by increasing hepatic antioxidant enzymes and decreasing MDA levels, while the butanol and *n*-hexane fractions did not considerably elevate the hepatic antioxidant enzymes. Data were expressed as the mean ± SD where $n = 10$. PPx and its fractions mitigate the recruitment of Kupffer cells (KCs) during acute hepatotoxicity.

(ANOVA), followed by Dunnett's *post hoc* test. $p < 0.05$ and $p < 0.01$ were considered to be significant.

RESULTS

Histopathology of the Liver Indicates Better Hepatoprotective Potential of the MeOH Extract of Pomegranate Peel Than That of Silymarin

Liver sections of the normal control group exhibited typical lobular architecture, with a central vein fenced by the hepatic cord of cells with clear spaces lined by elongated endothelial and Kupffer cells (**Table 1**; **Figures 2A,B**). In contrast, the CCl_4-treated group revealed loss of hepatic architecture with clear pale areas having degenerated and necrotic hepatocytes and the presence of inflammatory cells around the central vein with distinct nuclei (**Table 1**). This pointed toward the fact that the injurious free radical CCl_3^- is particularly generated only in the hepatocytes. Normal-shaped hepatocytes (**Figures 2C,D**) could also be perceived around the necrotic area, which could simply be identified because of their darker staining characteristic. Cells around the pale necrotic area exhibited hydrophic degeneration and ballooning hepatocytes (**Table 1**). Moreover, histopathological analysis (**Figure 3B**) had shown ~47% damage in the CCl_4-treated group. Liver samples acquired from the CCl_4^+ silymarin–treated group showed a substantially

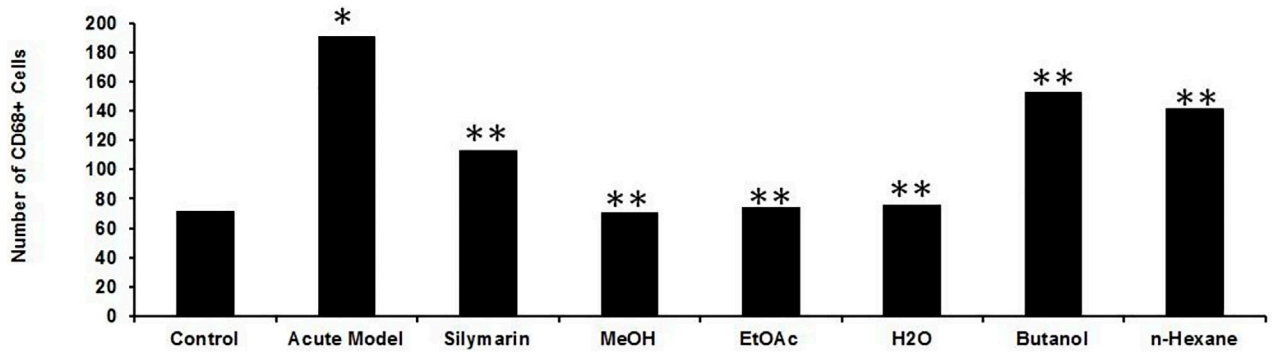

FIGURE 6 | Effect of *P. granatum* fractions on the recruitment of Kupffer cells (KCs). Immunohistochemistry was performed for different groups: CCl_4+ EtOAc fraction **(A–C)** or aqueous fraction **(D–F)**, butanol fraction **(G–I)**, and *n*-hexane fractions **(J–L)**. KCs that were positive **(A, D, G, J)** were presented by immunoreactivity. DAPI staining is shown in **(B, E, H, K)** for the nucleus, while the merged image is shown in **(C, F, I)**. The EtOAc **(A)** and H_2O **(D)** fractions have abrogated the increase in Kupffer cells in hepatotoxicity, but the butanol **(G)** and *n*-hexane **(J)** fractions increase the number of KCs drastically. Scale bar is 50 μm.

attenuated ($p < 0.001$) necrotic area around the central vein and a great decrease (**Figures 2E,F**) compared to the CCl_4 group (**Table 1**). Moreover, minimal hepatic damage (~10%) was observed by histopathological analysis (**Figure 3B**). Interestingly, the CCl_4+ Met-PPx completely prevented liver necrosis (**Table. 1**; **Figures 2G,H**) with 0% damage (**Figure 3B**). Therefore, the Met-PPx at an optimum dose of 100 mg/kg presented restoration of injury and hence showed hepatoprotective activity ($p < 0.001$) compared to the positive control silymarin (100 mg/kg).

Hepatoprotective Potential of the EtOAc and Aqueous Fractions of the Met-PPx

Figure 4 indicates the effect of different fractions of the Met-PPx on the histology of CCl_4-induced liver toxicity. The CCl_4+ EtOAc group had shown a similar protective effect to that of the Met-PPx, with restoration of the hepatic architecture with no sign of necrosis (**Table. 1**; **Figures 4A,B**), and presented 0% damage (**Figure 3B**). Even the liver architecture was in such a way that it was difficult to distinguish it from the untreated group. Likewise, the CCl_4+ aqueous group also completely abolished and showed normal arrangement of hepatocytes with no sign of necrosis (**Figures 4C,D**) and 0% damage (**Table 1**; **Figure 3B**). On contrary, more necrosis and massive inflammatory recruitment (**Table 1**) around the central vein was found in the CCl_4+ butanol group than in the positive control silymarin (**Figures 4E,F**). Histopathological investigation revealed ~29% damage (**Figure 3**) which is less than that in the CCl_4-treated group but more than that in the silymarin control. The CCl_4+ *n*-hexane group also indicated necrotic areas (**Table 1**) around the injurious place of the central vein with congestion of RBCs (**Figures 4G,H**).

PPx Alleviated Hepatic Enzyme Level

Several enzymes coming from the liver in the serum were used as useful biochemical markers for investigating early hepatotoxicity. After 48 h of CCl_4 intoxication, rats demonstrated a substantial increase in the levels of serum ALT, AST, and ALP as compared to the normal control (**Figure 3A**). The positive control silymarin at a dose of 100 mg/kg was not as effective in the reduction of hepatocellular damage as 100 mg/kg Met-PPx, which reduced ($p < 0.001$) the rise in the serum level of hepatic enzymes to a remarkable extent. However, it is interesting and noteworthy that in the silymarin-treated group, the level of enzymes was not completely halted down to the control, which represents some damage to the hepatocytes. Interestingly, the Met-PPx substantially stopped ($p < 0.001$) the rise in the level of serum enzymes and brought it down to control levels, indicating no damage to the parenchyma cells regardless of the CCl_4 treatment. The EtOAc fraction abrogated ($p < 0.001$) the elevation in serum enzymes. Similarly, the aqueous fraction also inhibited ($p < 0.001$) the increase in serum enzymes. However, the butanol and the *n*-hexane fractions did not considerably reduce the hepatic enzymes. These results strongly suggest that the hepatoprotective and free radical–quenching potential of the PP exists in the EtOAc and aqueous fraction due to the existence of bioactive compounds.

MDA is one of the main end products of lipid peroxidation, and its elevated level could be used as an indicator of hepatotoxicity. CCl_4 intoxication significantly elevated the MDA content while reducing GSH and SOD levels in the liver tissues, compared to the normal control group (**Figures 5A–C**), indicating that the CCl_4 injection induced severe oxidative stress. Treatment with Met-PPx and its EtOAc and aqueous fractions significantly attenuated this and were more effective than silymarin. Hepatic antioxidant enzyme levels were substantially increased (levels similar to those in the normal control) by Met-PPx and its EtOAc and aqueous fractions, which also significantly decreased MDA levels. In contrast, the butanol and the *n*-hexane fractions did not considerably increase the antioxidant activity and also showed high levels of MDA.

Inflammation of the liver is linked with activation of Kupffer cells (KCs) and their migration into the hepatic

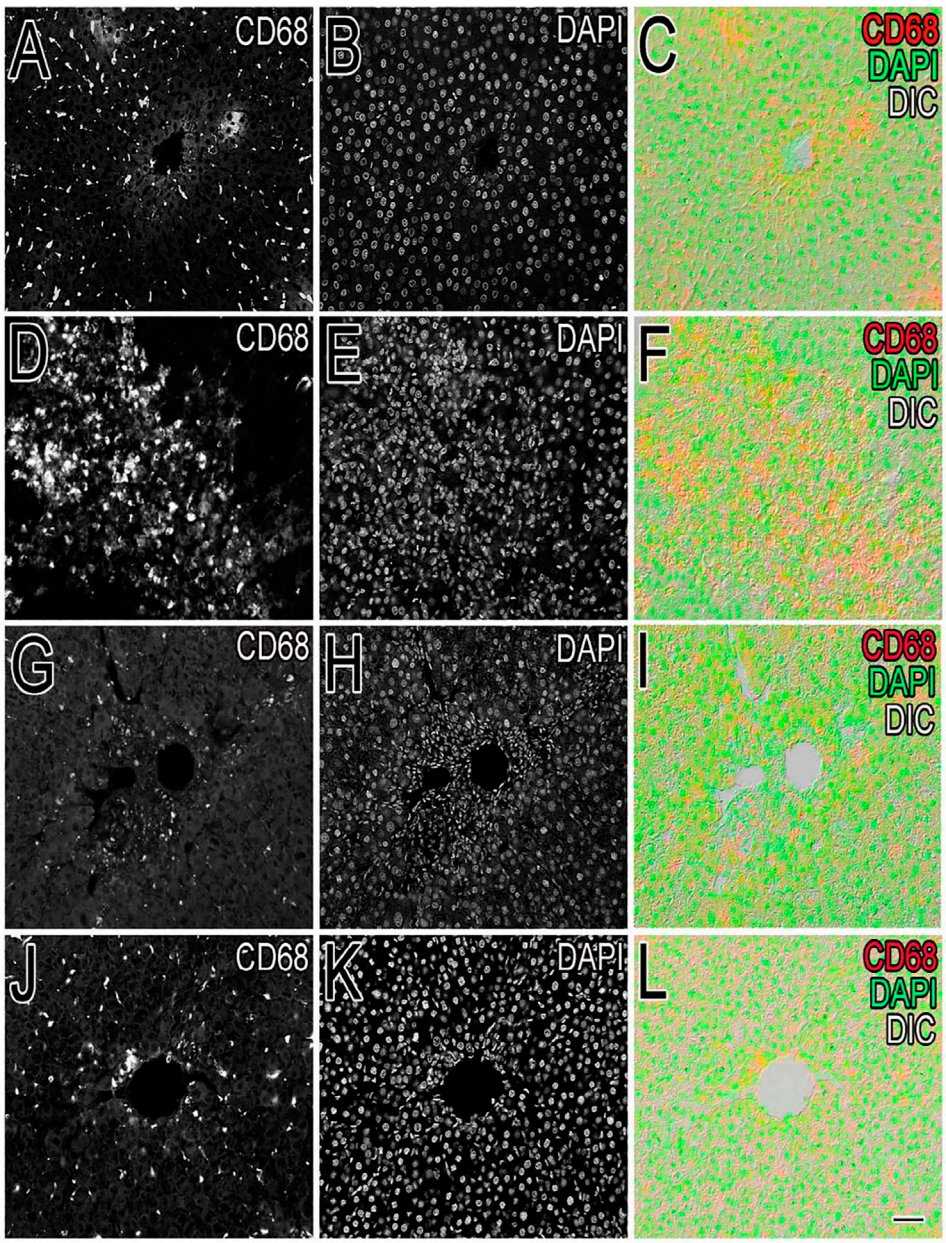

FIGURE 7 | Quantification of the Kupffer cells after *P. granatum* extract treatment on CCl_4-induced hepatotoxicity. After CCl_4 intoxication resulting in membrane damage, activation of the dormant KCs occurred along with the higher number KCs compared to the normal control group (*$p < 0.05$). This increase was somewhat prevented by silymarin treatment (**$p < 0.001$), and while the Met-PPX (**$p < 0.001$), EtOAc (**$p < 0.001$), and aqueous fraction (**$p < 0.001$) significantly reduced KCs down to control levels, the butanol and *n*-hexane fractions did not considerably decreased their number. Immunostaining of inducible nitric oxide synthase (iNOS).

cords where they secrete TNF- and IL-6, proinflammatory cytokines (Kiso et al., 2012). A particular KC marker, CD68, was used to monitor KC activation in CCl_4-intoxicated rats. In the normal control liver (**Figure 6**), a small number (71 ± 10) of quiescent KCs are restricted to the liver sinusoids only (**Figures 7A–C**). The liver section of the control group did not show considerable CD68 immunopositivity (**Figure 7A**). In contrast, strong ($p < 0.001$) CD68 expression (190 ± 8) was observed around the central vein of the CCl_4-intoxicated group (**Figures 7D–F**). CD68 immunoreactivity was observed mainly around the injured areas, presenting mostly pericentral staining. CD68 immunopositivity increased in the livers of CCl_4-intoxicated rats. Mixed infiltration of inflammatory cells (**Figure 7E**) was identified from elongated nuclei with DAPI staining around the central vein in the CCl_4-treated group. It is obviously known from

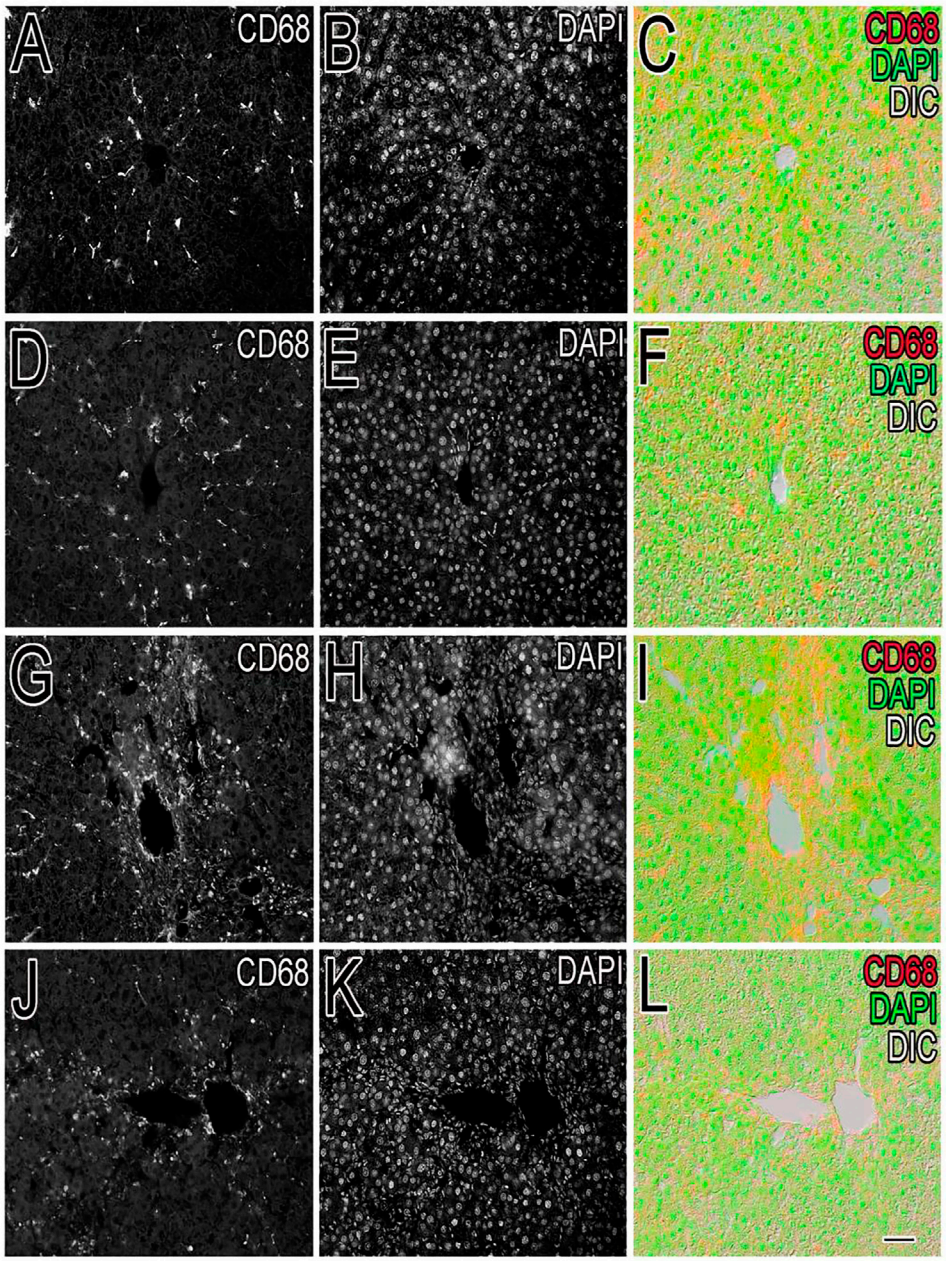

FIGURE 8 | Effect of *P. granatum* extract on the recruitment of Kupffer cells (KCs). Immunostaining of KCs in different experimental groups was performed. The number of Kupffer cells **(A, D, G, J)** was examined in the normal control **(A–C)**, CCl_4 **(D–F)**, silymarin-treated **(G–I)**, and Met-PPX **(J–L)** groups. DAPI was used for nucleus staining **(B, E, H, K),** while **(C, F, I, L)** shows the merge of DAPI + KCs. Considerably large number of KCs was found in the CCl_4-intoxicated group **(D)** which is abridged by silymarin **(G)**. Interestingly, the Met- PPx **(J)** significantly reduced ($p < 0.001$) KCs around the central vein, similar to the normal control group. Scale bar is 50 μm.

Figure 6 that treatment with silymarin has decreased ($p < 0.001$) the number of Kupffer cells (112 ± 10) compared to the intoxicated group. Moreover, an enhancement in the number of KCs surrounding the central vein and the pericentral region in the liver treated with silymarin was still higher ($p < 0.001$), relative to the control group (**Figures 7G–I**). Interestingly, the Met- PPx significantly reduced ($p < 0.001$) KCs (71 ± 9) around the central vein (**Figure 6**), similar to the normal control group. After CCl_4 intoxication, the activated KCs were recruited to the site of injury. The Met-PPx administration restricted the KCs to the sinusoidal spaces despite the CCl_4 treatment as supported by the immunohistochemistry (**Figures 7J–L**). The presence of polyphenolic compounds in the EtOAc fraction might significantly reduce ($p < 0.001$)

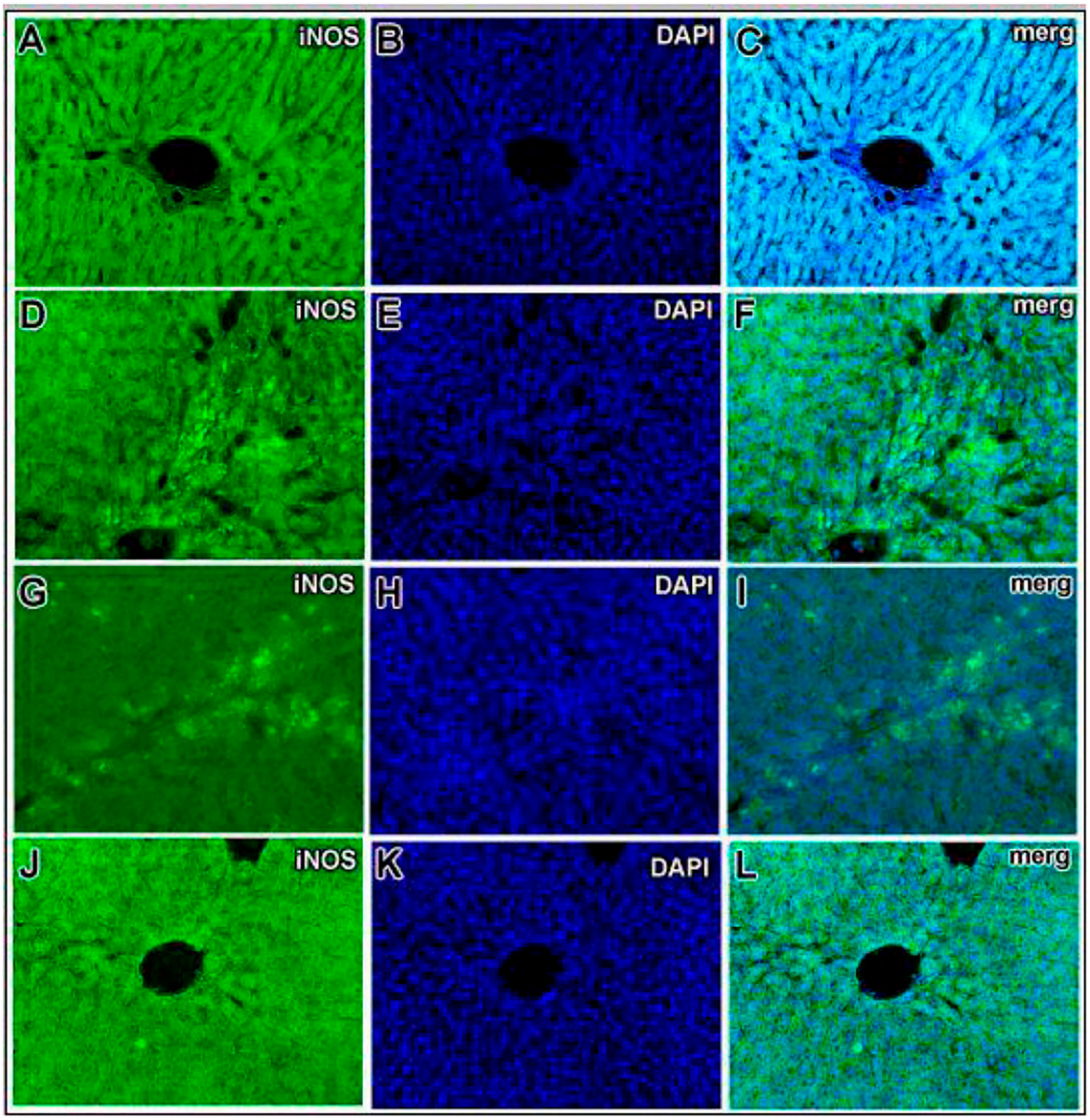

FIGURE 9 | Hepatic inducible nitric oxide synthase (iNOS) expression in CCl_4-induced liver injury. iNOS immunoreactivity was almost absent in the normal control **(A–C)**. Prominent iNOS immunoreactivity in the livers of the CCl_4-treated group **(D–F)** was observed. The CCl_4-treated group showed strong iNOS immunopositive hepatocyte nuclei around the central vein region. Presence of immunopositive cells for iNOS in the silymarin-treated group **(G–I)**. In the 100 mg kg^{-1} ethyl acetate and aqueous–treated group, only minute traces of iNOS immunopositivity around the central vein hepatocytes and endothelial cells **(J–L)** were identified.

CD68-positive (74 ± 8) and limited the KCs to the sinusoids, similar to the Met-PPx group as evident from immunohistochemistry (**Figures 7A–C**). Likewise, the aqueous fraction completely restricted ($p < 0.001$) the KCs (75 ± 9) (**Figure 6**) to the sinusoids (**Figures 8D–F**). Compared with normal control sections, the butanol group revealed a drastic increase in the number of KCs (153 ± 11) (**Figure 6**) around the central vein (**Figures 8G–I**). Similarly, the *n*-hexane–treated group showed a dramatic increase (141 ± 12) in the number of KCs (**Figures 6**, **7J–L**J–L**7J–L**).

Immunostaining of Inducible Nitric Oxide Synthase

To investigate the role of hepatic iNOS *in vivo*, a CCl_4-induced acute liver model of inflammation was used. In the control group, no apparent detection of iNOS expression was noticed by immunohistochemistry (**Figures 9A,B**), which was further confirmed from the merging of iNOS and DAPI as shown (**Figure 9C**). Moreover, quantification of the iNOS immunostained structure was identified and was measured under different conditions, showing a diminished number in

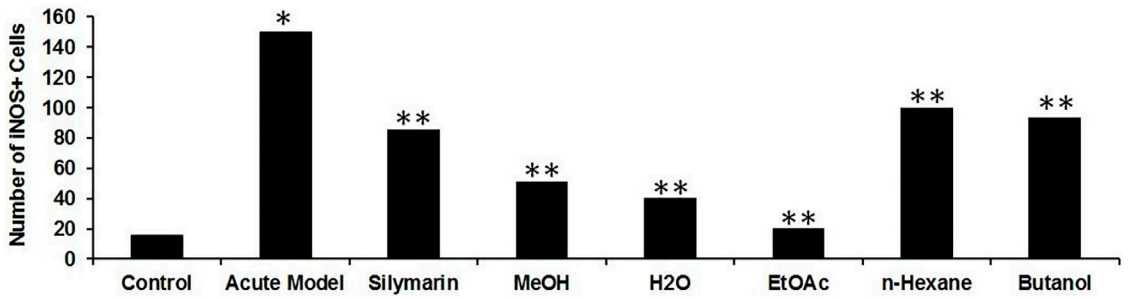

FIGURE 10 | Quantification of iNOS expressed immunoreactive cells upon CCl_4-induced hepatotoxicity. Injurious effect of CCl_4 intoxication causing central lobular damage and with continuous expression of iNOS in the stressed hepatocytes (*$p < 0.05$) in the CCl_4 group compared to the normal control. Due to the potential effect of silymarin, it was reduced somehow (**$p < 0.001$), and in contrast, the Met-PPX (**$p < 0.001$), EtOAc (**$p < 0.001$), and aqueous fraction (**$p < 0.001$) significantly abridged iNOS-positive immunostained cells to control levels, but in the *n*-hexane and butanol fractions, their number did not appreciably decline.

contrast to the CCl_4 group (**Figure 10**). After 24 h of administration of CCl_4, the liver-associated necroinflammation is at its peak, especially ALT. In the CCl_4-intoxicated model group, prominent expression of iNOS was observed and localized to the cytoplasmic content surrounding the hepatocytes' nuclei (**Figures 9D**, **10**). By double fluorescent microscopy, the enhanced expression and colocalization of iNOS and DAPI were uniformly confined in the surrounding central vein, which represents necrosis of hepatocytes (**Figures 9E**,**F**, **10**). The positive control silymarin group also presented the expression of iNOS in the central and pericentral hepatocytes (**Figures 9G**, **10**). The iNOS positively stained cells were scattered all around the central vein with signatures of necroinflammation (**Figures 9H,I**). In contrast, treatment with the ethyl acetate fraction showed negligible expression of iNOS (**Figures 9J**, **10**), whereas iNOS expression was further reduced in the at 100 mg kg^{-1} in merged image (**Figures 9L**, **10**). Moreover, hepatocyte and Kupffer cells' nuclei were immune-negative for iNOS in the normal group like the ethyl acetate– and aqueous-treated groups.

DISCUSSION

The current study was undertaken to determine the possible hepatoprotective, antioxidant, and anti-inflammatory potential of the pomegranate peel extract (PPx) and its fractions in the CCl_4-intoxicated rat model. Previous work has acknowledged the extensive pharmacological application of the pomegranate against a variety of diseases, particularly the effectiveness of its peel in abrogating the oxidative stress and curbing liver injury due to the presence of bioactive constituents. The antioxidant activity of the PG has been attributed to the presence of phenolic compounds having hydroxyl functional groups which act as potent hydrogen donors (Kulkarni et al., 2004). It has been suggested that peel powder and whey powder alone or synergistically exhibited antioxidant and hepatoprotective potential against CCl_4-induced liver injury in rats (Ashoush et al., 2013). Another report suggested that the polysaccharides from pomegranate peel had significant antioxidant and hepatoprotective ability against CCl_4-induced oxidative damage in mice (Zhai et al., 2018). In addition, the protective effects of pomegranate peel and seed extracts were demonstrated against CCl_4-induced hepatic fibrosis (Wei et al., 2015). Pomegranate extracts and genistein have significant anticancer effect through growth inhibition in human breast cancer (Jeune et al., 2005). Although a few studies have focused on the isolation of pure compounds from PP and their antioxidant activities *in vitro* and *in vivo*, there is a lack of investigation on the involvement of KCs in hepatotoxicity. Downregulation of KCs may be one of the key factors to halt the progression of CCl_4-induced hepatoxicity.

The CCl_4-induced hepatotoxicity model is extensively used for investigating the mechanisms of hepatotoxic effects such as necrosis, apoptosis, fibrosis, and hepatocellular carcinoma and for hepatoprotective drug screening (Pierce et al., 1987). Normally the hepatic lobules consist of the central vein surrounded by hepatic cords of cells and sinusoids. CCl_4 induces centrilobular necrosis of hepatocytes that can be detected by elevated levels of hepatic enzymes in the serum or histopathological study (Chen et al., 2017). It has been demonstrated previously that CCl_4 is metabolized in the hepatocytes by cytochrome P450 enzymes into the CCl_3 radical, which is further converted to the trichloromethyl peroxy radical in the presence of free oxygen. The highly reactive trichloromethyl peroxy radical subsequently binds to the polyunsaturated fatty acids of the cell membrane, resulting in peroxidative damage or stress. Oxidative stress plays a key role in the induction of hepatotoxicity by producing noxious lipid intermediates such as MDA and LPO that may interrupt the antioxidant defense, leading to hepatocyte necrosis (Brattin et al., 1985) and, ultimately, resulting in leakage and elevation of serum levels of enzymes, which is alleviated by the activities of SOD, GSH, and CAT (Kadiiska et al., 2005).

Elevation in the MDA content and levels of serum enzymes (ALT, AST, and ALP) and alleviated antioxidant enzyme activities, as evident in our study, indicates overproduction of free radicals due to failure of antioxidant defense mechanisms as a result of enhanced lipid peroxidation leading to loss of cell membrane integrity (Drotman and Lawhorn, 1978). Treatment

with Met-PPx decreased the MDA and LPO levels by enhancing antioxidant activities of SOD, GSH, and CAT to attenuate CCl_4-induced hepatotoxicity by reducing the oxidative stress. This extract also brought down the levels of AST, ALT, and ALP to corresponding normal values as compared to silymarin, which is a clue to the repair of hepatocyte damage and maintenance of the cell membrane and liver architecture. Likewise, EtOAC and the aqueous fractions enhanced the antioxidant activity and also alleviated the increase in serum enzymes. Nonetheless, the butanol and *n*-hexane fractions did not show satisfactory results. These biochemical findings were further supported by histopathological examination. These results suggest that the hepatoprotective effect of PPx and its fractions can be attributed to their antioxidative activities, also shown in previous studies (Singh et al., 2002).

Besides the aforementioned pathological aspects, inflammation is another important mechanism responsible for CCl_4-induced hepatotoxicity (Huang et al., 2017). Inflammation is linked with the activation of KCs. Normally KCs reside in a quiescent state in the sinusoids. Oxidative stress triggers the release of TNF-α from damaged hepatocytes. The damaged hepatocytes activate and recruit the KCs into the injured area around the central vein, where they release proinflammatory cytokines, such as TNF-α, TGF-β, and IL-6. These cytokines in turn activate NF-κB and COX-2, responsible for the production of NO and prostaglandins, respectively, causing nitrosative stress and contributing to the augmentation of CCl_4-induced hepatotoxicity (Kiso et al., 2012). We figured out that Met-PPx and its EtOAC and aqueous fractions overwhelm the inflammatory response by downregulating TNF-α and iNOS expression by attenuating oxidative stress and activation of KCs. Thus, the number of KCs around the central vein is reduced. However, butanol and *n*-hexane treatment showed a drastic increase in the number of KCs around the central vein, as evident from immunostaining, indicating that the active compound(s) is absent from these fractions.

CONCLUSION

From the aforementioned results of the current study, it is concluded that Met-PPx and its EtOAC and aqueous fractions have hepatoprotective potential to normalize the changes in serum markers by raising the activity of the endogenous antioxidant defense mechanisms to preclude oxidative stress by quenching free radicals in CCl_4-induced hepatotoxicity. Our findings also reveal that the Met-PPx and its EtOAC and aqueous fraction treatment significantly abrogated inflammatory response. Our work demonstrates that the hepatoprotective and free radical–quenching potential of the PP resides in the Met-PPx and its EtOAc and aqueous fractions due to the presence of bioactive compounds. Their use in precluding hepatotoxicity and ensuring the preserved structural integrity of the hepatocellular membrane deserves attention and further exploration.

DATA AVAILABILITY STATEMENT

The raw data supporting the conclusion of this article will be made available by the authors, without undue reservation.

ETHICS STATEMENT

The animal study was reviewed and approved by the Institutional Ethics Committee of COMSATS University, Islamabad. Written informed consent was obtained from the owners for the participation of their animals in this study.

AUTHOR CONTRIBUTIONS

RU, RAM, AmA, and AJ provided funding and conceived the study. AJ, HA, MK, and BNM designed and performed the experiments and collected and analyzed the data. HA, NK, and AJ wrote the first draft of the manuscript. AbA, SA, and SS critically edited the manuscript. All authors have read and approved the final version of the submitted manuscript.

FUNDING

All authors wish to thanks Researchers supporting Project (RSP-No-2021/119) at King Saud University, Riyadh, Saudi Arabia.

REFERENCES

Abid, M., Yaich, H., Cheikhrouhou, S., Khemakhem, I., Bouaziz, M., Attia, H., et al. (2017). Antioxidant Properties and Phenolic Profile Characterization by LC-MS/MS of Selected Tunisian Pomegranate Peels. *J. Food Sci. Technol.* 54 (9), 2890–2901. doi:10.1007/s13197-017-2727-0

Adhami, V. M., Khan, N., and Mukhtar, H. (2009). Cancer Chemoprevention by Pomegranate: Laboratory and Clinical Evidence. *Nutr. Cancer* 61 (6), 811–815. doi:10.1080/01635580903285064

Al-Jarallah, A., Igdoura, F., Zhang, Y., Tenedero, C. B., White, E. J., MacDonald, M. E., et al. (2013). The Effect of Pomegranate Extract on Coronary Artery Atherosclerosis in SR-BI/APOE Double Knockout Mice. *Atherosclerosis* 228 (1), 80–89. doi:10.1016/j.atherosclerosis.2013.02.025

Ali, H., Kabir, N., Muhammad, A., Shah, M. R., Musharraf, S. G., Iqbal, N., et al. (2014). Hautriwaic Acid as One of the Hepatoprotective Constituent of *Dodonaea viscosa*. *Phytomedicine* 21 (2), 131–140.

Anderson, M. E. (1985). Determination of Glutathione and Glutathione Disulfide in Biological Samples. *Methods Enzymol.* 113, 548–555. Academic Press. doi:10.1016/s0076-6879(85)13073-9

Ashoush, I. S., El-Batawy, O. I., and El-Shourbagy, G. A. (2013). Antioxidant Activity and Hepatoprotective Effect of Pomegranate Peel and Whey Powders in Rats. *Ann. Agric. Sci.* 58 (1), 27–32. doi:10.1016/j.aoas.2013.01.005

Bachoual, R., Talmoudi, W., Boussetta, T., Braut, F., and El-Benna, J. (2011). An Aqueous Pomegranate Peel Extract Inhibits Neutrophil Myeloperoxidase *In Vitro* and Attenuates Lung Inflammation in Mice. *Food Chem. Toxicol.* 49 (6), 1224–1228. doi:10.1016/j.fct.2011.02.024

Bandyopadhyay, A., López-Casillas, F., Malik, S. N., Montiel, J. L., Mendoza, V., Yang, J., et al. (2002). Antitumor Activity of a Recombinant Soluble Betaglycan in Human Breast Cancer Xenograft. *Cancer Res.* 62 (16), 4690–4695.

Banihani, S., Swedan, S., and Alguraan, Z. (2013). Pomegranate and Type 2 Diabetes. *Nutr. Res.* 33 (5), 341–348. doi:10.1016/j.nutres.2013.03.003

Bouroshaki, M. T., Sadeghnia, H. R., Banihasan, M., and Yavari, S. (2010). Protective Effect of Pomegranate Seed Oil on Hexachlorobutadiene-Induced Nephrotoxicity in Rat Kidneys. *Ren. Fail.* 32 (5), 612–617. doi:10.3109/08860221003778056

Bradford, M. M. (1976). A Rapid and Sensitive Method for the Quantitation of Microgram Quantities of Protein Utilizing the Principle of Protein-Dye Binding. *Anal. Biochem.* 72 (1-2), 248–254. doi:10.1006/abio.1976.9999

Brattin, W. J., Glende, E. A., Jr, and Recknagel, R. O. (1985). Pathological Mechanisms in Carbon Tetrachloride Hepatotoxicity. *J. Free Radic. Biol. Med.* 1 (1), 27–38. doi:10.1016/0748-5514(85)90026-1

Chen, Q., Zhan, Q., Li, Y., Sun, S., Zhao, L., Zhang, H., et al. (2017). Schisandra Lignan Extract Protects against Carbon Tetrachloride-Induced Liver Injury in Mice by Inhibiting Oxidative Stress and Regulating the NF-Kb and JNK Signaling Pathways. *Evid Based. Complement. Altern. Med.* 2017, 1–11. doi:10.1155/2017/5140297

Domitrović, R., Jakovac, H., and Blagojević, G. (2011). Hepatoprotective Activity of Berberine Is Mediated by Inhibition of TNF-α, COX-2, and iNOS Expression in CCl(4)-Intoxicated Mice. *Toxicology* 280 (1-2), 33–43. doi:10.1016/j.tox.2010.11.005

Domitrović, R., Jakovac, H., Milin, C., and Radosević-Stasić, B. (2009). Dose- and Time-dependent Effects of Luteolin on Carbon Tetrachloride-Induced Hepatotoxicity in Mice. *Exp. Toxicol. Pathol.* 61 (6), 581–589. doi:10.1016/j.etp.2008.12.005

Drotman, R. B., and Lawhorn, G. T. (1978). Serum Enzymes as Indicators of Chemically Induced Liver Damage. *Drug Chem. Toxicol.* 1 (2), 163–171. doi:10.3109/01480547809034433

El-Rashedy, A. H., Belal, S. K., Osman, H. E.-D., and Shehab, G. M. (2011). Protective Role of Pomegranate on Fatty Liver in Obesity: An Experimental Chemical & Histopathological Study. *Egypt. J. Hosp. Med.* 43, 162–172. doi:10.21608/ejhm.2011.16772

Hamoud, S., Hayek, T., Volkova, N., Attias, J., Moscoviz, D., Rosenblat, M., et al. (2014). Pomegranate Extract (POMx) Decreases the Atherogenicity of Serum and of Human Monocyte-Derived Macrophages (HMDM) in Simvastatin-Treated Hypercholesterolemic Patients: a Double-Blinded, Placebo-Controlled, Randomized, Prospective Pilot Study. *Atherosclerosis* 232 (1), 204–210. doi:10.1016/j.atherosclerosis.2013.11.037

Hong, M., Li, S., Tan, H. Y., Wang, N., Tsao, S. W., and Feng, Y. (2015). Current Status of Herbal Medicines in Chronic Liver Disease Therapy: the Biological Effects, Molecular Targets and Future Prospects. *Int. J. Mol. Sci.* 16 (12), 28705–28745. doi:10.3390/ijms161226126

Huang, Q. H., Xu, L. Q., Liu, Y. H., Wu, J. Z., Wu, X., Lai, X. P., et al. (2017). Polydatin Protects Rat Liver against Ethanol-Induced Injury: Involvement of CYP2E1/ROS/Nrf2 and TLR4/NF-B P65 Pathway. *Evidence-Based Complement. Altern. Med.* 2017, 1–14. doi:10.1155/2017/7953850

Huang, T. H., Peng, G., Kota, B. P., Li, G. Q., Yamahara, J., Roufogalis, B. D., et al. (2005). Anti-diabetic Action of Punica Granatum Flower Extract: Activation of PPAR-Gamma and Identification of an Active Component. *Toxicol. Appl. Pharmacol.* 207 (2), 160–169. doi:10.1016/j.taap.2004.12.009

Jeune, M. A., Kumi-Diaka, J., and Brown, J. (2005). Anticancer Activities of Pomegranate Extracts and Genistein in Human Breast Cancer Cells. *J. Med. Food* 8 (4), 469–475. doi:10.1089/jmf.2005.8.469

Kadiiska, M. B., Gladen, B. C., Baird, D. D., Germolec, D., Graham, L. B., Parker, C. E., et al. (2005). Biomarkers of Oxidative Stress Study II: Are Oxidation Products of Lipids, Proteins, and DNA Markers of CCl4 Poisoning? *Free Radic. Biol. Med.* 38 (6), 698–710. doi:10.1016/j.freeradbiomed.2004.09.017

Kaur, G., Jabbar, Z., Athar, M., and Alam, M. S. (2006). Punica Granatum (Pomegranate) Flower Extract Possesses Potent Antioxidant Activity and Abrogates Fe-NTA Induced Hepatotoxicity in Mice. *Food Chem. Toxicol.* 44 (7), 984–993. doi:10.1016/j.fct.2005.12.001

Khan, H., Jawad, M., Kamal, M. A., Baldi, A., Xiao, J., Nabavi, S. M., et al. (2018). Evidence and Prospective of Plant Derived Flavonoids as Antiplatelet Agents: Strong Candidates to Be Drugs of Future. *Food Chem. Toxicol.* 119, 355–367. doi:10.1016/j.fct.2018.02.014

Kiso, K., Ueno, S., Fukuda, M., Ichi, I., Kobayashi, K., Sakai, T., et al. (2012). The Role of Kupffer Cells in Carbon Tetrachloride Intoxication in Mice. *Biologic. Pharm. Bull.* 35, 980–983.

Kulkarni, A., Aradhya, S., and Divakar, S. (2004). Isolation and Identification of a Radical Scavenging Antioxidant - Punicalagin from Pith and Carpellary Membrane of Pomegranate Fruit. *Food Chem.* 87 (4), 551–557. doi:10.1016/j.foodchem.2004.01.006

Malik, A., Afaq, F., Sarfaraz, S., Adhami, V. M., Syed, D. N., and Mukhtar, H. (2005). Pomegranate Fruit Juice for Chemoprevention and Chemotherapy of Prostate Cancer. *Proc. Natl. Acad. Sci. U S A.* 102 (41), 14813–14818. doi:10.1073/pnas.0505870102

Moore, K. L., Dalley, A. F., and Agur, A. M. (2010). *Clinically Oriented Anatomy*. sixth ed. Philadelphia, USA: Lippincott Williams & Wilkins.

Moore, K. L., Dalley, A. F., and Agur, A. M. (2013). *Clinically Oriented Anatomy*. Philadelphia, USA: Lippincott Williams & Wilkins.

Olaleye, M. T., Akinmoladun, A. C., Ogunboye, A. A., and Akindahunsi, A. A. (2010). Antioxidant Activity and Hepatoprotective Property of Leaf Extracts of Boerhaavia Diffusa Linn against Acetaminophen-Induced Liver Damage in Rats. *Food Chem. Toxicol.* 48 (8-9), 2200–2205. doi:10.1016/j.fct.2010.05.047

Orgil, O., Schwartz, E., Baruch, L., Matityahu, I., Mahajna, J., and Amir, R. (2014). The Antioxidative and Anti-proliferative Potential of Non-edible Organs of the Pomegranate Fruit and Tree. *LWT - Food Sci. Techn.* 58 (2), 571–577. doi:10.1016/j.lwt.2014.03.030

Percival, M. (1998). Antioxidants. *Clinnutr Insights* 031, 1–4.

Pierce, R. A., Glaug, M. R., Greco, R. S., Mackenzie, J. W., Boyd, C. D., and Deak, S. B. (1987). Increased Procollagen mRNA Levels in Carbon Tetrachloride-Induced Liver Fibrosis in Rats. *J. Biol. Chem.* 262 (4), 1652–1658. doi:10.1016/s0021-9258(19)75686-5

Praneetha, P., Yellu, N. R., and Bobbala, R. K. (2019). Hepatoprotective Studies on Methanolic Extract Fractions of *Lindernia ciliata* and Development of Qualitative Analytical Profile for the Bioactive Extract. *Clin. Phytosci.* 5, 30.

Qureshi, N. N., Kuchekar, B. S., Logade, N. A., and Haleem, M. A. (2009). Antioxidant and Hepatoprotective Activity of Cordia Macleodii Leaves. *Saudi Pharm. J.* 17 (4), 299–302. doi:10.1016/j.jsps.2009.10.007

Rajeshkumar, S., Tamilarasan, B., and Sivakumar, V. (2015). Phytochemical Screening and Hepatoprotective Efficacy of Leaves Extracts of Annona Squamosa against Paracetamol Induced Liver Toxicity in Rats. *Int. J. Pharmacogn.* 2, 178–185. doi:10.13040/IJPSR.0975-8232.IJP.2(4).178-85

Rathi, A., Srivastava, A. K., Shirwaikar, A., Singh Rawat, A. K., and Mehrotra, S. (2008). Hepatoprotective Potential of Fumaria Indica Pugsley Whole Plant Extracts, Fractions and an Isolated Alkaloid Protopine. *Phytomedicine* 15 (6-7), 470–477. doi:10.1016/j.phymed.2007.11.010

Rechnagel, R. O., Glende, E. A., and Plaa, G. L. (1973). Carbon Tetrachloride Hepatotoxicity: an Example of Lethal Cleavage. *CRC Crit. Rev. Toxicol.* 2 (3), 263–297. doi:10.3109/10408447309082019

Singh, B., Singh, J. P., Kaur, A., and Singh, N. (2017). Phenolic Composition and Antioxidant Potential of Grain Legume Seeds: A Review. *Food Res. Int.* 101, 1–16. doi:10.1016/j.foodres.2017.09.026

Singh, R. P., Chidambara Murthy, K. N., and Jayaprakasha, G. K. (2002). Studies on the Antioxidant Activity of Pomegranate (Punica Granatum) Peel and Seed Extracts Using *In Vitro* Models. *J. Agric. Food Chem.* 50 (1), 81–86. doi:10.1021/jf010865b

Soliman, H. M., and Selim, A. O. (2012). Role of Hepatic Stellate Cells in Fibrogenesis in a Model of Pomegranate-Treated Fatty Liver Induced by Junk Food in Male Albino Rats Immunohistochemical and Electron Microscopic Study. *The Egypt. J. Histology* 35 (1), 54–66. doi:10.1097/01.ehx.0000410947.56955.e0

Stowe, C. B. (2011). The Effects of Pomegranate Juice Consumption on Blood Pressure and Cardiovascular Health. *Complement. Ther. Clin. Pract.* 17 (2), 113–115. doi:10.1016/j.ctcp.2010.09.004

Sun, F., Hamagawa, E., Tsutsui, C., Ono, Y., Ogiri, Y., and Kojo, S. (2001). Evaluation of Oxidative Stress during Apoptosis and Necrosis Caused by Carbon Tetrachloride in Rat Liver. *Biochim. Biophys. Acta* 1535 (2), 186–191. doi:10.1016/s0925-4439(00)00098-3

Vestena, A., Piton, Y., de Loretto Bordignon, S. A., Garcia, S., Arbo, M. D., Zuanazzi, J. A., et al. (2019). Hepatoprotective Activity of Verbena Litoralis, Verbena Montevidensis and Their Main Iridoid, Brasoside. *J. Ethnopharmacol.* 239, 111906. doi:10.1016/j.jep.2019.111906

Wei, X. L., Fang, R. T., Yang, Y. H., Bi, X. Y., Ren, G. X., Luo, A. L., et al. (2015). Protective Effects of Extracts from Pomegranate Peels and Seeds on Liver Fibrosis Induced by Carbon Tetrachloride in Rats. *BMC Complement. Altern. Med.* 15 (1), 389. doi:10.1186/s12906-015-0916-9

Wong, F. W., Chan, W. Y., and Lee, S. S. (1998). Resistance to Carbon Tetrachloride-Induced Hepatotoxicity in Mice Which Lack CYP2E1 Expression. *Toxicol. Appl. Pharmacol.* 153 (1), 109–118. doi:10.1006/taap.1998.8547

Xiao, J. (2017). Dietary Flavonoid Aglycones and Their Glycosides: Which Show Better Biological Significance? *Crit. Rev. Food Sci. Nutr.* 57 (9), 1874–1905. doi:10.1080/10408398.2015.1032400

Zhai, X., Zhu, C., Zhang, Y., Sun, J., Alim, A., and Yang, X. (2018). Chemical Characteristics, Antioxidant Capacities and Hepatoprotection of Polysaccharides from Pomegranate Peel. *Carbohydr. Polym.* 202, 461–469. doi:10.1016/j.carbpol.2018.09.013

Conflict of Interest: The authors declare that the research was conducted in the absence of any commercial or financial relationships that could be construed as a potential conflict of interest.

Publisher's Note: All claims expressed in this article are solely those of the authors and do not necessarily represent those of their affiliated organizations, or those of the publisher, the editors, and the reviewers. Any product that may be evaluated in this article, or claim that may be made by its manufacturer, is not guaranteed or endorsed by the publisher.

Advantages of publishing in Frontiers

OPEN ACCESS
Articles are free to read for greatest visibility and readership

FAST PUBLICATION
Around 90 days from submission to decision

HIGH QUALITY PEER-REVIEW
Rigorous, collaborative, and constructive peer-review

TRANSPARENT PEER-REVIEW
Editors and reviewers acknowledged by name on published articles

Frontiers
Avenue du Tribunal-Fédéral 34
1005 Lausanne | Switzerland

Visit us: www.frontiersin.org
Contact us: frontiersin.org/about/contact

REPRODUCIBILITY OF RESEARCH
Support open data and methods to enhance research reproducibility

DIGITAL PUBLISHING
Articles designed for optimal readership across devices

FOLLOW US
@frontiersin

IMPACT METRICS
Advanced article metrics track visibility across digital media

EXTENSIVE PROMOTION
Marketing and promotion of impactful research

LOOP RESEARCH NETWORK
Our network increases your article's readership